DISSERTATION

DEVELOPMENT AND APPLICATION OF NEW DIAGNOSTIC ASSAYS FOR THE DETECTION OF PRION PROTEINS IN TRANSMISSIBLE SPONGIFORM ENCEPHALOPATHIES

Submitted by

Toru Ishii

Graduate Degree Program in Cell and Molecular Biology

In partial fulfillment of the requirements

For the Degree of Doctor of Philosophy

Colorado State University

Fort Collins, Colorado

Summer 2018

Doctoral Committee:

Advisor: Glenn Telling

Howard Liber
Stephanie McGrath
Eric Ross
Mark Zabel

ABSTRACT

DEVELOPMENT AND APPLICATION OF NEW DIAGNOSTIC ASSAYS
FOR THE DETECTION OF PRION PROTEIN IN
TRANSNMISSIBLE SPONGIFORM ENCEPHALOPATHIES

Transmissible spongiform encephalopathies (TSEs), well known as prion diseases, are fatal neurodegenerative disorders in humans and animals, which a prion protein (PrP) mainly implicates with the TSE pathogenesis. The normal cellular PrP isoform, referred to as PrP^{C}, predominantly forms an α-helical structure. A structural alteration of the PrP^{C} isoform can misfold into the infectious and pathogenic PrP isoform, referred to as PrP^{Sc} (or PrP^{D} as disease-associated PrP). The PrP^{Sc} isoform consists of a β-sheet rich structure and accumulates in the central nervous system (CNS). The structural change and accumulation of this abnormal conformer alters physiochemical properties of the PrP^{C} isoform. However, the conversional mechanism from PrP^{C} to PrP^{Sc} isoforms is not clearly known. In general, the PrP^{C} structure has two conserved Asparagine (N)-glycosylation sites that generate four various glycosidic forms (unglycosyl, two differing monoglycosyl and diglycosyl). In preliminary studies, TSE-disease mice exhibited the increased detection of under-glycosylated PrP forms, compared to controls. Although protein glycosylation plays various structural and functional roles, the importance of these glycans is not clarified in TSE pathogeneses.

Recently, novel monoclonal antibodies (mAbs) against PrP molecules were reported. Of these mAbs, PRC7 mAb can recognize an unglycosyl form and one

monoglycosyl form (mono-1) of PrP molecules specifically. In addition, PRC7 mAb has a unique feature to require denaturation and renaturation of PrP molecules to recognize PrP^{Sc} isoforms. Since PRC7 mAb cannot react with a diglycosyl PrP form that an abundance of normal PrP^{C} isoforms express, PRC7 mAb preferentially detects PrP^{Sc} isoforms. Thus, these features of PRC7 mAb were applied to develop a sensitive enzyme-linked immunosorbent assay (ELISA) for the detection and quantification of under-glycosylated PrP forms in TSE-infected samples. My central hypothesis is that, the detection of under-glycosylated PrP forms is the hallmark of TSEs as diagnostic biomarkers for the disease progression.

Here, I propose that loss of full glycosylation is implicated in the pathological mechanisms of TSEs. For instance, glycosylation is involved in the maintenance of protein structure. Thus, its modulation can initiate unstable conditions for maintaining proper PrP^{C} conformations, which induce pathologic alterations of the PrP^{C} structure. These aberrant formations could lead functional impairments of normal PrP^{C} isoforms. In another aspect, the PrP^{Sc} isoform may lose glycans during the disease development of TSEs. Therefore, I assume that under-glycosylated PrP forms can be preferentially generated during the disease progression. To accomplish the proposed studies, I have developed two sensitive ELISA methods for the detection and quantification of PrP molecules in TSE-infected samples. Using the PRC7 and PRC5 mAbs as capture and detecting antibodies respectively, the 7-5 ELISA method specifically recognizes the certain under-glycosylated PrP forms that are significantly detected in TSE-infected materials. In addition, the D-5 ELISA method uses D18 anti-prion antibody as a capture antibody and has an exceptional capability to determine levels of only PrP^{C} or total PrP

molecules by different sample preparations. Using the D-5 ELISA method, I have detected the reduction of PrP^{C} levels in TSE-infected materials at terminal stages, whereas total PrP levels were increased. These results were similar observations to a recent article using the conformation-dependent immunoassay. Since my protocols do not require a proteinase K (PK) reagent, these ELISA methods will be ultimately beneficial for TSE diagnoses, especially for detecting PK-sensitive PrP^{Sc} forms. Furthermore, the ELISA approaches would contribute to understand the TSE pathogenesis under the specific detections of PrP^{Sc} isoforms, based on glycosylated forms for distinguishing PrP^{C} from PrP^{Sc} isoforms. This dissertation study will provide an innovative framework of the proposed projects that will achieve beneficial impacts into the fields of veterinary medicine, human medicine, and public health.

ACKNOWLEDGEMENTS

Many people contributed to the work described in this dissertation and I am very grateful to all of them. I am truly grateful to acknowledge Dr. Howard Liber, Dr. Paul Laybourn, and Ms. Lori Williams for their favorable supports, assistances, guidances, and encouragements during my graduate study in the Cell and Molecular Biology Graduate Program at Colorado State University. Their patience and acceptance helped me to achieve my goal and complete this dissertation. I would also like to deeply acknowledge Dr. Jodie Hanzlik, Dr. Kathy Partin, Dr. Stephanie McGrath, Ms. Kathleen Ivy, Ms. Sarma Sagarika, and Ms. Melissa Emerson. Their dedication and patience allowed for the successful progress in my graduate school life.

I would also like to gratefully thank Dr. Kristina Quynn in the CSU Writes, all staff advisers in the Writing Center, and Dr. Ann Hess in the Franklin A. Graybill Statistical Laboratory for draft writings and statistical analyses. Their valuable guidance, advice, and support promoted me to complete this dissertation. These CSU resources are extremely valuable for all students, especially for international students.

I am grateful to everyone in the Department of Microbiology, Immunology and Pathology, and all other CSU resources for your kind support and assistance. A special thanks is extended to Dr. Jifeng Bian and Dr. Julie Moreno for their scientific suggestions and reviews for this dissertation.

Finally, I would like to express gratitude to my PhD committee for guidance and understanding throughout my study. Without their acceptance, I would not be able to accomplish and fulfill my wishes and goals.

DEDICATION

I would like to dedicate this work to my wife, Yutaka Ishii. She has provided persistent support and great enthusiasm throughout my graduate studies in the US. I would also like to thank my daughters, Chihiro Sierra Ishii and Masaki Seda Ishii, who have given wonderful life for my wife and myself. Finally, I would like to dedicate this work to my parents, Shigeru and Kayoko Ishii, and my younger sister Miki Ishii, who have supported my dream and our lives in the US. Without their love and support, none of this study and degree program would have been possible.

TABLE OF CONTENTS

ABBREVIATIONS OF STANDARD PROTEINOGENIC AMINO ACIDS

Amino acid	Abbreviation (3 letters)	(1 letter)	Molecular Weight
Alanine	Ala	A	89.094
Arginine	Arg	R	174.203
Asparagine	Asn	N	132.119
Aspartic acid	Asp	D	133.104
Cysteine	Cys	C	121.154
Glutamic acid	Glu	E	147.131
Glutamine	Gln	Q	146.146
Glycine	Gly	G	75.067
Histidine	His	H	155.156
Isoleucine	Ile	I	131.175
Leucine	Leu	L	131.175
Lysine	Lys	K	146.189
Methionine	Met	M	149.208
Phenylalanine	Phe	F	165.192
Proline	Pro	P	115.132
Serine	Ser	S	105.093
Threonine	Thr	T	119.119
Tryptophan	Trp	W	204.228
Tyrosine	Tyr	Y	181.191
Valine	Val	V	117.148

CHAPTER 1

INTRODUCTION

Transmissible spongiform encephalopathies (TSE, TSEs), well known as prion diseases, are fatal neurodegenerative disorders in humans and animals, such as Creutzfeldt-Jacob disease (CJD) in humans, bovine spongiform encephalopathy (BSE) in cattle, chronic wasting disease (CWD) in elk, deer and moose, and scrapie in sheep and goat.[1-3] In general, TSEs are classified into three types: sporadic, genetic or infectious/acquired form. The characteristic features of the TSE pathology are observed in the central nervous system (CNS), especially in the brain, such as neuronal loss, spongiform degeneration and gliosis. Although these diseases develop slowly, TSE-affected individuals and animals suffer from impairments of CNS functions that propagated and accumulated pathogens induce behavioral and neurological abnormalities. Once onsets of clinical signs appear progressively, these mental and physical abnormalities deteriorate health conditions. The prevention of possible TSE transmissions between same and different species is critically important in public health and veterinary medicine. At present, no treatment is available to cure these diseases.

The relevant history of TSE most easily described through accounts of BSE in cattle, widely known as mad cow disease.[4-6] Since the BSE epidemic between the middle 1980s and early 2000s in the United Kingdom, Europe, North America and Japan, this disease has had serious attentions in public health and veterinary medicine through the world, especially for zoonotic transmissions (communicable infectious pathogens and diseases between animals and humans). The BSE epidemic has

influenced meat industry in economic and international trade. Through exposure to contaminated foods with BSE, its transmitted pathogens developed a new type of CJD in humans, described as Variant Creutzfeldt-Jacob disease (vCJD).[7-9] After these emerging outbreaks, preventions of BSE have been organized. As a result, the incidences of BSE and vCJD in the United Kingdom have decreased after these epidemic peaks in 1992 and 2000, respectively. However, the risks of BSE re-emergence and transmission to human and other animals still remain because of some limitations for detecting its pathogen by current TSE diagnoses.

While BSE outbreaks have been under surveillance in affected countries for the last decade, CWD has continuously expanded its outbreaks as a current progressive TSE problem through the world.[10,11] CWD is an emerging infectious disease in wild and captive cervid family (i.e. deer, elk and moose). In 1967, the first case of CWD was identified in captive deer in Northern Colorado. Since then, this infectious disease has been detected in 24 states of the United States and 3 provinces of Canada through North America. Until 2000, CWD was an endemic disease in these two countries. In late December 2000, however, the first CWD case outside the North America was detected in South Korea. This is also the first CWD detection in Asia. In the 1990s, several live elk were exported from CWD-contaminated farms in Canada to South Korea. Unfortunately, these CWD-exposed elk presumably became the infectious sources to spread its pathogens through a new country in a different continent. Alarmingly, the first European case of CWD was diagnosed in Norway in March 2016, which was also the first detection of natural CWD infection in a free-ranging reindeer through the world. The Norwegian Veterinary Institute has also detected three other CWD cases in 2016: one

moose in May, another moose in June, and one reindeer in August. These affected animals in Norway were found in wild natures. Since it is still unknown how CWD appears in Europe, the spread and outbreak of CWD internationally indicates a serious situation of TSE-related epidemics. The propagating factors of these CWD outbreaks have not been definitively investigated nor has the communicability of CWD pathogen to humans or the incidence of human TSE development caused by the infectious disease been confirmed.[12] The risk of CWD as zoonosis still remains under surveillance of public health and veterinary medicine. Given the spread of TSE etiology and propagation, investigations of its pathogenic mechanism would provide clear strategies for disease prevention and eradication.

The common molecular mechanism of TSE pathogeneses in multiple species (i.e. human, cattle, deer, sheep) is defined as the conformational conversion of prion protein (PrP) from normal cellular PrP isoform (PrP^{C}) to abnormally-misfolded infectious PrP isoform (PrP^{Sc}).[13-16] PrP^{C} is a monomer with predominantly α-helical structure, whereas PrP^{Sc} forms prone to oligomerization and aggregation with a β-sheet rich structure. At present, the mechanism of conversions from normal PrP^{C} to pathologic PrP^{Sc} isoforms is not clearly understood. However, the structural change to this abnormal conformer alters the physiochemical properties of PrP molecules as its cellular and molecular pathogenesis, and also accumulations of aggregated PrP^{Sc} agents in the CNS lead to the development of TSEs as like other neurodegenerative diseases. During the disease progression, the pathogenicity protein and its propagation disrupt normal functions of the brain and nervous systems in TSE-affected individuals and animals. These identifications indicate that the abnormal change of a proper PrP

structure is a key element to trigger the TSE development. The conformational alteration of PrP is an essential target to identify further TSE pathogeneses and analyze the pathogens in diagnoses. The basic processes of protein conformational development are necessary to demonstrate what is normal protein structure and abnormal change. Therefore, this introductory chapter is comprised of four sections with general and specific background information: 1) Protein structures, synthesis, glycosylations, and related pathologies; 2) Prion Protein and TSE pathogeneses (including aberrant PrP glycosylations; 3) Traditional TSE diagnoses and limitations; 4) Introduction to work in this dissertation research (novel anti-PrP monoclonal antibodies in house; research overview and specific aims). The order of these sections will make it easier to understand the projects in this dissertation as well as the strategies for future innovations.

Section 1: Protein structure, synthesis, glycosylation, and related pathologies

Fundamental Protein Structures

Proteins are macromolecules formed in three-dimensional structures, referred to as polypeptides, which consist of large assembled chains of amino acid residues.[17-19] The amino acid residue is synthesized with series of 20 different L-amino acids, which are encoded in a gene (genetic code). A covalent chemical bond, called peptide bonds, links two consecutive amino acid residues. During protein synthesis, the amino acid residues in protein are chemically modified for its property, folding, stability, and activity. This process is critical for developing a proper structure and preforming biological functions of the protein.

A protein structure is typically classified in four levels: primary, secondary, tertiary, quaternary structures.[17-19] The primary structure of a protein is specified as its unfolded liner sequence of amino acids in a polypeptide chain, which does not form the functional three-dimensional structure of a protein yet. Two consecutive amino acid monomers in a polypeptide chain are linked by peptide bonds, which are known as covalent chemical bonds (molecular bonds) for sharing electronic interactions between atoms. After this synthesis, these primary structures of polypeptide chains fold into different shapes at the second level.

The secondary structure is the general three-dimensional form of a local sub-structure of the polypeptide chains stabilized by hydrogen bonds, electrostatic attractions between atoms.[17-19] The definition of hydrogen bonds helps to explain a structural formation of a protein: “the hydrogen bond is an attractive interaction between a hydrogen atom from a molecule or a molecular fragment X-H in which X is more electronegative than H, and an atom or a group of atoms in the same or a different molecule, in which there is evidence of bond formation”.[20] Such secondary structures are defined by patterns of hydrogen bonds: α-helix and β-sheet are the two common types that have important roles in protein conformation. The α-helix forms a right-hand coiled or spiral conformation, the most prevalent element in local structures of proteins. Among the 20 L-amino acids, methionine, alanine, leucine, glutamine and lysine have high propensities to form α-helical structures, whereas proline, glycine, tyrosine, and serine have low propensities to adopt this spiral conformation. Proline and glycine have features to disrupt or interfere the conformational regularity of α-helix. Another common type, the β-sheet, forms a twisted and pleated sheet structure, consisted of two or more

hydrogen bonded β-stands. The β-stand is a single section of a polypeptide chain with amino acid residues in the β-sheet structure. Hydrogen-bonding interactions of adjacent β-stands in either parallel or antiparallel orientation form the β-sheet conformation. The β-strands in the truncal site of the β-sheet consist of large aromatic residues (i.e. tryptophan, tyrosine and phenylalanine) and β-branched amino acids (i.e. isoleucine, valine, and threonine): whereas proline is detected in the β-strands at the edge site of the β-sheet and introduces right-angle bends in the polypeptide.[21]

These secondary structures of α-helix and β-sheet fold together to create tertiary structure—a global three-dimensional conformation of a single and monomeric protein molecule.[17-19] Through this protein folding process, each protein achieves its specific native tertiary structure in order to function properly. A covalent bond, called disulfide bond (S-S bond, or disulfide bridge), links the thiol groups of two cysteine amino acids in this globular structure. The cysteine connection of disulfide bond has an important role to stabilize tertiary structure of a protein, and fold its proper conformation.

Quaternary structure is the protein complex that multimeric protein molecules with tertiary structures assemble.[17-19] In most proteins, proper assemblies of protein-protein interaction and protein complex formation provide conformational stability and perform biological functions. Thus, properly folded (tertiary) and assembled (quaternary) structures are essential conditions for functionalities to promote normal ability of a certain protein. Obviously, protein folding is a critical process in which each protein acquires its specific native global three-dimensional shape, referred to as a native state (native conformation or structure), to perform its proper function.

Environmental or other external/internal factors such as temperature, pH, voltage, ion concentration, or chemical reagents influence this native state of the folded and/or assembled protein conformation.[17-19] These factors disrupt three-dimensional protein conformations (secondary, tertiary and quaternary structures) and lead to an unfolded liner protein structure (primary structure). This unfolding process is called denaturation. After denaturation, a protein loses its functional activity because its native state conformation is already unfolded or disrupted, referred to as a denatured state. Although this denatured state is generally irreversible, an unfolding process could be reversible for some proteins in certain conditions when the denaturing factors are eliminated. Since denaturation does not alter peptide bonds of amino acid residues in a polypeptide chain, the primary structure of a protein remains intact and is capable of regaining its three-dimensional native conformation and function. This refolding process is called renaturation. Based on these folding and refolding mechanisms, proteins can maintain their proper native conformations and physiological functions. In other words, incorrect processes of these conformational mechanisms interfere protein homeostasis and initiate pathologic alterations of proteins in cellular and molecular environments.

Structural Abnormalities of Proteins as Pathological Features

The conformational change of the PrP molecule is the hallmark of TSE pathogeneses, which the natively folded isoform with a monomeric and α-helix rich structure alters to the abnormally misfolded isoform with an oligomeric/aggregable and β-sheet rich structure.[22] This pathological modification of the PrP structure induces aberrant propagations, aggregations and accumulations of the misfolded PrP. These

conditions dysregulate normal PrP functions and also generate toxic abilities of the abnormal PrP isoforms, causing damages and/or death to affected cells in the brain and nervous systems of TSE-affected individuals and animals.

Similar protein conformational abnormalities in TSEs have recently been identified in several major human diseases, such as Alzheimer's disease (AD), Parkinson's disease (PD), amyotrophic lateral sclerosis (ALS), Type II diabetes mellitus (Type II DM) and cataracts.[23-29] In these diseases, pathologies with disrupted native states and misfolded conformations of certain proteins have been identified. The TSE-like pathological mechanisms of these major diseases have gained serious awareness leading to innovations in advanced diagnoses and treatments, as well as understandings in protein physiology and pathology. Including TSEs, these types of protein conformation-associated diseases are referred to as protein misfolding diseases (PMD, PMDs: proteopathy, proteinopathy, or protein conformational disorder).

In PMD pathogeneses, several proteins have been identified their associations with certain diseases. [23-29] A specific protein is abnormally altered to misfolded structure that failures of its proper folding process induce. In this misfolded states, normal functions of the specific proteins are impaired because misfolded proteins can interfere with its protein physiology and proper protein assemblies to form protein-protein interactions and protein complexes. In fact, the misfolded proteins can induce disordered assemblies that lead to form massive aggregations and accumulations of the abnormal proteins. This pathological feature of a disordered proteinaceous assembly, called amyloid (amyloid fold or amyloid fibrils), is generally deposited extracellularly in tissues.[30-33] This aggregated proteinaceous formation disrupts tissue structures and

physiological functions of organs in the body. Subsequently, these pathological alterations trigger disease developments. Just like the characteristic feature of TSEs pathogeneses, amyloid formations in PMDs consist with aggregations of massive misfolded proteins. In most PMDs, secondary and/or tertiary structures (three-dimensional structures) of underlying misfolded proteins are altered conformationally from α-helix rich native state to β-sheet rich misfolded state.[23,27,34-38] Generations of aberrant isoforms of a certain protein progressively propagate its misfolded proteins. This propagation results in depositions of these aggregations in affected tissues and organs. Moreover, an abundance of misfolded proteins in PMD generates toxic abilities to affected tissues and organs, induced by cellular injuries and deaths. Thus, the misfolded conformation and deposition of disease-associated proteins are characterized as the hallmarks of PMD pathogeneses.[23-29] To understand the PMD pathogeneses and develop advanced diagnoses and therapies, it is essential to target misfolded proteins and aggregated proteinaceous assemblies in these diseases. Innovations of effective treatments and analytical methods for studying misfolded proteins and proteinaceous aggregates are still in progress. Future discoveries in TSE research will contribute to medical innovations in other PMDs, such as major human neurodegenerative disorders (i.e. AD, PD, and ALS).[39-41] To investigate new targeting approaches, distinguishing between normal and abnormal protein isoforms must be one of novel diagnostic and therapeutic applications in PMDs and TSEs. The fundamental mechanisms of normal protein syntheses are important to understand how new proteins is generated properly and why they might misfold abnormally.

Protein Synthesis and Glycosylation

Proper protein structures and conformations are essential for maintaining normal biology and physiology in cells, as well as functions of tissues and organs in the body.[17-19] During the protein synthesis, cells generate new proteins with accurate compositions, structures, and conformations, based on genetic information in deoxyribonucleic acid (DNA) that encodes a specific amino acid sequence of each certain protein. The processes of the protein synthesis are defined by the two steps of transcription and translation, which are initiated from the nuclei to cytoplasms in individual cells. Newly synthesized proteins are transported to appropriate locations for their functions, known as another step of translocation. Modifications regulate protein maturation conformationally and functionally, and also eliminate incorrectly synthesized proteins. Glycosylation is an essential modification for facilitating protein folding correctly and stabilizing protein structure functionally. The five-key stages of protein synthesis describe below to clarify its normal processes and some possible impairment.[17-19]

1) Transcription: In this initial stage of protein synthesis, the genetic information of proteins in DNA is copied (transcribed) to molecules of ribonucleic acids (RNA) with one strand of the DNA double helix, used as a template. This process in the nucleus is known as transcription, and this transcribed RNA molecule is called messenger RNA (mRNA).

2) Translation: The next stage of protein synthesis, called translation, takes place in the cytoplasm. mRNA enters from the nucleus to the cytoplasm where the mRNA interacts with a ribosome. This transcribed template of DNA is decoded by multiple ribosomes simultaneously for the protein synthesis. A ribosome forms two

subunits of ribosomal RNA (rRNA) molecules with a variety of ribosomal proteins. A small subunit determines the correct sequence of amino acids encoded in each mRNA. Another subunit is a large subunit that selects and assembles necessary amino acids to generate a polypeptide, which peptide bonds link amino acid residues in a long liner chain. Initially, the mRNA binds to a ribosome for translating the encoded specific amino acid sequence. For this interaction, transfer RNA (tRNA) molecules play a key role to specify the encoded specific amino acid sequence from mRNA and transport the corresponding amino acids to a ribosome for synthesizing new proteins.

Through transcription and translation, the correct sequence of amino acids is generated longer and assembled into a polypeptide—an unfolded liner structure known as the primary structure of a protein. In the following processes of protein synthesis, primary structures of newly synthesized proteins fold into three-dimensional conformations for holding their native state structures, described above as protein folding.

3) Translocation: Only qualified proteins are transported intracellularly or extracellularly to functionally appropriate locations at the end stage of protein synthesis. This protein transport, known as translocation, occurs during or after the processes of translation, called co-translational and post-translational translocations, respectively. To fold proper structures, newly synthesized proteins proceed through the quality controls in cellular mechanisms. Most proteins in eukaryotic cells (i.e. mammal and plant cells) are transported from a ribosome to the endoplasmic reticulum (ER), the Golgi apparatus (Golgi or Golgi complex) or endosome-lysosomal system through the co-translational translocation pathway. The post-translational translocation pathway is common in

prokaryotic organisms (i.e. bacterium and archaea). After translation has been completed, proteins are exported from a ribosome to the transporting destinations such as the ER (eukaryotes), plasma membrane (prokaryotes) or other organelles including mitochondria, chloroplast, and peroxisome via the post-translational translocation pathway. Through these translocation pathways, newly synthesized proteins in eukaryotic cells are assembled with a certain protein in the ER, called chaperone, which supports processes of proper protein folding and assembly. Chaperone proteins bind to these unfolded or partially folded proteins and assist their protein folding. This interaction with chaperone protects the newly synthesized proteins from aggregations with other molecules that form non-functional or abnormal protein assembly. Subsequently, only properly folded proteins contained in vesicles are transported to the Golgi apparatus for further enzymatic processes. These proteins are modified and sorted for transport to subsequent destinations in intracellular or extracellular sites for their functions, packaged by one of three different types of vesicles: exocytotic, secretory, and lysosomal.

4) Modification: During the protein synthesizing processes above, responsible cellular recourses facilitate new protein products to fold correctly and to stabilize their structures functionally. Concurrently, these end-stage products of protein synthesis are modified chemically before or after proteins are released from ribosomes, called co-translational and post-translational modifications, respectively. Mostly, proteins in eukaryotic cells are regulated by post-translational modification, which is associated with the quality control of protein synthesis. This modifying process is important for folding proteins properly and translocating new proteins to appropriate destinations

functionally in cellular networks. Specific modifications occur to the amino acid chains or the peptide termini (C-terminal and N-terminal) of proteins. One type of modification determines specific amino acids of a protein and catalyzes its linked peptide bonds by enzymes, called proteases. This proteolytic process breaks down the primary structure of a protein into small amino acids irreversibly, known as protein degradation, which prevents accumulations of damaged or misfolded proteins by the proteolytic reactions. These reactions can occur at various steps in the intracellular protein synthesis through the ER, the Golgi apparatus and the endosome-lysosomal or ubiquitin-mediated pathways during or after translation. Thus, impairments of protein degradation are involved in many disorders such as pancreatitis, rheumatoid arthritis, and Alzheimer's disease. Furthermore, another type of modification targets specific amino acid side chains of a protein chemically or spontaneously, with or without enzymes. The common processes of these modifications include glycosylation, phosphorylation, ubiquitination, methylation and acetylation. Generally, the post-translational modification in eukaryotic cells is incorporated in various cellular organelles and membranes such as the ER, the Golgi apparatus, and endosome-lysosomal system. Briefly, the ER, specifically the rough ER, is an important organelle for the quality control and modification of newly synthesized proteins. This organelle facilitates protein folding, enzymatic-proteolysis process, and protein glycosylation (called N-linked glycosylation) into the functional three-dimensional native structure of a protein. The Golgi apparatus plays key roles in enzymatic modifications for glycosylation (called O-linked glycosylation), degradation, and translocation of proteins. In the final stage of protein synthesis, the endosome-lysosomal system is an essential step. This system has functions in the proteolytic and

other modifications for protein maturation conformationally and functionally. Under the regulations of enzymatic cleavages, proteins acquire their active states from inactive forms, prior to transporting to intracellular destinations or secreting to cellular surface or extracellular space. Overall, hundreds of different proteins are newly synthesized in cells every single second, whereas almost 30% of new products are rapidly degraded within minutes of their syntheses.[42] These regulations indicate that the quality control of protein synthesis is a critically important mechanism for conformationally generating new normal proteins and expressing them to functionally appropriate locations for cellular biology and physiology. Also, this quality-control mechanism prevents aggressions and accumulations of damaged, misfolded or incompleted structural proteins. The balance of protein degradation and protein translocation maintains protein synthesis correctly in these intracellular systems through co- and post-translational modifications. Therefore, it is clear that the normal protein function is directly dependent on protein structure with proper folding and modifications. Seriously, failures of these processes can initiate impairments of normal functions in cells and eventually induce pathological developments.

5) Glycosylation: In the processes of protein synthesis, protein glycosylation is a key modification for most proteins in eukaryotic cells, to facilitate protein folding and stabilize protein structure functionally. Protein glycosylation is an enzyme-directed chemical reaction in which carbohydrates (sugar moieties or residues, referred to glycans and saccharides) are covalently attached by glycosidic bonds to specific amino acid residues in unfolded proteins (primary structures) during co- and post-translational modifications. A glycosylated protein, called a glycoprotein, is detected in many

organisms of eukaryotes and prokaryotes. The majority of newly synthesized proteins that proceed through the ER and Golgi apparatus are glycosylated. Generally, glycosylation in the ER is essential for monitoring protein folding as a checkpoint, whereas glycosylation in the Golgi apparatus contributes to protein translocation. Among various forms of carbohydrate-protein glycosidic linkages, major types of protein glycosylation are characterized by the two linkages based on binding sites of carbohydrates to specific amino acid residues: N-linked glycosylation and O-linked glycosylation. Briefly, N-linked glycosylation is the most common type of glycosylation, typically processed in the rough ER and the Golgi apparatus. Glycans are covalently attached to nitrogen atoms in the side chains of asparagine (Asn or N) that are adjacent to cysteine (Cys or C), serine (Ser or S) or threonine (Thr or T) followed by any amino acid except proline (Pro or P). For instance, the amino acid sequence of a N-linked glycosylation site is denoted as Asn-X-Cys or Asn-X-Ser in which X is any amino acid except Pro. Also, N-linked glycosylation has three main types, defined by formations of sugar residues and structures: high mannose, hybrid, and complex. O-linked glycosylation generally occurs only in the Golgi apparatus in which glycans bind to hydroxyl-oxygen atoms in the side chains of Ser (S), Thr (T), hydroxylysine (hLys), or hydroxylprotein acceptor site.[43] These amino acids are located in close proximity to Pro (P). O-linked glycosylation are categorized into seven major types listed below, based on the glycan-linked sites of amino acid residues and the types of carbohydrates. As the major structural components on cell membranes and secreted proteins, these N-linked and O-linked protein glycosylations have critical roles to facilitate proper structural folding and increase in their conformational stability. Thus, sites and forms of

glycosylation influence nascent liner proteins to fold into their secondary structures and stabilize conformations into their native states of tertiary and quaternary structures.[44] In fact, many proteins are not correctly folded without glycosylation because the glycosidic attachments assist the conformational stability for protein structure. In other words, glycosylated states are involved in the prevention and elimination of incorrectly folded proteins, which are proceeded to degradation. Given this process, glycosylation emerges an important process in the maintenance of correct protein conformations. Glycoproteins also interact with other specific proteins to initiate or modulate various essential biological mechanisms. As a result, glycosylation is a critical influence on the functions of glycoproteins and their assembled complexes in these mechanisms. Below, physiobiological and pathological features of N-linked and O-linked protein glycosylations are described.

N-linked glycosylation. During protein synthesis in the ER, the quality control of proteins occurs at any stage, such as translation, modification, assembly with chaperon, and transport. In the quality-controlling processes, N-linked glycosylation has essential endogenous functions as a checkpoint for the quality control in protein folding and selection through the ER. On attached proteins, this glycosylation provides stability as a structural component and modifies solubility against molecular environmental changes (i.e. temperature, and pH). In addition, a checkpoint function for protein degradation is closely linked to glycosylation states on attached proteins. As an exogenous function, the N-linked glycosylation directs transportation of glycoproteins and mediates cell-cell signaling, such as cell-cell and cell-matrix interaction. In the immune system, glycosylation has a role in cell-cell interactions of immune cells via lectins,

carbohydrate-binding proteins, which recognize specific carbohydrate residues on proteins in targeting cells. Furthermore, viruses propagate in infected cells and produce viral proteins linked with N-linked glycosylation.[45] This glycosidic structural component on viral proteins has a protective role to shield viruses from recognition by immune cells. For instance, human immunodeficiency virus (HIV) contains a high density of N-linked glycans on its envelope viral protein.[46] Parasites (i.e. Trypanosoma cruzi) also have similar strategies of immune evasion in glycoproteins.[47] In contrast, immune cells can determine dissimilar chemical compositions of glycosidic diversities between host proteins and viral/parasitic proteins. Thus, this immunological recognition by glycans operates as a functional barrier against cross-species transmissions of pathogens, such as zoonotic transmission.[45] Interestingly, current research indicates that this glycosylation-based self-recognition might be associated with underlying pathophysiological mechanisms in autoimmune diseases and organ transplant rejection. It is clear that N-linked glycosylation has protective functions for proteins and cells from intrinsic and extrinsic impairments. This glycosylation is also an essential checkpoint factor for self and non-self recognitions from infectious particles in transmissions and foreign materials from transplantations. Failures of this checkpoint factor impact the immune systems and the normal physiology in the body, which induce pathological development. In fact, defects of N-linked glycosylation or mutations of associated genes in this glycosylation have been detected in various disorders (i.e. congenital disorders of glycosylation in infants, the most known inherited glycosylation diseases). N-linked glycosylation-associated disorders cause pathological conditions particularly in the nervous system, such as ataxia, seizure, stroke, developmental delay, and other

neurological impairments. Therefore, it is enough to assume that N-linked glycosylation is a critically important factor to understand normal physiology and pathological developments in the nervous system.

O-linked glycosylation. The forms of O-linked glycosylation are defined by the glycosidic sites of amino acid residues on a protein and the types of carbohydrate moieties: glucose (Glc), galactose (Gal), mannose (Man), fucose (Fuc), N-acetylgalactosamine (GalNAc), N-acetylglucosamine (GlcNAc), and N-acetylneuraminic acid (NAHA, also known as sialic acid) (Lis H and Sharon N, 1993, European Journal of Biochemistry). The most common form of O-linked glycosylation is the attachment of GalNAc to Ser or Thr residues in a protein, known as the mucin-type or mucin glycoprotein, in which the abundance of mucus is secreted on cellular surfaces and in body fluids. This mucosal secretion is a highly concentrated carbohydrate. Proteoglycan is a characteristic glycoprotein that the GalNAc-attached form is involved in its protein synthesis. This protein has a critical role in the generation of components to form the extracellular matrix that is essential for cell-cell interactions. Genetic mutations in this glycosylation lead to cause some autosomal recessive disorders and autoimmune diseases.[48] Another form of the O-linked glycosylation is the GlcNAc-attached form, which only occurs to non-phosphorylated Ser or Thr residues. This form of glycoproteins in the nucleus and cytoplasm has a role of the interaction between O-glycosylation and phosphorylation. In addition, the GlcNAc-attached form has functions in transcription, translation, degradation and translocation, as well as a signal transduction pathway.[49] Interestingly, overexpression of the GlcNAc-attached form is involved in pathological mechanisms of insulin resistance and glucose toxicity in diabetes. Also, modifications of

this glycosylation have been recognized as the etiologies of neurodegenerative diseases and cancer development. This form has regulating roles for various oncogenic proteins and tumor suppressor proteins. An additional form, the attachment of Man to Ser or Thr, occurs specifically on certain proteins, called α-dystroglycans, in brain and muscle cells. It is known that impairments of this glycoprotein and its related enzymes are associated with the pathology of congenital muscular dystrophy, particularly in Duchene Muscular Dystrophy.[50,51] Other O-linked glycosylations of Fuc and Glc, the fourth and fifth forms, occurs between certain cysteines with repeats of epidermal growth factor (EGF) motifs in Notch proteins. Fuc attaches to Ser or Thr in between the second and third conserved cysteines, whereas Glc bonds to Ser in between the first and second conserved cysteines. This glycoprotein is essential in the Notch signaling pathway, which has an important role in various developmental processes in mammals. Thus, impairments of these forms affect regulations of this signaling pathway and initiate pathological developments of cancer (i.e. leukemia) and neurological disorders (i.e. cerebral autosomal dominant arteriopathy with subcortical infracts and leukoencephalopathy: CADASIL, the most common type of hereditary cerebral angiopathy/stroke disorder). As the sixth form, collagen is only the protein attached with Gal to its hLys residue. This form of O-linked glycosylation is required for proper functions of collagens as the major structural proteinous component in connective tissues. The impairments of collagen-sugar linkages are related to underlying pathological mechanisms in diabetes and autoimmune diseases, such as rheumatoid arthritis. The seventh form, O-linked glycosylation of NAHA, has an essential role to regulate activities of various intracellular proteins in the nucleus and cytoplasm.[52,53]

NAHA is involved in an important pathway of sugar metabolisms. Thus, impairments or genetic deficiencies of this form and/or associated enzymes affect these activities in the metabolic pathway, resulting in casing abnormalities in neurological and musculoskeletal disorders, such as congenital myastheniac syndrome, immunodeficiency syndrome, and adult-onset inclusion body myopathy (hereditary inclusion body myopathy).[54] Based on the information above, O-linked glycosylations are associated with cell-cell interactions and signaling pathways. Also, the impairments of the O-linked glycosylations are involved in immune-mediated pathological conditions. It provides a clear understanding that dysfunctions of this glycosylation type might affect regulations of immune systems. In addition, a genetic background of each protein influences its protein synthesis including glycosylation. Therefore, a genetic deficiency or mutation is closely related to incorrect processes of glycosylations in pathological developments of certain disorders.

Overall, proper protein structures and conformations are critically important for normal functions of proteins in cells, tissues, and organs in the body. Protein glycosylation is a key factor to maintain the quality control of protein synthesis and prevent abnormal protein generations. Physiologically, glycosylation states are involved in regulations of immune and nervous systems. In another aspect, the impairments of glycosylations are associated with pathological developments and disorders. It is now indispensable to recognize how much impaired glycosylations have been identified in multiple disorders at a time span from early neonatal to adult life.

Aberrant Glycosylation and Diseases

Recent studies describe that impairments of glycosylation pathways are underlying conditions in more than one hundred disorders in humans.[55-57] Since multiple genes are involved in glycosylation and associated enzymes (approximately 100 and 200 genes respectively), the large numbers of disorders by impaired glycosylation pathways might be unsurprising. These glycosylation-associated diseases are defined into congenital defects and acquired alterations of glycosylations.

Congenial defects of protein glycosylations implicate with various disorders, such as congenital disorders of glycosylations (CDG), congenital muscular dystrophies (CMD), and limb-girdle muscular dystrophies (LGMD).[58-60] Gene mutations that associate with glycosylations cause fatal neurological impairments, including cerebral, ocular, and muscular abnormalities.[61-63] In fact, gene mutations impair N-linked glycosylations in inherited neurological disorders, such as congenital myasthenic syndrome and schizophrenia.[64,65] Also, alterations of N-linked glycosylations have been identified in neurodevelopmental diseases, including autism spectrum disorder (ASD) and attention-deficit hyperactivity disorder (ADHD).[66,67] These findings indicate that N-linked glycosylations have essential roles in the regulation of the nervous and muscular systems.[68] Hence, the deficiency or alteration of protein glycosylations is a critical modulation influencing health conditions and causing pathological impairments. Failures or dysfunctions of glycosylations and associated pathways initiate developments and progressions of severe to fatal medical conditions.

Acquired alterations or abnormalities of glycosylations have also been detected in major human diseases, such as diabetes, and neurodegenerative diseases.

Here, I do not intend to summarize all protein glycosylations related to pathogeneses of these medical conditions. However, some key glycosylations will provide general perspective roles in the developments and progressions of these diseases.

1) Diabetes mellitus: Diabetes mellitus (DM) is a major metabolic disorder that disrupts glucose homeostasis.[69] The pancreas is the insulin-producing organ in which β cells in the islets of Langerhans release insulin upon physiological elevations of glucose levels in the blood. Hyperglycemia is a chronic condition with increased levels of glucose in the blood (high blood sugar), and eventually induces glucose toxicity that affects functions of the pancreas and other insulin-targeted peripheral tissues (i.e. muscle, liver and adipose tissue).[70,71] The dysfunction of β cells is a major etiology of DM and its complications, such as diabetic cardiomyopathy, nephropathy, retinopathy, and cardiovascular diseases.[72-80] To understand pathogeneses of the DM etiology, protein glycosylations are key molecular targets in β cells and other tissues, especially for insulin resistance in the Type II DM and .[81-83] For instance, N-linked glycosylation is involved in the DM pathogeneses.[84] An insulin receptor (N-linked glycoprotein on cell surfaces) has functions in the glucose uptake by insulin, as well as insulin-like growth factor (IGF) 1 and 2.[85] Bindings of insulin and its receptor play a regulating role of glucose homeostasis. Conditions of insulin receptors influence insulin sensitivity and resistance in cells. Decreases or defects of insulin receptors disrupt insulin binding and processing, which lead hyperglycemia, DM, and its complications.[86,87] Since N-linked glycosylations of insulin receptors have roles in intracellular processing and signal transduction, defects of the N-linked glycosylation affect on the receptor activity in glucose homeostasis.[88,89] Recent studies report an importance of N-linked glycosylation

on the receptor, especially in the kidneys.[78,79] Impairments of protein N-linked glycosylations can induce the pathological progression of diabetic nephropathy. Hence, glycosidic alterations are associated with in DM pathogeneses and disease developments, including insulin resistance, hyperglycemia, and complications. Thus, proteomics approaches target protein glycosidic statuses in DM diagnostic innovations.[90] Profiling glycosylations is now referred as to glycomics.[91] Screening states of glycosylations on certain proteins is a useful application to determine pre-diabetes and DM conditions in patients.[92-94] Therefore, a glycosylation-targeting diagnosis is an important strategy to establish novel analytical methods.[95,96] New investigations will provide further advances to understand roles of protein glycosylations in pathological etiology.

2) Alzheimer's disease: Current researches have proposed Alzheimer's disease (AD) as a new "Type III" DM, based on similar pathogeneses to DM, such as impaired metabolisms of insulin and glucose in brains.[97-99] Insulin and its signaling are involved in various functions of brains including cognition and memory, which AD patients decline.[100] Hyperglycemia and glucose tolerance are significant conditions in patients with AD.[101-103] Also, altered glucose metabolisms cause cognitive impairments in brains, which are associated with the underlying causes of neurodegenerative pathologies in the AD development.[103-105]

In PMDs, AD is the major neurodegenerative disorder in humans that has serious global impacts internationally because it is the most common cause of dementia.[97-99] Both hyperglycemia and hypoglycemia are well known risk factors of cognitive dysfunctions and dementia. Similar to the pathologic PrP agent, certain proteins (i.e.

amyloid-β (Aβ) peptide and tau protein) that link to the AD etiology misfold and aggregate in brains. Aβ is a proteolytic fragment of amyloid precursor protein (APP), an integral membrane protein expressed in various tissues and concentrated in synapses of neurons.[106] Tau protein is a microtubule-associated protein that is abundantly accumulated in axons of neurons but less expressed in other cells and tissues.[107] The misfolding and aggregations of these certain molecules are the major pathologic hallmarks of AD. Aberrant Aβ and tau protein compose amyloid plaques and neurofibrillary tangles, respectively. The abnormal accumulations of these aggregated proteins toxically impair the nervous system and eventually induce the AD development.

As described above, the Type II DM is one of the PMDs that islet amyloid polypeptide (IAPP) misfolds and accumulates in the pancreas like abnormal PrP feature, and its aggregation affects the function of β cells toxically.[108-110] Recent studies report the pathological link between Type II DM and AD in which DM is a risk factor of the AD development.[111-116] Insulin and its signaling are key regulators to form amyloid plaques and neurofibrillary tangles. In fact, insulin-resistant conditions and impaired signaling progress the accumulation and deposition of Aβ in brains of AD patients.[99,100] The disease-associated proteins in Type II DM and AD alter conformationally from α-helix to β-sheet rich structures, which are characteristic features of amyloid deposits.[117] The aggregations and accumulations of the misfolded proteins are potentials of disease transmission and propagation.[118] These pathologic features of protein abnormalities and deposits are the hallmarks of PMDs.

Similar to DM, these AD pathogeneses are also associated with modifications of protein glycosylations. Defects and aberrances of protein glycosylations have been

reported in AD.[76, 119] APP is well known as a precursor molecule of Aβ.[120] Even though APP is a single molecule, this protein derived from human cerebrospinal fluid (CSF) consists of both N-linked and O-linked glycosylations.[121] N-linked glycans are functionally important to regulate transports and secretions of APP. Increases of N-linked glycans enhance secretions of APP and its metabolites.[122,123] Thus, inhibitions or defects in N-linked glycosylations reduce APP transports and secretions. In addition, mutations of APP alter N-linked glycosylations but increase O-linked GlcNAc glycosylations.[124] In AD patients, this glycosidic increase on APP upregulates mRNA expressions of GlcNAc transferase III (GnT-III), which is the responsible enzyme for synthesizing GlcNAc residues in their brains.[125] The enzymatic upregulation induces increases of soluble APPα, whereas Aβ generations are decreased. This mechanism indicates protective effects of APP glycosylations for brains against Aβ generations and accumulations. Normally, O-linked GlcNAc glycosylations are abundant in neurons.[126] However, decreases or impairments of O-linked GlcNAc glycosylations have been found in AD brains. The decreases are associated with impaired metabolisms of insulin and glucose, and increased expressions of the enzyme O-linked GlcNAc transferase (OGT) that catalyzes the addition of GlcNAc residues in O-linked glycosidic linkages.[127,128] Eventually, these aberrant alterations disrupt functions of O-linked GlcNAc glycosylations and affect stability, activity, expression, and interactions of glycoproteins.[129,130] In consequence, altered protein glycosylations could initiate abnormalities and AD development.

Tau proteins in non-AD brains only express O-linked GlcNAc glycosylations, which have functions to prevent the proteins from aberrant phosphorylation, paired

helical filament, and tangle formation.[131-133] In contrast, the tau proteins in AD brains alter glycosylations of both N-linked and O-linked glycans.[134] The glycosidic abnormalities in AD brains could be caused by reductions of the enzymes that remove N-linked glycans.[119] To assemble neurofibrillary tangles, N-linked glycosylations promote formations of tau proteins with paired helical filament or hyperphosphorylation, which highly contain truncated glycans.[135,136] Aberrant N-linked glycosylations of tau proteins induce more susceptibility to phosphorylation but are less prone to dephospohorylation.[134] Thus, the N-linked glycosidic abnormality leads hyperphosphorylation of tau proteins.[137] In addition to the abnormal N-linked glycosylation, modifications of O-linked GlcNAc glycosylations are detected on tau proteins in AD brains that have 4-fold decreased levels.[138,139] Glucose metabolism regulates protein O-linked GlcNAc glycosylations that control phosphorylation of tau proteins.[140] Therefore, an impaired-glucose uptake in the brain induces decreases and dysfunctions of O-linked GlcNAc glycosylations that reciprocally increase hyperphosphorylation of tau proteins and neurofibrillary tangles.[141-143] These dysregulations result in the development of AD pathology.

Overall, alterations of N-linked and O-linked glycosylations could trigger pathologic modifications and aggregations of tau proteins, called tauopathy, in neurofibrillary tangles initiating AD development. Impaired glucose metabolism is associated with aberrant protein aggregation and accumulation in AD. Interestingly, recent articles discuss an association between DM and amyotrophic lateral sclerosis (ALS) by a large population study in Sweden.[144-146] This study suggests that impaired energy metabolisms including insulin and glucose are risk factors of ALS. Other studies

also identify similar glycosylation patterns of AD in ALS, such as reduced O-linked GlcNAc glycans, increased N-linked glycans, and hyperphosphorylated proteins.[147,148] Thus, the disease development of ALS could be related to dysregulations of protein glycosylations and phosphorylations. According to all of the information in this Section 1, it is obvious that an alteration or impairment of glycosylations is one of the hallmarks in PMDs and a characteristic feature in neurodegenerative diseases. Because of PMDs, pathologic modifications of glycosylations could be associated with structural aberrations and misfoldings of disease-associated proteins. Using concepts of glycomics and glycoproteomics, targeting glycosylation states on disease-associated proteins is a practical approach for diagnostic and therapeutic innovations and for elucidating undefined pathogeneses in PMDs including neurodegenerative diseases. The upcoming Section 2 describes background information of prion proteins and abnormalities in TSE pathogeneses including glycosylations of normal and pathologic PrP. Aberrant N-linked glycosylations are key modulators of disease development and progression in TSEs.[149-152] Alterations of glycosidic states are essential targets of TSE diagnoses to distinguish normal and abnormal PrP, as well as to evaluate infected states, disease development and prognoses.

Section 2: Prion Protein and TSE Pathogeneses

Normal prion protein isoform

Prion protein (PrP) is an N-linked glycoprotein on a cell membrane, and cellular prion protein isoform (PrP^C) is a normal prion protein that is monomeric, detergent soluble and protease sensitive. PrP^C is encoded by its gene (PRNP in humans and

Prnp in mice) located on the short (p) arm of chromosome 20 in humans (at position 13: 20p13), which corresponds to chromosome 2 in mice.[153] PrP^C consists of α-helix-rich structures mostly with two N-linked glycans (diglycosyl form). PrP^C is abundantly expressed in tissues of the central nervous system (CNS), especially in several regions of the brain, such as olfactory bulb, striatum, hippocampus, and prefrontal cortex.[154,155] PrP^C mainly localizes on the cellular membrane, and its expression has been detected in neurons, extraneural tissues, and glial cells in the CNS.[156-159] Conversely, neocortical, hippocampal, and thalamic neurons show intracellular expressions of PrP^C in these cytosols.[160,161] Cerebellar neurons, however, do not express this protein in their cytosols. A recent study identified that mitochondria in healthy mouse brains expresses PrP^C with diglycosyl N-linked glycans that is localized to inner mitochondrial membranes.[162] This finding indicates, in a natural state, PrP^C exists intracellularly in brain mitochondria. The intracellular PrP^C might influence mitochondrial functions physiologically and pathologically. Since intracellular accumulations of altered PrP isoforms are strongly neurotoxic and cause neurodegeneration, the cytosolic PrP^C expressions in these neurons might be associated with molecular pathogeneses of TSEs.[163-165] Furthermore, PrP^C expressions have been identified in the peripheral nervous system, and other non-CNS organs and tissues, such as the heart, muscles, spleen, lungs, gastrointestinal tract, skin, kidneys, and lymphoid tissues.[157,159,167-169] Recent dental research reports that the PrP^C interacts with neurotransmitters, such as dopamine and serotonin, in tooth development, maintenance, and abnormality.[170-174] Therefore, systemic expressions of PrP^C throughout the body indicate its functional importance in organ physiology.

PrP Structure and Glycosylation

PrP with N-linked glycans consists of approximately 250 amino acids in a length of its primary sequence.[14] On a 253 amino acid sequence in human (and hamster) numbering, residues 1 to 124 form (NH_2)-terminal (N-terminal) region. Residues 1 to 22 consist of the primary-amino signal peptide of N-terminal. Residues 23 to 124 are composed of the flexible N-terminal domain that consists of five or six repeats of eight glycine-rich residues (PHGGGWGQ) known as the octapeptide repeat region, acting as binding sites of divalent metal ions, such as copper, iron, zinc, nickel and manganese.[72,175-177] Recent studies determine that metal imbalances in the brain influence physiological functions of PrP molecules. These functional disruptions are possibly related to TSE pathogenesis.[177] Furthermore, residues 125 to 253 form the carboxylic acid (COOH)-terminal (C-terminal) region. Residues 125 to 228 constitute the globular-structure domain in the C-terminal. Through proper folding, the tertiary structure of PrP forms a globular domain with three α-helices (corresponding to residues 144-154, 173-194, and 200-228) and two antiparallel β-strand sheets (residues 128-131, and 161-164) in the C-terminal.[178-180] In addition, a large rigid loop links the second β-strand sheet (β-sheet 2) to the second α-helix (α-helix 2), known as a β2-α2 loop (residues 165-175) that has intriguing structural properties for stabilizing tertiary structures of PrP and folding these proper conformations.[179-182] Recent studies propose this well-structured loop as a pathologic key factor of PrP conformational abnormalities, species barriers, and transmission in TSEs.[183-187] At last, residues 232 to 253 form the hydrophobic peptide in the C-terminal.

During protein syntheses, the following post-translational modifications occur to PrP molecules: 1) removals of both N- and C-terminal signal peptides, 2) additions of glycophosphatidylinositol (GPI) membrane anchors, 3) formations of disulfide bands, and 4) attachments of N-linked glycans.[188,189] After the cleavage of the N-terminal signal peptide and C-terminal hydrophobic peptide, the residue 231 in the C-terminal of PrP links a GPI membrane anchor that tethers a PrP to a specific-membrane microdomain of a cellular membrane (a plasma membrane). This microdomain is known as a lipid raft that is a cholesterol- and glycosphinogolipid-rich region and associates with signal transduction mechanisms.[190,191] The cysteine (Cys) connection of one disulfide bond exists between Cys 179 on the α-helix 2 and Cys 214 on the α-helix 3 in human and hamster PrP numbering (178 and 213 in mouse PrP numbering).[192,193] This disulfide bond stabilizes a tertiary structure of PrP and folds its proper conformation. In the process of N-linked glycosylation, glycans attach to two asparagine (Asn or N) residues located on the α-helices 2 and 3 (i.e. respectively, 180 and 196 in mouse PrP numbering; 181 and 197 in human and hamster) in the amino acid sequence of the PrP structure.[194] This N-linked glycosylation generates four various forms of glycosylated PrP: 1) unglycosyl, 2) monoglycosyl at 180 = mono1, 3) monoglycosyl at 196 = mono2, and 4) diglycosyl at 180 and 196.[195] Typically, an abundance of normal PrP^C has the diglycosyl form (2 glycans). During these post-translational modifications in the ER and Golgi, the PrP sequence is shortened to almost 200 amino acids in length (209 in human) for its maturation.[14] Eventually, the mature PrP is transported from the Golgi to the cell membrane for its functions.[196]

Although the mechanisms of these N-linked glycans on PrP are not completely understood, it is recognized that glycosylation plays various structural and functional roles in proteins.[197] For example, N-linked glycosylation is involved in the maintenance of PrP structure, and thus modulations of the N-linked glycosylation may lead to change a protein conformation.[197] In fact, mutation or truncation of N-linked glycans interferes with protein folding and structure.[198,199] Also, intracellular accumulations of unglycosyl proteins cause cytotoxicity that associates with molecular pathogeneses of neurodegeneration.[200] In TSEs, it is suggested that N-linked glycans on normal PrP isoforms contribute to disease phenotypes. For instance, transgenic mice lacking a glycan at either one of the two consensus sites for N-linked glycosylation of PrP show more sensitivity to the infections of TSEs.[201] This infectious sensitivity indicates that the loss of N-linked glycans on PrP is involved in the pathological mechanisms of prion diseases. Moreover, the absence of a diglycosyl PrP form is reported in cell culture models, and in brain tissues derived from human patients with TSEs.[150,202] In addition, abnormal patterns of PrP glycosylation are detected by in vivo models of scrapie, with an increased ratio of under-glycosylated forms (unglycosyl and/or monoglycosyl form = 0 or 1 glycan), but a decrease in diglycosyl forms.[203] Although a normal PrP^{C} isoform mostly localizes on a cell membrane, both PrP^{C} with aberrant N-linked glycans and abnormal PrP^{Sc} isoforms exhibit intracellularly.[204] This intracellular proteinous accumulation causes cytotoxicity.[165,166]

In spite of numerous studies about the expression profiles of the glycosylated forms of PrP, the importance of the glycosylation in TSEs is not fully clarified.[205] As a result, it is a pathobiological curiosity why glycans on PrP are lost during the disease

development. A possible reason is that alterations in states of glycosylation could cause PrP abnormalities and provoke TSE developments. Another feasible reason is that N-linked glycosylation may play a significant role in prion pathogenesis by selective glycosyl forms. Therefore, N-linked glycosylation and its states are innovative targets to clarify different properties of normal and abnormal PrP isoforms. This dissertation project focuses on analytical and diagnostic aspects for distinguishing abnormal PrP isoforms with certain states of aberrant glycosylations. To establish the aims of the project, in-house anti-PrP antibodies are utilized to identify and to measure PrP molecules in TSEs.

PrP Functions

PrP abnormalities in TSEs have been largely studied, and three Novel Prize winners were awarded in TSE and related research fields: Dr. Daniel Carleton Gajdusek (Physiology or Medicine) in 1976; Dr. Stanley B. Prusiner (Physiology or Medicine) in 1997; and Dr. Kurt Wüthrich (Chemistry) in 2002.[206,207] While abnormalities of PrP have been well-documented, in contrast, normal functions of PrP^C have yet to be determined clearly, and their physiological importance has been controversial.[208] PrP-knocked out (PrP-KO) transgenic (Tg) mice have been used to determine functional roles of PrP^C in normal physiology.[209-212] At the initial stage of these investigations, an availability of various breed lines of PrP-KO Tg mice was limited.[209,210] These mice lacking PrP expressions were clinically normal and also did not show clear onsets or symptoms of disease development.[209,210,213] In addition, PrP-KO Tg mice with inoculations of TSE-infected materials did not develop any clinical signs of the diseases.[214,215] Hence, it has

been recognized as evidence that the Tg mice lacking PrP are prone to maintain non-disease conditions and are also not susceptible to TSE infections. These observations have implied that PrP^C and their functions are non-essential molecules and regulators in biology and physiology of CNS and other organ systems for the survival of the laboratory mice.[209,210,216,217] Therefore, PrP^C researches have paid less attention to determine deficiencies and modifications of normal PrP physiological functions, compared to dysfunctions by abnormal PrP pathogeneses in TSEs.

Current studies have increasingly reported associations of PrP^C with major human disorders, such as AD,[218-225] cancers,[226-231] and DM.[232-234] These identifications have sparked exploratory investigations of undefined PrP functions in normal physiology, as well as pathophysiology. Furthermore, several studies have revealed clinical abnormalities in various available breed lines of PrP-KO Tg mice, such as dysregulations of circadian and sleep rhythms, deficiencies in cognition and olfaction, and alterations in the immunological system.[235-241] Clinical abnormalities in these mice are observed as strain-phenotype dependences in PrP-deficient Tg mouse breed lines.[242-245] As mentioned above, the PrP-KO Tg mouse breed lines that were initially utilized to determine PrP functions did not show physiological or developmental aberrations.[209,210,213] These findings indicate that different gene-targeting strategies for generating Tg mouse lines with PrP deficits influence PrP functions in mouse physiology. However, recent studies have identified spontaneously impaired conditions and drug sensitivities in these breed lines.[237,245-260] Therefore, pleiotropic regulators might be associated with PrP functions in physiology. Although the investigations of PrP

functions still remain open, several clinical and physiological phenotypes attributable to PrP deficits have been identified from PrP-KO Tg mouse studies.

The most recognized PrP^C function is known as a copper interaction and transporter.[13, 219,261-268] Impairments of copper homeostasis in nervous systems cause some inherited disorders of copper metabolism, and neurodegenerative diseases.[269-271] In copper metabolism and homeostasis, PrP^C isoforms are highly interacted with copper ion (Cu^{2+}).[219,261-263] On the PrP^C structure, Cu^{2+}-binding sites are localized in the octapeptide repeat region at the flexible unstructured N-terminal.[175,176,264,265] Since PrP^C can chelate Cu^{2+}, this protein is considered as an antioxidant to protect cells from oxidative damages, and reduce cellular reactive oxygen species (ROS) that comprise of radical and non-radical oxygen species.[272-275] In fact, PrP-KO mice and their cultured neural cells exhibited the increased sensitivity to oxidative stress.[276-283] Also, brains of PrP-KO mice decreased copper levels and numbers of mitochondria per cell.[276-278]. The majority of mitochondria were morphologically abnormal.[278] These reports indicate that PrP^C may have protective function for cells from oxidative damage.

Here, I do not intend to summarize all PrP functions for focusing on the dissertation topics. However, some PrP functions could be implicated with the TSE disease developments and progressions, as listed in following areas: neurotransmission system[159,284-295]; cellular proliferation, differentiation, death, and survival[296-299]; myelin maintenance property[245,300,301]; neuroprotection[297,302-304]; phenotypes of sleep, behavior, and memory[235,305-308]; and non-nervous systems (i.e. the immune, muscular, cardiovascular, gastrointestinal systems)[309-314].

Overall, PrP^C expressions and functions are essential factors and regulators for cellular biology and neurophysiology in the CNS and PNS. The loss or alteration of PrP^C isoforms would influence neurological functions, leading to aberrant impairments and disease developments, such as neurodegenerative disorders. To understand PrP^C implications in pathogenic mechanisms of functional failures, the measurements of PrP^C expressions and alterations would be beneficial to determine physical impairments, abnormalities, disease developments and prognoses in longitudinal terms. This dissertation study will provide the practical prospects for these analytical applications.

PrP polymorphisms and aberrant variants

1) Normal variants with disease implications: In the human PrP^C gene, some polymorphisms of normal variants are not pathogenic, but influential factors on the susceptibility to sporadic, inherited, and infectious forms of TSEs, and the phenotypic properties of these diseases.[315,316] The polymorphism at the codon 129 is the common normal variant that codes either methionine (Met: M) or valine (Val: V), which this polymorphism is usually denoted as M129V. In the Caucasian population, approximately 50% of people have homozygous variations of either M (40%) or V (10%) at the codon 129. However, the codon 129 genotypes are significant factors for increasing the developmental risks of CJD and its phenotypic variations, including PRNP mutations and inheritances.[317-323] Also, the codon 129 homozygosis strongly implicates with acquired forms of TSEs, such as kuru, variant CJD (vCJD), and iatrogenic CJD. [324-329] For instance, 70% of sporadic CJD (sCJD) patients exhibit homozygous expressions with M or V at the codon 129 (MM, VV). Remarkably, 100% of

vCJD patients express only M homozygotes (MM). In contrast, the heterozygosis (MV) at the codon 129 is a resistant factor to CJD developments. CJD patients with MV variant at the codon 129 tend to prolong onsets of the disease until late ages, compared with those with the homozygosis (MM or VV). This protective efficiency of the MV heterozygosity is considered as in relation to the protein-protein interactions in PrP^{Sc} transmissions between homologous species.[317,330,331] In addition, the codon 129 variants in PRNP implicate with other neurological disorders that are not associated with TSEs. The VV homozygosis at the codon 129 is a risk factor to elicit early onsets in AD patients.[332,333] Conversely, another study indicated the protective efficiency of the V allele homozygosis (VV) and heterozygosis (MV) at the codon 129 that reduce 13% from the developmental risk of AD and extend prolonged-disease onsets, especially in elder patients over 65 years olds, compared to people with the MM variants.[334] In Down syndrome patients, this VV variant progressively aggravates their cognitive impairments.[335] Even in healthy individuals, the VV variant is involved in the age-related declines of cognitive and long-term memory functions during adulthood and senescence.[336-338] Moreover, the MM homozygosis at the codon 129 is associated with exacerbations of neurological impairments in senior patients with Wilson disease, an autosomal recessive inherited disorder of copper metabolism and accumulation, whereas the patients with VV or MV variant exhibit the early disease onset.[339,340] Although the PRNP 129 polymorphism is causally related to neurological impairments, these underlying mechanisms are uncertain yet.

Another non-pathogenic polymorphism has been reported at the codon 219 in the human PrP^{C} gene.[341,342] This 219 variant accounts for approximately 6% of the

Japanese population, coding either glutamic acid (Glu: E) or lysine (Lys: K), denoted as E219K for this polymorphism.[316,341] Since the 219 heterozygosis is not detected in sCJD patients, this variant should have a protective property against PrP^{Sc} transmissions and conversions.[343] In fact, the E219K ability was confirmed in cell cultures and transgenic mice with this variant, which also inhibited conversions of co-expressed wild-type PrP^{C} to PrP^{Sc} in mice.[344,345] One study reported a similar protective effect of the E219K variant in mouse models with human PrP 219K or mouse PrP 218K (corresponding to human 219K in the murine numbering) against sCJD transmissions.[346] Interestingly, PrP^{C} isoforms with these KK variants converted into PrP^{Sc} isoforms in the mice under vCJD infections, whereas the PrP^{C} expressions with E219K heterozygosis (EK) were protective to the PrP^{Sc} conversion in the infections. Additionally, PrP^{C} isoforms with other 219 heterozygotes (E0, K0: 0 = null) in mice were susceptible to the PrP^{Sc} conversion. These outcomes suggest that the EK variant at the codon 219 in human PrP isoforms promotes the heterozygous inhibition and resistance to PrP^{Sc} transmission and conversion.

Furthermore, during the last decade, researchers have investigated a new protective polymorphism of human PRNP against a TSE disease in a certain community at the Okapa District of the Eastern Highlands Province, Papua New Guinea.[347,348] In this region, the ritual cannibalism causes transmissions of the human TSE among people in the Fore tribe, called kuru. As like CJD, the people with the codon 129 homozygosis (MM or VV) are susceptible to the epidemic of kuru, especially for the MM homozygotes.[329,349] In contrast, those with the heterozygous variant (M129V) are resistant to the disease exposures. Recent studies reported that the Fore people have

acquired a new naturally occurring variant of PrP gene at the codon 127 against the disease, over 10 generations[347,348] In the highly disease-exposed areas, people predominantly present the heterozygotes of glycine (Gly: G) and V at the codon 127 (G127V). Although the codon 129 MM homozygote is a common PRNP allele in the Fore communities, people with this variant exclusively exhibit the V allele at the codon 127. This alteration from G to V allele is considered as the result of a missense mutation, a point mutation at the codon 127. Since this 127 polymorphism is not detected in the kuru patients as well as people in the non kuru-epidemic regions, the G127V heterozygous variant must be a protective allele and resistant factor against kuru. In addition, this protective property of the variant has been confirmed in mouse studies, which the V allele at the codon 127 demonstrates complete resistances to PrP^{Sc} transmission, conversion and disease development against CJD and kuru infections.[348] These outcomes provide a new scope of treatment and prevention for TSEs, as well as other neurodegenerative diseases and protein-misfolding disorders.

Instead of PRNP in humans, mouse PrP gene is denoted as Prnp or Prn-p, which also exhibits polymorphisms.[350] Mice expressing PrP-A allotype are common breeds such as FVB/n and C57BL6: mouse prion protein gene $Prnp^{a}$ is the s7 allele of the sinc locus and encodes leucine (abbreviated as Leu or L) at the codon 108 and threonine (abbreviated as Thr or T) at the codon 189 of the mouse PrP open reading frame (ORF). In contrast, VM/DK is a mouse breed expressing PrP-B allotype: mouse prion protein gene $Prnp^{b}$ is the p7 allele of the sinc locus and encodes phenylalanine (abbreviated as Phe or F) at the codon 108 and valine (abbreviated as Val or V) at the codon 189 of the moPrP ORF. Inoculations of TSE-infected isolates provoke shorter incubation periods

in the PrP-A allotype mice, but longer incubation periods in the PrP-B allotype mice.[351,352] The mouse polymorphisms also influence aggregation tendency, strain adaptability, and conformational variability in TSE disease developments.[353] Moreover, another study identified a novel mouse Prnp polymorphism at the codon 108 with F and 189 with T in the MAI/Pas breed, denoted as the PrP-C allotype that prolonged the TSE incubation times longer than the PrP-B allotype mice.[354] These phenomena suggest that the two amino-acid residues in primary structures of the Prnp allotypes modulate the incubation-times differences and the disease developments of TSE infections.

Moreover, small ruminants (i.e. sheep and goats) also exhibit various non-pathogenic polymorphisms of PrP^C genes that also link to disease susceptibilities and implications of TSEs. In the sheep PrP^C gene, polymorphisms at three codons are associated with the occurrence of classic scrapie: the codon 136 with either alanine (Ala: A) or V, denoted as A136V; the codon 154 with either arginine (Arg: R) or histidine (His: H), denoted as R154H; and the codon 171 with glutamine (Gln: Q), R, or H, denoted as Q171R/H.[355,356] The ovine susceptibility to classic scrapie links to the 136V (codon/amino acid: codon 136 with V), 154R, 171Q and 171H, whereas the 136A, 154H, 171R are resistant to scrapie infection.[357-362] Among the 12 possible combinations of these polymorphisms, the following five alleles are common in the notation of the codons 136, 154, and 171: ARQ (=136A-154R-171Q), ARR, AHQ, ARH, and VRQ.[360,363] The predominance of these five alleles is dependent on sheep breeds.[364] Although the incident factors of these variations are not well understood, ovine ARR and AHQ are resistant alleles to classic scrapie.[364,365] In contrast, ARQ, ARH, and VRQ are susceptible alleles. Combinations of these five alleles consist of 15 PrP^C genotypes total,

commonly found in sheep. Among these 15 genotypes, the scrapie susceptibility varies from the complete resistance to the extreme susceptibility.[366] The ovine ARR/ARR and AHQ/VRQ alleles are significant genotypes for resistances to classic scrapie. In contrast, the ARQ/ARQ, AHQ/AHQ and VRQ/VRQ homozygous genotypes in sheep are the greater risk factors for the etiology of classic scrapie, in addition to other VRQ heterozygous genotypes with ARQ or AHQ (i.e. ARQ/VRQ, ARH/VRQ). Sheep with these susceptible genotypes are prone to present the morbidity and mortality of classic scrapie at younger ages: the risk peaks at the 2-year ages in VRQ/VRQ and ARH/VRQ sheep, and at the 3-year ages in ARQ/VRQ sheep. Although these susceptible sheep decrease the scrapie risks during 4 and 5 years of ages, the second risk peak rises from 6-year age. Furthermore, the genetic susceptibility to atypical scrapie in sheep is different from classic scrapie. Many cases of atypical scrapie are frequently diagnosed in sheep with the ARR/ARR homozygote that is a resistant genotype to classic scrapie.[367,368] In addition to the polymorphisms at the codons 154 (R or H) and 171 (Q, R, or H), variants at the codon 141 (L or F) implicate with the disease risk and occurrence.[369,370] Mostly, sheep carrying F at the codon 141 with ARQ (A141FRQ; AFRQ) have the highest incidence for atypical scrapie, as well as sheep with the AHQ/AHQ homozygote.[368] Also, sheep carrying L at this codon with ARQ and/or ARR (i.e. A141LRQ; ALRQ, A141LRR; ALRR) are susceptible to atypical scrapie. Thus, polymorphisms in the ovine PrP^C gene are critical aspects for the strategies in scrapie control and eradication from sheep flocks, including breeding schemes and genetic selections.

Interestingly, goats have the excessive variability in PrP^C genes that presents more than 50 polymorphisms.[371] These allelic viabilities of the caprine PrP^C gene are widely dependent on breeds, regions, and countries. Against scrapie infections, caprine resistances have been evaluated in several polymorphisms at certain PrP alleles, such as the codons 142, 143, 146, 151, 211, and 222.[372-374] The codons 142 with M (142M), 143 with R (143R), and 151 with H (151H) have moderate properties for scrapie protections. The codon 211 with Q (211Q) has a property to decrease conversion rates from PrP^C to PrP^{Sc} isoforms. Moreover, the codons 146 with aspartic acid (Asp: D) (146D), 146 with serine (Ser: S) (146S), 222 with lysine (Lys: K) (222K) significantly reduce the PrP conversion rates. Potentially, these three variants are protective against scrapie infections. Under experimental infections in goats and transgenic mice, the 222K variant is an essential resistant factor against classic ovine scrapie and bovine/caprine BSE isolates.[375-377] In addition, the latest studies have revealed that the classic scrapie agent in goat milk could transmit to sheep via oral routes, especially carrying the codon 141 polymorphisms.[370,378] Although the genetic diversity in the PrP^C gene has been investigated numerously in goats, their breeding programs with genetic selections against scrapie infections have not been under development yet.[379] Thus, outbreaks of scrapie will seriously affect to the goat industries (i.e. meat, milk, and mohair productions) and economic situations through the world, and possibly spreading and disturbing sheep industries. Under the surveillance and disease control, it is critically important to detect infected goats from flocks for preventing and eradicating the scrapie epidemics.

In addition to the TSE susceptibility and resistance in homologous species, the variability of PrP alleles is a pivotal factor to influence the cross-species transmissions of TSEs.[380,381] In small ruminants, for instance, PrP^C genes of sheep and goats are highly polymorphic, which these species share amino acid polymorphisms at the certain codons, including Q101R, G127S, H143R, N146S, R151H, R154H, R211Q, T219I (I = isoleucine/Ile), and Q220H. The substitutions of identical amino acids at these codons could be associated with the mechanisms in transmissions and propagations of scrapie agents between sheep and goats. Moreover, the polymorphic variations of octapeptide repeats in PrP^C structures are also risk factors for the TSE transmission in these small ruminants, as well as its susceptibility.[380-383] Overall, the diversity of these genetic backgrounds could be related to the conformational changes from normal PrP^C isoforms to abnormal or pathogenic agents in new hosts, which facilitate PrP^{Sc} transmissions and propagations passing through homogeneous and heterogeneous species.

2) Insoluble and PK-resistant variant of PrP^{Sc} isoform: Prion is the etiological agent of TSEs, termed from “proteinaceous infectious only.”.[384] According to the protein-only hypothesis, this infectious agent does not consist of nucleic acids for its self-replications and propagations in which normal PrP^C isoforms are the necessary molecules.[214,385] An abnormal isoform of PrP^C molecule is called scrapie prion protein (PrP^{Sc}) that is capable of converting normal PrP^C structure to its altered conformation.[384] PrP^C structure has been investigated at its atomic level, but the high-resolution structure and related modifications of post-translational chemical factors are not clearly found in this abnormal structure alteration.[386,387] However, limited data from low-resolution structural methods suggest particular differences between PrP^C and PrP^{Sc}

conformations.[388-390] According to studies using infrared spectroscopy and circular dichroism spectroscopy, an abundant composition of PrP^{C} structure is α-helices (42%) with a fractional content of β-sheets (3%). In contrast, β-sheets (>43%) consist largely of an abnormal PrP^{Sc} structure, and the PrP^{Sc} structure with truncated N-terminals contains an increased fraction of β-sheets (>54%). However, the definitive structural differentiation between these normal and altered isoforms is not elucidated yet, although numerous studies have investigated the PrP conformational conversion.[390,391] In fact, many in vivo studies have not succeeded experimentally to recapitulate the transformation of PrP^{C} isoforms to its amyloidogenic PrP^{Sc} aggregations, under the protein-only hypothesis. Thus, large evidences propose implications of other macromolecules in the mechanism of the PrP conformational alteration.[392,393] Since multiple factors, described above, interact with PrP^{C} isoforms for various important functions in physiology, it is not questionable that these influential factors might facilitate the conversional process of normal PrP^{C} to infectious PrP^{Sc} structures.[394-397] Nevertheless, inoculations of recombinant PrP aggregates can develop sicknesses in wild-type and transgenic mice, under deficient conditions of cofactors.[398-400] Another experimental approach, protein misfolding cyclic amplification (PMCA) assay, has also provided in vitro proofs of the protein-only hypothesis.[401-403] In this assay, seeds of PrP^{Sc} aggregates interact and template with PrP^{C} substrates for converting and replicating to infectious PrP^{Sc} particles. In fact, the PMCA assay generated the formation of bacterially expressed recombinant PrP particles into PK-resistant conformations and aggregations.[394,404] Intracerebral inoculations of these PrP particles induced neurological disease developments in mice. Thus, these observations are still

supportive aspects for the protein-only hypothesis in the PrP structural transformation and TSE pathogenesis.

In TSE pathogenesis, the conformational conversion is the critical molecular process that α-helix rich PrP^{C} structures alter to β-sheet rich PrP^{Sc} compositions and aggregations. This β-sheet rich PrP^{Sc} structure acquires greater conformational stability and aggregational ability. The PrP^{Sc} isoform holds unconventional properties that are insoluble and resistant to inactivation by high pressures and temperatures, as well as chemical agents (i.e. proteinase K: PK), ultraviolet exposures, and radiation irradiations.[405,406] Moreover, aggregated PrP^{Sc} complexes are capable of forming amyloid fibrils that locate and accumulate in extracellular spaces and intracellular vesicular compartments.[407] These proteinous aggregates and fibrils release small particles that potentially behave as templates for other PrP^{C} molecules to recruit into the PrP^{Sc} complexes. PrP^{C} molecules that consist of an identical sequence to PrP^{Sc} isoforms could be integrated into further formations of amyloid fibrils.

In addition to the PrP^{Sc} conformations and aggregations, inoculations of PrP^{Sc} isolates from different TSE sources present varieties of pathological behaviors in new hosts with unique phenotypes, even if they are genetically identical.[39,408,409] Interestingly, each TSE source transmits consistently its distinctive features of disease developments in infected syngeneic hosts histologically and clinically, such as prion infectivity, incubation times, lesional regions and distributions of PrP^{Sc} depositions in the CNS. Based on these phenomena, disease phenotypes of the infectious particles are defined as “prion strains” or “strains” of PrP^{Sc} isoforms. These strain-dependent features indicate that varieties of pathological PrP^{Sc} conformations are imparted onto the host

PrP^C structures. Hence, the infectious particles can adopt different PrP conformations with a biochemical property of each strain, leading to capabilities for developing characteristic features of diseases.[39,410,411] These mechanisms implicate with the interaction of each strain with host polymorphisms (i.e. the codon 129 in human PRNP) and provoke phenotypic plethora. Interestingly, the strain-base phenotypes are also observed in AD, clinically and histologically.[412-414]

Several researches have revealed evidence that glycosylation states and relative proportions of four glycosyl forms (unglycosyl, mono-1 glycosyl, mono-2 glycosyl, and diglycosyl) contribute to molecular identities and diversities of PrP^{Sc} strains.[415] In fact, different PrP^{Sc} strains exhibit distinct proportions of PrP glycoforms by western blot analyses.[409,417] For instance, glycoform-specific ratios and differences are beneficial to distinguish phenotypes between sCJD and sporadic fatal insomnia (sFI) in patients with the same polymorphism (MM) at the codon 129.[418] Furthermore, the electrophoretic mobility of PK-resistance fraction is a specific classification for PrP^{Sc} strain differentiations.[419] Upon PK digestion, distinct fragments of PK-resistant PrP^{Sc} fractions can elucidate various degrees of the mobility in gel electrophoresis. The strain distinguishment can denote different resistances and cleavage sites against PK digestion among various PrP^{Sc} conformations. Even in sCJD, its subtypes exhibit different mobility of PK-resistant PrP^{Sc} fragments.[420-424] Also, distinctive molecular subtypes between iatrogenic CJD (iCJD) and sCJD patients are identified by the codon 129 polymorphisms and biochemical properties of PrP^{Sc} strain differences.[425,426] In addition to human TSEs including CJD, FFI and kuru, animal TSEs (i.e. BSE, CWD and scrapie) exhibit different PK-resistant PrP^{Sc} fragments among PrP^{Sc} strains.[321,427-435]

Thus, the detection of these characteristic fragments is an essential approach for profiling the molecular types of PrP^{Sc} strains. Possibly, the uses of several anti-PrP antibodies would be accurate to determine the strain differences rather than a single antibody, because of targeting variegated conformations among PrP^{Sc} strains.[436]

3) PK-sensitive variant of PrP^{Sc} isoform: PK is a serine protease that enzymatically cleaves proteins, and as described above, PrP^{C} isoforms are sensitive to this proteolytic enzyme.[437] This protein degradation enables TSE detection to eliminate these normal proteins from testing samples, specifically for detecting abnormal PrP^{Sc} isoforms, because of its partial resistance to PK digestion through α-helix rich to β-sheet rich structural transition. In contrast, PK truncates PrP^{Sc} isoform aminoterminally into its small portion, termed as PrP27-30 or $PrP^{27\text{-}30}$ that ranges in molecular weights (MW) between 27-30 kilodaltons (kDa). Thus, the standard methods in TSE diagnosis and PrP^{Sc} analysis have specified to detect this fragment. In general, this partial PK resistance has been considered as a characteristic feature of the conformational stabilities that PrP^{Sc} isoforms possess. During the last two decades, however, accumulating evidence suggests another variant of an infectious PrP^{Sc} isoform that is sensitive to PK exposures.[410,438-441] In human TSE study, sCJD brains exhibit both PK-sensitive and -resistant PrP^{Sc} variants.[442] The PK-sensitive PrP^{Sc} ($senPrP^{Sc}$) variant accounts for approximately 90% factions of the entire PrP molecules in the gray and white matters of brains from sCJD patients.[439] Interestingly, variant CJD (vCJD) brains also exhibit similar outcomes of this sensitive variant in the sCJD patients.[443] These detections of the $senPrP^{Sc}$ variant in these two subtypes of CJD cases seem to be related to the polymorphism at the codon 129 of the PRNP gene, especially for CJD

patients with the V homozygotes or heterozygotes. In familial CJD (fCJD) patients with 144-base pair (bp) insertion mutations, the senPrP^{Sc} variant predominantly exhibits in pathognomonic PrP patches of the cerebellum, in which the PK-resistant PrP^{Sc} (resPrP^{Sc}) variant is undetectable.[445] Thus, the senPrP^{Sc} variant must possess equivalent properties to implicate infectivity and neurotoxicity in TSE pathogenesis, as comparable to the resPrP^{Sc} variant. Furthermore, GSS brains constitute abundant portions of the senPrP^{Sc} variant.[442] Although the pathogenic role of the senPrP^{Sc} variant is not elucidated yet, this molecule is predominantly detected in the brains from variably protease-sensitive prionopathy (VPSPr: a sporadic human TSE) patients with the codon 129 VV homozygotes, whereas the resPrP^{Sc} variant is deficit.[446-448] Interestingly, PK treatment diminishes approximately 90% quantities of total PrP^{Sc} isoforms, detected in the brain tissues from scrapie-infected sheep with the VRQ or ARQ genotypes.[449] This finding indicates the majority of PrP^{Sc} isoforms is the senPrP^{Sc} variant. Thus, it is a serious concern that the use of PK arises potential risks for false-negative outcomes in TSE diagnoses and PrP^{Sc} analyses, because the use of PK would digest the senPrP^{Sc} variant and overlook its detection. In addition, the concentration and stability of the senPrP^{Sc} variant is associated with incubation periods and progression rates of TSEs, which seem to be implicated with the codon 129 polymorphisms and glycoform states.[410,450,451] In fact, the senPrP^{Sc} variant with the VV homozygous genotype and unglycosyl form (no glycan) is predisposed to have shorter survival times in sCJD patients, compared to the patients with MM homozygotes. These findings indicate that the senPrP^{Sc} variant is a critical modulator in TSE pathogenesis. Consequently, this

variant should be a valuable biomarker to determine disease developments and progressions.

To study about the senPrP^{Sc} variant, a thermostable neutral metalloproteinase enzyme, called thermolysin, is an applicable reagent to isolate its fractions from rodent and human brains, combined with applications of differential centrifugation.[440,444,452] As differed from the PK ability, thermolysin hydrolytically cleaves peptide bonds of a protein that contain the hydrophobic amino acids, such as A, V, I, L, M, and F (in the MW ordering). Preferentially, this enzyme truncates the N-terminus of these hydrophobic residues on proteins. Although thermolysin degrades normal PrP^{C} isoforms into little pieces, PrP^{Sc} isoforms are resistant to its proteolytic effect and can maintain these full-length forms. These isolation studies contribute to determine the comparable properties of the senPrP^{Sc} variant to the resPrP^{Sc} variant, such as infectivity and incubation times. Moreover, PMCA technology can amplify the senPrP^{Sc} variant as a seed in this in vitro replication, which indicates its propagative ability under the protein-only hypothesis. Understandably, PK treatment eradicates these pathogenic properties of the isolated senPrP^{Sc} particles with the thermolysin applications above.

The results from the sedimentation velocity method and PMCA also indicate similar structural properties of senPrP^{Sc} and resPrP^{Sc} variants from amplified monomers.[440,453] Ratios of senPrP^{Sc} and resPrP^{Sc} variants are dependent on TSE strains. The productions of variant differences are associated with sizes of the monomers in these strains, but not the biochemical structures of aggregates. In fact, small PrP^{Sc} aggregates are low MW and sensitive to proteolysis, but the increases of these complex sizes apparently provoke the typical biochemical properties of the

resPrP^{Sc} variant. Moreover, the aggregate sizes are correlated to the seeding potency and conformation-converting activity, which are highly exhibited in small aggregates/oligomers of the isolated fractions.[454] In sCJD patients, the continuum of PrP^{Sc} aggregates varies from less than 20 to more than 600 PrP^{Sc} molecules. The most effective initiators of the PrP^{C} conversions to abnormal conformations are small oligomers with masses equivalent to 20-78 molecules of PrP^{Sc} isoforms. In contrast, the increases of aggregate sizes reduce the seeding efficacy of sCJD PrP^{Sc} molecules. Thus, smaller aggregates possess higher seeding potency in the conformational conversion and replicative process. Since these efficient aggregates are PK sensitive, the senPrP^{Sc} variant must be possessive to form smaller oligomeric aggregations or complexes, whereas the resPrP^{Sc} variant consists of larger formations.[453] Possibly, the generations of the senPrP^{Sc} variant are associated with the strain-dependent features, as influenced by sizes of monomer and aggregates that each strain retains characteristically.

Some researchers have proposed another model of PrP^{Sc} formation that promotes the existence of a hypothetical lethal PrP variant (PrP^{L}), as opposed to the PrP^{C}-as-receptor mediating model of PrP^{Sc} toxicity.[39,454-458] The PrP^{L} variant is explained as a toxic intermediate or byproduct of the PrP conversions from PrP^{C} to PrP^{Sc} isoforms, as well as during the PrP replication, under a template-associated progression of the protein-only hypothesis. This toxic PrP^{L} variant is a small oligomer that induces neurotoxicity and neurodegeneration.[39] Conceivably, the small aggregate is a causal molecule of protein misfolding and disease initiation.[454] In fact, the accumulated concentrations of PrP^{L} generations link to neurotoxicity and clinical onsets of diseases,

as well as states of subclinical infections.[455,456,460-462] Rapid increases of PrP^{L} levels implicate with shorter incubation periods and survival times in mouse models of TSEs. In addition, an alternative aspect postulates that the PrP^{L} variant is not an intermediate product in the pathway to be a mature PrP^{Sc} isoform. Although the mature PrP^{Sc} isoform plays as a surface template of the PrP conversions from normal to abnormal conformation, the small PrP^{L} oligomers could be formed from the mature PrP^{Sc} isoforms.[463] Although the PrP^{L} variant is not physically defined, this lethal variant could be identical to PrP^{Sc} isoforms and modulate signals to cause neurotoxicity arising from the mature abnormal molecules. In mouse studies, kinetic measurements of the PrP^{Sc} infectivity indicate its plateau phase in brains, prior to developing clinical onsets of diseases at the latent period. Possibly, hypothetical PrP^{L} variants induce these accumulations that would be initiators for clinical onsets of diseases. This phenomenon could be switched from the phase 1 (a clinically silent exponential phase: autocatalytic production of infectivity, with reaching rapidly to a maximal prion titer) to the phase 2 (a clinically toxic phase: activated pathway for PrP^{L} generations, without an increase of infectious PrP^{Sc} propagations). According to the model of PrP propagation and toxicity, two distinct phases occurs: 1) replications of nontoxic PrP^{Sc} molecules (infectious PrP^{Sc} particles) until these accumulations saturate to a plateau phase as depended on levels of PrP^{C} expressions, and 2) a continuous plateau phase of PrP^{Sc} infectivity, but the initiation of PrP^{L} generation and formation/accumulation as in proportional to the PrP^{C} concentration. This new model of PrP pathology is based on the uncoupling of infectivity and toxicity in the two distinctive phases. A further study proposes the generations of the toxic PrP^{L} oligomers with the PrP^{C} downregulation in the duration of latent periods,

when prion propagation saturates during the template-assisted progression from PrP^{C} to PrP^{Sc} conversion.[464] Conversely, there are arguments to the PrP^{L} hypothesis because of extrapolated interpretations in these proposed models above.[459,465] However, the concept of the PrP^{L} variant overlaps with features of the $senPrP^{Sc}$ variant. If this pathogenic PrP particle could be one of the $senPrP^{Sc}$ variant, the PrP^{C} expression and dysfunction would influence controls against neurotoxic signals arising from PrP^{Sc} isoforms, especially these small toxic PrP^{Sc} oligomers. Hence, the decreases of PrP^{C} expression and function impair or sensitize neurons against PrP^{Sc} toxicity.

In addition to TSEs and other neurodegeneration disorders, numerous studies have reported the implication of PrP expressions in cancer pathogenesis, including progression, drug resistance, and proteinous amyloidogenesis.[230,231,466-471] An intriguing study revealed that cancer cells in TSE-infected mice highly express the $senPrP^{Sc}$ variant, but not the $resPrP^{Sc}$ variant.[472] These malignant cells with the $senPrP^{Sc}$ variant possess aggressive behaviors in proliferation and metastasis, leading to progressive exacerbation. Thus, I hypothesize that TSE-infected cells expressing the $senPrP^{Sc}$ variant have these cancer-like behaviors through the disease course. These cells can propagate and migrate locally and systemically with aggressive behaviors in TSE pathogenesis, as like cancer stem cells. This pathogenic feature should be different from general properties of the PrP^{Sc} infectivity, in which the $senPrP^{Sc}$ variant might have unique biochemical features. Overall, the existence of the $senPrP^{Sc}$ variant directs the necessity and importance of non-PK-based methods for detecting and understanding TSEs as well as other major disorders. The $senPrP^{Sc}$ variant is a valuable target to

further investigate the unknown mechanisms of disease developments and progressions.

4) Insoluble and aggregative variant of PrP^C isoform: The PrP^C isoform is known as soluble, monomeric and protease sensitive features, expressed abundantly in the CNS of humans and animals as normal.[1] However, the existence of an insoluble aggregate of PrP^C isoforms has been reported in humans and cultured neuronal cells.[473,474] This new PrP^C isoform is termed insoluble PrP^C ($iPrP^C$) variant that forms a monomeric, dimeric, oligomeric, or multimeric structure, and is resistant to PK digestion even under high concentrations. In human brains without TSE infections, the $iPrP^C$ variant accounts for approximately 25% of the total PrP^C expression. The gene 5 protein (g5p) and sodium phosphotugstate (NaPTA) are reagents that specifically bind to structurally altered PrP molecules, but not to normal PrP^C isoforms.[442,475] These affinities of the reagents enable isolations of the $iPrP^C$ variant. The g5p is a single-stranded DNA binding protein that has an avidity to interact with nucleic acids.[476] This binding ability was also utilized to isolate PrP^{Sc} isoforms and $iPrP^C$ aggregates. However, this proteinaceous reagent might have a specificity to interact with aggregated oligomers and complexes.[477-479]

For detecting the $iPrP^C$ variant, two anti-PrP monoclonal antibodies (mAbs), 1E4 and 3F4, were applied.[473,480] 1E4 mAb binds to its epitope on the residues 97 to 105 in the PrP sequence, whereas 3F4 mAb interacts to the residues 106 to 112. Although these epitopes were adjacent, the $iPrP^C$ variant showed a high affinity to 1E4 mAb, but a low affinity to 3F4 mAb.[150,474] These different reactivities of the two mAbs might indicate some conformation alterations in the region of these binding epitopes. The residues 91

to 120 in the PrP sequence are known as the region implicated in the PrP^{C}-PrP^{Sc} conversion.[481] Thus, I assume that $iPrP^{C}$ variant has structural changes in the 3F4 epitopic residues, because 3F4 mAb declined its binding affinity. Under immunofluorescence microscopic detections with 1E4 mAbs, the PK-resistant $iPrP^{C}$ aggregates predominantly localized in the cytoplasm around the nucleus, although PrP^{C} isoforms generally express on cell surfaces and sensitize to PK exposures.[150,482] These results suggest that the $iPrP^{C}$ variant has a unique conformation and localization, compared to PrP^{C} and PrP^{Sc} isoforms. In addition, the researchers in these $iPrP^{C}$ studies also isolated the oligomers of soluble and insoluble PrP^{C} isoforms from healthy human brains.[475] Thus, they intriguingly hypothesized the chameleon-like abilities of PrP^{C} isoforms in conformations.[482] Possibly, the $iPrP^{C}$ variant with the unique abilities might be involved in the TSE pathogenesis, especially in hosts for mechanisms of the PrP^{Sc} infection and the PrP^{C}-PrP^{Sc} conversion. In fact, in addition to PrP^{Sc} isoforms, 1E4 mAb detected the $iPrP^{C}$ variant in VPSPr patients with MM or MV polymorphisms at the codon 129 of PPRP gene, as well as fCJD patients with the mutation from V to I at the codon 180.[150,446,483]

Furthermore, the same group investigated the cleavage sites of the PK-resistant PrP fragment from brains of VPSPr patients.[434] The cleavage site for the N-terminal localized within the residues 99 to 101, while the C-termial cleavage site was detected between the residues 152 and 157. In addition, 1E4 mAb detected the $iPrP^{C}$ variant in human brains without TSE infections, although the PrP^{Sc} isoforms in the VPSPr and fCJD brains above reacted with this anti-PrP antibody. Interestingly, the same research group also revealed a potential implication of the $iPrP^{C}$ variant as the main PrP

conformer for interacting with amyloid β42 (Aβ42) aggregates in brains from AD patients.[484] Three years later, another group reported this iPrP^{C}-Aβ42 assembly in the AD pathogenesis.[485] Additionally, the cytosolic inclusions of PrP^{C} aggregations were detected in the β-islet cells of pancreases in rat models of DM, classified as PMD including TSEs and AD.[233] These findings suggest the pathogenic roles of the iPrP^{C} variant and PrP^{C} aggregate in neurodegenerative diseases and PMD. Thus, detections of the iPrP^{C} variant would be valuable molecular targets to evaluate potential risks and disease developments of TSEs and other PMD.

According to the report from an ischemic stroke study, moreover, detected PrP^{C} molecules were resistant to formic acids and heat.[486] Possibly, these PrP^{C} molecules altered conformational properties under hypoxic conditions. In ischemic brains, PrP^{C} molecules at the infarct regions highly aggregated with resistance to protease treatments.[304,487] These implicated factors could arise from low-pH environments that hypoxia and ischemia induced. In fact, acidic pH induced the conversion of the soluble PrP^{C} isoform into the iPrP^{C} variant in brain samples from humans.[486] Therefore, it is a pivotal importance to investigate the in vivo roles of this insoluble protein, especially for the implication of pH with the PrP conformation in physiology and pathology. This mechanism could be related to the chameleon-like abilities of the PrP^{C} isoform above.

At last, highly α-helical proteinous conformers are involved in the cytotoxicity in PMDs. These intermediate monomers have been detected in aggregations (amyloid plaques) of amyloidogenic proteins, such as Aβ in AD, α-synuclein in PD, and islet amyloid polypeptide (IAPP) in Type II DM.[489-492] A formation of highly α-helical protein is prone to induce aggregations locally, which leads a β-sheet rich formation

intermolecularly.[493] For instance, the progression of amyloid formation in DM is proportional to the amount of highly α-helical IAPP[494.495] However, biological significances of the intermediates still remain to be determined. In a recombinant PrP study, a monomeric and highly α-helical intermediate form of PrP molecules is the most neurotoxic substance on various types of cultured neuronal cells, on cerebellar brain slices, and in mouse brains, although oligomers of recombinant PrP molecules are also neurotoxic.[496] Similar to PrP^{Sc} isoforms, this intermediate PrP monomer exhibits insolubility and PK resistance, in spite of its higher α-helical structure as like normal PrP^{C} isoforms. The intermediate monomer also causes autophagic and apoptotic cell death. Interestingly, it induces cytotoxicity without endogenous PrP expressions in neuronal cells. In addition, the PrP-induced toxicity implicates into the autopgaolysosomal degradation pathway in neuronal cells and mouse brain with TSE infections. This recombinant PrP study suggests that the toxic monomer is an independent product of the PrP^{Sc} isoform during its infection and replication, or a generated molecule during the structural transitions of normal PrP^{C} to aberrant PrP^{Sc} conformations. These findings of the monomeric highly α-helical intermediate PrP form are consistent with features of the $iPrP^{C}$ and PrP^{L} variants. Consequently, the investigations of novel PrP mechanisms would continue as a fascinating field in biology, physiology and medicine. As a reminder, however, it is still a serious risk that the use of PK might result in non-accurate analyses for PrP^{Sc} detections and TSE diagnoses.

Overall, the PrP polymorphism is associated with the biochemical property of PrP^{Sc} strain differences and the underlying mechanism of PrP conformational changes and stabilities, including the PK sensitivity and PrP glycoform state.[39,410,411,425,450,451] As

described above, the codon 129 polymorphism implicates with the susceptibility and disease phenotype: note, the codon 132 in elk corresponds to the codon 129 in humans.[317,324,497-501] In addition, the glycoforms of VPSPr brain samples displayed the lack of diglycosyl PrP^{Sc} forms, but the high expression of mono-1 glycosyl forms (a single glycan at the glycosidic residue 181).[150] This glycoform pattern is similar to fCJD cases with the PRNP mutation at the codon 180 from valine/V to isoleucine/I (V180I). These physiochemical and biological properties of VPSPr agents might have possible associations with fCJD agents with the V180I allele.[448] In addition to this fCJD form, biochemical and neuropathological features of VPSPr resembled GSS and some sCJD forms. Feasibly, glycosidic deficits at the 180 residues could be attributable to clinicopathologic manifestations as well as conformational changes from normal PrP^{C} to abnormal PrP^{Sc} structures. These findings suggested that under-glycosylated PrP^{Sc} forms were implicated with TSE pathogeneses. Importantly, the lack of glycosylations could link to the PrP conformational instability that might induce sensitivities to PK digestions. Therefore, the uses of protease reagents would increase risks of false negative results in PrP^{Sc} analyses and TSE diagnoses. Incidentally, the existence of PK-sensitive PrP^{Sc} agents would cause potential occurrences of the iatrogenic PrP^{Sc} transmission to other patients via surgical and medical interventions including blood transfusions, organ transplantations, and instruments contaminated with the pathogens. For this transmissive concern and risk, the screening of glycosylation states would be essential targets as biomarkers to identify PrP^{Sc} existences and contaminations in donors, products, and equipments. In this dissertation, the proposed analytical methods

would provide practical approaches to detect PK-sensitive PrP^{Sc} pathogens selectively and specifically.

PrP glycosylations in TSE diseases

Glycosylation is the most common post-translational modification, which processes the addition of a carbohydrate moiety to a protein, lipid, and other organic molecules in cells endogenously or exogenously.[502,503] In the co-translational and/or post-translational mechanisms, enzymatic modifications intimately commit the regulation of glycosidic processes, specifically for sites and substrates.[504] Certainly, glycans secreted from glycoproteins influence various properties of proteins, such as solubility. Glycans localized on cell surfaces are also involved in numerous fundamental biological processes, such as cell-cell adhesions, cell-matrix interaction, cellular metabolisms, and intra- and inter-cellular signalings.[505,506] Thus, the loss or dysregulation of glycosylations affects normal functions in the cellular physiology. In fact, altered glycosylations induce pathological modifications and several diseases, such as cancers and neurodegenerative disorders.[507] In neurodegenerative diseases, modifications of different glycoproteins influence neural activity.[508,509] Some glycosyltransferases, responsible enzymes for the biosynthesis of glycans, are essential for neural development. These enzymatic dysfunctions implicate with neuropathological manifestations. Consequently, aberrant glycosylations modify the normal neural migration, leading to congenital neurological or neuromuscular disorders, such as muscular dystrophy.[509] In TSEs, a research group reported a declined activity of a Golgi glycosyltransferase (N-acetylglocosaminyltransferease III; GnTIII) in cells that generate

PrP^{Sc} isoforms.[510-511] This enzymatic reduction induced different proportions of glycans between PrP^{C} and PrP^{Sc} molecules: 11% smaller bisected glycans, 5% greater triantennary glycans, and 10% greater tetra-antennary glycans in the N-linked glycosylation of PrP^{Sc} molecules, compared to PrP^{C} isoforms. Thus, the GnTIII-related enzymatic modulation might be attributable to cause the aberrant glycosylations and the TSE pathogeneses.

In addition, glycosylations promote the stability of proteins in that an increased amount of oligosaccharide delivers a higher free-energy barrier for preventing the pathologic conformational conversions from PrP^{C} to PrP^{Sc} isoforms.[197,512] The inhibition or attenuation of glycosylations induces the aberrant PrP conversions. On the electrophoretic gel, the intensity of a diglycosyl PrP^{Sc} fragment is the smallest band in the sCJD form.[197] This result suggests that the majority of diglycosyl PrP^{C} isoforms might not convert to PrP^{Sc} isoforms. Hence, under-glycosylated PrP^{C} forms could be prone to modulate conformations.[514] Tunicamycin, an antibiotic that can remove glycans, inhibited the N-linked glycosylation, resulting in the acceleration of PrP^{Sc} formations in scrapie-infected cells and the acquisition of PrP^{Sc} properties in transfected cells with PRNP mutations.[514,515] In familial TSE forms, a deletion or alteration of the PrP glycosylation is a frequent phenomenon, because of naturally occurring mutations in PRNP.[150,516-518] In fCJD forms with PRNP mutations of V180I or T183A, diglycosyl forms of PK-resistant PrP^{Sc} fragments are generally undetectable, because these mutations cause the loss of a glycosidic site.[517,518] Hence, the amino acid substitutions at these codons abolish or alter a N-linked glycosylation at the codon 181 in the human PrP structure. Also, mutations affecting the PrP^{C} glycosidic sites induce accumulations of

insoluble PrP isoforms.[475,482] Other PRNP mutations (i.e. D178N, F198S, E200K) also modulate glycoform ratios that induce pathogenic changes in PrP^{C} structures.[323,519] Therefore, the underlying substitutions of amino acids in PRNP mutations directly impact PrP^{Sc} transformations.[511,520] Similar to the fCJD form with the V180I mutation, VPSPr pathogenesis has a glycoform-selective prion formation pathway even without PRNP mutations.[150,447,483] These two diseases notably lose both diglycosyl and monoglycosyl (the codon 181) PrP^{Sc} forms. Moreover, altered PrP glycosylations influence the binding affinity or reactivity of anti-PrP mAbs to PrP^{Sc} agents in VPSPr materials because of conformational conversions to abnormal PrP structures.[150] Accordingly, VPSPr should be the first TSE disease where the alterations of glycosylations cause structural abnormalities of PrP molecules.[521]

In in vitro experiments, glycosylations present the property to maintain PrP conformations.[515] On the exogenous PrP^{C} molecules, mutations of the N-linked glycosidic sites (the codons 181 and 197 in humans; 180 and 196 in mice) on PrP structures interfere glycosylations, resulting in alterations of conformations and properties from PrP^{C} to PrP^{Sc} molecules, such as PK resistance. These findings indicate that the loss of the N-linked glycosylation modulates the PrP^{C} sequence and structure that intrinsically adopt a β-sheet conformation. In contrast, cells treated with tunicamycin did not exhibit abnormal modulations for properties of the endogenous PrP^{C} molecules.[514] Also, PrP overexpressions provoked protein aggregations intrinsically as property alterations[522]. To investigate the glycosidic implications in TSEs, the unglycosyl form of short PrP peptides was synthesized from the helix-2 domain (the residues 175-195) of the PrP structure.[523] This unglycosyl peptide rapidly acquired a β-sheet structure

that subsequently formed amyloid fibrils. In contrast, the same peptide sequence with N-linked glycans (glycosylated peptide) significantly declined fibril formations. In another study, PrP peptides that synthesized with O-linked glycans also ensured similar observations.[524] Although the PrP^{C} structure does not have O-linked glycans naturally, this study suggests that glycosylations alter the kinetic equilibrium between monomeric PrP^{C} and aggregated PrP^{Sc} molecules. Moreover, the glycosylation does not link to properties of PrP^{Sc} agents in propagations and infections. In scrapie-infection studies, the large productions of unglycosyl PrP^{C} forms via tunicamycin treatment did not prevent PrP^{Sc} formations in murine neuroblastoma N2a cells.[514] However, unglycosylated mutations of PrP^{C} molecules (substitutions of asparagine to glutamine at the codon 180 and 196 in mouse numbering) caused susceptibilities to TSE infections in uninfected N2a cells.[525] In scrapie-infected N2a cells and transgenic mice, mutations of the glycosidic consensus sequences in the PrP^{C} structure affected subcellular locations of PrP^{C} molecules and enhanced susceptibility to infections[526].

In the PrP^{Sc} conversion, the glycosylation state can significantly modulate the interaction of host PrP^{C} isoforms with invasive PrP^{Sc} seeds. Especially in different species, the glycosylation is an influential factor at the initial binding occasion of the PrP^{C}-PrP^{Sc} interaction. For crossing the species barrier between hamsters and mice, hamster PrP^{Sc} seeds can introduce a species-specific amino acid residue into host mice. Subsequently, these seeds can initiate the conversions of mouse PrP^{C} molecules to abnormal conformations more readily when the host PrP^{C} molecules are unglycosylated forms.[514,527,528] Conversely, the glycosylations of host PrP^{C} molecules block the interaction with PrP^{Sc} seeds. Even in the cell-free conversion assay, the glycosylation

state of PrP^{C} molecules influence the conformation of the PrP^{Sc} agents.[205,529] In the cross-species conversion reaction, an unglycosyl PrP^{C} form enhances the efficiency of the PrP^{Sc} conversion. This reaction should be attributable to an increased capability of the unglycosyl PrP^{C} forms binding to the PrP^{Sc} seeds. Thus, the presence of the full glycosylation can inhibit or modulate the interactions of PrP^{C} to PrP^{Sc} agents. Hence, the glycosylation states of host PrP^{C} molecules are determinant influencers for the compatibility of amino acid sequences in the PrP^{C}-PrP^{Sc} interaction and conversion over glycosylation states.

In fact, the glycoform patterns of PK-resistant PrP^{Sc} fragments exhibit different patterns among the disease forms in the CJD classification.[420] Among TSE strains or subtypes, the composition and proportion of the glycans exhibit different glycoform patterns.[510,530,531] The vCJD cases have abundances of diglycosyl forms, which cattle with classic BSE also dominantly express. In contrast, atypical BSE cases exhibit different glycoform patterns of PrP^{Sc} fragments from the classical BSE cases, but more atypical BSE cases resemble the glycosidic patterns of sCJD cases in humans.[420,532,533] Both atypical BSE and sCJD cases predominately express monoglycosyl PrP^{Sc} forms. These differences arise from PrP^{Sc} conformation and glycosylation that implicate with the molecular basis of TSE strain diversities. The properties that each strain maintains are stably transmissible and reproducible in the new host.[331] In inoculated mice, PK-resistant PrP^{Sc} fragments maintain the TSE strain-specific sizes and glycosylation patterns upon transmissions.[325] These specific glycoform patterns influence strain properties, such as incubation periods and neuropathology.[410,534] Transmissions of vCJD materials into mice generated PrP^{Sc} fragment sizes and glycoform ratios, similar

to classic BSE.[535] In the molecular basis of TSE pathogeneses, these strain properties are also associated with host-specific factors, such as the primary PrP^C structure and host-specific glycosylation.

Attachments of N-glycosylation to proteins are initiated in the ER lumen. Intriguingly, a glycopohosphatidyl-inositol (GPI) attachment to the PrP^C molecule occurs in the ER lumen.[528] The GPI moiety for the C-terminal membrane anchorage could be a required factor for the initiation of N-glycosylation to of the PrP^C molecule.[536] The GPI anchor also facilitates translocations of glycosylated PrP^C molecules through the secretory pathway to cell membranes. Thus, a deficiency or dysregulation of the GPI anchor synthesis is influential for N-glycan attachments to proteins. Indeed, these impaired processes are observed in some severe and lethal diseases, such as congenital disorders of glycosylation.[537-540] Hence, the GPI anchor could be involved as an essential role for proper PrP glycosylations.

In glycoproteins, cell surfaces could be the pivotal sites for the initiation of neurodegeneration, because the PrP^C isoform functions on the cell membrane as a single molecule.[541,542] Since the GPI anchors are involved in aberrant PrP^{Sc} transformations, the conditions of the PrP glycosylation critically implicate with the TSE development, classification, and strain characterization. In transgenic mice, mutations of the glycosidic consensus sites altered the subcellular localization of PrP^C isoforms and the susceptibly to TSE infections.[526,543] Alerted subcellular localizations induced the TSE-strain dependence for infection and propagation. Intriguingly, monoglycosyl PrP^{Sc} isoforms could be attributable to the molecular mechanisms of host susceptibilities to TSE infections and PrP^{Sc} conversions.[544] In fact, the mutation of the first glycosidic site

provoked intracellular PrP^{Sc} accumulations into neuronal cell bodies.[204,545] Since the two N-link glycosidic sites localize in the structured globular domain at the C-terminal of the PrP structure, the loss of glycans might alter the protein conformation.

Overall, the PrP glycosylation is a key regulatory mechanism to control several pathophysiological processes in TSEs. Because glycans maintain various biological efficiencies, the glycosidic deficiency links to the loss of PrP^{C} functions, such as neuroprotection.[546,547] The PrP^{C} dysfunctions would alter cellular microenvironments, leading to neurodegeneration and disease development.[548] These pathogenic changes might gain toxicities in cells.[458,549-551] Thus, the recognition of certain glycosylated PrP forms would specifically discriminate PrP^{Sc} agents and determine unidentified TSE pathogeneses including strain differences. Consequently, glycobiology has been an increasing subject to discover the implication of glycosylations in various disease researches.[552-558] For these clinicopathologic implications, investigations have challenged to meet the needs for high specificity, sensitivity and capacity of analytical approaches. In this dissertation, the established analytical methods have utilized characteristic features of the in-house anti-PrP mAbs that have conformation dependences for PrP recognition specifically. In fact, one mAb binds specifically to unglycosyl and monoglycosyl (mono-1) PrP forms.

Section 3: Traditional TSE diagnoses and limitations

PrP^{Sc} detections in TSE diseases

1) Current and traditional methods: Currently, the detection of abnormal PrP^{Sc} isoforms in brains accomplishes definitive diagnoses of TSEs. In general, autopsy is the

most common procedure to obtain brain tissue samples from TSE-affected patients and animals. While brain biopsy is an available procedure technically at ante mortem, World Health Organization (WHO) does not recommend this intervention for suspected TSE cases, because of the risk for pathogen contaminations to instruments and further iatrogenic transmissions.[559] Upon autopsy, histological and immunehistochemical analyses of brain tissues are standard examinations for definitive diagnoses of TSEs.[560] In all TSEs, the general features of neuropathology commonly include reactive gliosis, neuronal loss, spongiform change, and PrP^{Sc} depositions. Some neuropathological features can distinguish subtypes of TSEs, especially between sCJD and vCJD cases. PrP^{Sc} depositions are detected in amyloid plaques, called Kure plaques.[560] This plaque is found in Kuru patients, sCJD patients with the MV2 subtype, and GSS patients. In vCJD cases, a dense core of PrP^{Sc} immunopositive deposition forms a plaque, surrounded by vacuoles of spongiform changes, known as florid plaque.[561] In addition, vCJD brains exhibit multiple small plaques, but not associated with spongiform changes. Thus, the existences of florid plaques are useful features to confirm the vCJD form, which allows distinguishing from the sCJD form.[561]

While several methods have been innovated to detect TSE pathogens at ante mortem, definitive diagnoses of TSE are still based on tissue examinations at post mortem. Since PrP^{Sc} agents are transmissible pathogens in the same species and between different species, proper precautions must be undertaken to minimize a potential risk of exposures to the pathogen, especially for handling brains or related samples.[562] In general, brains from patients with CJD suspicions should be handled in a Class II Biological Safety Cabinet in a specialized Biosafety Level II facility for sCJD and

fCJD cases, and a Level III facility for vCJD cases. For vCJD cases, tonsils and lymphatic tissues are potential samples to detect PrP^{Sc} accumulations at ante mortem.[327,563-565] However, sCJD and fCJD cases do not exhibit PrP^{Sc} expressions in tonsils. Thus, PrP^{Sc} detections in these tissues via biopsy could differentiate suspected patients affected with either vCJD or other forms of human TSE diseases at ante mortem. In tonsils derived from vCJD cases, PrP^{Sc} expressions might be detectable even before developing clinical onsets. The spleen is also another organ that expresses PrP^{Sc} agents in TSE patients even with asymptomatic phases of the vCJD form.[566] Nevertheless, pathogen contaminations to instruments during biopsy and surgical procedures are serious concerns for potential risks of iatrogenic transmissions.

After collecting tissue samples, the western blot analysis should be one of the most common methods for PrP^{Sc} detection.[562] This method requires the use of PK reagent in preparations of testing brain or tissue homogenates. PK digestion enables to differentiate abnormal PrP^{Sc} agents from normal PrP^{C} isoforms. Because the pathogenic proteins are partially PK resistant and the normal proteins are completely sensitive, PrP^{C} isoform should not be measurable in non-TSE infected tissues.[2] Hence, only PK-resistant PrP^{Sc} agents would be detectable in TSE-affected or contaminated samples. This enzymatic digestion generates a C-terminal core fragment from the PrP^{Sc} isoform, called PrP27-30. Using anti-PrP mAbs, western blot analysis detects a PrP27-30 fragment as a PrP^{Sc} agent. In addition to an advantage that does not need large amounts of testing samples, this analytical method can distinguish subtypes of PrP^{Sc} isoforms in different variants or strains of TSEs, especially for human CJDs combined with the PRNP genotypes, such as the codon 129 polymorphism, genetic mutations,

and characteristic histopathological features.[562] Although western blot analyses can provide detectable sensitivities of PK-resistant PrP^{Sc} agents for definitive diagnoses, immunohistochemistry can evaluate resolutions of anatomical lesions and PrP^{Sc} distributions throughout the whole brain structures. Compared to western blot analyses, a detection sensitivity of immunohistochemistry is lower, because a background reactivity of PrP^{C} isoforms interferes with analytical resolutions. However, this issue could be overcome with paraffin-embedded and formalin-fixed tissue sections that are heated and pre-treated with formic acid and hydrolytic autoclaving.[562] These processes can eliminate PrP^{C} immunereactivities and expose PrP^{Sc} depositions. Therefore, western blot and immunohistochemistry are absolutely imperative as routine tools to detect PrP^{Sc} agents for definitive diagnosis.

For human TSE cases, diagnostic imaging and electrophysiological examinations may define TSE features, but each form of human diseases present differently.[567] Magnetic resonance imaging (MRI) and electroencephalogram (EEG) examinations can provide differential diagnoses between vCJD and sCJD forms at ante mortem[568] MRI is a unique imaging tool for CJD differentiations. In MRI evaluations, vCJD patients mostly pronounce signal enhancements in the posterior thalamus, called the pulvinar sign.[569] Since approximately 80% of vCJD cases present this sign, it has been included in the diagnostic criteria for vCJD. However, sCJD patients do not have signaling enhancements in the posterior thalamus. Thus, the presence of the pulvinar sign is a significant distinction between vCJD and sCJD forms, which is an essential aspect from public health. In addition, 60-80% of sCJD cases exhibit the hyper signal intensity in the basal ganglia.[567,570] Based on MRI evaluations, signal alterations in brains correlate with

molecular subtypes of the sCJD form.[571] Thus, advanced imaging would contribute to the earlier diagnosis for CJD patients.

Furthermore, EEG could be another tool to distinguish between vCJD and sCJD cases. Periodic sharp wave complexes (PSWCs) are characteristic patterns of EEG in the sCJD form, accounting for 60-70% of patients.[572-576] PSWCs can be detectable as early as 3 weeks after their disease onsets. Between two types of the sCJD form in the codon 129 genotypes, most common subtypes of type 1 (MM1, MV1) show PSWCs, while other subtypes (VV1, VV2, MM2, MV2) do not show.[577,578] Possibly, the codon 129 polymorphism might be an influential factor of the characteristic EEG pattern in sCJD cases.[579] In addition, fCJD patients with the codon 200 or 210 mutations exhibit this EEG pattern during the disease course.[580,581] In FFI cases, the EEG polysomnography might determine changing patterns in association with clinical symptoms during the course of disease progression.[582,583] No diagnostic EEG pattern is found in GSS, iCJD, and vCJD patients.[567]

2) Limitations of current diagnostic methods: Spongiform change is known as a histological feature of TSEs, but not all cases exhibit this pathogenic alteration. In fact, various other diseases also cause this alteration or vacuolar degeneration in affected brains, such as AD, some neurodegenerative lysosomal disorders with autophagic vacuoles (i.e. neuronal ceroid lipofuscinoses, Battern disease, Niemann-Pick disease, aspartylglucosaminuria), canine distemper, avian vacuolar myelinopathy, progressive multifocal leukoencephalopathy (John Cunningham virus infection), cerebral autosomal dominant arteriopathy with subcortical infracts and leukoencephalopathy (a hereditary stroke disorder), Krabbe disease (an inherited fatal lysosomal disease, also known as

globoid cell leukodystrophy or galactosylceramide lipidosis,), and toxic spongiform leukoencephalopathy.[584-591] Thus, the detection of vacuoles is not a sole decisive evidence for the TSE definitive diagnosis.

The most significant limitation for the TSE identification could be the definitive diagnosis at post mortem after autopsy. Without autopsy, this limitation could be a possible source of the iatrogenic PrP^{Sc} transmission if suspicious individuals donated bloods, tissues, and organs before the definitive diagnosis. Even for animals, necropsy would a critical procedure to prevent the PrP^{Sc} contamination to food products and its oral transmissions to humans and other animals. Furthermore, MRI and EEG are great diagnostic applications for neurological disorders. However, the MRI and EEG observations differ from each CJD case at ante mortem. These diagnostic results might differ from histological confirmations as TSEs at post mortem.[592] Even if observing clinical progressions of TSE-like features, the PrP^{Sc} existence in brains should be necessary to confirm for definitive diagnosis. For this purpose of the PrP^{Sc} detection, PK reagents have been used to isolate the pathogenic proteins from its normal form. Conversely, recent studies have accumulated evidences of PK-sensitive PrP^{Sc} isoforms that are mostly implicated with TSE pathogeneses, such as infection, neurotoxicity, disease progression and lethal outcomes. [440,434,445,448,449,59-596] Thus, the use of PK reagents would cause potential risks of missing the pathogens in PrP^{Sc} analyses or TSE diagnoses. In other words, novel innovations are pivotal for the PrP^{Sc} detection at ante mortem or the asymptomatic phase.

New technologies have provided capable tests of detecting subtle amounts of pathogens via the amplifications of PrP^{Sc} seeds from PrP^{C} substrates.[597-601] Several

analyses have been examined for clinical TSE patients at ante mortem, leading to a probable diagnosis for TSEs and a differential diagnosis for clarifying other neurodegenerative diseases.[602-605] In bioassays, long incubation periods are impractical for infectious studies until animals initiate disease onsets over months to years. This is the major barrier of the TSE research. In contrast, the cycles for the PrP^{Sc} amplification and conversion take from hours to days. Hence, these advanced methods can overcome the major issue in bioassays. Thus, these analytical tools can contribute to the early detections of PrP^{Sc} particles in testing materials from TSE-affected individuals and animals. However, several questions arise for these methodologies, such as processing cycles under higher temperatures.[60-610] These temperatures are at 42°C or higher that are causative factors for thermal protein degradations and irreversible structural instabilities.[611-613] Since these processing cycles continue hours to days, degraded proteins could be produced and might link to conformational changes of PrP particles. In addition, the new methods do not have a system as like the degradation pathway in cells during the protein synthesis.[614-617] Hence, the protein quality control is not available for eliminating incompleted or misfolded PrP structures in these methodologies. Moreover, repeated cycles of the PrP amplification and conversion might be similar to overproductions of PrP molecules in cells. It is known that the PrP overexpression induces the high possibility of protein aggregations.[522]. In fact, substances for amplifications in these experimental approaches are recombinant PrP molecules that are usually unglycosyl forms. Thus, the structures of these substrates could be susceptible to conformational conversions via templates of PrP^{Sc} seeds. In the methods for PrP^{Sc} amplification, another common substrate is the brains from

transgenic mice generating PrP overexpression that should contain numerous PrP^{C} molecules. Because of high PrP productions, many immature forms should be generated in these brains, especially those in cells intracellularly for processing full glycosylations through the protein synthesis. In addition, the methods for PrP amplifications and conversions do not have any systems to evaluate and eliminate the error of synthesized proteins with incorrect structure or misfolded conformation. Thus, increased cycles of the protein amplification might raise chances to generate insoluble PrP forms. For this point, WB requires PK reagent to determine amplified molecules. However, the presence of insoluble PrP^{C} forms and these aggregations might result in false negative observations as PrP^{Sc} isoforms. In a case when PrP^{Sc} seeds are PK sensitive, amplified molecules might maintain this feature. Hence, PK digestion for WB preparations would eliminate this pathogen potentially.

3) A proposing strategy to detect PrP^{Sc} isoforms effectively: To differentiate PrP^{Sc} agents from the abundance of PrP^{C} isoforms, one strategy could be a methodology for these conformational differences. One method is known as the conformation dependent assay or immunoassay.[410,439,449,619-622] Although developments of immunological reagents and methods have attempted the capability of selecting these soluble and insoluble PrP isoforms, anti-PrP mAbs specifically distinguishing the PrP^{Sc} conformation are not available. Thus, detergents (i.e. guanidine hydrochloride) have ben used to denature proteins.[623-626] The conformation of PrP^{Sc} isoforms is resistant to denaturation at lower concentrations of detergents, whereas PrP^{C} isoforms are sensitive and soluble for detergents. Hence, increased concentrations of detergents can denature the normal proteins in testing samples that lose native structures.[627-629] As

a result, only insoluble proteins would remain persistently in the samples and maintain these resistant conformations for detecting in assays using anti-PrP mAbs.[453,630-633] In this dissertation, established methods for PrP^{Sc} analyses utilized the guanidine-mediated differentiation for innovating an experimental strategy without the use of PK reagents.

4) Enzyme-linked immunosorbent assay (ELISA) for detecting PrP^{Sc} isoforms: ELISA methods have been widely used as diagnostic tools in medicine and research because of these high sensitivities and strong specificities. Compared to western blot (WB) and immuneprecipitation (IP), the advantages of ELISA methods are the ability to test greater numbers of samples at the same time, and detect very low or unknown concentrations of targeted antigens. In general, ELISA procedures are quick, convenient and safe (i.e. no radioactive substance). Several ELISA methods are routinely applied for PrP detections in tissue samples, followed by PK digestion of PrP^{C} isoforms for specific detection of PrP^{Sc} isoforms that are generally resistant to the PK reagent.[634,635] This enzyme is also used for sample preparations in WB and IP procedures. PK digestion has been widely used in PrP^{Sc} analysis and TSE detection, whereas non-PK protocols of these standard analyses are limited in TSEs. Nevertheless, the existence of PK-sensitive PrP^{Sc} agents has been reported, and some studies suggest that a significant amount of the PrP^{Sc} agent is PK sensitive.[449,453] Therefore, the use of PK reagents for PrP^{Sc} detections has potential risks to produce the false negative results in the traditional PK-based diagnostic methods. In the public health aspect, these risks are serious concerns for food safety and zoonotic transmission, especially for BSE and vCJD implications. To overcome this critical

limitation of PK-based tests, the development of novel assays to detect PrP^{Sc} agents is required to avoid the use of PK reagents and ultimately improve the sensitivity and specificity.

Section 4: Introduction to work in this dissertation research

Research Overview

The overreaching goal of this dissertation is to establish novel analytical systems for TSE diagnoses. TSEs, well known as prion diseases, are fatal neurodegenerative disorders in humans and animals, caused by the accumulation of the misfolded PrP isoform, referred to as PrP^{Sc}.[2,3,28,637] The normal cellular PrP isoform, called PrP^{C}, comprises a monomeric and predominant α-helical structure. The abnormal conformational conversion of the normal PrP^{C} isoform misfolds into the pathogenic PrP^{Sc} isoform that configures an aggregation-prone β-sheet rich structure. This structural change renders the PrP^{Sc} isoform to be protease resistant and detergent insoluble, whereas the PrP^{C} isoform is sensitive to PK reagents and soluble to detergents. Through long incubation periods, accumulations of aggregated PrP^{Sc} isoforms in the CNS implicate with the TSE disease development. Because of the structural modification, this abnormal conformer also alters the physiochemical properties of PrP^{C} isoforms. However, the transformational mechanism from PrP^{C} to PrP^{Sc} isoforms is not clearly known.

In general, the N-linked glycosylation is a covalent attachment of glycans to the carboxamido nitrogen on asparagine (N) residues on proteins.[640,641] The PrP^{C} structure composes two N-linked glycans, conserved at amino acid residues 180 and 196 in mice

(181 and 197 in humans).[642-645] Glycosidic variances generate four different forms of PrP glycosylations: unglycosyl, monoglycosyl at 180/181 (mice/humans), monoglycosyl at 196/197, and diglycosyl forms. While the expression profiles of the glycosylated PrP forms have been studied, the role of the glycosylation and its importance is not clarified in TSEs.[205] Conversely, glycosylation plays various structural and functional roles in proteins.[511] For example, mutation or truncation of N-linked glycans interferes with protein folding.[119,512,646] Since glycosylation has a role in the maintenance of the PrP^C structure, the modulation of the N-linked glycosylation may lead to protein conformational changes. In TSEs, N-linked glycans on the normal PrP^c isoform link to the disease phenotype. In fact, transgenic mice lacking a glycan at either one of the two consensus sites for N-linked glycosylation on the PrP^C isoforms present more susceptibilities to the TSE infection.[201] Therefore, the loss of N-linked glycans from the PrP structure should be involved in the pathological mechanisms of TSEs. Moreover, the absence of a diglycosyl PrP form is reported in cell culture models and brain tissues from TSE-affected patients.[150,202] Also, in vivo models of scrapie exhibited abnormal glycosylation patterns of PrP molecules. These observations showed an increased ratio of under-glycosylated forms, but a decrease of diglycosyl forms.[203] In the preliminary studies, TSE-affected mice exhibited increased detections of under-glycosylated PrP forms in brains, compared to controls (unpublished data). However, it is not clear why glycans on PrP molecules are lost during the disease development. Possibly, the alteration of glycosylation states may play a significant role in the TSE pathogenesis by selective glycosyl forms.

This dissertation research proposes that the under-glycosylated forms of PrP molecules are preferentially generated during TSE disease development, resulting in the increased efficiency of the conformational conversion of PrP^{C} to PrP^{Sc} isoforms. Conversely, the tools to specifically determine the glycosylation state of PrP^{Sc} isoforms have been limited. Therefore, it is important to develop new and sensitive methods for detecting specific glycosylated PrP^{Sc} forms. The targeting approach to the under-glycosylated state of PrP^{Sc} isoforms will reveal the molecular mechanisms in the selection of certain glycosylated forms for the PrP conformational conversion. These studies will identify molecular mechanisms of the PrP transformation providing insight for the development of innovative diagnostic methods and effective treatments against TSEs.

Among the in-house productions of antibodies, two novel anti-PrP mAbs, PRC5 and PRC7, react with discontinuous epitopes in the structured globular domain of a PrP molecule.[195] Interestingly, PRC7 specifically recognizes an unglycosyl form and one monoglycosyl form of PrP molecules. As another unique feature, PRC7 requires denaturation and renaturation of PrP molecules to recognize PrP^{Sc} isoforms. In addition, PRC7 cannot recognize a diglycosyl form of PrP molecules that an abundance of normal PrP^{C} isoforms expresses. Consequently, PRC7 preferentially detects PrP^{Sc} isoforms. To innovate new analytical systems specifically for PrP^{Sc} isoforms, developments of sensitive ELISA protocols utilized the PRC5 and PRC7 features of conformational-dependent reactivities. The use of PRC7 would enable the detection and quantification of under-glycosylated PrP forms in TSE-infected samples.

The central hypothesis is that, the detection of under-glycosylated forms of PrP molecules is a hallmark of TSEs as a diagnostic biomarker for prion disease progression. Here, I propose that the loss of full glycosylation implicates with the pathological mechanisms of TSEs. For instance, glycosylation is involved in the maintenance of protein structures. Thus, its modulation can initiate unstable conditions for maintaining proper PrP conformation, which induces pathologic alterations of PrP structures. These aberrant formations could impair functions of normal PrP^{C} isoforms. Another aspect of glycosylation is that PrP^{Sc} isoforms may lose glycans during the TSE developments. Therefore, I assume that under-glycosylated PrP forms can be preferentially generated during the disease progression. To accomplish the proposed studies, two sensitive ELISA methods were developed for the detection and quantification of PrP^{Sc} isoforms in TSE-infected samples.

Using the PRC7 and PRC5 mAbs as capture and detecting antibodies respectively, 7-5 ELISA specifically recognizes the two certain under-glycosylated PrP forms, significantly detected in TSE-infected materials. In addition, D-5 ELISA uses D18 anti-prion antibody as a capture antibody and has an exceptional capability to determine levels of only PrP^{C} or total PrP molecules by different sample preparations. Using the D-5 ELISA method, TSE-infected materials at terminal stages decreased PrP^{C} levels, whereas total PrP levels were increased. These results correspond to a recent article using the conformation-dependent immunoassay (CDI).[647] Since the established protocols do not require PK reagents, these ELISA methods will be ultimately beneficial for TSE diagnoses, especially for detecting PK-sensitive PrP^{Sc} agents. In addition, the Sandwich ELISA approaches would contribute to understanding the TSE pathogenesis

by detecting PrP^{Sc} isoforms, specifically based on glycosylated forms and distinguishing PrP^{C} isoforms from PrP^{Sc} agents. The following Specific Aims will provide an innovative framework of the dissertation research that will result in beneficial impacts for the fields of veterinary medicine, human medicine, and public health.

Aims of Study

Specific Aim 1 (Chapter 2): Development and optimization of a new ELISA approach, based on novel properties of the PRC7 mAb. I determined the capabilities of PRC5 and PRC7 in ELISA approaches, using recombinant PrP particles and brain homogenate samples from mouse models of TSEs. These mAbs were capable of reacting with these samples in both Indirect and Sandwich ELISA methods. These experiments identified the specificity for the productions of under-glycosylated PrP forms during the TSE development. To develop an optimized ELISA protocol, I attempted various approaches: i.e. mAb coating concentrations, sample denaturation/non-denaturation, sample protein concentrations, temperature, etc.

Specific Aim 2 (Chapter 3): Determination of the 7-5 ELISA method to detect disease-associated PrP in mouse models of TSEs. I hypothesized that the 7-5 ELISA method could detect under-glycosylated PrP forms in TSE-infected samples from different species. For this aim, I examined PrP^{Sc} isoforms in tissue samples from various transgenic mouse models of TSEs at terminal stages. The D-5 ELISA method also could determine modulations of PrP^{C} levels and total PrP levels in the testing murine samples. These outcomes developed new sensitive methods for evaluating various

PrP^{Sc} strains, TSE-infectious states, species differences, and generations of under-glycosylated PrP forms in TSEs.

Specific Aim 3 (Chapter 4): Evaluation of the utility of 7-5 ELISA as a diagnostic tool for TSEs in cervids. I hypothesized that under-glycosylated PrP forms were preferentially generated during the disease progression of chronic wasting disease (CWD), a naturally occurring infectious prion disease in cervid animals. The sensitivity of the 7-5 ELISA method would determine under-glycosylated PrP forms in collected samples from CWD-infected and uninfected cervids. The D-5 ELISA method was also a sensitive analytical tool to measure PrP^{C} levels and total PrP levels from the collected samples. These investigations determined the generation of under-glycosylated PrP forms in CWD and the modulation of PrP^{C} and total PrP levels. These alterations should implicate with the disease development, comparing to its negative samples and controls.

REFERENCES

1. Prusiner SB. The prion diseases. *Brain Pathol* 1998;8:499–513.
2. Prusiner SB. Prions. *Proc Natl Acad Sci USA* 1998;95:13363–83.
3. Colby DW, Prusiner SB. Prions. *Cold Spring Harb Perspect Biol* 2011;3:a006833.
4. Taylor DM, Woodgate SL. Bovine spongiform encephalopathy: the causal role of ruminant-derived protein in cattle diets. *Rev - Off Int Epizoot* 1997;16: 187–98.
5. Nathanson N, Wilesmith J, Griot C. Bovine spongiform encephalopathy (BSE): causes and consequences of a common source epidemic. *Am J Epidemiol* 1997;145:959–69.
6. Harman JL, Silva CJ. Bovine spongiform encephalopathy. *J Am Vet Med Assoc* 2009;234:59–72.
7. Ramasamy I, Law M, Collins S, Brooke F. Organ distribution of prion proteins in variant Creutzfeldt-Jakob disease. *Lancet Infect Dis* 2003;3:214–22.
8. Ironside JW, Head MW. Variant Creutzfeldt-Jakob disease and its transmission by blood. *J Thromb Haemost* 2003;1:1479–86.
9. Ironside JW, Head MW. Variant Creutzfeldt-Jakob disease: risk of transmission by blood and blood products. *Haemophilia* 2004;10 Suppl 4:64–9.
10. Miller MW, Williams ES. Chronic wasting disease of cervids. *Curr Top Microbiol Immunol* 2004;284:193–214.
11. Sigurdson CJ. A prion disease of cervids: chronic wasting disease. *Vet Res* 2008;39:41.
12. Belay ED, Maddox RA, Williams ES, Miller MW, Gambetti P, Schonberger LB. Chronic wasting disease and potential transmission to humans. *Emerging Infect Dis* 2004;10:977–84.
13. Brown DR, Qin K, Herms JW, Madlung A, Manson J, Strome R, *et al.* The cellular prion protein binds copper in vivo. *Nature* 1997;390:684–7.
14. Hegde RS, Mastrianni JA, Scott MR, DeFea KA, Tremblay P, Torchia M, *et al.* A transmembrane form of the prion protein in neurodegenerative disease. *Science* 1998;279:827–34.
15. Priola SA, Chesebro B, Caughey B. Biomedicine. A view from the top--prion diseases from 10,000 feet. *Science* 2003;300:917–9.
16. Weissmann C. The state of the prion. *Nat Rev Microbiol* 2004;2:861–71.
17. Lodish H, Berk A, Zipursky SL, Matsudaira P, Baltimore D, Darnell J. *Molecular Cell Biology*. 4th ed. W. H. Freeman; 2000.
18. Alberts B, Johnson A, Lewis J, Raff M, Roberts K, Walter P. *Molecular Biology of the Cell*. 4th ed. Garland Science; 2002.
19. Berg JM, Tymoczko JL, Stryer L, Berg JM, Tymoczko JL, Stryer L. *Biochemistry*. 5th ed. W H Freeman; 2002.
20. Arunan E, Desiraju GR, Klein RA, Sadlej J, Scheiner S, Alkorta I, *et al.* Definition of the hydrogen bond (IUPAC Recommendations 2011). *Pure and Applied Chemistry* 2011;83:1637–1641.

21. Richardson JS, Richardson DC. Natural beta-sheet proteins use negative design to avoid edge-to-edge aggregation. *Proc Natl Acad Sci USA* 2002;99:2754–9.
22. Prusiner SB. Shattuck lecture--neurodegenerative diseases and prions. *N Engl J Med* 2001;344:1516–26.
23. Carrell RW, Lomas DA. Conformational disease. *Lancet* 1997;350:134–8.
24. Walker LC, LeVine H. The cerebral proteopathies: neurodegenerative disorders of protein conformation and assembly. *Mol Neurobiol* 2000;21:83–95.
25. Walker LC, LeVine H. The cerebral proteopathies. *Neurobiol Aging* 2000;21:559–61.
26. Chiti F, Dobson CM. Protein misfolding, functional amyloid, and human disease. *Annu Rev Biochem* 2006;75:333–66.
27. Luheshi LM, Crowther DC, Dobson CM. Protein misfolding and disease: from the test tube to the organism. *Curr Opin Chem Biol* 2008;12:25–31.
28. Prusiner SB. Biology and genetics of prions causing neurodegeneration. *Annu Rev Genet* 2013;47:601–23.
29. Westermark GT, Fändrich M, Lundmark K, Westermark P. Noncerebral Amyloidoses: Aspects on Seeding, Cross-Seeding, and Transmission. *Cold Spring Harb Perspect Med* 2018;8:.
30. Wisniewski HM, Sadowski M, Jakubowska-Sadowska K, Tarnawski M, Wegiel J. Diffuse, lake-like amyloid-beta deposits in the parvopyramidal layer of the presubiculum in Alzheimer disease. *J Neuropathol Exp Neurol* 1998;57:674–83.
31. Sipe JD, Cohen AS. Review: history of the amyloid fibril. *J Struct Biol* 2000;130:88–98.
32. Glabe CG. Common mechanisms of amyloid oligomer pathogenesis in degenerative disease. *Neurobiol Aging* 2006;27:570–5.
33. Gadad BS, Britton GB, Rao KS. Targeting oligomers in neurodegenerative disorders: lessons from α-synuclein, tau, and amyloid-β peptide. *J Alzheimers Dis* 2011;24 Suppl 2:223–32.
34. Selkoe DJ. Folding proteins in fatal ways. *Nature* 2003;426:900–4.
35. Ito D, Suzuki N. Conjoint pathologic cascades mediated by ALS/FTLD-U linked RNA-binding proteins TDP-43 and FUS. *Neurology* 2011;77:1636–43.
36. Eisenberg D, Jucker M. The amyloid state of proteins in human diseases. *Cell* 2012;148:1188–203.
37. Jucker M, Walker LC. Self-propagation of pathogenic protein aggregates in neurodegenerative diseases. *Nature* 2013;501:45–51.
38. Wolozin B, Apicco D. RNA binding proteins and the genesis of neurodegenerative diseases. *Adv Exp Med Biol* 2015;822:11–5.
39. Collinge J, Clarke AR. A general model of prion strains and their pathogenicity. *Science* 2007;318:930–6.
40. Colby DW, Prusiner SB. De novo generation of prion strains. *Nat Rev Microbiol* 2011;9: 771–7.
41. Walker LC. Proteopathic Strains and the Heterogeneity of Neurodegenerative Diseases. *Annu Rev Genet* 2016;50:329–46.

42. Schubert U, Antón LC, Gibbs J, Norbury CC, Yewdell JW, Bennink JR. Rapid degradation of a large fraction of newly synthesized proteins by proteasomes. *Nature* 2000;404:770–4.
43. Lis H, Sharon N. Protein glycosylation. Structural and functional aspects. *Eur J Biochem* 1993;218:1–27.
44. Petrescu A-J, Milac A-L, Petrescu SM, Dwek RA, Wormald MR. Statistical analysis of the protein environment of N-glycosylation sites: implications for occupancy, structure, and folding. *Glycobiology* 2004;14:103–14.
45. Crispin M, Harvey DJ, Bitto D, Bonomelli C, Edgeworth M, Scrivens JH, *et al.* Structural plasticity of the Semliki Forest virus glycome upon interspecies transmission. *J Proteome Res* 2014;13:1702–12.
46. Quiñones-Kochs MI, Buonocore L, Rose JK. Role of N-linked glycans in a human immunodeficiency virus envelope glycoprotein: effects on protein function and the neutralizing antibody response. *J Virol* 2002;76:4199–211.
47. Freire-de-Lima L, Oliveira IA, Neves JL, Penha LL, Alisson-Silva F, Dias WB, *et al.* Sialic acid: a sweet swing between mammalian host and Trypanosoma cruzi. *Front Immunol* 2012;3:356.
48. Freeze HH, Ng BG. Golgi glycosylation and human inherited diseases. *Cold Spring Harb Perspect Biol* 2011;3:a005371.
49. Hart GW, Slawson C, Ramirez-Correa G, Lagerlof O. Cross talk between O-GlcNAcylation and phosphorylation: roles in signaling, transcription, and chronic disease. *Annu Rev Biochem* 2011;80:825–58.
50. Hewitt JE. Abnormal glycosylation of dystroglycan in human genetic disease. *Biochim Biophys Acta* 2009;1792:853–61.
51. Endo T. Glycobiology of α-dystroglycan and muscular dystrophy. *J Biochem* 2015;157:1–12.
52. Zachara NE, Hart GW. Cell signaling, the essential role of O-GlcNAc! *Biochim Biophys Acta* 2006;1761:599–617.
53. Jensen PH, Kolarich D, Packer NH. Mucin-type O-glycosylation--putting the pieces together. *FEBS J* 2010;277:81–94.
54. Willems AP, van Engelen BGM, Lefeber DJ. Genetic defects in the hexosamine and sialic acid biosynthesis pathway. *Biochim Biophys Acta* 2016;1860:1640–54.
55. Freeze HH, Eklund EA, Ng BG, Patterson MC. Neurological aspects of human glycosylation disorders. *Annu Rev Neurosci* 2015;38:105–25.
56. Hennet T, Cabalzar J. Congenital disorders of glycosylation: a concise chart of glycocalyx dysfunction. *Trends Biochem Sci* 2015;40:377–84.
57. Jaeken J. Congenital disorders of glycosylation. *Handb Clin Neurol* 2013;113:1737–43.
58. Jaeken J, Vanderschueren-Lodeweyckx M, Casaer P, Snoeck L, Corbeel L, Eggermont E, *et al.* Familial psychomotor retardation with markedly fluctuating serum prolactin, FSH and GH levels, partial TBG-deficiency, increased serum arylsulphatase A and increased CSF protein: a new syndrome?: 90. *Pediatric Research* 1980;14:179.
59. Jaeken J. Congenital disorders of glycosylation. *Ann N Y Acad Sci* 2010;1214:190–8.

60. Freeze HH, Eklund EA, Ng BG, Patterson MC. Neurology of inherited glycosylation disorders. *Lancet Neurol* 2012;11:453–66.
61. Pearl PL, Krasnewich D. Neurologic course of congenital disorders of glycosylation. *J Child Neurol* 2001;16:409–13.
62. Sparks Susan E. Inherited Disorders of Glycosylation. *ELS* 2007.
63. Praissman JL, Wells L. Mammalian O-mannosylation pathway: glycan structures, enzymes, and protein substrates. *Biochemistry* 2014;53:3066–78.
64. Cossins J, Belaya K, Hicks D, Salih MA, Finlayson S, Carboni N, *et al.* Congenital myasthenic syndromes due to mutations in ALG2 and ALG14. *Brain* 2013;136:944–56.
65. Mueller TM, Haroutunian V, Meador-Woodruff JH. N-Glycosylation of GABAA receptor subunits is altered in Schizophrenia. *Neuropsychopharmacology* 2014;39:528–37.
66. Dwyer CA, Esko JD. Glycan susceptibility factors in autism spectrum disorders. *Mol Aspects Med* 2016;51:104–14.
67. Pivac N, Knezević A, Gornik O, Pucić M, Igl W, Peeters H, *et al.* Human plasma glycome in attention-deficit hyperactivity disorder and autism spectrum disorders. *Mol Cell Proteomics* 2011;10:M110.004200.
68. Scott H, Panin VM. The role of protein N-glycosylation in neural transmission. *Glycobiology* 2014;24:407–17.
69. Kitabchi AE, Umpierrez GE, Miles JM, Fisher JN. Hyperglycemic crises in adult patients with diabetes. *Diabetes Care* 2009;32:1335–43.
70. Rossetti L, Giaccari A, DeFronzo RA. Glucose toxicity. *Diabetes Care* 1990;13:610–30.
71. Robertson RP, Harmon J, Tran PO, Tanaka Y, Takahashi H. Glucose toxicity in beta-cells: type 2 diabetes, good radicals gone bad, and the glutathione connection. *Diabetes* 2003;52:581–7.
72. Brownlee M. Biochemistry and molecular cell biology of diabetic complications. *Nature* 2001;414:813–20.
73. Brownlee M. The pathobiology of diabetic complications: a unifying mechanism. *Diabetes* 2005;54:1615–25.
74. Laczy B, Hill BG, Wang K, Paterson AJ, White CR, Xing D, *et al.* Protein O-GlcNAcylation: a new signaling paradigm for the cardiovascular system. *Am J Physiol Heart Circ Physiol* 2009;296:H13-28.
75. Fülöp N, Marchase RB, Chatham JC. Role of protein O-linked N-acetyl-glucosamine in mediating cell function and survival in the cardiovascular system. *Cardiovasc Res* 2007;73:288–97.
76. Issad T, Masson E, Pagesy P. O-GlcNAc modification, insulin signaling and diabetic complications. *Diabetes Metab* 2010;36:423–35.
77. Darley-Usmar VM, Ball LE, Chatham JC. Protein O-linked β-N-acetylglucosamine: a novel effector of cardiomyocyte metabolism and function. *J Mol Cell Cardiol* 2012;52:538–49.
78. Liljedahl L, Pedersen MH, Norlin J, McGuire JN, James P. N-glycosylation proteome enrichment analysis in kidney reveals differences between diabetic mouse models. *Clin Proteomics* 2016;13:22.

79. Ravidà A, Musante L, Kreivi M, Miinalainen I, Byrne B, Saraswat M, *et al.* Glycosylation patterns of kidney proteins differ in rat diabetic nephropathy. *Kidney Int* 2015;87:963–74.
80. Peterson SB, Hart GW. New insights: A role for O-GlcNAcylation in diabetic complications. *Crit Rev Biochem Mol Biol* 2016;51:150–61.
81. Stanaway S.E.R.S., Gill G.V. Protein glycosylation in diabetes mellitus: biochemical and clinical considerations. *Practical Diabetes International* 2000;17:21–5.
82. Ohtsubo K, Takamatsu S, Gao C, Korekane H, Kurosawa TM, Taniguchi N. N-Glycosylation modulates the membrane sub-domain distribution and activity of glucose transporter 2 in pancreatic beta cells. *Biochem Biophys Res Commun* 2013;434:346–51.
83. Liu K, Paterson AJ, Chin E, Kudlow JE. Glucose stimulates protein modification by O-linked GlcNAc in pancreatic beta cells: linkage of O-linked GlcNAc to beta cell death. *Proc Natl Acad Sci USA* 2000;97:2820–5.
84. Bastian W, Zhu J, Way B, Lockwood D, Livingston J. Glycosylation of Asn397 or Asn418 is required for normal insulin receptor biosynthesis and processing. *Diabetes* 1993;42:966–74.
85. Ward CW, Lawrence MC. Ligand-induced activation of the insulin receptor: a multi-step process involving structural changes in both the ligand and the receptor. *Bioessays* 2009;31:422–34.
86. Collier E, Carpentier JL, Beitz L, Carol H, Taylor SI, Gorden P. Specific glycosylation site mutations of the insulin receptor alpha subunit impair intracellular transport. *Biochemistry* 1993;32:7818–23.
87. Tiwari S, Singh RS, Li L, Tsukerman S, Godbole M, Pandey G, *et al.* Deletion of the insulin receptor in the proximal tubule promotes hyperglycemia. *J Am Soc Nephrol* 2013;24:1209–14.
88. Hwang JB, Frost SC. Effect of alternative glycosylation on insulin receptor processing. *J Biol Chem* 1999;274:22813–20.
89. Hwang JB, Hernandez J, Leduc R, Frost SC. Alternative glycosylation of the insulin receptor prevents oligomerization and acquisition of insulin-dependent tyrosine kinase activity. *Biochim Biophys Acta* 2000;1499:74–84.
90. Mayer TK, Freedman ZR. Protein glycosylation in diabetes mellitus: a review of laboratory measurements and of their clinical utility. *Clin Chim Acta* 1983;127:147–84.
91. Varki A, Cummings RD, Esko JD, Stanley P, Hart GW, Aebi M, *et al.*, editors. *Essentials of Glycobiology*. 3rd ed. Cold Spring Harbor (NY): Cold Spring Harbor Laboratory Press; 2015.
92. Torres CR, Hart GW. Topography and polypeptide distribution of terminal N-acetylglucosamine residues on the surfaces of intact lymphocytes. Evidence for O-linked GlcNAc. *J Biol Chem* 1984;259:3308–17.
93. Comer FI, Vosseller K, Wells L, Accavitti MA, Hart GW. Characterization of a mouse monoclonal antibody specific for O-linked N-acetylglucosamine. *Anal Biochem* 2001;293:169–77.
94. Snow CM, Senior A, Gerace L. Monoclonal antibodies identify a group of nuclear pore complex glycoproteins. *J Cell Biol* 1987;104:1143–56.

95. Hahne H, Gholami AM, Kuster B. Discovery of O-GlcNAc-modified proteins in published large-scale proteome data. *Mol Cell Proteomics* 2012;11:843–50.
96. Hahne H, Kuster B. Discovery of O-GlcNAc-6-phosphate modified proteins in large-scale phosphoproteomics data. *Mol Cell Proteomics* 2012;11:1063–9.
97. de la Monte SM. Type 3 diabetes is sporadic Alzheimer's disease: mini-review. *Eur Neuropsychopharmacol* 2014;24:1954–60.
98. Ahmed S, Mahmood Z, Zahid S. Linking insulin with Alzheimer's disease: emergence as type III diabetes. *Neurol Sci* 2015;36:1763–9.
99. Kandimalla R, Thirumala V, Reddy PH. Is Alzheimer's disease a Type 3 Diabetes? A critical appraisal. *Biochim Biophys Acta* 2017;1863:1078–89.
100. Bedse G, Di Domenico F, Serviddio G, Cassano T. Aberrant insulin signaling in Alzheimer's disease: current knowledge. *Front Neurosci* 2015;9:204.
101. Ohara T, Doi Y, Ninomiya T, Hirakawa Y, Hata J, Iwaki T, *et al.* Glucose tolerance status and risk of dementia in the community: the Hisayama study. *Neurology* 2011;77:1126–34.
102. Talbot K, Wang H-Y. The nature, significance, and glucagon-like peptide-1 analog treatment of brain insulin resistance in Alzheimer's disease. *Alzheimers Dement* 2014;10:S12-25.
103. Mattishent K, Loke YK. Bi-directional interaction between hypoglycaemia and cognitive impairment in elderly patients treated with glucose-lowering agents: a systematic review and meta-analysis. *Diabetes Obes Metab* 2016; 18:135–41.
104. Whitmer RA, Karter AJ, Yaffe K, Quesenberry CP, Selby JV. Hypoglycemic episodes and risk of dementia in older patients with type 2 diabetes mellitus. *JAMA* 2009;301:1565–72.
105. González-Reyes RE, Aliev G, Ávila-Rodrigues M, Barreto GE. Alterations in Glucose Metabolism on Cognition: A Possible Link Between Diabetes and Dementia. *Curr Pharm Des* 2016;22:812–8.
106. Priller C, Bauer T, Mitteregger G, Krebs B, Kretzschmar HA, Herms J. Synapse formation and function is modulated by the amyloid precursor protein. *J Neurosci* 2006;26:7212–21.
107. Shin RW, Iwaki T, Kitamoto T, Tateishi J. Hydrated autoclave pretreatment enhances tau immunoreactivity in formalin-fixed normal and Alzheimer's disease brain tissues. *Lab Invest* 1991;64:693–702.
108. Costes S, Langen R, Gurlo T, Matveyenko AV, Butler PC. β-Cell failure in type 2 diabetes: a case of asking too much of too few? *Diabetes* 2013;62:327–35.
109. Mukherjee A, Morales-Scheihing D, Butler PC, Soto C. Type 2 diabetes as a protein misfolding disease. *Trends Mol Med* 2015;21:439–49.
110. Mukherjee A, Soto C. Prion-Like Protein Aggregates and Type 2 Diabetes. *Cold Spring Harb Perspect Med* 2017;7:.
111. Yang Y, Song W. Molecular links between Alzheimer's disease and diabetes mellitus. *Neuroscience* 2013;250:140–50.
112. Barbagallo M, Dominguez LJ. Type 2 diabetes mellitus and Alzheimer's disease. *World J Diabetes* 2014;5:889–93.

113. Li X, Song D, Leng SX. Link between type 2 diabetes and Alzheimer's disease: from epidemiology to mechanism and treatment. *Clin Interv Aging* 2015;10:549–60.
114. Walker JM, Harrison FE. Shared Neuropathological Characteristics of Obesity, Type 2 Diabetes and Alzheimer's Disease: Impacts on Cognitive Decline. *Nutrients* 2015;7:7332–57.
115. Mittal K, Katare DP. Shared links between type 2 diabetes mellitus and Alzheimer's disease: A review. *Diabetes Metab Syndr* 2016;10:S144-149.
116. Alam F, Islam MA, Sasongko TH, Gan SH. Type 2 Diabetes Mellitus and Alzheimer's Disease: Bridging the Pathophysiology and Management. *Curr Pharm Des* 2016;22:4430–42.
117. Ashraf GM, Greig NH, Khan TA, Hassan I, Tabrez S, Shakil S, *et al.* Protein misfolding and aggregation in Alzheimer's disease and type 2 diabetes mellitus. *CNS Neurol Disord Drug Targets* 2014;13:1280–93.
118. Moreno-Gonzalez I, Soto C. Misfolded protein aggregates: mechanisms, structures and potential for disease transmission. *Semin Cell Dev Biol* 2011;22:482–7.
119. Schedin-Weiss S, Winblad B, Tjernberg LO. The role of protein glycosylation in Alzheimer disease. *FEBS J* 2014;281:46–62.
120. Turner PR, O'Connor K, Tate WP, Abraham WC. Roles of amyloid precursor protein and its fragments in regulating neural activity, plasticity and memory. *Prog Neurobiol* 2003;70:1–32.
121. Saito F, Yanagisawa K, Miyatake T. Soluble derivatives of beta/A4 amyloid protein precursor in human cerebrospinal fluid are both N- and O-glycosylated. *Brain Res Mol Brain Res* 1993;19:171–4.
122. McFarlane I, Georgopoulou N, Coughlan CM, Gillian AM, Breen KC. The role of the protein glycosylation state in the control of cellular transport of the amyloid beta precursor protein. *Neuroscience* 1999;90:15–25.
123. Nakagawa K, Kitazume S, Oka R, Maruyama K, Saido TC, Sato Y, *et al.* Sialylation enhances the secretion of neurotoxic amyloid-beta peptides. *J Neurochem* 2006;96:924–33.
124. Akasaka-Manya K, Manya H, Sakurai Y, Wojczyk BS, Spitalnik SL, Endo T. Increased bisecting and core-fucosylated N-glycans on mutant human amyloid precursor proteins. *Glycoconj J* 2008;25:775–86.
125. Akasaka-Manya K, Manya H, Sakurai Y, Wojczyk BS, Kozutsumi Y, Saito Y, *et al.* Protective effect of N-glycan bisecting GlcNAc residues on beta-amyloid production in Alzheimer's disease. *Glycobiology* 2010;20:99–106.
126. Zhu Y, Shan X, Yuzwa SA, Vocadlo DJ. The emerging link between O-GlcNAc and Alzheimer disease. *J Biol Chem* 2014;289:34472–81.
127. Lozano L, Lara-Lemus R, Zenteno E, Alvarado-Vásquez N. The mitochondrial O-linked N-acetylglucosamine transferase (mOGT) in the diabetic patient could be the initial trigger to develop Alzheimer disease. *Exp Gerontol* 2014;58:198–202.
128. Yuzwa SA, Vocadlo DJ. O-GlcNAc and neurodegeneration: biochemical mechanisms and potential roles in Alzheimer's disease and beyond. *Chem Soc Rev* 2014;43:6839–58.

129. Lefebvre T, Guinez C, Dehennaut V, Beseme-Dekeyser O, Morelle W, Michalski J-C. Does O-GlcNAc play a role in neurodegenerative diseases? *Expert Rev Proteomics* 2005;2:265–75.
130. Yang YR, Suh P-G. O-GlcNAcylation in cellular functions and human diseases. *Adv Biol Regul* 2014;54:68–73.
131. Yuzwa SA, Shan X, Macauley MS, Clark T, Skorobogatko Y, Vosseller K, *et al.* Increasing O-GlcNAc slows neurodegeneration and stabilizes tau against aggregation. *Nat Chem Biol* 2012;8:393–9.
132. Yuzwa SA, Cheung AH, Okon M, McIntosh LP, Vocadlo DJ. O-GlcNAc modification of tau directly inhibits its aggregation without perturbing the conformational properties of tau monomers. *J Mol Biol* 2014;426:1736–52.
133. Graham DL, Gray AJ, Joyce JA, Yu D, O'Moore J, Carlson GA, *et al.* Increased O-GlcNAcylation reduces pathological tau without affecting its normal phosphorylation in a mouse model of tauopathy. *Neuropharmacology* 2014;79:307–13.
134. Liu F, Zaidi T, Iqbal K, Grundke-Iqbal I, Merkle RK, Gong CX. Role of glycosylation in hyperphosphorylation of tau in Alzheimer's disease. *FEBS Lett* 2002;512:101–6.
135. Wang JZ, Grundke-Iqbal I, Iqbal K. Glycosylation of microtubule-associated protein tau: an abnormal posttranslational modification in Alzheimer's disease. *Nat Med* 1996;2:871–5.
136. Sato Y, Naito Y, Grundke-Iqbal I, Iqbal K, Endo T. Analysis of N-glycans of pathological tau: possible occurrence of aberrant processing of tau in Alzheimer's disease. *FEBS Lett* 2001;496:152–60.
137. Liu F, Zaidi T, Iqbal K, Grundke-Iqbal I, Gong C-X. Aberrant glycosylation modulates phosphorylation of tau by protein kinase A and dephosphorylation of tau by protein phosphatase 2A and 5. *Neuroscience* 2002;115:829–37.
138. Dias WB, Hart GW. O-GlcNAc modification in diabetes and Alzheimer's disease. *Mol Biosyst* 2007;3:766–72.
139. Liu F, Shi J, Tanimukai H, Gu J, Gu J, Grundke-Iqbal I, *et al.* Reduced O-GlcNAcylation links lower brain glucose metabolism and tau pathology in Alzheimer's disease. *Brain* 2009;132:1820–32.
140. Liu F, Iqbal K, Grundke-Iqbal I, Hart GW, Gong C-X. O-GlcNAcylation regulates phosphorylation of tau: a mechanism involved in Alzheimer's disease. *Proc Natl Acad Sci USA* 2004;101:10804–9.
141. Li X, Lu F, Wang J-Z, Gong C-X. Concurrent alterations of O-GlcNAcylation and phosphorylation of tau in mouse brains during fasting. *Eur J Neurosci* 2006;23:2078–86.
142. Gong C-X, Liu F, Grundke-Iqbal I, Iqbal K. Impaired brain glucose metabolism leads to Alzheimer neurofibrillary degeneration through a decrease in tau O-GlcNAcylation. *J Alzheimers Dis* 2006;9:1–12.
143. Deng Y, Li B, Liu F, Iqbal K, Grundke-Iqbal I, Brandt R, *et al.* Regulation between O-GlcNAcylation and phosphorylation of neurofilament-M and their dysregulation in Alzheimer disease. *FASEB J* 2008;22:138–45.

144. Mariosa D, Kamel F, Bellocco R, Ye W, Fang F. Association between diabetes and amyotrophic lateral sclerosis in Sweden. *Eur J Neurol* 2015;22:1436–42.
145. Kawada T. Type 2 diabetes and amyotrophic lateral sclerosis. *Eur J Neurol* 2016;23:e9.
146. Mariosa D, Fang F. Response to the letter 'Type 2 diabetes and amyotrophic lateral sclerosis'. *Eur J Neurol* 2016;23:e26.
147. Shan X, Vocadlo DJ, Krieger C. Reduced protein O-glycosylation in the nervous system of the mutant SOD1 transgenic mouse model of amyotrophic lateral sclerosis. *Neurosci Lett* 2012;516:296–301.
148. Gonçalves M, Tillack L, de Carvalho M, Pinto S, Conradt HS, Costa J. Phosphoneurofilament heavy chain and N-glycomics from the cerebrospinal fluid in amyotrophic lateral sclerosis. *Clin Chim Acta* 2015;438:342–9.
149. Goh AX-H, Li C, Sy M-S, Wong B-S. Altered prion protein glycosylation in the aging mouse brain. *J Neurochem* 2007;100:841–54.
150. Xiao X, Yuan J, Haïk S, Cali I, Zhan Y, Moudjou M, *et al.* Glycoform-selective prion formation in sporadic and familial forms of prion disease. *PLoS ONE* 2013;8:e58786.
151. Wiseman FK, Cancellotti E, Piccardo P, Iremonger K, Boyle A, Brown D, *et al.* The glycosylation status of PrPC is a key factor in determining transmissible spongiform encephalopathy transmission between species. *J Virol* 2015;89:4738–47.
152. Katorcha E, Makarava N, Savtchenko R, Baskakov IV. Sialylation of the prion protein glycans controls prion replication rate and glycoform ratio. *Sci Rep* 2015;5:16912.
153. Sparkes RS, Simon M, Cohn VH, Fournier RE, Lem J, Klisak I, *et al.* Assignment of the human and mouse prion protein genes to homologous chromosomes. *Proc Natl Acad Sci USA* 1986;83:7358–62.
154. Salès N, Rodolfo K, Hässig R, Faucheux B, Di Giamberardino L, Moya KL. Cellular prion protein localization in rodent and primate brain. *Eur J Neurosci* 1998;10:2464–71.
155. Fournier JG. Nonneuronal cellular prion protein. *Int Rev Cytol* 2001; 208:121–60.
156. Kretzschmar HA, Prusiner SB, Stowring LE, DeArmond SJ. Scrapie prion proteins are synthesized in neurons. *Am J Pathol* 1986;122:1–5.
157. Bendheim PE, Brown HR, Rudelli RD, Scala LJ, Goller NL, Wen GY, *et al.* Nearly ubiquitous tissue distribution of the scrapie agent precursor protein. *Neurology* 1992;42:149–56.
158. Moser M, Colello RJ, Pott U, Oesch B. Developmental expression of the prion protein gene in glial cells. *Neuron* 1995;14:509–17.
159. Ford MJ, Burton LJ, Li H, Graham CH, Frobert Y, Grassi J, *et al.* A marked disparity between the expression of prion protein and its message by neurones of the CNS. *Neuroscience* 2002;111:533–51.
160. Lainé J, Marc ME, Sy MS, Axelrad H. Cellular and subcellular morphological localization of normal prion protein in rodent cerebellum. *Eur J Neurosci* 2001;14:47–56.

161. Mironov A, Latawiec D, Wille H, Bouzamondo-Bernstein E, Legname G, Williamson RA, *et al.* Cytosolic prion protein in neurons. *J Neurosci* 2003;23:7183–93.
162. Faris R, Moore RA, Ward A, Race B, Dorward DW, Hollister JR, *et al.* Cellular prion protein is present in mitochondria of healthy mice. *Sci Rep* 2017;7:41556.
163. Ma J, Wollmann R, Lindquist S. Neurotoxicity and neurodegeneration when PrP accumulates in the cytosol. *Science* 2002;298:1781–5.
164. Ma J, Lindquist S. Conversion of PrP to a self-perpetuating PrPSc-like conformation in the cytosol. *Science* 2002;298:1785–8.
165. Chiovitti K, Corsaro A, Thellung S, Villa V, Paludi D, D'Arrigo C, *et al.* Intracellular accumulation of a mild-denatured monomer of the human PrP fragment 90-231, as possible mechanism of its neurotoxic effects. *J Neurochem* 2007;103:2597– 609.
166. Norstrom EM, Ciaccio MF, Rassbach B, Wollmann R, Mastrianni JA. Cytosolic prion protein toxicity is independent of cellular prion protein expression and prion propagation. *J Virol* 2007;81:2831–7.
167. Horiuchi M, Yamazaki N, Ikeda T, Ishiguro N, Shinagawa M. A cellular form of prion protein (PrPC) exists in many non-neuronal tissues of sheep. *J Gen Virol* 1995;76 (Pt 10):2583–7.
168. Aguzzi A, Heikenwalder M. Pathogenesis of prion diseases: current status and future outlook. *Nat Rev Microbiol* 2006;4:765–75.
169. Petit CSV, Besnier L, Morel E, Rousset M, Thenet S. Roles of the cellular prion protein in the regulation of cell-cell junctions and barrier function. *Tissue Barriers* 2013;1:e24377.
170. Schneider K, Korkmaz Y, Addicks K, Lang H, Raab WH-M. Prion protein (PrP) in human teeth: an unprecedented pointer to PrP's function. *J Endod* 2007;33:110–3.
171. Khan Q-E-S, Press CM, Sehic A, Landin MA, Risnes S, Osmundsen H. Expression of prion gene and presence of prion protein during development of mouse molar tooth germ. *Eur J Oral Sci* 2010;118:559–65.
172. Zhang Y, Kim S-O, Opsahl-Vital S, Ho SP, Souron J-B, Kim C, *et al.* Multiple effects of the cellular prion protein on tooth development. *Int J Dev Biol* 2011;55:953–60.
173. Dimitrova-Nakov S, Baudry A, Harichane Y, Collet C, Marchadier A, Kellermann O, *et al.* Deletion of serotonin 2B receptor provokes structural alterations of mouse dental tissues. *Calcif Tissue Int* 2014;94:293–300.
174. Baudry A, Alleaume-Butaux A, Dimitrova-Nakov S, Goldberg M, Schneider B, Launay J-M, *et al.* Essential Roles of Dopamine and Serotonin in Tooth Repair: Functional Interplay Between Odontogenic Stem Cells and Platelets. *Stem Cells* 2015;33:2586–95.
175. Stöckel J, Safar J, Wallace AC, Cohen FE, Prusiner SB. Prion protein selectively binds copper(II) ions. *Biochemistry* 1998;37:7185–93.
176. Whittal RM, Ball HL, Cohen FE, Burlingame AL, Prusiner SB, Baldwin MA. Copper binding to octarepeat peptides of the prion protein monitored by mass spectrometry. *Protein Sci* 2000;9:332–43.

177. Choi CJ, Kanthasamy A, Anantharam V, Kanthasamy AG. Interaction of metals with prion protein: possible role of divalent cations in the pathogenesis of prion diseases. *Neurotoxicology* 2006;27:777–87.
178. Schätzl HM, Da Costa M, Taylor L, Cohen FE, Prusiner SB. Prion protein gene variation among primates. *J Mol Biol* 1995;245:362–74.
179. Zahn R, Liu A, Lührs T, Riek R, von Schroetter C, López García F, *et al.* NMR solution structure of the human prion protein. *Proc Natl Acad Sci USA* 2000;97:145–50.
180. Damberger FF, Christen B, Pérez DR, Hornemann S, Wüthrich K. Cellular prion protein conformation and function. *Proc Natl Acad Sci USA* 2011;108:17308–13.
181. Christen B, Damberger FF, Pérez DR, Hornemann S, Wüthrich K. Structural plasticity of the cellular prion protein and implications in health and disease. *Proc Natl Acad Sci USA* 2013;110:8549–54.
182. Dutta A, Chen S, Surewicz WK. The effect of β2-α2 loop mutation on amyloidogenic properties of the prion protein. *FEBS Lett* 2013;587:2918–23.
183. Sigurdson CJ, Joshi-Barr S, Bett C, Winson O, Manco G, Schwarz P, *et al.* Spongiform encephalopathy in transgenic mice expressing a point mutation in the β2-α2 loop of the prion protein. *J Neurosci* 2011;31:13840–7.
184. Bett C, Fernández-Borges N, Kurt TD, Lucero M, Nilsson KPR, Castilla J, *et al.* Structure of the β2-α2 loop and interspecies prion transmission. *FASEB J* 2012;26:2868–76.
185. Kurt TD, Bett C, Fernández-Borges N, Joshi-Barr S, Hornemann S, Rülicke T, *et al.* Prion transmission prevented by modifying the β2-α2 loop structure of host PrPC. *J Neurosci* 2014;34:1022–7.
186. Kurt TD, Jiang L, Bett C, Eisenberg D, Sigurdson CJ. A proposed mechanism for the promotion of prion conversion involving a strictly conserved tyrosine residue in the β2-α2 loop of PrPC. *J Biol Chem* 2014;289:10660–7.
187. Kurt TD, Jiang L, Fernández-Borges N, Bett C, Liu J, Yang T, *et al.* Human prion protein sequence elements impede cross-species chronic wasting disease transmission. *J Clin Invest* 2015;125:1485–96.
188. Maiti NR, Surewicz WK. The role of disulfide bridge in the folding and stability of the recombinant human prion protein. *J Biol Chem* 2001;276:2427–31.
189. Lu B-Y, Chang J-Y. A 3-disulfide mutant of mouse prion protein expression, oxidative folding, reductive unfolding, conformational stability, aggregation and isomerization. *Arch Biochem Biophys* 2007;460:75–84.
190. Stahl N, Borchelt DR, Hsiao K, Prusiner SB. Scrapie prion protein contains a phosphatidylinositol glycolipid. *Cell* 1987;51:229–40.
191. Lewis V, Hooper NM. The role of lipid rafts in prion protein biology. *Front Biosci (Landmark Ed)* 2011;16:151–68.
192. Turk E, Teplow DB, Hood LE, Prusiner SB. Purification and properties of the cellular and scrapie hamster prion proteins. *Eur J Biochem* 1988;176:21–30.
193. Lu B-Y, Chang J-Y. A 3-disulfide mutant of mouse prion protein expression, oxidative folding, reductive unfolding, conformational stability, aggregation and isomerization. *Arch Biochem Biophys* 2007;460:75–84.

194. Haraguchi T, Fisher S, Olofsson S, Endo T, Groth D, Tarentino A, *et al.* Asparagine-linked glycosylation of the scrapie and cellular prion proteins. *Arch Biochem Biophys* 1989;274:1–13.
195. Kang H-E, Weng CC, Saijo E, Saylor V, Bian J, Kim S, *et al.* Characterization of conformation-dependent prion protein epitopes. *J Biol Chem* 2012;287:37219–32.
196. Harris DA. Trafficking, turnover and membrane topology of PrP. *Br Med Bull* 2003;66:71–85.
197. Rudd PM, Wormald MR, Wing DR, Prusiner SB, Dwek RA. Prion glycoprotein: structure, dynamics, and roles for the sugars. *Biochemistry* 2001;40:3759–66.
198. Varki A. Biological roles of oligosaccharides: all of the theories are correct. *Glycobiology* 1993;3:97–130.
199. Ermonval M, Duvet S, Zonneveld D, Cacan R, Buttin G, Braakman I. Truncated N-glycans affect protein folding in the ER of CHO-derived mutant cell lines without preventing calnexin binding. *Glycobiology* 2000;10:77–87.
200. Kang S-W, Yoon S-Y, Park J-Y, Kim D-H. Unglycosylated clusterin variant accumulates in the endoplasmic reticulum and induces cytotoxicity. *Int J Biochem Cell Biol* 2013;45:221–31.
201. Neuendorf E, Weber A, Saalmueller A, Schatzl H, Reifenberg K, Pfaff E, *et al.* Glycosylation deficiency at either one of the two glycan attachment sites of cellular prion protein preserves susceptibility to bovine spongiform encephalopathy and scrapie infections. *J Biol Chem* 2004;279:53306–16.
202. Zou RS, Fujioka H, Guo J-P, Xiao X, Shimoji M, Kong C, *et al.* Characterization of spontaneously generated prion-like conformers in cultured cells. *Aging (Albany NY)* 2011;3:968–84.
203. Chen L, Yang Y, Han J, Zhang B-Y, Zhao L, Nie K, *et al.* Removal of the glycosylation of prion protein provokes apoptosis in SF126. *J Biochem Mol Biol* 2007;40:662–9.
204. Rogers M, Taraboulos A, Scott M, Groth D, Prusiner SB. Intracellular accumulation of the cellular prion protein after mutagenesis of its Asn-linked glycosylation sites. *Glycobiology* 1990;1:101–9.
205. Lawson VA, Collins SJ, Masters CL, Hill AF. Prion protein glycosylation. *J Neurochem* 2005;93:793–801.
206. Zetterström R. The discovery of misfolded prions as an infectious agent. *Acta Paediatr* 2010;99:1910–3.
207. Palmer AG, Patel DJ. Kurt Wüthrich and NMR of biological macromolecules. *Structure* 2002;10:1603–4.
208. Sakudo A, Onodera T, Suganuma Y, Kobayashi T, Saeki K, Ikuta K. Recent advances in clarifying prion protein functions using knockout mice and derived cell lines. *Mini Rev Med Chem* 2006;6:589–601.
209. Büeler H, Fischer M, Lang Y, Bluethmann H, Lipp HP, DeArmond SJ, *et al.* Normal development and behaviour of mice lacking the neuronal cell-surface PrP protein. *Nature* 1992;356:577–82.
210. Manson JC, Clarke AR, Hooper ML, Aitchison L, McConnell I, Hope J. 129/Ola mice carrying a null mutation in PrP that abolishes mRNA production are developmentally normal. *Mol Neurobiol* 1994;8:121–7.

211. Weissmann C, Aguzzi A. Perspectives: neurobiology. PrP's double causes trouble. *Science* 1999;286:914–5.
212. Weissmann C, Flechsig E. PrP knock-out and PrP transgenic mice in prion research. *Br Med Bull* 2003;66:43–60.
213. Lipp HP, Stagliar-Bozicevic M, Fischer M, Wolfer DP. A 2-year longitudinal study of swimming navigation in mice devoid of the prion protein: no evidence for neurological anomalies or spatial learning impairments. *Behav Brain Res* 1998;95:47–54.
214. Büeler H, Aguzzi A, Sailer A, Greiner RA, Autenried P, Aguet M, *et al.* Mice devoid of PrP are resistant to scrapie. *Cell* 1993;73:1339–47.
215. Sailer A, Büeler H, Fischer M, Aguzzi A, Weissmann C. No propagation of prions in mice devoid of PrP. *Cell* 1994;77:967–8.
216. Weissmann C, Büeler H. A mouse to remember. *Cell* 2004;116:S111-113, 2 p following S113.
217. Zan Q, Wen B, He Y, Wang Y, Xu S, Qian J, *et al.* Complete sequence data support lack of balancing selection on PRNP in a natural Chinese population. *J Hum Genet* 2006;51:451–4.
218. Soto C, Estrada LD. Protein misfolding and neurodegeneration. *Arch Neurol* 2008;65:184–9.
219. La Mendola D, Mendola DL, Pietropaolo A, Pappalardo G, Zannoni C, Rizzarelli E. Prion proteins leading to neurodegeneration. *Curr Alzheimer Res* 2008;5:579–90.
220. Nygaard HB, Strittmatter SM. Cellular prion protein mediates the toxicity of beta-amyloid oligomers: implications for Alzheimer disease. *Arch Neurol* 2009;66:1325–8.
221. Zou W-Q, Xiao X, Yuan J, Puoti G, Fujioka H, Wang X, *et al.* Amyloid-beta42 interacts mainly with insoluble prion protein in the Alzheimer brain. *J Biol Chem* 2011;286:15095–105.
222. Guest WC, Plotkin SS, Cashman NR. Toward a mechanism of prion misfolding and structural models of PrP(Sc): current knowledge and future directions. *J Toxicol Environ Health Part A* 2011;74:154–60.
223. Laurén J. Cellular prion protein as a therapeutic target in Alzheimer's disease. *J Alzheimers Dis* 2014;38:227–44.
224. Béland M, Bédard M, Tremblay G, Lavigne P, Roucou X. Aβ induces its own prion protein N-terminal fragment (PrPN1)-mediated neutralization in amorphous aggregates. *Neurobiol Aging* 2014;35:1537–48.
225. Collinge J. Mammalian prions and their wider relevance in neurodegenerative diseases. *Nature* 2016;539:217–26.
226. Liang J, Kong Q. α-Cleavage of cellular prion protein. *Prion* 2012;6:453–60.
227. Yang X, Zhang Y, Zhang L, He T, Zhang J, Li C. Prion protein and cancers. *Acta Biochim Biophys Sin (Shanghai)* 2014;46:431–40.
228. Martin-Lannerée S, Hirsch TZ, Hernandez-Rapp J, Halliez S, Vilotte J-L, Launay J-M, *et al.* PrP(C) from stem cells to cancer. *Front Cell Dev Biol* 2014;2:55.
229. Santos TG, Lopes MH, Martins VR. Targeting prion protein interactions in cancer. *Prion* 2015;9:165–73.

230. Corsaro A, Bajetto A, Thellung S, Begani G, Villa V, Nizzari M, *et al.* Cellular prion protein controls stem cell-like properties of human glioblastoma tumor-initiating cells. *Oncotarget* 2016;7:38638–57.
231. Wang Y, Yu S, Huang D, Cui M, Hu H, Zhang L, *et al.* Cellular Prion Protein Mediates Pancreatic Cancer Cell Survival and Invasion through Association with and Enhanced Signaling of Notch1. *Am J Pathol* 2016;186:2945–56.
232. Atouf F, Scharfmann R, Lasmezas C, Czernichow P. Tight hormonal control of PrP gene expression in endocrine pancreatic cells. *Biochem Biophys Res Commun* 1994;201:1220–6.
233. Strom A, Wang G-S, Reimer R, Finegood DT, Scott FW. Pronounced cytosolic aggregation of cellular prion protein in pancreatic beta-cells in response to hyperglycemia. *Lab Invest* 2007;87:139–49.
234. Strom A, Wang G-S, Scott FW. Impaired glucose tolerance in mice lacking cellular prion protein. *Pancreas* 2011;40:229–32.
235. Tobler I, Gaus SE, Deboer T, Achermann P, Fischer M, Rülicke T, *et al.* Altered circadian activity rhythms and sleep in mice devoid of prion protein. *Nature* 1996;380:639–42.
236. Tobler I, Deboer T, Fischer M. Sleep and sleep regulation in normal and prion protein-deficient mice. *J Neurosci* 1997;17:1869–79.
237. Criado JR, Sánchez-Alavez M, Conti B, Giacchino JL, Wills DN, Henriksen SJ, *et al.* Mice devoid of prion protein have cognitive deficits that are rescued by reconstitution of PrP in neurons. *Neurobiol Dis* 2005;19:255–65.
238. Isaacs JD, Jackson GS, Altmann DM. The role of the cellular prion protein in the immune system. *Clin Exp Immunol* 2006;146:1–8.
239. Zomosa-Signoret V, Arnaud J-D, Fontes P, Alvarez-Martinez M-T, Liautard J-P. Physiological role of the cellular prion protein. *Vet Res* 2008;39:9.
240. Balducci C, Beeg M, Stravalaci M, Bastone A, Sclip A, Biasini E, *et al.* Synthetic amyloid-beta oligomers impair long-term memory independently of cellular prion protein. *Proc Natl Acad Sci USA* 2010;107:2295–300.
241. Petit CSV, Besnier L, Morel E, Rousset M, Thenet S. Roles of the cellular prion protein in the regulation of cell-cell junctions and barrier function. *Tissue Barriers* 2013;1:e24377.
242. Sakaguchi S, Katamine S, Nishida N, Moriuchi R, Shigematsu K, Sugimoto T, *et al.* Loss of cerebellar Purkinje cells in aged mice homozygous for a disrupted PrP gene. *Nature* 1996;380:528–31.
243. Gerlai R. Gene-targeting studies of mammalian behavior: is it the mutation or the background genotype? *Trends Neurosci* 1996;19:177–81.
244. Weissmann C. PrP effects clarified. *Curr Biol* 1996;6:1359.
245. Nishida N, Tremblay P, Sugimoto T, Shigematsu K, Shirabe S, Petromilli C, *et al.* A mouse prion protein transgene rescues mice deficient for the prion protein gene from purkinje cell degeneration and demyelination. *Lab Invest* 1999;79:689–97.
246. Collinge J, Whittington MA, Sidle KC, Smith CJ, Palmer MS, Clarke AR, *et al.* Prion protein is necessary for normal synaptic function. *Nature* 1994;370:295–7.

247. Whittington MA, Sidle KC, Gowland I, Meads J, Hill AF, Palmer MS, *et al.* Rescue of neurophysiological phenotype seen in PrP null mice by transgene encoding human prion protein. *Nat Genet* 1995;9:197–201.
248. Manson JC, Hope J, Clarke AR, Johnston A, Black C, MacLeod N. PrP gene dosage and long term potentiation. *Neurodegeneration* 1995;4:113–4.
249. Herms JW, Kretzchmar HA, Titz S, Keller BU. Patch-clamp analysis of synaptic transmission to cerebellar purkinje cells of prion protein knockout mice. *Eur J Neurosci* 1995;7:2508–12.
250. Lledo PM, Tremblay P, DeArmond SJ, Prusiner SB, Nicoll RA. Mice deficient for prion protein exhibit normal neuronal excitability and synaptic transmission in the hippocampus. *Proc Natl Acad Sci USA* 1996;93:2403–7.
251. Colling SB, Khana M, Collinge J, Jefferys JG. Mossy fibre reorganization in the hippocampus of prion protein null mice. *Brain Res* 1997;755:28–35.
252. Walz R, Amaral OB, Rockenbach IC, Roesler R, Izquierdo I, Cavalheiro EA, *et al.* Increased sensitivity to seizures in mice lacking cellular prion protein. *Epilepsia* 1999;40:1679–82.
253. Pereira GS, Walz R, Bonan CD, Battastini AM, Izquierdo I, Martins VR, *et al.* Changes in cortical and hippocampal ectonucleotidase activities in mice lacking cellular prion protein. *Neurosci Lett* 2001;301:72–4.
254. Walz R, Castro RMRPS, Velasco TR, Carlotti CG, Sakamoto AC, Brentani RR, *et al.* Cellular prion protein: implications in seizures and epilepsy. *Cell Mol Neurobiol* 2002;22:249–57.
255. Curtis J, Errington M, Bliss T, Voss K, MacLeod N. Age-dependent loss of PTP and LTP in the hippocampus of PrP-null mice. *Neurobiol Dis* 2003;13:55–62.
256. Asante EA, Li Y-G, Gowland I, Jefferys JGR, Collinge J. Pathogenic human prion protein rescues PrP null phenotype in transgenic mice. *Neurosci Lett* 2004;360:33–6.
257. Maglio LE, Perez MF, Martins VR, Brentani RR, Ramirez OA. Hippocampal synaptic plasticity in mice devoid of cellular prion protein. *Brain Res Mol Brain Res* 2004;131:58–64.
258. Maglio LE, Martins VR, Izquierdo I, Ramirez OA. Role of cellular prion protein on LTP expression in aged mice. *Brain Res* 2006;1097:11–8.
259. Baumann F, Tolnay M, Brabeck C, Pahnke J, Kloz U, Niemann HH, *et al.* Lethal recessive myelin toxicity of prion protein lacking its central domain. *EMBO J* 2007;26:538–47.
260. Rangel A, Burgaya F, Gavín R, Soriano E, Aguzzi A, Del Río JA. Enhanced susceptibility of Prnp-deficient mice to kainate-induced seizures, neuronal apoptosis, and death: Role of AMPA/kainate receptors. *J Neurosci Res* 2007;85:2741–55.
261. Brown DR. Copper and prion diseases. *Biochem Soc Trans* 2002;30:742–5.
262. Varela-Nallar L, González A, Inestrosa NC. Role of copper in prion diseases: deleterious or beneficial? *Curr Pharm Des* 2006;12:2587–95.
263. Gasperini L, Meneghetti E, Legname G, Benetti F. In Absence of the Cellular Prion Protein, Alterations in Copper Metabolism and Copper-Dependent Oxidase Activity Affect Iron Distribution. *Front Neurosci* 2016;10:437.

264. Bonomo RP, Cucinotta V, Giuffrida A, Impellizzeri G, Magri A, Pappalardo G, *et al.* A re-investigation of copper coordination in the octa-repeats region of the prion protein. *Dalton Trans* 2005:150–8.
265. Bonomo RP, Pappalardo G, Rizzarelli E, Santoro AM, Tabbì G, Vagliasindi LI. Nitrogen oxide interaction with copper complexes formed by small peptides belonging to the prion protein octa-repeat region. *Dalton Trans* 2007:1400–8.
266. Di Natale G, Grasso G, Impellizzeri G, La Mendola D, Micera G, Mihala N, *et al.* Copper(II) interaction with unstructured prion domain outside the octarepeat region: speciation, stability, and binding details of copper(II) complexes with PrP106-126 peptides. *Inorg Chem* 2005;44:7214–25.
267. Osz K, Nagy Z, Pappalardo G, Di Natale G, Sanna D, Micera G, *et al.* Copper(II) interaction with prion peptide fragments encompassing histidine residues within and outside the octarepeat domain: speciation, stability constants and binding details. *Chemistry* 2007;13:7129–43.
268. Di Natale G, Osz K, Nagy Z, Sanna D, Micera G, Pappalardo G, *et al.* Interaction of copper(II) with the prion peptide fragment HuPrP(76-114) encompassing four histidyl residues within and outside the octarepeat domain. *Inorg Chem* 2009;48:4239–50.
269. Waggoner DJ, Bartnikas TB, Gitlin JD. The role of copper in neurodegenerative disease. *Neurobiol Dis* 1999;6:221–30.
270. Gaggelli E, Kozlowski H, Valensin D, Valensin G. Copper homeostasis and neurodegenerative disorders (Alzheimer's, prion, and Parkinson's diseases and amyotrophic lateral sclerosis). *Chem Rev* 2006;106:1995–2044.
271. Macreadie IG. Copper transport and Alzheimer's disease. *Eur Biophys J* 2008;37:295–300.
272. Brown DR, Clive C, Haswell SJ. Antioxidant activity related to copper binding of native prion protein. *J Neurochem* 2001;76:69–76.
273. Rachidi W, Vilette D, Guiraud P, Arlotto M, Riondel J, Laude H, *et al.* Expression of prion protein increases cellular copper binding and antioxidant enzyme activities but not copper delivery. *J Biol Chem* 2003;278:9064–72.
274. Dupiereux I, Falisse-Poirrier N, Zorzi W, Watt NT, Thellin O, Zorzi D, *et al.* Protective effect of prion protein via the N-terminal region in mediating a protective effect on paraquat-induced oxidative injury in neuronal cells. *J Neurosci Res* 2008;86:653–9.
275. Malaisé M, Schätzl HM, Bürkle A. The octarepeat region of prion protein, but not the TM1 domain, is important for the antioxidant effect of prion protein. *Free Radic Biol Med* 2008;45:1622–30.
276. Brown DR, Qin K, Herms JW, Madlung A, Manson J, Strome R, *et al.* The cellular prion protein binds copper in vivo. *Nature* 1997;390:684–7.
277. Wong BS, Liu T, Li R, Pan T, Petersen RB, Smith MA, *et al.* Increased levels of oxidative stress markers detected in the brains of mice devoid of prion protein. *J Neurochem* 2001;76:565–72.
278. Miele G, Jeffrey M, Turnbull D, Manson J, Clinton M. Ablation of cellular prion protein expression affects mitochondrial numbers and morphology. *Biochem Biophys Res Commun* 2002;291:372–7.

279. Klamt F, Dal-Pizzol F, Conte da Frota ML, Walz R, Andrades ME, da Silva EG, *et al.* Imbalance of antioxidant defense in mice lacking cellular prion protein. *Free Radic Biol Med* 2001;30:1137–44.
280. Wong BS, Pan T, Liu T, Li R, Gambetti P, Sy MS. Differential contribution of superoxide dismutase activity by prion protein in vivo. *Biochem Biophys Res Commun* 2000;273:136–9.
281. Brown DR, Nicholas RSJ, Canevari L. Lack of prion protein expression results in a neuronal phenotype sensitive to stress. *J Neurosci Res* 2002;67:211–24.
282. Waggoner DJ, Drisaldi B, Bartnikas TB, Casareno RL, Prohaska JR, Gitlin JD, *et al.* Brain copper content and cuproenzyme activity do not vary with prion protein expression level. *J Biol Chem* 2000;275:7455–8.
283. Hutter G, Heppner FL, Aguzzi A. No superoxide dismutase activity of cellular prion protein in vivo. *Biol Chem* 2003;384:1279–85.
284. Ford MJ, Burton LJ, Morris RJ, Hall SM. Selective expression of prion protein in peripheral tissues of the adult mouse. *Neuroscience* 2002;113:177–92.
285. Mouillet-Richard S, Ermonval M, Chebassier C, Laplanche JL, Lehmann S, Launay JM, *et al.* Signal transduction through prion protein. *Science* 2000;289:1925–8.
286. Khosravani H, Zhang Y, Tsutsui S, Hameed S, Altier C, Hamid J, *et al.* Prion protein attenuates excitotoxicity by inhibiting NMDA receptors. *J Cell Biol* 2008;181:551–65.
287. Khosravani H, Zhang Y, Tsutsui S, Hameed S, Altier C, Hamid J, *et al.* Prion protein attenuates excitotoxicity by inhibiting NMDA receptors. *J Gen Physiol* 2008;131:i5.
288. Beraldo FH, Arantes CP, Santos TG, Queiroz NGT, Young K, Rylett RJ, *et al.* Role of alpha7 nicotinic acetylcholine receptor in calcium signaling induced by prion protein interaction with stress-inducible protein 1. *J Biol Chem* 2010;285:36542–50.
289. Beraldo FH, Arantes CP, Santos TG, Machado CF, Roffe M, Hajj GN, *et al.* Metabotropic glutamate receptors transduce signals for neurite outgrowth after binding of the prion protein to laminin γ1 chain. *FASEB J* 2011;25:265– 79.
290. Resenberger UK, Harmeier A, Woerner AC, Goodman JL, Müller V, Krishnan R, *et al.* The cellular prion protein mediates neurotoxic signalling of β-sheet-rich conformers independent of prion replication. *EMBO J* 2011;30:2057–70.
291. You H, Tsutsui S, Hameed S, Kannanayakal TJ, Chen L, Xia P, *et al.* Aβ neurotoxicity depends on interactions between copper ions, prion protein, and N-methyl-D-aspartate receptors. *Proc Natl Acad Sci USA* 2012;109:1737–42.
292. Petit-Paitel A, Ménard B, Guyon A, Béringue V, Nahon J-L, Zsürger N, *et al.* Prion protein is a key determinant of alcohol sensitivity through the modulation of N-methyl-D-aspartate receptor (NMDAR) activity. *PLoS ONE* 2012;7:e34691.
293. Um JW, Nygaard HB, Heiss JK, Kostylev MA, Stagi M, Vortmeyer A, *et al.* Alzheimer amyloid-β oligomer bound to postsynaptic prion protein activates Fyn to impair neurons. *Nat Neurosci* 2012;15:1227–35.

294. Um JW, Kaufman AC, Kostylev M, Heiss JK, Stagi M, Takahashi H, *et al.* Metabotropic glutamate receptor 5 is a coreceptor for Alzheimer aβ oligomer bound to cellular prion protein. *Neuron* 2013;79:887–902.
295. Hernandez-Rapp J, Martin-Lannerée S, Hirsch TZ, Pradines E, Alleaume-Butaux A, Schneider B, *et al.* A PrP(C)-caveolin-Lyn complex negatively controls neuronal GSK3β and serotonin 1B receptor. *Sci Rep* 2014;4:4881.
296. Kikuchi Y, Kakeya T, Yamazaki T, Takekida K, Nakamura N, Matsuda H, *et al.* G1-dependent prion protein expression in human glioblastoma cell line T98G. *Biol Pharm Bull* 2002;25:728–33.
297. Steele AD, Emsley JG, Ozdinler PH, Lindquist S, Macklis JD. Prion protein (PrPc) positively regulates neural precursor proliferation during developmental and adult mammalian neurogenesis. *Proc Natl Acad Sci USA* 2006;103:3416– 21.
298. Ermonval M, Petit D, Le Duc A, Kellermann O, Gallet P-F. Glycosylation-related genes are variably expressed depending on the differentiation state of a bioaminergic neuronal cell line: implication for the cellular prion protein. *Glycoconj J* 2009;26:477–93.
299. Lee YJ, Baskakov IV. The cellular form of the prion protein guides the differentiation of human embryonic stem cells into neuron-, oligodendrocyte-, and astrocyte-committed lineages. *Prion* 2014;8:266–75.
300. Bremer J, Baumann F, Tiberi C, Wessig C, Fischer H, Schwarz P, *et al.* Axonal prion protein is required for peripheral myelin maintenance. *Nat Neurosci* 2010;13:310–8.
301. Nuvolone M, Hermann M, Sorce S, Russo G, Tiberi C, Schwarz P, *et al.* Strictly co-isogenic C57BL/6J-Prnp-/- mice: A rigorous resource for prion science. *J Exp Med* 2016;213:313–27.
302. Weise J, Crome O, Sandau R, Schulz-Schaeffer W, Bähr M, Zerr I. Upregulation of cellular prion protein (PrPc) after focal cerebral ischemia and influence of lesion severity. *Neurosci Lett* 2004;372:146–50.
303. Sakurai-Yamashita Y, Sakaguchi S, Yoshikawa D, Okimura N, Masuda Y, Katamine S, *et al.* Female-specific neuroprotection against transient brain ischemia observed in mice devoid of prion protein is abolished by ectopic expression of prion protein-like protein. *Neuroscience* 2005;136:281–7.
304. Weise J, Sandau R, Schwarting S, Crome O, Wrede A, Schulz-Schaeffer W, *et al.* Deletion of cellular prion protein results in reduced Akt activation, enhanced postischemic caspase-3 activation, and exacerbation of ischemic brain injury. *Stroke* 2006;37:1296–300.
305. Nishida N, Katamine S, Shigematsu K, Nakatani A, Sakamoto N, Hasegawa S, *et al.* Prion protein is necessary for latent learning and long-term memory retention. *Cell Mol Neurobiol* 1997;17:537–45.
306. Lugaresi E, Tobler I, Gambetti P, Montagna P. The pathophysiology of fatal familial insomnia. *Brain Pathol* 1998;8:521–6.
307. Cagampang FR, Whatley SA, Mitchell AL, Powell JF, Campbell IC, Coen CW. Circadian regulation of prion protein messenger RNA in the rat forebrain: a widespread and synchronous rhythm. *Neuroscience* 1999;91:1201–4.

308. Mallucci G, Collinge J. Update on Creutzfeldt-Jakob disease. *Curr Opin Neurol* 2004;17:641–7.
309. Dürig J, Giese A, Schulz-Schaeffer W, Rosenthal C, Schmücker U, Bieschke J, *et al.* Differential constitutive and activation-dependent expression of prion protein in human peripheral blood leucocytes. *Br J Haematol* 2000;108: 488–95.
310. Nico PBC, de-Paris F, Vinadé ER, Amaral OB, Rockenbach I, Soares BL, *et al.* Altered behavioural response to acute stress in mice lacking cellular prion protein. *Behav Brain Res* 2005;162:173–81.
311. Tsutsui S, Hahn JN, Johnson TA, Ali Z, Jirik FR. Absence of the cellular prion protein exacerbates and prolongs neuroinflammation in experimental autoimmune encephalomyelitis. *Am J Pathol* 2008;173:1029–41.
312. Haddon DJ, Hughes MR, Antignano F, Westaway D, Cashman NR, McNagny KM. Prion protein expression and release by mast cells after activation. *J Infect Dis* 2009;200:827–31.
313. Hidaka K, Shirai M, Lee J-K, Wakayama T, Kodama I, Schneider MD, *et al.* The cellular prion protein identifies bipotential cardiomyogenic progenitors. *Circ Res* 2010;106:111–9.
314. Martin GR, Keenan CM, Sharkey KA, Jirik FR. Endogenous prion protein attenuates experimentally induced colitis. *Am J Pathol* 2011;179:2290–301.
315. Owen F, Poulter M, Collinge J, Crow TJ. A codon 129 polymorphism in the PRIP gene. *Nucleic Acids Res* 1990;18:3103.
316. Petraroli R, Pocchiari M. Codon 219 polymorphism of PRNP in healthy Caucasians and Creutzfeldt-Jakob disease patients. *Am J Hum Genet* 1996;58:888–9.
317. Palmer MS, Dryden AJ, Hughes JT, Collinge J. Homozygous prion protein genotype predisposes to sporadic Creutzfeldt-Jakob disease. *Nature* 1991;352:340–2.
318. Dlouhy SR, Hsiao K, Farlow MR, Foroud T, Conneally PM, Johnson P, *et al.* Linkage of the Indiana kindred of Gerstmann-Sträussler-Scheinker disease to the prion protein gene. *Nat Genet* 1992;1:64–7.
319. Poulter M, Baker HF, Frith CD, Leach M, Lofthouse R, Ridley RM, *et al.* Inherited prion disease with 144 base pair gene insertion. 1. Genealogical and molecular studies. *Brain* 1992;115 (Pt 3):675–85.
320. Goldfarb LG, Petersen RB, Tabaton M, Brown P, LeBlanc AC, Montagna P, *et al.* Fatal familial insomnia and familial Creutzfeldt-Jakob disease: disease phenotype determined by a DNA polymorphism. *Science* 1992;258:806–8.
321. Monari L, Chen SG, Brown P, Parchi P, Petersen RB, Mikol J, *et al.* Fatal familial insomnia and familial Creutzfeldt-Jakob disease: different prion proteins determined by a DNA polymorphism. *Proc Natl Acad Sci USA* 1994;91:2839–42.
322. Alperovitch A, Zerr I, Pocchiari M, Mitrova E, de Pedro Cuesta J, Hegyi I, *et al.* Codon 129 prion protein genotype and sporadic Creutzfeldt-Jakob disease. *Lancet* 1999;353:1673–4.

323. Hainfellner JA, Parchi P, Kitamoto T, Jarius C, Gambetti P, Budka H. A novel phenotype in familial Creutzfeldt-Jakob disease: prion protein gene E200K mutation coupled with valine at codon 129 and type 2 protease-resistant prion protein. *Ann Neurol* 1999;45:812–6.
324. Collinge J, Palmer MS, Dryden AJ. Genetic predisposition to iatrogenic Creutzfeldt-Jakob disease. *Lancet* 1991;337:1441–2.
325. Collinge J, Beck J, Campbell T, Estibeiro K, Will RG. Prion protein gene analysis in new variant cases of Creutzfeldt-Jakob disease. *Lancet* 1996;348:56.
326. Zeidler M, Stewart G, Cousens SN, Estibeiro K, Will RG. Codon 129 genotype and new variant CJD. *Lancet* 1997;350:668.
327. Hill AF, Butterworth RJ, Joiner S, Jackson G, Rossor MN, Thomas DJ, *et al.* Investigation of variant Creutzfeldt-Jakob disease and other human prion diseases with tonsil biopsy samples. *Lancet* 1999;353:183–9.
328. Lee HS, Brown P, Cervenáková L, Garruto RM, Alpers MP, Gajdusek DC, *et al.* Increased susceptibility to Kuru of carriers of the PRNP 129 methionine/methionine genotype. *J Infect Dis* 2001;183:192–6.
329. Mead S, Stumpf MPH, Whitfield J, Beck JA, Poulter M, Campbell T, *et al.* Balancing selection at the prion protein gene consistent with prehistoric kurulike epidemics. *Science* 2003;300:640–3.
330. Prusiner SB, Scott M, Foster D, Pan KM, Groth D, Mirenda C, *et al.* Transgenetic studies implicate interactions between homologous PrP isoforms in scrapie prion replication. *Cell* 1990;63:673–86.
331. Collinge J, Palmer MS, Sidle KC, Hill AF, Gowland I, Meads J, *et al.* Unaltered susceptibility to BSE in transgenic mice expressing human prion protein. *Nature* 1995;378:779–83.
332. Dermaut B, Croes EA, Rademakers R, Van den Broeck M, Cruts M, Hofman A, *et al.* PRNP Val129 homozygosity increases risk for early-onset Alzheimer's disease. *Ann Neurol* 2003;53:409–12.
333. Golanska E, Hulas-Bigoszewska K, Rutkiewicz E, Styczynska M, Peplonska B, Barcikowska M, *et al.* Polymorphisms within the prion (PrP) and prion-like protein (Doppel) genes in AD. *Neurology* 2004;62:313–5.
334. He J, Li X, Yang J, Huang J, Fu X, Zhang Y, *et al.* The association between the methionine/valine (M/V) polymorphism (rs1799990) in the PRNP gene and the risk of Alzheimer disease: an update by meta-analysis. *J Neurol Sci* 2013;326:89–95.
335. Del Bo R, Comi GP, Giorda R, Crimi M, Locatelli F, Martinelli-Boneschi F, *et al.* The 129 codon polymorphism of the prion protein gene influences earlier cognitive performance in Down syndrome subjects. *J Neurol* 2003;250: 688–92.
336. Berr C, Richard F, Dufouil C, Amant C, Alperovitch A, Amouyel P. Polymorphism of the prion protein is associated with cognitive impairment in the elderly: the EVA study. *Neurology* 1998;51:734–7.
337. Croes EA, Dermaut B, Houwing-Duistermaat JJ, Van den Broeck M, Cruts M, Breteler MMB, *et al.* Early cognitive decline is associated with prion protein codon 129 polymorphism. *Ann Neurol* 2003;54:275–6.

338. Papassotiropoulos A, Wollmer MA, Aguzzi A, Hock C, Nitsch RM, de Quervain DJ-F. The prion gene is associated with human long-term memory. *Hum Mol Genet* 2005;14:2241–6.
339. Grubenbecher S, Stüve O, Hefter H, Korth C. Prion protein gene codon 129 modulates clinical course of neurological Wilson disease. *Neuroreport* 2006;17:549–52.
340. Merle U, Stremmel W, Gessner R. Influence of homozygosity for methionine at codon 129 of the human prion gene on the onset of neurological and hepatic symptoms in Wilson disease. *Arch Neurol* 2006;63:982–5.
341. Furukawa H, Kitamoto T, Tanaka Y, Tateishi J. New variant prion protein in a Japanese family with Gerstmann-Sträussler syndrome. *Brain Res Mol Brain Res* 1995;30:385–8.
342. Tanaka Y, Minematsu K, Moriyasu H, Yamaguchi T, Yutani C, Kitamoto T, *et al.* A Japanese family with a variant of Gerstmann-Sträussler-Scheinker disease. *J Neurol Neurosurg Psychiatry* 1997;62:454–7.
343. Shibuya S, Higuchi J, Shin RW, Tateishi J, Kitamoto T. Codon 219 Lys allele of PRNP is not found in sporadic Creutzfeldt-Jakob disease. *Ann Neurol* 1998;43:826–8.
344. Crozet C, Lin Y-L, Mettling C, Mourton-Gilles C, Corbeau P, Lehmann S, *et al.* Inhibition of PrPSc formation by lentiviral gene transfer of PrP containing dominant negative mutations. *J Cell Sci* 2004;117:5591–7.
345. Perrier V, Kaneko K, Safar J, Vergara J, Tremblay P, DeArmond SJ, *et al.* Dominant-negative inhibition of prion replication in transgenic mice. *Proc Natl Acad Sci USA* 2002;99:13079–84.
346. Hizume M, Kobayashi A, Teruya K, Ohashi H, Ironside JW, Mohri S, *et al.* Human prion protein (PrP) 219K is converted to PrPSc but shows heterozygous inhibition in variant Creutzfeldt-Jakob disease infection. *J Biol Chem* 2009;284:3603–9.
347. Mead S, Whitfield J, Poulter M, Shah P, Uphill J, Campbell T, *et al.* A novel protective prion protein variant that colocalizes with kuru exposure. *N Engl J Med* 2009;361:2056–65.
348. Asante EA, Smidak M, Grimshaw A, Houghton R, Tomlinson A, Jeelani A, *et al.* A naturally occurring variant of the human prion protein completely prevents prion disease. *Nature* 2015;522:478–81.
349. Mead S, Whitfield J, Poulter M, Shah P, Uphill J, Beck J, *et al.* Genetic susceptibility, evolution and the kuru epidemic. *Philos Trans R Soc Lond, B, Biol Sci* 2008;363:3741–6.
350. Cortez LM, Kumar J, Renault L, Young HS, Sim VL. Mouse prion protein polymorphism Phe-108/Val-189 affects the kinetics of fibril formation and the response to seeding: evidence for a two-step nucleation polymerization mechanism. *J Biol Chem* 2013;288:4772–81.
351. Westaway D, Mirenda CA, Foster D, Zebarjadian Y, Scott M, Torchia M, *et al.* Paradoxical shortening of scrapie incubation times by expression of prion protein transgenes derived from long incubation period mice. *Neuron* 1991;7:59–68.

352. Carlson GA, Ebeling C, Yang SL, Telling G, Torchia M, Groth D, *et al.* Prion isolate specified allotypic interactions between the cellular and scrapie prion proteins in congenic and transgenic mice. *Proc Natl Acad Sci USA* 1994;91:5690–4.
353. Cortez LM, Sim VL. Implications of prion polymorphisms. *Prion* 2013;7:276–9.
354. Lloyd SE, Thompson SR, Beck JA, Linehan JM, Wadsworth JDF, Brandner S, *et al.* Identification and characterization of a novel mouse prion gene allele. *Mamm Genome* 2004;15:383–9.
355. Hunter N, Moore L, Hosie BD, Dingwall WS, Greig A. Association between natural scrapie and PrP genotype in a flock of Suffolk sheep in Scotland. *Vet Rec* 1997;140:59–63.
356. Baylis M, Goldmann W. The genetics of scrapie in sheep and goats. *Curr Mol Med* 2004;4:385–96.
357. Laplanche JL, Chatelain J, Westaway D, Thomas S, Dussaucy M, Brugere-Picoux J, *et al.* PrP polymorphisms associated with natural scrapie discovered by denaturing gradient gel electrophoresis. *Genomics* 1993;15:30–7.
358. Westaway D, Zuliani V, Cooper CM, Da Costa M, Neuman S, Jenny AL, *et al.* Homozygosity for prion protein alleles encoding glutamine-171 renders sheep susceptible to natural scrapie. *Genes Dev* 1994;8:959–69.
359. Hunter N, Goldmann W, Smith G, Hope J. The association of a codon 136 PrP gene variant with the occurrence of natural scrapie. *Arch Virol* 1994;137:171–7.
360. Ikeda T, Horiuchi M, Ishiguro N, Muramatsu Y, Kai-Uwe GD, Shinagawa M. Amino acid polymorphisms of PrP with reference to onset of scrapie in Suffolk and Corriedale sheep in Japan. *J Gen Virol* 1995;76 (Pt 10):2577–81.
361. Hunter N, Foster JD, Goldmann W, Stear MJ, Hope J, Bostock C. Natural scrapie in a closed flock of Cheviot sheep occurs only in specific PrP genotypes. *Arch Virol* 1996;141:809–24.
362. Hunter N, Goldmann W, Foster JD, Cairns D, Smith G. Natural scrapie and PrP genotype: case-control studies in British sheep. *Vet Rec* 1997;141: 137–40.
363. Belt PB, Muileman IH, Schreuder BE, Bos-de Ruijter J, Gielkens AL, Smits MA. Identification of five allelic variants of the sheep PrP gene and their association with natural scrapie. *J Gen Virol* 1995;76 (Pt 3):509–17.
364. Eglin RD, Warner R, Gubbins S, Sivam SK, Dawson M. Frequencies of PrP genotypes in 38 breeds of sheep sampled in the National Scrapie Plan for Great Britain. *Vet Rec* 2005;156:433–7.
365. Tongue SC, Pfeiffer DU, Warner R, Elliott H, Del Rio Vilas V. Estimation of the relative risk of developing clinical scrapie: the role of prion protein (PrP) genotype and selection bias. *Vet Rec* 2006;158:43–50.
366. Baylis M, Chihota C, Stevenson E, Goldmann W, Smith A, Sivam K, *et al.* Risk of scrapie in British sheep of different prion protein genotype. *J Gen Virol* 2004;85:2735–40.
367. Lühken G, Buschmann A, Groschup MH, Erhardt G. Prion protein allele A136 H154Q171 is associated with high susceptibility to scrapie in purebred and crossbred German Merinoland sheep. *Arch Virol* 2004;149:1571–80.

368. Lühken G, Buschmann A, Brandt H, Eiden M, Groschup MH, Erhardt G. Epidemiological and genetical differences between classical and atypical scrapie cases. *Vet Res* 2007;38:65–80.
369. Moum T, Olsaker I, Hopp P, Moldal T, Valheim M, Moum T, *et al.* Polymorphisms at codons 141 and 154 in the ovine prion protein gene are associated with scrapie Nor98 cases. *J Gen Virol* 2005;86:231–5.
370. Konold T, Phelan LJ, Donnachie BR, Chaplin MJ, Cawthraw S, González L. Codon 141 polymorphisms of the ovine prion protein gene affect the phenotype of classical scrapie transmitted from goats to sheep. *BMC Vet Res* 2017;13:122.
371. Curcio L, Sebastiani C, Di Lorenzo P, Lasagna E, Biagetti M. Review: A review on classical and atypical scrapie in caprine: Prion protein gene polymorphisms and their role in the disease. *Animal* 2016;10:1585–93.
372. Acutis PL, Colussi S, Santagada G, Laurenza C, Maniaci MG, Riina MV, *et al.* Genetic variability of the PRNP gene in goat breeds from Northern and Southern Italy. *J Appl Microbiol* 2008;104:1782–9.
373. Eiden M, Soto EO, Mettenleiter TC, Groschup MH. Effects of polymorphisms in ovine and caprine prion protein alleles on cell-free conversion. *Vet Res* 2011;42:30.
374. White SN, Reynolds JO, Waldron DF, Schneider DA, O'Rourke KI. Extended scrapie incubation time in goats singly heterozygous for PRNP S146 or K222. *Gene* 2012;501:49–51.
375. Lacroux C, Perrin-Chauvineau C, Corbière F, Aron N, Aguilar-Calvo P, Torres JM, *et al.* Genetic resistance to scrapie infection in experimentally challenged goats. *J Virol* 2014;88:2406–13.
376. Aguilar-Calvo P, Espinosa JC, Pintado B, Gutiérrez-Adán A, Alamillo E, Miranda A, *et al.* Role of the goat K222-PrP(C) polymorphic variant in prion infection resistance. *J Virol* 2014;88:2670–6.
377. Aguilar-Calvo P, Fast C, Tauscher K, Espinosa J-C, Groschup MH, Nadeem M, *et al.* Effect of Q211 and K222 PRNP Polymorphic Variants in the Susceptibility of Goats to Oral Infection With Goat Bovine Spongiform Encephalopathy. *J Infect Dis* 2015;212:664–72.
378. Konold T, Thorne L, Simmons HA, Hawkins SAC, Simmons MM, González L. Evidence of scrapie transmission to sheep via goat milk. *BMC Vet Res* 2016;12:208.
379. Vitale M, Migliore S, La Giglia M, Alberti P, Di Marco Lo Presti V, Langeveld JPM. Scrapie incidence and PRNP polymorphisms: rare small ruminant breeds of Sicily with TSE protecting genetic reservoirs. *BMC Vet Res* 2016;12:141.
380. Goldmann W. PrP genetics in ruminant transmissible spongiform encephalopathies. *Vet Res* 2008;39:30.
381. Vaccari G, Panagiotidis CH, Acin C, Peletto S, Barillet F, Acutis P, *et al.* State-of-the-art review of goat TSE in the European Union, with special emphasis on PRNP genetics and epidemiology. *Vet Res* 2009;40:48.

382. Goldmann W, Ryan K, Stewart P, Parnham D, Xicohtencatl R, Fernandez N, *et al.* Caprine prion gene polymorphisms are associated with decreased incidence of classical scrapie in goat herds in the United Kingdom. *Vet Res* 2011;42:110.
383. Goldmann W, Marier E, Stewart P, Konold T, Street S, Langeveld J, *et al.* Prion protein genotype survey confirms low frequency of scrapie-resistant K222 allele in British goat herds. *Vet Rec* 2016;178:168.
384. Prusiner SB. Novel proteinaceous infectious particles cause scrapie. *Science* 1982;216:136–44.
385. Brandner S, Isenmann S, Raeber A, Fischer M, Sailer A, Kobayashi Y, *et al.* Normal host prion protein necessary for scrapie-induced neurotoxicity. *Nature* 1996;379:339–43.
386. Stahl N, Baldwin MA, Teplow DB, Hood L, Gibson BW, Burlingame AL, *et al.* Structural studies of the scrapie prion protein using mass spectrometry and amino acid sequencing. *Biochemistry* 1993;32:1991–2002.
387. Riek R, Hornemann S, Wider G, Billeter M, Glockshuber R, Wüthrich K. NMR structure of the mouse prion protein domain PrP(121-231). *Nature* 1996;382:180–2.
388. Safar J, Roller PP, Gajdusek DC, Gibbs CJ. Conformational transitions, dissociation, and unfolding of scrapie amyloid (prion) protein. *J Biol Chem* 1993;268:20276–84.
389. Pan KM, Baldwin M, Nguyen J, Gasset M, Serban A, Groth D, *et al.* Conversion of alpha-helices into beta-sheets features in the formation of the scrapie prion proteins. *Proc Natl Acad Sci USA* 1993;90:10962–6.
390. Riesner D. Biochemistry and structure of PrP(C) and PrP(Sc). *Br Med Bull* 2003;66:21–33.
391. Requena JR, Wille H. The structure of the infectious prion protein: experimental data and molecular models. *Prion* 2014;8:60–6.
392. Caughey B, Baron GS. Prions and their partners in crime. *Nature* 2006;443:803–10.
393. Fasano C, Campana V, Zurzolo C. Prions: protein only or something more? Overview of potential prion cofactors. *J Mol Neurosci* 2006;29:195–214.
394. Wang F, Wang X, Yuan C-G, Ma J. Generating a prion with bacterially expressed recombinant prion protein. *Science* 2010;327:1132–5.
395. Gill AC, Agarwal S, Pinheiro TJT, Graham JF. Structural requirements for efficient prion protein conversion: cofactors may promote a conversion-competent structure for PrP(C). *Prion* 2010;4:235–42.
396. Hooper NM. Glypican-1 facilitates prion conversion in lipid rafts. *J Neurochem* 2011;116:721–5.
397. Deleault NR, Piro JR, Walsh DJ, Wang F, Ma J, Geoghegan JC, *et al.* Isolation of phosphatidylethanolamine as a solitary cofactor for prion formation in the absence of nucleic acids. *Proc Natl Acad Sci USA* 2012;109:8546–51.
398. Legname G, Baskakov IV, Nguyen H-OB, Riesner D, Cohen FE, DeArmond SJ, *et al.* Synthetic mammalian prions. *Science* 2004;305:673–6.

399. Colby DW, Giles K, Legname G, Wille H, Baskakov IV, DeArmond SJ, *et al.* Design and construction of diverse mammalian prion strains. *Proc Natl Acad Sci USA* 2009;106:20417–22.
400. Makarava N, Kovacs GG, Bocharova O, Savtchenko R, Alexeeva I, Budka H, *et al.* Recombinant prion protein induces a new transmissible prion disease in wild-type animals. *Acta Neuropathol* 2010;119:177–87.
401. Soto C, Castilla J. The controversial protein-only hypothesis of prion propagation. *Nat Med* 2004;10 Suppl:S63-67.
402. Castilla J, Saá P, Hetz C, Soto C. In vitro generation of infectious scrapie prions. *Cell* 2005;121:195–206.
403. Soto C. Prion hypothesis: the end of the controversy? *Trends Biochem Sci* 2011;36:151–8.
404. Wang F, Wang X, Ma J. Conversion of bacterially expressed recombinant prion protein. *Methods* 2011;53:208–13.
405. Alper T, Haig DA, Clarke MC. The exceptionally small size of the scrapie agent. *Biochem Biophys Res Commun* 1966;22:278–84.
406. Alper T, Cramp WA, Haig DA, Clarke MC. Does the agent of scrapie replicate without nucleic acid? *Nature* 1967;214:764–6.
407. Rambaran RN, Serpell LC. Amyloid fibrils: abnormal protein assembly. *Prion* 2008;2:112–7.
408. Bartz JC, Dejoia C, Tucker T, Kincaid AE, Bessen RA. Extraneural prion neuroinvasion without lymphoreticular system infection. *J Virol* 2005;79:11858–63.
409. Aguzzi A, Heikenwalder M, Polymenidou M. Insights into prion strains and neurotoxicity. *Nat Rev Mol Cell Biol* 2007;8:552–61.
410. Safar J, Wille H, Itri V, Groth D, Serban H, Torchia M, *et al.* Eight prion strains have PrP(Sc) molecules with different conformations. *Nat Med* 1998;4: 1157–65.
411. Aguzzi A. Understanding the diversity of prions. *Nat Cell Biol* 2004;6:290–2.
412. Meyer-Luehmann M, Coomaraswamy J, Bolmont T, Kaeser S, Schaefer C, Kilger E, *et al.* Exogenous induction of cerebral beta-amyloidogenesis is governed by agent and host. *Science* 2006;313:1781–4.
413. Cohen ML, Kim C, Haldiman T, ElHag M, Mehndiratta P, Pichet T, *et al.* Rapidly progressive Alzheimer's disease features distinct structures of amyloid-β. *Brain* 2015;138:1009–22.
414. Cohen M, Appleby B, Safar JG. Distinct prion-like strains of amyloid beta implicated in phenotypic diversity of Alzheimer's disease. *Prion* 2016;10:9–17.
415. Parchi P, Capellari S, Chen SG, Petersen RB, Gambetti P, Kopp N, *et al.* Typing prion isoforms. *Nature* 1997;386:232–4.
416. Helenius A, Aebi M. Intracellular functions of N-linked glycans. *Science* 2001;291:2364–9.
417. Khalili-Shirazi A, Summers L, Linehan J, Mallinson G, Anstee D, Hawke S, *et al.* PrP glycoforms are associated in a strain-specific ratio in native PrPSc. *J Gen Virol* 2005;86:2635–44.

418. Pan T, Colucci M, Wong BS, Li R, Liu T, Petersen RB, *et al.* Novel differences between two human prion strains revealed by two-dimensional gel electrophoresis. *J Biol Chem* 2001;276:37284–8.
419. Bessen RA, Marsh RF. Distinct PrP properties suggest the molecular basis of strain variation in transmissible mink encephalopathy. *J Virol* 1994;68: 7859–68.
420. Collinge J, Sidle KC, Meads J, Ironside J, Hill AF. Molecular analysis of prion strain variation and the aetiology of 'new variant' CJD. *Nature* 1996;383: 685–90.
421. Parchi P, Giese A, Capellari S, Brown P, Schulz-Schaeffer W, Windl O, *et al.* Classification of sporadic Creutzfeldt-Jakob disease based on molecular and phenotypic analysis of 300 subjects. *Ann Neurol* 1999;46:224–33.
422. Puoti G, Giaccone G, Rossi G, Canciani B, Bugiani O, Tagliavini F. Sporadic Creutzfeldt-Jakob disease: co-occurrence of different types of PrP(Sc) in the same brain. *Neurology* 1999;53:2173–6.
423. Hill AF, Joiner S, Wadsworth JDF, Sidle KCL, Bell JE, Budka H, *et al.* Molecular classification of sporadic Creutzfeldt-Jakob disease. *Brain* 2003;126:1333–46.
424. Polymenidou M, Stoeck K, Glatzel M, Vey M, Bellon A, Aguzzi A. Coexistence of multiple PrPSc types in individuals with Creutzfeldt-Jakob disease. *Lancet Neurol* 2005;4:805–14.
425. Uro-Coste E, Cassard H, Simon S, Lugan S, Bilheude J-M, Perret-Liaudet A, *et al.* Beyond PrP res type 1/type 2 dichotomy in Creutzfeldt-Jakob disease. *PLoS Pathog* 2008;4:e1000029.
426. Uro-Coste E, Cassard H, Simon S, Lugan S, Bilheude J-M, Perret-Liaudet A, *et al.* Beyond PrP9res) type 1/type 2 dichotomy in Creutzfeldt-Jakob disease. *PLoS Pathog* 2008;4:e1000029.
427. Parchi P, Castellani R, Capellari S, Ghetti B, Young K, Chen SG, *et al.* Molecular basis of phenotypic variability in sporadic Creutzfeldt-Jakob disease. *Ann Neurol* 1996;39:767–78.
428. Parchi P, Giese A, Capellari S, Brown P, Schulz-Schaeffer W, Windl O, *et al.* Classification of sporadic Creutzfeldt-Jakob disease based on molecular and phenotypic analysis of 300 subjects. *Ann Neurol* 1999;46:224–33.
429. Parchi P, Zou W, Wang W, Brown P, Capellari S, Ghetti B, *et al.* Genetic influence on the structural variations of the abnormal prion protein. *Proc Natl Acad Sci USA* 2000;97:10168–72.
430. Benestad SL, Sarradin P, Thu B, Schönheit J, Tranulis MA, Bratberg B. Cases of scrapie with unusual features in Norway and designation of a new type, Nor98. *Vet Rec* 2003;153:202–8.
431. Biacabe A-G, Jacobs JG, Bencsik A, Langeveld JPM, Baron TGM. H-type bovine spongiform encephalopathy: complex molecular features and similarities with human prion diseases. *Prion* 2007;1:61–8.
432. Angers RC, Kang H-E, Napier D, Browning S, Seward T, Mathiason C, *et al.* Prion strain mutation determined by prion protein conformational compatibility and primary structure. *Science* 2010;328:1154–8.

433. Perrott MR, Sigurdson CJ, Mason GL, Hoover EA. Evidence for distinct chronic wasting disease (CWD) strains in experimental CWD in ferrets. *J Gen Virol* 2012;93:212–21.
434. Pirisinu L, Nonno R, Esposito E, Benestad SL, Gambetti P, Agrimi U, *et al.* Small ruminant nor98 prions share biochemical features with human gerstmann-sträussler-scheinker disease and variably protease-sensitive prionopathy. *PLoS ONE* 2013;8:e66405.
435. Poggiolini I, Saverioni D, Parchi P. Prion protein misfolding, strains, and neurotoxicity: an update from studies on Mammalian prions. *Int J Cell Biol* 2013;2013:910314.
436. Telling G. Study of prion types questions classification system. *Lancet Neurol* 2005;4:788–9.
437. Silva CJ, Vázquez-Fernández E, Onisko B, Requena JR. Proteinase K and the structure of PrPSc: The good, the bad and the ugly. *Virus Res* 2015;207:120–6.
438. Yakovleva O, Janiak A, McKenzie C, McShane L, Brown P, Cervenakova L. Effect of protease treatment on plasma infectivity in variant Creutzfeldt-Jakob disease mice. *Transfusion* 2004;44:1700–5.
439. Safar JG, Geschwind MD, Deering C, Didorenko S, Sattavat M, Sanchez H, *et al.* Diagnosis of human prion disease. *Proc Natl Acad Sci USA* 2005;102:3501–6.
440. Pastrana MA, Sajnani G, Onisko B, Castilla J, Morales R, Soto C, *et al.* Isolation and characterization of a proteinase K-sensitive PrPSc fraction. *Biochemistry* 2006;45:15710–7.
441. D'Castro L, Wenborn A, Gros N, Joiner S, Cronier S, Collinge J, *et al.* Isolation of proteinase K-sensitive prions using pronase E and phosphotungstic acid. *PLoS ONE* 2010;5:e15679.
442. Zou W-Q, Zheng J, Gray DM, Gambetti P, Chen SG. Antibody to DNA detects scrapie but not normal prion protein. *Proc Natl Acad Sci USA* 2004;101: 1380–5.
443. Jones M, Peden AH, Prowse CV, Gröner A, Manson JC, Turner ML, *et al.* In vitro amplification and detection of variant Creutzfeldt-Jakob disease PrPSc. *J Pathol* 2007;213:21–6.
444. Cronier S, Gros N, Tattum MH, Jackson GS, Clarke AR, Collinge J, *et al.* Detection and characterization of proteinase K-sensitive disease-related prion protein with thermolysin. *Biochem J* 2008;416:297–305.
445. Xiao X, Cali I, Dong Z, Puoti G, Yuan J, Qing L, *et al.* Protease-sensitive prions with 144-bp insertion mutations. *Aging (Albany NY)* 2013;5:155–73.
446. Gambetti P, Dong Z, Yuan J, Xiao X, Zheng M, Alshekhlee A, *et al.* A novel human disease with abnormal prion protein sensitive to protease. *Ann Neurol* 2008;63:697–708.
447. Zou W-Q, Puoti G, Xiao X, Yuan J, Qing L, Cali I, *et al.* Variably protease-sensitive prionopathy: a new sporadic disease of the prion protein. *Ann Neurol* 2010;68:162–72.

448. Peden AH, Sarode DP, Mulholland CR, Barria MA, Ritchie DL, Ironside JW, *et al.* The prion protein protease sensitivity, stability and seeding activity in variably protease sensitive prionopathy brain tissue suggests molecular overlaps with sporadic Creutzfeldt-Jakob disease. *Acta Neuropathol Commun* 2014;2:152.
449. Thackray AM, Hopkins L, Bujdoso R. Proteinase K-sensitive disease-associated ovine prion protein revealed by conformation-dependent immunoassay. *Biochem J* 2007;401:475–83.
450. Kim C, Haldiman T, Cohen Y, Chen W, Blevins J, Sy M-S, *et al.* Protease-sensitive conformers in broad spectrum of distinct PrPSc structures in sporadic Creutzfeldt-Jakob disease are indicator of progression rate. *PLoS Pathog* 2011;7:e1002242.
451. Kim C, Haldiman T, Surewicz K, Cohen Y, Chen W, Blevins J, *et al.* Small protease sensitive oligomers of PrPSc in distinct human prions determine conversion rate of PrP(C). *PLoS Pathog* 2012;8:e1002835.
452. Owen JP, Maddison BC, Whitelam GC, Gough KC. Use of thermolysin in the diagnosis of prion diseases. *Mol Biotechnol* 2007;35:161–70.
453. Tzaban S, Friedlander G, Schonberger O, Horonchik L, Yedidia Y, Shaked G, *et al.* Protease-sensitive scrapie prion protein in aggregates of heterogeneous sizes. *Biochemistry* 2002;41:12868–75.
454. Silveira JR, Raymond GJ, Hughson AG, Race RE, Sim VL, Hayes SF, *et al.* The most infectious prion protein particles. *Nature* 2005;437:257–61.
455. Hill AF, Joiner S, Linehan J, Desbruslais M, Lantos PL, Collinge J. Species-barrier-independent prion replication in apparently resistant species. *Proc Natl Acad Sci USA* 2000;97:10248–53.
456. Kaneko K, Ball HL, Wille H, Zhang H, Groth D, Torchia M, *et al.* A synthetic peptide initiates Gerstmann-Sträussler-Scheinker (GSS) disease in transgenic mice. *J Mol Biol* 2000;295:997–1007.
457. Solomon IH, Huettner JE, Harris DA. Neurotoxic mutants of the prion protein induce spontaneous ionic currents in cultured cells. *J Biol Chem* 2010;285:26719–26.
458. Sandberg MK, Al-Doujaily H, Sharps B, Clarke AR, Collinge J. Prion propagation and toxicity in vivo occur in two distinct mechanistic phases. *Nature* 2011;470:540–2.
459. Aguzzi A, Falsig J. Prion propagation, toxicity and degradation. *Nat Neurosci* 2012;15:936–9.
460. Race R, Raines A, Raymond GJ, Caughey B, Chesebro B. Long-term subclinical carrier state precedes scrapie replication and adaptation in a resistant species: analogies to bovine spongiform encephalopathy and variant Creutzfeldt-Jakob disease in humans. *J Virol* 2001;75:10106–12.
461. Thackray AM, Klein MA, Aguzzi A, Bujdoso R. Chronic subclinical prion disease induced by low-dose inoculum. *J Virol* 2002;76:2510–7.
462. Thackray AM, Klein MA, Bujdoso R. Subclinical prion disease induced by oral inoculation. *J Virol* 2003;77:7991–8.

463. Sandberg MK, Al-Doujaily H, Sharps B, Clarke AR, Collinge J. Prion propagation and toxicity in vivo occur in two distinct mechanistic phases. *Nature* 2011;470:540–2.
464. Mays CE, van der Merwe J, Kim C, Haldiman T, McKenzie D, Safar JG, *et al.* Prion Infectivity Plateaus and Conversion to Symptomatic Disease Originate from Falling Precursor Levels and Increased Levels of Oligomeric PrPSc Species. *J Virol* 2015;89:12418–26.
465. Solomon IH, Huettner JE, Harris DA. Neurotoxic mutants of the prion protein induce spontaneous ionic currents in cultured cells. *J Biol Chem* 2010;285:26719–26.
466. Antony H, Wiegmans AP, Wei MQ, Chernoff YO, Khanna KK, Munn AL. Potential roles for prions and protein-only inheritance in cancer. *Cancer Metastasis Rev* 2012;31:1–19.
467. Checler F, Alves da Costa C. p53 in neurodegenerative diseases and brain cancers. *Pharmacol Ther* 2014;142:99–113.
468. Yang X, Zhang Y, Zhang L, He T, Zhang J, Li C. Prion protein and cancers. *Acta Biochim Biophys Sin (Shanghai)* 2014;46:431–40.
469. Zafar S, Behrens C, Dihazi H, Schmitz M, Zerr I, Schulz-Schaeffer WJ, *et al.* Cellular prion protein mediates early apoptotic proteome alternation and phospho-modification in human neuroblastoma cells. *Cell Death Dis* 2017;8:e2557.
470. Lee JH, Yun CW, Lee SH. Cellular Prion Protein Enhances Drug Resistance of Colorectal Cancer Cells via Regulation of a Survival Signal Pathway. *Biomol Ther (Seoul)* 2017.
471. Ghosh S, Salot S, Sengupta S, Navalkar A, Ghosh D, Jacob R, *et al.* p53 amyloid formation leading to its loss of function: implications in cancer pathogenesis. *Cell Death Differ* 2017;24:1784–98.
472. Krasemann S, Neumann M, Szalay B, Stocking C, Glatzel M. Protease-sensitive prion species in neoplastic spleens of prion-infected mice with uncoupling of PrP(Sc) and prion infectivity. *J Gen Virol* 2013;94:453–63.
473. Yuan J, Xiao X, McGeehan J, Dong Z, Cali I, Fujioka H, *et al.* Insoluble aggregates and protease-resistant conformers of prion protein in uninfected human brains. *J Biol Chem* 2006;281:34848–58.
474. Yuan J, Dong Z, Guo J-P, McGeehan J, Xiao X, Wang J, *et al.* Accessibility of a critical prion protein region involved in strain recognition and its implications for the early detection of prions. *Cell Mol Life Sci* 2008;65:631–43.
475. Xiao X, Yuan J, Zou W-Q. Isolation of soluble and insoluble PrP oligomers in the normal human brain. *J Vis Exp* 2012.
476. Brayer GD, McPherson A. Mechanism of DNA binding to the gene 5 protein of bacteriophage fd. *Biochemistry* 1984;23:340–9.
477. Marsh RF, Malone TG, Semancik JS, Lancaster WD, Hanson RP. Evidence for an essential DNA component in the Scrapie agent. *Nature* 1978;275: 146–7.
478. Narang HK, Asher DM, Gajdusek DC. Evidence that DNA is present in abnormal tubulofilamentous structures found in scrapie. *Proc Natl Acad Sci USA* 1988;85:3575–9.

479. Sklaviadis T, Akowitz A, Manuelidis EE, Manuelidis L. Nuclease treatment results in high specific purification of Creutzfeldt-Jakob disease infectivity with a density characteristic of nucleic acid-protein complexes. *Arch Virol* 1990;112:215–28.
480. Zou W-Q, Langeveld J, Xiao X, Chen S, McGeer PL, Yuan J, *et al.* PrP conformational transitions alter species preference of a PrP-specific antibody. *J Biol Chem* 2010;285:13874–84.
481. Emwas A-HM, Al-Talla ZA, Guo X, Al-Ghamdi S, Al-Masri HT. Utilizing NMR and EPR spectroscopy to probe the role of copper in prion diseases. *Magn Reson Chem* 2013;51:255–68.
482. Zou W-Q, Zhou X, Yuan J, Xiao X. Insoluble cellular prion protein and its association with prion and Alzheimer diseases. *Prion* 2011;5:172–8.
483. Zou W-Q, Gambetti P, Xiao X, Yuan J, Langeveld J, Pirisinu L. Prions in variably protease-sensitive prionopathy: an update. *Pathogens* 2013;2:457–71.
484. Zou W-Q, Xiao X, Yuan J, Puoti G, Fujioka H, Wang X, *et al.* Amyloid-beta42 interacts mainly with insoluble prion protein in the Alzheimer brain. *J Biol Chem* 2011;286:15095–105.
485. Dohler F, Sepulveda-Falla D, Krasemann S, Altmeppen H, Schlüter H, Hildebrand D, *et al.* High molecular mass assemblies of amyloid-β oligomers bind prion protein in patients with Alzheimer's disease. *Brain* 2014;137: 873–86.
486. Zou W-Q, Cashman NR. Acidic pH and detergents enhance in vitro conversion of human brain PrPC to a PrPSc-like form. *J Biol Chem* 2002;277:43942–7.
487. McLennan NF, Brennan PM, McNeill A, Davies I, Fotheringham A, Rennison KA, *et al.* Prion protein accumulation and neuroprotection in hypoxic brain damage. *Am J Pathol* 2004;165:227–35.
488. Shyu W-C, Lin S-Z, Chiang M-F, Ding D-C, Li K-W, Chen S-F, *et al.* Overexpression of PrPC by adenovirus-mediated gene targeting reduces ischemic injury in a stroke rat model. *J Neurosci* 2005;25:8967–77.
489. Hebda JA, Miranker AD. The interplay of catalysis and toxicity by amyloid intermediates on lipid bilayers: insights from type II diabetes. *Annu Rev Biophys* 2009;38:125–52.
490. Abedini A, Raleigh DP. A role for helical intermediates in amyloid formation by natively unfolded polypeptides? *Phys Biol* 2009;6:015005.
491. Kirkitadze MD, Condron MM, Teplow DB. Identification and characterization of key kinetic intermediates in amyloid beta-protein fibrillogenesis. *J Mol Biol* 2001;312:1103–19.
492. Anderson VL, Ramlall TF, Rospigliosi CC, Webb WW, Eliezer D. Identification of a helical intermediate in trifluoroethanol-induced alpha-synuclein aggregation. *Proc Natl Acad Sci USA* 2010;107:18850–5.
493. Abedini A, Raleigh DP. A critical assessment of the role of helical intermediates in amyloid formation by natively unfolded proteins and polypeptides. *Protein Eng Des Sel* 2009;22:453–9.
494. Knight JD, Hebda JA, Miranker AD. Conserved and cooperative assembly of membrane-bound alpha-helical states of islet amyloid polypeptide. *Biochemistry* 2006;45:9496–508.

495. Saraogi I, Hebda JA, Becerril J, Estroff LA, Miranker AD, Hamilton AD. Synthetic alpha-helix mimetics as agonists and antagonists of islet amyloid polypeptide aggregation. *Angew Chem Int Ed Engl* 2010;49:736–9.
496. Zhou M, Ottenberg G, Sferrazza GF, Lasmézas CI. Highly neurotoxic monomeric α-helical prion protein. *Proc Natl Acad Sci USA* 2012;109:3113–8.
497. McLean CA, Storey E, Gardner RJ, Tannenberg AE, Cervenáková L, Brown P. The D178N (cis-129M) 'fatal familial insomnia' mutation associated with diverse clinicopathologic phenotypes in an Australian kindred. *Neurology* 1997;49:552–8.
498. Bugiani O, Giaccone G, Piccardo P, Morbin M, Tagliavini F, Ghetti B. Neuropathology of Gerstmann-Sträussler-Scheinker disease. *Microsc Res Tech* 2000;50:10–5.
499. Hamir AN, Gidlewski T, Spraker TR, Miller JM, Creekmore L, Crocheck M, *et al.* Preliminary observations of genetic susceptibility of elk (Cervus elaphus nelsoni) to chronic wasting disease by experimental oral inoculation. *J Vet Diagn Invest* 2006;18:110–4.
500. O'Rourke KI, Spraker TR, Zhuang D, Greenlee JJ, Gidlewski TE, Hamir AN. Elk with a long incubation prion disease phenotype have a unique PrPd profile. *Neuroreport* 2007;18:1935–8.
501. Moore SJ, Vrentas CE, Hwang S, West Greenlee MH, Nicholson EM, Greenlee JJ. Pathologic and biochemical characterization of PrPSc from elk with PRNP polymorphisms at codon 132 after experimental infection with the chronic wasting disease agent. *BMC Vet Res* 2018;14:80.
502. Apweiler R, Hermjakob H, Sharon N. On the frequency of protein glycosylation, as deduced from analysis of the SWISS-PROT database. *Biochim Biophys Acta*1999;1473:4–8.
503. Kim EH, Misek DE. Glycoproteomics-based identification of cancer biomarkers. *Int J Proteomics* 2011;2011:601937.
504. Karve TM, Cheema AK. Small changes huge impact: the role of protein posttranslational modifications in cellular homeostasis and disease. *J Amino Acids* 2011;2011:207691.
505. Helenius A, Aebi M. Intracellular functions of N-linked glycans. *Science* 2001;291:2364–9.
506. Kobata A. Glycobiology in the field of aging research--introduction to glycogerontology. *Biochimie* 2003;85:13–24.
507. Wei X, Li L. Comparative glycoproteomics: approaches and applications. *Brief Funct Genomic Proteomic* 2009;8:104–13.
508. Lowe JB, Marth JD. A genetic approach to Mammalian glycan function. *Annu Rev Biochem* 2003;72:643–91.
509. Endo T. Structure, function and pathology of O-mannosyl glycans. *Glycoconj J* 2004;21:3–7.
510. Rudd PM, Endo T, Colominas C, Groth D, Wheeler SF, Harvey DJ, *et al.* Glycosylation differences between the normal and pathogenic prion protein isoforms. *Proc Natl Acad Sci USA* 1999;96:13044–9.
511. Rudd PM, Wormald MR, Wing DR, Prusiner SB, Dwek RA. Prion glycoprotein: structure, dynamics, and roles for the sugars. *Biochemistry* 2001;40:3759–66.

512. Joao HC, Dwek RA. Effects of glycosylation on protein structure and dynamics in ribonuclease B and some of its individual glycoforms. *Eur J Biochem* 1993;218:239–44.
513. Wormald MR, Dwek RA. Glycoproteins: glycan presentation and protein-fold stability. *Structure* 1999;7:R155-160.
514. Taraboulos A, Rogers M, Borchelt DR, McKinley MP, Scott M, Serban D, *et al.* Acquisition of protease resistance by prion proteins in scrapie-infected cells does not require asparagine-linked glycosylation. *Proc Natl Acad Sci USA* 1990;87:8262–6.
515. Lehmann S, Harris DA. Blockade of glycosylation promotes acquisition of scrapie-like properties by the prion protein in cultured cells. *J Biol Chem* 1997;272:21479–87.
516. Nitrini R, Rosemberg S, Passos-Bueno MR, da Silva LS, Iughetti P, Papadopoulos M, *et al.* Familial spongiform encephalopathy associated with a novel prion protein gene mutation. *Ann Neurol* 1997;42:138–46.
517. Grasbon-Frodl E, Lorenz H, Mann U, Nitsch RM, Windl O, Kretzschmar HA. Loss of glycosylation associated with the T183A mutation in human prion disease. *Acta Neuropathol* 2004;108:476–84.
518. Chasseigneaux S, Haïk S, Laffont-Proust I, De Marco O, Lenne M, Brandel J-P, *et al.* V180I mutation of the prion protein gene associated with atypical PrPSc glycosylation. *Neurosci Lett* 2006;408:165–9.
519. Capellari S, Parchi P, Russo CM, Sanford J, Sy MS, Gambetti P, *et al.* Effect of the E200K mutation on prion protein metabolism. Comparative study of a cell model and human brain. *Am J Pathol* 2000;157:613–22.
520. Rosenmann H, Talmor G, Halimi M, Yanai A, Gabizon R, Meiner Z. Prion protein with an E200K mutation displays properties similar to those of the cellular isoform PrP(C). *J Neurochem* 2001;76:1654–62.
521. Das AS, Zou W-Q. Prions: Beyond a Single Protein. *Clin Microbiol Rev* 2016;29:633–58.
522. Fioriti L, Dossena S, Stewart LR, Stewart RS, Harris DA, Forloni G, *et al.* Cytosolic prion protein (PrP) is not toxic in N2a cells and primary neurons expressing pathogenic PrP mutations. *J Biol Chem* 2005;280:11320–8.
523. Bosques CJ, Imperiali B. The interplay of glycosylation and disulfide formation influences fibrillization in a prion protein fragment. *Proc Natl Acad Sci USA* 2003;100:7593–8.
524. Chen P-Y, Lin C-C, Chang Y-T, Lin S-C, Chan SI. One O-linked sugar can affect the coil-to-beta structural transition of the prion peptide. *Proc Natl Acad Sci USA* 2002;99:12633–8.
525. Korth C, Kaneko K, Prusiner SB. Expression of unglycosylated mutated prion protein facilitates PrP(Sc) formation in neuroblastoma cells infected with different prion strains. *J Gen Virol* 2000;81:2555–63.
526. DeArmond SJ, Sánchez H, Yehiely F, Qiu Y, Ninchak-Casey A, Daggett V, *et al.* Selective neuronal targeting in prion disease. *Neuron* 1997;19:1337–48.
527. Priola SA, Lawson VA. Glycosylation influences cross-species formation of protease-resistant prion protein. *EMBO J* 2001;20:6692–9.

528. Rudd PM, Merry AH, Wormald MR, Dwek RA. Glycosylation and prion protein. *Curr Opin Struct Biol* 2002;12:578–86.
529. Lawson VA, Priola SA, Wehrly K, Chesebro B. N-terminal truncation of prion protein affects both formation and conformation of abnormal protease-r esistant prion protein generated in vitro. *J Biol Chem* 2001;276:35265–71.
530. Stimson E, Hope J, Chong A, Burlingame AL. Site-specific characterization of the N-linked glycans of murine prion protein by high-performance liquid chromatography/electrospray mass spectrometry and exoglycosidase digestions. *Biochemistry* 1999;38:4885–95.
531. Parchi P, Capellari S, Gambetti P. Intracerebral distribution of the abnormal isoform of the prion protein in sporadic Creutzfeldt-Jakob disease and fatal insomnia. *Microsc Res Tech* 2000;50:16–25.
532. Biacabe A-G, Laplanche J-L, Ryder S, Baron T. Distinct molecular phenotypes in bovine prion diseases. *EMBO Rep* 2004;5:110–5.
533. Casalone C, Zanusso G, Acutis P, Ferrari S, Capucci L, Tagliavini F, *et al.* Identification of a second bovine amyloidotic spongiform encephalopathy: molecular similarities with sporadic Creutzfeldt-Jakob disease. *Proc Natl Acad Sci USA* 2004;101:3065–70.
534. Somerville RA. Host and transmissible spongiform encephalopathy agent strain control glycosylation of PrP. *J Gen Virol* 1999;80 (Pt 7):1865–72.
535. Hill AF, Desbruslais M, Joiner S, Sidle KC, Gowland I, Collinge J, *et al.* The same prion strain causes vCJD and BSE. *Nature* 1997;389:448–50, 526.
536. Walmsley AR, Zeng F, Hooper NM. Membrane topology influences N-glycosylation of the prion protein. *EMBO J* 2001;20:703–12.
537. Ioffe E, Stanley P. Mice lacking N-acetylglucosaminyltransferase I activity die at mid-gestation, revealing an essential role for complex or hybrid N-linked carbohydrates. *Proc Natl Acad Sci USA* 1994;91:728–32.
538. Schachter H. Congenital disorders involving defective N-glycosylation of proteins. *Cell Mol Life Sci* 2001;58:1085–104.
539. Freeze HH. Update and perspectives on congenital disorders of glycosylation. *Glycobiology* 2001;11:129R-143R.
540. Holada K, Simak J, Risitano AM, Maciejewski J, Young NS, Vostal JG. Activated platelets of patients with paroxysmal nocturnal hemoglobinuria express cellular prion protein. *Blood* 2002;100:341–3.
541. Rogers M, Yehiely F, Scott M, Prusiner SB. Conversion of truncated and elongated prion proteins into the scrapie isoform in cultured cells. *Proc Natl Acad Sci USA* 1993;90:3182–6.
542. Campana V, Caputo A, Sarnataro D, Paladino S, Tivodar S, Zurzolo C. Characterization of the properties and trafficking of an anchorless form of the prion protein. *J Biol Chem* 2007;282:22747–56.
543. DeArmond SJ, Qiu Y, Sànchez H, Spilman PR, Ninchak-Casey A, Alonso D, *et al.* PrPc glycoform heterogeneity as a function of brain region: implications for selective targeting of neurons by prion strains. *J Neuropathol Exp Neurol* 1999;58:1000–9.

544. Neuendorf E, Weber A, Saalmueller A, Schatzl H, Reifenberg K, Pfaff E, *et al.* Glycosylation deficiency at either one of the two glycan attachment sites of cellular prion protein preserves susceptibility to bovine spongiform encephalopathy and scrapie infections. *J Biol Chem* 2004;279:53306–16.
545. Moudjou M, Treguer E, Rezaei H, Sabuncu E, Neuendorf E, Groschup MH, *et al.* Glycan-controlled epitopes of prion protein include a major determinant of susceptibility to sheep scrapie. *J Virol* 2004;78:9270–6.
546. Roucou X, Gains M, LeBlanc AC. Neuroprotective functions of prion protein. *J Neurosci Res* 2004;75:153–61.
547. Ohtsubo K, Marth JD. Glycosylation in cellular mechanisms of health and disease. *Cell* 2006;126:855–67.
548. Kovacs GG, Budka H. Prion diseases: from protein to cell pathology. *Am J Pathol* 2008;172:555–65.
549. Forloni G, Angeretti N, Chiesa R, Monzani E, Salmona M, Bugiani O, *et al.* Neurotoxicity of a prion protein fragment. *Nature* 1993;362:543–6.
550. Harris DA, True HL. New insights into prion structure and toxicity. *Neuron* 2006;50:353–7.
551. Simoneau S, Rezaei H, Salès N, Kaiser-Schulz G, Lefebvre-Roque M, Vidal C, *et al.* In vitro and in vivo neurotoxicity of prion protein oligomers. *PLoS Pathog* 2007;3:e125.
552. Hakomori S. Glycosylation defining cancer malignancy: new wine in an old bottle. *Proc Natl Acad Sci USA* 2002;99:10231–3.
553. Fuster MM, Esko JD. The sweet and sour of cancer: glycans as novel therapeutic targets. *Nat Rev Cancer* 2005;5:526–42.
554. Reis CA, Osorio H, Silva L, Gomes C, David L. Alterations in glycosylation as biomarkers for cancer detection. *J Clin Pathol* 2010;63:322–9.
555. Markowska AI, Cao Z, Panjwani N. Glycobiology of ocular angiogenesis. *Glycobiology* 2014;24:1275–82.
556. Cheon Y-P, Kim C-H. Impact of glycosylation on the unimpaired functions of the sperm. *Clin Exp Reprod Med* 2015;42:77–85.
557. Wani WY, Chatham JC, Darley-Usmar V, McMahon LL, Zhang J. O-GlcNAcylation and neurodegeneration. *Brain Res Bull* 2017;133:80–7.
558. Wani WY, Ouyang X, Benavides GA, Redmann M, Cofield SS, Shacka JJ, *et al.* O-GlcNAc regulation of autophagy and α-synuclein homeostasis; implications for Parkinson's disease. *Mol Brain* 2017;10:32.
559. Zeidler M, Gibbs CJ, Meslin F-X, Response WHOD of E and PA and. WHO manual for strengthening diagnosis and surveillance of Creutzfeldt-Jakob disease 1998.
560. Kretzschmar HA. Diagnosis of prion diseases. *Clin Lab Med* 2003;23:109–28, viii.
561. Ward HJT, Head MW, Will RG, Ironside JW. Variant Creutzfeldt-Jakob disease. *Clin Lab Med* 2003;23:87–108.
562. Zou W, Colucci M, Gambetti P, Chen SG. Characterization of prion proteins. *Methods Mol Biol* 2003;217:305–14.
563. Hill AF, Zeidler M, Ironside J, Collinge J. Diagnosis of new variant Creutzfeldt-Jakob disease by tonsil biopsy. *Lancet* 1997;349:99–100.

564. Schreuder BE, van Keulen LJ, Vromans ME, Langeveld JP, Smits MA. Tonsillar biopsy and PrPSc detection in the preclinical diagnosis of scrapie. *Vet Rec* 1998;142:564–8.
565. Hilton DA, Fathers E, Edwards P, Ironside JW, Zajicek J. Prion immunoreactivity in appendix before clinical onset of variant Creutzfeldt-Jakob disease. *Lancet* 1998;352:703–4.
566. Peden AH, Head MW, Ritchie DL, Bell JE, Ironside JW. Preclinical vCJD after blood transfusion in a PRNP codon 129 heterozygous patient. *Lancet* 2004;364:527–9.
567. Zerr I, Poser S. Clinical diagnosis and differential diagnosis of CJD and vCJD. With special emphasis on laboratory tests. *APMIS* 2002;110:88–98.
568. Zeidler M, Gibbs CJ, Meslin F-X, Response WHOD of E and PA and. WHO manual for strengthening diagnosis and surveillance of Creutzfeldt-Jakob disease 1998.
569. Zeidler M, Sellar RJ, Collie DA, Knight R, Stewart G, Macleod MA, *et al.* The pulvinar sign on magnetic resonance imaging in variant Creutzfeldt-Jakob disease. *Lancet* 2000;355:1412–8.
570. Zerr I. Human prion diseases: progress in clinical trials. *Brain* 2013;136:996–7.
571. Zerr I, Kallenberg K, Summers DM, Romero C, Taratuto A, Heinemann U, *et al.* Updated clinical diagnostic criteria for sporadic Creutzfeldt-Jakob disease. *Brain* 2009;132:2659–68.
572. Zerr I, Pocchiari M, Collins S, Brandel JP, de Pedro Cuesta J, Knight RS, *et al.* Analysis of EEG and CSF 14-3-3 proteins as aids to the diagnosis of Creutzfeldt-Jakob disease. *Neurology* 2000;55:811–5.
573. Sanchez-Valle R, Nos C, Yagüe J, Graus F, Domínguez A, Saiz A, *et al.* Clinical and genetic features of human prion diseases in Catalonia: 1993- 2002. *Eur J Neurol* 2004;11:649–55.
574. Pauri F, Amabile G, Fattapposta F, Pierallini A, Bianco F. Sporadic Creutzfeldt-Jakob disease without dementia at onset: clinical features, laboratory tests and sequential diffusion MRI (in an autopsy-proven case). *Neurol Sci* 2004;25:234–7.
575. Visani E, Agazzi P, Scaioli V, Giaccone G, Binelli S, Canafoglia L, *et al.* FVEPs in Creutzfeldt-Jacob disease: waveforms and interaction with the periodic EEG pattern assessed by single sweep analysis. *Clin Neurophysiol* 2005;116:895–904.
576. Wieser HG, Schindler K, Zumsteg D. EEG in Creutzfeldt-Jakob disease. *Clin Neurophysiol* 2006;117:935–51.
577. Castellani RJ, Colucci M, Xie Z, Zou W, Li C, Parchi P, *et al.* Sensitivity of 14-3-3 protein test varies in subtypes of sporadic Creutzfeldt-Jakob disease. *Neurology* 2004;63:436–42.
578. Collins SJ, Sanchez-Juan P, Masters CL, Klug GM, van Duijn C, Poleggi A, *et al.* Determinants of diagnostic investigation sensitivities across the clinical spectrum of sporadic Creutzfeldt-Jakob disease. *Brain* 2006;129:2278–87.

579. Binelli S, Agazzi P, Canafoglia L, Scaioli V, Panzica F, Visani E, *et al.* Myoclonus in Creutzfeldt-Jakob disease: polygraphic and video-electroencephalography assessment of 109 patients. *Mov Disord* 2010;25:2818–27.
580. Lowden MR, Scott K, Kothari MJ. Familial Creutzfeldt-Jakob disease presenting as epilepsia partialis continua. *Epileptic Disord* 2008;10:271–5.
581. Appel SA, Chapman J, Prohovnik I, Hoffman C, Cohen OS, Blatt I. The EEG in E200K familial CJD: relation to MRI patterns. *J Neurol* 2012;259:491–6.
582. Castellani RJ, Colucci M, Xie Z, Zou W, Li C, Parchi P, *et al.* Sensitivity of 14-3-3 protein test varies in subtypes of sporadic Creutzfeldt-Jakob disease. *Neurology* 2004;63:436–42.
583. Gao C, Shi Q, Tian C, Chen C, Han J, Zhou W, *et al.* The epidemiological, clinical, and laboratory features of sporadic Creutzfeldt-Jakob disease patients in China: surveillance data from 2006 to 2010. *PLoS ONE* 2011;6:e24231.
584. Smith TW, Anwer U, DeGirolami U, Drachman DA. Vacuolar change in Alzheimer's disease. *Arch Neurol* 1987;44:1225–8.
585. Chang YJ, Tsai CH, Chen CJ. Leukoencephalopathy after inhalation of heroin vapor. *J Formos Med Assoc* 1997;96:758–60.
586. Thomas NJ, Meteyer CU, Sileo L. Epizootic vacuolar myelinopathy of the central nervous system of bald eagles (Haliaeetus leucocephalus) and American coots (Fulica americana). *Vet Pathol* 1998;35:479–87.
587. Kriegstein AR, Shungu DC, Millar WS, Armitage BA, Brust JC, Chillrud S, *et al.* Leukoencephalopathy and raised brain lactate from heroin vapor inhalation ('chasing the dragon'). *Neurology* 1999;53:1765–73.
588. Koussa S, Zabad R, Rizk T, Tamraz J, Nasnas R, Chemaly R. [Vacuolar leucoencephalopathy induced by heroin: 4 cases]. *Rev Neurol (Paris)* 2002;158:177–82.
589. Amude AM, Alfieri AA, Alfieri AF. Clinicopathological findings in dogs with distemper encephalomyelitis presented without characteristic signs of the disease. *Res Vet Sci* 2007;82:416–22.
590. Sulzer D, Mosharov E, Talloczy Z, Zucca FA, Simon JD, Zecca L. Neuronal pigmented autophagic vacuoles: lipofuscin, neuromelanin, and ceroid as macroautophagic responses during aging and disease. *J Neurochem* 2008;106:24–36.
591. Tung Y-T, Wang B-J, Hu M-K, Hsu W-M, Lee H, Huang W-P, *et al.* Autophagy: a double-edged sword in Alzheimer's disease. *J Biosci* 2012;37:157–65.
592. Donahue JE, Hanna PA, Hariharan S. Autopsy-proven Creutzfeldt-Jakob disease in a patient with a negative 14-3-3 assay and nonspecific EEG and MRI. *Neurol Sci* 2004;24:411–3.
593. Cronier S, Gros N, Tattum MH, Jackson GS, Clarke AR, Collinge J, *et al.* Detection and characterization of proteinase K-sensitive disease-related prion protein with thermolysin. *Biochem J* 2008;416:297–305.

594. Jansen C, Head MW, van Gool WA, Baas F, Yull H, Ironside JW, *et al.* The first case of protease-sensitive prionopathy (PSPr) in The Netherlands: a patient with an unusual GSS-like clinical phenotype. *J Neurol Neurosurg Psychiatry* 2010;81:1052–5.
595. Sajnani G, Silva CJ, Ramos A, Pastrana MA, Onisko BC, Erickson ML, *et al.* PK-sensitive PrP is infectious and shares basic structural features with PK-resistant PrP. *PLoS Pathog* 2012;8:e1002547.
596. Fiorini M, Bongianni M, Monaco S, Zanusso G. Biochemical Characterization of Prions. *Prog Mol Biol Transl Sci* 2017;150:389–407.
597. Kocisko DA, Come JH, Priola SA, Chesebro B, Raymond GJ, Lansbury PT, *et al.* Cell-free formation of protease-resistant prion protein. *Nature* 1994;370:471–4.
598. Saborio GP, Permanne B, Soto C. Sensitive detection of pathological prion protein by cyclic amplification of protein misfolding. *Nature* 2001;411:810–3.
599. Soto C, Anderes L, Suardi S, Cardone F, Castilla J, Frossard M-J, *et al.* Pre-symptomatic detection of prions by cyclic amplification of protein misfolding. *FEBS Lett* 2005;579:638–42.
600. Colby DW, Zhang Q, Wang S, Groth D, Legname G, Riesner D, *et al.* Prion detection by an amyloid seeding assay. *Proc Natl Acad Sci USA* 2007;104:20914–9.
601. Atarashi R, Satoh K, Sano K, Fuse T, Yamaguchi N, Ishibashi D, *et al.* Ultrasensitive human prion detection in cerebrospinal fluid by real-time quaking-induced conversion. *Nat Med* 2011;17:175–8.
602. Castilla J, Saá P, Soto C. Detection of prions in blood. *Nat Med* 2005;11: 982–5.
603. Saá P, Castilla J, Soto C. Presymptomatic detection of prions in blood. *Science* 2006;313:92–4. 1
604. Park JH, Choi YG, Lee YJ, Park SJ, Choi HS, Choi KC, *et al.* Real-Time Quaking-Induced Conversion Analysis for the Diagnosis of Sporadic Creutzfeldt-Jakob Disease in Korea. *J Clin Neurol* 2016;12:101–6. 1
605. Cramm M, Schmitz M, Karch A, Mitrova E, Kuhn F, Schroeder B, *et al.* Stability and Reproducibility Underscore Utility of RT-QuIC for Diagnosis of Creutzfeldt-Jakob Disease. *Mol Neurobiol* 2016;53:1896–904.
606. Barria MA, Gonzalez-Romero D, Soto C. Cyclic amplification of prion protein misfolding. *Methods Mol Biol* 2012;849:199–212.
607. Morales R, Duran-Aniotz C, Diaz-Espinoza R, Camacho MV, Soto C. Protein misfolding cyclic amplification of infectious prions. *Nat Protoc* 2012;7: 1397–409.
608. Sano K, Satoh K, Atarashi R, Takashima H, Iwasaki Y, Yoshida M, *et al.* Early detection of abnormal prion protein in genetic human prion diseases now possible using real-time QUIC assay. *PLoS ONE* 2013;8:e54915.
609. Schmitz M, Cramm M, Llorens F, Müller-Cramm D, Collins S, Atarashi R, *et al.* The real-time quaking-induced conversion assay for detection of human prion disease and study of other protein misfolding diseases. *Nat Protoc* 2016;11:2233–42.

610. Kang H-E, Mo Y, Abd Rahim R, Lee H-M, Ryou C. Prion Diagnosis: Application of Real-Time Quaking-Induced Conversion. *Biomed Res Int* 2017;2017:5413936.
611. Becktel WJ, Schellman JA. Protein stability curves. *Biopolymers* 1987;26:1859–77.
612. Li JJ, Dewey WC. Relationship between thermal tolerance and protein degradation in temperature-sensitive mouse cells. *J Cell Physiol* 1992;151:310–7.
613. Bischof JC, He X. Thermal stability of proteins. *Ann N Y Acad Sci* 2005;1066:12–33.
614. Cuervo AM, Wong ESP, Martinez-Vicente M. Protein degradation, aggregation, and misfolding. *Mov Disord* 2010;25 Suppl 1:S49-54.
615. Ciechanover A, Kwon YT. Degradation of misfolded proteins in neurodegenerative diseases: therapeutic targets and strategies. *Exp Mol Med* 2015;47:e147.
616. Jackson MP, Hewitt EW. Cellular proteostasis: degradation of misfolded proteins by lysosomes. *Essays Biochem* 2016;60:173–80.
617. Ciechanover A, Kwon YT. Protein Quality Control by Molecular Chaperones in Neurodegeneration. *Front Neurosci* 2017;11:185.
618. Fioriti L, Dossena S, Stewart LR, Stewart RS, Harris DA, Forloni G, *et al.* Cytosolic prion protein (PrP) is not toxic in N2a cells and primary neurons expressing pathogenic PrP mutations. *J Biol Chem* 2005;280:11320–8.
619. Bellon A, Seyfert-Brandt W, Lang W, Baron H, Gröner A, Vey M. Improved conformation-dependent immunoassay: suitability for human prion detection with enhanced sensitivity. *J Gen Virol* 2003;84:1921–5.
620. Subramanian S, Madhavadas S, Balasubramanian P. Influence of conformational antibodies on dissociation of fibrillar amyloid beta (A beta 1-42) in vitro. *Indian J Exp Biol* 2009;47:309–13.
621. Choi YP, Peden AH, Gröner A, Ironside JW, Head MW. Distinct stability states of disease-associated human prion protein identified by conformation-dependent immunoassay. *J Virol* 2010;84:12030–8.
622. Choi YP, Gröner A, Ironside JW, Head MW. Comparison of the level, distribution and form of disease-associated prion protein in variant and sporadic Creutzfeldt-Jakob diseased brain using conformation-dependent immunoassay and Western blot. *J Gen Virol* 2011;92:727–32.
623. Grathwohl KU, Horiuchi M, Ishiguro N, Shinagawa M. Sensitive enzyme-linked immunosorbent assay for detection of PrP(Sc) in crude tissue extracts from scrapie-affected mice. *J Virol Methods* 1997;64:205–16.
624. Meyer RK, Oesch B, Fatzer R, Zurbriggen A, Vandevelde M. Detection of bovine spongiform encephalopathy-specific PrP(Sc) by treatment with heat and guanidine thiocyanate. *J Virol* 1999;73:9386–92.
625. Kang S-C, Li R, Wang C, Pan T, Liu T, Rubenstein R, *et al.* Guanidine hydrochloride extraction and detection of prion proteins in mouse and hamster prion diseases by ELISA. *J Pathol* 2003;199:534–41.

626. Dabaghian RH, Barnard G, McConnell I, Clewley JP. An immunoassay for the pathological form of the prion protein based on denaturation and time resolved fluorometry. *J Virol Methods* 2006;132:85–91.
627. Kocisko DA, Lansbury PT, Caughey B. Partial unfolding and refolding of scrapie-associated prion protein: evidence for a critical 16-kDa C-terminal domain. *Biochemistry* 1996;35:13434–42.
628. Peretz D, Scott MR, Groth D, Williamson RA, Burton DR, Cohen FE, *et al.* Strain-specified relative conformational stability of the scrapie prion protein. *Protein Sci* 2001;10:854–63.
629. Callahan MA, Xiong L, Caughey B. Reversibility of scrapie-associated prion protein aggregation. *J Biol Chem* 2001;276:28022–8.
630. Caughey B, Raymond GJ, Kocisko DA, Lansbury PT. Scrapie infectivity correlates with converting activity, protease resistance, and aggregation of scrapie-associated prion protein in guanidine denaturation studies. *J Virol* 1997;71:4107–10.
631. McKenzie D, Bartz J, Mirwald J, Olander D, Marsh R, Aiken J. Reversibility of scrapie inactivation is enhanced by copper. *J Biol Chem* 1998;273:25545–7.
632. McCutcheon S, Hunter N, Houston F. Use of a new immunoassay to measure PrPSc levels in scrapie-infected sheep brains reveals PrP genotype-specific differences. *J Immunol Methods* 2005;298:119–28.
633. Sun Y, Makarava N, Lee C-I, Laksanalamai P, Robb FT, Baskakov IV. Conformational stability of PrP amyloid fibrils controls their smallest possible fragment size. *J Mol Biol* 2008;376:1155–67.
634. Gavier-Widén D, Stack MJ, Baron T, Balachandran A, Simmons M. Diagnosis of transmissible spongiform encephalopathies in animals: a review. *J Vet Diagn Invest* 2005;17:509–27.
635. Lukan A, Vranac T, Curin Šerbec V. TSE diagnostics: recent advances in immunoassaying prions. *Clin Dev Immunol* 2013;2013:360604.
636. Nazor KE, Kuhn F, Seward T, Green M, Zwald D, Pürro M, *et al.* Immunodetection of disease-associated mutant PrP, which accelerates disease in GSS transgenic mice. *EMBO J* 2005;24:2472–80.
637. Stahl N, Prusiner SB. Prions and prion proteins. *FASEB J* 1991;5:2799–807.
638. Prusiner SB. Molecular biology and pathogenesis of prion diseases. *Trends Biochem Sci* 1996;21:482–7.
639. Ryou C. Prions and prion diseases: fundamentals and mechanistic details. *J Microbiol Biotechnol* 2007;17:1059–70.
640. Breitling J, Aebi M. N-linked protein glycosylation in the endoplasmic reticulum. *Cold Spring Harb Perspect Biol* 2013;5:a013359.
641. Aebi M. N-linked protein glycosylation in the ER. *Biochim Biophys Acta* 2013;1833:2430–7.
642. Ermonval M, Mouillet-Richard S, Codogno P, Kellermann O, Botti J. Evolving views in prion glycosylation: functional and pathological implications. *Biochimie* 2003;85:33–45.
643. Deignan ME, Prior M, Stuart LE, Comerford EJ, McMahon HEM. The structure function relationship for the Prion protein. *J Alzheimers Dis* 2004;6:283–9.

644. Lawson VA, Collins SJ, Masters CL, Hill AF. Prion protein glycosylation. *J Neurochem* 2005;93:793–801.
645. Yusa S, Oliveira-Martins JB, Sugita-Konishi Y, Kikuchi Y. Cellular prion protein: from physiology to pathology. *Viruses* 2012;4:3109–31.
646. Varki A. Biological roles of oligosaccharides: all of the theories are correct. *Glycobiology* 1993;3:97–130.
647. Mays CE, Kim C, Haldiman T, van der Merwe J, Lau A, Yang J, *et al.* Prion disease tempo determined by host-dependent substrate reduction. *J Clin Invest* 2014;124:847–58.

CHAPTER 2

DEVELOPMENT AND OPTIMIZATION OF A NEW ELISA APPROACH, BASED ON NOVEL PROPERTIES OF THE PRC7 MAB

Summary

TSEs are fatal neurodegenerative disorders that transmit horizontally and environmentally in humans and animals. Various analytical methods have been developed for PrP^{Sc} analyses and TSE diagnoses. However, each method has both advantages and limitations.[1,2] In fact, PK-sensitive PrP^{Sc} existences and these pathogenic influences have been reported in TSE disease developments.[3-5] Thus, the traditional TSE diagnostic methods using PK reagents have potential risks for false negative results. To overcome some limitations of the current TSE diagnoses, this Chapter 2 attempts to establish new analytical methods for PrP^{Sc} detections. For these purposes, the in-house anti-PrP mAbs of PRC5 and PRC7 were evaluated for applications in Indirect and Sandwich ELISA methods. Both mAbs were capable of detecting recombinant prion protein (RecPrP) of elk and mouse species by the Indirect ELISA application. In addition, these mAbs proved significant capabilities of detecting these RecPrP molecules by the Sandwich ELISA application that composed of the capture PRC7 antibody and the detecting PRC5 antibody. Without PK reagents, this Sandwich ELISA application could detect higher PrP levels in brain homogenates (BH) from TSE-diseased mice, compared to non-infected controls. To improve detectable abilities for PrP^{Sc} isoforms, various preparations and conditions were determined with RecPrP and BH samples to optimize the Sandwich ELISA protocol with PRC7 and

PRC5 mAbs. Furthermore, this Chapter study defines the characteristic feature of the established Sandwich ELISA protocol that is the conformation-dependent PrP recognition.

Introduction

The early detections and preventions of TSEs are critically important to eradicate further epidemic incidences throughout the world. In this dissertation, the overreaching goal set aims to establish new analytical systems for TSE diagnoses without the use of PK reagents. For these aims, ELISA applications utilized features of two anti-PrP monoclonal antibodies (mAbs), PRC5 and PRC7. PRC7 mAb specifically recognizes an unglycosyl form and one monoglycosyl form (mono-1: amino acid residue 180 on mouse) of PrP molecules.[6] In contrast, PRC7 mAb cannot recognize a diglycosyl form of PrP molecules, which the abundance of PrP^{C} isoforms normally express this glycosidic state during non-infected states. In preliminary studies of western blot (WB) assay, PRC7 mAb preferentially detected unglycosyl and mono-1 glycosyl PrP expressions in BH samples from TSE-inoculated mice, while non-infected BH controls did not exhibit clearly (unpublished data). Hence, PRC7 mAb might react selectively with PrP^{Sc} isoforms, but not PrP^{C} isoforms.

WB or immnoprecipitation (IP) assay has been applied to study the PrP glycosylation using some other anti-PrP antibodies.[7-10] However, these methods have limitations, such as time consumption and sensitivity. Compared to WB and IP assays, the ELISA method has the advantaged ability to test greater numbers of samples at the same time, and to detect very low or unknown concentrations of targeted antigens.

Thus, the ELISA method has been widely used as a diagnostic tool in medicine and research because of its high sensitivity and strong specificity. In general, ELISA procedures are quick, convenient, and safe (i.e. no radioactive substance). Several ELISA applications are used routinely for PrP detections in tissue samples with the PK treatment. It is well known that PrP^{C} isoforms are sensitive to this reagent, whereas PrP^{Sc} isoforms are partially resistant.[1,2] Thus, the PK reagent has been a common material specifically for detecting PrP^{Sc} isoforms in TSE research and diagnosis, including WB and IP assays. For this reason, non-PK protocols of these standard methods are extremely limited in TSEs. However, the existence of PK-sensitive PrP^{Sc} agents have been reported, and some studies suggest that significant amounts of PrP^{Sc} isoforms are PK sensitive.[3,4] Therefore, the uses of PK reagents have potential risks of the false negative results for PrP^{Sc} detections in the traditional TSE diagnostic methods. This is a serious concern for food safety and zoonotic transmission in public health. To overcome this critical potential of PK-based analyses, the development of novel assays is required to avoid the use of PK reagents, but to ultimately improve the sensitivity and specificity for PrP^{Sc} detections.

For innovations of more advanced methods in the PrP^{Sc} detection and quantification, anti-PrP mAbs PRC7 (IgG1 isotype) and PRC5 (IgG2a isotype) were applied to develop new sensitive ELISA protocols that can react with PrP^{Sc} isoforms specifically and distinguish glycosylated forms. The established Sandwich ELISA method utilizes the unique properties of PRC7 mAb, named the “7-5 ELISA” method that comprises PRC7 and PRC5 mAbs as the capture and detection antibodies, respectively. Without the use of PK reagents, this new method can detect PrP^{Sc}

isoforms in BH samples from several different species. Thus, the 7-5 ELISA method will be ultimately beneficial for detecting PK-sensitive PrP^{Sc} pathogens in TSE diagnostic investigations as well as for understanding TSE pathogenesis in research. Moreover, the novel 7-5 ELISA method will be the first-reported Sandwich ELISA protocol as specifically capable of the PrP^{Sc} detection and its glycosidic distinguishment. An innovative framework of the dissertation projects is provided in the following.

Materials and Methods

Antibodies

In 2012, Kang HE, et.al, reported the generation and characterization of novel anti-PrP mAbs: PRC1, PRC5, PRC7, and PRC9.[6] This dissertation study evaluates the utilities of PRC5 (IgG2a isotype) and PRC7 (IgG1 isotype) mAbs to develop new ELISA protocols for detecting abnormal misfolding PrP (PrP^{Sc}) agents in the diagnosis of transmissible spongiform encephalopathy (TSE). PRC5 and PRC7 mAbs bind to discontinuous epitopes in the structured globular domain of the PrP molecule. Thus, these mAbs have conformational dependences for the PrP recognition. PRC5 mAb can react with all four glycosylated states of the PrP primary structure: 1) unglycosyl= no glycan at the amino acid residues either 180 or 196; 2) mono-1 glycosyl= a single glycan at the amino acid residue 180; 3) mono-2 glycosyl= one glycan at the amino acid residue 196; and 4) diglycosyl= two glycans at both 180 and 196 amino acid residues, in mouse PrP numbering.[11,12] In contrast, PRC7 mAb only recognizes unglycosyl and mono-1 glycosyl forms of PrP molecules. In general, an abundance of PrP^{C} isoforms consists of a diglycosyl form in a non-TSE infected or healthy state. However, TSE-

infected individuals tend to generate under-glycosylated (no or one glycan) PrP forms.[13] Thus, the use of PRC7 mAb would be specifically capable of determining TSE infectious states by under-glycosylated states. To address this feature, PRC5 and PRC7 mAbs were paired for a conformation- and glycosylation-dependent approach to detect PrP^{Sc} isoforms selectively in the Sandwich ELISA method. In addition, horseradish peroxidase (HRP) conjugated secondary antibodies were applied: Sheep anti-Mouse IgG conjugated with HRP (NXA931, GE Healthcare Life Sciences, Pittsburgh, Pennsylvania, USA) for Indirect ELISA applications, Goat anti-Mouse IgG1 conjugated HRP when PRC7 is a detecting antibody in the Sandwich ELISA application (Cat#40126, Alpha Diagnostic Intl. Inc., San Antonio, Texas, USA), and Goat anti-mouse IgG2a conjugated with HRP (Cat#40127, Alpha Diagnostic Intl. Inc., San Antonio, Texas, USA) for a detecting antibody PRC5 in the Sandwich ELISA method.

Indirect ELISA approach

A protein concentration of each recombinant prion protein (RecPrP) sample was measured by the ultramicroplate reader (ELx808 Absorbance Reader, BioTek Instruments, Inc, Winooski, Vetmont, USA) using the Pierce™ BCA Protein Assay Kit (Thermo Fisher Scientific Inc. Massachusetts, USA). Based on the BCA results, recombinant mouse and elk PrP samples synthesized in house were diluted with a coating buffer (0.05 M Carbonate-Bicarbonate buffer in distilled water) to 400µg/ml protein concentration.[6] For denaturation, the same volume of 8 molar (M) guanidine hydrochloride (GdnHCL; G3272, Sigma-Aldrich Co. LLC, St. Louis, Missouri, USA) in 1X TBS-Tween (TBST) buffer (50mM Tris, 150mM NaCl, 0.05% Tween-20 in distilled

water, pH 7.6) was applied to each prepared RecPrP sample to be 4M concentration during denaturation (protein concentration 200μg/ml) for 15 minutes at room temperature (RT) or testing temperatures (ºC). Denatured samples were diluted ten fold with the coating buffer to be 100μg/ml. Subsequently, serial dilutions of these samples were prepared with the same buffer. For non-denatured samples, 400μg/ml protein concentration of each prepared RecPrP sample was diluted with the same volume of 1X TBST buffer to be 200μg/ml protein concentration. Followed by incubation for 15 minutes at RT or testing temperature (ºC) as matching to a paired sample of the denaturing process, the sample was diluted with a coating buffer to be 100μg/ml and serial dilutions. 100μl of each prepared sample was coated into wells (n=2 for each dilution of a sample) on ELISA plates (Nunc MaxiSorp® flat-bottom 96-well plate, Thermo Fisher Scientific, Rochester, New York, USA). Coated total proteins per well were as follows: 0.48, 0.97, 1.95, 3.90, 7.81, 15.62, 31.25, 62.5, 125, 250, 500 and 1000ng. Also, bovine serum albumin (BSA: Sigma-Aldrich Co. LLC, St. Louis, Missouri, USA) was examined as a control, at the same amounts of total proteins for each dilution. After incubating ELISA plates with these samples overnight at 4ºC, all solutions were removed from the plates. For a blocking process, 200μl of 1X phosphate buffered saline (PBS: no calcium and magnesium, HyClone Laboratories, Inc. GE Healthcare Life Sciences, Logan, Utah, USA) with 3% BSA was added into each well. Followed by 1-hour incubation at 37ºC, each plate was washed three to five times with 1X TBST buffer by a plate washer (the Finstruments^{TM} Microplate Washer, MTX Lab Systems, Inc. Vienna, Virginia, USA). After removing all solutions from plates, 100μl of each primary antibody (PRC5 1:5,000 and PRC7 1:250 dilutions in 1% BSA-containing PBS)

was added into certain wells on the plates. Followed by incubation at 37ºC for 1 hour, the secondary antibody was added to all the testing wells after removing solutions from the plates and washing three times with 1X TBST by the washer. The plates with the secondary antibody were incubated at 37ºC for 1 hour. Subsequently, all solutions were removed from the plates. After washing seven times with 1X TBST by the washer, ABTS® Peroxidase Substrate was applied under the manufacturer's protocol for developing a color reaction. At 405nm, the ultramicroplate reader measured an O.D. value of each well on the plates.

Sandwich ELISA approach

PRC7 and PRC5 mAbs were applied as capture and detecting antibodies, respectively, for establishing a new Sandwich ELISA protocol, called the 7-5 ELISA method. Prior to experiments, testing ELISA plates were prepared with coating a known quantity of each capture antibody. The stock solution of PRC7 mAb was diluted with a coating buffer to be 20μg/ml concentration. 100μl of the diluted PRC7 solution was added into each well on the ELISA plate, and incubated overnight at 4°C. For blocking non-specific binding sites on the well surface, all solutions were removed from the plate. Subsequently, 200μl of 3% BSA-containing PBS was added into each well on the ELISA plate. After 1-hour incubation at 37°C, all solutions were cleared from the plate. Next, the plate was washed three times with 1X TBST buffer using the washer. Each prepared sample coated the wells on the plate, then were incubated overnight at 4°C. The sample-coated plate was emptied and washed three times with 1X TBST. A detecting antibody (i.e. PRC5 mAb, 1mg/ml) was prepared at 1:5,000 into a dilution

buffer (1% BSA-containing PBS without calcium and magnesium). 100µl of the diluted detecting antibody was added per well on the ELISA plate, and then incubated for 1 hour at 37°C. A secondary antibody (Goat Anti-Mouse IgG2 HRP conjugate, 1mg/ml) was prepared at 1:5,000 in a dilution buffer. After evacuating and washing the plate three times with 1X TBST, 100µl of the diluted secondary antibody was used to coat all testing wells. Followed by an incubation for 1 hour at 37°C, the plate was drained and washed seven times with 1X TBST. Under the manufacturer's protocol, ABTS® Peroxidase Substrate was applied for an enzymatic color development. To determine the presence and quantity of antigen by the chemical reaction, the ultramicro plate reader measured the plate for the absorbency of each well at a wavelength of 405nm.

Preparation of brain homogenates

Brain samples isolated from uninfected and TSE-infected mice were stored at -80°C. These samples were repeatedly extruded by aspirations using 18-gauge and serial fine syringe needles in cold 1X PBS (lacking calcium and magnesium) to be a 10% (or 20%) brain homogenate (BH), preparing and testing ELISA, WB assay, and other future experiments. Each TSE-inoculation study with mouse information was recorded in the laboratory database of the Prion Research Center at Colorado State University (CSU). The tested murine BH samples in this chapter are listed in the following table (Table 1). In addition, BH samples from uninfected mice were prepared as controls for comparison with each study mouse group: PrP-KO (no PrP), FVB/n (wild-type MousePrP), Tg5037 (ElkPrP E226), Tg1536 (DeerPrP), Tg3533 (OvinePrP ARQ), and Tg4166 (OvinePrP VRQ). Also, information of brain and other tissue

samples collected from uninfected mice are available in the database (i.e. dates of birth and tissue collection).

Table 1. TSE-inoculated mouse brain homogenate samples

Study Group	Mouse	TSE	Inoculation	Animal
SK-01	FVB/n (wild-type)	Mouse-adapted Scrapie RML*	IC ** 1% BH	D541
RA-150	Tg5037 (ElkPrP E226)	CWD*** Bala05-0308	IC 10^{-4} diluted BH	b581, b582
RA-154	Tg1536 (DeerPrP)	CWD Bala05-0308	IC 10^{-4} diluted BH	b694
CLC-04	Tg5037 (ElkPrP E226)	CWD Bala05-0308	IC 1% BH	F447
CLC-05	Tg1536 (DeerPrP)	CWD Bala05-0308	IC 1% BH	F476
KG-49	Tg3533 (OvinePrP ARQ)	Scrapie 48x38	IC 1% BH	5060
KG-50	Tg3533 (OvinePrP ARQ)	Scrapie SSBP/1	IC 1% BH	5064
KG-51	Tg3533 (OvinePrP ARQ)	Scrapie CH1641	IC 1% BH	5075
KG-62	Tg3533 (OvinePrP ARQ)	Scrapie US Goat Isolate	IC 1% BH	5520
KG-98	Tg4166 (OvinePrP VRQ)	Scrapie SSBP/1	IC 1% BH	6369
JB-66	Tg3533 (OvinePrP ARQ)	Scrapie Colorado Scrapie	IC 1% BH	F1208

*RML: Rocky Mountain Laboratory mouse-adapted scrapie strain

**IC: intracerebral inoculation (30ul BH).

***CWD: Chronic Wasting Disease

Preparation of tissue samples for 7-5 ELISA method

Followed by the manufacturer's protocol of the BCA Protein Assay Kit (Pierce™ BCA Protein Assay Kit), protein concentrations of BH samples were measured by the ultramicroplate reader. To prepare a final protein concentration 200μg/ml of each analyte, a BH sample was aliquoted into an eppendorf tube and diluted with 1X PBS to be 4mg/ml initially. For denaturation, the prepared BH sample and 8M GdnHCL in 50mM Tris buffer were mixed as 1:1 ratio, and incubated at 37°C with agitation by Thermomixer (Eppendorf AG, Hamburg, Germany) for 15 minutes or testing times: 4M GdnHCL during the denaturation. For evaluating lower concentrations of GdnHCL, two times higher concentration of GdnHCL solution was prepared. The same volumes of the GdnHCL and BH samples were mixed to be half concentration of GdnHCL: i.e. 6M GdnHCL to be 3M. These applications were also tested with guanidine thiocyanate (GdnSCN: Fisher Scientific, Fair Lawn, New Jersey, USA). After the incubation, the denatured sample was immediately diluted ten times with 1% BSA-containing PBS. At the final step, a protein concentration of the sample was 200μg/ml: the residue of GdnHCL was 0.4M concentration in the sample. 100μl of the prepared sample (200μg/ml) was coated per well (total protein = 20μg per well) on the prepared ELISA plate with the capture antibody. The sample-coated ELISA plate was stored at 4°C overnight. Subsequent procedures were performed under the Sandwich ELISA approach described above. All these preparations also evaluated RecPrP (mouse and elk) analyte by the 7-5 ELISA method. Note: tested protein concentrations of these RecPrP are listed in the following Results section.

Enhancement of PrP detections by the Sandwich ELISA approach

To enhance PrP detections by the Sandwich ELISA method, a detergent, Triton X^{TM}-100 Electrophoresis (TX100; Fisher Scientific, Fiar Lawn, New Jersey, USA), was applied at the pre-denaturation step in the sample preparation. For coating the final protein concentration 200μg/ml of a testing sample, a BH sample was prepared with 10% increase of protein concentration, compared with the sample preparation described above: i.e. 4mg/ml to 4.4mg/ml. The prepared BH sample was mixed with its 10% volume of 10% TX100-containing PBS (no calcium and magnesium) to be 1% TX100 in the sample in an eppendorf tube. This sample mixture was incubated for 1 hour at 37°C with agitation (BH protein concentration 4mg/ml). During optimizing an application of TX100 or its testing conditions for the 7-5 ELISA protocol, several conditions were modified, such as reagent concentrations in PBS (i.e. 0% TX100 means only 1X PBS), incubation times, and temperatures. Followed by this TX100 incubation, subsequent processes after the denaturation step were performed as described above under the sample preparation procedures for the Sandwich ELISA method.

Conformation-dependent reactivity of the 7-5 ELISA method for PrP detections

PRC7 and PRC5 mAbs have conformational-dependences for binding to PrP molecules. To evaluate these characteristic reactivities in the 7-5 ELISA method, β-mercaptoethanol (βME: 2-Mercaptoethanol, Bio-Rad Laboratories, Inc. Hercules, California, USA) was used to cleave disulfide bonds of structured globular domains in PrP molecules. This chemical application disrupts protein folding and stability, and eventually causes unfolding structures. After the denaturation step in the sample

preparations, 50mM βME in PBS was added into BH samples (βME-treated), whereas only PBS was used for βME-untreated BH samples. These BH samples were incubated for 30 minutes at 55°C and diluted to be 200μg/ml protein concentration (βME 2.56mM as final concentration). In addition, the positive sample controls for the 7-5 ELISA method were prepared without βME and incubation under the current protocol above. To analyze these samples by the 7-5 ELISA method, 100μl of each prepared analyte was coated on the ELISA plate with PRC7 capture antibody and incubated at 4°C overnight. Additional procedures were preformed from the blocking process under the Sandwich ELISA approach above.

Results

Indirect ELISA approach with recombinant PrP

Using RecPrP samples, the utility of PRC7 and PRC5 mAbs was assessed in ELISA methods. As an initial approach, these mAbs were tested by the Indirect ELISA method using RecElkPrP and RecMousePrP. Bovine Serum Albumin (BSA) was used as a control. These samples were diluted for the following range of protein per well (duplicate for each amount): 0.48, 0.97, 1.95, 3.90, 7.81, 15.62, 31.25, 62.5, 125, 250, 500 and 1000ng. All prepared samples were coated onto wells of an ELISA plate, followed by incubations with each primary antibody PRC7 or PRC5 mAb, secondary antibody (Rabbit anti-Mouse IgG conjugated with horseradish peroxidase HRP), and ABTS® Peroxidase Substrate for color development. Both PRC7 and PRC5 mAbs detected the RecPrP samples, compared to the control (Figures 2-1.A and B).

Since these results indicated that PRC7 and PRC5 mAbs reacted with native elk and mouse PrP^C structures, the next assessment was the effect of protein denaturants on detections by the Indirect ELISA method. The RecPrP samples denatured with 4M GdnHCL showed similar O.D. values as non-denatured RecPrP samples. Because both mAbs have binding features to discontinuous conformation-dependent epitopes in the structured globular domain of the PrP molecule, these results suggested that RecPrP particles, once denatured, renature to these native structures that reinstate the conformation of these epitopes.[6] Subsequently, the influence of sample-coating times was evaluated between 30 minutes and 1 hour at RT. This experiment found that longer coating enhanced detections of lower amounts of PrP molecules by both PRC7 and PRC5 mAbs for these recombinant elk and mouse PrP agents (Figures 2-1.C to J).

A.

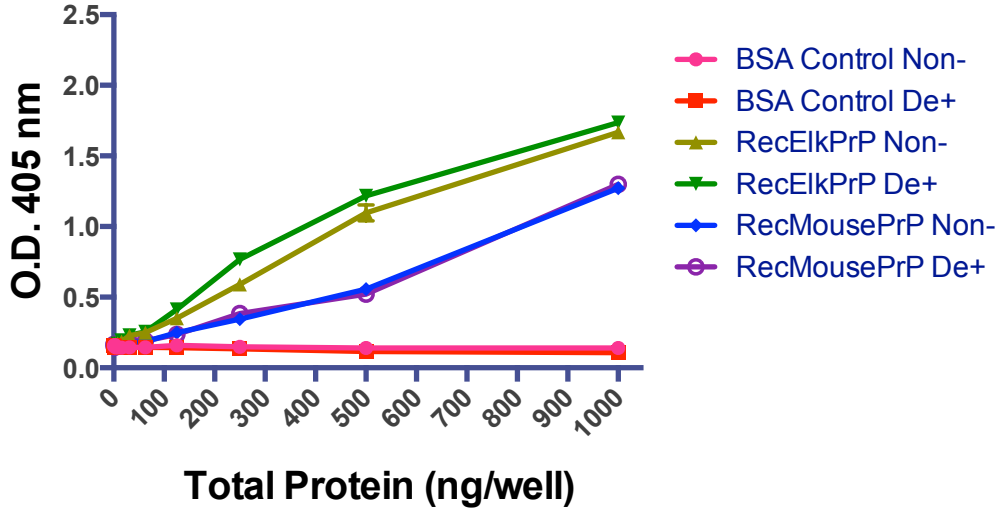
O.D. 405 nm
2.5
2.0
1.5
1.0
0.5
0.0
0
100
200
300
400
500
600
700
800
900
1000
Total Protein (ng/well)
BSA Control Non-
BSA Control De+
RecElkPrP Non-
RecElkPrP De+
RecMousePrP Non-
RecMousePrP De+

B.

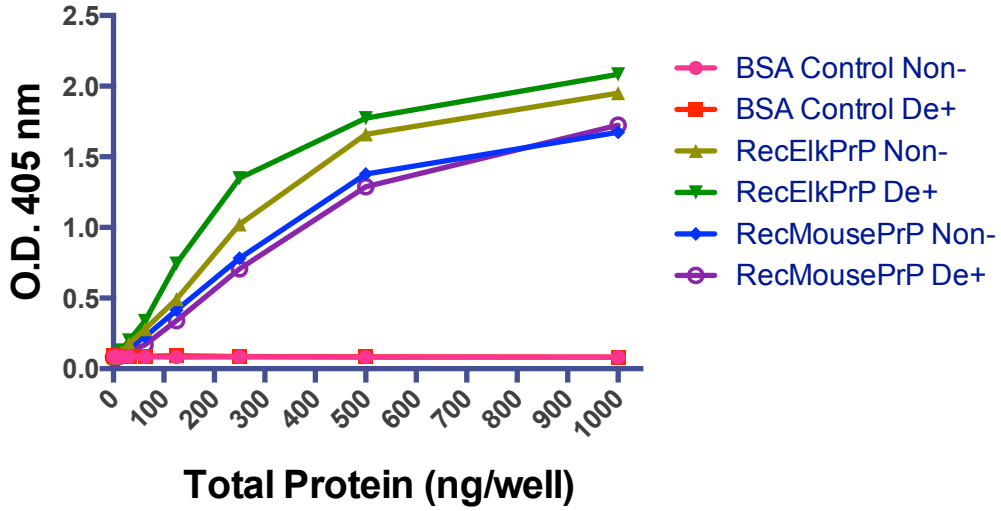
O.D. 405 nm
2.5
2.0
1.5
1.0
0.5
0.0
0
100
200
300
400
500
600
700
800
900
1000
Total Protein (ng/well)
BSA Control Non-
BSA Control De+
RecElkPrP Non-
RecElkPrP De+
RecMousePrP Non-
RecMousePrP De+

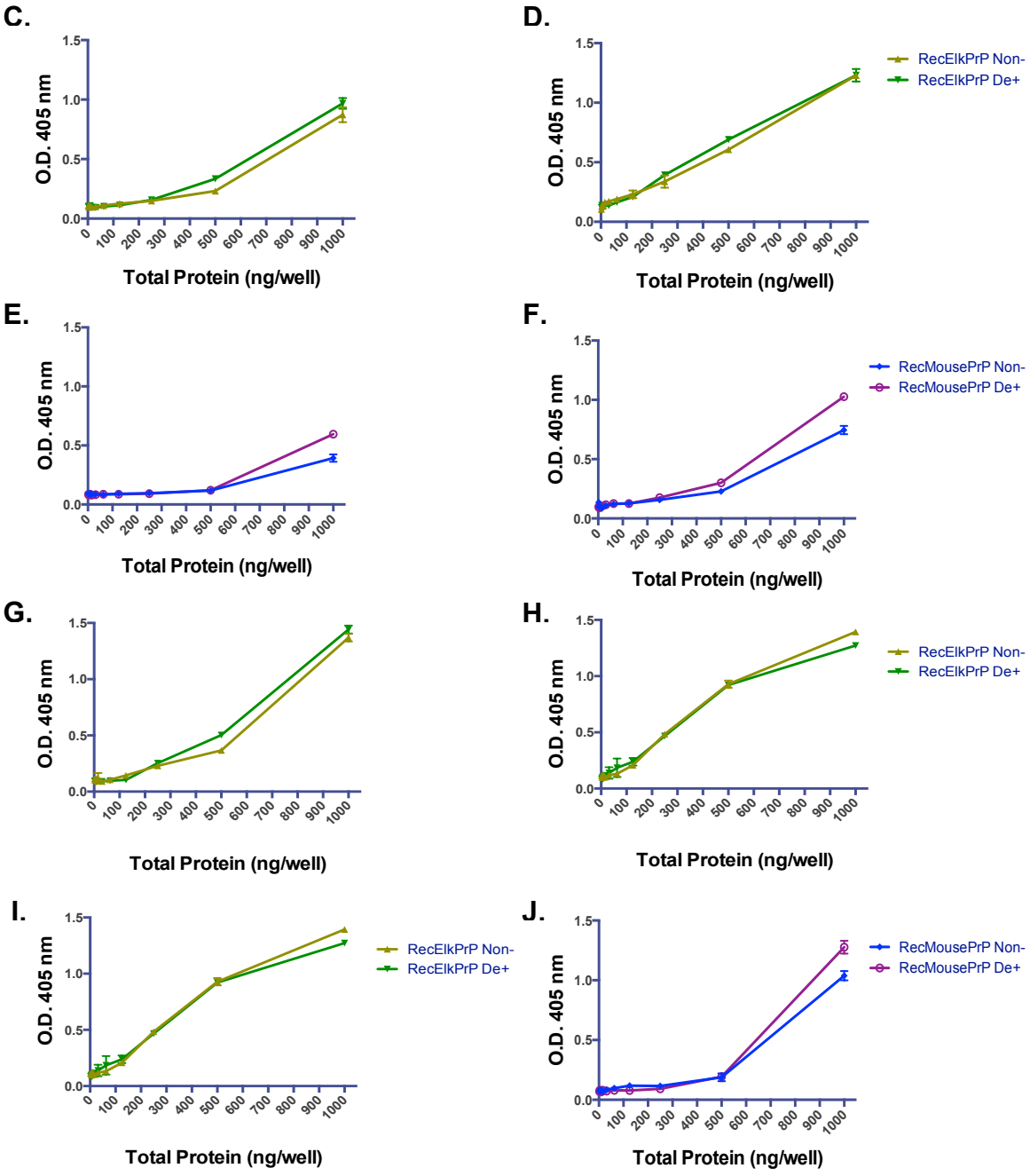

Figure 2-1. Indirect ELISA approaches of PRC7 and PRC5 mAbs.
(A) PRC7 and (B) PRC5, testing with BSA, RecElkPrP, and RecMousePrP
(C) PRC7 with denatured (De+) RecElkPrP for the sample-coating time
30 minutes at RT. (D) PRC7 with De+ RecElkPrP, 1 hour. (E) PRC7 with
De+ RecMousePrP, 30 minutes. (F) PRC7 with De+ RecMousePrP, 1 hour.
(G) PRC5 with De+ RecElkPrP, 30 minutes.(H) PRC5 mAb with De+ RecElkPrP,
1 hour. (I) PRC5 with De+ RecMousePrP, 30 minutes.(J) PRC5 with De+
RecMousePrP, 1 hour. (duplicate for each amount per analyte: well numbers = 2).

Initial Application of the 7-5 ELISA method with recombinant PrP

Based on the capabilities of PRC7 and PRC5 mAbs (IgG1 and IgG2a isotypes respectively) in the Indirect ELISA method, these anti-PrP mAbs were applied to establish a new Sandwich ELISA protocol, called as the 7-5 ELISA method under the order of PRC7 and PRC5 mAbs as capture and detecting antibodies, respectively. Three different conditions were examined using RecElkPrP: 1) non-denaturation, 2) denaturation with 4M GdnHCL at 85°C, or 3) denaturation with 4M GdHCL at RT. This 7-5 ELISA method detected RecElkPrP for all of the three sample conditions. For the RecPrP analyte, denaturant and temperature did not show influence to detect PrP molecules by the 7-5 ELISA method (Figure 2-2). Since the tested RecPrP samples have non-glycosylated structures, there is no limitation for detecting PrP molecules by PRC7 mAbs, which only bind to unglycosyl and mono-1 glycosyl forms of PrP molecules.

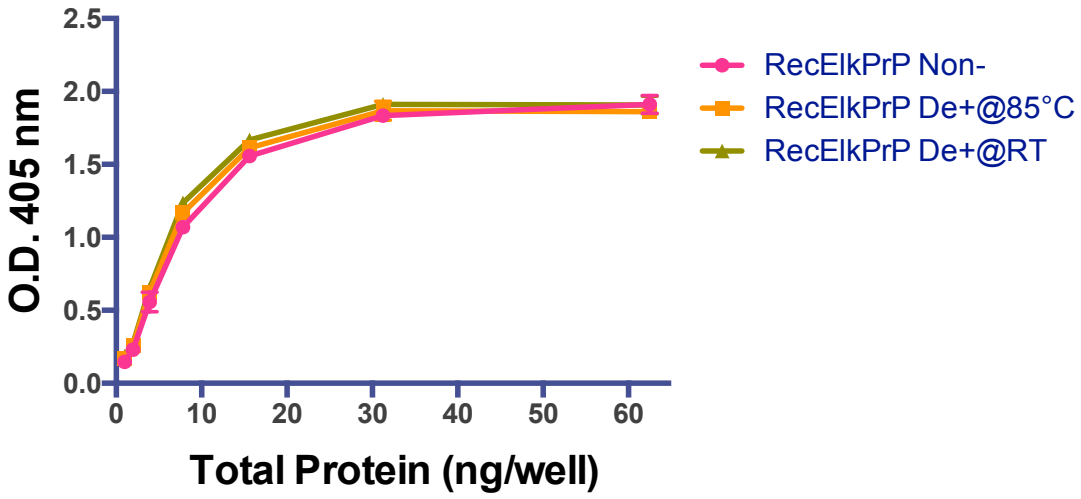

Figure 2-2. Sandwich ELISA approach of PRC7 and PRC5 mAbs. RecElkPrP with non-denaturation (pink and circle), denaturation at 85°C (orange and square), and denaturation at RT (green and triangle). n=2 for each total protein of a sample.

Qualification of PRC5 mAb as a capture antibody in the 5-7 ELISA approach

In opposed to the 7-5 ELISA method, PRC5 mAb was tested as a capture antibody for a Sandwich ELISA approach with PRC7 mAb as a detecting antibody. This alternative antibody order as the 5-7 ELISA approach could detect RecPrP compared to BSA control. However, its O.D. value is much lower than results from the 7-5 ELISA and Indirect ELISA methods of PRC5 mAb under the same amounts of the tested total protein (Figure 2-3.A). In addition, this alternative application showed a potential to cause higher detectable backgrounds, based on O.D values including the BSA control (Figure 2-3.B). Comparing to the 7-5 ELISA results, the 5-7 ELISA approach could not distinguish PrP molecules between RML (Rocky Mountain Laboratory mouse-adapted scrapie)-infected and uninfected materials (Figures 2-3.C and D). Therefore, the application of the 5-7 ELISA approach may not be useful to detect PrP molecules in TSE-infected materials under the protocol procedure for the 7-5 ELISA method at this experimental point. Therefore, the development and optimization of the 7-5 ELISA protocol were concentrated specifically and selectively for PrP detections in TSE-infected materials.

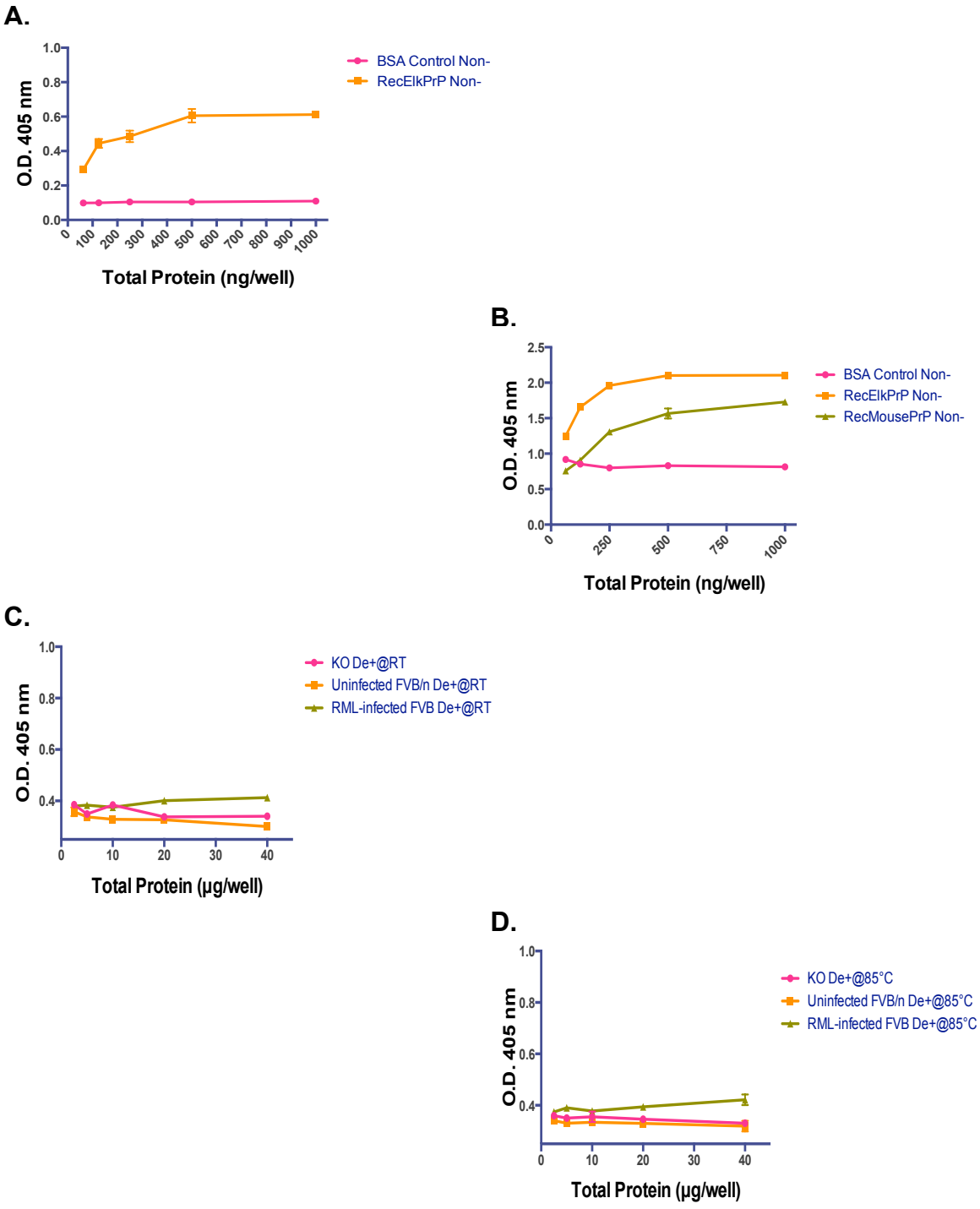

Figure 2-3. The 5-7 ELISA approach with different conditions.
(A) RecElkPrP with non-denaturation, (B) RecElkPrP and RecMousePrP with non-denaturation, (C) mouse BH samples with denaturation at RT, and (D) mouse BH samples with denaturation at 85°C. (n=2 for each prepared sample at a total protein)

Denaturation and temperature optimization for the 7-5 ELISA method

Combinations of three different concentrations of GdnHCL (0, 2, or 4M) with two temperatures (RT or 85°C) were applied to denature BH samples from PrP-KO, uninfected and RML-infected FVB/n mice. These results showed that GdnHCL enhanced PrP detections in the infected samples with the denaturation using 4M GdnHCL at RT, which measured the highest O.D. value (Figures 2-4.A and B). Procedures of 85°C incubation and/or non-denaturation are less effective for PrP detections in the 7-5 ELISA method (Figures 2-4.C to E).

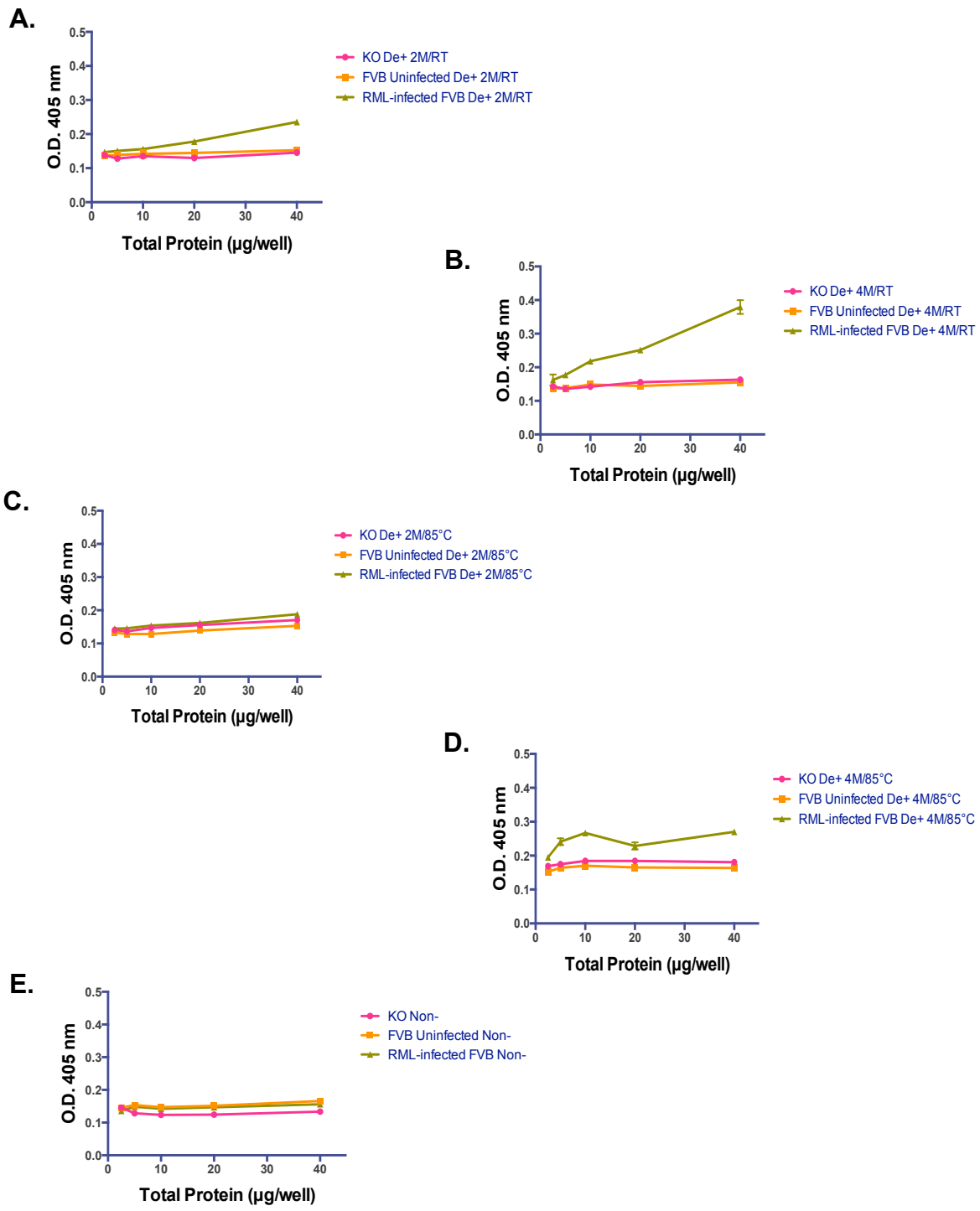

Figure 2-4. GdnHCL concentration and temperature are influential factors for denaturation to detect PrP levels in TSE-infected murine BH samples.
(A) 2M GdnHCL denaturation at RT, (B) 4M GdnHCL denaturation at RT, (C) 2M GdnHCL denaturation at 85°C, (D) 4M GdnHCL denaturation at 85°C, and (E) non-denaturation. (n=2 for each prepared sample at a total protein)

Optimized Concentration of Capture Antibody in the 7-5 ELISA method

To find an optimized concentration of the capture antibody, various concentrations of PRC7 mAb (1, 2.5, 5 and 10μg/ml) were accessed with different total protein levels (2.5, 5, 10, 20, and 40μg per well) of mouse BH samples from uninfected PrP-KO and RML-infected FVB/n mice. The 7-5 ELISA method only detected PrP molecules in the denatured sample from the infected mouse, whereas this method did not detect higher PrP levels in the samples from the knockout or non-denatured infected mouse (Figures 2-5.A to D). In fact, the 10μg/ml PRC7-coating concentration showed the highest O.D. values to detect PrP levels in the infected sample.

A subsequent experiment increased coating concentrations of PRC7 mAb (5, 10, 20, and 30μg/ml) for testing the same brain samples at total protein levels, 10, 20, and 40μg per well (Figures 2-5.E to H). The coating mAb concentrations 20 and 30μg/ml showed equivalent O.D. values for denatured RML-infected samples (Figure 2-5.H).

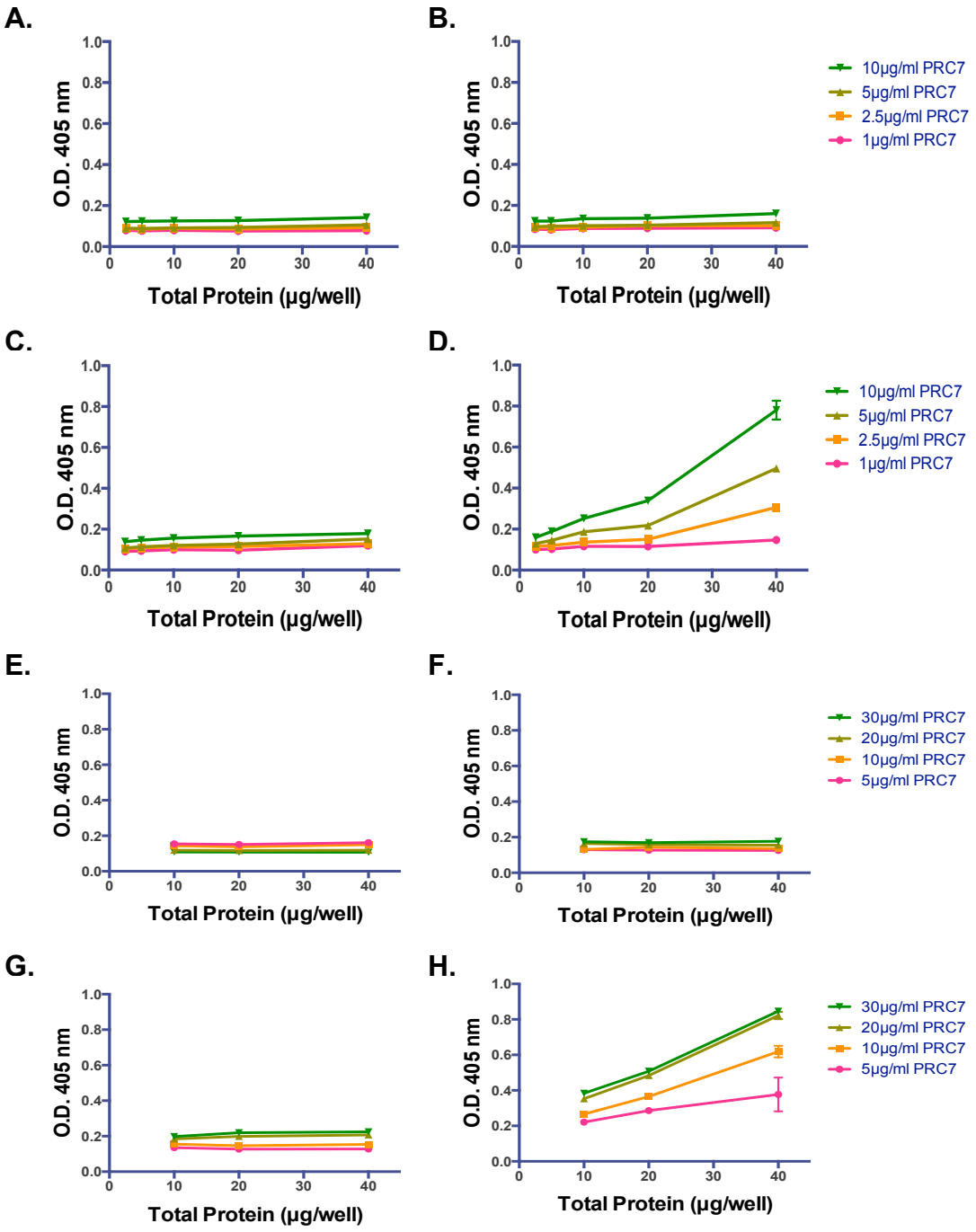

Figure 2-5. Optimized Concentration of PRC7 mAb as Capture Antibody in the range for the 7-5 ELISA method. 1-10µg/ml concentrations: (A) PrP-KO mouse BH sample with non-denaturation, (B) PrP-KO with denaturation at RT, (C) RML-inoculated FVB mouse BH sample with non-denaturation, and (D) RML-inoculated FVB with denaturation at RT. 5-30µg/ml concentrations: (E) PrP-KO mouse BH sample with non-denaturation, (F) PrP-KO with denaturation at RT, (G) RML-inoculated FVB mouse BH sample with non-denaturation, and (H) RML-inoculated FVB with denaturation at RT. (n=2, each total protein amount)

Addition of Triton X-100 to enhance PrP detections in the 7-5 ELISA method

Selecting the 20μg/ml as a coating concentration of PRC7 mAb, the 7-5 ELISA method allowed for detections of PrP levels only in the infected material with denaturation, whereas no detection in the controls of PrP-KO and uninfected FVB/n mice (Figure 2-6.A). However, the detected PrP level in the infected analyte was not a significant high value. To improve the PrP detection in TSE-infected materials, an additional detergent Triton X-100 (TX100) was evaluated for its possible effects in the 7-5 ELISA method, such as the cell lyses, the permeabilization of cell membranes, and the solubilization of membrane proteins.[14] The 1% TX100 addition into testing samples was examined at two different time points before or after denaturation procedures (pre- or post-denaturation). For the pre-denaturation time point, samples with 1% TX100 were initially incubated for one hour at RT. Subsequently, 4M GdnHCL was added into these incubated samples for denaturation, and additionally incubated 15 minutes at RT. For preparing non-denatured controls, the same volume of a diluent buffer (50mM Tris) was added into non-denaturing samples, instead of GdnHCL. The processes of post-denaturation were performed through the opposite direction of pre-denaturation samples by the following: denaturation with 4M GdnHCL in samples for 15 minutes, and then 1-hour incubation with the TX100 addition as 1% in the sample. In non-denatured samples, TX100 did not enhance PrP detections in the infected material at either adding points of this reagent (Figure 2-6.B). However, the TX100 addition at the pre-denaturation time point increased the PrP detection in the infected material, compared to the infected sample without this detergent. In contrast, the infected sample with the TX100 treatment at the post-denaturation time point decreased the O.D. value

(Figure 2-6.B and C). Hence, the use of TX100 should be effective prior to denaturation for higher PrP detections.

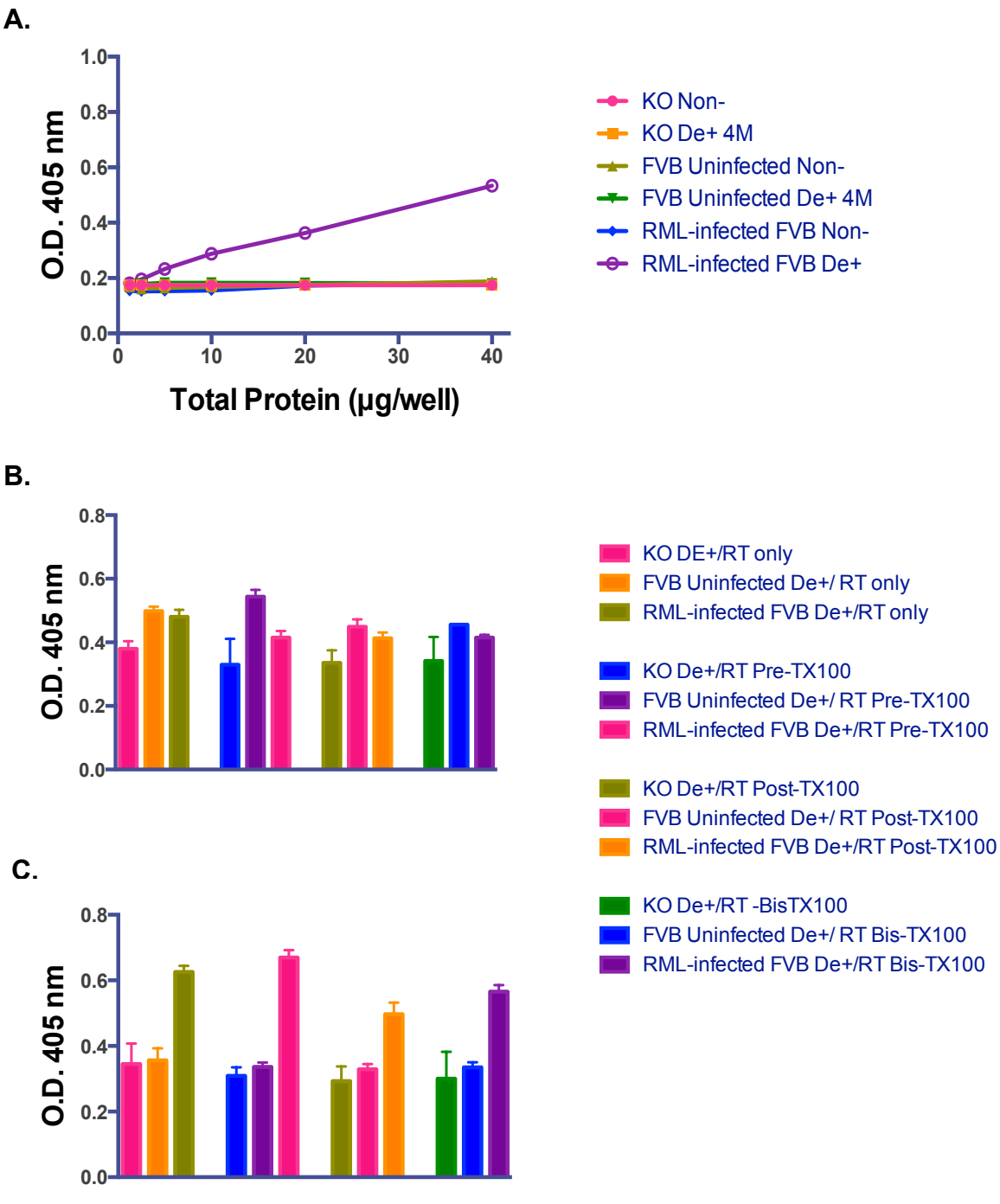

Figure 2-6. Applications of TX100 for enhancing PrP detections in RML-infected murine analyte. (A) PRC7 20µg/ml with denatured BH samples from PrP-KO, uninfected FVB/n and RML-infected FVB/n mice, without TX100 (n=2, each total protein amount). Under the 7-5 ELISA protocol, (B) non-denaturation and (C) denaturation with 4M GdnHCL. Additions of TX100 were compared at pre-denaturation, post-denaturation, or both time points (n=3, each sample category).

Triton X-100 enhances PrP detections in brain homogenates from CWD-infected transgenic mice in the 7-5 ELISA method

Based on the results from the RML-infected mouse BH samples above (Figures 2-4 to 2-6), the same procedure and sample preparation were applied to uninfected transgenic mice expressing elk PrP (referred as Tg5037) and CWD-infected Tg5037 mice. However, the 7-5 ELISA method could not detect PrP levels in the BH samples from the CWD-infected mice and the uninfected mice. To overcome this issue, TX100 was used to enhance the PrP detection in CWD-infected materials. For testing this detergent at three different percentages 0, 1, or 5% (0% = only PBS), the following conditions were also applied to sample preparations: 1) non-denaturation, 2) denaturation, and 3) incubation at RT or 85°C. As the same application in Sections 2 and 3, two time points (pre- or post-denaturation) were tested for adding 1% TX100 into testing samples and incubating 1 hour at RT. Wells in these ELISA plates were duplicated for each category. In non-denatured sample preparations, the 7-5 ELISA method did not show clear differences for O.D. values between infected and uninfected materials under these two temperatures (Figure 2-7.A and B). In contrast, denatured samples at RT with 1% TX100 at pre-denaturation enhanced the PrP detection in the CWD-infected material, compared to uninfected and KO mouse samples (Figure 2-7.C). Moreover, denaturation at 85°C was ineffective, which may be due to the high temperature because of the cloud point of TX100, known to be 66°C (Figure 2-7.D). Compared to the condition of 0% TX100 with denaturation at RT, the PrP detection in the CWD-infected material was enhanced with 1% TX100 (Figure 2-7.E). Note: a cloud point is the temperature at which an aqueous solution of a water-soluble surfactant (i.e.

TX100) starts to solidify molecular agglomerates, resulting in cloudy precipitations.[15] Thus, a cloud point influences a phase separation, stability, and effect of a surfactant during its use.

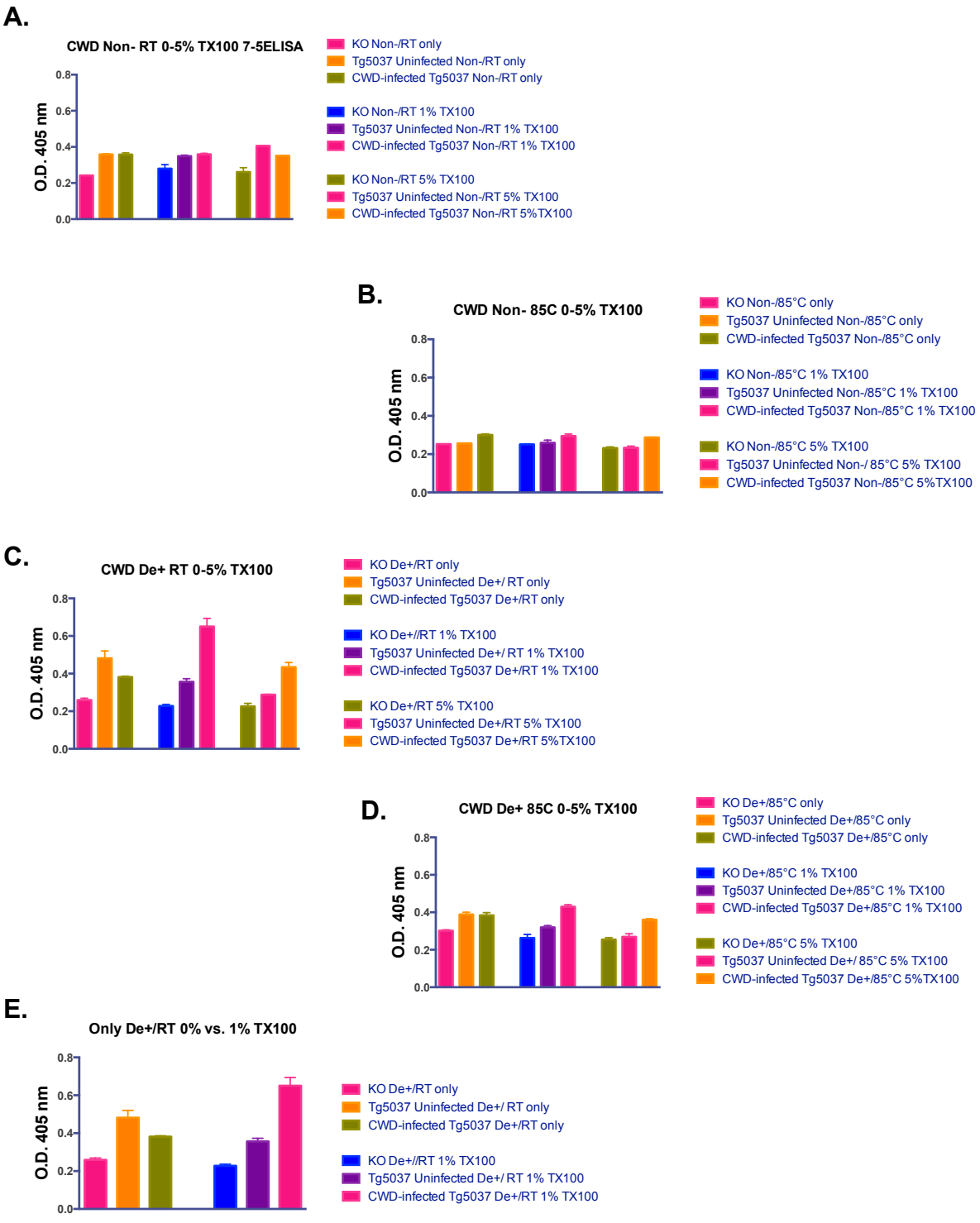

Figure 2-7. TX100 enhances PrP detections in CWD-infected murine analyte. Under the 7-5 ELISA protocol testing with 0, 1, or 5% TX100 concentration, (A) non-denaturation at RT, (B) non-denaturation at 85°C, (C) denaturation at RT, (D) denaturation at 85°C, (E) comparison of 0% (left side) and 1%(right side) TX100 at RT incubation and denaturation. (n=3, each sample category)

Optimizations of incubation times and temperatures with TX100 and GdnHCL

In order to evaluate the optimal conditions of TX100 in the 7-5 ELISA method, three concentrations (0, 0.5, and 1%) of this detergent were initially tested at different incubation times (1 hour vs. 16 hours) and temperatures (RT vs. 37°C). For each sample group, a same temperature was applied for incubations of TX100 treatment and GdnHCL denaturation: i.e. the A sample at RT for TX100 and GdnHCL, and the B sample at 37°C for TX100 and GdnHCL. Through the 1-hour incubation with 0.5 or 1% TX100 and a subsequent incubation with GdnHCL denaturation for 15 minutes, the 37°C incubation temperature enhanced higher O.D. values for PrP detections in CWD-infected materials, compared to the RT incubations (Figures 2-8.A and B). In contrast, the 16-hour incubation with TX100 showed opposite results, whereas the 1-hour TX100 incubation detected higher O.D. values in the infected material (Figures 2-8.C and D). Therefore, this shorter TX100 incubation with 37°C can be practical for further applications of the 7-5 ELISA method as laboratory procedures and diagnostic applications. Furthermore, several denaturation times of GdnHCL were compared to the 15-minute incubation in the all experiments above. Prior to the denaturation, all samples were incubated with 0.5% TX100 at 37°C for 1 hour. Following this TX100 treatment, these samples were denatured with GdnHCL, testing for 10, 15, 30 or 60-minute incubation. Measured by the 7-5 ELISA method, the denatured samples for the 15-minute incubation showed the peak of PrP detections in CWD-infected material, whereas longer incubations decreased O.D. values (Figure 2-8.E). In addition, the 7-5 ELISA method showed higher O.D. values of PrP detections in CWD-infected material with treatments of TX100 for 1 hour and GdnHCL for 15 minutes, compared to non-

denatured samples with 0.5% TX100 at 37°C (Figure 2-8.F). These results indicated that the 7-5 ELISA method required denaturation for PrP^{Sc} detections in TSE-infected materials.

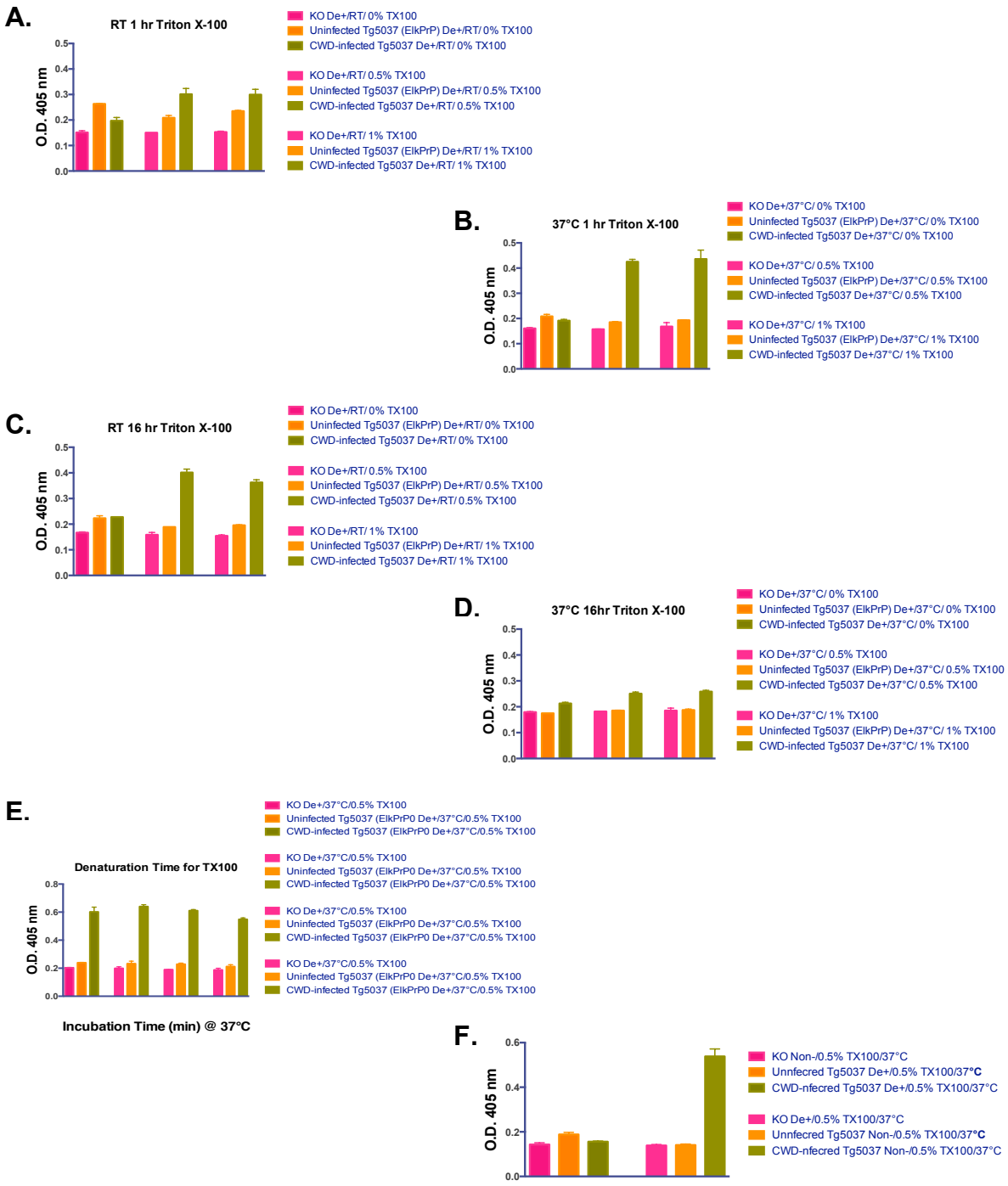

Figure 2-8. Optimizations of sample-incubation times and temperatures with TX100 and GdnHCL for PrP detections in CWD-infected murine BH samples. Under the 7-5 ELISA protocol, (A) 1-hour TX100 incubation at RT, (B) 1-hour TX100 incubation at 37°C, (C) 16-hour TX100 incubation at RT, (D) 16-hour TX100 incubation at 37°C, (E) comparison of GdnHCL-incubation time (10, 15, 30, and 60 minutes) with 1-hour TX100 incubation at 37°C, and (F) Comparison of non-denatured and denatured-murine BH samples with 0.5% TX100 and GdnHCL, 1-hour incubations at 37°C. (n=3, each sample category)

Optimization of incubation temperatures and agitation for sample preparations

To compare the effective sample preparations from the 7-5 ELISA method using CWD-infected materials above, the identified procedures were applied to BH samples from RML-infected FVB/n, uninfected FVB/n, and PrP-KO mice. Briefly, prepared BH samples were incubated with TX100 for 1 hour and 4M GdnHCL denaturation for 15 minutes, at either RT or 37°C. These testing samples were agitated at 800rpm in the Thermomixer (eppendorf) throughout these incubations. This approach attempted to obtain consistent protocol for minimizing influences from sample types, such as among species, TSE strains, and other experimental variables. Another notable modification was changing dilutions of the detecting antibody PRC5 mAb from 1:2,000 (Figures 2-9.A and B) to 1:5,000 (Figures 2-9.C and D). Compared to controls in testing ELISA-plate wells, the 1:2,000 dilution of the PRC5 concentration showed color developments in the infected materials faster than the 1:5,000 dilution (Figures 2-9.A to D). Conversely, the 1:5,000 dilution enhanced PrP detections in the PrP^{Sc}-contained materials. These results could be arisen from a higher binding probability of the secondary antibody to PRC5 mAb, which could induce quicker reactions for color development. In fact, color changes occurred in the controls because the secondary antibody can bind to murine IgG2a in the testing mouse samples. Based on these results, the 7-5 ELISA method was applied to protein-dose dependent responses for the samples with the 0.5% TX100 treatment (Figure 2-9.E). Clearly, these modifications above enhanced detectable levels of PrP molecules in TSE-infected materials by the 7-5 ELISA method.

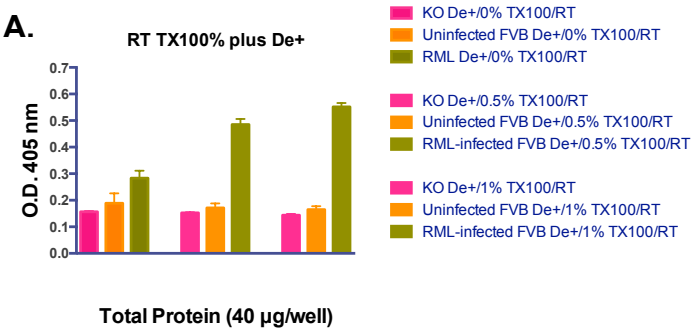
A.
RT TX100% plus De+
O.D. 405 nm
0.7
0.6
0.5
0.4
0.3
0.2
0.1
0.0
KO De+/0% TX100/RT
Uninfected FVB De+/0% TX100/RT
RML De+/0% TX100/RT
KO De+/0.5% TX100/RT
Uninfected FVB De+/0.5% TX100/RT
RML-infected FVB De+/0.5% TX100/RT
KO De+/1% TX100/RT
Uninfected FVB De+/1% TX100/RT
RML-infected FVB De+/1% TX100/RT
Total Protein (40 µg/well)

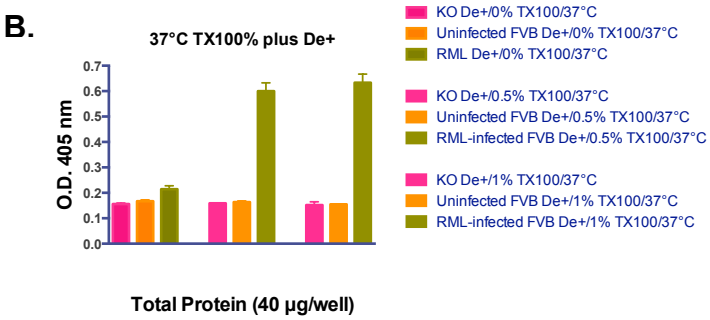
B.
37°C TX100% plus De+
O.D. 405 nm
0.7
0.6
0.5
0.4
0.3
0.2
0.1
0.0
KO De+/0% TX100/37°C
Uninfected FVB De+/0% TX100/37°C
RML De+/0% TX100/37°C
KO De+/0.5% TX100/37°C
Uninfected FVB De+/0.5% TX100/37°C
RML-infected FVB De+/0.5% TX100/37°C
KO De+/1% TX100/37°C
Uninfected FVB De+/1% TX100/37°C
RML-infected FVB De+/1% TX100/37°C
Total Protein (40 µg/well)

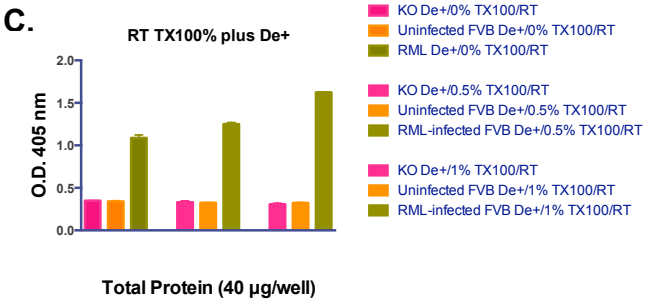
C.
RT TX100% plus De+
O.D. 405 nm
2.0
1.5
1.0
0.5
0.0
KO De+/0% TX100/RT
Uninfected FVB De+/0% TX100/RT
RML De+/0% TX100/RT
KO De+/0.5% TX100/RT
Uninfected FVB De+/0.5% TX100/RT
RML-infected FVB De+/0.5% TX100/RT
KO De+/1% TX100/RT
Uninfected FVB De+/1% TX100/RT
RML-infected FVB De+/1% TX100/RT
Total Protein (40 µg/well)

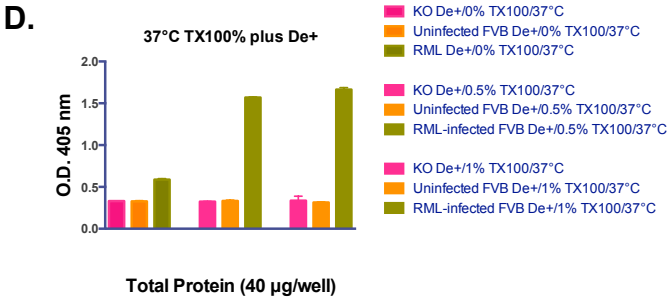
D.
37°C TX100% plus De+
O.D. 405 nm
2.0
1.5
1.0
0.5
0.0
KO De+/0% TX100/37°C
Uninfected FVB De+/0% TX100/37°C
RML De+/0% TX100/37°C
KO De+/0.5% TX100/37°C
Uninfected FVB De+/0.5% TX100/37°C
RML-infected FVB De+/0.5% TX100/37°C
KO De+/1% TX100/37°C
Uninfected FVB De+/1% TX100/37°C
RML-infected FVB De+/1% TX100/37°C
Total Protein (40 µg/well)

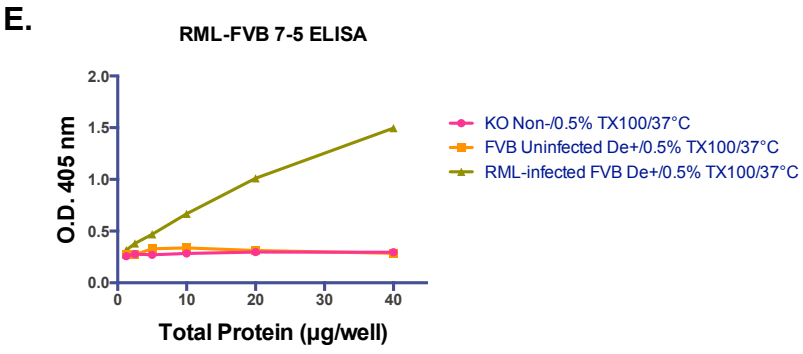
E.
RML-FVB 7-5 ELISA
O.D. 405 nm
2.0
1.5
1.0
0.5
0.0
0
10
20
30
40
KO Non-/0.5% TX100/37°C
FVB Uninfected De+/0.5% TX100/37°C
RML-infected FVB De+/0.5% TX100/37°C
Total Protein (µg/well)

Figure 2-9. Optimizations of sample-incubation times and temperatures with TX100 and GdnHCL for PrP detections in RML-infected murine BH analyte. PRC5 mAb applications at (A) 1:2,000 dilution with TX100 and GdnHCL incubations at RT, (B) 1:2,000 dilution with TX100 and GdnHCL incubations at 37°C, (C) 1:5,000 dilution with TX100 and GdnHCL incubations at RT, (D) 1:5,000 dilution with TX100 and GdnHCL incubations at 37°C, (E) PRC5 mAb 1:5,000 application with 0.5% TX100 and denaturation with 1-hour incubation at 37°C. (n=3, each analyte category or amount)

Comparisons of sample incubation times for the 7-5 ELISA method

In the Figure 2-1, sample-coating times were compared using RecPrP with PRC7 and PRC5 mAbs by the Indirect ELISA method. These results indicated that longer coating times enhanced detections of RecPrP by these mAbs, especially for lower amounts of the antigens (Figures 2-1.C to J). Under the developed protocol of the 7-5 ELISA method above, incubations for samples-coating times were evaluated. Note: PRC7 capture antibody was already coated on each well of the testing ELISA plate as a preparation. This experiment included the following murine BH samples: RML-inoculated FVB/n mice, controls (uninfected FVB/n and PrP-KO mice), and TSE-inoculated transgenic mice with PrP expressions of deer (Tg1536), elk (Tg5037), or sheep (Tg3533 with alanine (Ala: A) at the amino acid residue 136). Compared to the 1-hour sample incubation, the overnight (16 hours) sample incubation enhanced the PrP detection in all of the TSE-infected materials, while no significant increase of PrP detections in the control samples (Figures 2-10.A and B). In contrast, the 6-hour sample incubation exhibited an equivalent O.D. value of PrP detections in the RML-infected sample, compared to the overnight sample incubation (Figure 2-10.C). Therefore, 6-hour sample incubation could be applicable to save time consumption for urgent or emergency cases that would require rapid TSE diagnoses. However, the overnight incubation should be practical for time scheduling in daily laboratory works.

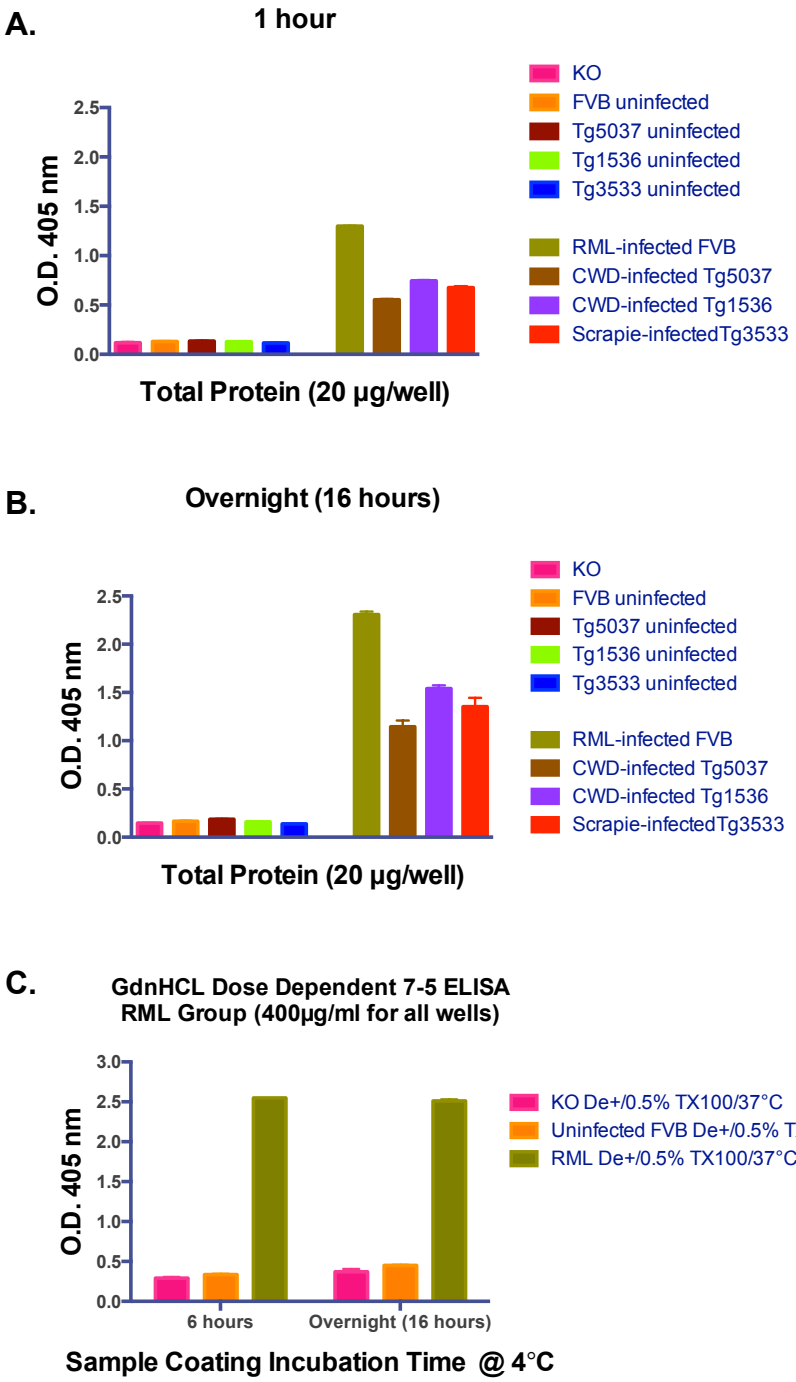

Figure 2-10. Comparisons of sample-incubation times for the 7-5 ELISA method. (A) 1-hour incubation at 4°C, (B) 16-hour incubation at 4°C, and (C) compared incubations of 6 hours and 16 hours at 4°C. (n=3, each sample category with 20µg total protein amount)

Conformation-dependent reactivity of the 7-5 ELISA method for the PrP detection

PRC7 and PRC5 mAbs are described as conformation-dependent antibodies against PrP molecules.[6] In mouse PrP numbering, PRC5 mAb binds to the amino acid residues A132 and N158 constituting a discontinuous epitope. PRC7 mAb recognizes the residues Y154 and Q185 constituting a discontinuous epitope. These residues acquire the proximity that requires for antibody recognitions in tertiary structures of PrP^C isoforms. Therefore, the reactivities of these two mAbs are dependent on the PrP conformation. These reactivities of conformation-dependent antibodies were evaluated by the WB assay with and without proteinase K, using BH samples from RML-infected wild-type mice in the presence or absence of β-mercaptoethanol (βME).[6] βME is a reducing agent, commonly used to cleave disulfide bonds that consist of structured globular domains in proteins. Disulfide bonds play an important role for protein folding and stability. In fact, the WB assay reduced PrP detections in the presence of βME with the uses of PRC7 and PRC5 mAbs. These observations indicated the characteristic features of these mAbs, which recognized discontinues epitopes with conformational-dependences reactivities. Based on the WB results, βME was applied to evaluate the conformation-dependent reactivity of the 7-5 ELISA method for PrP detections. Initially, BH samples from RML-infected and control mice were incubated for one-hour incubation with 0.5% TX100 and 15-minute with 4M GdnHCL. 50mM βME in PBS was added into a βME-treated (+) sample, whereas only PBS addition for a βME untreated (-) sample. Subsequently, these βME samples were incubated for 30 minutes at 55°C. The positive control was prepared without this βME addition and incubation, as under the current protocol. Intriguingly, by the 7-5 ELISA method could not detect PrP levels in

RML-infected samples with the βME treatment, as an equivalent O.D. value to the controls (Figure 2-11). Hence, PRC7 and PRC5 mAbs could not react with PrP molecules because βME disrupted disulfide bands and globular structures of PrP conformations. Therefore, it is obvious that the 7-5 ELISA method has the property of conformational dependence for PrP detections. Compared to the positive controls of the RML-infected sample, the infected sample with non-βME treatment (PBS only) decreased O.D. value for PrP detections. This outcome might link to the extra incubation time for the βME treatment with higher temperature. Possibly, this additional incubation could induce further denaturations to the sample. As mentioned in Section 2-8, longer denaturation times decreased O.D. values of PrP detections in TSE-infected materials (Figure 2-8.E).

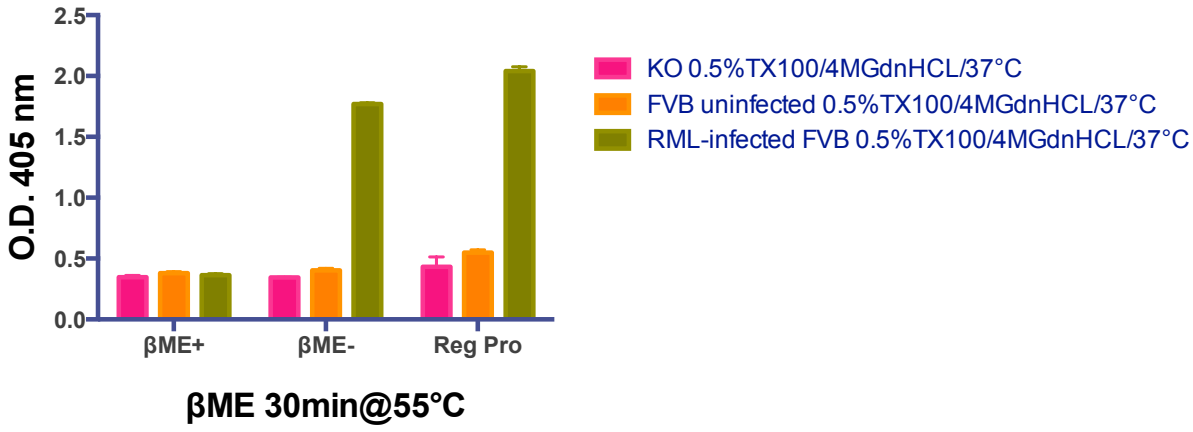

Figure 2-11. The 7-5 ELISA method has a conformation-dependent reactivity for the PrP detection in RML-infected murine analyte. (n=3, each analyte with 20μg total protein amount)

Comparisons of two denaturants in the 7-5 ELISA method

Guanidine hydrochloride (GdnHCL) and guanidine isothiocyanate (GdnSCN) are common denaturants in the TSE research field for measuring PrP^{Sc} isoforms.[16-18] The effectiveness of these denaturants was compared under sample preparations for the 7-5 ELISA method. Testing samples were denatured with different concentrations of GdnHCL (0-4M) or GdnSCN (0-3M) for 15 minutes at 37°C incubation. In the GdnHCL study, the 4M concentration showed the highest O.D. value of PrP detections in the TSE-infected material (Figure 2-12.A). However, the 2M GdnHCL concentration showed the reduced O.D. value, compared to lower concentrations. This phenomenon was also observed in the repeated experiment (Figure 2-12.B). In the GdnSCN study, the 3M concentration showed the highest O.D. value of PrP detections in the infected material (Figure 2-12.C). However, GdnSCN was less effective to detect PrP levels by the 7-5 ELISA method, compared to GdnHCL. To confirm a potential negative effect of TX100 to GdnSCN, 0% (only PBS) and 0.5% TX100 treatments were compared for the same samples above. After the 1-hour incubation at 37°C, these samples were denatured with 3M GdnSCN. These results found that 0.5% TX100 enhanced PrP detections in the infected material (Figure 2-12.D). Hence, TX100 did not interfere the effect of GdnSCN in the 7-5 ELISA method. Therefore, GdnHCL is a proper reagent for sample denaturation in the 7-5 ELISA protocol than GdnSCN. The use of TX100 also enhanced efficacies of denaturants for PrP detections in TSE-infected materials by the 7-5 ELISA method.

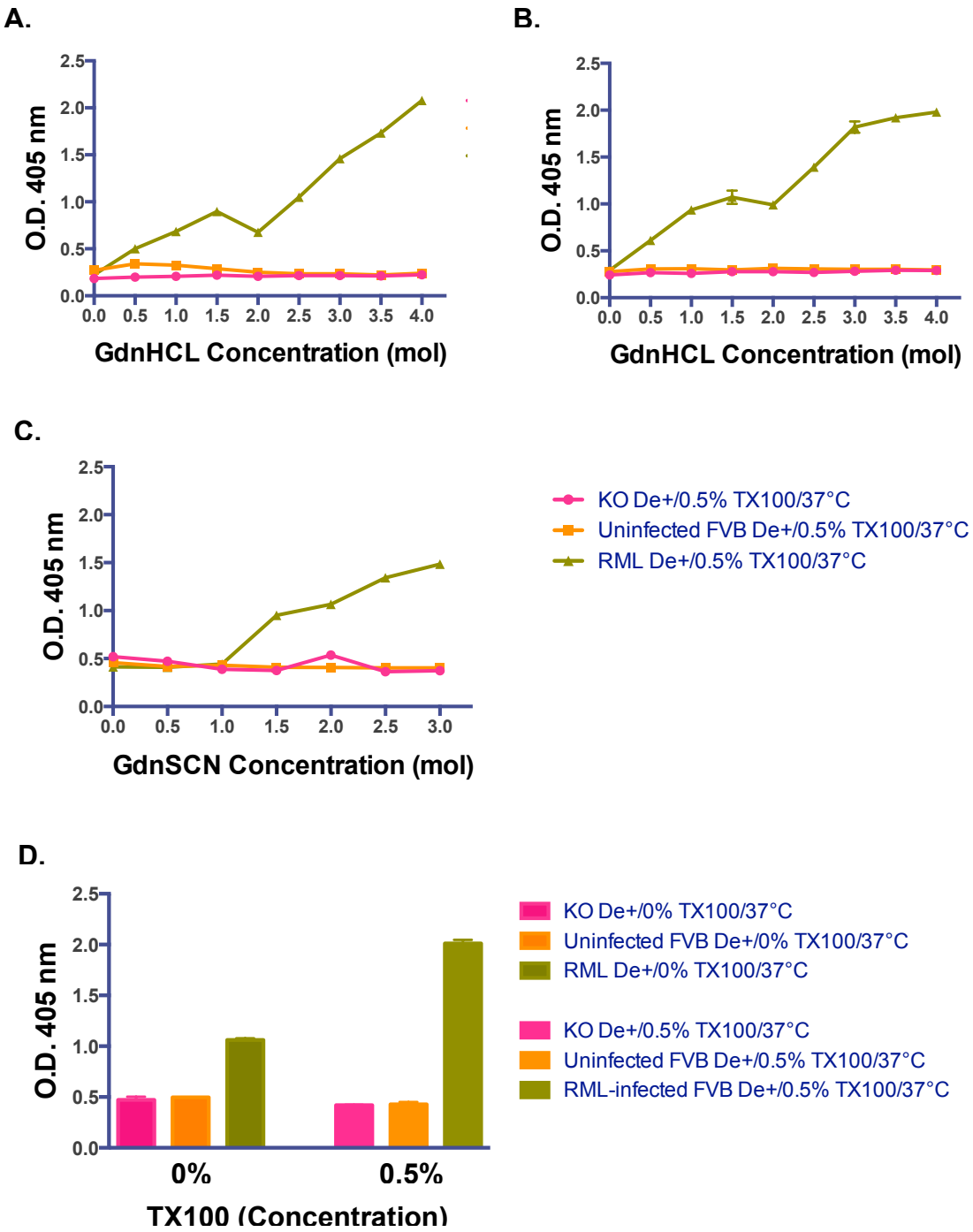

Figure 2-12. Comparison of GdnHCL and GdnSCN for the sample denaturation in the 7-5 ELISA method. (A) GdnHCL-dose dependence, (B) Repeated evaluation of GdnHCL-dose dependence, (C) GdnSCN-dose dependence, (D) TX100 application with GdnSCN denaturation. (n=2, each analyte with 40μg total protein amount)

Higher temperature incubations with both denaturants using the 7-5 ELISA method

Previously, sample denaturations were evaluated at different temperatures: RT, 37°C and 85°C. For the next step, samples for the 7-5 ELISA method were denatured with 4M GdnHCL or 3M GdnSCN at different temperatures between 37°C and 85°C. In GdnHCL, 67°C incubation showed slightly higher O.D. values in the CWD-infected materials, compared to lower temperatures (Figure 2-13.A). In contrast, GdnSCN decreased O.D. values in the infected samples along with increased temperatures (Figure 2-13.B). Potentially, a GdnSCN treatment might not require a heating process for samples, measured by the 7-5 ELISA method. For a further analysis, temperatures 37, 65, 75, and 85°C were evaluated for sample denaturations with 4M GdnHCL. As a result, these temperatures did not show clear differences for PrP detections in the infected materials (Figure 2-13.C). Hence, 37°C should produce an equivalent effect to higher temperatures for PrP detections in denatured TSE-infected materials.

A.

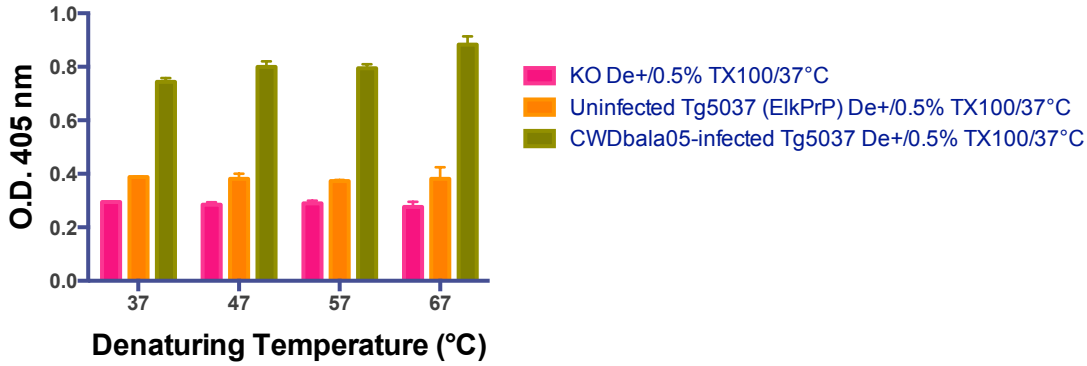

B.

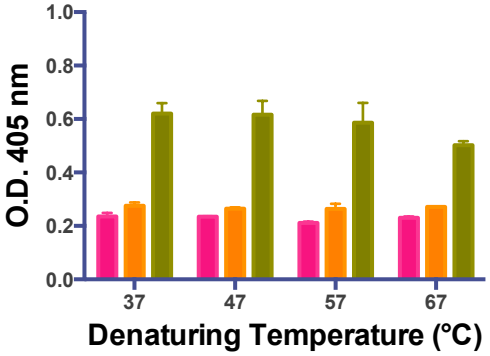

C.

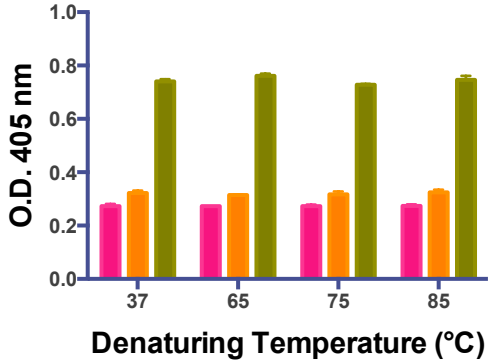

Figure 2-13. Influences of high denaturing temperatures for PrP detections. For the sample preparation under the 7-5 ELISA protocol, (A) 4M GdnHCL denaturation, (B) 3M GdnSCN denaturation, and (C) repeated evaluation with 4M GdnHCL denaturation. (n=3, each analyte with 40µg total protein amount)

Efficacy of TX100 when using recombinant PrP in the 7-5 ELISA method

To evaluate the TX100 effectiveness for PrP detections, this detergent was treated with recombinant PrP that is composed of a native PrP-globular structure. For the 7-5 ELISA method, the following four different conditions were applied to RecElkPrP, RecMousePrP, and a BSA control: A) no TX100 and GdnHCL reagent, B) only 0.5% TX100 treatment without GdnHCL, C) only 4M GdnHCL denaturation without TX100, and D) both 0.5% TX100 and 4M GdnHCL reagents (Figures 2-14.A to D). These procedures were performed by the following incubations: 1 hour for TX100 and 15 minutes for GdnHCL at 1,000 rpm agitation and 37°C. The TX100-only treatment (B condition) enhanced detections of RecPrP even at lower amounts of total proteins, compared to no treatment (A condition) (Figures 2-14.A and B). In addition, both treatments (D condition) induced higher RecPrP detections than only GdnHCL denaturation (C condition) (Figures 2-14.C and D). Based on these results, the TX100 treatment demonstrated the ability to enhance PrP detections. Also, this detergent has an effect to enhance or prolong GdnHCL denaturation for RecPrP structures. Therefore, the TX100 application could be useful as a selective approach to detect abnormal PrP structures with GdnHCL denaturation.

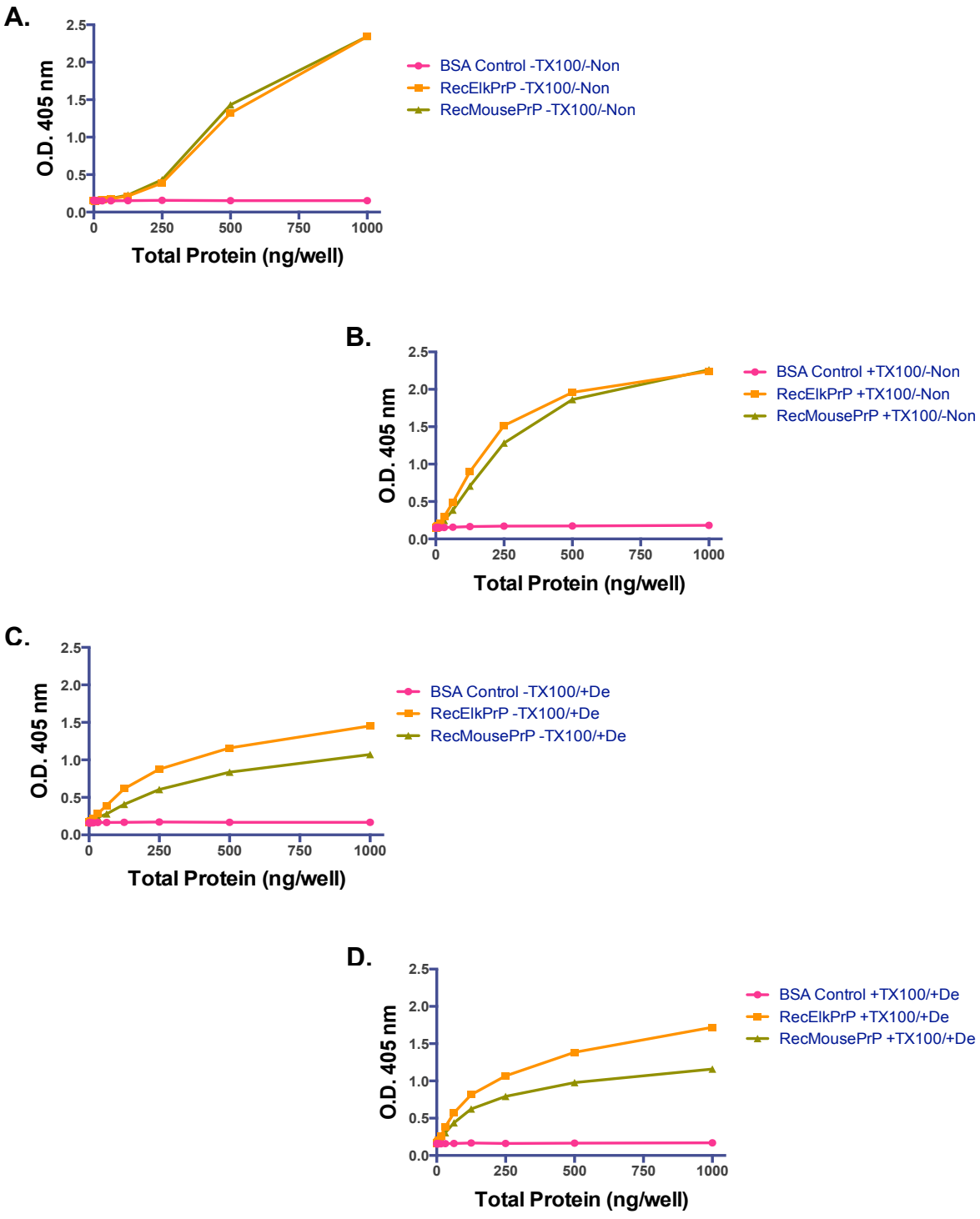

Figure 2-14. Evaluation of TX100 efficacy for recombinant PrP in the 7-5 ELISA method. For the sample preparation of RecMouse PrP under the 7-5 ELISA protocol, applications of (A) no TX100 and GdnHCL reagent, (B) only 0.5% TX100 treatment without GdnHCL, (C) only 4M GdnHCL denaturation without TX100, and (D) both 0.5% TX100 and 4M GdnHCL reagents.

Denaturant effects for recombinant PrP by the 7-5 ELISA method

In the GdnHCL-dose dependent evaluation, 0.5% TX100 was added to all testing samples for the 1-hour incubation process at 37°C prior to denaturations. After that, RecElkPrP and RecMousePrP were denatured with different concentrations of GdnHCL (0, 1, 2, 3, or 4M). Evaluated by the 7-5 ELISA method, both RecElkPrP and RecMousePrP samples showed the highest O.D. values with 0M GdnHCL denaturation (Figures 2-15.A and B). Among 1-4M GdnHCL denaturations, the 7-5 ELISA method measured subtle differences for PrP detections in these samples among the denaturant concentration, especially for RecElkPrP. According to the Section 2-2 result, GdnHCL denaturation and temperature were no influential in RecElkPrP, compared to non-denatured condition (Figure 2-2). Hence, the denaturation was a minimal effect for detections of this RecPrP sample. However, 0M-denatured RecElkPrP with Triton-X 100 showed a higher O.D. value than denatured analyte (Figure 2-15.A). Therefore, these results suggested that the pre-treatment with Triton-X 100 enhanced an efficiency of GdnHCL denaturation. In addition, the denatured RecMousePrP with 2M GdnHCL reduced the O.D. value, compared to this analyte with other GdnHCL concentrations (Figure 2-15.B). This phenomenon was also observed in the GdnHCL-dose dependent study with RML-infected mouse BH samples (Figures 2-12.A and B). Thus, the decreased PrP detection with 2M GdnHCL might be a unique reaction in MousePrP.

A.

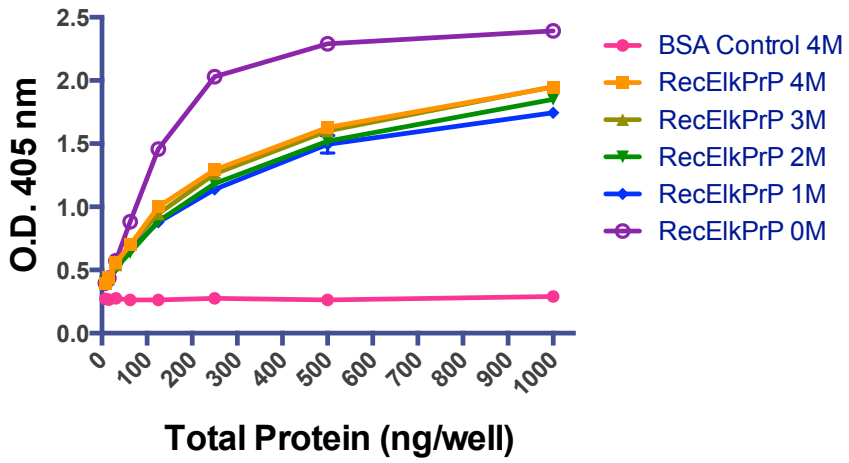

B.

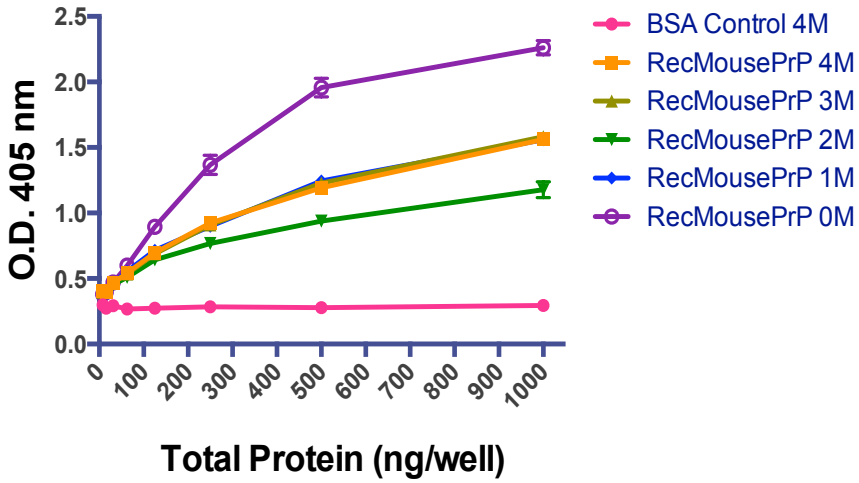

Figure 2-15. GdnHCL-dose dependent responses in RecPrP by the 7-5 ELISA method. (A) RecElkPrP and (B) RecMousePrP (n=2 for each prepared sample at a total protein).

Effective GdnHCL concentrations for mouse brain homogenates in the 7-5 ELISA method

The 7-5 ELISA method analyzed dose-dependent responses of GdnHCL to four different protein amounts of BH samples from three TSE-infected mouse study groups. Including PrP-KO mice for each group, these study groups were 1) RML-infected and uninfected FVB mice, 2) CWD-infected and uninfected Tg5037 (ElkPrP) mice, and 3) CWD-infected and uninfected Tg1536 (DeerPrP) mice. Prior to denaturations, all prepared samples were treated with 0.5% TX100 for 1 hour at 37°C with 1,000 rpm agitation. For all TSE-infected samples in the three study groups, the highest protein amounts exhibited the peaks of O.D. values at 5M GdnHCL, whereas 6M GdnHCL decreased the values (Figures 2-16.A to C). These outcomes indicated that the range of 4-5M GdnHCL concentrations could be adequate to detect PrP agents in TSE-infected materials. Notably, over 5M GdnHCL concentrations have potentials to decrease PrP detections. Therefore, the GdnHCL denaturation should maintain between 4-5M concentrations for sample preparations under the 7-5 ELISA protocol.

A.

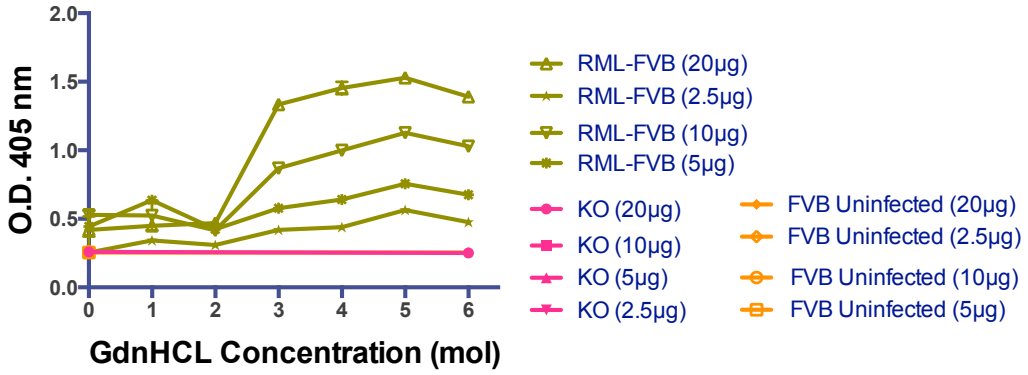

B.

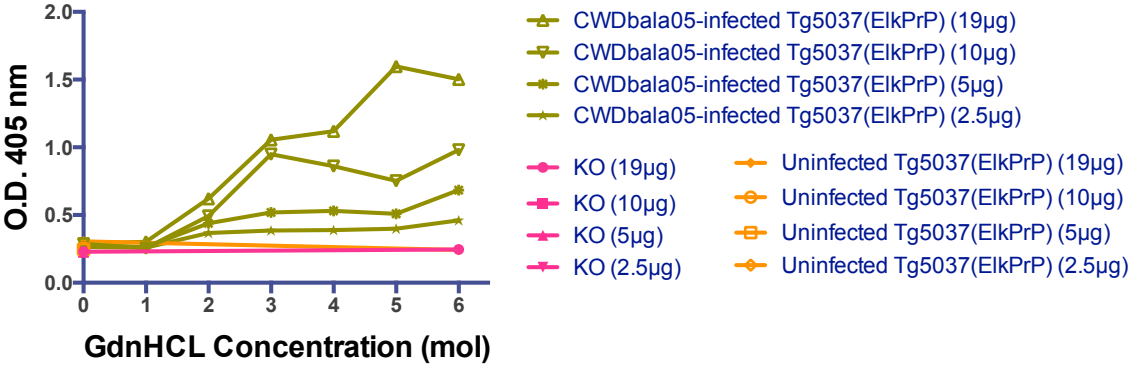

C.

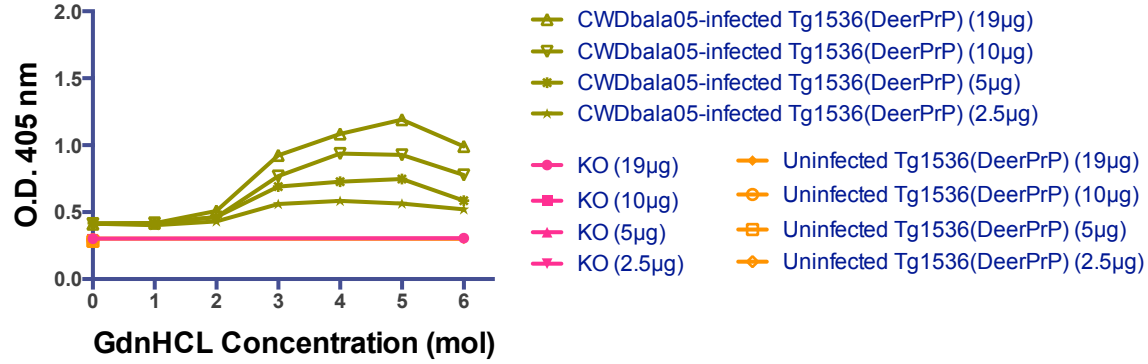

Figure 2-16. GdnHCL-dose dependences to different protein amounts of TSE-infected murine BH materials in the 7-5 ELISA method. BH samples of PrP-KO mouse with (A) RML-infected and uninfected FVB mice, (B) CWD-infected and uninfected Tg5037 (ElkPrP) mice, and (C) CWD-infected and uninfected Tg1536 (DeerPrP) mice. (n=3, each dose).

Efficacy of TX100 for PrP detections in brain homogenates from CWD-inoculated transgenic mice by the 7-5 ELISA method

To enhance PrP detections in CWD-infected materials, four different concentrations of TX100 (0.5, 1, 2.5, and 5%) were tested with BH samples from transgenic mice with expressing cervid PrP. These samples with each TX100 concentration were incubated for 1 hour or 2 hours. After these TX100 treatments, all testing samples were denatured with 4M GdnHCL for 15 minutes. The 7-5 ELISA method measured that the controls of PrP-KO mice, uninfected Tg5037 mice (elk PrP expression), and uninfected Tg1563 mice (deer PrP expression) did not have clear differences for O.D. values by the TX100 treatments and incubation times (Figures 2-17.A to C). In contrast, the 1% TX100 treatment exhibited the peak of PrP detections in both CWD-infected Tg5037 and Tg1536 murine BH samples. However, higher TX100 concentrations decreased PrP detections (Figures 2-17.D and E). Therefore, the 1% TX100 should be applicable for enhancing PrP detections in mouse BH samples by the 7-5 ELISA method.

A.

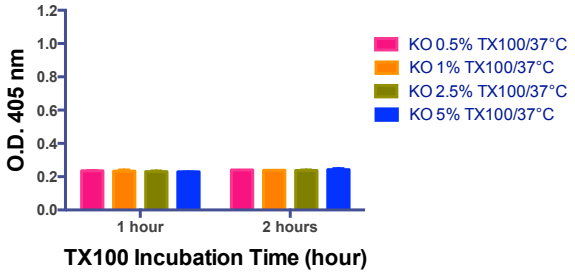
O.D. 405 nm
1.2
1.0
0.8
0.6
0.4
0.2
0.0
1 hour
2 hours
TX100 Incubation Time (hour)
KO 0.5% TX100/37°C
KO 1% TX100/37°C
KO 2.5% TX100/37°C
KO 5% TX100/37°C

B.

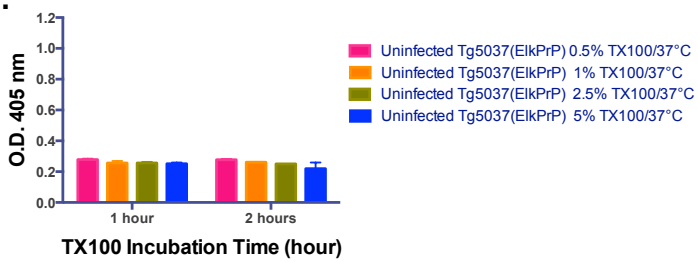
O.D. 405 nm
1.2
1.0
0.8
0.6
0.4
0.2
0.0
1 hour
2 hours
TX100 Incubation Time (hour)
Uninfected Tg5037(ElkPrP) 0.5% TX100/37°C
Uninfected Tg5037(ElkPrP) 1% TX100/37°C
Uninfected Tg5037(ElkPrP) 2.5% TX100/37°C
Uninfected Tg5037(ElkPrP) 5% TX100/37°C

C.

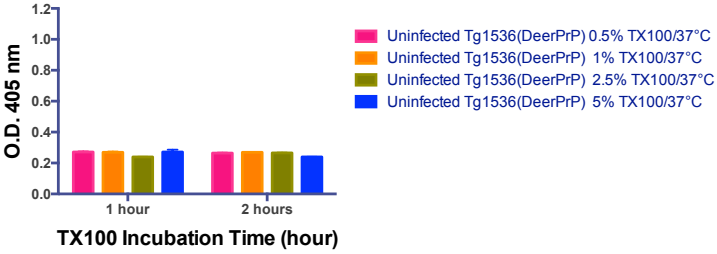
O.D. 405 nm
1.2
1.0
0.8
0.6
0.4
0.2
0.0
1 hour
2 hours
TX100 Incubation Time (hour)
Uninfected Tg1536(DeerPrP) 0.5% TX100/37°C
Uninfected Tg1536(DeerPrP) 1% TX100/37°C
Uninfected Tg1536(DeerPrP) 2.5% TX100/37°C
Uninfected Tg1536(DeerPrP) 5% TX100/37°C

D.

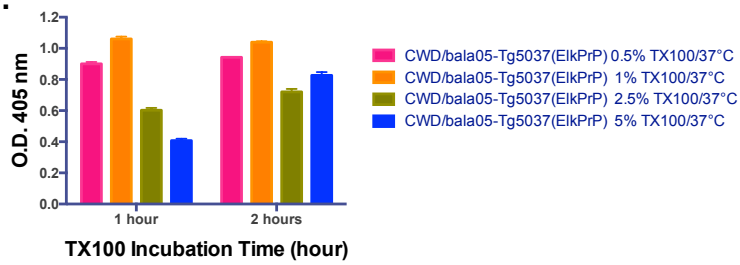
O.D. 405 nm
1.2
1.0
0.8
0.6
0.4
0.2
0.0
1 hour
2 hours
TX100 Incubation Time (hour)
CWD/bala05-Tg5037(ElkPrP) 0.5% TX100/37°C
CWD/bala05-Tg5037(ElkPrP) 1% TX100/37°C
CWD/bala05-Tg5037(ElkPrP) 2.5% TX100/37°C
CWD/bala05-Tg5037(ElkPrP) 5% TX100/37°C

E.

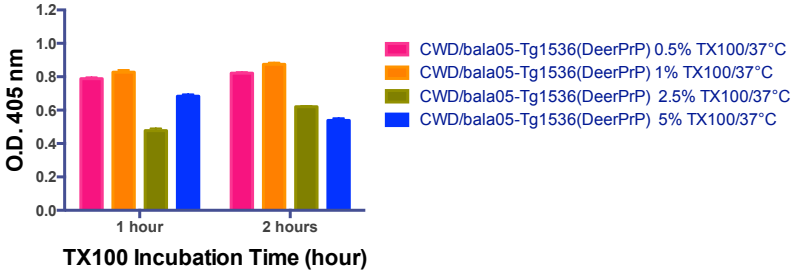
O.D. 405 nm
1.2
1.0
0.8
0.6
0.4
0.2
0.0
1 hour
2 hours
TX100 Incubation Time (hour)
CWD/bala05-Tg1536(DeerPrP) 0.5% TX100/37°C
CWD/bala05-Tg1536(DeerPrP) 1% TX100/37°C
CWD/bala05-Tg1536(DeerPrP) 2.5% TX100/37°C
CWD/bala05-Tg1536(DeerPrP) 5% TX100/37°C

Figure 2-17. TX100 efficacy under different concentrations and incubation times in the 7-5 ELISA method. (A) PrP-KO mouse BH samples,
(B) Uninfected Tg5037 mouse BH samples, (C) Uninfected Tg1536 mouse BH samples, (D) CWD(Bala05)-infected Tg5037 mouse BH samples,
(E) CWD(Bala05)-infected Tg1536 mouse BH samples. (n=3, each sample category with 20μg total protein amount)

1% TX100 application to RML-infected murine brain homogenate in the 7-5 ELISA method

Based on the experiments above, 1% TX100 was the most effective concentration for PrP detections in CWD-infected materials by the 7-5 ELISA method. However, RML-infected materials exhibited similar PrP levels with 0.5% and 1% TX100 incubations at 37°C. To confirm the 1% TX100 concentration as the optimized 7-5 ELISA protocol, this detergent was re-evaluated with BH samples from RML-infected mouse and its controls (uninfected FVB/n and PrP-KO mice). Initially, these BH samples were incubated with 1% TX100 for 1 hour at 37°C, and subsequently denatured with 5M GdnHCL for 15 minutes at 37°C. After ten-time dilutions, these prepared samples were further diluted in a range from 0.625µg to 160µg total proteins per well (each well number = duplicate), evaluating for protein-dose dependent responses in the 7-5 ELISA method. The efficacy of TX100 was obvious to detect PrP agents in the infected material, based on the previous results in this chapter. Between 0.625µg and 20µg total proteins, the dose responses showed a linear range on the curve (Figure 2-18.A). For the TX100 incubations, different times were previously tested at 1, 2, or 3 hours, or overnight. The 1-hour incubation was the most effective and convenient time for PrP detections. To determine minimal incubation times for enhancing the 1% TX100 efficacy, its treatment was tested for shorter incubation times (5, 10, 20, 30, 40, 50, or 60 minutes) using the same brain samples above. After these time-point incubations, all samples were denatured with 5M GdnHCL for 15 minutes at 37°C. Followed by the 10-time dilutions, the 20µg total protein of each prepared sample was coated per well (triplicate for each incubation time and individual). Among these time points, the infected

sample did not exhibit significant differences for O.D. values of PrP detections (Figure 2-18.B). However, these results suggested that at least 40 minutes of the TX100 incubation should be applicable as a minimum.

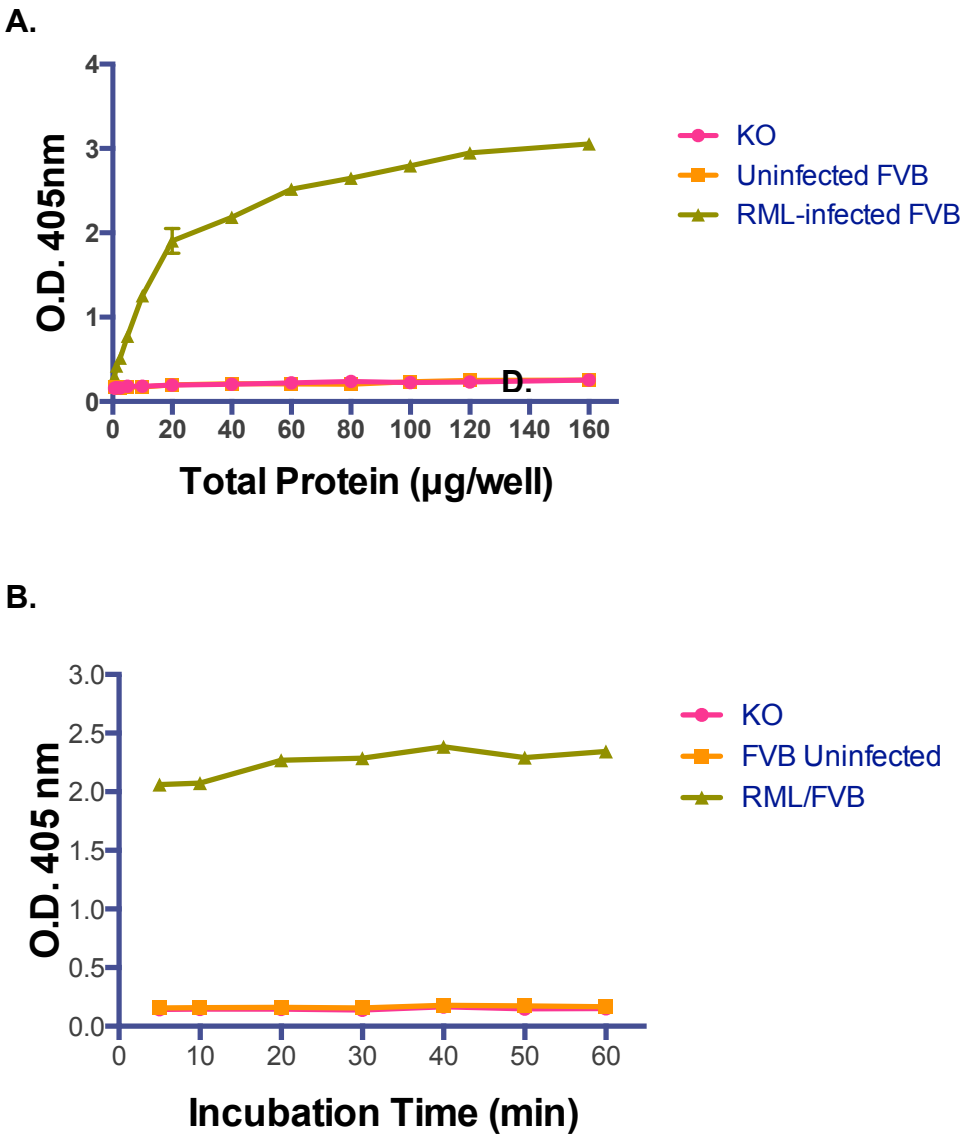

Figure 2-18. TX100 effects for PrP detections in RML-infected murine analyte in the 7-5 ELISA method. (A) protein-dose dependent responses, and (B) incubation-time dependent evaluation of TX100 with testing samples. (n=3, each sample category)

Application of the optimized 7-5 ELISA protocol to scrapie-infected transgenic mice

For further analyses of the 7-5 ELISA method, its optimized protocol was tested with BH samples from scrapie-inoculated transgenic mice expressing ovine PrP. These murine samples were derived from the following past bioassay in KG study numbers: KG-49 (sheep scrapie 48x35), KG-50 (sheep scrapie SSBP/1), KG-51 (sheep scrapie CH1641/4), and KG-62 (US goat scrapie 76/12/22). The background information of these four scrapie strains are described below. The three strains (SSBP/1, 48x35, and CH1641/4) were originally isolated at the Neuropathogenesis Unit (NPU), Edinburgh in the United Kingdom. The SSBP/1 isolate originated from three sheep that naturally developed scrapie. Mixed homogenates of these brains were inoculated into other sheep for passages, mainly in the Cheviot breed (Dickinson et al., 1989). The sheep scrapie 48x35 was the isolate from a scrapie-developed Cheviot sheep expressing a heterozygous VRQ/ARQ genotype with Leucine (abbreviated as Leu/L) at the codon 141 in the ARQ allele of the PrP gene. Another scrapie isolate CH1641 was derived from a Cheviot sheep with natural scrapie infection. The US goat scrapie 76/12/22 isolate originated from a US goat with an experimental scrapie inoculation, provided by Dr. Jason Bartz at Creighton University (Omaha, Nebraska, USA). For the transmission analyses, the KG bioassay inoculated these scrapie isolates intracerebrally into Tg3533 mice expressing ovine PrP (ARQ) that is composed of alanine (Ala: A) at amino acid residue 136.

For this scrapie experiment, one mouse brain from each KG experiment was evaluated by the 7-5 ELISA method. The animal numbers of tested Tg3553 mice were

the following: #5060 (48x35 in KG-49), #5064 (SSBP/1 in KG-50), #5075 (CH1641/4 in KG-51), and #5520 (US goat scrapie 76/12/22 in KG-62). Moreover, one mouse brain (animal number #6369) from the KG-98 study (the transmission of SSBP/1 sheep scrapie) was analyzed. This transgenic mouse Tg4166 (Ovine VRQ) expressed sheep PrP with valine (abbreviated as Val or V) at amino acid residue 136. Since PRC5 mAb does not bind sheep PrP with Valine at the amino acid residue 136, the VRQ sheep PrP sample was a negative control for the 7-5 ELISA method. Other controls included BH samples from PrP-KO, uninfected Tg3533 (Ovine ARQ) and Tg4166 (Ovine VRQ) mice. Briefly, all BH samples were treated with 1% TX100 for 1 hour at 37°C, and then denatured with 5M GdnHCL for 15 minutes at 37°C. Subsequently, these prepared samples were diluted 10 times to be 200μg/ml protein concentration. 100μl of each diluted sample was coated per well (total 20μg/well; duplicate for each mouse) for the 7-5 ELISA analyses. All samples from the scrapie-infected Tg3533 mice showed higher O.D. values of PrP detections, compared to the controls (Figure 2-19).

However, these detections were lower values, compared to the previous experiment of another isolate Colorado Scrapie in Tg3533 mouse in Section 2-10 (Figure 2-10.B). These different detections might indicate quantitative estimations or determinations of PrP levels by the 7-5 ELISA method, as depended on individual variances. To analyze this possibility, additional numbers of mice from scrapie bioassay would be necessary. Notably, the KG study samples have been stored over a decade, and also transferred from another institute to CSU. In contrast, the inoculum experiments with the Colorado Scrapie isolate were performed at CSU. Then, mouse brains were tested by the 7-5 ELISA method shortly after these tissue collections

(shorter storage times). Potentially, the sample storage time and condition might be a causal factor to decrease PrP detections. In addition, the 7-5 ELISA method could not measure PrP levels in the SSBP/1 scrapie-infected Tg4166 (Ovine VRQ) mouse because of the PRC5 property. Therefore, the 7-5 ELISA method can be utilized to detect scrapie infections in sheep with a non-Valine background at the amino acid residue 136 of PrP genes.

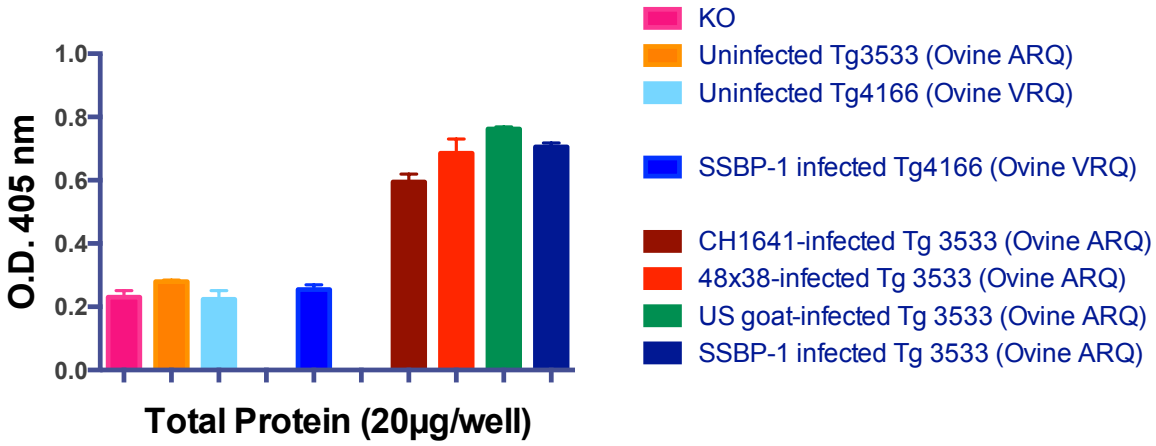

Figure 2-19. The 7-5 ELISA method is capable of detecting PrP levels in BH samples from scrapie-infected transgenic mice. (n=3, each sample with 20µg total protein amount)

Discussions

Several different analytical methods have been used to diagnose TSE infections. However, each method has both advantages and limitations for PrP^{Sc} detections, based on technical processes.[1,2] This thesis established objectives to develop novel analytical methods that overcome some of the current limitations for TSE diagnoses. These investigations anticipated promoting the identification of underlying mechanisms in TSEs. For these fundamental aims, the ELISA approach was selected to develop an analytical and diagnostic tool with high sensitivity and strong specificity for PrP^{Sc} detections. Compared to western blot (WB) and immnoprecipitation (IP) assays, ELISA methods are capable of testing greater numbers of samples at the same time and also detecting very low or unknown amounts of targeted antigens. In general, the ELISA method is quick, convenient and safe (i.e. no radioactive substance). Thus, several ELISA approaches are used routinely for PrP detections in tissue samples, with PK treatment for PrP^{C} digestions and for specific PrP^{Sc} detections.[1,2] Since the PrP^{Sc} isoform is generally known as partially resistant to the PK reagent, this enzyme has been utilized in sample preparations for TSE diagnoses including WB and IP assays for identifying PK-resistant PrP or PrP^{Sc} agents. Thus, non-PK protocols of these common analytical methods are extremely limited in TSEs. However, some studies suggest that significant amounts of PrP^{Sc} isoforms are PK sensitive, which highly implicate neurotoxic mechanisms in the TSE pathogenesis.[3-5] Therefore, the PK application for PrP^{Sc} detections has potential risks to produce false negative results in the traditional PK-based diagnostic methods. This is a serious concern for food safety and zoonotic transmission, especially for BSE. To overcome this critical limitation of PK-based tests,

the development of new PrP^{Sc} detectable assays is required to avoid the PK reagent and ultimately improve the sensitivity and specificity.

PRC7 and PRC5 mAbs are the in-house products of new anti-PrP mAbs.[6] PRC7 mAb specifically recognizes both unglycosyl and one monoglycosyl (mono-1: amino acid residue 180 for mouse) forms of PrP molecules. Conversely, PRC7 mAb cannot recognize a diglycosyl PrP form that is in abundance during non-infected states. Therefore, PRC7 mAb preferentially detects the under-glycosylated form of PrP molecules. According to the preliminary studies, PRC7 mAb detected under-glycosylated PrP forms in infected samples from TSE-inoculated mice by WB assay (unpublished data). Since WB and IP assays have limitations such as time consumption and analytical sensitivity, the development of more advanced methods was aimed using PRC7 and PRC5 mAbs for the PrP detection and quantification in TSE-infected samples. Based on the characteristic feature of PRC7 mAb that react with two of the under-glycosylated PrP forms in TSE-infected materials, the establishment of a new ELISA method with more sensitivity was attempted for detecting certain glycosylated PrP^{Sc} forms.

In order to evaluate capabilities of PRC7 and PRC5 mAbs for ELISA applications, these antibodies were initially tested by the Indirect ELISA method using recombinant prion protein (RecPrP) samples (Figure 2-1). These two mAbs were capable of PrP detections in different species (elk and mouse) under the Indirect ELISA approach. In addition, denatured RecPrP samples must be renatured to these native conformations because these O.D. values were similar to non-denatured samples, in that PRC7 and PRC5 mAbs were conformation-dependent antibodies (Figure 2-1). To

increase the specificity of PrP detections, these antibodies were examined by the Sandwich ELISA approach. However, the use of PRC7 mAb had a potential restriction to detect large amounts of PrP molecules in testing samples by the Sandwich ELISA method, because of its selective reactivity to unglycosyl and mono-1 glycosyl PrP forms. Thus, the combination of PRC7 and PRC5 mAbs for the Sandwich ELISA approach was determined using RecPrP with different sample preparations. In fact, the Sandwich ELISA approach with the capture PRC7 and detecting PRC5 antibodies (the 7-5 ELISA method) showed PrP detections under RecPrP-dose dependences for both elk and mouse species. Similar to the results from the Indirect ELISA method, denaturation did not influence PrP detections by the 7-5 ELISA method, compared to the non-denatured preparation. Since the incubation temperatures also did not show differences for the denaturation state, it is obvious that the 7-5 ELISA method can recognize renatured PrP structures after the sample denaturation (Figure 2-2).

In contrast, the 5-7 ELISA approach (the reverse order of PRC7 and PRC5 mAbs in Sandwich ELISA) did not detect PrP levels, specifically in TSE-infected murine materials (Figure 2-3). However, this ELISA approach reacted with RecElkPrP and RecMousePrP samples that were non-glycosylated forms. These results indicated that the capture antibody PRC5 mAb bound to all four glycosylated PrP forms in BH samples, whereas PrP molecules with unglycosyl and/or mono-1 glycosyl forms were possibly less captured by this mAb. Therefore, the detecting antibody PRC7 mAb could not have a greater chance to bind with these two glycosylated PrP forms. In the 7-5 ELISA method, conversely, PRC7 mAb captured only unglycosyl and/or mono-1 glycosyl PrP forms, and then PRC5 mAb detected all captured PrP molecules. As

reported, TSE infections tend to increase generations of under-glycosylated PrP forms in affected animals.[10] Thus, the selective capture by mAbs against under-glycosylated PrP forms must be an analytical tool, specifically for PrP^{Sc} detections in TSE-infected materials. Hence, under-glycosylated PrP forms are candidate biomarkers to diagnose the TSE infection state and disease progression. Consequently, the 7-5 ELISA method has a potential utility as a novel analytical system in TSE diagnosis.

Evaluated by the 7-5 ELISA method, higher concentrations of GdnHCL increased PrP detections in TSE-infected materials, while extremely higher temperatures (85°C) reduced O.D. values of PrP levels (Figure 2-4). These results reflected thermal influence and protein degradation. In general, thermal injury and protein denaturation are initiated around 42-45°C, and increased temperatures progress protein degradation faster.[19] In fact, proteins are prone to lose stabilities at temperatures 40°C and above, which induce unfolding protein structures.[20] For the PrP conformational stability, the midpoint of denaturation temperatures is different between PrP^{C} and PrP^{Sc} isoforms in that the abnormal structure has a higher heat tolerance than the wild-type protein.[21] At elevated temperatures, therefore, the denaturation procedure might cause irreversibility for the PrP renaturation and conformation, possibly resulting in degradation of the damaged protein.

Followed by optimizing steps for sample preparations, the 7-5 ELISA method could increase its capability to detect PrP levels in BH samples from TSE-infected mice. Higher amounts of the PRC7 capture antibody would increase chances for capturing many unglycosyl and mono-1 glycosyl PrP forms in the tested samples (Figure 2-5). In addition, the supplemental use of detergents enhanced PrP detections in TSE-infected

materials (Figure 2-6). The efficacy of TX100 was obvious for CWD-infected Tg5037 (ElkPrP) mouse samples (Figure 2-7). In the TSE research, several different detergents (i.e. sodium dodecyl sulfate, sodium deoxycholate) have been applied to enhance PrP^{Sc} detections in TSE-infected materials and to analyze PrP phenotypes and glycosylation profiles.[22,23] However, various experimental factors are influential for the PrP detectability, such as detergent types and concentrations, PK reagents, host species, TSE strains, and analytical methods. Thus, it is important to select effective detergents for enhancing PrP detections through the development and optimization of the 7-5 ELISA method. In fact, the TX100 application at the pre-denaturation showed the increase of PrP detections (Figure 2-6). The 1% TX100 obviously enhanced O.D values of PrP levels in CWD-infected Tg5037 mouse BH samples, compared to the 0% and 5% TX100 concentrations (Figure 2-7). In contrast, the 7-5 ELISA method could not detect PrP levels in CWD-infected materials without the TX100 treatment. These outcomes reflected previous reports that efficacies of detergents were dependent on detergent concentrations, TSE strains, and host species.[22,23] In addition, denaturation at higher temperatures diminished PrP detections (Figure 2-7). Possibly, elevated incubation temperatures caused irreversible conditions for protein structural renaturation as an excessive effect of the thermal denaturation. However, the 37°C temperature for TX100 and GdnHCL treatments enhanced PrP detections in CWD-infected materials during certain incubation times: 1 hour with TX100, and 15 minutes with GdnHCL (Figure 2-8). However, longer incubation times reduced O.D. values of PrP detections in the infected samples. For the TX100 concentration, 1% concentration was less influential by temperatures for PrP detections in RML-infected murine materials, although 0.5% and

1% concentrations showed similar O.D values (Figure 2-9). Therefore, 1% TX100 concentration could be appropriate to prevent temperature-related declines of PrP detections in the 7-5 ELISA method. In addition to the incubation temperature and detergent, sample-coating times on ELISA plates were also an influencing factor to obtain accurate results for PrP^{Sc} detections. The 6-hour incubation could provide equivalent captures of PrP molecules by the PRC7 mAb, compared to the overnight incubation (Figure 2-10). Nevertheless, the 1-hour sample incubation was also detectable for the TSE-infection state. The application of shorter incubations would be applied when rapid TSE diagnosis is required.

In the 7-5 ELISA method for PrP detections, β-mercaptoethanol (βME) cleaved disulfide bonds in conformational globular domains of PrP structures, resulting in the loss of protein folding and stability (Figure 2-11). Since PRC7 and PRC5 mAbs in the 7-5 ELISA method are conformation-dependent features for PrP detections, this analytical method could not recognize PrP levels in βME-treated BH samples from RML-infected mouse, whereas the samples with non-βME treatment showed higher O.D. values for PrP detections (Figure 2-11). These outcomes indicated that the conformational-dependent ELISA approach only detected PrP molecules with structural conditions, but not for unfolding states. In addition, PRC7 mAb and the 7-5 ELISA method only detect unglycosyl and mono-1 glycosyl PrP forms. Based on these findings, under-glycosylated PrP conformations might be less stable for maintaining protein structures because of no protection by glycans. During the developmental processes of the 7-5 ELISA protocol, it was obvious that this analytical method required denaturation for PrP detections in TSE-infected materials. As PRC7 and PRC5 mAbs

have conformational-dependent reactivities to PrP molecules, detected targets by the 7-5 ELISA method must be renatured after denaturation to their structural conformations. In the conformational experiment for PrP detections in Section 2-11, βME was applied to the BH samples after denaturation (Figure 2-11). This βME treatment disabled renaturing abilities of denatured PrP molecules and eventually induced unfolded conditions. In neurodegenerative diseases including TSEs, unfolded protein responses are the central role of pathological mechanisms for disturbing the protein folding.[24,25] In fact, a recent study identified that partially unfolded PrP forms were in the process of conformational conversions to misfolded PrP structures.[26] According to these recent findings, I propose that under-glycosylated forms of PrP molecules are immature or intermediate conformations in an alteration from PrP^{C} to PrP^{Sc} isoforms and/or during newly PrP^{Sc} replications and generations. Furthermore, I suspect that under-glycosylated PrP^{Sc} isoforms or immature/intermediate conformers are fully or partially unfolding conditions. Since PRC7 mAb and the 7-5 ELISA method could not detect under-glycosylated PrP forms without denaturants, the sample dilution after denaturation would reduce its efficiency, leading to a renaturation process for these unfolding PrP^{Sc} forms to PrP^{C} or its equivalent structure. As a future direction I hypothesize, the PrP glycosylation state changes during different disease stages of TSE pathogeneses, especially for under-glycosylated PrP forms. To investigate the kinetics of under-glycosylated PrP formations during the PrP^{Sc} replication and generation, the 7-5 ELISA method would be capable of determining the modulation of glycosylated PrP forms in TSE-mouse models, through different time points in the TSE disease development. Thus, the 7-5 ELISA method will be applicable as a sensitive

analytical tool to measure PrP glycosidic alterations and expressional modulations. In further experiments, a longitudinal approach will identify the kinetic changes of PrP glycosylations and implications in the TSE disease course.

In general, GdnSCN is a stronger protein denaturant than GdnHCL. Thus, it has been widely used in various biological samples for denaturation. However, the comparison studies of GdnSCN and GdnHCL indicated that the 7-5 ELISA method exhibited a higher efficacy of GdnHCL for PrP detections in TSE-infected materials. In the literature, GdnHCL has a unique feature that inhibits propagation, replication, and aggregation of PrP^{Sc} isoforms in cellular models.[27-29] These studies indicated the GdnHCL treatment cured PrP-generating phenotypes of cells from abnormal PrP^{Sc} to normal PrP^{C} isoforms. Although mechanisms of GdnHCl-mediated PrP conformational modifications are not confirmed yet, the 7-5 ELISA results suggest that denatured PrP^{Sc} conformers with GdnHCL would renature to PrP^{C} or PrP^{C}-like structures (Figure 2-12). GdnHCL might not interrupt this reversible effect of the PrP conformation higher than GdnSCN. Thus, the 7-5 ELISA method requires GdnHCL denaturation for under-glycosylated PrP^{Sc} isoforms in TSE-infected materials for detecting PrP^{C} or PrP^{C}-like conformations after spontaneous renaturation. Moreover, the 85°C incubation for GdnHCL denaturation reduced PrP detections in TSE-infected BH samples in Section 2-4 (Figure 2-4). However, this experiment was performed without a TX100 addition prior to this denaturation. In contrast, when TX100 was pre-incubated before the denaturation step, temperatures between 37 and 87°C with certain ranges for the denaturation (GdnHCL) did not show clear influences for PrP detections in the infected samples at all tested temperatures (Figure 2-13). Possibly, the TX100 detergent might

have a potential to assist the renaturation of denatured PrP^{Sc} structures to normal PrP^{C} or PrP^{C}-like conformations.

Compared to no detergent (PBS only) and denaturant (50mM Tris buffer only) in Section 2-14, TX100 treatment enhanced O.D. values of RecPrP detections without GdnHCL (Figure 2-14). All tested samples were incubated for certain times so that thermal denaturations were possibly induced to the proteins. Thus, TX100 might mediate the protein renaturation to native conformational structures. In contrast, denatured RecPrP samples with 4M GdnHCL decreased O.D. values, while the TX100 addition still enhanced detections of denatured PrP samples (Figure 2-14). Since RecPrP is a native PrP^{C} structure without glycans, it should be less stable for maintaining its α-helix rich conformation after suffering denaturants and/or other experimental and environmental influences. Therefore, some denatured RecPrP samples might lose the ability for protein folding, which the 7-5 ELISA method detected lower O.D. values in GdnHCL-denatured samples than the non-denatured condition. On the other hand, under-glycosylated PrP^{Sc} conformers in TSE-infected mammal tissue samples might show more stability to detergents and denaturants because of β-sheet rich structures as misfolding PrP conformers.

For verifying the influential concern of denaturation, GdnHCL-dose dependent responses were evaluated with RecPrP samples by the 7-5 ELISA method (Figure 2-15). In fact, GdnHCL decreased O.D. values of PrP detections in denatured RecElkPrP and RecMousePrP samples, compared to the 0M treatment (only PBS with 0.5% TX100 during incubations). Interestingly, the 2M GdnHCL reduced the O.D. value of RecMousePrP more than other concentrations (Figure 2-15). These observations

indicated that some denatured RecPrP molecules could not renature to native folding structures. Since PRC7 and PRC5 mAbs are conformation-dependent antibodies, the 7-5 ELISA method cannot bind to unfolded conditions of RecPrP molecules if denatured samples do not renature.

Furthermore, the 7-5 ELISA experiment in Section 2-16 evaluated GdnHCL-dose dependent responses for the proper range of denaturant concentrations to enhance PrP detections in TSE-infected materials, using different TSE strains and host species (Figure 2-16). Notably, the highest GdnHCL concentration showed decreases of O.D. values in TSE-infected samples, compared to the lower dose treatments. This observation indicated that the denaturant-dose dependent applications also revealed an additional approach of the 7-5 ELISA method for a conformational stability assay. This new application would be utilized to determine TSE strain differences. As future directions for the 7-5 ELISA method, the use of other denaturants (i.e. GdnSCN, Urea) and PK reagents could be applied to the conformational stability assay that would provide more opportunity to evaluate various observations among TSE strains and species origins.

For an effective application of a TX100 detergent, 0.5-1% concentrations promoted PrP detections in CWD-infected samples from both Tg5037 (ElkPrP) and Tg1536 (DeerPrP) mice. In contrast, higher TX100 concentrations needed longer incubation times, but declined PrP detections in the infected materials, compared to the 0.5-1% concentrations (Figure 2-17). In fact, the 1% TX100 showed the highest PrP detections under shorter incubations in these two transgenic mouse lines with CWD infection states. Thus, the 1% concentration could be a proper use for BH samples from

transgenic mice with cervid PrP expressions in the 7-5 ELISA protocol. It was obvious that the 1% TX100 application enhanced PrP detections in BH samples from RML-infected FVB/n mice, compared to previous results which the same samples were treated with different TX100 concentrations at the 5M GdnHCL during denaturation (Figures 2-16 and 2-18). Therefore, it is practical to select and maintain the 1% concentration for sample preparations in the 7-5 ELISA protocol as a current optimized TX100 application.

Furthermore, the optimized condition of the 7-5 ELISA protocol was examined with BH samples from Scrapie-infected transgenic mice with sheep PrP expressions. This analytical method detected higher PrP levels of all four different scrapie strains in the tested mice with sheep ARQ PrP expressions. However, this experiment also confirmed the limitation of the 7-5 ELISA method that could not detect PrP levels in a transgenic mouse BH sample with ovine VRQ PrP expressions, because PRC5 mAb does not react to PrP molecules with VRQ alleles.[6] Therefore, it would be necessary to check the background information of the amino acid residue at 136 in testing sheep samples, when the 7-5 ELISA method would be applied in future diagnostic situations.

Overall, the experiments in this chapter determined the condition of Sandwich ELISA protocol using the in-house anti-PrP mAbs. In the 7-5 ELISA method, PRC7 and PRC5 mAbs can be utilized to detect PrP agents in TSE-infected materials specifically. In fact, this Sandwich ELISA method is capable of detecting RecPrP samples and PrP levels in BH samples from TSE-mouse models. This result indicated that the detected PrP molecule was unglycosyl and/or mono-1 glycosyl forms, because PRC7 mAb only reacted to these two forms. Based on all findings above, the 7-5 ELISA method clarified

the specificity of under-glycosylated PrP productions in the TSE disease development. As hypothesized, the detection of an under-glycosylated PrP form can be a valuable diagnostic biomarker for the TSE infection state and disease progression. In the Chapter 3, thereafter, the 7-5 ELISA method was examined by multiple approaches to optimize its protocol. Using BH samples from various transgenic mouse models of TSEs at terminal stages, the 7-5 ELISA method was capable of detecting under-glycosylated PrP forms in TSE-infected samples among various influential factors, such as different species, TSE strains, and infectious states.

In another aspect, the 7-5 ELISA method exhibited analytical limitations for PrP detections.[6] PRC7 mAb does not recognize human, hamster and bovine PrP molecules due to amino acid differences at the antibody-binding site (Y154 and Q185 constitute a discontinuous epitope). In addition, PRC5 mAb is not capable of detecting sheep PrP molecules with Valine at the residue 136. To overcome these limitations and develop specific antibodies distinguishing each glycosylation state, the productions of new anti-PrP mAbs for multiple species are future directions for TSE diagnostic innovations. Newly generated antibodies will be applicable to develop more advanced diagnostic methods for TSE infections in the future.

REFERENCES

1. Gavier-Widén D, Stack MJ, Baron T, Balachandran A, Simmons M. Diagnosis of transmissible spongiform encephalopathies in animals: a review. *J Vet Diagn Invest* 2005;17:509–27.
2. Lukan A, Vranac T, Curin Šerbec V. TSE diagnostics: recent advances in immunoassaying prions. *Clin Dev Immunol* 2013;2013:360604.
3. Tzaban S, Friedlander G, Schonberger O, Horonchik L, Yedidia Y, Shaked G, *et al.* Protease-sensitive scrapie prion protein in aggregates of heterogeneous sizes. *Biochemistry* 2002;41:12868–75.
4. Tzaban S, Friedlander G, Schonberger O, Horonchik L, Yedidia Y, Shaked G, *et al.* Protease-sensitive scrapie prion protein in aggregates of heterogeneous sizes. *Biochemistry* 2002;41:12868–75.
5. Thackray AM, Hopkins L, Bujdoso R. Proteinase K-sensitive disease-associated ovine prion protein revealed by conformation-dependent immunoassay. *Biochem J* 2007;401:475–83.
6. Kang H-E, Weng CC, Saijo E, Saylor V, Bian J, Kim S, *et al.* Characterization of conformation-dependent prion protein epitopes. *J Biol Chem* 2012;287:37219–32.
7. Neuendorf E, Weber A, Saalmueller A, Schatzl H, Reifenberg K, Pfaff E, *et al.* Glycosylation deficiency at either one of the two glycan attachment sites of cellular prion protein preserves susceptibility to bovine spongiform encephalopathy and scrapie infections. *J Biol Chem* 2004;279:53306–16.
8. Zou RS, Fujioka H, Guo J-P, Xiao X, Shimoji M, Kong C, *et al.* Characterization of spontaneously generated prion-like conformers in cultured cells. *Aging (Albany NY)* 2011;3:968–84.
9. Xiao X, Yuan J, Haïk S, Cali I, Zhan Y, Moudjou M, *et al.* Glycoform-selective prion formation in sporadic and familial forms of prion disease. *PLoS ONE* 2013;8:e58786.
10. Chen L, Yang Y, Han J, Zhang B-Y, Zhao L, Nie K, *et al.* Removal of the glycosylation of prion protein provokes apoptosis in SF126. *J Biochem Mol Biol* 2007;40:662–9.
11. Stimson E, Hope J, Chong A, Burlingame AL. Site-specific characterization of the N-linked glycans of murine prion protein by high-performance liquid chromatography/electrospray mass spectrometry and exoglycosidase digestions. *Biochemistry* 1999;38:4885–95.
12. Tuzi NL, Cancellotti E, Baybutt H, Blackford L, Bradford B, Plinston C, *et al.* Host PrP glycosylation: a major factor determining the outcome of prion infection. *PLoS Biol* 2008;6:e100.
13. Rudd PM, Endo T, Colominas C, Groth D, Wheeler SF, Harvey DJ, *et al.* Glycosylation differences between the normal and pathogenic prion protein isoforms. *Proc Natl Acad Sci USA* 1999;96:13044–9.
14. Koley D, Bard AJ. Triton X-100 concentration effects on membrane permeability of a single HeLa cell by scanning electrochemical microscopy (SECM). *Proc Natl Acad Sci USA* 2010;107:16783–7.

15. Akbaş H, Boz M, Batigöç C. Study on cloud points of Triton X-100-cationic gemini surfactants mixtures: a spectroscopic approach. *Spectrochim Acta A Mol Biomol Spectrosc* 2010;75:671–7.
16. Meyer RK, Oesch B, Fatzer R, Zurbriggen A, Vandevelde M. Detection of bovine spongiform encephalopathy-specific PrP(Sc) by treatment with heat and guanidine thiocyanate. *J Virol* 1999;73:9386–92.
17. Kang S-C, Li R, Wang C, Pan T, Liu T, Rubenstein R, *et al.* Guanidine hydrochloride extraction and detection of prion proteins in mouse and hamster prion diseases by ELISA. *J Pathol* 2003;199:534–41.
18. Concha-Marambio L, Diaz-Espinoza R, Soto C. The extent of protease resistance of misfolded prion protein is highly dependent on the salt concentration. *J Biol Chem* 2014;289:3073–9.
19. Bischof JC, He X. Thermal stability of proteins. *Ann N Y Acad Sci* 2005;1066:12–33.
20. Becktel WJ, Schellman JA. Protein stability curves. *Biopolymers* 1987;26:1859–77.
21. Kong Q, Mills JL, Kundu B, Li X, Qing L, Surewicz K, *et al.* Thermodynamic stabilization of the folded domain of prion protein inhibits prion infection in vivo. *Cell Rep* 2013;4:248–54.
22. Breyer J, Wemheuer WM, Wrede A, Graham C, Benestad SL, Brenig B, *et al.* Detergents modify proteinase K resistance of PrP^{Sc} in different transmissible spongiform encephalopathies (TSEs). *Vet Microbiol* 2012;157:23–31.
23. Kuczius T, Groschup MH. Regional phenotypes of cellular prion proteins in human brains identified by differential detergent solubility. *Brain Res* 2013;1507:19–27.
24. Halliday M, Mallucci GR. Review: Modulating the unfolded protein response to prevent neurodegeneration and enhance memory. *Neuropathol Appl Neurobiol* 2015;41:414–27.
25. Scheper W, Hoozemans JJM. The unfolded protein response in neurodegenerative diseases: a neuropathological perspective. *Acta Neuropathol* 2015;130:315–31.
26. Moulick R, Das R, Udgaonkar JB. Partially Unfolded Forms of the Prion Protein Populated under Misfolding-promoting Conditions: CHARACTERIZATION BY HYDROGEN EXCHANGE MASS SPECTROMETRY AND NMR. *J Biol Chem* 2015;290:25227–40.
27. Eaglestone SS, Ruddock LW, Cox BS, Tuite MF. Guanidine hydrochloride blocks a critical step in the propagation of the prion-like determinant [PSI(+)] of Saccharomyces cerevisiae. *Proc Natl Acad Sci USA* 2000;97:240–4.
28. Ferreira PC, Ness F, Edwards SR, Cox BS, Tuite MF. The elimination of the yeast [PSI+] prion by guanidine hydrochloride is the result of Hsp104 inactivation. *Mol Microbiol* 2001;40:1357–69.
29. Ness F, Ferreira P, Cox BS, Tuite MF. Guanidine hydrochloride inhibits the generation of prion “seeds” but not prion protein aggregation in yeast. *Mol Cell Biol* 2002;22:5593–605.

CHAPTER 3

DETERMINATION OF THE 7-5 ELISA METHOD TO DETECT DISEASE-ASSOCIATED PRP AGENTS IN MOUSE MODELS OF TSES

Summary

This Chapter 3 expanded the 7-5 ELISA method to test more BH samples from various transgenic-mouse models of different TSE diseases, including CWD, TME, GSS, and scrapie. The 7-5 ELISA method was exceptionally capable of detecting PrP^{Sc} isoforms in these murine BH samples. These results indicated the abundant existences of under-glycosylated PrP^{Sc} forms at the terminal stage of the disease course in mice. Hence, TSE-infected brains were prone to generate under-glycosylated PrP^{Sc} forms throughout different species and with various PrP^{Sc} isolates. Intriguingly, different TSE isolates exhibited variances for PrP^{Sc} detections in quantities and stabilities among inoculated hosts. Thus, the 7-5 ELISA method might distinguish diversities of strain differences, based on the detections of under-glycosylated PrP^{Sc} specificities. In addition, this analytical assay validated another capability to estimate PrP^{Sc} infectivity and titration, in comparison to results from the cervid prion cell assay (CPCA) with PRC7. Therefore, the glycosidic deficit on the PrP conformation should implicate with the TSE pathogenesis. The unstable structures of under-glycosylated PrP forms might link to conformational alterations of the normal PrP^{C} structure to the pathologic isoform. Furthermore, the D-5 ELISA method, which used a D18 anti-PrP antibody as a capture antibody, demonstrated an exceptional capability to determine levels of only PrP^{C} molecules or total PrP/PrP^{Sc} agents by a single change in sample preparations. Without

denaturation, the D-5 ELISA method detects the decrease of PrP^{C} levels in BH samples from TSE-infected materials at terminal stages. In contrast, these samples with denaturation exhibited increases of total PrP levels by the D-5 ELISA method. These results proved that the D-5 ELISA approach was capable of analyzing the modulations of normal PrP^{C} and abnormal PrP^{Sc} levels in a same animal with TSE diseases. The PrP^{C}-PrP^{Sc} modulations should be implicated with the pathological dysfunction, development and progression among various TSE diseases, strains and species backgrounds.

Introduction

The typical TSE bioassay involves the intracerebral inoculation of PrP^{Sc}-contained materials into rodents, such as wild-type mice or genetically modified mice (transgenic mice) with PrP expressions of the pathogen-donor or recipient species.[1-9] Through slow and imprecise incubation periods, inoculated PrP^{Sc} agents replicate and propagate in infected animals, resulting in developments of TSE disease onsets and progressions. Brains in affected hosts exhibit accumulations of pathogenic PrP^{Sc} agents. Using brain samples derived from past mouse bioassays in the CSU Prion Research Center, the 7-5 ELISA and the D-5 ELISA methods determined disease-associated PrP agents in various mouse models of TSEs at terminal stages. As hypothesized, the 7-5 ELISA method would detect under-glycosylated PrP forms in TSE-infected murine BH samples from different species backgrounds. These detections can indicate prominent generations of under-glycosylated PrP forms during the disease progression. In addition, this new sensitive method would be applicable to evaluate

various PrP^{Sc} isolates and trains, TSE-infectious states, species differences, and generations of under-glycosylated PrP forms. Furthermore, the D-5 ELISA method has the property to measure only PrP^{C} levels or total PrP levels in the testing samples. This analytical feature would be capable of evaluating PrP^{C}-PrP^{Sc} modulations and variances through the disease courses. In fact, the loss of PrP^{C} isoforms might be a causative factor of the functional abnormality in TSE-infected animals. Ultimately, the 7-5 ELISA and the D-5 ELISA methods would indicate aspects of the TSE pathogenesis. Possibly, glycosidic deficits implicate with pathological alterations of PrP conformations. Because of the important role of glycosylation, its modulation would affect the stability of protein structures. Subsequently, this unstable condition can alter the PrP structure abnormally. These aberrant formations would impair PrP^{C} functions in physiology, and eventually cause pathogenic alterations. Therefore, the evaluation of PrP^{C} and PrP^{Sc} modulations is a valuable analysis to monitor disease stages and prognoses. The generation of under-glycosylated PrP forms must be the characteristic feature of TSEs as a diagnostic biomarker for disease infection and progression. In this dissertation, the 7-5 ELISA and D-5 ELISA methods will demonstrate the exceptional capabilities of analyzing PrP detections and modulations in the TSE disease development.

Materials and Methods

Preparation of Brain Homogenates

The TSE mouse models with certain PrP^{Sc} inocula are listed (Table 2). These TSE-infected murine brains have been stocked at -80°C after tissue collections. The information of each inoculation study, animal, and tissue collection date was recorded in

the server database of the CSU Prion Research Center. Note: RML = Rockies Mountain Laboratory; CWD = chronic wasting disease; TME = transmissible mink encephalopathy; Dr. RB = Dr. Richard Bessen (Colorado State University); Dr. MZ = Dr. Mark Zabel (Colorado State University); RA150 = a passage of CWD Bala05 (elk brain) into Tg5037 mice (inoculated BH from the mouse B581); RA-154 = a passage of CWD Bala05 (elk brain) into Tg1536 mice (inoculated BH from the mouse B691); RA-86 = a passage of CWD 99W12389 (elk brain) into Tg5037 mice (inoculated BH from the mouse #7581); RA-78 = a passage of CWD 04-0306 (elk brain) into Tg5037 mice (inoculated BH rom the mouse #7455).

The testing mouse brains were homogenated by repeated extrusions using different sizes of syringe needles to 20% concentrations with cold 1X phosphate-buffered saline (PBS: no calcium and magnesium, HyClone Laboratories, Inc. GE Healthcare Life Sciences, Logan, Utah, USA). Aliquots of these BH samples in eppendorf tubes were stored at -80°C after the preparation. In addition, BH samples from PrP-KO mice and uninfected wild-type or transgenic mice were used as controls to TSE-infected mice in each study: PrP-KO (no PrP), FVB/n (wild-type MousePrP), C57BL6 (wild-type MousePrP), Tg5037 (ElkPrP E226), Tg1536 (DeerPrP), Tg3533 (OvinePrP ARQ), and TgF431 (MinkPrP).

Table 2. List of tested murine brain samples and inocula

Study/Provider	Mice	BH inocula of TSE
SK-01	FVB/n (MousePrP)	RML mouse-adapted scrapie
CLC-04	Tg5037 (ElkPrP)	RA-150/ CWD Bala05 (elk)
CLC-05	Tg1536 (DeerPrP)	RA-154/ CWD Bala05 (elk)
JB-66	Tg3533 (OvineARQ PrP)	Colorado Scrapie (sheep)
VK-11	TgF431 (MinkPrP)	TME #58 NBP 950825 (mink)
VK-18	TgF431 (MinkPrP)	TME 941031 (mink)
VK-20	TgF431 (MinkPrP)	TME 941201 (mink)
Dr. RB	C57BL6 (MousePrP)	22L mouse-adapted scrapie
Dr. RB	VM/Dk (MousPrP allotype B)	87V mouse-adapted scrapie
Dr. MZ	C57BL6 (MousePrP)	D10 mouse-adapted CWD
ES-02	Tg1536 (DeerPrP)	CWD 08W-11,741 (moose)
ES-03	Tg5037 (ElkPrP)	CWD 08W-11,741 (moose)
KG-18	Tg1536 (DeerPrP)	CWD strain 99W12389 (elk)
RA-26	Tg1536 (DeerPrP)	CWD Bala04-0306 (elk)
GT-142	Tg5037 (ElkPrP)	RA-86/ CWD 99W12389 (elk)
GT-143	Tg5037 (ElkPrP)	RA-78/ CWD Bala04-0306 (elk)

Applied 7-5 ELISA protocol to murine BH samples

Initially, PRC7 mAb was diluted to 20μg/ml concentration in a coating buffer (0.05M Carbonate-Bicarbonate in distilled water). 100μl of the prepared PRC7 solution was coated into each well on ELISA plates (Nunc MaxiSorp® flat-bottom 96-well plate, Thermo Fisher Scientific, Rochester, New York, USA), and subsequently incubated at 4°C overnight. After emptying the plates gently, 200μl PBS with 3% bovine serum albumin (BSA: Sigma-Aldrich Co. LLC, St. Louis, Missouri, USA) was added into each well for blocking non-specific binding sites on well surfaces. Following an incubation at 37°C for one hour and a removal of all solutions, the plate was washed three times with 1X TBS-Tween (TBST) buffer (50mM Tris, 150mM NaCl, 0.05% Tween-20 in distilled water, pH 7.6) by a plate washer (the Finstruments^{TM} Microplate Washer, MTX Lab Systems, Inc. Vienna, Virginia, USA). 100μl of each prepared BH sample was coated into designated wells on the plate. After incubating overnight at 4°C, the plate was evacuated and washed three times with 1X TBST by the washer. 1:5,000 dilution of PRC5 mAb was prepared using a dilution buffer (1% BSA-containing PBS without calcium and magnesium). 100μl of the prepared PRC5 solution was added into each emptied well on the ELISA plate as a detecting antibody. Following an incubation of one hour at 37°C, the plate was cleared, washed three times with 1X TBST by the plate washer, and gently emptied. Thereafter, a horseradish peroxidase (HRP)-conjugated secondary antibody (Goat Anti-Mouse IgG2a HRP conjugate, 1 mg/ml, Alpha Diagnostic Intl. Inc. Texas, USA) was diluted in a dilution buffer (1:5,000 ratio), and 100μl of the diluted secondary antibody was added into all testing wells. Following an incubation of one hour at 37°C and a removal of all solutions, the plate was washed seven times with

1X TBST by the washer. To evaluate an enzymatic reaction and color development, ABTS® Peroxidase Substrate (KPL, Inc. Maryland, USA) was applied under the manufacturer's protocol. Using an ultramicroplate reader (ELx808 Absorbance Reader, BioTek Instruments, Inc, Winooski, Vermont, USA), the absorbency of each well on the plate was analyzed at a wavelength of 405nm.

Sample preparations for the 7-5 ELISA method

In this Chapter 3, most materials of Sandwich ELISA experiments were analyzed with the final protein concentration of 200μg/ml mouse BH samples, proceeded by the following steps: 1) dilution of BH sample with 1X PBS to be 5.87mg/ml, 2) addition of 10% volume of 10% Triton X-100 (TX100) solution to be 1% concentration, 3) denaturation using 5M GdnHCL, 4) 10-time dilution with 1% BSA-containing PBS, and 5) sample coating on an ELISA plate. For planning to coat 100μl of the prepared BH sample (200μg/ml) per well (total protein 20μg each well) for triplicate, the final volume of each analyte was prepared to be 400μl. At the first step, 13.5μl of BH sample (5.87mg/ml) diluted by PBS (no calcium and magnesium) was mixed with 1.5μl of 10% TX100 in PBS (= total 15μl volume of 5.33mg/ml protein concentration with 1% TX100). This mixture was incubated for 1 hour at 37°C with 1,000 rpm agitation. Subsequently, 25μl of 8M GdnHCL (G3272, Sigma-Aldrich Co. LLC, St. Louis, Missouri, USA) in 1X TBST buffer (50mM Tris, 150mM NaCl, 0.05% Tween-20 in distilled water, pH 7.6) was added into the incubated 15μl BH sample. The total sample volume was 40μl of BH sample (2mg/ml) with 5M GdnHCL, which were then incubated for 15 minutes at 37°C with 1,000 rpm agitation. Then, the denatured sample was diluted with 360μl of a

dilution buffer (1% BSA-containing PBS: no calcium and magnesium). The total sample volume was 400µl of the BH sample (200µg/ml) with 0.5M GdnHCL. Then, 100µl of each prepared BH sample (200µg/ml) was coated per well (total protein 20µg each well) on the ELISA plate with pre-coatings of a capture antibody. The sample-coated plate was incubated overnight at 4°C. From the next blocking step, all other procedures were performed under the Sandwich ELISA method described above.

Cervid prion-cell assay

In 2014, Bian et al. reported the methodology of cervid prion-cell assay (CPCA).[10,11] This method can be performed conveniently for titration of TSE infections in various species backgrounds. CPCA has an equivalent sensitivity to mouse bioassay and scrapie cell assay (SCA or standard scrapie cell assay) for evaluating infectivity and its titration of TSE strains.[10-12] In addition, CPCA is capable of overcoming limitations of bioassay, such as processing times. CPCA utilizes a multiscreen 96-well filtration plate with filter membranes (0.45µm) on the bottoms of wells (an enzyme-linked immunospot (ELISpot) assay plate, Millipore, Billerica, Massachusetts 01821). In the CPCA experiment, it is essential to prepare fresh solutions daily, prior to starting any procedures with an ELISpot plate. Also, these solutions must be ultracleaned and filtered with 0.22µm pore membrane of a vacuum filtration system (Corning Incorporated-Life Sciences, Tewksbury, Massachusetts).

1) Activation of an ELISpot plate: Filter membranes on an ELISpot plate need to be activated before use. 100µl of 70% ethanol in ultrapure water was added into each well and incubated one minute at room temperature (RT) in a cell/tissue culture hood.

Immediately, ethanol was vacuumed from all filter membranes on the plate, washed twice with 150µl of 1X PBS and vacuumed each time. After adding 50µl of 1X PBS per well, the plate was gently tapped to cover the entire surface of each filter membrane for all wells. This is a critical point to maintain moisture on the membranes. Followed by vacuuming for one minute, the ELISpot plate was washed twice with 50µl of 1X PBS per well and vacuumed. After the second wash, it is important to vacuum the plate for one minute and re-vacuum to remove moisture from all wells. Subsequently, the well-vacuumed plate was dried at 50°C for one hour or until all membranes completely dried (membranes would be white when dried completely). After placing a lid on the dried ELISpot plate, it was wrapped with Saran Wrap to store in a -20°C freezer.

2) Preparation of Analyte: Based on a sample type and experimental aim, CPCA has two applications for testing analyte using an ELISpot plate. This study analyzed the infection of TSE-inoculated mouse BH samples into cultured cells, and the chronically TSE-infected cell lines and control cell lines. These two sample preparations were performed prior to transferring cells onto activated ELISpot plates.

Infection to RK13 cells

Preparation of brain homogenates and testing plate: According to the CPCA protocol (modified CPCA Protocol June 2013 in the lab database), The BH sample of a TSE-infected animal was prepared to be 10% (w/v) in PBS, and subsequently, its serial dilutions were made. For CWD or mouse-adapted prion analyte, the starting concentration of the serial dilutions was 0.1%: for reference, the 1% concentration can be applied to other TSE-infected materials for improving and enhancing PrP^{Sc} detections by CPCA. BH samples of SB-63 Tg1536 (DeerPrP) and RA116 Tg5037

(ElkPrP) mice were utilized as TSE-positive controls on CPCA. Both bioassay studies were applied with the same CWD prion inoculum (012-09442). 100µl of each diluted BH solution was coated per well of certain testing spots on a 96-well tissue culture (TC) plate (triplicate for each dilution). In a cell/tissue culture hood without ultraviolet light, this BH-coated TC plate with a lid cover was incubated for one hour at RT. Followed by aspirations of the coated BH solutions from all wells, the TC plate was washed twice with 1X PBS (no calcium and magnesium) and then emptied. Subsequently, the TC plate was placed in the hood for desiccating the membranes of all wells for two hours at RT or until completely dried. After that, the BH-coated TC plate was completely wrapped with Saran Wrap and stored at 4°C.

Plate cells onto the BH-coated TC plate: In the CPCA protocol, RK13 cells with PrP expressions of mouse, deer, or elk were utilized for TSE infections. RK13 cell line is a rabbit kidney epithelial cell line (ATCC, Manassas, Virginia, USA), in which its PrP expression is primarily undetectable. For the TSE research, this original cell line was stably transfected with vectors for developing a new cell line with PrP expressions.[10] In this CPCA study, RKM7 (mouse PrP), Deer5E9-S1 (deer PrP) and RKE (Elk21-#3: elk PrP) were applied. For a PrP-negative control, RKV (RK13 cells only transfected with a empty vector: no PrP expression) was included. These cell lines were grown with DMEM (10% fetal bovine serum: FBS, 1µg/ml penicillin, 100U/ml streptomycin, and 1µg/ml puromycin) in TC dishes or T75 flasks. Before transferring cells, the cold-storage plate should be placed at RT for 20-30 minutes. To test these cell lines by CPCA, 100µl of 20,000 cells was placed per well on the BH-coated TC plate. For obtaining higher PrP^{Sc} detections, the TC plate with cells was maintained in a

carbon dioxide (CO_2) incubator (5%) at 37°C for four weeks. The cell culture medium was changed weekly. In order to include positive controls for CPCA in the TC plate, Deer 5E9-S1 cells were added into the BH-coated wells of the SB-63 Tg1536 (DeerPrP) sample; RKE (Elk21-#3) cells were placed into the prepared wells of the RA116 Tg5037 (ElkPrP) sample. For the negative-control wells that were coated with these TSE-positive BH materials, RKV cells were added because the wells would not develop PrP replication and generation.

Transfer cells onto an ELISpot plate: At the end of the four-week TSE infections, the TC plate with coated cells was washed with 100µl of trypsin per well, and then aspirated gently in a cell culture hood. After adding another 100µl trypsin per well, the TC plate was incubated for five minutes in the CO_2 incubator, prior to collecting adhesion cells from wells. Six wells were randomly selected, and then cell numbers were counted twice for each well (total 12-time measurements). Based on the average cell numbers from the 12-time counts, 20,000 cells were transferred from each well on the TC plate to its matching site on an activated ELISpot plate (i.e. cells from the well "A1" on TC plate were transferred to the well "A1" on an ELISpot plate).

Chronically TSE-infected cells and control cells

SMB cells: After the inoculation of the mouse-adapted scrapie strain Chandler, the SMB cell line was originally isolated from the brain of the mouse when it showed clinical signs.[13] PrP^{Sc} expressions were detected in SMB cells even after continuous passages. Thus, the SMB cell line has been used as chronically TSE-infected cells. The SMB-PS cell line was established as a control that SMB cells were treated with pentosan sulphate (PS). Since SMB-PS cells permanently lost PrP^{Sc} generations even

after 50 passages, it was considered as a cured cell line.[14] These cell lines were maintained in culture with medium (10% FBS, and 1μg/ml penicillin, 100 U/ml streptomycin) in a 5% CO_2 incubator at 37°C.

TSE-infected RK13 cells: Using the transfected RK13 cell lines with stable PrP expressions described above, chronically TSE-infected cell models were established.[10] These TSE-infected cells chronically generate detectable amounts of PrP^{Sc} isoforms. The RKM7 cell line with mouse PrP expressions is highly susceptible to TSE infection. RML-RKM7 cells were isolated from RKM cells infected with a mouse-adapted scrapie strain RML.[11] Elk^+ cells were isolated from infected RKE cells with CWD positive elk brain (012-09442) and this cell line expresses PrP^{Sc} isoforms chronically.[10] The RKV cell line is RK13 cells stably transfected only with empty vectors. In addition to these uninfected/cured and infected cells, this non-PrP expressing cell line was included as a control of non-TSE infection and non-PrP^{Sc} generation. These cells were maintained with DMEM (10% FBS, 1μg/ml penicillin, 100U/ml streptomycin, and 1μg/ml puromycin) in TC dishes or T75 flasks in a CO_2 incubator (5%) at 37°C.

Transfer cells onto an ELISpot plate: Confluent cell monolayer of a dish/flask was washed twice with cold 1X PBS and then trypsinized. After counting numbers of collected cells, 20,000 cells of each cell line were placed per well (wells = triplicate) into assigned sites on an activated ELISpot plate.

3) Enzymatic cell digestion: Proteinase K (PK) was utilized to detect PrP^{Sc} molecules in TSE-infected cells on the ELISpot plate. Cells in PK-positive wells were enzymatically digested with 5μg/ml of the PK reagent (Roche Diagnosis, Indianapolis, USA) in a cell lysis buffer (CLB: 50mM Tris (pH 8.0), 150mM NaCl, 0.5% sodium

deoxycholate, 0.5% Igepal CA-630). 60µl of the PK reagent in CLB was added into each PK-positive well on the ELISpot plate. Subsequently, the plate was covered with a lid cover. A humidified chamber was prepared and filled with 1X PBS (no calcium and magnesium) up to its quarter-inch level. Two empty pipet tip racks was placed into the humidified chamber. After the ELISpot plate was put on the racks, the chamber was closed with a lid, and then placed on a shaker in an oven to incubate for 90 minutes at 37°C. Next, the ELISpot plate was vacuumed to empty all wells. To terminate this enzymatic digestion, 150µl of 2mM phenylmethylsulfonyl fluoride (PMSF: AMRESCO LLC, Solon, Ohio, USA) was added into all PK-positive wells. The ELISpot plate was placed into the humidified chamber, incubated on an orbital shaker at RT for twenty minutes, and finally vacuumed. For the protein denaturation, 120µl of 3M GdnSCN (Fisher Scientific, Fair Lawn, New Jersey, USA) in 10mM Tris-HCl (pH 8.0) was added into each well. The ELISPot plate was incubated on the shaker at RT for 10 minutes (note: this incubation time should not be exceeded). Immediately after the incubation, the plate was vacuumed. 160µl of 1X PBS was added into all wells to wash filter membranes. Additionally, this washing and vacuuming procedure was repeated four times.

4) Immunodetection: In a blocking procedure, 160µl of 5% SuperBlock (Pierce, Rockford, Illinois) in ultrapure water was added into each well on the ELISpot plate. After covering with a lid, the plate was placed in the humidified chamber and incubated for one hour at RT on an orbital shaker. After vacuuming the plate, 60µl of a diluted anti-prion antibody (i.e. 6H4 = 1:20,000, PRC5 = 1:3,000, PRC7 = 1:2,000-3,000) in fresh 1X TBST was added into each designated well. In this Chapter 3, 1:2,000 dilution of PRC7

mAb was used for the CPCA experiments. The ELISpot plate was covered with a lid and placed into the humidified chamber. This incubation was performed overnight at 4°C on a rotating shaker in a refrigerator as recommended, or for one hour at RT on a rotating shaker as an alternative way. By flicking the plate, coated antibody solutions were removed from wells. For washing all wells, 160µl of fresh 1X TBST was added and then removed by flicking the plate. This procedure was repeated three times. At the same time, a secondary antibody, alkaline phosphatase (AP)-conjugated Goat anti-Mouse IgG antibody (Southern Biotechnology Associates, Birmingham, AL), was prepared as 1:5,000 dilution in fresh 1X TBST. After the fourth wash with 1X TBST, the plate was completely vacuumed, and immediately, 60µl of the prepared secondary antibody solution was added into each well on the ELISpot plate. The plate was covered with a lid and placed on empty pipet racks in a chamber without liquids for maintaining moisture. After incubating the plate for one hour at RT on a shaker gently, the secondary antibody solutions were flicked out from the plate. 160µl of fresh 1X TBST was added into each well to wash the plate. For each wash, the plate was flicked to remove 1X TBST. After repeating this washing procedure four times, fresh 1X PBS (no calcium and magnesium) was added into all wells as a final wash (the fifth time). After vacuuming the plate completely, a plastic drain was removed from the bottom of the ELISpot plate, and then the bottom area was gently rinsed with 1X PBS one time for eliminating residual agents. To dry the plate completely, it was placed on a bench overnight, and covered loosely with a large kimwipe paper (Kimberly-Clark Professional, Roswell, GA). For color developments, a tablet of an AP-conjugate substrate kit (NBT/BCIP Tablets, Roche Diagnosis, Indianapolis, USA) was prepared in 10ml

ultrapure water. 60µl of the prepared AP-conjugate substrate solution was added into each well at RT. Subsequently, the ELISpot plate was hidden in the dark for color development. When color change was detected, the plate was flipped to stop the reaction, and then washed with 160µl of water twice. The plate was flipped to remove all solutions. To dry the plate completely, it was placed in a 4°C refrigerator overnight, without stacking plates when multiple plates were used. Imaging scans were performed using ImmunoSpot S6-V analyzer (Cellular Technology Ltd, Shaker Heights, Ohio). Spot numbers of color-developed cells were measured by ImmunoSpot5 software (Cellular Technology Ltd, Shaker Heights, Ohio). The titer of the PrP^{Sc} detection was based on calculated numbers of color spot-forming TSE-infected cells (or cervid prion cells: CPC) per gram of an applied BH sample.

5) Tested reagents for modifying the CPCA protocol to utilize PRC7 mAb: To improve the utility of PRC7 mAb in the CPCA protocol described above, the following reagents were applied for permeabilization, enzymatic digestion, or denaturation. Tested conditions of each reagent in the CPCA experiments are described in the Result section.

Permeabilization = Triton® X-100 (TX100, Fisher Scientific, Fair Lawn, New Jersey, USA), Tween® 20 (Fisher Scientific, Fair Lawn, New Jersey, USA), and Saponin (Sigma-Aldrich, Inc. St. Luis, MO, USA).

Enzymatic digestion = proteinase K (PK, Roche Diagnosis, Indianapolis, USA), PMSF (AMRESCO LLC, Solon, Ohio, USA), and cell lysis buffer (CLB, pH 8.0) that contains 50mM Tris (Tris Base, Fisher Scientific, Fair Lawn, New Jersey, USA), 150mM Sodium Chloride (NaCl, Acros Organics, Thermo Fisher Scientific, Fair Lawn, New

Jersey, USA), 0.5% IGEPAL® CA-630 (Sigma-Aldrich, Inc. St. Luis, MO, USA), and 0.5% Sodium Deoxycholate (Sigma-Aldrich, Inc. St. Luis, MO, USA) in filtered distilled water.

Denaturation = guanidine thiocyanate (GdnSCN, Fisher Scientific, Fair Lawn, New Jersey, USA), and guanidine hydrochloride (GdnHCL, Sigma-Aldrich, Inc. St. Luis, MO, USA).

New Sandwich ELISA protocol for detecting PrP^C molecules

Based on the 7-5 ELISA protocol described above, other capture antibodies were evaluated to establish a new Sandwich ELISA method without the detergent and denaturant (TX100 and GdnHCL respectively), which can detect normal PrP^C molecules, predominantly with a diglycosyl form. Tested anti-PrP antibodies were the following: 6H4 (Prionics, Schlieren, Switzerland), PRC5 mAb, and D18 Fab Ab (both in-house productions). To prevent protein degradation during experiments, a protease inhibitor product (cOmplete, Roche Diagnostics, Indianapolis, IN, USA) was added into buffers under the manufacture's direction: sample dilution buffer, blocking buffer, and dilutions of detecting and secondary antibodies. 10% BH samples from uninfected homozygous Tg4112 (MousePrP overexpression) and PrP-KO mice were applied for these Sandwich ELISA experiments. Technical applications in this study will be described in the Results section.

The D-5 ELISA method and its comparative evaluations with other capture antibodies

A pair of D18-PRC5 antibodies was capable of detecting PrP^C agents sensitively by this Sandwich ELISA approach, now called the D-5 ELISA method. D18 Fab Ab requires denaturation to detect PrP27-30 rods by ELISA and IP experiments.[15] This new D-5 ELISA method examined the following BH samples with denaturation (n=1 each mouse category): RML-inoculated FVB/n, RML-inoculated C57BL6, and 22L-inoculated C57BL6 mice, and their controls (PrP-KO, uninfected FVB/n, uninfected C57BL6). All processes were performed by the 7-5 ELISA protocol, except the capture antibody D18 Fab Ab. The D-5 ELISA method was optimized by the same approaches for the 7-5 ELISA development, described in Chapter 2 and 3 above.

In comparison with the D18 Fab Ab, the following anti-PrP antibodies were determined as capture antibodies under the D-5 ELISA protocol: PRC7 (in house), 6H4 (Prionics, Schlieren, Switzerland), POM2 (Prionatis AG, Alpnach Dorf, Switzerland), SAF-32 (Cayman Chemical, Michigan, USA[16]), and mAb132 (kindly provided by Dr. Motohiro Horiuchi, Hokkaido University, Japan[17,18]). Tested applications of these antibodies will be described in the Results section. BH samples of RML-inoculated FVB/n, uninfected FVB/n, and PrP-KO mice (n=1) were applied to this experiment with and without detergent and denaturant for measuring PrP^{Sc} or only PrP^C levels respectively. Furthermore, the D-5 ELISA approach with or without detergent and denaturant was examined with TSE-inoculated mouse models expressing different PrP species: RML-inoculated FVB/n, CWD-inoculated Tg1563 (ElkPrP), CWD-inoculated Tg5037 (ElkPrP), CWD-inoculaed gene-targeted mouse (ElkPrP), Colorado Scrapie-

inoculated Tg3533 (SheepPrP), TME-inoculated TgF431 (MinkPrP) mice, and these control mice.

Enhancement of PrP detections in TSE-infected materials by the novel Sandwich ELISA methods

To improve sensitivity and selectivity of PrP measurements by the new Sandwich ELISA applications, the 7-5 ELISA and D-5 ELISA methods, the following reagents were utilized: Proteinase K (PK: Roche Diagnosis, Indianapolis, USA), cell lysis buffer (CLB: 50 mM Tris (pH 8.0), 150mM NaCl, 0.5% sodium deoxycholate, 0.5% Igepal CA-630), phenylmethylsulfonyl fluoride (PMSF: AMRESCO LLC, Solon, Ohio, USA), Triton® X-100 (TX100: Fisher Scientific, Fair Lawn, New Jersey, USA), Sarkosyl (Fisher Scientific, Fair Lawn, New Jersey, USA), sodium hydroxide (NaOH: Fisher Scientific, Fair Lawn, New Jersey, USA), sodium chloride (NaCl: Acros Organics, Thermo Fisher Scientific, Fair Lawn, New Jersey, USA), monosodium phosphate (also named as monobasic sodium phosphate and sodium dihydrogen phosphate, NaH_2PO_4: Sigma-Aldrich, Inc. St. Luis, MO, USA), sodium bicarbonate ($NaHCO_3$: Sigma-Aldrich, Inc. St. Luis, MO, USA), sodium carbonate (Na_2CO_3: Sigma-Aldrich, Inc. St. Luis, MO, USA), carbonate-bicarbonate buffer-capsule (contains both Na_2CO_3 and $NaHCO_3$ in equilibrium: Sigma-Aldrich, Inc. St. Luis, MO, USA), sodium deoxycholate (deoxycholic acid sodium salt, DOC: Sigma-Aldrich, Inc. St. Luis, MO, USA), and sodium dodecyl sulfate (SDS: Fisher Scientific, Fair Lawn, New Jersey, USA). Applications of each reagent and tested mouse BH samples will be described in the Result section.

Applications of the new Sandwich ELISA methods to detect PK-sensitive PrP^{Sc} agents

The Tg464 mouse breed line is a transgenic animal model of Gerstmann-Sträussler-Scheinker (GSS) syndrome, an autosomal-dominant inherited prion disease in humans. Although this GSS mouse model spontaneously develops clinical and pathological features of GSS, these mice generate PK-sensitive PrP molecules.[19] Therefore, standard PrP^{Sc} analyses using PK reagents are not applicable to Tg464 mice. Since the 7-5 ELISA and D-5 ELISA protocols do not use PK reagents, these approaches should be capable of detecting the enzyme-sensitive PrP molecule. Under the current optimized protocols of these Sandwich ELISA methods with or without detergent and denaturant, BH samples from Tg464 mice at different ages (pre-clinical sign: 61, 81, 142 days) and with clinical signs (KN-35 study: 1% BH sample from a spontaneously GSS-developed Tg464 mouse was inoculated into 40-day ages of young Tg464 mice that were at non-clinical condition) were examined to measure detectable levels of PrP^{Sc} and PrP^{C} isoforms, as well as PrP modulations at each time-point base. WB also analyzed the BH samples using the protocol, previously reported.[11,20,21] According to the protocol and these references, 100μg/ml of the PK reagent in cold lysis buffer was applied to each BH sample for 1 hour at 37°C, and subsequently terminated with PMSF (2 μM at a final concentration in each digested sample) for PK digestions. After the 10-minute boiling of prepared samples, proteins were resolved by SDS-PAGE and then transferred to Immobilon-FL PVDF (Polyvinylidene Difluoride) membranes (Millipore, Billerica, USA). Primary mAbs were applied to probe these membranes, followed by a HRP–conjugated anti-mouse secondary antibody (GE Healthcare, Little

Chalfont, UK). Proteins were visualized by chemiluminescence using ECL Plus (GE Healthcare, Piscataway, USA) and an FLA-5000 scanner (Fujifilm Life Science, Woodbridge, USA).

Results

Sensitivity of the 7-5 ELISA method for PrP detections in TSE-infected mouse models

Using the optimized 7-5 ELISA conditions that I described in the previous chapter, the sensitivity of this method was determined for PrP detections in brain samples from RML-infected FVB/n mice, uninfected FVB/n mice, and PrP-KO mice in which the PrP gene was disrupted by homologous recombination, also referred to as *Prnp*$^{0/0}$ mice. Using the 7-5 ELISA method, total protein levels in each sample were determined, and these reactivities were compared over an equivalent range of concentrations ranging from 0.06µg to 20µg. Triplicate replicates of each sample were analyzed to assess technical reproducibility. The lowest amount still showed subtle differences between the infected and control samples ($P<0.0001$) (Figure 3-1.A). For the further analysis of the assay sensitivity, the 7-5 ELISA method was tested with the range from 0.01ng to 20ng total proteins (wells = triplicate as technical replicates for each sample) for PrP detections in the same sample group above. Even in picogram amounts, the 7-5 ELISA method detected subtle levels of PrP molecules in the infected sample (Figure 3-1.B). To confirm the specificity of the 7-5 ELISA method, PRC7 was replaced with a non-specific murine IgG1 antibody as a capture antibody. These comparison experiments assessed reactivity from the same BH samples, using 20µg

per well. The Sandwich ELISA approach with the IgG1 Ab and PRC5 mAb did not show differences among these samples. (Figure 3-1.C). These results suggest that the 7-5 ELISA method has the sensitivity for detecting subtle PrP amounts in TSE-infected BH materials, even lower than 1μg total protein.

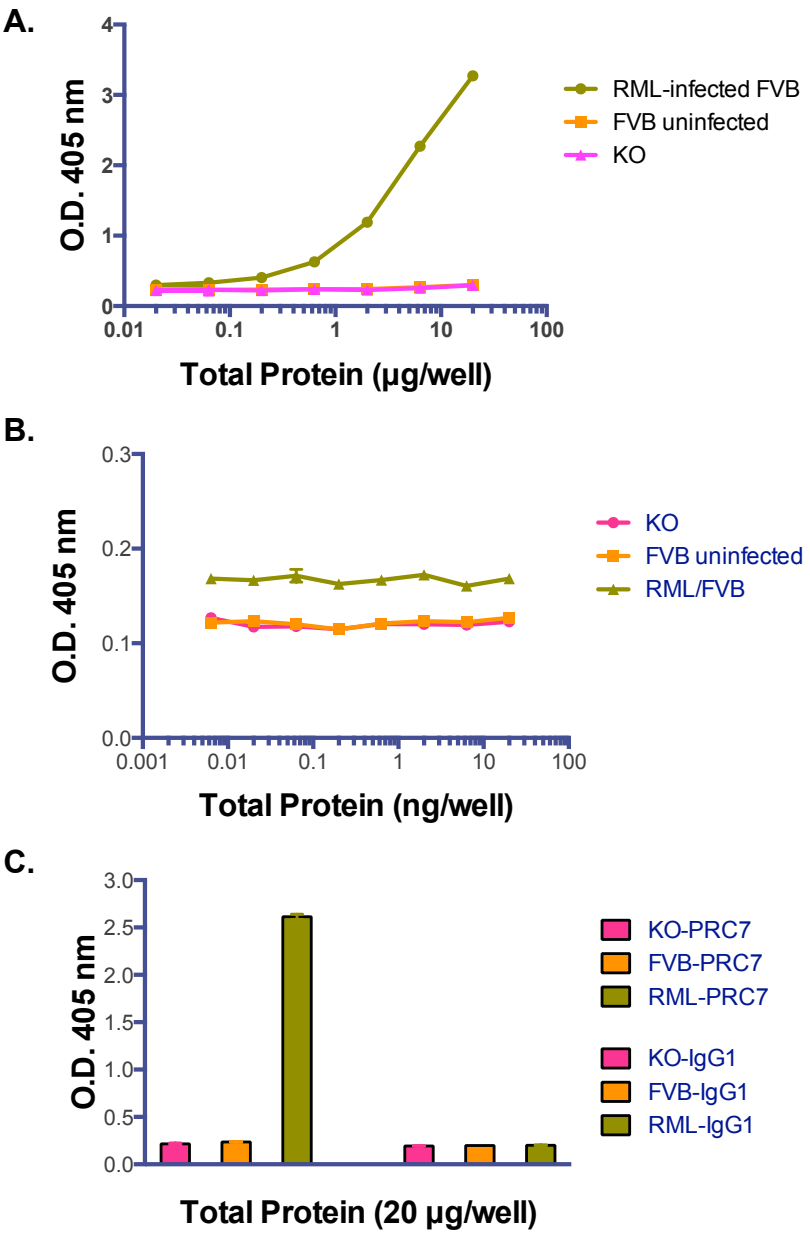

Figure 3-1. Sensitivity of the 7-5 ELISA method for PrP detections.
(A) Half-log dilutions of proteins from murine BH samples of PrP-KO, uninfected FVB/n, and RML-infected FVB/n (n=3, each total protein amount from 0.06µg to 20µg), (B) Protein-dose dependent responses of lower half-log dilutions in range from 0.01ng to 20ng total proteins (n=3, each total protein amount), and (C) Comparisons of PRC7 mAb (left) and IgG1 antibody (right) as capture antibodies in Sandwich ELISA approaches (n=3, each sample with 20µg total protein amount).

Biological replicates of TSE-mouse models for PrP detections by the 7-5 ELISA method

To evaluate PrP variances among mice, the 7-5 ELISA method was tested with three different groups of the following TSE-mouse models: 1) RML-inoculation in FVB/n mice, 2) CWD-inoculation in Tg5037 (ElkPrP) mice, and 3) CWD-inoculation in Tg1536 (DeerPrP) mice. The mean ± SEM of sick dates for these three mice in each inoculated experiment was 1) 129.33 ±2.33 for RML-FVB/n, 2) 263.33±45.88 for CWD-Tg5037, and 3) 401.33±1.76 for CWD-Tg1536. Each testing group contained nine total animals from TSE-infected mice, uninfected mice, and PrP-KO mice: three mice were from each mouse category. Using these BH samples, the 7-5 ELISA method exhibited significantly higher O.D. values of PrP detections in all TSE-infected mice (Figures 3-2.A to C). Statistically, p values of Infected vs. KO or uninfected mice were following: RML-FVB/n vs. KO or Uninfected as $p < 0.0001$ for both; CWD-Tg5037 vs. KO or Uninfected as $p = 0.00024$, and 0.0027 respectively; CWD-Tg1536 vs. KO or Uninfected as $p = 0.0056$, and 0.0059 respectively. These results indicated the specificity of the 7-5 ELISA method for PrP detections in TSE-infected brain materials. In addition, the 7-5 ELISA method measured high quantities of under-glycosylated PrP forms in these analyte. As hypothesized, hence, the loss or deficit of the PrP glycosylation occurred during the TSE disease development in mice.

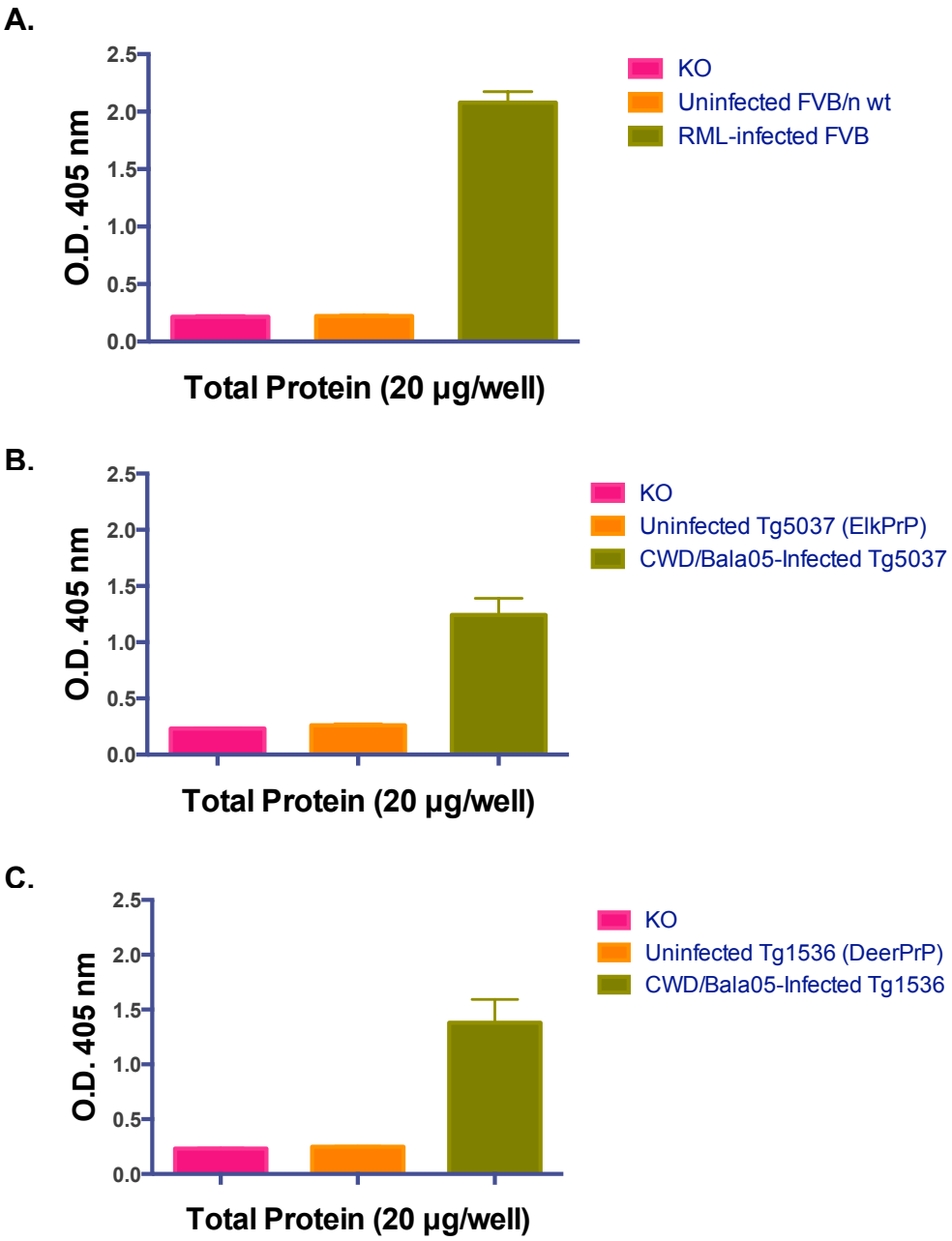

Figure 3-2. PrP detections in TSE-inoculated murine brain analyte by the 7-5 ELISA method. Biological replicates (n= three mice, each category). (A) RML-inoculated FVB/n mouse, (B) CWD(Bala05)-inoculated Tg5037 mouse, and (C) CWD(Bala05)-inoculated Tg1536 mouse.

Capability of the 7-5 ELISA method for PrP detections from multiple species in TSE-mouse models

PRC7 mAb is only capable of reacting to an unglycosyl form and one mono glycosyl form (mono-1: one glycan at 180 amino acid residue) of PrP molecules.[20] Because of this characteristic feature, the 7-5 ELISA method specifically recognizes these two under-glycosylated PrP forms that are significantly detected in TSE-infected materials (Figures 3-2.A to C). For further analyses, the 7-5 ELISA method was applied for testing BH samples from five different TSE mouse models: 1) RML-inoculation in FVB/n mice, 2) CWD-inoculation in Tg5037 (ElkPrP) mice, 3) CWD-inoculation in Tg1536 (DeerPrP) mice, 4) Sheep scrapie-inoculation in Tg3533 mice (OvineARQ PrP: alanine (Ala: A) at the residue 136), and 5) Transmissible mink encephalopathy (TME)-inoculation in TgF431 (MinkPrP) mice. Each TSE model included BH samples from its uninfected wild-type or transgenic mice. The 5th Group of TME contained BH samples from uninfected mink. These 7-5 ELISA analyses evaluated higher quantities of under-glycosylated PrP forms as a hallmark of TSEs and a diagnostic biomarker of the disease progression. This approach also determined the capability of this method for detecting PrP molecules in different species. Initially, testing BH samples were treated with 1% TX100 for one hour, and then denatured with 5M GdnHCL for 15 minutes at 37°C, with 1,000 rpm agitation for both incubation times. After 10-time dilutions, the prepared samples contained 60μg total proteins. To determine protein-dose dependent responses of PrP detections, these final samples were additionally diluted to the range from 2.5 μg to 50μg total proteins. Thereafter, all prepared samples were coated on PRC7-coated ELISA plates (well numbers = triplicate for each amount). After an

incubation on the ELISA plates at 4°C overnight, the wells with samples on ELISA plates were blocked with 3% BSA-containing PBS for one hour at 37°C. Then, the detecting antibody PRC5 and secondary antibody were applied to the wells, and incubated 1 hour at 37°C for each antibody. After color development with ABTS® Peroxidase Substrate (under the manufacture's protocol), the ELISA plates were read by the plate reader for measuring O.D. values of PrP detections in each sample. Based on the results from the protein-dose dependent responses (total proteins from 2.5μg to 60μg per well with triplicate), higher detections of the under-glycosylated PrP forms were significant in all tested TSE-infected materials by the 7-5 ELISA method (Figures 3-3.A to E). These results indicated that these certain forms of PrP molecules were generated in animals with TSE infections. Thus, the 7-5 ELISA method should be a powerful application to detect PrP molecules in multiple species. Also, this method was applicable to the PrP detection in various TSEs. However, a TME-infected mouse exhibited lower O.D. values than other TSE-infected samples. This finding suggested that the mouse with TME inoculation might not generate much under-glycosylated PrP forms. In another prospect, the sick date of this TME-infected mouse was 93 days (mean sick date = 108.5 days in its study group), which were shorter than those of other tested samples with TSE inoculations. Therefore, this short incubation period for the disease development may have not generated or accumulated under-glycosylated PrP forms in mice with the TME inoculation. Moreover, the 7-5 ELISA method measured some PrP detections in uninfected TgF431 with mink PrP expressions, compared to a PrP-KO mouse. Because of PrP overexpressions, this transgenic mouse breed line may produce under-glycosylated PrP forms in normal conditions, compared to wild-type

mice. Thus, transgenic mice with PrP overexpressions should normally express some levels of PrP molecules with the glycosidic impairment or immature process.

A.

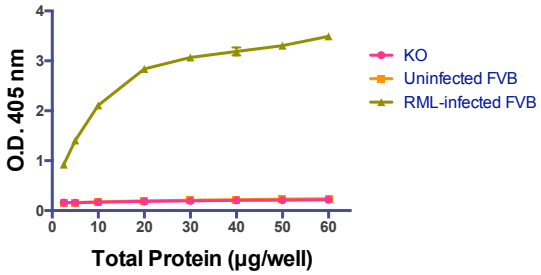
O.D. 405 nm
Total Protein (µg/well)
KO
Uninfected FVB
RML-infected FVB

B.

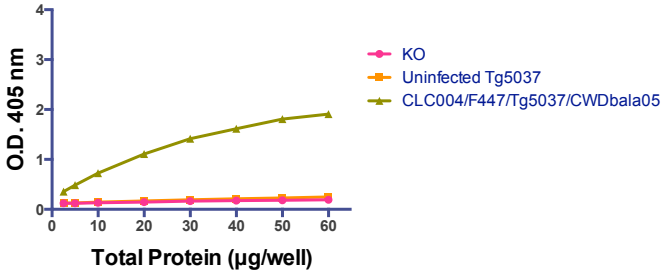
O.D. 405 nm
Total Protein (µg/well)
KO
Uninfected Tg5037
CLC004/F447/Tg5037/CWDbala05

C.

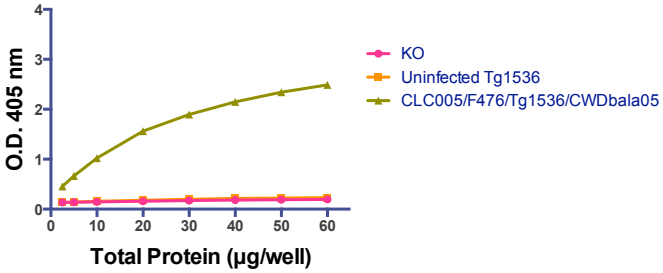
O.D. 405 nm
Total Protein (µg/well)
KO
Uninfected Tg1536
CLC005/F476/Tg1536/CWDbala05

D.

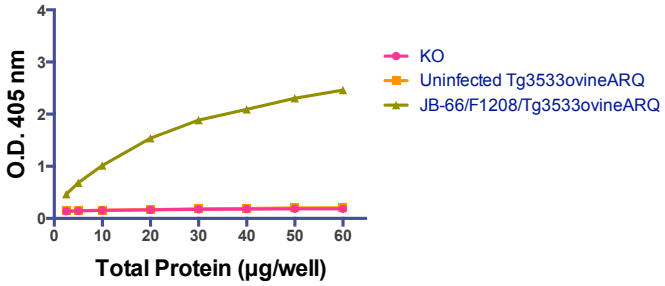
O.D. 405 nm
Total Protein (µg/well)
KO
Uninfected Tg3533ovineARQ
JB-66/F1208/Tg3533ovineARQ

E.

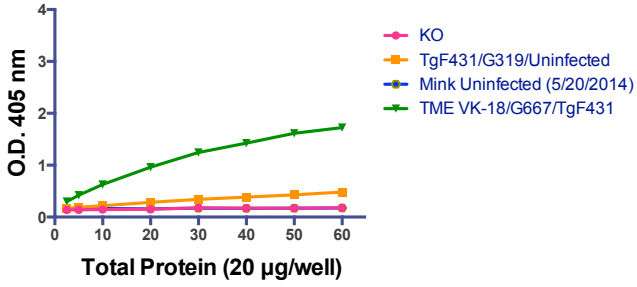
O.D. 405 nm
Total Protein (20 µg/well)
KO
TgF431/G319/Uninfected
Mink Uninfected (5/20/2014)
TME VK-18/G667/TgF431

Figure 3-3. Protein-dose responses of PrP detections in BH samples from mouse models with five different TSE strains by the 7-5 ELISA method. (A) RML-inoculation in FVB/n, (B) CWD-inoculation in Tg5037 (ElkPrP), (C) CWD-inoculation in Tg1536 (DeerPrP), (D) Sheep scrapie-inoculation in Tg3533 (OvineARQ), and (E) TME-inoculation in TgF431 (MinkPrP) mice. (n=3, each total protein in range from 2.5 μg to 50μg per well)

PrP detections in various mouse-adapted TSE strains by the 7-5 ELISA method

The RML strain of mouse-adapted scrapie was used in processes of the 7-5 ELISA development and optimization. For further analyses, the 7-5 ELISA method measured PrP detections in BH samples from other mouse-adapted TSE strains: 22L (mouse-adapted scrapie in C57BL6 mouse), 87V (mouse-adapted scrapie in VM/Dk expressing PrP allotype B) and D10 (mouse-adapted CWD in FVB/n mice primary and passaged into C57BL6 mice secondary). Firstly, these BH samples were treated with 1% TX100, then denatured with 5M GdnHCL, and incubated for 1 hour and 15 minutes at 37°C respectively, with 1,000rpm agitation. At the final step of the sample preparations, the total protein 20µg of the prepared sample treated at each GdnHCL dose was coated on ELISA plate wells, in which PRC7 mAb was coated previously (triplicate for each individual). For controls, uninfected PrP-KO (FVB/Prnp$^{0/0}$), FVB/n and C57BL6 mice were included. An RML-infected FVB/n mouse was also contained as a positive control of TSE-infected samples. The 7-5 ELISA results showed higher O.D. values in all tested TSE-infected mouse BH samples, compared to uninfected controls (Figure 3-4.A).

However, the PrP detection in the 87V-infected sample was almost twice less than other TSE samples. The same BH samples from these mouse-adapted prions were analyzed by Western blot that showed similar results to this 7-5 ELISA experiment above (data not shown). Therefore, the 7-5 ELISA protocol can be utilized to analyze detections and quantifications of PrP molecules in TSE-mouse models. For the 87V strain and VM/Dk mouse background, several possibilities can be considered for low PrP detections by the ELISA analysis. Potentially, this result suggested that the 87V

strain showed the sensitivity or resistance to denaturation, and 5M GdnHCL was not effective for its PrP detections. To investigate this possibility, the 7-5 ELISA method was determined by GdnHCL-dose dependent responses for the PrP detection in various mouse-adapted TSE strains. Based on the 7-5 ELISA protocol, BH samples from the tested mice above were prepared with different concentrations of GdnHCL (0, 1, 2, 3, 4, 5, 6, or 7M). After the final procedure of the sample preparations, 20μg total protein of each prepared sample was coated on wells for PRC7-coated ELISA plates (well numbers = triplicate for each individual at each GdnHCL dose). The 7-5 ELISA results detected that the 22L prion strain showed the highest O.D. values of PrP detections with 2M GdnHCL, whereas other strains required 3-4M GdnHCL for reaching to the peak of the O.D. values (Figures 3-4.B to E). However, the 87V-infected BH analyte decreased the O.D. value of PrP detections when denatured with 5M GdnHCL and higher concentrations. This observation could be related to the conformational stability of the 87V strain, indicated by its tolerance level to denaturation. As described above, both PRC7 and PRC5 mAbs bind to these epitopes in the structured globular domain at the C terminal of the PrP structure. Thus, these results might suggest conformational differences in or around the mAb-biding sites among TSE strains and PrP allotypes. For further studies, the 7-5 ELISA method would have potential applications for analyzing biochemical properties in TSE-strain differences, such as a conformational stability assay using various denaturants and other reagents.

A.

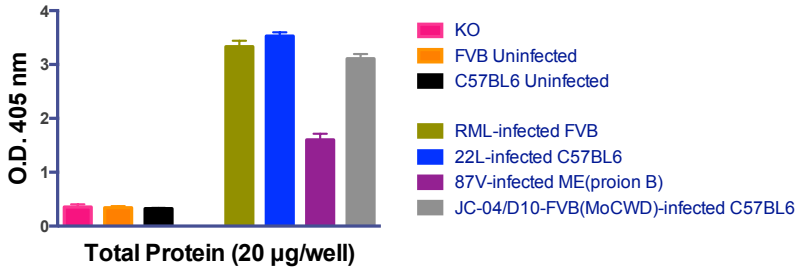
O.D. 405 nm
Total Protein (20 µg/well)
KO
FVB Uninfected
C57BL6 Uninfected
RML-infected FVB
22L-infected C57BL6
87V-infected ME(proion B)
JC-04/D10-FVB(MoCWD)-infected C57BL6

B.

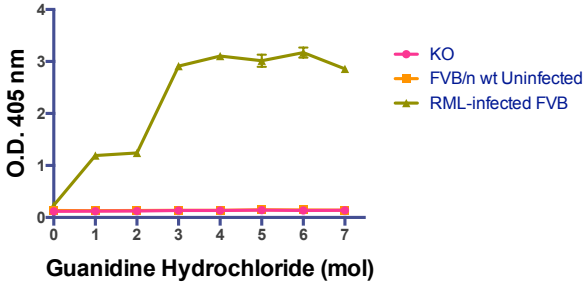
O.D. 405 nm
Guanidine Hydrochloride (mol)
KO
FVB/n wt Uninfected
RML-infected FVB

C.

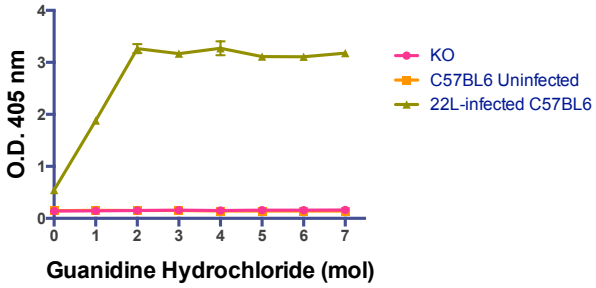
O.D. 405 nm
Guanidine Hydrochloride (mol)
KO
C57BL6 Uninfected
22L-infected C57BL6

D.

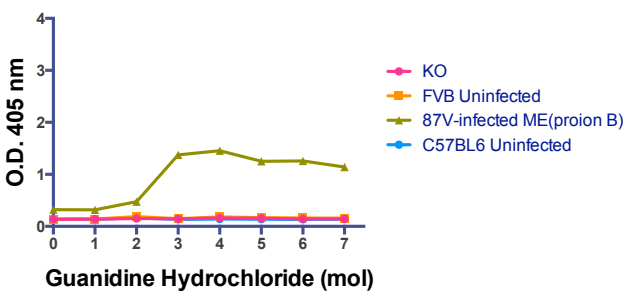
O.D. 405 nm
Guanidine Hydrochloride (mol)
KO
FVB Uninfected
87V-infected ME(proion B)
C57BL6 Uninfected

E.

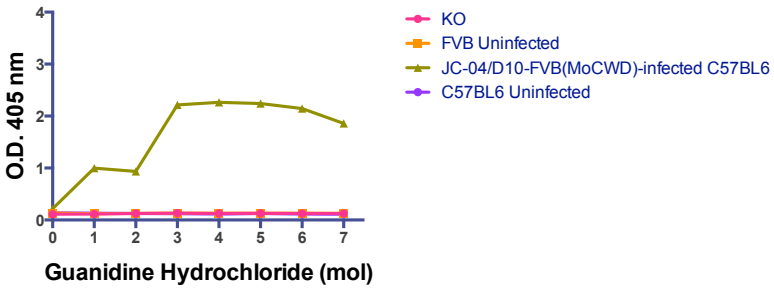
O.D. 405 nm
Guanidine Hydrochloride (mol)
KO
FVB Uninfected
JC-04/D10-FVB(MoCWD)-infected C57BL6
C57BL6 Uninfected

Figure 3-4. Comparisons of PrP detections among four different mouse-adapted scrapie strains. The 7-5 ELISA method measured GdnHCL-dose dependent responses of PrP levels in BH samples from TSE-mouse models:
(B) RML, (C) 22L, (D) 87V, and (E) D10. (n=3, each GdnHCL dose with 20μg total protein per well)

Variances of detectable PrP levels in CWD mouse models by the 7-5 ELISA method

Primarily, the following six mouse model studies were evaluated for transmissible properties of inoculated CWD isolates: 1) ES-02, 2) ES-03, 3) KG-18, 4) RA-26, 5) GT-142, and 6) GT-143. For the 7-5 ELISA studies, each study group included BH samples of three CWD-infected mice. Controls were PrP-KO, uninfected Tg1536 (DeerPrP) and Tg5037 (ElkPrP) mice. These hemizygous $Tg1536^{+/-}$ and $Tg5037^{+/-}$ mice generate approximately five-fold higher levels of PrP expressions in their brains than the wild-type mice (FVB/n). The PrP structure between deer and elk is one difference at the amino acid residue 226, which consists of glutamine (abbreviated as Gln or Q) in deer, but glutamic acid (abbreviated as Glu or E) in elk. A recent study indicated that the residue 226 was localized in α-helix 3 and consisted of the β2-α2 loop in the globular domain of the PrP structure.[22] This domain implicated with the PrP^{Sc} replication and CWD pathogenesis. Thus, conformational compatibility at this amino acid residue should be associated with rearrangements of PrP structures between deer and elk.

1) PrP detections of moose CWD isolates in transgenic mouse models: In wild nature, five diagnosed cases of moose with CWD infections have been reported: three cases in Jackson County, Colorado[23]; one case in Star Valley, Wyoming; another case in Hilda, Alberta, Canada (no peer-review article for the cases in Wyoming and Canada but these information are available by internet searches). These moose cases with natural transmissions were found in CWD-endemic areas for other cervids, such as deer and elk. It is known that primary PrP structures in deer (Odocoileus species) and Shira's moose (Alces alces shirasi) are identical. Thus, CWD transmissions between

these species could be a potential infectious route. Thus, one publication determined an experimental inoculum of the brain tissue sample from a CWD-infected captive mule deer into three moose (captive Shiria's moose) via oral transmission.[24] In the mouse-model studies of ES-02 and ES-03, a brain tissue sample from the CWD-infected moose (08W-11,741: one of the three CWD-infected moose above) was inoculated into Tg1536 (DeerPrP) and Tg5037 (ElkPrP) mice, respectively. BH samples from these moose CWD-infected mice and controls (uninfected cervidized transgenic mice and PrP-KO mice) were tested with the 7-5 ELISA method. In addition, the inoculated brain sample of the moose CWD isolate was included for this analysis. The total protein 20μg of each prepared sample was coated on a well (triplicate for each individual) on a 7-5 ELISA plate. These analyses measured higher O.D. values of PrP detections in all infected mice from the two studies, compared to the controls (Figure 3-5.A and B). In fact, the infected Tg1536 (DeerPrP) mice exhibited higher levels of PrP detections than the infected Tg5037 (ElkPrP) mice and the CWD-infected moose brain sample (Figure 3-5.C). These findings suggested the transmissible property of the moose CWD isolate to deer and elk through the species barrier. Also, this inoculum might behave like a deer CWD pathogen in the transgenic mice with deer PrP expressing because of the identical primary PrP structure in deer and moose. Thus, the PrP^{Sc} propagation of the moose CWD agents could be more prominent in Tg1536 mice than Tg5037 mice. However, the disease incubation time in Tg5037 mice was shorter than Tg1536 mice: mean incubation times ± SEM, 286.33±15.56 days (Tg5037 in ES-03 study), and 322.00±10.03 days (Tg1536 in ES-02 study). Based on these 7-5 ELISA results, the shorter incubation time of the CWD-infected Tg5037 mice might indicate the

susceptibility of elk to the moose CWD transmission and the early or progressive disease development. In this point, it is not clear if generations and accumulations of under-glycosylated PrP^{Sc} forms were limited in the infected Tg5037 mice during the disease development. In the previous article, transmissions of several different CWD isolates were evaluated in these transgenic mice.[25] Compared to the Tg1536 (DeerPrP) mice with CWD inoculations, the infected Tg5037 (ElkPrP) mice exhibited faster incubation times for all tested CWD isolates derived from deer or elk. Depending on inocula, the infected group of Tg5037 mice was 24-148 day shorter for disease-incubation periods than that of Tg1536 mice. Therefore, the Tg5037 mouse with elk PrP expressions is prone to exhibit faster disease development and progressions after CWD inoculations. In another aspect, Tg5037 mice with the moose CWD inocula might generate preferentially diglycosyl and/or mono-2 glycosyl PrP forms, which PRC7 mAb in the 7-5 ELISA method cannot recognize. To determine this possibility, WB is applicable with the same samples from the moose CWD-inoculation studies.

2) CWD inocula isolated from elk into Tg1536 (DeerPrP) mice: The two prevalent types of CWD strains exhibited different pathological, biological and biochemical features.[26] The CWD type 1 is the strain, progressing the disease development in short incubation periods with bilaterally symmetric lesions of its histological distribution in brain. In contrast, the features of the CWD type 2 are long incubation periods with asymmetrical distribution of PrP^{Sc} agents in brains. However, these CWD strains have similar biochemical characteristics. According to WB results, the proportions of various glycosylated PrP forms were equivalent among mice infected with CWD type 1 (n=44) and type 2 (n=14) strains.[26] The dose-dependent responses for

GdnHCL were similar properties between transgenic mice with deer or elk PrP expressions inoculated with CWD type 1 and 2. In addition, inoculations of CWD strains from elk (Elk CWD) to Tg1536 (DeerPrP) mice showed unstable responses for maintaining the strain types of the CWD inocula, and caused mixtures of pathological features of CWD type 1 and type 2 in brains, referred as strain mixtures or CWD type 3. However, the inoculated Elk CWD developed the features of the inoculated strain types in Tg5037 (ElkPrP) mice. This observation indicated stable propagations of inoculated Elk CWD strains in the same species.[26] These features of CWD transmissions can be arisen as different primary PrP structures in deer and elk at the amino acid residue 226, mentioned above.

The following inoculations of mouse models were previously performed to analyze pathologic characters of Elk CWD transmissions using Tg1536 (DeerPrP) mice.[26] One of the CWD inocula was 99W12389, originally from CWD-infected elk in the Sybille Wildlife Research Unit at the Wyoming Game and Fish Department. This strain was evaluated as a CWD type 1. Bala04/04-0306 was another CWD inoculum, derived from elk naturally affected with CWD in Saskatchewan, Canada, and identified as a type 2 strain. Briefly, the KG-18 study was an inoculation of the CWD strain 99W12389 (Type 1) into Tg1536 (DeerPrP) mice; the RA-26 study was an inoculation of the CWD strain Bala04/04-0306 (Type 2) into Tg1536 (DeerPrP) mice; the GT-142 study was a passage of 99W12389 (Type-1)-inoculated Tg5037 (ElkPrP) mouse brain (RA-86 study) into Tg1536 (DeerPrP) mice; and the GT-143 study was a passage of Bala04/04-0306 (Type 2)-inoculated Tg5037 (ElkPrP) mouse brain (RA-78 study) into Tg1536 (DeerPrP) mice. Using three mouse brain homogenates from each study above (except the GT-

143 study had four mice), the 7-5 ELISA method analyzed PrP detections in these CWD mouse models. The onsets of clinical signs and terminal-disease conditions were diagnosed in all infected mice. Controls included PrP-KO, uninfected Tg1536 (DeerPrP) and Tg5037 (ElkPrP) mice (n=3 for each as biological replications). This 7-5 ELISA experiment was performed under the same procedures in the moose CWD study above. As an outcome, the 7-5 ELISA method measured higher O.D. values of PrP detections in all infected materials, compared to the controls. However, PrP detectable levels varied among the three individuals in each study. To evaluate these ELISA results, other analyses (i.e. WB and dot blot) can be useful to compare variances of PrP levels in tested samples by each inoculation study. In general, the PK reagent is utilized in these two blotting methods as a common reagent in TSE research. Potentially, the use of PK reagents may influence biochemical properties of tested samples, inducing different responses. In fact, the WB did not distinguish differences between CWD type 1 and type 2 strains among large numbers of infected mice, when treated with PK reagents.[26] Since the 7-5 ELISA method can analyze PrP detections under its PK-free protocol, this method may recognize subtle type-base differences and other possible observations.

In the KG-18 study, infected Tg1536 (DeerPrP) mice showed higher PrP detections, as indicating the replication and propagation of PrP^{Sc} molecules derived from the 99W12389 Elk CWD strain (Type 1) inocula (Figure 3-5.D). This phenomenon also occurred in the infected mice from the GT-142 study (Figure 3-5.E): a passage of the 99W12389-inoculated Tg5037 (ElkPrP) mouse brain (from the RA-86 study) into Tg1536 (DeerPrP) mice. The O.D. values of infected mice in the GT-142 study were 2-3

folds higher than those in the KG-18 study. These results indicated that the Tg5037 mouse-passaged Elk CWD type 1 strain could increase propagations of its PrP^{Sc} agents in transgenic mice with deer PrP expressions. However, incubation periods in the GT-142 study were approximately twice longer than those in the first passage of the CWD type 1 strain in the KG-18 study: mean incubation time ± SEM; 417.83±36.74 days in the GT-142 study; and 229.88±8.62 days in the KG-18 study. Possibly, the prolonged incubation period in the GT-142 study was implicated with unstable and delayed propagations of the Elk CWD type 1 strain by deer PrP. Also, the strain mixtures of pathology (CWD type 3 by a deer PrP) might cause different features of disease developments.

In comparison with the RA-26 study that was the inoculation of the CWD type 2 strain Bala04/04-0306 into Tg1536 (DeerPrP) mice, higher O.D. values of PrP detections were measured in infected Tg1536 mice of the GT-143 study (a passage of Bala04/04-0306-inoculated Tg5037 (ElkPrP) mouse brain from the RA-78 study) (Figure 3-5.F and G). These measurements suggested that the transmission of the CWD type 2 strain into Tg5037 mice could enhance PrP^{Sc} propagations in transgenic mice with deer PrP expressions. Notably, the incubation times between these two studies were not very different: mean incubation time ± SEM; 280.71±5.25 days in the RA-26 study; and 291.13±15.17 days in the GT-143 study. Hence, the CWD type 2 strain may have stable properties in PrP^{Sc} propagations with deer PrP molecules, compared to the CWD type 1 strain. Overall, the 7-5 ELISA experiments in this section demonstrated influential consequences of structural differences at the residue 226 on the globular domain of the cervid PrP structure. The biochemical difference in CWD-strain types should link to the

PrP^{Sc} transmissible property of CWD pathogens for interspecies and the pathological features.

A.

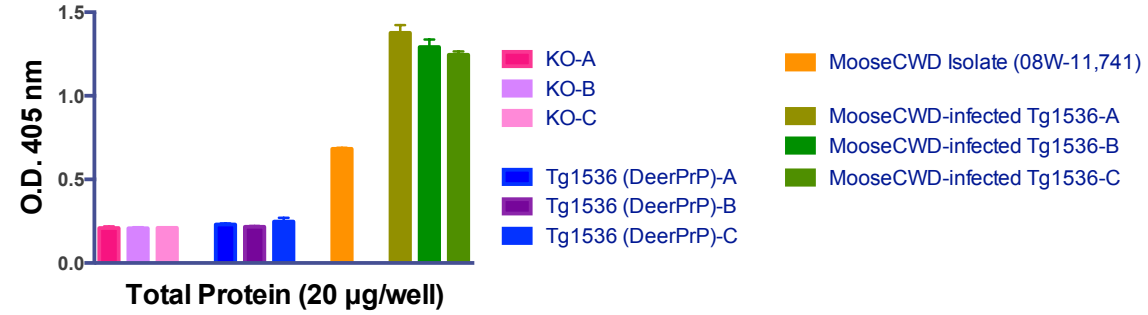
1.5
1.0
0.5
0.0
O.D. 405 nm
Total Protein (20 µg/well)
KO-A
KO-B
KO-C
Tg1536 (DeerPrP)-A
Tg1536 (DeerPrP)-B
Tg1536 (DeerPrP)-C
MooseCWD Isolate (08W-11,741)
MooseCWD-infected Tg1536-A
MooseCWD-infected Tg1536-B
MooseCWD-infected Tg1536-C

B.

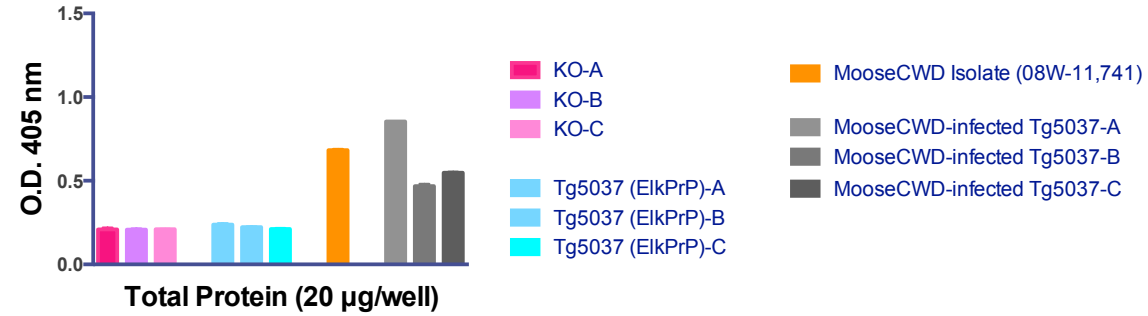
1.5
1.0
0.5
0.0
O.D. 405 nm
Total Protein (20 µg/well)
KO-A
KO-B
KO-C
Tg5037 (ElkPrP)-A
Tg5037 (ElkPrP)-B
Tg5037 (ElkPrP)-C
MooseCWD Isolate (08W-11,741)
MooseCWD-infected Tg5037-A
MooseCWD-infected Tg5037-B
MooseCWD-infected Tg5037-C

C.

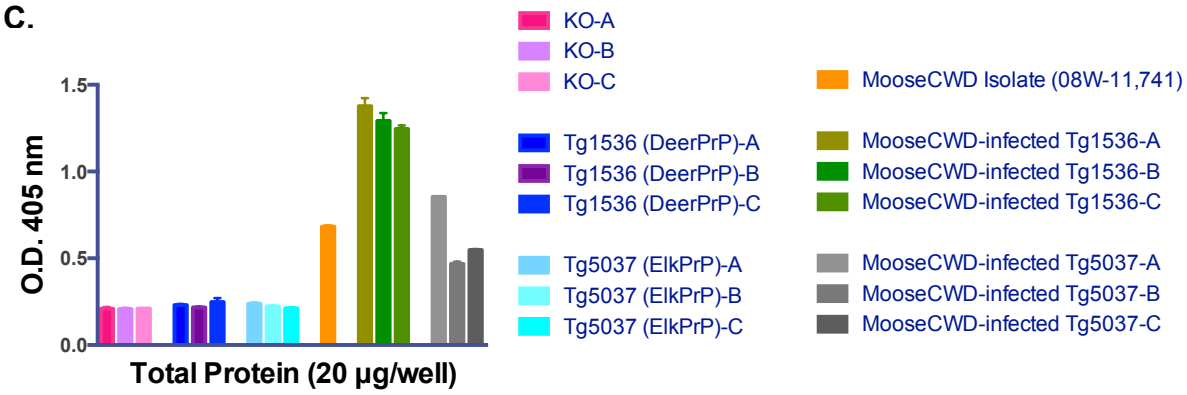
1.5
1.0
0.5
0.0
O.D. 405 nm
Total Protein (20 µg/well)
KO-A
KO-B
KO-C
Tg1536 (DeerPrP)-A
Tg1536 (DeerPrP)-B
Tg1536 (DeerPrP)-C
Tg5037 (ElkPrP)-A
Tg5037 (ElkPrP)-B
Tg5037 (ElkPrP)-C
MooseCWD Isolate (08W-11,741)
MooseCWD-infected Tg1536-A
MooseCWD-infected Tg1536-B
MooseCWD-infected Tg1536-C
MooseCWD-infected Tg5037-A
MooseCWD-infected Tg5037-B
MooseCWD-infected Tg5037-C

D.

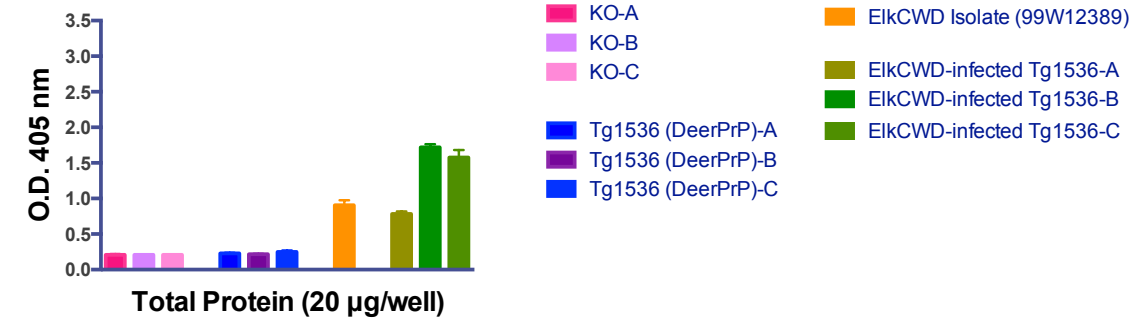
O.D. 405 nm
3.5
3.0
2.5
2.0
1.5
1.0
0.5
0.0
Total Protein (20 µg/well)
KO-A
KO-B
KO-C
Tg1536 (DeerPrP)-A
Tg1536 (DeerPrP)-B
Tg1536 (DeerPrP)-C
ElkCWD Isolate (99W12389)
ElkCWD-infected Tg1536-A
ElkCWD-infected Tg1536-B
ElkCWD-infected Tg1536-C

E.

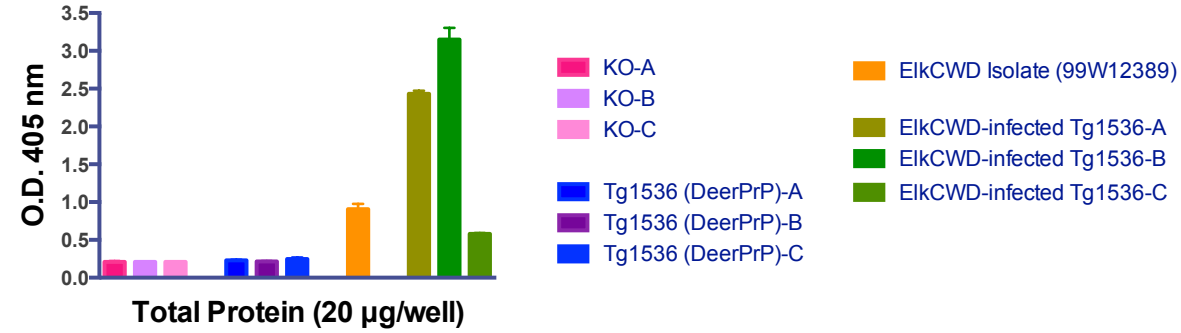
O.D. 405 nm
3.5
3.0
2.5
2.0
1.5
1.0
0.5
0.0
Total Protein (20 µg/well)
KO-A
KO-B
KO-C
Tg1536 (DeerPrP)-A
Tg1536 (DeerPrP)-B
Tg1536 (DeerPrP)-C
ElkCWD Isolate (99W12389)
ElkCWD-infected Tg1536-A
ElkCWD-infected Tg1536-B
ElkCWD-infected Tg1536-C

F.

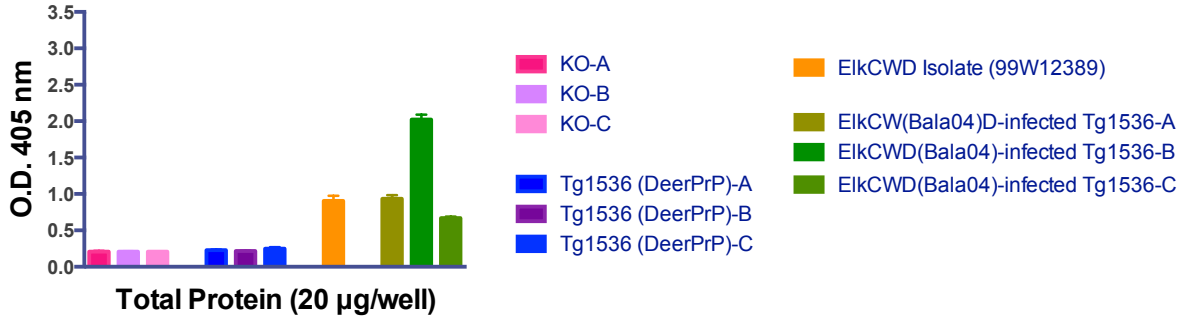
O.D. 405 nm
3.5
3.0
2.5
2.0
1.5
1.0
0.5
0.0
Total Protein (20 µg/well)
KO-A
KO-B
KO-C
Tg1536 (DeerPrP)-A
Tg1536 (DeerPrP)-B
Tg1536 (DeerPrP)-C
ElkCWD Isolate (99W12389)
ElkCW(Bala04)D-infected Tg1536-A
ElkCWD(Bala04)-infected Tg1536-B
ElkCWD(Bala04)-infected Tg1536-C

G.

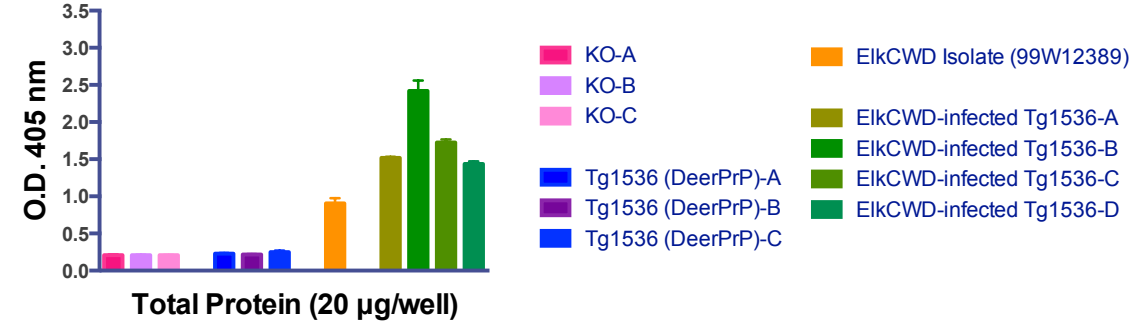
O.D. 405 nm
3.5
3.0
2.5
2.0
1.5
1.0
0.5
0.0
Total Protein (20 µg/well)
KO-A
KO-B
KO-C
Tg1536 (DeerPrP)-A
Tg1536 (DeerPrP)-B
Tg1536 (DeerPrP)-C
ElkCWD Isolate (99W12389)
ElkCWD-infected Tg1536-A
ElkCWD-infected Tg1536-B
ElkCWD-infected Tg1536-C
ElkCWD-infected Tg1536-D

Figure 3-5. PrP detections of moose-isolated CWD inocula in transgenic mouse models with cervid PrP expressions by the 7-5 ELISA method. Measured PrP levels in BH samples from (A) Tg1536 (deerPrP) mice and (B) Tg5037 (elkPrP) mice with inoculations of moose-isolated CWD brain materials. (C) comparisons of Moose-CWD inoculum, and infected mice. PrP detections in BH samples from Tg1536 (deerPrP) mice with Type-1 CWD inocula (elk-isolated CWD strain, 99W12389): (D) KG-18 inoculation study, and (E) GT-142 inoculation study. PrP detections in Tg1536 (deerPrP) mice with Type-2 CWD inocula (elk-isolated CWD strain, Bala04): (F) RA-26 inoculation study, and (G) GT-143 inoculation study. (n=3, each sample with 20μg total protein per well)

PrP detections in TME-inoculated transgenic mice by the 7-5 ELISA method

Previously, three isolates of transmissible mink encephalopathy (TME) from minks were kindly provided by Dr. Jason Bartz, Creighton University, Omaha, Nebraska, USA. These three TME inocula were 1) #58 NBP 950825, 2) 10^{-5} cloned TME 941031, and 3) 10^{-5} cloned TME 941201. Note: the laboratory database recorded these brain samples as 8/25/95, 10/31/94, and 12/1/94. However, I confirmed with Dr. Bartz about the correct notation as the order of Year/Month/Day, by e-mail communications. These TME mink brain samples were the cloned isolates by a serial passage of the Stetsonville TME souse, derived from a mixture of several brains from TME-affected minks.[3] Although the laboratory database does not have clear background information of the three TME clones in minks, such as clinical signs and neuropathology, passages of these TME isolates showed both clinical signs of hyper and drowsy strains in Syrian golden hamsters (e-mail communications with Dr. Jason Bartz). In this section study, the 7-5 ELISA method measured BH samples of the three TME clones under its optimized protocol, described above. Controls included PrP-KO mice, uninfected FVB/n mice, and uninfected TgF431 (MinkPrP) mice. On a prepared ELISA plate, a well contained total protein 20μg of each sample (triplicate). The 7-5 ELISA method results indicated that all TME isolates exhibited higher O.D. values of PrP levels, compared to the control BH samples (Figure 3-6.A). However, the TME 941031 and 941201 isolates had much higher PrP levels than the #58 NBP 950825. These observations suggested that these two TME isolates prominently generated unglycosyl and mono-1 glycosyl PrP forms during the disease developments. As noted above, all tested isolates were clones of the same TME source, originated from a

pooled brain sample of different disease minks in the same affected ranch.[3] Thus, it is possible that these cloned isolates exhibit different phenotypes or strain dependences (e-mail communications with Dr. Jason Bartz). To determine these possible differences in the three isolates, further studies analyzed BH samples from mouse models with TME inoculations.

In the past mouse bioassay, three TME isolates were inoculated into transgenic mice with mink PrP expressions, referred to as TgF431 expressing an equivalent PrP level to wild-type mouse FVB/n: 1) VK-11 study with #58 NBP 950825 inoculation (scrapie sick date: mean ± SEM = 262.14±16.9 days); 2) VK-18 study with TME 941031 inoculation (108.5±3.24 days); 3) VK-20 study with TME 941101 inoculation (123.25±3.44 days). Intriguingly, these sick date records indicated that the #58 NBP 950825 isolate had a prolonged incubation period at least twice longer than the TME 941031 and 941201 isolates. Based on the 7-5 ELISA results from the three TME isolates, #58 NBP 950825 exhibited approximately twice lower O.D. value of unglycosyl and mono-1 glycosyl PrP forms than other isolates (Figure 3-6.A). As hypothesized, therefore, these outcomes indicated that generations of under-glycosylated PrP forms could implicate with the disease development and progression in TME.

In the 7-5 ELISA experiments, three mice of each TME-inoculated study were tested. Three uninfected TgF431 mice were used as a non-TME control; one PrP-KO mouse and one uninfected FVB/n mouse were also included as negative controls of the 7-5 ELISA method. In addition, the three TME inocula were examined to compare with these TME-infected mouse models. Under the optimized 7-5 ELISA protocol, BH samples from all of these samples above were processed. At the final step, these

prepared samples were coated into ELISA plate wells (= triplicate for each sample: total protein 20µg per well). All TME-inoculated mouse BH samples showed higher O.D. values of PrP detections, compared to uninfected TgF431 mice and other negative controls: p-values by group means for Uninfected TgF431 vs. TME-study were p= 0.0007 (VK-11 = #58 NBP 950825), p= 0.0002 (VK-18 = TME 941031), and p= 0.0016 (VK-20 = TME 941201) (Figures 3-6.B to D). However, the TME mouse models exhibited lower O.D. values than each inoculum of a TME isolate from affected mink. This observation could be associated with the first transmission passage of these cloned TME isolates through the species barrier, even though the inoculated mice had mink PrP expressions. Instead of PrP molecules, other murine factors might interfere or interact with the inocula for these mink-PrP^{Sc} replication. Moreover, the O.D. values between 0.6 and 1.0 in TME-inoculated mice indicated threshold amounts or levels of PrP^{Sc} generations and/or accumulations that caused clinical signs of neurological impairments and disease progressions to terminal stages for the TgF431 (MinkPrP) mouse line. Since the inoculation studies with the TME 941031 and 941201 isolates had twice shorter incubation periods than the #58 NBP 950825 isolate, generating and accumulating times of under-glycosylated PrP^{Sc} forms could be proportional to TME-incubation periods and disease progressions.

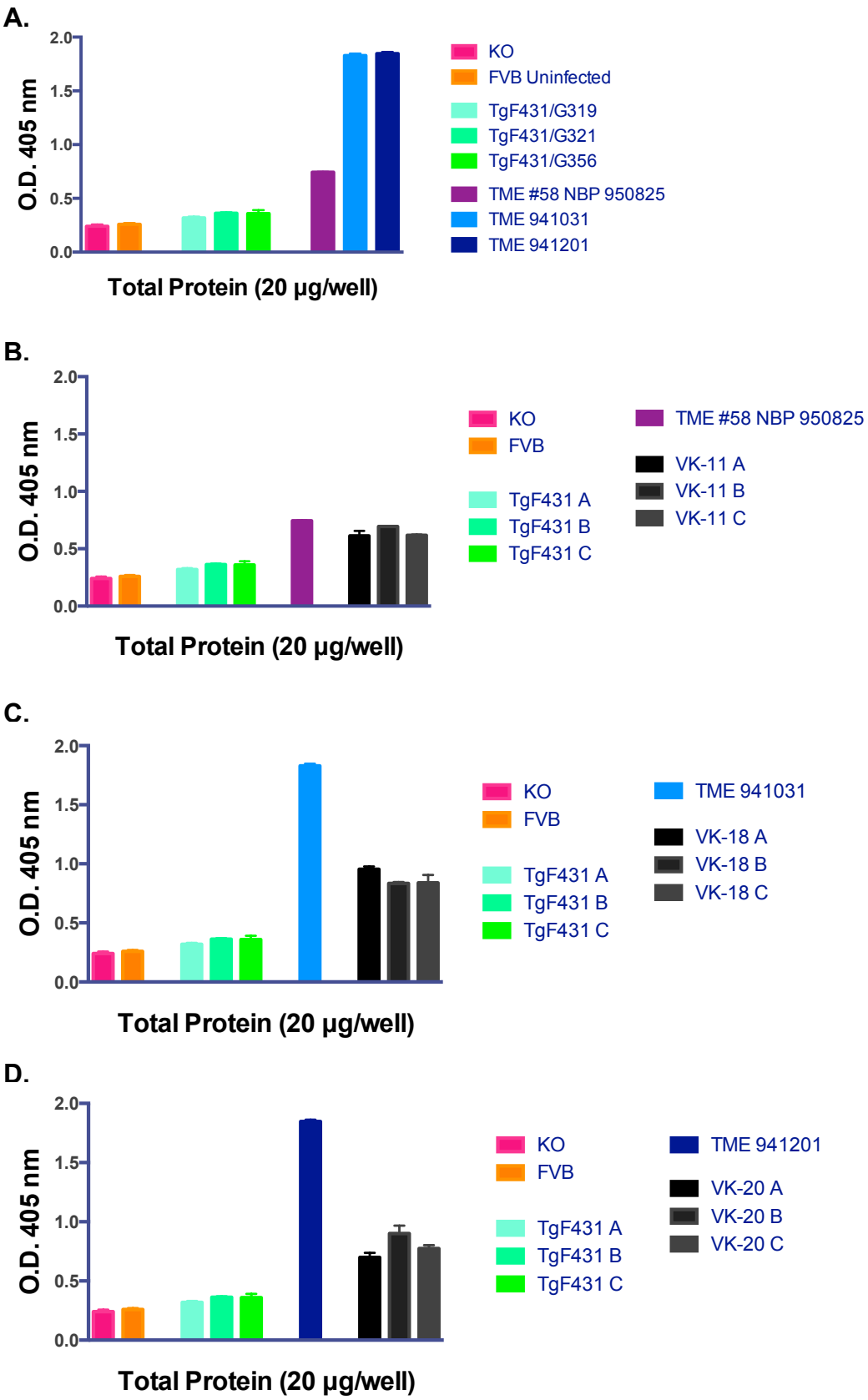
A.
O.D. 405 nm
2.0
1.5
1.0
0.5
0.0
Total Protein (20 µg/well)
KO
FVB Uninfected
TgF431/G319
TgF431/G321
TgF431/G356
TME #58 NBP 950825
TME 941031
TME 941201
B.
O.D. 405 nm
Total Protein (20 µg/well)
KO
FVB
TgF431 A
TgF431 B
TgF431 C
TME #58 NBP 950825
VK-11 A
VK-11 B
VK-11 C
C.
O.D. 405 nm
Total Protein (20 µg/well)
KO
FVB
TgF431 A
TgF431 B
TgF431 C
TME 941031
VK-18 A
VK-18 B
VK-18 C
D.
O.D. 405 nm
Total Protein (20 µg/well)
KO
FVB
TgF431 A
TgF431 B
TgF431 C
TME 941201
VK-20 A
VK-20 B
VK-20 C

Figure 3-6. Mink PrP detections by the 7-5 ELISA method.
(A) three TME inocula, BH samples from TgF431(minkPrP) mice with three TME inocula: (B) VK-11 study with #58 NBP 950825 inoculation, (C) VK-18 study with TME 941031 inoculation, and (D) VK-20 study with TME 941101 inoculation. (n=3, each sample with 20μg total protein per well)

Pilot application of the 7-5 ELISA method as comparison of CPCA

Bioassay has been utilized to assess infectivity and its titration of TSE prion strains. However, this *in vivo* approach has limitations, such as time consumption and cost. Dr. Charles Weissmann's group established a cell assay, referred to as scrapie cell assay (SCA) or standard scrapie cell assay.[12] SCA is equivalently sensitive to mouse bioassay for titrating prion infectivity using cell culture models, by ten-fold faster processing times. On the other hand, this cellular assay restricts applications only for mouse-adapted scrapie prion strains, because of the use of murine cell lines with mouse PrP expressions. To overcome this limitation, Dr. Jifeng Bian, an assistant professor at CSU, reported a new cell-base quantitative method, called cervid prion-cell assay (CPCA).[10,11] The methodology of CPCA was described in the Materials and Method of this Chapter. Briefly, this method is performed conveniently for necessary processes to establish TSE infections in cell culture models, compared to the SCA procedure. Moreover, a rabbit kidney epithelial cell line RK13 (ATCC, Manassas, Virginia, USA) was utilized to generate stably transfected RK13 cells expressing PrP of elk, deer, sheep, mouse, mink or others. Primarily, the RK13 cells do not have detectable levels of PrP expressions. The establishment of these transfect RK13 cells has promoted the CPCA application, which is a capable method to develop susceptible cell culture models for infection and replication of a testing TSE strain in its corresponding species of PrP expressions.[10] However, CPCA and SCA generally require a 4-week incubation period of a TSE infection in cell culture models to assess its proper infectivity and titer. For overcoming this time consuming issue, detectable PrP^{Sc} levels in a TSE-infected brain material by the 7-5 ELISA method should be correlated

with the infectivity, titrated by CPCA from the cell culture models with TSE infection of the same sample. If this correlation appeared, the 7-5 ELISA method would have a potential utility for titrating prion infectivity. Since this ELISA procedure can be completed within 2-3 days, the time consumption for analyzing prion infectivity would be ten times less than CPCA and SCA methods. As noted above, SCA is ten-fold faster than bioassay. Therefore, this ELISA approach might be 100 times faster than bioassay for analyzing infectivity and titration of TSE prion strains.

Ms. Carla Calvi, a former research coordinator in the CSU Prion Research Center, examined CPCA with RK13 cells expressing cervid PrP using multiple brain homogenates from CWD-infected transgenic mouse models. According to her CPCA outcomes, two study groups (the inoculation studies RA-24 and SB-41) showed different titers between the tested samples from each inoculation study (Figure 3-7.A). In the RA-24 study using a CWD inoculum Bala02-0306, derived from elk brain with subclinical signs but pathologically TSE positive, the hemizygous Tg1536 (DeerPrP) mouse #5695 had a lower titer value than the mouse #5696. In the SB-41 study using a CWD inoculum H92 derived from a deer brain, the hemizygous Tg1536 (DeerPrP) mouse #3684 had a lower titer value than the mouse #3685. Thus, these results indicated that infectivity of the inoculum could be different among animals even in the same study group. However, it was unknown what factors could be involved in this observation. As an initial approach, the 7-5 ELISA method measured PrP levels in these four CWD-infected BH samples. Controls included PrP-KO and uninfected Tg1536 mice. Intriguingly, the low-titer animals showed lower O.D. values of PrP detections, compared to the high-titer animals, at total protein 20μg per well as triplicate

for each sample (Figure 3-7.B). In fact, these detectable differences between the samples in the same inoculation study were similar patterns to the CPCA data by Ms. Calvi. Therefore, the 7-5 ELISA method might have a potential application to estimate prion infectivity and titer of a TSE-infected material, in comparison with the bioassay and cell culture model. For a further pilot study, CPCA evaluated prion infectivity and titer of the CWD-infected materials from transgenic mice tested in the Figure 3-5 above: RA-26, KG-18, GT-142, and GT-143.

Under the guidance of Dr. Bian, CPCA was performed using RK13 cells expressing deer PrP and calculated titers for each tested sample. The anti-PrP antibody for this cellular assay was 6H4 mAb, commonly used in TSE research (Prionics, Schlieren, Switzerland). Interestingly, these two experimental methods suggested that the infected samples with higher O.D. values have higher titers by CPCA (Figures 3-7.C and D). Although these observations were still pilot data among the tested BH samples by the 7-5 ELISA and CPCA experiments, the 7-5 ELISA approach can be utilized as an alternatively rapid method to estimate infectivities and titers of testing TSE-infected materials. Therefore, it is an appropriate direction for continuing further experiments that evaluate prion infectivity and titer by the 7-5 ELISA method, and develop its additional valuable application in TSE research.

A.

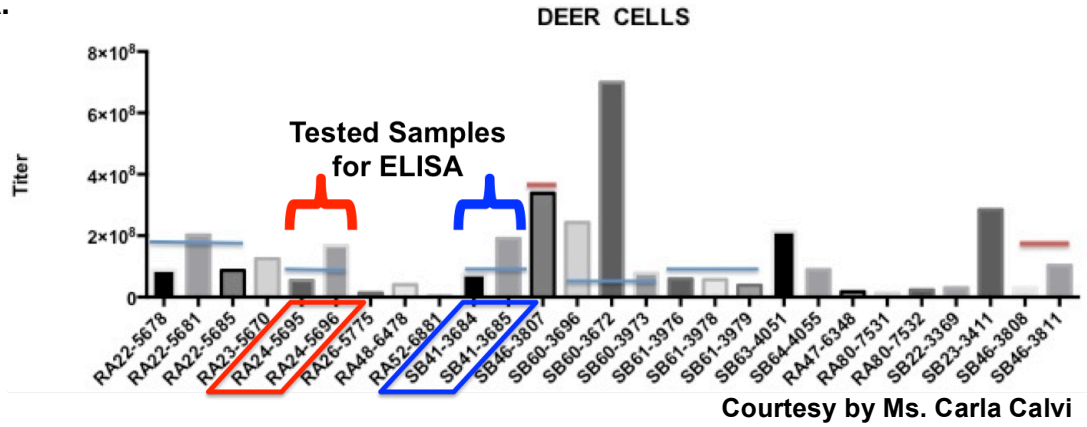

Courtesy by Ms. Carla Calvi

B.

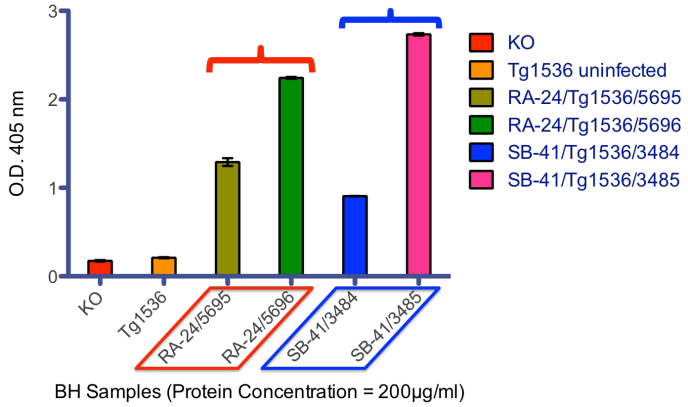

BH Samples (Protein Concentration = 200µg/ml)

C.

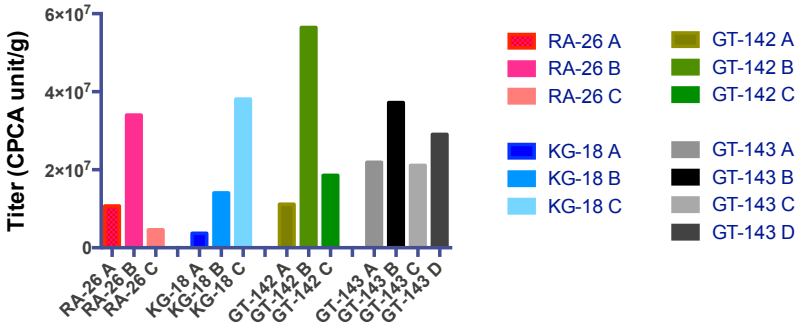

D.

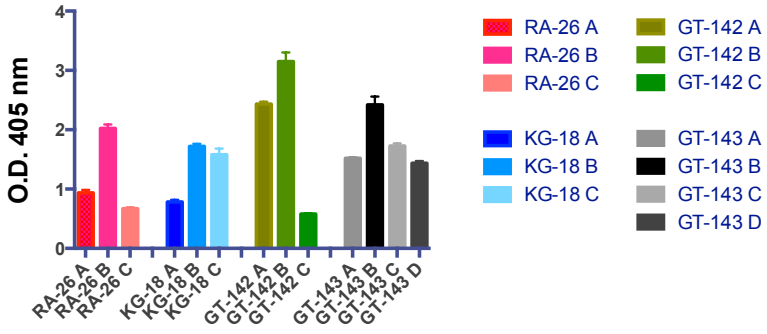

Total Protein (20 µg/well)

Figure 3-7. Comparisons of CPCA and the 7-5 ELISA method.
(A) PrP titers from CPCA results, using RK13 cells with CWD infections.
(B) PrP detections in selected murine BH samples with CWD infections that CPCA tested, (C) PrP titers in CPCA results using RK13 cells, infected with CWD inocula from four bioassays, and (D) PrP detections in murine BH samples from four CWD bioassays that CPCA tested. (n=3, each sample with 20µg total protein per well)

Potential utility of the 7-5 ELISA method for monitoring prion infectivity and titration

Furthermore, the CPCA method evaluated an infectivity and titration of the mouse-adapted scrapie prion strain RML with RK13 cells expressing mouse PrP, using the RML-infected mouse brain homogenate, which was the same sample in the Figure 3-1 (Figure 3-1.A). For analyzing prion infectivity and titer of the RML-infected FVB/n BH sample, the CPCA experiment obtained titers 4.64×10^8 CPCA unit/g. The unit value for the nanogram (ng) protein amount was 0.464 CPCA unit/ng (i.e. 4.64×10^8 CPCA unit/g; 4.64×10^5 CPCA unit/mg; 4.64×10^2 CPCA unit/μg). This value was applied to calculate infectivity per total protein in the half log protein-dose study of the RML-infected murine material in the study of the Figure 3-1 (Table 3). Combined with the half log data by the 7-5 ELISA method, the obtained titer was scaled at each protein concentration of the tested RML-inoculated FVB/n mouse BH sample, and these two data showed similar patterns of curve lines (Figure 3-8).

Table 3. Calculations for Titers

Total Protein (ng/well)	Calculations	Titers (unit/ng)
6.324	x 0.464 SCA unit/ng	2.9348
20	x 0.464 SCA unit/ng	9.28
63.25	x 0.464 SCA unit/ng	29.348
200	x 0.464 SCA unit/ng	92.8
632.5	x 0.464 SCA unit/ng	293.48
2,000	x 0.464 SCA unit/ng	928
6,325	x 0.464 SCA unit/ng	2934.8
20,000	x 0.464 SCA unit/ng	9280

4.64×10^8 CPCA unit/g = 4.64×10^5 SCA unit/mg = 4.64×10^2 SCA unit/μg
= **0.464 SCA unit/ng**

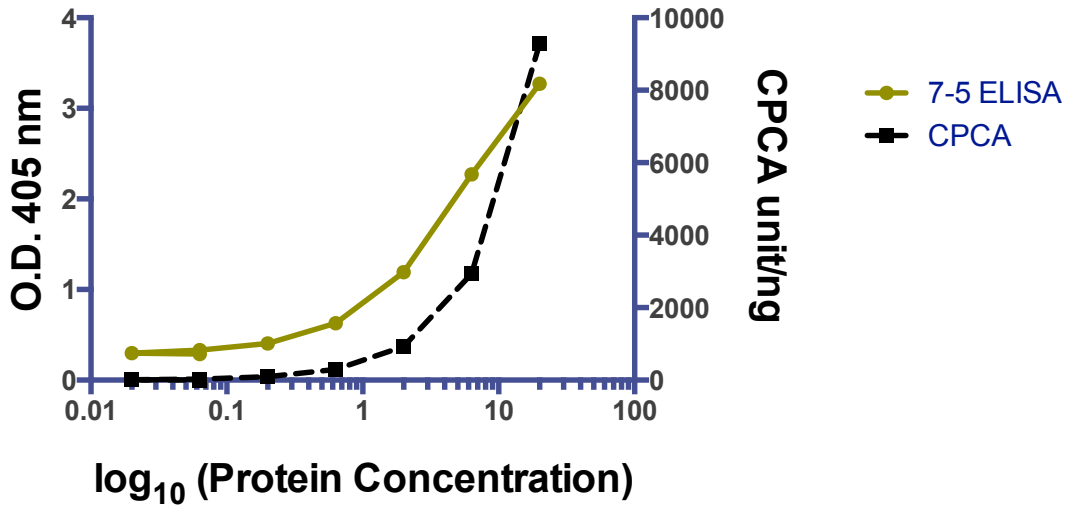

Figure 3-8. Comparisons of CPCA and the 7-5 ELISA method. Evaluations of the PrP titration of RML infectivity with RK13 cells in CPCA, and PrP detections in RML-inoculated FVB/n murine BH samples by the 7-5 ELISA method. (n=3, each total protein amount).

Modified protocol for the PRC7 utility into CPCA testing with SMB cells

The 7-5 ELISA approach presented a potential utility to estimate prion infectivity and titer as an alternative method of *in vitro* and *in vivo* assays. However, the CPCA results above were based on PrP detections by another anti-PrP mAb 6H4. Since 6H4 can react with all four glycosylated PrP forms, the utility of the 7-5 ELISA method might not be simply compared with outcomes from different experiments unless PRC7 and PRC5 were applied. In the Sandwich ELISA approach, PRC7 only captures unglycosyl and mono-1 glycosyl PrP forms. Thus, an evaluation of the PRC7 application in CPCA was necessary for proper comparisons of its data with the 7-5 ELISA results using the same analyte. According to Dr. Bian, the PRC7 application was not successful in his past CPCA experiments, compared to other common anti-PrP antibodies such as 6H4. Also, PRC5 was prone to cause higher color-background issues on membranes of ELISpot plates. In the CPCA procedures, however, cellular samples were denatured with 3M GdnSCN at RT for 10 minutes. As described above, the GdnSCN denaturation with lower temperature and/or shorter incubation times was less effective to detect PrP molecules in the 7-5 ELISA method. For the undefined utility of PRC7 in past CPCA results, a new working hypothesis also proposed that under-glycosylated PrP molecules were immature forms localized in intracellular domains rater than on cell surfaces, and that glycosylation states may be changed during the transportation of PrP molecules from intracellular domains to cell surfaces. Therefore, additional permeabilizations for cellular membranes would facilitate chances of PRC7 reacting with intracellular PrP molecules in testing cells. For these fundamental purposes, different cell lines and TSE strains were examined under the following sample conditions: 1) permeabilization with

different detergents; 2) PK digestions or non-PK digestions; and 3) denaturations with GdnSCN or GdnHCL.

1) Permeabilization: In the immunocytochemistry (ICC) protocol for TSE-infected cells that Ms. Calvi obtained from Dr. Bessen and used, digitonin (a toxin derived from the poisonous foxglove plant Digitalis purpurea) was applied for cellular permeabilization. However, this detergent is a costly reagent and requires one-hour incubation time on the protocol. Since other detergents have been used for permeabilizing cell membranes for ICC, other effective chemicals were tested for PRC7 in the CPCA application. In an initial approach, Triton X-100 (TX100), Tween 20, and saponin were tested under different concentrations and incubation times, but not including digitonin. PBS was used as a dilution buffer, and the control was the only PBS addition. Note: Sarkosyl was not included in this experiment, although this reagent is one of the common detergents in the TSE research. The following study with the Figure 3-16 explains the negative efficacy of Sarkosyl for the 7-5 ELISA method.

2) PK digestion: the 7-5 ELISA protocol does not require the use of proteinase K (PK) for PrP detections in TSE-infected materials. Under-glycosylated PrP^{Sc} forms are commonly detected in the infected analyte, but not usually generated in uninfected individuals and animals. In addition, non-PK application allows recognizing PK-sensitive PrP^{Sc} forms. However, the PK treatment is one of the procedures in CPCA for detecting PK-resistant PrP agents in TSE-infected cells. To evaluate the PK efficacy for the PRC7 application in CPCA, PK-treated (PK 1mg/ml in cell lysis buffer (CLB); final concentration 5µg/ml during incubation with samples) and non-treated (CLB only) conditions were determined at 37°C for 1 hour. Note: CLB contained 50mM Tris pH 8.0,

150mM NaCl, 0.5% IGEPAL-CA630 and 0.5% Sodium Deoxycholate. Since IGEPAL-CA630 is a similar detergent to TX100 and NP-40, it might induce permeabilization on cell membranes.

3) Denaturation: GdnSCN and GdnHCL were compared at different concentrations. Tris-HCL buffer was a dilution buffer for these denaturants: 10mM for GdnSCN in CPCA, but 50mM for GdnHCL in the 7-5 ELISA method. Potentially, different denaturants and buffer concentrations might have influenced the PRC7 application in CPCA. To determine efficacies of PRC7 in CPCA, various conditions of denaturations were tested with the following two cell lines: 1) the scrapie-infected SMB cell line, derived from the brain of a disease mouse after an inoculation with the mouse-adapted scrapie strain Chandler [13]; 2) the SMB-PS cell line, which is the permanently cured SMB cell line by the pentosan sulphate (PS) treatment, and PrP^{Sc} expressions are no longer detectable over 50 passages.[14]

For permeabilizations of cell membranes on SMB and SMB-PS cell lines, four different conditions were applied: 1) PBS only, 2) 0.1% TX100, 3) 0.1% Tween 20, and 4) 0.1% saponin. These detergents were diluted in PBS. On the ELISpot plates, cells were incubated with each detergent condition for 30 minutes at RT. Then, the cells were digested with final concentration 5μg/ml of the PK reagent for 1 hour at 37°C, whereas only CLB was added for non-PK treated cells. The PK digestion was terminated by additions of PMSF 2mM in PBS for each well, with incubations at RT for 20 minutes. Consequently, all cells on ELISpot plates were denatured with different doses of either GdnSCN (0, 1.5, 3M) or GdnHCL (0, 2, 4M). These denaturants were prepared with 10mM Tris-HCL buffer, and 0M condition was the only buffer addition. The incubation

time for the denaturation was 10 minutes at RT. Subsequent procedures were completed under the CPCA protocol. Based on all outcomes from these CPCA experiments, the GdnHCL denaturation with detergents enhanced PrP detections under PK-treated SMB cells, whereas the GdnSCN with detergents decreased (Figures 3-9.A to F). Intriguingly, saponin showed the highest spot numbers, compared to other detergent conditions. Also, low doses of these detergents without PK treatment did not show clear differences for spot numbers between SMB and SMB-PS cells. In contrast, the higher doses of GdnHCL and GdnSCN presented more differences for spot numbers between these cell lines. In fact, 0.1%-detergent permeabilization enhanced spot numbers in SMB cells, but decreased in SMB-PS cells. For 0M denaturant with additions of either 10mM or 50mM Tris-HCL buffer, the combination of saponin with the 50mM Tris-HCL buffer did not influence spot numbers in SMB cells between PK-digested and non-treated conditions. In contrast, other combinations of detergents and buffers decreased detections of spot numbers. These outcomes suggested that saponin with 4M GdnHCL denaturation can be useful for the PRC7 application in CPCA. Possibly, 50mM Tris-HCL buffer is a better concentration of a dilution buffer for GdnHCL in CPCA, as well as the 7-5 ELISA method. Furthermore, PRC7 detected stained spots of PrP expressions in SMB-PS cells without PK treatment, although these cells did not generate PK-resistant PrP molecules. This finding indicated that these detections were unglycosyl and/or mono-1 glycosyl PrP forms, frequently identified in TSE-infected materials. Hence, the SMB-PS cells still exhibited the under-glycosylated state even after cured for PrP^{Sc} generations. Thus the cured cells might not have had normal functions or full-recovered conditions for PrP syntheses. Probably, the under-

glycosylation state in SMB-PS cells should be one of the reasons that the cured cells were susceptible to re-infections of different scrapie strains.[14]

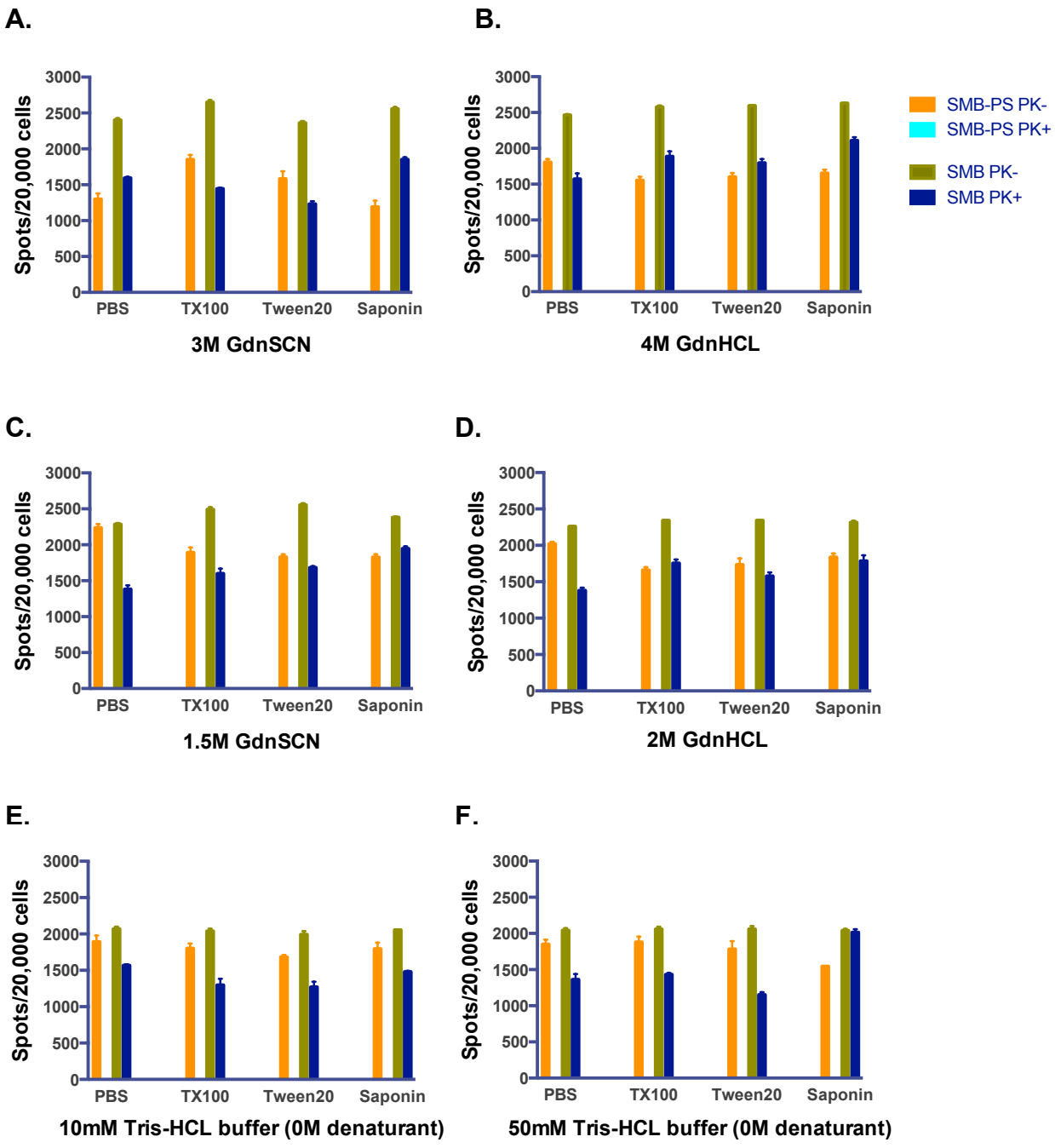

Figure 3-9. Efficacies of detergents for PrP detections in SMB cells with PRC7 mAb by CPCA. Comparisons of PBS, TX100, Tween20, and Saponin (0.1% concentration for each detergent), under different dinaturations with (A) 3M GdnSCN, (B) 4M GdnHCL, (C) 1.5M GdnSCN, (D) GdnHCL, (E) 0M (10mM Tris-HCL), and (F) 0M (50mM Tris-HCL).

Detergent efficacies for PrP detections in RML-infected RKM cells with PRC7 mAb by CPCA

For additional evaluations of the PRC7 application, the transfected mouse-PrP expressing RK13 cells (RKM7 cells) and its chronically infected cells with a mouse-adapted scrapie strain RML (RML-RKM7 cells) were tested in CPCA.[11] RKV cells were the RK13 cells stably transfected with empty vector, and were included in a control for non-PrP expression and non-TSE infection. As described above, a RK13 cell line (ATCC, Manassas, Virginia, USA) originated from rabbit kidney epithelial cells line and originally does not have PrP expressions. Transfecting this parent cell line, RKM7 cells with stable PrP expressions were generated previously. Using these cells, the four different detergent conditions (PBS only, 0.1% concentration of TX100, Tween20 or saponin) were compared with two different incubation times (10 minutes vs. 30 minutes at RT). Also, PK-treated and non-treated conditions were determined under the procedure (including PMSF) in the SMB cells. Denaturations of the cells were processed with 4M GdnHCL in 10mM Tris-HCL buffer for 10 minutes at RT. These results indicated that the 30-minute incubation with PBS, TX100, or Tween20 reduced spot numbers in RML-RKM7 cells with PK digestion, compared to the 10-minute incubations (Figures 3-10.A and B). Interestingly, saponin with these incubation times did not show clear differences for spot numbers in the infected cells with PK treatment. Thus, saponin with 10-minute incubation can be an applicable condition for PRC7 in CPCA. Instead of the 0.1% concentration, moreover, the 0.2% concentration of these four-detergent conditions were determined with the 10-minute incubation time, followed by the same procedures above in CPCA. This experiment found that an increased

concentration of the detergents reduced detectable spot numbers in PK-treated RML-RKM7 cells, especially with saponin, compared to the 0.1% concentration (Figures 3-10.A and C). Therefore, the 0.1% detergent concentration with the 10-minute incubation could be a practical condition of the permeabilization for the PRC7 application in CPCA.

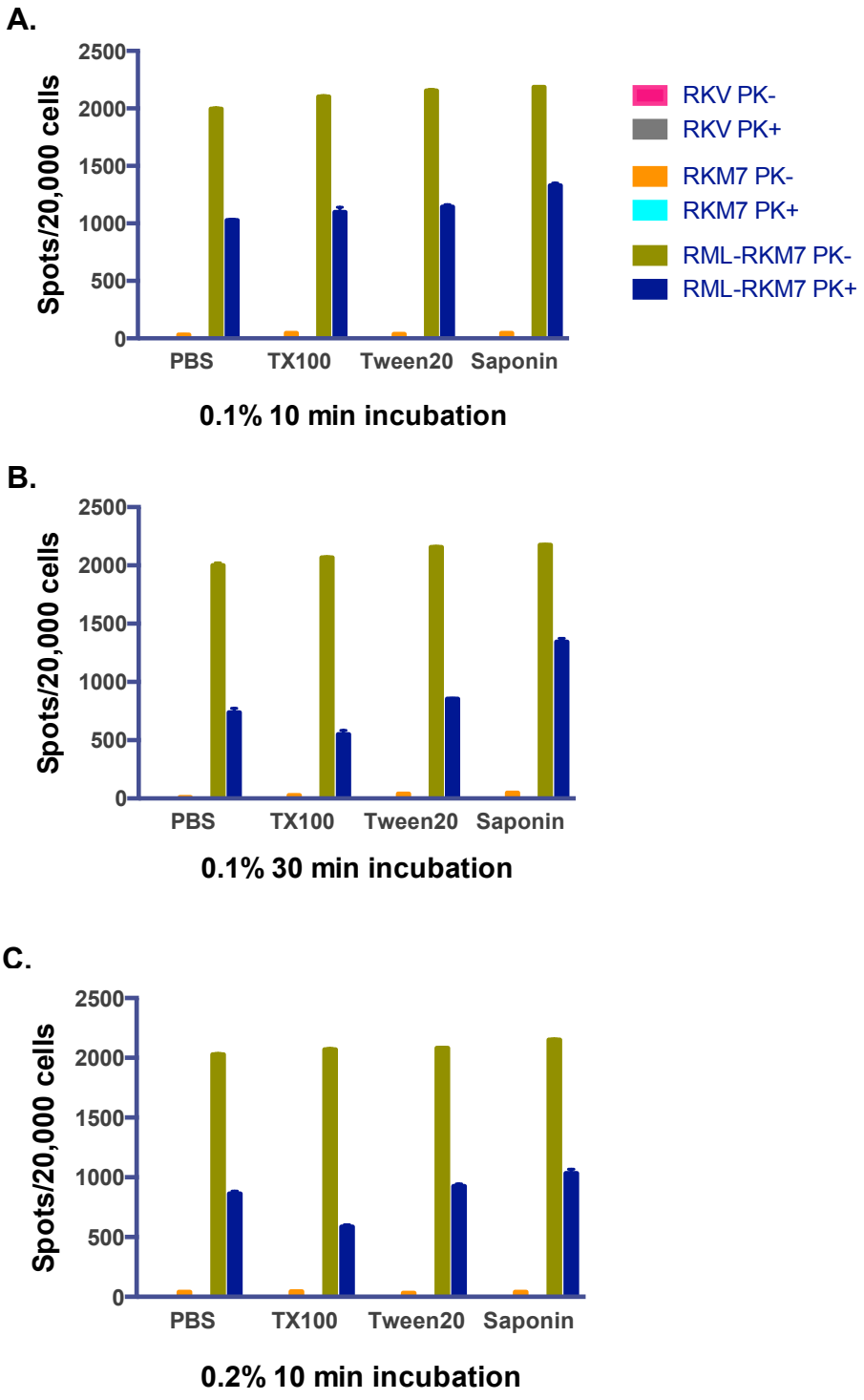

Figure 3-10. Efficacies of detergents for PrP detections in RML-RKM cells with PRC7 mAb by CPCA. Comparisons of PBS, TX100, Tween20, and Saponin (0.1% concentration of each), under different incubations for (A) 10 minutes and (B) 30 minutes. (C) 0.2% detergent concentration with 10-minute incubation.

Detergent efficacies for PrP detections in CWD-infected RK Elk cells with PRC7 mAb by CPCA

The efficacies of the tested detergents and conditions were evaluated with another TSE using PRC7 in CPCA. For this aim, the following cell lines were included: the transfected elk-PrP expressing RK13 cells (RKE cells), and its chronically infected cells (Elk^+ cells) with brain homogenates derived from the CWD-positive elk brain (isolated sample: 012-09442).[10] RKV cells were the negative control of the PrP expression and TSE infection. As the first approach, the same procedures in RML-RKM cells above were applied to RKE cells, Elk^+ cells, and RKV cells: the four different detergent conditions (PBS only, 0.1% concentration of TX100, Tween20 or saponin) with incubation for either 10 minutes or 30 minutes at RT. Also, PK and PMSF procedures were same as the SMB cells and RML-RKM7 cells above. GdnHCL was prepared in 10mM Tris-HCL buffer and its final concentration was 4M. Cells were denatured with 10 minutes at RT. In contrast to SMB cells and RML-RKM cells with TSE infections, the uninfected RKE cells showed higher spot numbers without the PK digestion than the CWD-infected Elk^+ cells (Figures 3-11.A to C). This outcome suggested that the CPCA protocol required the PK reagent for PrP^{Sc} detections in transfected RK13 cells with PrP expressions. Although the 30-minute incubation with detergents decreased spot numbers in the uninfected cells without the PK digestion, this condition did not enhance increases of spot numbers in the CWD-infected cells both with and without PK treatments. Therefore, an efficacy of Tris-HCL buffer was evaluated for GdnHCL. Instead of 10mM Tris-HCL buffer, 50mM concentration was applied. In the experiments with SMB cells above, 50mM Tris-HCL buffer enhanced

spot numbers in cells with PK and saponin treatments, compared to 10mM (Figures 3-9.E and F). Followed by the same procedures with 50mM Tris-HCL buffer for GdnHCL, RKV, RKE, and Elk^{+} cells were examined with PRC7 in CPCA. In fact, this buffer modification increased spot numbers in the CWD-infected cells with all detergents, especially for saponin (Figure 3-11.C).

Based on the optimization of the 7-5 ELISA protocol, the utility of PRC7 mAb was explored to CPCA. Importantly, the results from the all three cell groups above indicated existences of PK-sensitive PrP forms in TSE-infected cells, in comparison of PK-treated and non-treated conditions. Moreover, the PK-sensitive PrP forms must be unglycosyl and/or mono-1 glycosyl forms because of the PRC7 property. Thus, the CPCA approach with PRC7 mAb revealed the increased generation of under-glycosylated PrP forms in cell culture models of TSE-infection states. Although the final concentration of PK reagents was 5μg/ml, PK-sensitive PrP^{Sc} forms were still susceptible to this concentration. Therefore, the optimized PK concentration might be different for detecting maximum levels of PrP^{Sc} agents by PRC7 mAb in CPCA. As a future direction, a PK-dose dependent study would be required. The following study with the Figure 3-15 describes PK-dose dependent responses in the 7-5 ELISA method, using mouse BH samples. This result would be useful for optimizing PK concentrations for PRC7 mAb in CPCA.

Furthermore, additional permeabilizations for cellular membranes enhanced detectable spot numbers of PrP expressions in TSE-infected cells with the tested detergents, especially saponin. These results could overcome the previous limitation of the PRC7 application to CPCA. Hence, PRC7 mAb increased PrP detections in tested

cells. Thus, this PrP detection endorsed the working hypothesis that the intracellular PrP molecules were under-glycosylated forms, which might be immature structures and will be fully glycosylated during its transportation from intracellular to cell surface.

In addition to all outcomes in the studies with the Figures 3-9, 3-10, and 3-11, further optimizations would be beneficial to develop a new utility of the 7-5 ELISA approach for infectivity and titration of TSE strains. For instance, the following experiments can be practical to initiate: 1) saponin and other reagents for the permeabilization under different concentrations, incubation times, temperatures, and buffers; 2) GdnHCL for denaturation to find optimized conditions by its dose-dependence, incubation times, and temperatures; and 3) the PK digestion with different buffers because its dilution buffer CLB contains IGEPAL-CA630 and Sodium Deoxycholate. Since IGEPAL-CA630 is a similar detergent to TX100 and NP-40, an extra permeabilization might occur during the PK digestion. Potentially, IGEPAL-CA630 and Sodium Deoxycholate might influence PrP detections by PRC7 mAb in CPCA. Therefore, the CLB without IGEPAL-CA630 and Sodium Deoxycholate should be compared with PBS only for PK preparations. These outcomes will more confirm the effects of saponin and other tested detergents for the PRC7 application in CPCA.

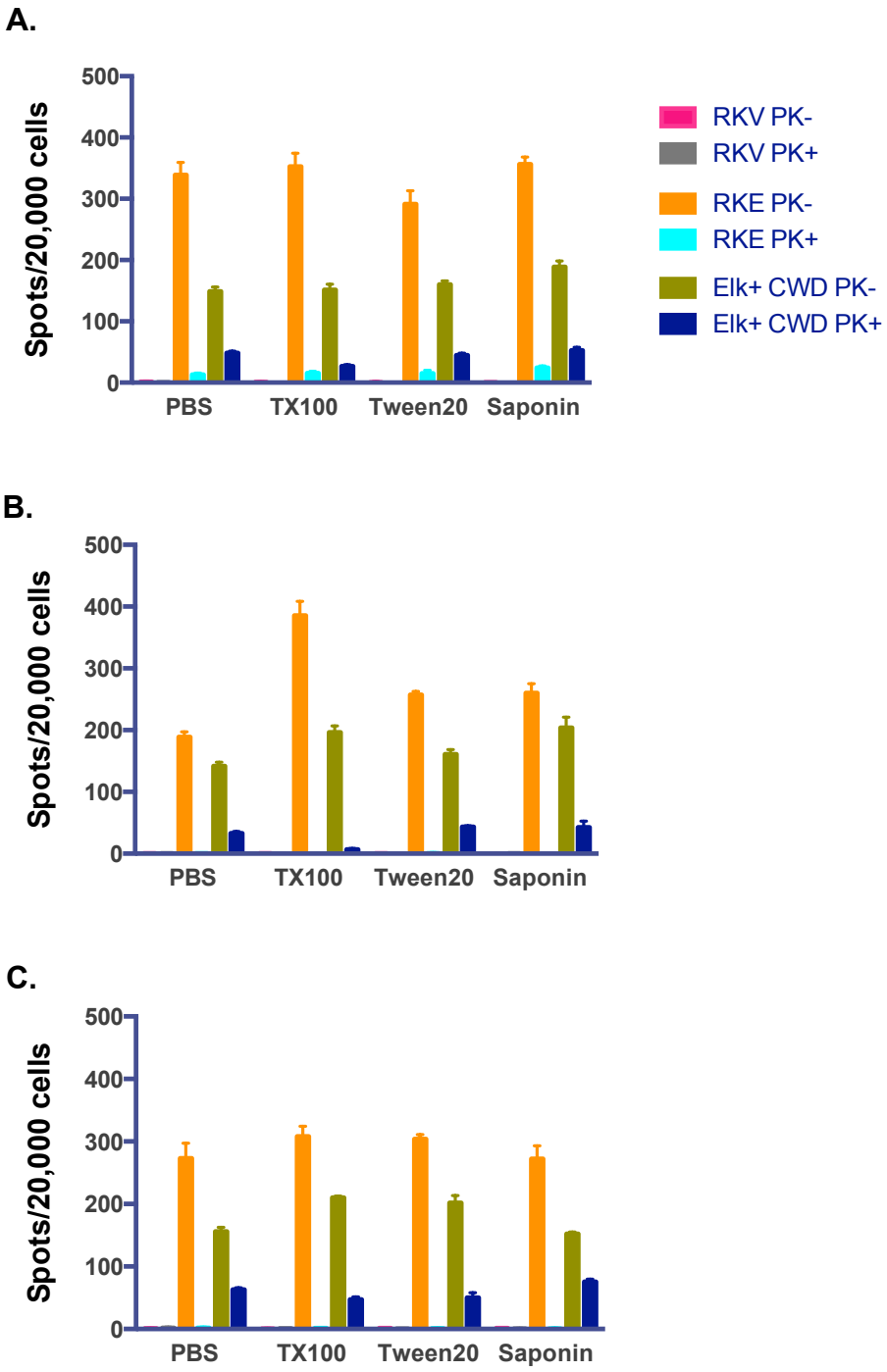

Figure 3-11. Efficacies of detergents for PrP detections in CWD-infected Elk^{+} cells with PRC7 mAb by CPCA. Comparisons of PBS, TX100, Tween20, and Saponin (0.1% concentration of each), under different conditions with (A) 10-minute incubation with 10mM Tris-HCL buffer for GdnHCL, (B) 30-minute incubation with 10mM Tris-HCL buffer for GdnHCL, and (C) 10-minute incubation with 50mM Tris-HCL buffer for GdnHCL.

New ELISA approach for PrP^C detections

Instead of targeting PrP^{Sc} agents in TSE-infected materials, an additional ELISA approach is capable of measuring only PrP^C molecules. Initially, Dr. Richard Bessen, a former faculty in the Department of Microbiology, Immunology and Pathology at Colorado State University, talked with me about his finding. Briefly, Dr. Bessen's laboratory detected lower mRNA expression levels of the Prnp gene in the tested TSE-infected mouse tissue samples using a quantitative polymerase chain reaction (qPCR) method, compared to uninfected controls. Thus, we discussed capabilities of the 7-5 ELISA method for testing these mouse samples for only PrP^C expressions and for determining the correlation of Prnp gene expressions and PrP^C levels in the same samples. Since a diglycosyl form is the most abundant PrP^C conformation, PRC7 and the 7-5 ELISA method are inefficient approaches for targeting normal PrP^C molecules. Thus, 6H4 mAb, a well-known anti-PrP antibody in TSE research that recognizes all four glycosylated PrP forms, was an alternate antibody for this Sandwich ELISA trial, as a replacement of PRC7.

In the pilot study, Sandwich ELISA approaches with 6H4 and PRC5 mAbs evaluated three infected and three uninfected mouse nasal tissue samples from Dr. Bessen's laboratory as a blind study. Under sample procedures without Triton X-100 and denaturation, both orders of these antibodies were examined as capture and detecting antibodies in the ELISA approaches: 6H4-PRC5 ELISA and PRC5-6H4 ELISA applications. Both ELISA measurements revealed lower O.D. values of PrP detections in all infected materials than the uninfected samples (data are not present here). This result was a similar observation to Dr. Bessen's identification above. Therefore, these

Sandwich ELISA methods with the two anti-prion mAbs found the decrease of PrP levels in TSE-infected materials. However, it was not clear if these PrP detections were only PrP^C or total PrP amounts in the mouse tissue samples.

For further approaches to develop new Sandwich ELISA applications for only PrP^C detections, the following experiments included the D18 prion-specific recombinant antibody (fragment antigen-binding antibody = Fab Ab: Fab fragment is an antibody lacking the Fc, or constant region) as a candidate for establishing a new ELISA protocol, in addition to 6H4 and PRC5 mAbs. As previously reported, the D18 Fab Ab presented a unique feature applying to ELISA methods that required sample denaturation with guanidine thiocyanate (GdnSCN) to detect PrP27-30 rods.[15] PrP27-30 was an isolate, purified from hamster-adapted scrapie prions and incorporated into liposomes. The PrP27-30 property in scrapie PrP^{Sc} agents has been identified as the protease-resistant core of infectious PrP^{Sc} isoforms that has an essential role in the TSE infectivity and pathogenesis.[27,28] Intriguingly, the D18 Fab Ab could not react to the PrP27-30 rods without the denaturation step by ELISA methods.[15] In addition, the same research group published a therapeutic potential of the D18 Fab Ab that bound to normal PrP^C isoforms for preventing these interactions with abnormal PrP^{Sc} isoforms.[29] In this study, tested samples were not denatured with GdnSCN or other denaturants, such as guanidine hydrochloride (GdnHCL). Thus, I anticipated a potential that the D18 Fab Ab would be capable of detecting only PrP^C molecules, when testing samples are not denatured.

Combined with the anti-PrP antibodies 6H4, PRC5 and D18, three different Sandwich ELISA applications were initially determined with the following orders of

capture and detecting antibodies: 6H4-PRC5, D18-PRC5, and PRC5-D18. Each capture antibody was coated into ELISA plate wells: 100µl of its 5µg/ml concentration per well (= 0.5µg/well). For PrP^C detections, testing samples were not treated with any detergents or denaturants. To reduce possible degradations of PrP^C molecules, sample handlings and preparations were carefully performed on ice or at 4°C. For the same purpose, a protease inhibitor product (cOmplete, Roche Diagnostics, Indianapolis, IN, USA) was added into buffers of sample dilution, blocking process, and detecting and secondary antibodies: one tablet of this protease inhibitor cocktail for 50 ml volume of an extraction solution at the manufacture's direction. At first, these testing ELISA applications determined protein-dilution dependence using 10% BH samples of uninfected homozygous Tg4112 mice (MousePrP overexpression) and PrP-KO mice. According to the laboratory database, a hemizygous Tg4112 mouse line expresses 2-4 times higher PrP levels, compared to a wild-type FVB/n mouse. The Tg4112 BH sample was diluted by the PrP-KO BH sample: the volume proportions were prepared from 30% to 100% Tg4112 BH (= from 70% to 0% PK-KO mouse BH) with each 10% increase. These prepared samples were added into wells on the ELISA plates, pre-coated with each capture antibody. Subsequent procedures were the same as the 7-5 ELISA protocol, except handling on ice. Consequently, the three Sandwich ELISA experiments detected high O.D. values of PrP^C expressions in all tested samples, but no difference displayed from 30% to 100% Tg4112 sample proportion. These observations must be associated with PrP overexpressions in this mouse breed line (data not present). Therefore, the three ELISA candidates were re-evaluated using 1% BH of Tg4112 and PrP-KO mice by the same procedures above. The Tg4112 BH dilution with PrP-KO BH

samples was modified from 0% to 100% Tg4112 BH volume proportion (= 100% to 0% KO mouse BH volume) with each 10% increase. 50µl of each diluted Tg4112/PrP-KO BH sample was coated on ELISA plate wells (duplicate for each sample proportion). Since 1% BH was estimated as 1mg/ml (= 1µg/µl), 50µl of 100% Tg4112 BH sample proportion should be approximately 50µg total protein per well. All three ELISA applications measured PrP^C detections of the lowest and highest O.D. values at 0% and 100% Tg4112 BH volume proportion, respectively (Figure 3-12.A). At the 0% Tg4112 BH volume proportion (= only PrP-KO mouse sample), the D18-PRC5 ELISA experiment showed the lowest background of O.D. value that was less than 0.1 (Figure 3-12.B). In contrast, its opposite order PRC5-D18 ELISA application exhibited the highest background over 0.4 O.D. value. Compared to the 6H4-PRC5 ELISA approach, the D18-PRC5 ELISA method analyzed equivalent PrP^C detections in all volume proportions (Figure 3-12.A). In addition, D18 and PRC5 antibodies are available to generate in house. Therefore, these in-house antibodies were selected to measure PrP^C expressions by a new Sandwich ELISA protocol, named as the **"D-5 ELISA"** method.

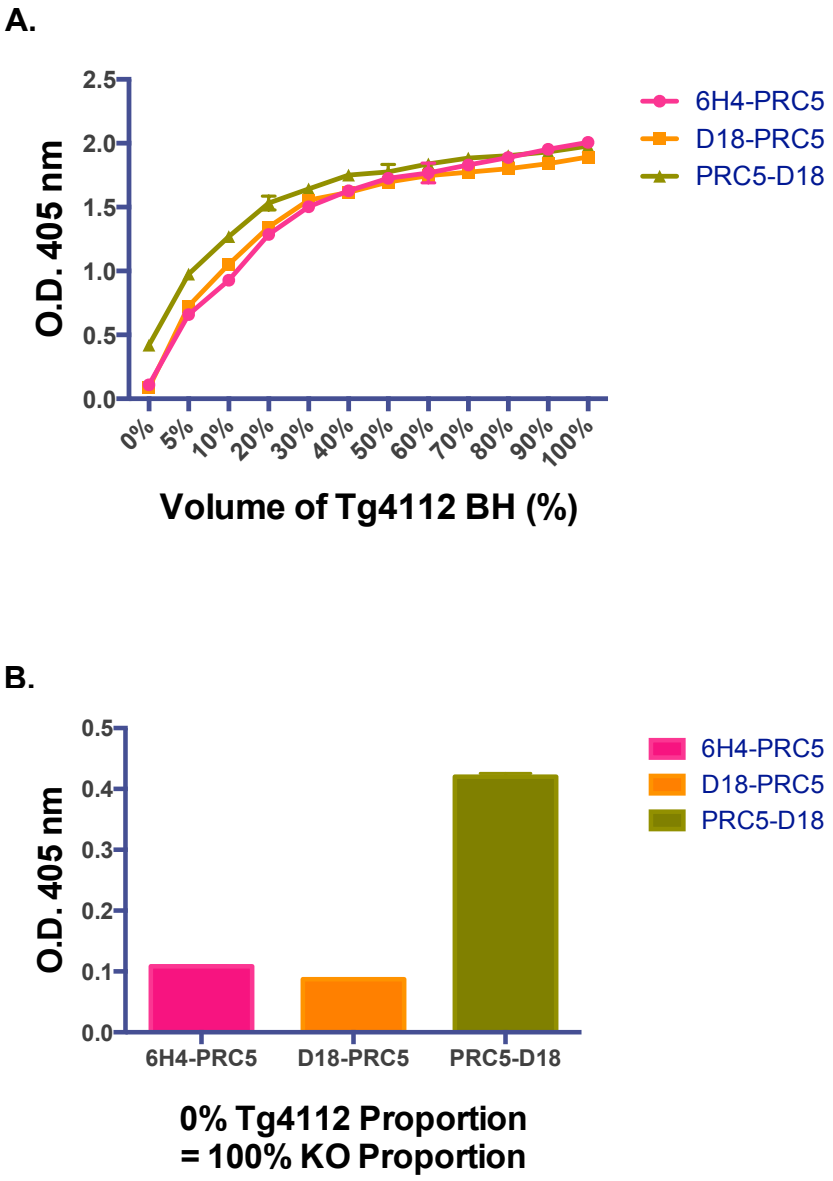

Figure 3-12. PrP^C detections by three anti-PrP antibody applications for Sandwich ELISA approaches. Tested samples were serial dilutions of the Tg4112 BH sample with the PrP-KO BH sample. (A) 0% to 100% Tg4112 BH volume proportion (= 100% to 0% KO mouse BH volume) with each 10% increase; (B) 0% Tg4112 proportion = 100% PrP-KO proportion (n=2, each proportion)

Application of the D-5 ELISA method for PrP analyses in TSE-infected materials

The D18 Fab Ab is capable of detecting PrP27-30 rods in denatured samples by ELISA and IP experiments.[15] Under the non-denatured condition, however, a Sandwich ELISA approach with this Ab measured high PrP levels in BH samples from an uninfected Tg4112 mouse with murine PrP overexpressions, but not from a PrP-KO mouse. Hence, these findings indicated that the D18 Fab Ab could detect PrP^C expressions in the uninfected brain by an ELISA method without denaturation. To determine D18 features, two Sandwich ELISA approaches (D18-PRC5 and PRC5-D18) were applied for the following mouse BH samples: PrP-KO, uninfected FVB/n, RML-inoculated FVB/n, uninfected C57BL6, RML-inoculated C57BL6, and 22L-inoculated C57BL6 mice (n=1 for each mouse). Followed by the optimized 7-5 ELISA protocol, two groups of these samples were prepared for denaturation with either 0M GdnHCL (only 50mM Tris buffer as non-denaturant) or 5M GdnHCL, and then incubated for 15 minutes at 37°C. In this experiment, the concentration of coated capture antibodies was 5μg/ml (= 0.5μg in 100μl per well). Also, buffers containing protease inhibitor cocktail (one tablet in 50mL) were used for sample dilution, blocking step, and detecting and secondary antibodies. In the 5M GdnHCL denaturation group, both ELISA approaches detected high PrP levels in all infected materials (Figures 3-13.A and B). However, the PRC5-D18 Sandwich ELISA approach exhibited higher background, as predicted from CPCA studies. In contrast, the 0M GdnHCL condition showed lower O.D. values in these infected samples than uninfected controls by the two ELISA approaches (Figures 3-13.C and D). Since the D18 Fab Ab requires denaturation to measure PrP27-30 rods, these O.D. values in non-denatured conditions denoted only PrP^C detections. These

results indicated that the denaturation step in the D-5 ELISA method would be an influential factor to measure either only PrP^{C} or total PrP (including PrP^{Sc}) levels. Also, TSE-infected mice had decreased PrP^{C} levels in the disease course to the terminal stage, whereas large amounts of PrP^{Sc} agents were generated (Figures 3-13.A and C).

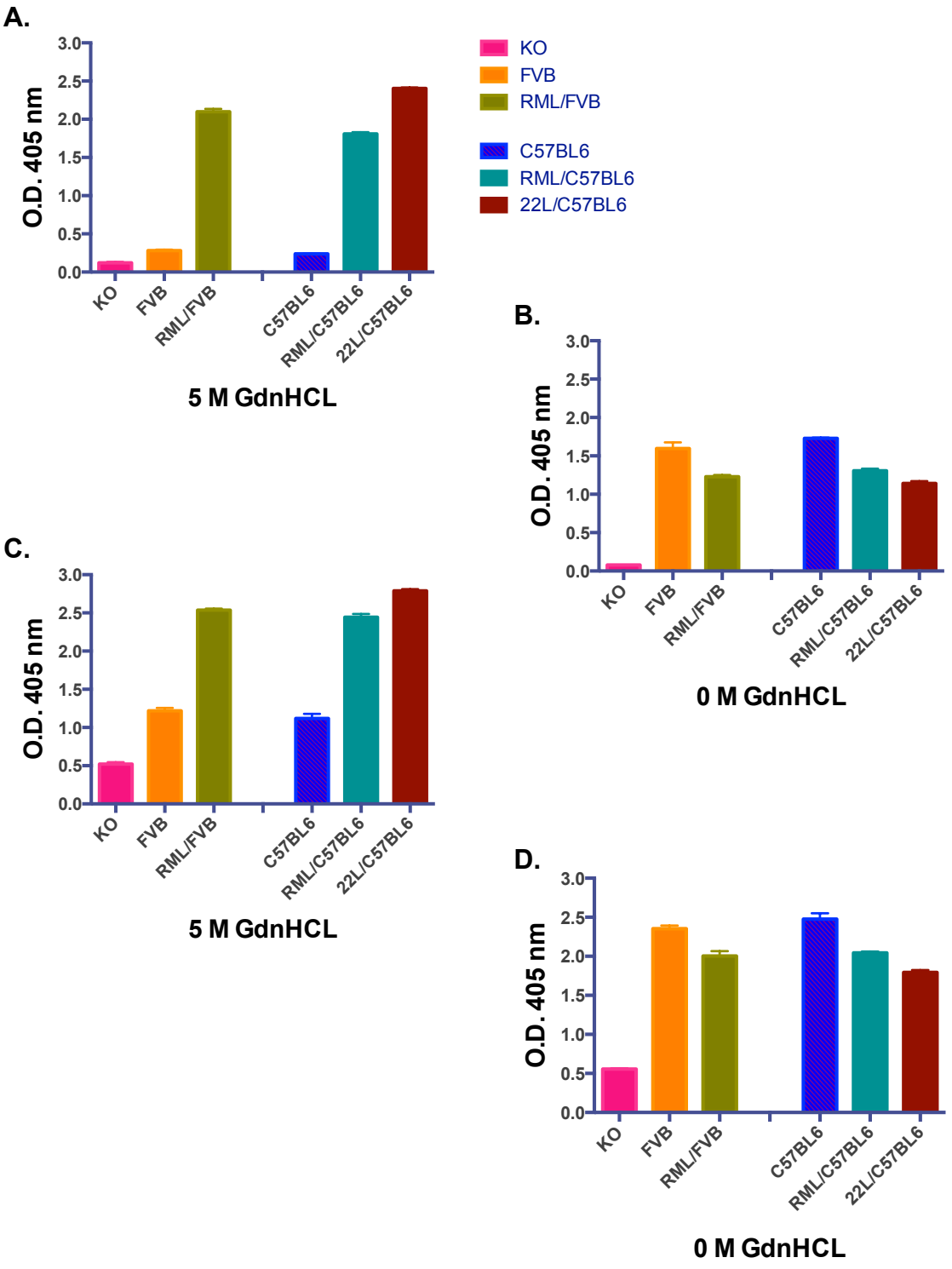

Figure 3-13. PrP detections in TSE-infected murine BH materials using the D-5 ELISA method. Sandwich ELISA applications of D18-PRC5 mAbs for denatured samples with (A) 5M GdnHCL denaturation and (B) 0M GdnHCL; the application of PRC5-D18 mAbs for the samples with (C) 5M GdnHCL denaturation and (D) 0M GdnHCL. (n=3, each sample, 20µg total protein per well)

Optimization of the D18 Fab Ab as the capture antibody in the D-5 ELISA method

To optimize a coating concentration of the D18 Fab Ab as the capture antibody, the same tested procedures in the study with the Figure 2-2 were applied for the D-5 ELISA method under sample preparations with non-denaturation and denaturation. The 96-well plates for the D-5 ELISA method were prepared for each denaturation state. Initially, the D18 Fab Ab was diluted to concentrations 0.5, 1, 2.5, and 5 μg/ml. 100 μl of each antibody concentration was coated into wells as triplicate: final total Ab amounts were 0.05, 0.1, 0.25, and 0.5μg per well. Testing mouse BH samples included a RML-inoculated FVB/n mouse, an uninfected FVB/n mouse, and a PrP-KO mouse (n=1). For the non-denatured experiment, BH samples were only diluted with PBS containing a protease inhibitor to be a protein concentration 200μg/ml. Then, 100μl of each diluted sample were coated into wells (triplicate) on a prepared ELISA plate for each capture antibody concentration. Total protein of each sample was 20μg per well. For the denatured experiment, BH samples were treated with 5M GdnHCL under the optimized protocol of the 7-5 ELISA method. At the final step of the sample preparation, these denatured samples were diluted. 100μl of each diluted sample (200μg/ml protein concentration) was added into the wells for each capture antibody concentration. Subsequent procedures were followed by the 7-5 ELISA protocol. In addition, further concentrations of the D18 Fab Ab at 5, 10, 20, and 30μg/ml were evaluated under the procedures above. In the denatured experiment, the 5μg/ml concentration of the D18 Fab Ab showed the highest O.D value for PrP detections in the RML-infected material (Figure 3-14.A). At higher D18 concentrations, the O.D. values of both infected and uninfected BH samples seemed to reach the signal plateaus between 10 and 20μg/ml

concentrations (Figure 3-14.B). In the non-denatured experiment, an uninfected FVB/b mouse showed higher PrP detections than the infected samples at all concentrations of the D18 capture antibody. The signal plateaus of O.D. values were also observed between the 10 and 20μg/ml antibody concentrations (Figure 3-14.C and D). These results suggested that the 10μg/ml concentration of the D18 Fab Ab should be practical for the D-5 ELISA method, but the 20μg/ml concentration would be a proper application for both denatured and non-denatured sample conditions. In fact, the 7-5 ELISA method also contained the 20μg/ml concentration of a PRC7 capture antibody. To compare these two Sandwich ELISA approaches, therefore, the 20μg/ml concentration was also applied for a capture D18 antibody in the further D-5 ELISA experiments.

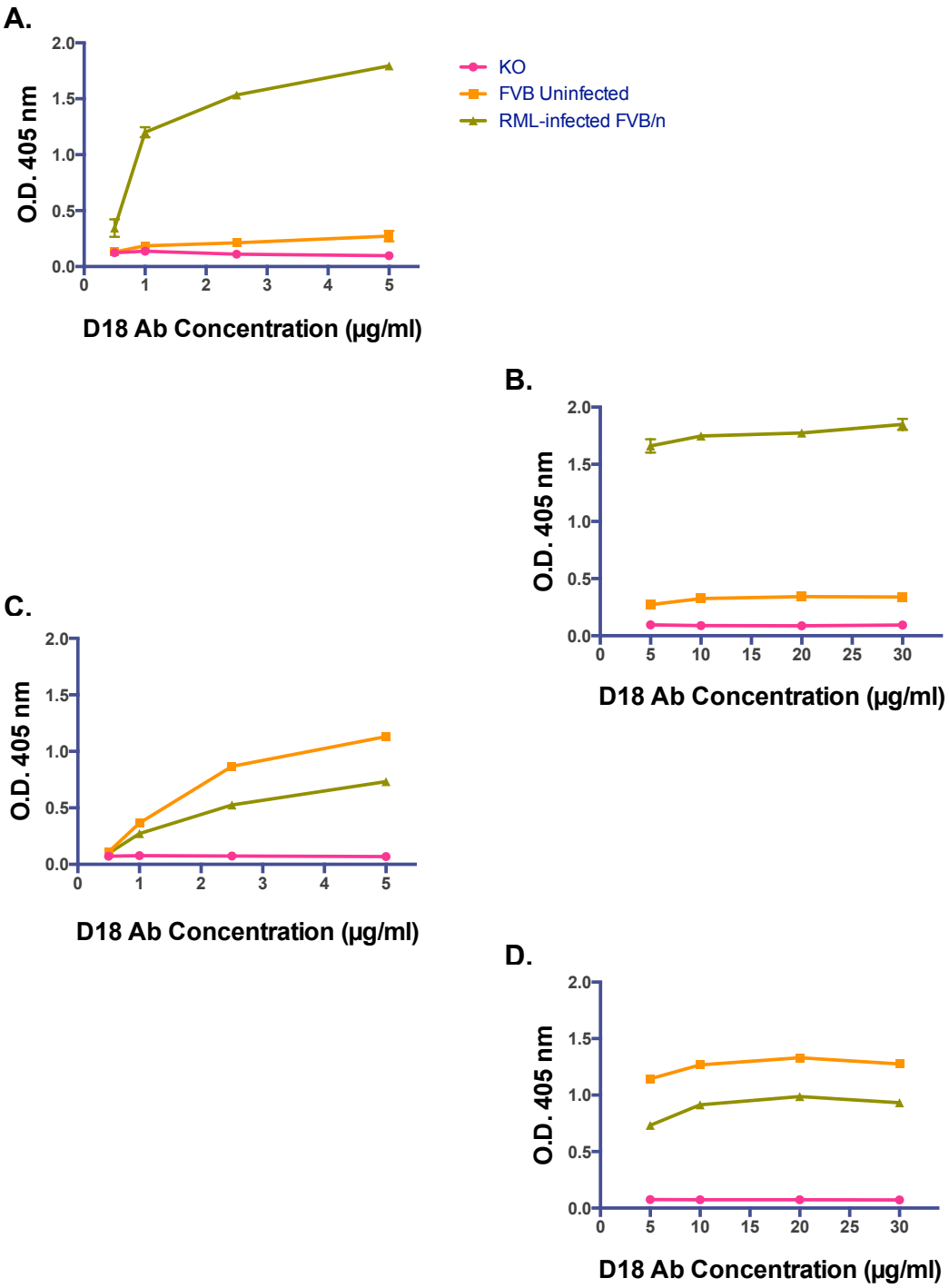

Figure 3-14. Optimizations of coating amounts as the capture antibody D18 Fab Ab in the D-5 ELISA method. Testing with denatured samples and D18 concentration (per well) in the range of (A) 0.5-5µg/ml, and (B) 5-30µg/ml. Testing with non-denatured samples and D18 concentration (per well) in the range of (C) 0.5-5µg/ml, and (D) 5-30µg/ml. (n=3, each concentration with 20µg total protein amount of each sample)

Comparisons of two denaturants in the D-5 ELISA method

As described above, the study of the Figure 2-9 compared the effectiveness of GdnHCL and GdnSCN for the sample denaturations in the 7-5 ELISA protocol. For optimizing the D-5 ELISA method, these denaturants were again evaluated for sample denaturations using 5M GdnHCL and 3M GdnSCN. Testing mouse BH samples included a RML-inoculated FVB/n mouse, an uninfected FVB/n mouse, and a PrP-KO mouse (n=1 for each). After the treatment with 1% TX100 at 37°C incubation for one hour, these BH samples were denatured with either 5M GdnHCL or 3M GdnSCN for 15 minutes at 37°C. Each denatured sample contained a protein concentration of 2mg/ml, which subsequently was 10 times diluted by PBS with 1% BSA and protease inhibitor to be 200µg/ml. 100µl of each diluted sample was added into wells of ELISA plates with pre-coating of the D18 Fab Ab 20µg/ml concentration. The total protein of each sample was 20µg per well at the final step. Similar to the 7-5 ELISA results in the study of the Fugire 2-9, the GdnHCL denaturation showed at least 1.5 times higher O.D. value of the PrP detection in the infected material, compared to the GdnSCN treatment (Figure 3-15.A and B). In addition, the 7-5 ELISA experiment evaluated the same prepared BH samples as a comparative control (Figure 3-15.C and D). These outcomes indicated the preferable effect of GdnHCL as a denaturant in the D-5 ELISA method.

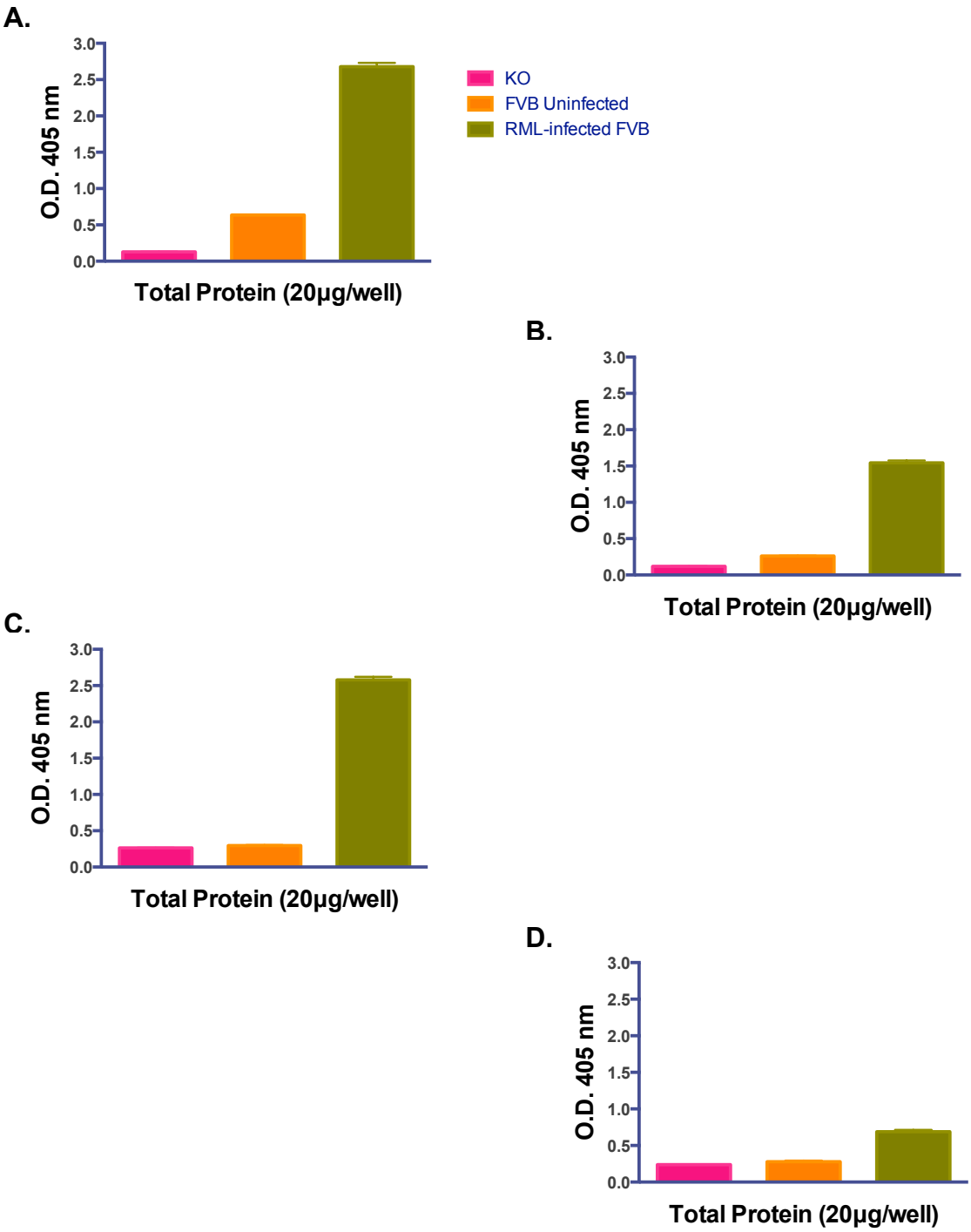

Figure 3-15. Comparisons of denaturant efficacies for PrP detections in RML-infected murine BH analyte by the D-5 ELISA method.
Under the sample preparation protocol, the D-5 ELISA method with (A) 5M GdnHCL, and (B) 3M GdnSCN; the 7-5 ELISA method with (C) 5M GdnHCL, and (D) 3M GdnSCN. (n=3, each sample with 20µg total protein amount per well)

GdnHCL-dose dependent responses for PrP detections in the D-5 ELISA method

To optimize a GdnHCL concentration in the D-5 ELISA method, its different concentrations (0-6M) were determined with BH samples from a RML-inoculated FVB/n mouse, an uninfected FVB/n mouse, and a PrP-KO mouse (n=1 for each). All procedures were performed under the optimized 7-5 ELISA protocol. Controls for the denaturing procedures were non-denatured samples, which were only diluted by PBS with 1% BSA and protease inhibitor to be 200μg/ml protein concentration. The samples for 0M GdnHCL only contained 50mM Tris, whereas other GdnHCL concentrations were applied into the testing samples for each concentration. These prepared samples were then denatured for 15 minutes at 37°C incubation. At the final step of the sample preparations, all denatured samples were diluted 10 times by PBS with 1% BSA and protease inhibitor: the final protein concentration was 200μg/ml. 100μl of each prepared sample was coated into wells (triplicate: total protein 20μg per well) on the plate for the D-5 ELISA method. In this GdnHCL-dose dependent experiment, the infected material presented the plateaus of O.D. values from the 4M GdnHCL (Figure 3-16.A).

In comparison to the D18 Fab Ab, another anti-PrP mAb POM2 (Prionatis AG, Alpnach Dorf, Switzerland) was tested for this GdnHCL-dose dependence as a capture antibody (0.5μg/ml concentration; coated 0.05μg per well) in the Sandwich ELISA approach. POM2 mAb has four binding epitopes (four alternative non-competing epitopes: 58-64, 66-72, 74-80, 82-88) in the octarepeat peptide region at the unstructured flexible N-terminal domain of the PrP structure. In contrast, the D18 Fab Ab binds to the epitopes 133-157 in the structured C-terminal globular domain. In the Sandwich ELISA approach, the combination of POM2-PRC5 antibodies showed higher

O.D. values of PrP detections in the uninfected samples with and without denaturation, compared to the PrP-KO analyte (Figures 3-16.A and B). However, all detected PrP levels were not very different among tested GdnHCL doses. These results indicated that denaturation did not influence the octarepeat peptide region of the PrP^C structure, because the N-terminal was a liner domain where POM2 mAb bound to its epitopes. In contrast, the D-5 ELISA results indicated that both uninfected and infected samples decreased PrP^C detections in a comparison of non-denatured and 0M-denatured samples at 37°C incubation and/or 50mM Tris (a dilution buffer of GdnHCL) (Figure 3-16.A). Since the D18 Fab Ab binds to the globular structure domain, these procedures could influence the PrP structure or its conformational stability. Hence, this observation suggested that denatured PrP^C molecules might require longer renaturation times to fold native structures. These renaturation times might be longer than the process of sample coatings, immediately after the denaturation and subsequent ten-fold dilution in the sample preparation. Overall, GdnHCL is a proper denaturant applying to the sample preparation in the D-5 ELISA protocol. At least 4M concentration is necessary to enhance higher PrP detections in TSE-infected materials.

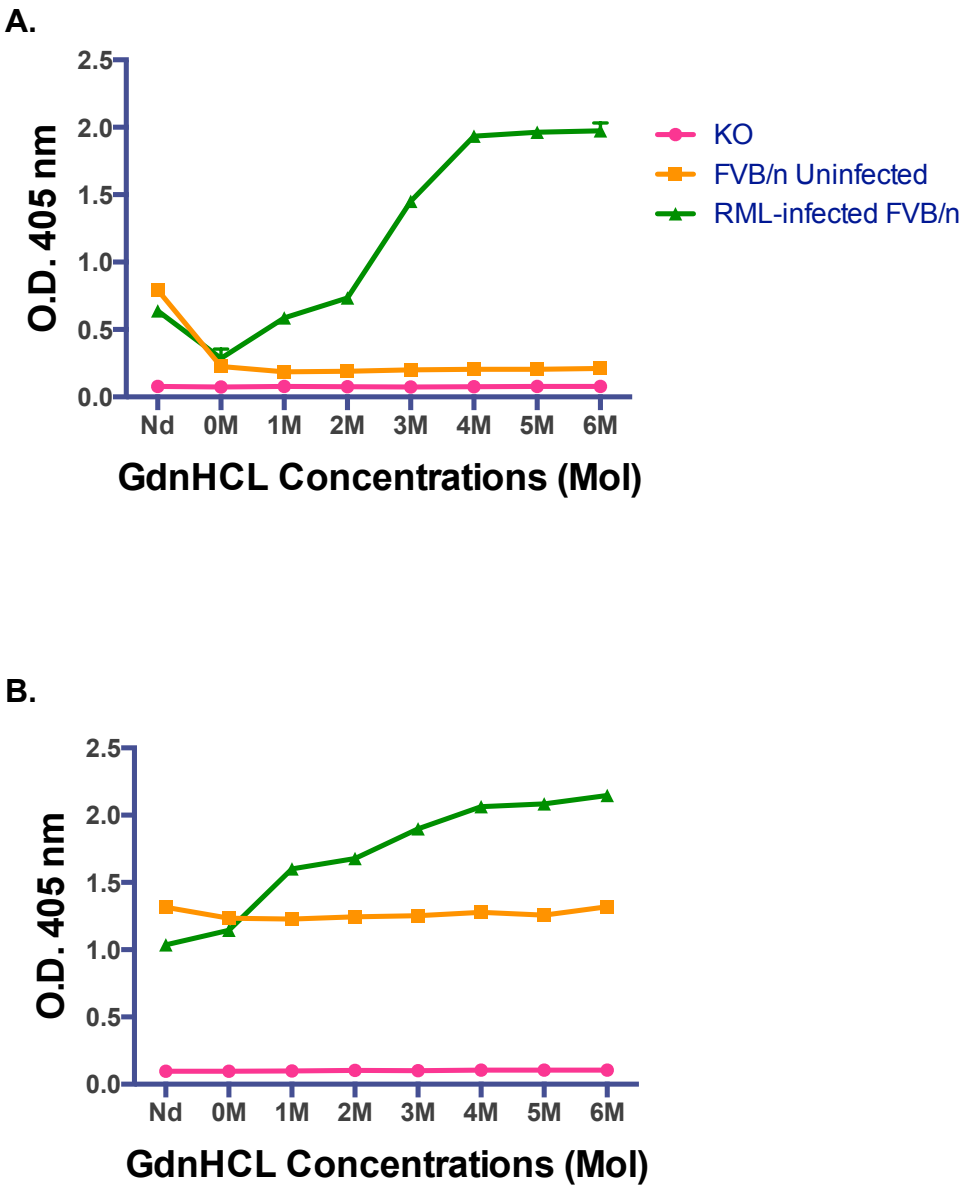

Figure 3-16. GdnHCL-dose dependent responses in RML-infected murine BH samples. (A) the D-5 ELISA method, compared to (B) POM2 mAb as a capture antibody with the detecting antibody PRC5 mAb. (n=3, each sample with 20µg total protein amount per well)

Renaturation times of denatured PrP molecules

Presumably, the renaturing process of a denatured PrP molecule should initiate immediately after the ten-time dilution step. Nevertheless, its completion times might influence binding chances of the capture antibodies to the targeted molecules in ELISA plate wells. To determine potential influences of PrP renaturation times, the D-5 ELISA and 7-5 ELISA methods examined the time-point evaluations of sample coatings into wells on prepared plates. Testing BH samples included a RML-inoculated FVB/n mouse, an uninfected FVB/n mouse, and a PrP-KO mouse (n=1 for each). These samples were denatured with 5M GdnHCL, and then diluted by PBS with a 1% BSA and protease inhibitor to be the 200μg/ml protein concentration. Subsequently, 100μl of each prepared sample was coated into wells (triplicate: total protein 20μg per well) on prepared ELISA plates with pre-coated D18 or PRC7. The sample coating was done at the following times after the sample dilution: 0 (immediately after the dilution), 5, 10, 20, 30, 40, 50, and 60 minutes as post-denaturation periods. Both D-5 ELISA and 7-5 ELISA experiments showed the highest O.D. values of PrP detections in the infected material at the 0 minute time points (Figure 3-17.A and B). In contrast, longer waiting times for the sample coating reduced the PrP detection, especially in the 7-5 ELISA method. Possibly, the reduced PrP detection was related to re-aggregations or clusterizations of renatured PrP^{Sc} molecules in the infected material through the delay of sample coatings. Furthermore, PrP degradations were also possible occasions, because the under-glycosylated PrP forms that PRC7 recognized should be unstable protein structures. Overall, these results suggested a quick procedure for sample coatings into ELISA plates, immediately after denaturation.

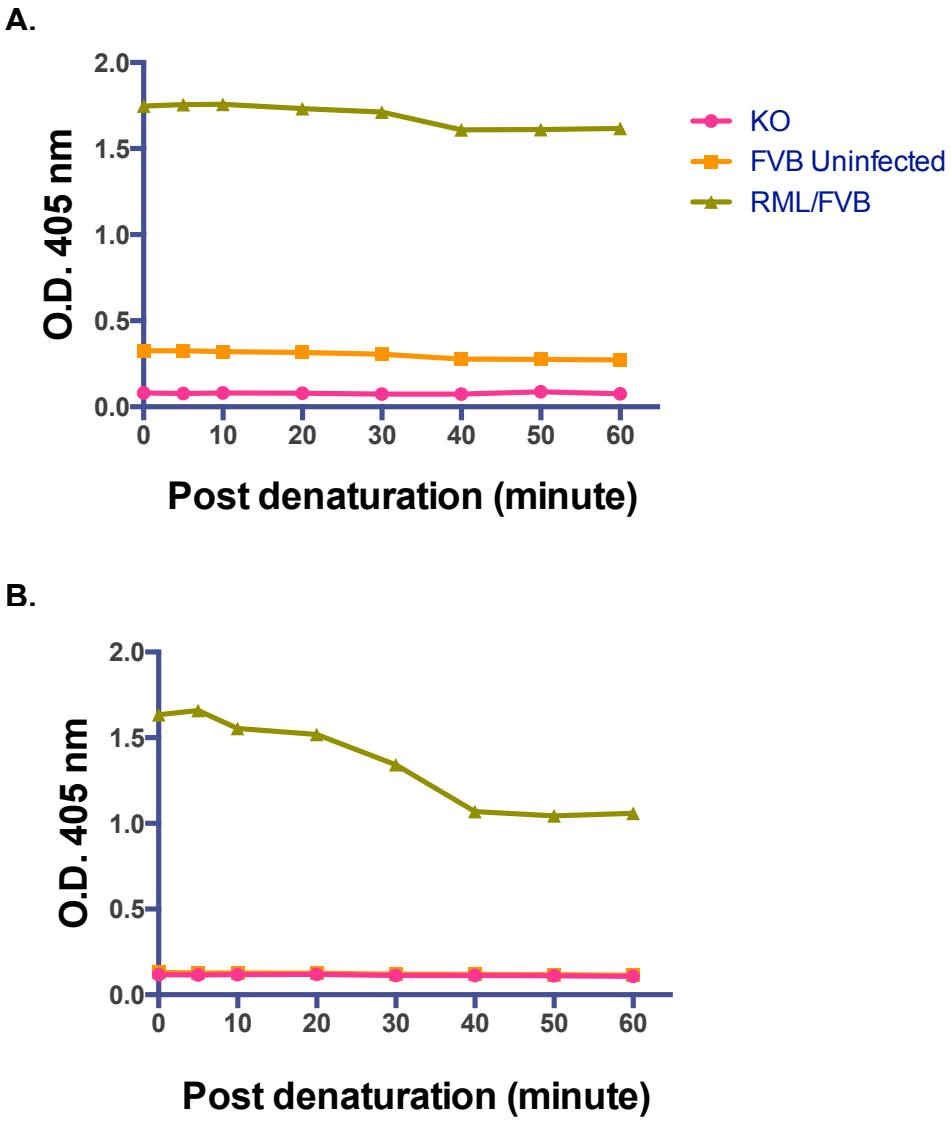

Figure 3-17. Evaluations of renaturation times for denatured PrP molecules in RML-infected murine BH samples. Tested times of sample coatings after the 10-time dilution: 0 (immediately after the dilution), 5, 10, 20, 30, 40, 50, and 60 minutes as post-denaturation periods. (A) the D-5 ELISA method, and (B) the 7-5 ELISA method(n=3 per a time point with each sample, 20μg total protein per well)

Comparisons of multiple capture antibodies in the Sandwich ELISA approach

The 7-5 ELISA and D-5 ELISA protocols have innovated molecular diagnostic applications for PrP detections in TSEs. To evaluate these analytical specificities, other anti-PrP antibodies were compared as capture antibodies under the same protocols: 6H4 (Prionics, Schlieren, Switzerland), POM2 (Prionatis AG, Alpnach Dorf, Switzerland), SAF-32 (Cayman Chemical, Michigan, USA[16]), and mAb132 (kindly provided by Dr. Motohiro Horiuchi, Hokkaido University, Japan[17,18]). According to the company product information and/or related publications, the following amino acid positions in the PrP structure are binding epitopes of these antibodies:

- PRC7 (IgG1) = discontinuous epitopes 154-185 in structured globular domain of C terminus (mouse PrP numbering)
- D18 (Fab) = discontinuous epitopes 133-157 in structured globular domain of C terminus (mouse PrP numbering)
- 6H4 (IgG1) = linear epitopes 144-152 in structured globular domain of C terminus (human PrP numbering)
- POM2 (IgG1) = linear epitopes 58-64, 66-72, 74-80, 82-88 as four alternative non-competing epitopes in the octarepeat region of unstructured flexible domain at N terminus (mouse PrP numbering)
- SAF-32 (IgG2b) = linear epitopes 59-89 in the octarepeat region of unstructured flexible domain at N terminus (mouse PrP numbering)
- mAb 132 (IgG1) = linear epitopes 119-127 in hydrophobic core region adjacent to the cleavage of unstructured and structured domains between N and C termini (mouse PrP numbering)

A concentration and amount for coating each capture antibody are listed below, based on the ELISA protocols in this dissertation, or the recommended application from each company and related publication mentioned above.

- PRC7: 100µl of 20µg/ml Ab per well = 2µg/well
- D18: 100µl of 20µg/ml Ab per well = 2µg/well
- 6H4: 100µl of 1µg/ml Ab per well = 0.1µg/well
- POM2: 100µl of 0.5µg/ml Ab per well = 0.05µg/well
- SAF-32: 100µl of 0.5µg/ml Ab per well = 0.05µg/well
- mAb132: 100µl of 0.5µg/ml Ab per well = 0.05µg/well

A detecting antibody was PRC5 mAb (1mg/ml concentration in a stock). PRC5 mAb was used at a dilution of 1:5,000 ratio with PBS containing 1% BSA and protease inhibitor. 100µl of the diluted PRC5 mAb solution was added into each well (1:5,000 = 0.2µg/ml; 100µl of 0.2µg/ml Ab per well = 0.02µg/well).

- PRC5 (IgG2a) = discontinuous epitopes 132-158 in structured globular domain of C terminus (mouse PrP numbering)

For the Sandwich ELISA approach using multiple capture antibodies, testing BH samples included a RML-inoculated FVB/n mouse, an uninfected FVB/n mouse, and a PrP-KO mouse (n=1 for each). All sample preparations were performed under the optimized 7-5 ELISA protocol (including the D-5 ELISA method) for both denatured and non-denatured conditions. These BH samples for denaturation were initially treated with 1% TX100 for one hour at 37°C with an agitation of 1,000 rpm, followed by an

incubation with 5M GdnHCL at 37°C with an agitation of 1,000 rpm for 15 minutes. Subsequently, all denatured samples were diluted ten folds with PBS containing 1% BSA and protease inhibitor to be 200μg/ml protein concentration. For the non-denatured sample experiment, the BH samples were only diluted with PBS containing 1% BSA and protease inhibitor to be 200μg/ml protein concentration. To evaluate protein-dose dependences, these diluted BH samples from both denatured and non-denatured conditions were additionally diluted to prepare lower protein concentrations with the PBS buffer above, and another prepared PBS diluent with GdnHCL to be 0.5M in each sample: 10μg/ml, 5μg/ml, 2.5μg/ml, 1.25μg/ml, 0.625μg/ml, 0.3125μg/ml, and 0.15625μg/ml. Following these diluting procedures, 100μl of each sample was added into wells (quadruplicate: total protein 20μg per well) on an ELISA plate pre-coated with each capture antibody. After an overnight incubation of these ELISA plates at 4°C, all necessary procedures were completed under the optimized 7-5 ELISA protocol.

1) Denatured BH samples: The 7-5 ELISA method showed high O.D. value of PrP detections in denatured BH samples from the RML-inoculated FVB/n mouse, but not for uninfected and PrP-KO mice (Figure 3-18.A). As described in the study with the Figure 3-12 (Figure 3-12.A) above, the D-5 ELISA method was equivalent to the 6-5 ELISA approach for PrP detections in the TSE-infected sample (Figure 3-18.B and C). Both ELISA approaches also detected some PrP^C amounts in the uninfected FVB/n mouse even with denaturation. These observations might have indicated that denaturations in the optimized protocol were not enough to eliminate PrP^C molecules, such as denaturant concentration, incubation time and temperature. In fact, similar

results were also observed in the study of the Figure 3-16 for the GdnHCL-dose dependent study of the D-5 ELISA method (Figure 3-16.A).

Interestingly, the POM2-PRC5 ELISA application showed unique data that the uninfected BH sample exhibited much a higher O.D. value of the PrP detection, compared to the 7-5 ELISA, D-5 ELISA and 6-5 ELISA results (Figure 3-18.D). In addition, the detected PrP level of the infected sample was only 1.5-2 times higher than the level in the uninfected sample. This observation could be associated with the epitope sites of the POM2 mAb in the octarepeat region at the N terminal of the PrP structure. Since the N terminal is the unstructured flexible domain, denaturation might be less influential for the PrP^{C} conformation or its stability. Possibly, the flexible PrP domain is not very different between normal and abnormal PrP isoforms.

Similar to the POM2 mAb, the epitope site of the SAF-32 mAb also localizes in the octarepeat region at the N terminal. In the SAF-32-PRC5 ELISA approach, it is interesting that the SAF-32 mAb showed a lower PrP detection in the infected sample, compared to the POM2-PRC5 ELISA experiment (Figure 3-18.E). As described above, the POM2 mAb has four different bindings epitopes in the octarepeat region, which might provide much higher binding chances of POM2 mAb to PrP molecules, compared to the SAF-32 mAb with only one binding epitope.

Unexpectedly, the mAb 132 antibody did not measure PrP levels in all tested BH samples (Figure 3-18.F). This result might be related to sample preparations under the applied protocols, which might not be suitable for this antibody. In fact, a previous study reported that the mAb 132 antibody detected PrP^{Sc} agents in Indirect ELISA methods, when samples were denatured with 6M GdnHCL for a longer incubation, 60 minutes.[17]

However, the denaturation in this comparative experiment was processed with 5M GdnHCL for 15 minutes. According to another article from Dr. Horiuchi's laboratory, 5M GdnSCN was applied for the experiments with the mAb 132 antibody and TSE-infected cell cultures.[18] In the Prion 2015 conference at CSU, Fort Collins, Colorado, his group presented the poster about a cell-base ELISA method using the mAb 132 antibody.[30] Further publications reported the optimized protocols of the mAb 132 application for PrP^{Sc} detections.[31-33] The sample preparations in the mAb 132 protocols were different from the 7-5 and D-5 ELISA methods.

2) Non-denatured BH samples: The 7-5 ELISA method could not detect PrP levels in all tested analyte under non-denatured condition, because the PRC7 mAb required denaturation and renaturation of PrP^{Sc} isoforms to fold native PrP^{C} structures or these equivalent conformations (Figure 3-18.G). In general, the abundance of normal PrP^{C} isoforms in healthy individuals and animals are diglycosyl forms that the PRC7 mAb cannot react. In contrast, the D-5 ELISA and 6-5 ELISA approaches detected higher PrP^{C} levels in the uninfected sample, compared to the infected sample (Figures 3-18.H and I). These measurements indicated that the RML infection and disease development decreased PrP^{C} levels in the inoculated mouse brain. Nevertheless, the POM2-PRC5 ELISA approach with the non-denaturation presented limited differences of PrP detections between infected and uninfected samples (Figure 3-18.J). These results suggested that the RML infection and disease progression might have affected the structured globular domain with which D18 and 6H4 mAbs bound. The unstructured domain with which the POM2 mAb reacted might have no or less influence through the disease development.

Furthermore, the SAF-32 and mAb132 mAbs were not applicable to determine PrP levels in tested samples under the non-denatured condition (Figures 3-18.K and L). In fact, the mAb 132 was reported as a PrP^{Sc}-specific antibody.[18] Thus, this anti-PrP mAb has to be less reactive to PrP^{C} isoforms. Even with denaturation, PrP^{C} molecules did not expose the binding epitopes of the mAb 132 in uninfected cells.[18] Possibly, immediately after a denaturing process, refolded PrP^{C} structures may prevent the interaction with this antibody. These observations should be associated with different experimental preparations and conditions. Hence, sample preparations and experimental conditions are influential factors for the protein conformation and renaturation, which affect binding epitopes of testing antibodies on targeting molecules.

Overall, the PrP detection is dependent on the conformation and its modification between PrP^{C} and PrP^{Sc} isoforms, influenced by the binding epitopes of applied anti-PrP antibodies. Based on the outcomes in this study section, the selection and combination of capture and detecting antibodies are key applications in Sandwich ELISA approaches. In this method, the combination of anti-PrP antibodies that bind epitopes in the structured globular domain could be better selections to measure higher PrP detections in TSE-infected materials. Therefore, the 7-5 ELISA and D-5 ELISA approaches have practical utilities to identify PrP^{Sc} isoforms in TSE diagnoses, and also to measure PrP^{C} levels, compared to other tested capture antibodies.

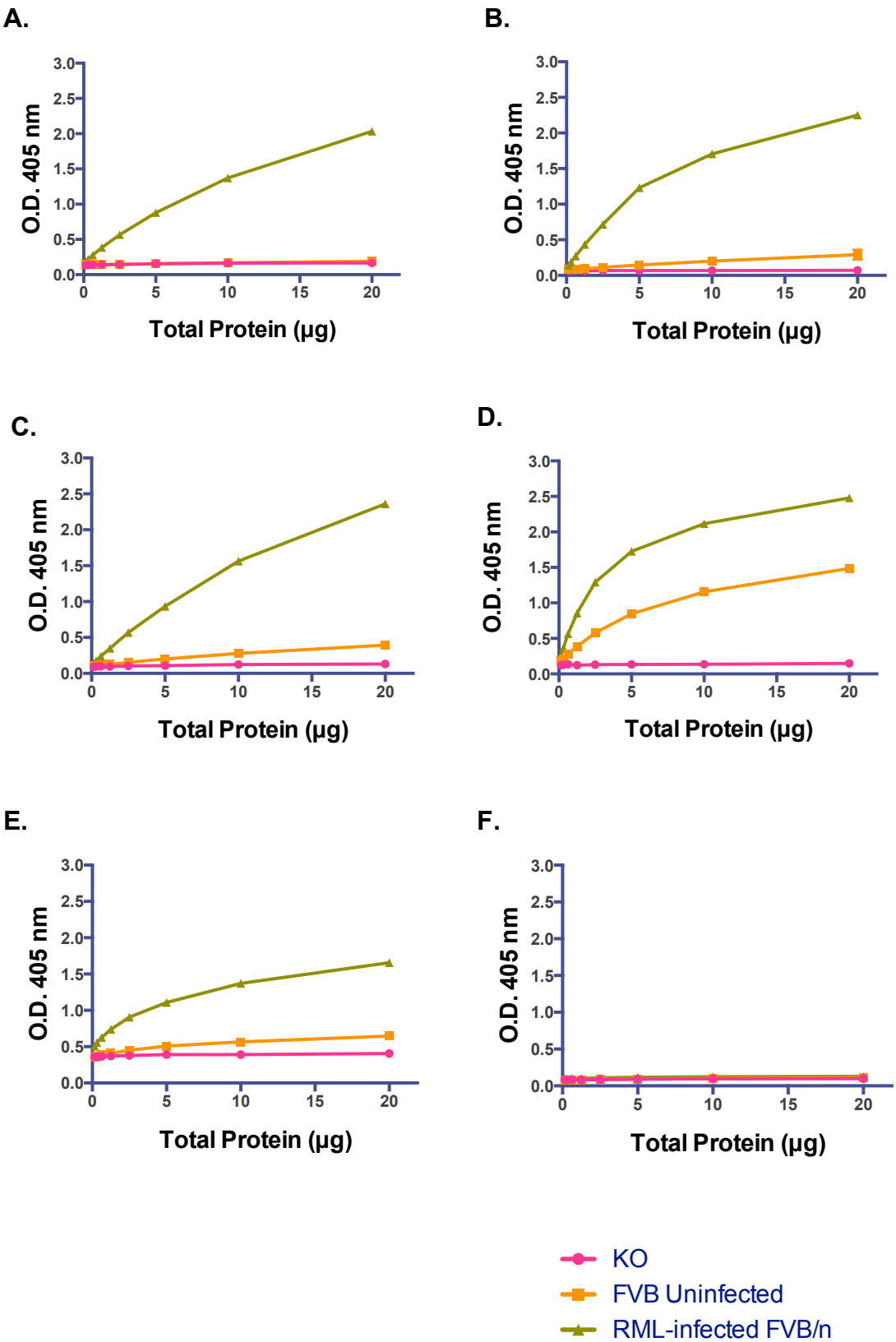
A.
B.
C.
D.
E.
F.
O.D. 405 nm
Total Protein (µg)
0.0
0.5
1.0
1.5
2.0
2.5
3.0
0
5
10
15
20
KO
FVB Uninfected
RML-infected FVB/n

G.

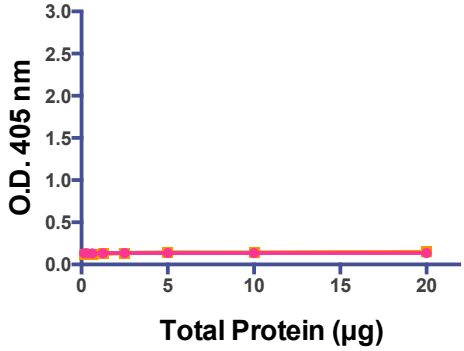
O.D. 405 nm
3.0
2.5
2.0
1.5
1.0
0.5
0.0
0
5
10
15
20
Total Protein (µg)

H.

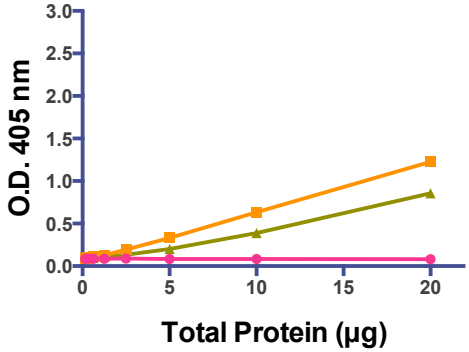
O.D. 405 nm
3.0
2.5
2.0
1.5
1.0
0.5
0.0
0
5
10
15
20
Total Protein (µg)

I.

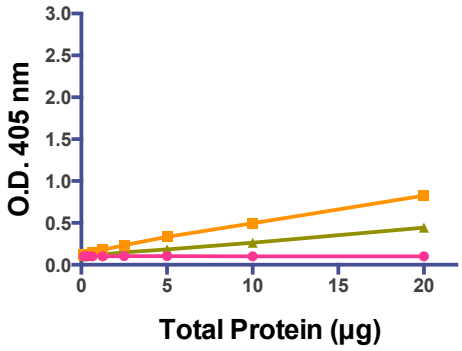
O.D. 405 nm
3.0
2.5
2.0
1.5
1.0
0.5
0.0
0
5
10
15
20
Total Protein (µg)

J.

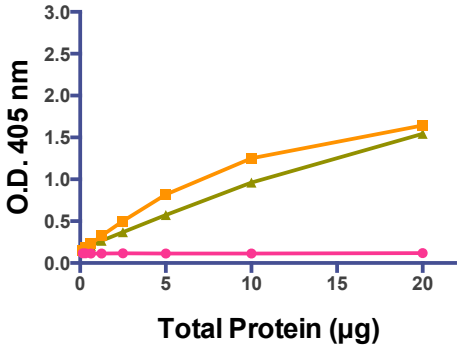
O.D. 405 nm
3.0
2.5
2.0
1.5
1.0
0.5
0.0
0
5
10
15
20
Total Protein (µg)

K.

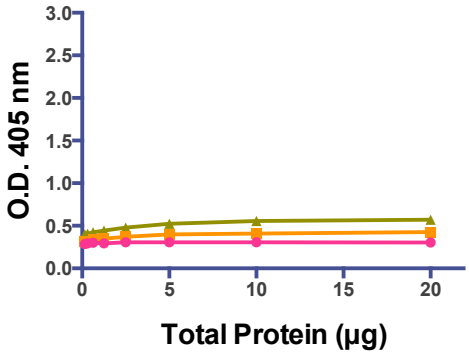
O.D. 405 nm
3.0
2.5
2.0
1.5
1.0
0.5
0.0
0
5
10
15
20
Total Protein (µg)

L.

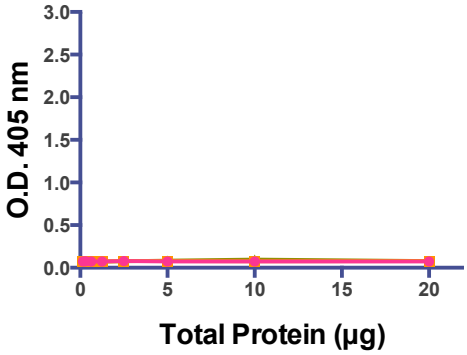
O.D. 405 nm
3.0
2.5
2.0
1.5
1.0
0.5
0.0
0
5
10
15
20
Total Protein (µg)

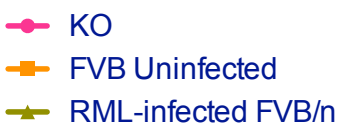
KO
FVB Uninfected
RML-infected FVB/n

Figure 3-18. Comparisons of multiple capture antibodies in protein-dose dependent responses under the Sandwich ELISA approach. Using a RML-infected murine BH analyte and its control samples, six different anti-PrP antibodies were tested as capture antibodies with the detecting antibody PRC5 mAb.
For denatured BH materials, capture antibodies were (A) PRC7 mAb, (B) D18 Ab, (C) 6H4 mAb, (D) POM2 mAb, (E) SAF-32 mAb, and (F) the mAb 132.
for non-denatured BH materials, capture antibodies were (G) PRC7 mAb, (H) D18 Ab, (I) 6H4 mAb, (J) POM2 mAb, (K) SAF-32 mAb, and (L) the mAb 132.
(n=3 per total protein amount for each sample)

Comparisons of the 7-5 ELISA and D-5 ELISA methods for PrP detections in TSE-mouse models expressing different PrP species

In this dissertation, four Sandwich ELISA systems were established for PrP detections. First, the 7-5 ELISA method detects PrP levels in TSE-infected mouse BH samples with 5M GdnHCL denaturation. Specifically, this method can measure unglycosyl and mono-1 glycosyl PrP forms that are predominantly generated in TSE-infected animals, but not in healthy or non-TSE-infected hosts. Thus, the 7-5 ELISA method is capable of analyzing TSE infections by glycosylation states. Second, the D-5 ELISA method detects PrP^{Sc} molecules (or total PrP levels) in denatured BH samples from TSE-infected mice. This analytical feature is based on the D18 property that requires a sample denaturation for PrP^{Sc} detection. This method has a competent ability to analyze TSE infections by detectable PrP levels in denatured BH samples. Third, the D-5 ELISA method without denaturation only recognizes PrP^{C} levels in BH samples. In TSE-mouse models, uninfected BH samples exhibit higher PrP^{C} levels than TSE-infected BH samples. These results indicate the decreases of PrP^{C} molecules during the TSE disease development and progression in infected hosts. Thus, modifications of PrP^{C} levels could be implicated with the TSE pathogenesis. Additionally, the 7-5 ELISA method without denaturation might be applicable to evaluate the generation of unglycosyl and mono-1 glycosyl PrP^{C} forms in testing BH samples, as the fourth system. The detection of under-glycosylated PrP forms might indicate an impairment of the PrP glycosylation, leading to unstable PrP structures and conformational alterations.

To compare the analytical properties of these four Sandwich ELISA systems, protein-dose dependent approaches were determined by various TSE mouse models

with different PrP species. These comparison studies included the following TSE-infected mouse models: 1) RML-inoculation in FVB/n mouse, 2) CWD (elk CWD brain sample Bala05-0308)-inoculation in Tg1536 (DeerPrP) mouse, 3) CWD (Bala05-0308)-inoculation in Tg5037 (ElkPrP) mouse, 4) CWD (elk CWD brain sample 99W12389)-inoculated gene-targeted (GTE) M2elk mouse expressing Elk PrP, 5) Sheep scrapie (Colorado Scrapie)–inoculation in Tg3533 (OvineARQ PrP) mouse, and 6) TME (941031)-inoculation in TgF431 (MinkPrP) mouse. Controls were BH samples from a PrP-KO mouse, an uninfected wild-type mouse, and a transgenic or gene-targeted mouse matching to each TSE-inoculated mouse model.

Samples preparations for the 7-5 ELISA and D-5 ELISA methods were described above. For the denatured preparation, these BH samples were initially treated with 1% TX100 for one hour at 37°C with 1,000rpm agitation, and then denatured with 5M GdnHCL for 15 minutes at 37°C with 1,000rpm agitation. After that, the denatured samples were 10 times diluted with 1% BSA-containing PBS. The final protein concentration of these diluted BH samples was 200μg/ml (= total protein 20μg in 100μl). For protein-dose dependent studies, the samples were further diluted to be 100, 50, 25, 12.5, 6.25, 3.125 and 1.5625 μg/ml concentrations (= total protein 10, 5, 2.5, 1.25, 0.625, 0.3125, and 0.15625 μg in 100μl respectively). Subsequently, 100μl of each prepared sample was added into wells for each category on ELISA plates with pre-coated capture antibodies, either PRC7 or D18. Furthermore, the non-denatured preparation did not include any treatment with TX100, GdnHCL, and heat incubation, prior to coating the samples on the prepared ELISA plates. Hence, BH samples were only diluted with PBS that contained 1% BSA and protease inhibitor to be the final

protein concentration 200μg/ml. These prepared samples were additionally diluted to the lower protein concentrations above. Lastly, 100μl of each diluted sample was added into wells for each category on the ELISA plates. After the ELISA plates with samples were incubated at 4°C overnight, the subsequent processes were performed under the optimized 7-5 ELISA and D-5 ELISA protocols.

1) RML-inoculated FVB/n Group: The tested RML-infected material was a BH sample derived from a mouse with a terminal disease condition in the inoculation study SK-01. For the denatured BH samples, the 7-5 ELISA and D-5 ELISA methods detected higher O.D. values of PrP levels in the RML-inoculated mouse, compared to uninfected FVB/n and PrP-KO mice (Figures 3-19.A and B). In addition, the D-5 method showed higher PrP level in this infected sample than the 7-5 ELISA method. This finding could be associated with the different features of the capture antibodies on these two ELISA approaches: the PRC7 mAb only recognizes unglycosyl and mono-1 glycosyl PrP forms, whereas the D18 Fab Ab reacts to all four varieties of glycosyl PrP forms. For screening the existence of abnormal PrP agents, the D-5 ELISA method has a practical utility in diagnostic purposes. The D-5 ELISA method also presented PrP detections in uninfected samples with denaturation. This detected O.D. value should be PrP^{C} molecules that the denatured process did not eliminate, or denatured molecules refolded to native PrP conformations. Furthermore, the 7-5 ELISA method did not detect PrP levels in non-denatured BH samples, because PRC7 requires denaturation and renaturation of a PrP^{Sc} agent to be a PrP^{C} or its equivalent conformation (Figure 3-19.C). In contrast, the D-5 ELISA method detected PrP levels in both uninfected and RML-infected BH samples (Figure 3-19.D). As described above, the uninfected BH sample

showed approximately a two-fold higher O.D. value of the PrP^C level than the infected BH sample. This observation suggested the decrease of the PrP^C amount or generation/synthesis in the infected mouse during disease development and progression of the RML mouse-adapted scrapie prion strain. Moreover, the lower PrP^C detection in the RML-infected mouse might imply structural modifications in the binding epitopes or these regions of D18 and/or PRC5 antibodies on the PrP^C conformation, which antibodies lose binding activities to targeted molecules.

2) CWD-inoculated Tg1536 (DeerPrP) group: The group of CWD (elk CWD brain isolate Bala05-0308)-infected transgenic mouse with deer PrP expressions (the inoculation study CLC-005) exhibited the similar patterns of PrP detections. Both the 7-5 ELISA and D-5 ELISA methods measured the elevated PrP levels in the CWD-infected BH sample under the denatured condition (Figures 3-19.E and F). Also, the D-5 ELISA method showed a higher O.D. value of PrP detection in the infected sample than the 7-5 ELISA results. Under the non-denatured condition, the 7-5 ELISA method did not show clear differences of PrP detections between uninfected and CWD-infected materials (Figure 3-19.G). However, the 7-5 EILSA method measured subtle PrP levels in the uninfected Tg1536 mouse BH sample, in comparison to the infected Tg1536 and PrP-KO mice. Statistically, the difference of O.D. values between the uninfected and infected samples was $p < 0.02\text{-}0.0001$ from total proteins 2.5μg to 20μg, as a technical replication (well number = 4 for each mouse and total protein amount). At this point, it is not clarified if the 7-5 ELISA method detected under-glycosylated PrP forms in the uninfected Tg1536 BH sample. However, this detection might indicate that transgenic mice naturally generate PrP molecules with glycosidic deficiency or immaturity.

Furthermore, the D-5 ELISA method measured almost a two-fold higher PrP^C level in the uninfected Tg1536 mouse BH sample than the infected material under the non-denatured condition (Figure 3-19.H). These results are the same outcomes in the RML-infected mouse group described above.

3) CWD-inoculated Tg5037 (ElkPrP) group: The CWD (elk CWD brain isolate Bala05-0308)-inoculated transgenic mouse with elk PrP expressions (the inoculation study CLC-004) showed similar outcomes to the RML-FVB/n and CWD-Tg1536 (DeerPrP) groups above (Figures 3-19.I to L). The 7-5 ELISA method detected differences of PrP levels between uninfected and CWD-infected mouse BH samples under the non-denatured condition (Figure 3-19.K). The O.D. value of the uninfected Tg5037 mouse was higher than the infected mouse and PrP-KO mouse. Based on a technical replication (well numbers = 4 for each individual), p values were $p < 0.02$-0.0001 from total protein 1.25μg to 20μg for the uninfected vs. infected material, statistically. Thus, these observations indicated that transgenic mouse breed lines with cervid PrP overexpressions naturally generated unglycosyl and/or mono-1 glycosyl PrP forms in healthy condition or non-TSE infected status. Intriguingly, the 7-5 ELISA method also measured the decreased level of under-glycosylated PrP^C forms in the CWD-infected material, compared to the uninfected and PrP-KO mouse analyte. Hence, these PrP^C molecules might have altered to denaturation-resistant agents, such as abnormal PrP^{Sc} isoforms during the CWD infection and its PrP^{Sc} replication. As hypothesized, this PrP analytical approach suggested the implication of under-glycosylated PrP forms in the CWD pathogenesis. These observations supported the

exceptional sensitivity of the 7-5 ELISA method to detect the two under-glycosylated PrP forms at low amounts of total protein in tested samples.

4) CWD-inoculated GTE M2elk (ElkPrP) group: Previously, this inoculation study JC-10 applied gene-targeted (GT) mice with elk PrP expressions for a bioassay of a CWD isolate (elk CWD brain 99W12380). Transgenic mice with cervid PrP expressions, such as Tg1536 (DeerPrP) and Tg5037 (ElkPrP) mouse breed lines, predominantly overexpress these proteins in the nervous system, compared to wild-type mice. In contrast, this newly developed GT mouse breed line exhibits elk PrP expressions throughout the body including peripheral sites. Also, elk PrP expressions in this mouse are equivalent levels to a wild-type mouse. For the PrP measurement, both 7-5 ELISA and D-5 ELISA experiments detected the elevated PrP level in the denatured BH sample of a CWD-inoculated GT mouse (Figures 3-19.M and N). Also, the D-5 ELISA method showed higher O.D. values than the 7-5 ELISA method. These results were similar observations to those from the CWD (Bala05-0308) inoculation in transgenic mice with cervid PrP expressions above. In contrast, the 7-5 ELISA method did not measure PrP^C levels in the non-denatured BH samples from the infected and uninfected GT mice, compared to the PrP-KO mouse analyte (Figure 3-19.O). This observation was similar to the RML-inoculated FVB/n mouse group (a wild-type mouse breed line), but different from the studies of CWD-inoculated transgenic mice with cervid PrP expressions above. Therefore, the PrP^C detections by the 7-5 ELISA method could be specific phenomena in non-denatured BH samples from transgenic mice with PrP overexpressions. However, the D-5 ELISA method identified the decreased PrP^C

detection in the non-denatured BH sample from the CWD-infected GT mouse, as equal to the outcomes of other tested groups above (Figure 3-19.P).

5) Sheep scrapie-inoculated Tg3533 (OvineARQPrP) group: In a past bioassay (the JB-66 study), a sheep scrapie brain isolate Colorado Scrapie was inoculated into Tg3533 (OvineARQ PrP) mice whose brains were collected and stored after disease developments. Under the denatured condition, the 7-5 ELISA and D-5 ELISA method detected the elevated O.D. values of PrP levels in the Scrapie-inoculated BH sample (Figures 3-19.Q and R). The reason that the D-5 ELISA method could measure higher PrP levels than another method should link to the property of the D18 Fab Ab for binding to all four glycosyl PrP forms. In contrast, the PRC7 mAb only reacts to two of these forms. However, the PrP measurements by the 7-5 ELISA method revealed the prominent generations of unglycosyl and/or mono-1 glycosyl PrP forms in TSE-infected animals. Since the majority of PrP^C molecules hold diglycosyl forms, the loss of glycan(s) could be a specific observation in the TSE disease development and progression. As hypothesized, therefore, the expressional pattern of the PrP glycosylation could be a potential candidate as a biomarker to diagnose and monitor individuals and animals for the infection, disease development, progression, and prognosis of these fatal neurodegenerative disorders. In addition, the 7-5 ELISA method detected small PrP^C levels in the non-denatured BH samples from the uninfected and infected Tg3533 mice, compared to the PrP-KO mouse (Figure 3-19.S). These similar detections were also recognized in the transgenic mouse studies above. However, the detected PrP^C levels of the uninfected and infected Tg3533 mice exhibited similar O.D. values. Because of the PrP overexpression in these transgenic mouse breed lines,

higher generations of under-glycosyled PrP forms could be possible in their normal and healthy conditions, but non-existent or rare in wild-type and gene-targeted mouse breed lines. Lastly, the D-5 ELISA method detected a lower PrP^C level in the non-denatured BH sample from the Scrapie-infected mouse (Figure 3-19.T). This PrP^C reduction was a common observation in TSE-infected animals by the D-5 ELISA method above. Therefore, the loss of PrP^C molecules should be related to the TSE disease state.

6) TME-inoculated TgF431 (MinkPrP) group: In the study of the Figure 3-6 above, the 7-5 ELISA experiments analyzed BH samples of the three different mink TME isolates and from these inoculated TgF431 mice: inoculation studies VK-11, VK-18, and VK-20. The 7-5 ELISA method detected higher PrP levels in denatured BH samples from three mice (biological replication n= 3; well number= 3 for each mouse) of each TME-inoculation study (Figures 3-6.A to D). However, the O.D. values of all tested TME-infected mice were around 1.0 or lower (total 9 mice: 3 for each study). Thus, these observations indicated that TME pathogens replicated less in the TgF341 mice but caused the disease progression in the hosts to terminal stages. As described above, however, the 7-5 ELISA method is only capable of detecting unglycosyl and mono-1 glycosyl PrP forms after denaturation and renaturation. Therefore, it was possible that these TME-infected TgF431 mice generated more diglycosyl and/or mono-2 glycosyl PrP forms. To evaluate this possibility, the D-5 ELISA method would be useful for obtaining further information and understanding the TME pathobiology.

The inoculation study VK-18 was a bioassay of the TME-affected mink brain isolate (TME 941031) into Tg431 transgenic mice with mink PrP^C expressions. PrP levels in TgF431 mice are equivalent to those in wild-type FVB/n mice. In this study

section of the protein-dose dependent ELISA experiment, both the 7-5 ELISA and D-5 ELISA methods measured PrP levels in the denatured BH sample from the TME-infected material (VK-18), but this O.D. value was lower than 1.0 (Figures 3-19.U and V). These results were similar to the data in the study with the Figure 3-6 above. Therefore, the TME mink brain isolate 941031 should have limited the replication and generation of unglycosyl and mono-1 glycosyl PrP^{Sc} forms in the infected TgF431 (MinkPrP) mice, whereas this inoculum exhibited approximately 2.0 of the O.D. value in the 7-5 ELISA method (Figure 3-6.A). Unexpectedly, non-denatured BH samples of the uninfected and TME-infected TgF431 mice showed much higher O.D. values than the PrP-KO mouse (Figures 3-19.W and X). Intriguingly, both the 7-5 ELISA and D-5 ELISA results showed that these non-denatured BH samples had almost the same O.D. values of PrP levels between the uninfected and infected mice at all tested total proteins.

In comparison to these TME results, the 7-5 ELISA method in this study section showed only small PrP^{C} detections in non-denatured BH samples from uninfected and infected conditions of other transgenic mice expressing different PrP species (Figures 3-19.G to S). Also, these experiments indicated the decreased PrP^{C} detection in TSE-infected analyte. Hence, the TgF431 mink-PrP expressing mice might have developed different responses in the TME infection and pathogenesis, compared to transgenic mouse groups with other TSE inoculations. However, it is still possible that TME-infected TgF431 mice reduced diglycosyl PrP^{C} forms but generated under-glycosylated PrP^{C} forms during the TME disease development. These PrP^{C} modifications might impair functions of this normal protein, leading to pathological developments during the TSE disease development.

To understand these observations in TgF431 mice and TME inoculations, the 7-5 experiment re-analyzed the same tested BH samples above and a new uninfected normal mink brain (kindly provided by Dr. Jason Bartz, Creighton University, Omaha, Nebraska, USA). Under the denatured condition, this re-evaluation revealed no PrP detection in the normal mink brain as equivalent to the PrP-KO mouse (Figure 3-19.Y). In contrast, the 7-5 ELISA method detected a higher PrP level in the denatured BH sample of the uninfected TgF431 mouse, compared to the PrP-KO mouse and the uninfected mink. Although the PrP expressional level of this transgenic mouse breed line is equivalent to a wild-type mouse FVB/n, the Tg431 mouse generated under-glycosylated PrP forms like other transgenic mice with PrP overexpressions (Figures 3-6.A to D, 3-19.Y). Hence, the tested transgenic mouse breed lines in this dissertation should be predisposed naturally to generate under-glycosylated PrP forms.

Overall, the 7-5 ELISA and D-5 ELISA methods are useful applications to detect various species of PrP expressions in TSE-mouse models. In the TSE disease development, the infected mice decreased PrP^{C} detections at their terminal stages. In addition, the tested transgenic mouse breed lines above might generate some PrP^{C} forms with partial resistances to GdnHCL, and possibly other denaturants too. These PrP forms might not have native PrP^{C} conformations but equivalent to these structures with which the PRC7 mAb can react after denaturation and renaturation. However, it is not clear yet how much this potential PrP^{C} conformer is an influential factor for the TSE infection and disease development in transgenic mice bioassays.

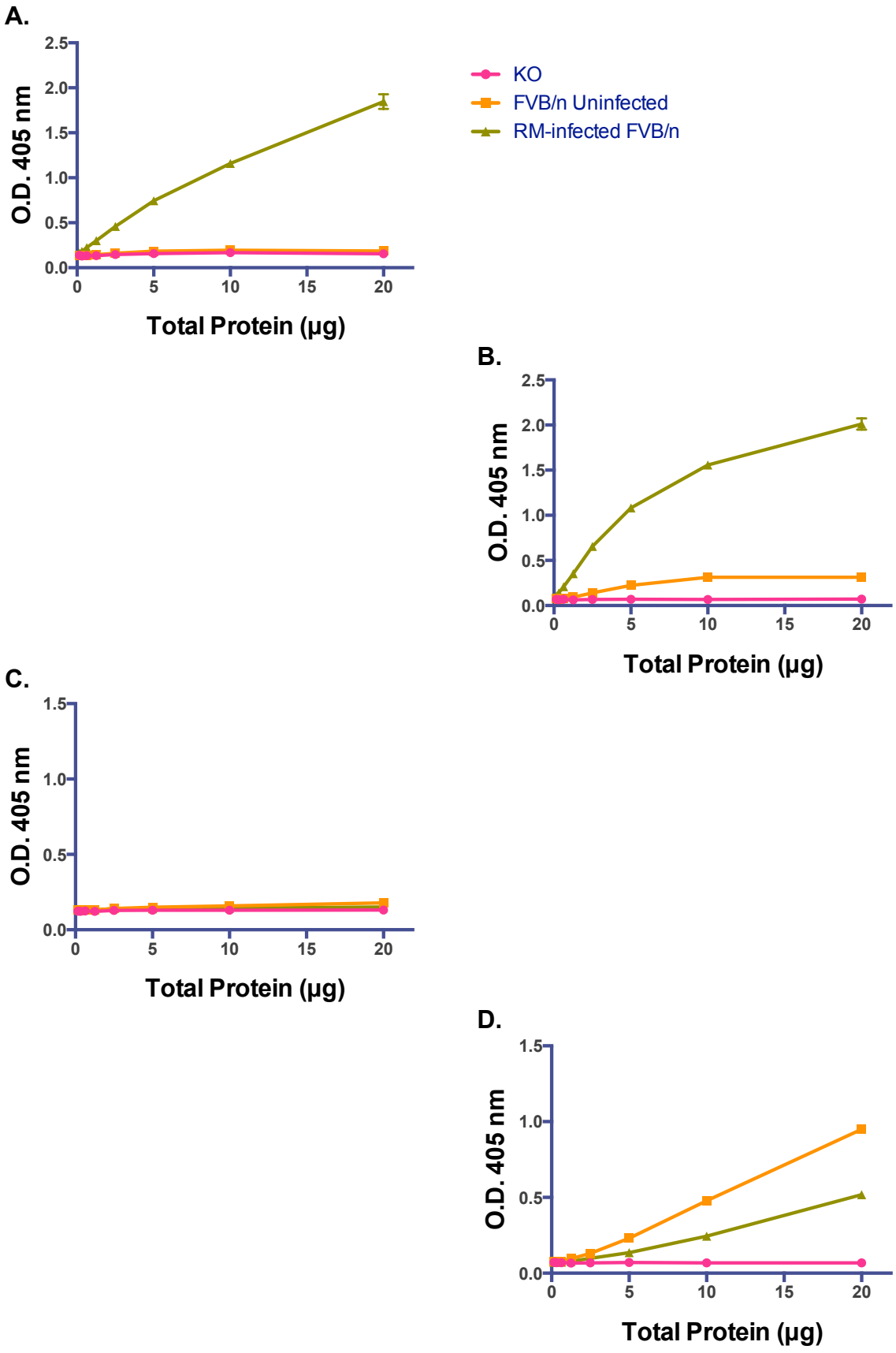
A.
O.D. 405 nm
2.5
2.0
1.5
1.0
0.5
0.0
0
5
10
15
20
Total Protein (µg)
KO
FVB/n Uninfected
RM-infected FVB/n
B.
O.D. 405 nm
Total Protein (µg)
C.
O.D. 405 nm
Total Protein (µg)
D.
O.D. 405 nm
Total Protein (µg)

E.

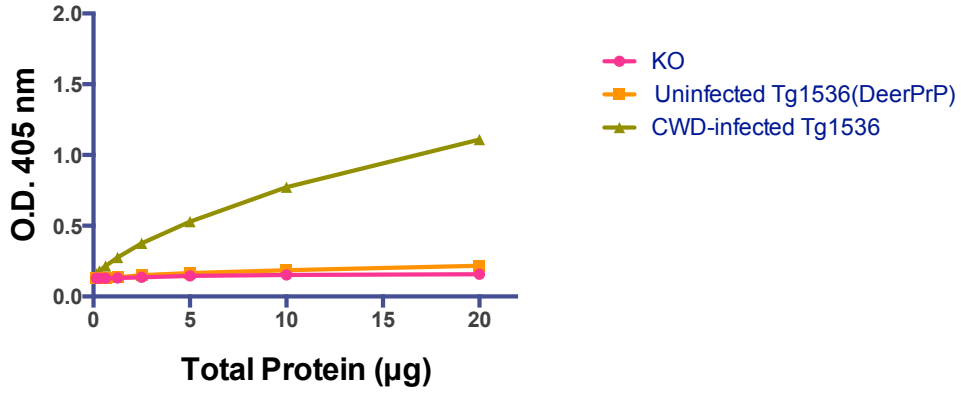
KO
Uninfected Tg1536(DeerPrP)
CWD-infected Tg1536
O.D. 405 nm
2.0
1.5
1.0
0.5
0.0
0
5
10
15
20
Total Protein (µg)

F.

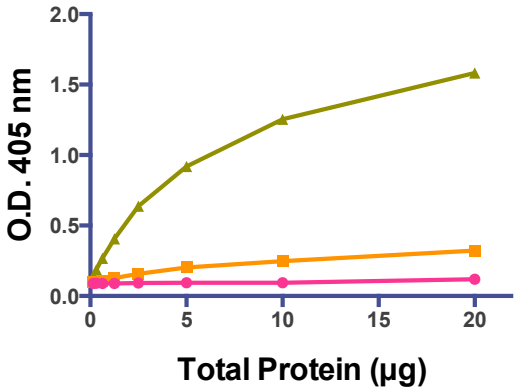
O.D. 405 nm
2.0
1.5
1.0
0.5
0.0
0
5
10
15
20
Total Protein (µg)

G.

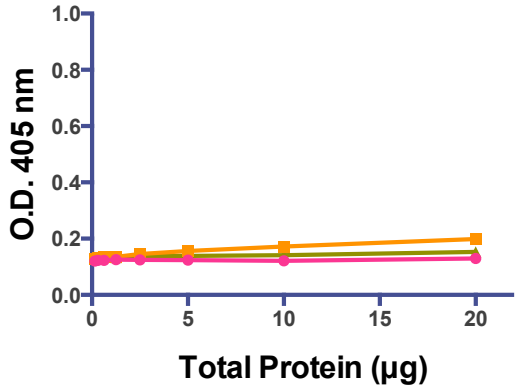
O.D. 405 nm
1.0
0.8
0.6
0.4
0.2
0.0
0
5
10
15
20
Total Protein (µg)

H.

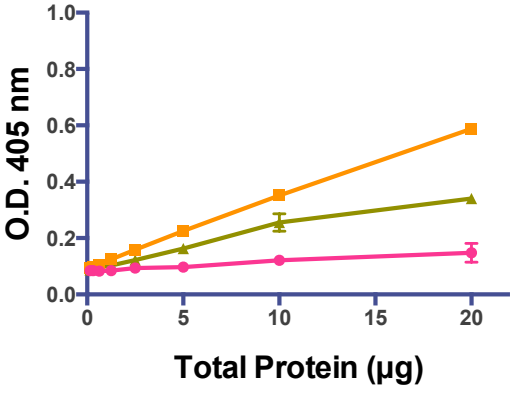
O.D. 405 nm
1.0
0.8
0.6
0.4
0.2
0.0
0
5
10
15
20
Total Protein (µg)

I.

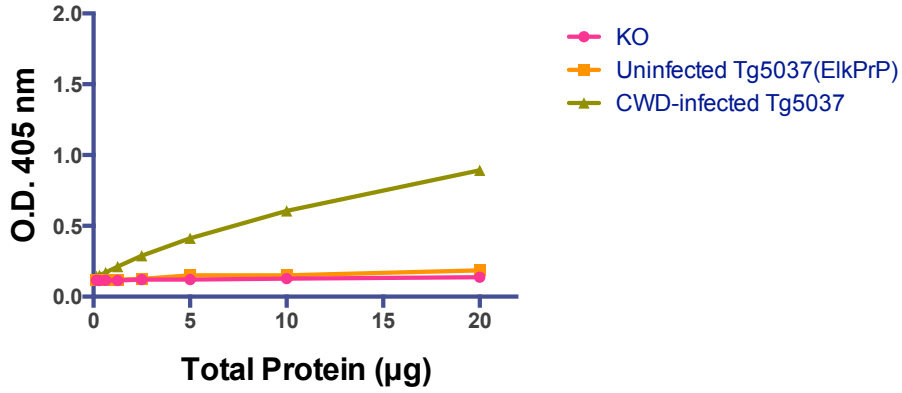
KO
Uninfected Tg5037(ElkPrP)
CWD-infected Tg5037
O.D. 405 nm
2.0
1.5
1.0
0.5
0.0
0
5
10
15
20
Total Protein (µg)

J.

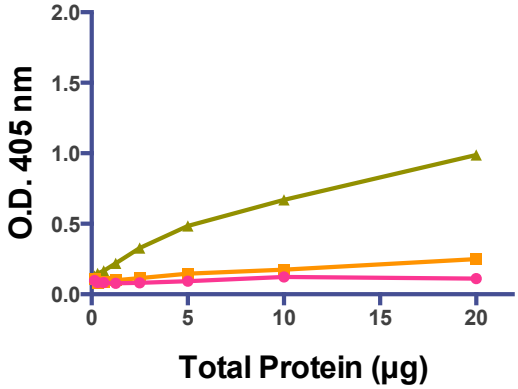
O.D. 405 nm
2.0
1.5
1.0
0.5
0.0
0
5
10
15
20
Total Protein (µg)

K.

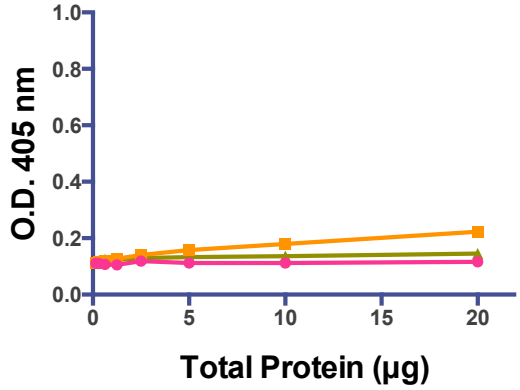
O.D. 405 nm
1.0
0.8
0.6
0.4
0.2
0.0
0
5
10
15
20
Total Protein (µg)

L.

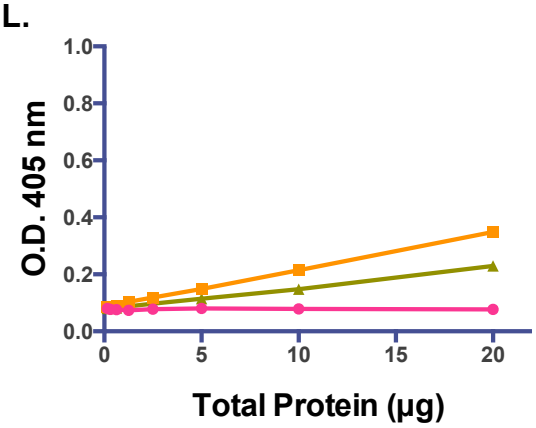
O.D. 405 nm
1.0
0.8
0.6
0.4
0.2
0.0
0
5
10
15
20
Total Protein (µg)

M.

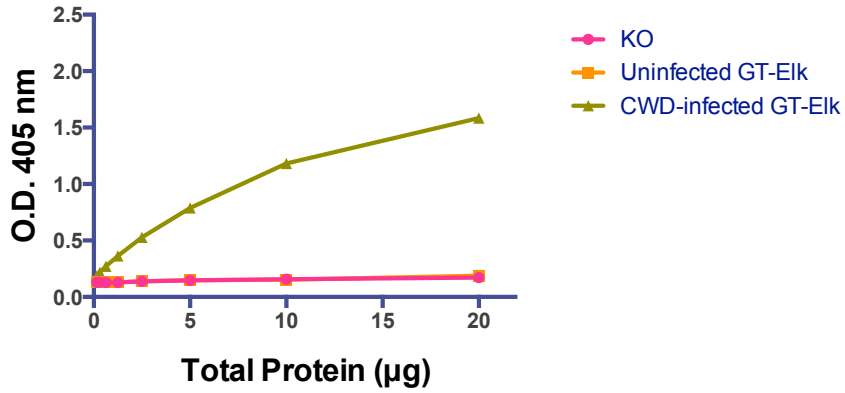
KO
Uninfected GT-Elk
CWD-infected GT-Elk
O.D. 405 nm
2.5
2.0
1.5
1.0
0.5
0.0
0
5
10
15
20
Total Protein (µg)

N.

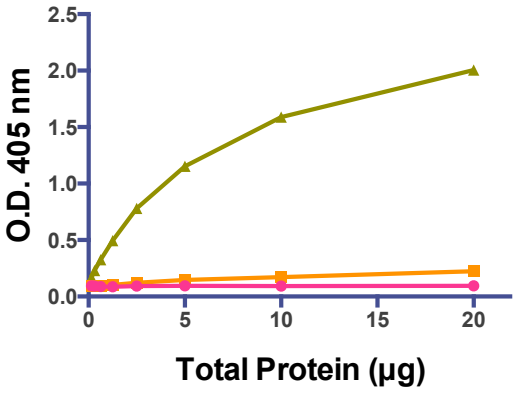
O.D. 405 nm
2.5
2.0
1.5
1.0
0.5
0.0
0
5
10
15
20
Total Protein (µg)

O.

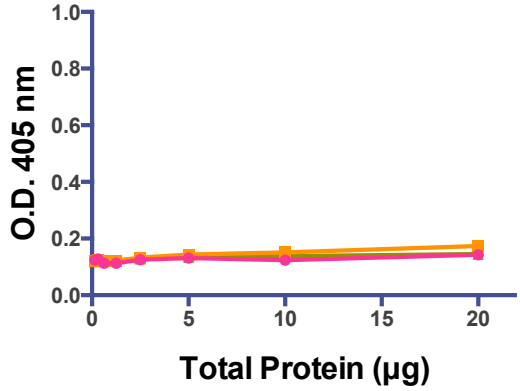
O.D. 405 nm
1.0
0.8
0.6
0.4
0.2
0.0
0
5
10
15
20
Total Protein (µg)

P.

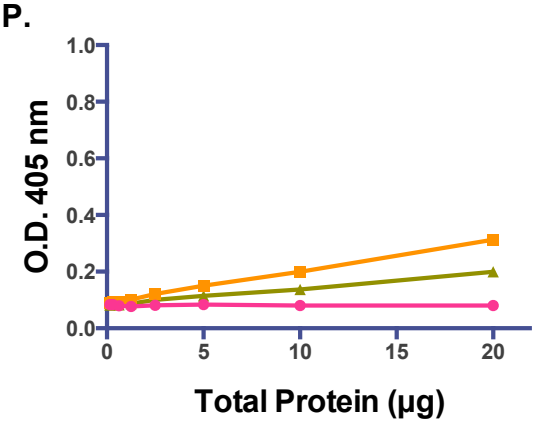
O.D. 405 nm
1.0
0.8
0.6
0.4
0.2
0.0
0
5
10
15
20
Total Protein (µg)

Q.

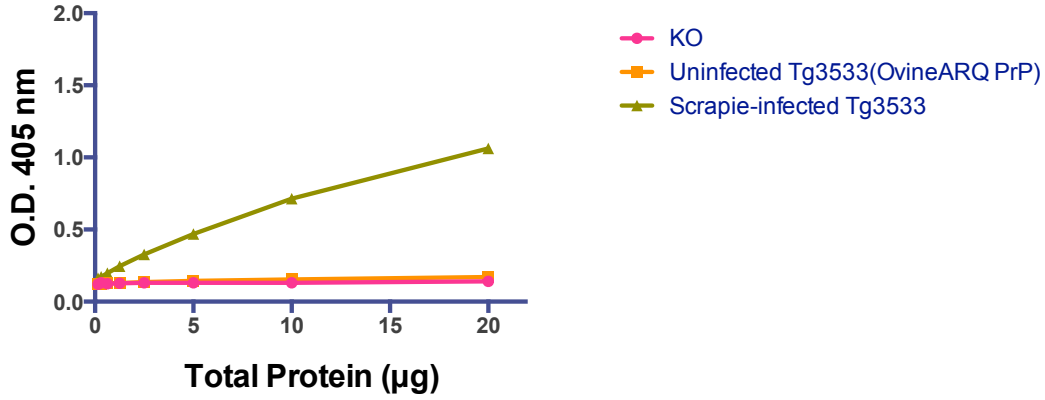
KO
Uninfected Tg3533(OvineARQ PrP)
Scrapie-infected Tg3533
O.D. 405 nm
2.0
1.5
1.0
0.5
0.0
0
5
10
15
20
Total Protein (µg)

R.

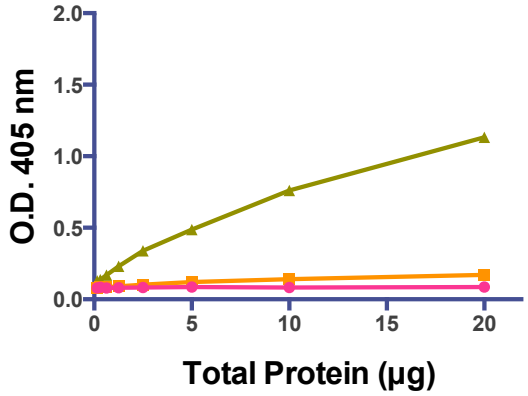
O.D. 405 nm
2.0
1.5
1.0
0.5
0.0
0
5
10
15
20
Total Protein (µg)

S.

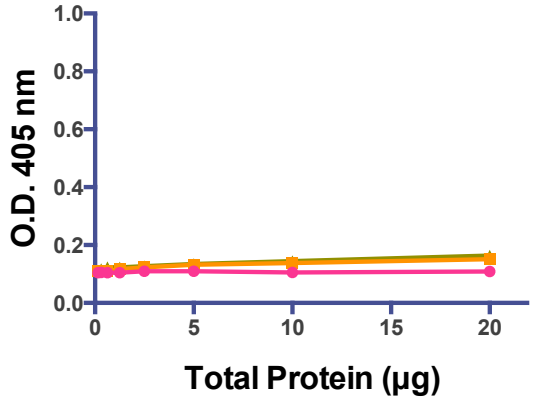
O.D. 405 nm
1.0
0.8
0.6
0.4
0.2
0.0
0
5
10
15
20
Total Protein (µg)

T.

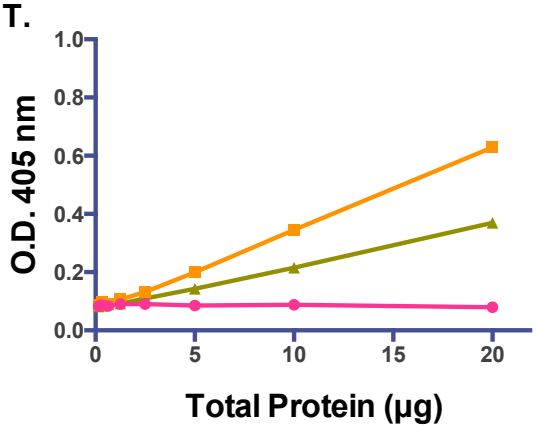
O.D. 405 nm
1.0
0.8
0.6
0.4
0.2
0.0
0
5
10
15
20
Total Protein (µg)

U.

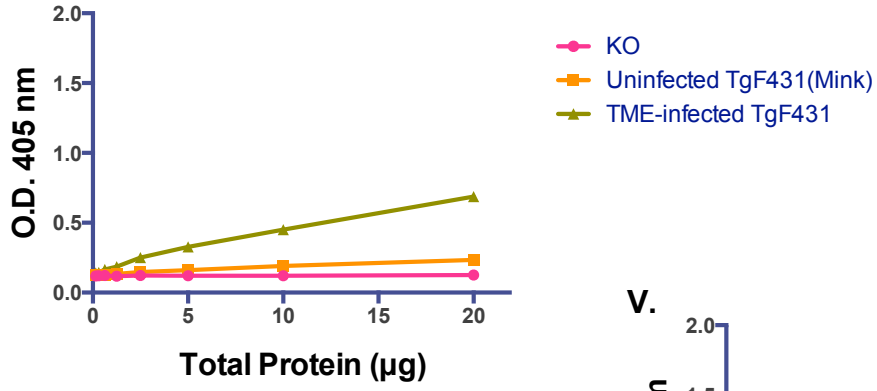
O.D. 405 nm
2.0
1.5
1.0
0.5
0.0
0
5
10
15
20
Total Protein (µg)
KO
Uninfected TgF431(Mink)
TME-infected TgF431

V.

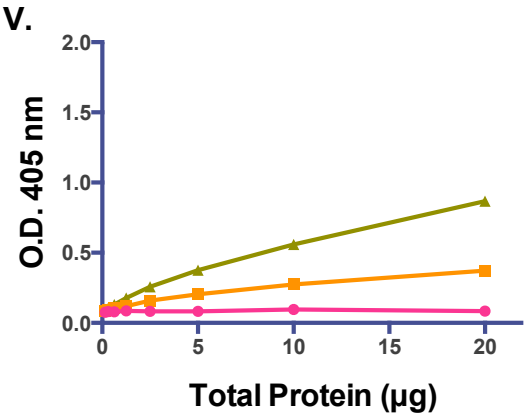
O.D. 405 nm
2.0
1.5
1.0
0.5
0.0
0
5
10
15
20
Total Protein (µg)

W.

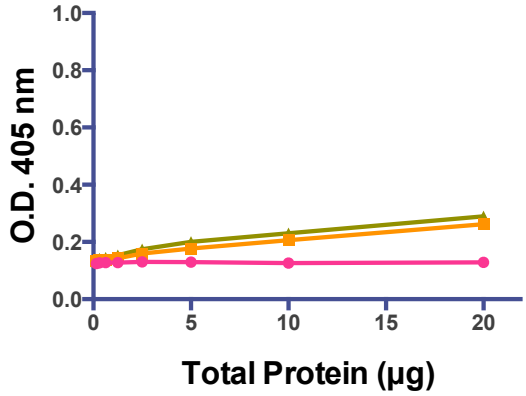
O.D. 405 nm
1.0
0.8
0.6
0.4
0.2
0.0
0
5
10
15
20
Total Protein (µg)

X.

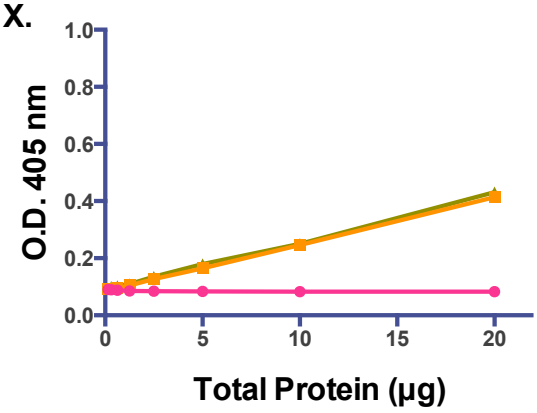
O.D. 405 nm
1.0
0.8
0.6
0.4
0.2
0.0
0
5
10
15
20
Total Protein (µg)

Y.

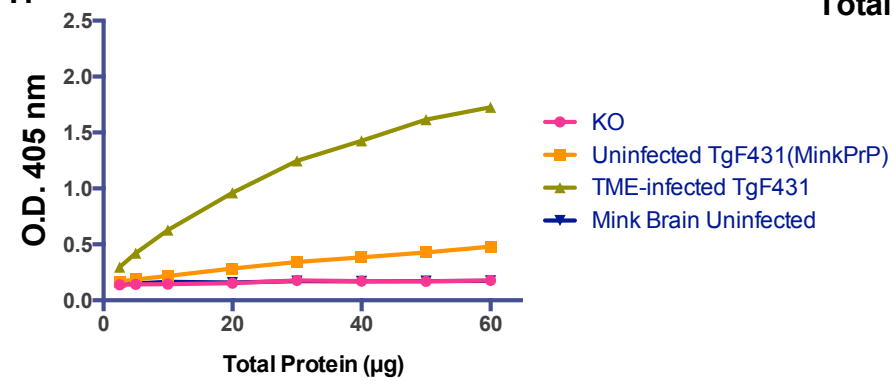
O.D. 405 nm
2.5
2.0
1.5
1.0
0.5
0.0
0
20
40
60
Total Protein (µg)
KO
Uninfected TgF431(MinkPrP)
TME-infected TgF431
Mink Brain Uninfected

Figure 3-19. Protein-dose dependent responses for PrP detections in BH samples from TSE-inoculated mouse models under different sample preparations.
RML-inoculated FVB/n BH analyte and its control samples:
(A) the 7-5 ELISA method with denaturation, (B) the D-5 ELISA method with denaturation, (C) the 7-5 ELISA method with non-denaturation, and (D) the D-5 ELISA method with non-denaturation.
CWD-inoculated Tg1536(DeerPrP) BH analyte and its control samples:
(E) the 7-5 ELISA method with denaturation, (F) the D-5 ELISA method with denaturation, (G) the 7-5 ELISA method with non-denaturation, and (H) the D-5 ELISA method with non-denaturation.
CWD-inoculated Tg5037(ElkPrP) BH analyte and its control samples:
(I) the 7-5 ELISA method with denaturation, (J) the D-5 ELISA method with denaturation, (K) the 7-5 ELISA method with non-denaturation, and (L) the D-5 ELISA method with non-denaturation.
CWD-inoculated GT(ElkPrP) BH analyte and its control samples:
(M) the 7-5 ELISA method with denaturation, (N) the D-5 ELISA method with denaturation, (O) the 7-5 ELISA method with non-denaturation, and (P) the D-5 ELISA method with non-denaturation.
Scrapie-inoculated Tg3533(OvineARQ PrP) BH analyte and its control samples: (Q) the 7-5 ELISA method with denaturation, (R) the D-5 ELISA method with denaturation, (S) the 7-5 ELISA method with non-denaturation, and (T) the D-5 ELISA method with non-denaturation.
TME-inoculated TgF431(MinkPrP) BH analyte and its control samples:
(U) the 7-5 ELISA method with denaturation, (V) the D-5 ELISA method with denaturation, (W) the 7-5 ELISA method with non-denaturation, (X) the D-5 ELISA method with non-denaturation, and (Y) the 7-5 ELISA method with denaturation including uninfected mink BH sample. (n=3 per total protein amount for each sample)

Proteinase K-dose dependent responses for PrP detections in the 7-5 ELISA and D-5 ELISA methods

Under the non-denatured condition, the D-5 ELISA method detected the decrease of PrP^{C} levels in infected materials from TSE-mouse models, compared to those uninfected mouse controls. In addition, the D-5 ELISA method measured small levels of PrP detections in uninfected materials even under 5M GdnHCL denaturation. However, it was not confirmed if the D-5 ELISA method detected only PrP^{C} molecules under non-denaturation and what PrP molecules the uninfected transgenic mice exhibited in their denatured BH samples. According to a common theory of prion propagation, abnormal PrP^{Sc} proteins behave as templates for converting normal PrP^{C} proteins into the misfolded isoform by changing their conformations. The templates guide the misfolding of more normal proteins into the pathologic PrP conformation. These newly formed PrP molecules can then go on to convert more proteins as new templates. These consequences trigger a chain reaction that produces large amounts of the PrP^{Sc} isoform. In addition, PrP molecules with conformational alterations acquire resistances to protease, denaturation by chemical and physical agents, radiation, and others. Thus, the decreased PrP^{C} levels in TSE-infected animals could be associated with the structural conversions of normal PrP^{C} to misfolded PrP^{Sc} forms. These conversions would reduce total amounts of PrP^{C} molecules, compared to uninfected mice. In addition, the D-5 ELISA method might indicate that the detected PrP level in the denatured BH samples from uninfected transgenic mice reflects the tolerance of the PrP structure against 5M GdnHCL. Possibly, detected PrP^{C} molecules have alternative forms of the native PrP^{C} structure, as spontaneously generated in transgenic mice.

To understand the existing PrP molecules that the D-5 ELISA method measured in the denatured BH samples from uninfected transgenic mice, the D-5 ELISA method was applied to test both denatured and non-denatured BH samples of a hemizygous Tg4112 mouse breed line with murine PrP^C overexpressions: 2-4 folds higher than a wild-type FVB/n mouse. The PrP levels that the 7-5 ELISA and D-5 ELISA methods detected in the non-denatured BH samples could be the same types of the existing PrP molecules in the denatured samples the D-5 detected above. Other testing BH samples included PrP-KO, uninfected FVB/n and RML-inoculated FVB/n mice. The final amount of total protein was 20μg per well (n=3 as technical replication) for each mouse. Prior to these D-5 ELISA experiments, a working prediction was that the uninfected Tg4112 mouse BH sample with the same species of PrP expressions would not exhibit detectable PrP levels under denatured and non-denatured conditions, as similar to the observations in uninfected wild-type mice. However, the Tg4112 mouse BH sample showed much higher detections of PrP levels in both denatured and non-denatured procedures (Figures 3-20.A and B). Under the denatured condition, the O.D. value of the uninfected Tg4112 mouse was closely high to that of the RML-infected murine material. Hence, this result indicated that the Tg4112 mouse naturally generated resistant PrP molecules to the high concentration of GdnHCL denaturation. In contrast, both uninfected FVB/n and Tg4112 mice showed higher PrP levels than the infected mouse under the non-denaturation procedure; the Tg4112 mouse exhibited an elevated O.D. value in comparison to the uninfected FVB/n mouse. Thus, these unpredicted outcomes suggested that the tested transgenic mouse breed lines spontaneously

generate both native and unknown PrP^C molecules because of the tolerance to denaturation.

Uninfected transgenic mouse breed lines with PrP overexpressions spontaneously presented developments and progressions of clinical neurological signs and neuromuscular degenerations.[34] In fact, the laboratory database has records of some spontaneous disease cases in the in-house uninfected transgenic mouse breed lines (i.e. Tg4112). These evidences suggested that PrP or PrP^C overexpressions are irregular conditions that might trigger dysfunctions in the nervous system. Thus, the PrP overproduction and/or accumulation must be pathologic or toxic conditions to mice, but not dependent on either PrP^C or PrP^{Sc} isoform to cause functional impairments. Furthermore, intermediate conformers between PrP^C and PrP^{Sc} isoforms have been found in uninfected brains and cultured cells.[35-38] These newly PrP conformers were spontaneously generated with the PrP^{Sc}-like characteristics of insoluble aggregation and resistance to proteolysis, which the N-linked glycosylation status of the PrP conformation could be involved in these unusual PrP generations. Therefore, the GdnHCL-resistant PrP conformers in the uninfected Tg4112 mouse might result from irregularly alterations in protein foldings or syntheses during PrP overproductions in natural conditions.

For further analyses for the generation of non-native PrP conformers in uninfected Tg4112 mice, proteinase K (PK) was applied to sample preparations for ELISA experiments. This approach would evaluate the presence of PK-resistant PrP molecules in uninfected Tg4112 mice. For this experimental aim, the D-5 ELISA and 7-5 ELISA methods examined the same tested BH samples above (PrP-KO, uninfected

FVB/n, uninfected Tg4112, and RML-infected FVB/n mice) under both denatured and non-denatured conditions with or without the PK digestion. Since the established Sandwich ELISA protocol did not include the PK treatment, the following sample preparations were applied.

1) Low dose of PK treatment:

Denaturation: BH samples were treated with 2.5μg/ml PK concentration in PBS with 1% TX100 and 0.1% Sarkosyl (denoted as PK+), whereas PBS with only 1% TX100 was added into non-PK treating samples (denoted as PK-). These samples were incubated at 37°C for one hour with 1,000rpm agitation, followed by an addition of PMSF (2mM) for PK+ samples and PBS for PK- samples. After the incubation on ice for 10 minutes, all samples were denatured with 5M GdnHCL, and then 10 times diluted by PBS with 1% BSA and protease inhibitor to be final protein concentration 200μg/ml under the optimized ELISA protocol.

Non-denaturation: PK+ BH samples were treated as the processes above until the PMSF step. Subsequently, the PK+ samples were diluted by PBS with 1% BSA and protease inhibitor to be final protein concentration 200μg/ml. PK- samples were prepared under the optimized protocol, and diluted by the PBS solution to be 200μg/ml. 100μl of each prepared sample from these procedures was coated onto respective wells (n=3 as a technical replication: each well contained total protein 20μg of a prepared sample.) on ELISA plates pre-coated with either D18 or PRC7 capture antibody. All of following procedures were completed under the optimized ELISA protocol.

For the lower PK dose experiment, the D-5 ELISA and 7-5 ELISA methods measured the existence of PrP molecules in the uninfected FVB/n and Tg4112 BH

samples under the denatured and non-denatured conditions, compared to the non-PK treated results (Figures 15-C to 15-J). In addition, the 7-5 ELISA method detected high PrP levels of uninfected Tg4112 BH samples under denatured and non-denatured conditions with and without the PK treatment (Figure 15-G to 15-J). These results indicated that Tg4112 mice generated under-glycosylated PrP forms with some resistances to high GdnHCL and low PK concentrations. Therefore, the detected PrP^{C} molecule might have the PK tolerance to 2.5μg/ml concentration that was not effective for protein digestions. Hence, these consequences suggested that the generation of under-glycosylated PrP forms concurrently occurred with the production of non-native PrP conformers in the Tg4112 mouse. Since the loss of glycans is involved in causing fatal diseases (i.e. congenital defect of glycan) and sensitizing cells to apoptosis, the overproduction and accumulation of under-glycosylated PrP forms can be factors affecting health conditions, especially for maintaining normal functions in nervous systems that contain abundances of PrP^{C} levels.

2) Higher dose of PK treatment:

Denaturation: Instead of the 2.5μg/ml PK and 0.1% Sodium-lauroyl sarkosinate (Sarkosyl) concentrations above, PBS with 50μg/ml PK concentration in 2% Sarkosyl was applied to PK+ BH samples. Sarkosyl is a detergent commonly used in the TSE research for purifying protease-resistant PrP molecules from TSE-infected materials.[39] In the WB protocol of this dissertation, 2% of this detergent was used in sample preparations with the PK reagent. However, Sarkosyl inhibits interactions of PrP^{C} and PrP^{Sc} isoforms by polymerizing synthetic peptide fragments of PrP molecules.[40] In contrast, PK- BH samples were prepared with only 1% TX100-containing PBS. After a

sample incubation for one hour with 1,000rpm agitation at 37°C, PMSF (2mM) was added into PK+ samples, whereas only PBS was applied for PK- samples. Following sample incubation on ice for 10 minutes, denaturation with 5M GdnHCL was performed for these samples. Denatured samples were ten-times diluted by PBS with 1% BSA and protease inhibitor to be a final protein concentration of 200μg/ml under the optimized ELISA protocol.

Non-denaturation: PK and PMSF treatments were performed for PK+ samples, which were then diluted with PBS containing 1% BSA and protease inhibitor to be 200μg/ml. PK- samples were diluted with the same PBS solution to be the 200μg/ml final protein concentration.

As described in the lower PK treatment above, sample coating and subsequent procedures were performed under the optimized ELISA protocol. For the denatured sample condition in the D-5 ELISA experiment, the higher PK concentration eliminated PrP detections in uninfected FVB/n and Tg4112 mouse BH samples, whereas the RML-infected FVB/n BH sample was resistant to this PK dose (Figures 3-20.K and L). Thus, the detected PrP molecules in these uninfected mice were possibly neither PrP^{Sc} nor the intermediate PrP conformers mentioned above, but still tolerant to 5M GdnHCL. For the non-denatured condition, in contrast, the D-5 ELISA method could not detect any PrP levels in all tested BH samples with the PK treatment (Figures 3-20.M and N). Hence, the D-5 ELISA method detected PK-sensitive PrP molecules under the non-denaturation, which must be only PrP^{C} isoforms, especially for the uninfected samples. Possibly, the limited response of the lower PK dose was associated with the structural stability of the abundant PrP^{C} isoforms with diglycosylations (Figures 3-20.C to G).

Intriguingly, the 7-5 ELISA method showed the reduction of an O.D. value in the denatured BH sample of RML-infected FVB/n mouse with the high PK dose (Figures 3-20.O and P). This decreased O.D. value indicated the instability of under-glycosylated PrP^{Sc} forms during the PK treatment. These PrP^{Sc} forms might be less resistant to the PK digestion, compared to diglycosyl PrP^{Sc} agents. In fact, the denatured RML-infected BH sample did not affect PrP detections with the PK treatment by the D-5 ELISA method that detected all four glycosyl PrP forms (Figures 3-20.K and L). Therefore, the difference of PK-treated PrP levels between these two ELISA methods indicated the existence of PK-sensitive PrP^{Sc} agents, known as equivalently infectious to PK-resistant PrP^{Sc} agents in the same TSE strain.[41-43]

In addition, the 7-5 ELISA method detected the under-glycosylated PrP forms with GdnHCL tolerance in the Tg4112 BH sample without PK treatment, but the higher PK dose eliminated the PrP detection (Figures 3-20.O to R). These outcomes suggested that under-glycosylated PrP forms could be predisposed to lose these conformational stabilities against the increasing PK doses. In addition, the Tg4112 mouse generated large amounts of under-glycosylated PrP forms with GdnHCL tolerance, which exhibited a similar O.D. value to the TSE-infected material (Figure 3-20.O). Thus, these PrP forms might have generated the PrP oligomerization or aggregation for maintaining these conformational stabilities or tolerances to influential factors. It is curious that transgenic mouse breed lines with PrP overexpressions have this phenomenon, rather than misfolding of the PrP^{C} structure. These protein-complex formations might preserve PrP molecules from direct exposures to denaturants or other chemicals. Thus, the 7-5 ELISA method detected under-glycosylated forms of the

preserved PrP molecules in the formations. In addition, uninfected wild-type mouse breed lines (FVB/n and C57BL6: Figures 3-19.A and C) and several uninfected transgenic mice exhibited GdnHCL-tolerant PrP^{C} molecules. If these murine PrP^{C} molecules have some conformational modifications from the native PrP^{C} structures, these altered agents could have acquired some resistance to denaturation, similar to PrP^{Sc} isoforms. Thus, the denaturation-tolerant PrP^{C} forms might interact with the PrP^{Sc} templates for pathogen replications and propagations. Eventually, these interactions would develop more tolerance to exposures from local and systemic environments, leading to continuous productions of abnormal PrP agents.

A.

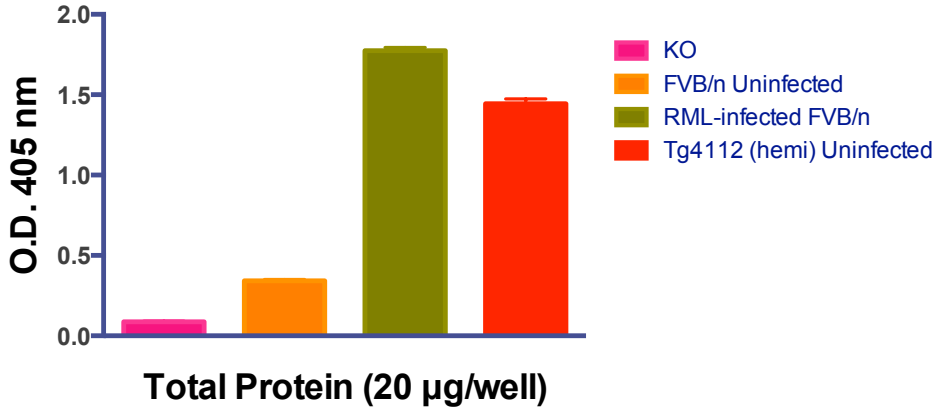
2.0
1.5
1.0
0.5
0.0
O.D. 405 nm
Total Protein (20 µg/well)
KO
FVB/n Uninfected
RML-infected FVB/n
Tg4112 (hemi) Uninfected

B.

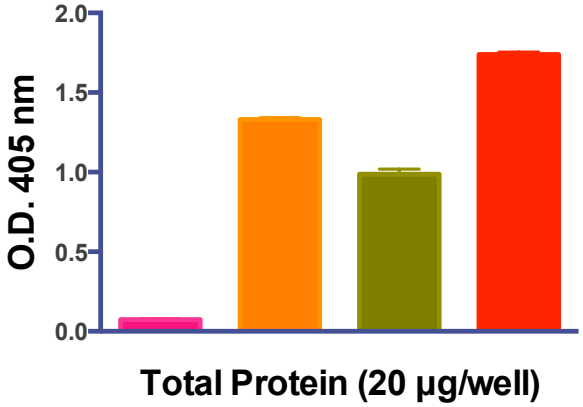
2.0
1.5
1.0
0.5
0.0
O.D. 405 nm
Total Protein (20 µg/well)

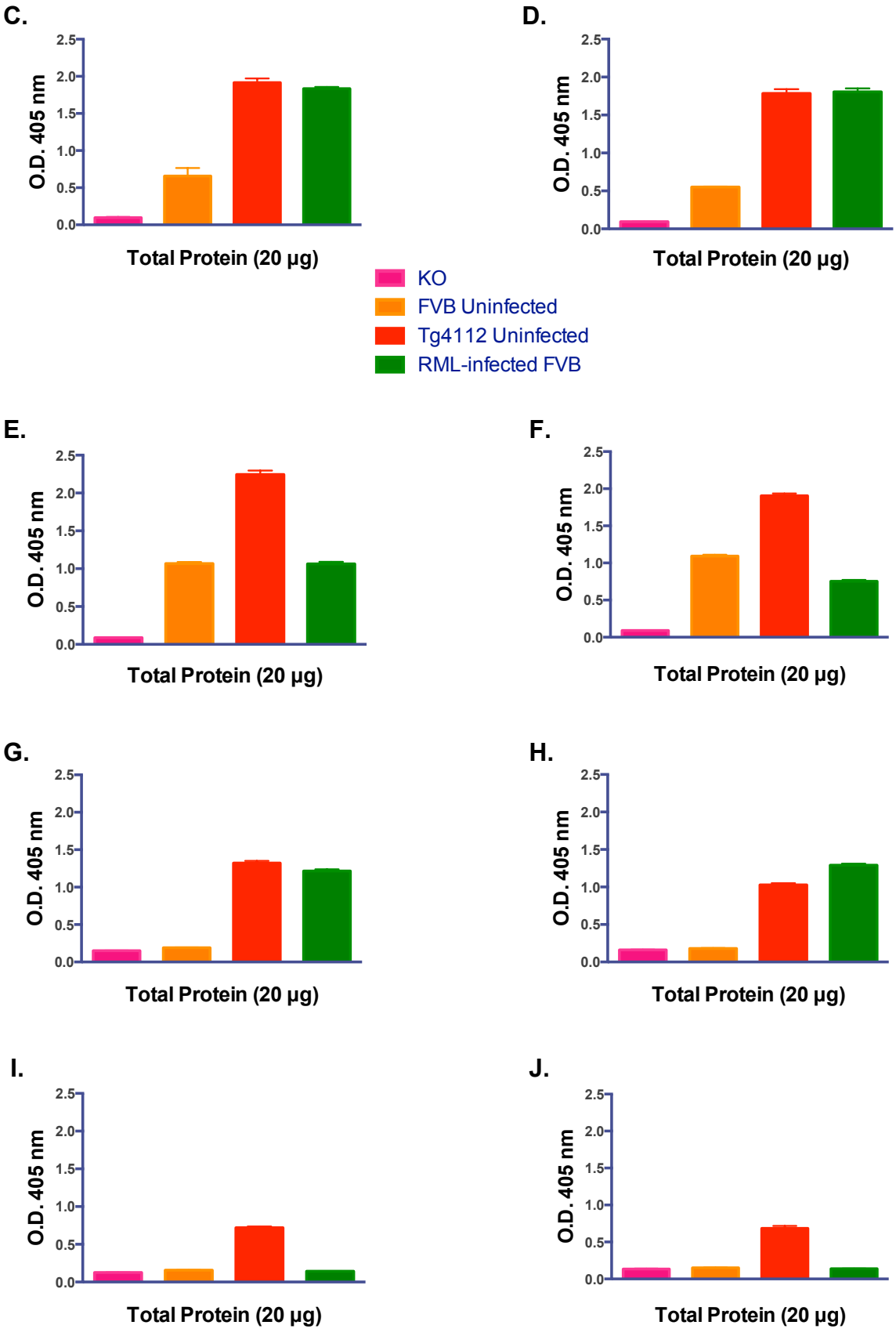
C.
D.
O.D. 405 nm
2.5
2.0
1.5
1.0
0.5
0.0
Total Protein (20 µg)
KO
FVB Uninfected
Tg4112 Uninfected
RML-infected FVB
E.
F.
G.
H.
I.
J.

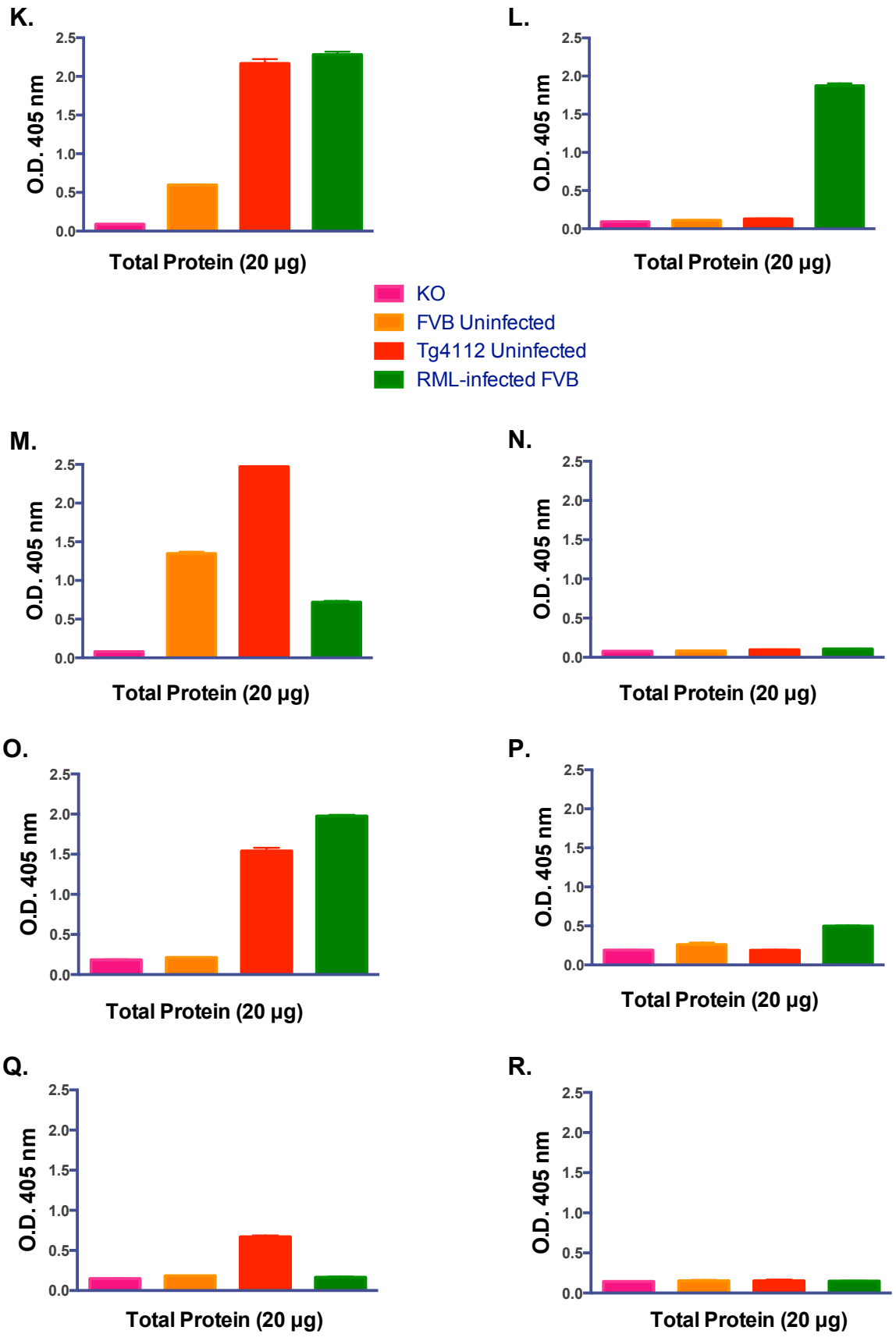
K.
L.
O.D. 405 nm
2.5
2.0
1.5
1.0
0.5
0.0
Total Protein (20 µg)
KO
FVB Uninfected
Tg4112 Uninfected
RML-infected FVB
M.
N.
O.
P.
Q.
R.

Figure 3-20. PrP detections in BH samples from a hemizygous Tg4112 mouse with murine PrP^C overexpressions. The **D-5 ELISA method,** testing with (A) denatured and (B) non-denatured mouse BH samples.
The **D-5 ELISA method**, evaluating the BH samples with (C) non-PK but denaturation, (D) low PK with denaturation, (E) non-PK and non-denaturation, and (F) low PK with non-denaturation. The **7-5 ELISA method**, testing with (G) non-PK but denaturation, (H) low PK with denaturation, (I) non-PK and non-denaturation, and (J) low PK with non-denaturation.
The **D-5 ELISA method**, testing with (K) non-PK but denaturation, (L) high PK with denaturation, (M) non-PK and non-denaturation, and (N) high PK with non-denaturation. The **7-5 ELISA method**, evaluating (O) non-PK but denaturation, (P) high PK with denaturation, (Q) non-PK and non-denaturation, and (R) high PK with non-denaturation. (n=3, each sample with 20μg total protein per well)

PK digestions for sub-clinical cases in TSE-mouse models

According to the laboratory database, the endpoint experiment of the elk CWD brain isolate Bala05-0308 infection was determined in Tg5037 (ElkPrP) mice for the estimation of prion titer. For this purpose, the CWD isolate was prepared from 10^{-1} to 10^{-10} dilutions in 10-fold increments. These prepared inocula were injected intracerebrally into a Tg5037 mouse group (n=8) at each dilution point. In this inoculation study, the endpoint of the TSE infection was examined as the dilution point, which half of the inoculated mice in a group developed clinical signs of the disease in relation to the inoculum. The RA-150 study was one of these endpoint experiments where the 10^{-4} diluted CWD isolate was inoculated into Tg5037 (ElkPrP) mice. As an outcome, three mice developed clinical signs but other three mice did not show (2 of the 8 mice were dead). Tissues from these disease mice (animal numbers b581, b582, b586) with clinical signs were collected at terminal disease stages. The 7-5 ELISA method examined these brains as a biological replication (n=3) in the study section with the Figure 3-2 (Figure 3-2.B). Three other mice without clinical signs were euthanized at 16 months following the inoculations. To determine if modifications of PrP^{C} and PrP^{Sc} levels were involved in the disease development, the D-5 ELISA and 7-5 ELISA methods evaluated these mouse brains with subclinical conditions. In addition, an efficacy of PK digestions was determined in these CWD-inoculated Tg5037 mouse BH samples by these Sandwich ELISA methods, followed by the same sample preparations and experimental procedures from the higher PK-dose study as described above. The application of PK digestions would identify the existence of PK-resistant PrP agents in these sub-clinical conditions of CWD-inoculated mice. For these ELISA experiments,

two (animal numbers b583 and b584) of these subclinical mice were tested with and without denaturation and PK digestion. Also, this experiment included mouse BH samples from PrP-KO, uninfected Tg5037, and the CWD-inoculated Tg5037 at terminally disease condition in RA-150 study (animal number b582). The D-5 ELISA and 7-5 ELISA methods analyzed these prepared samples under the optimized protocol: respective wells for each sample contains 20μg of total protein per well on ELISA plates as described above.

Under the denaturation without PK digestions, the D-5 ELISA and 7-5 ELISA methods detected a high PrP level in the BH sample from the CWD-infected mouse with the disease condition (Figures 3-20.A and C). Using the PK reagent, these ELISA approaches only detected a PK-resistant PrP level in the denatured BH sample from the terminal-stage mouse (Figures 3-20.B and D). In contrast, O.D. values of the sub-clinical mice were similar to the uninfected Tg5037 mice with and without the PK treatment (Figures 3-20.A and D). These results indicated that the subclinical mice did not have prion replication even inoculated with the CWD isolate.

In contrast, the subclinical mice exhibited increased PrP^C levels in their BH samples under the non-denatured condition (no addition of Tris buffer or incubation with heating) in comparison to the uninfected sample, while the CWD-positive sample decreased (Figures 3-20.E and G). With the PK treatment, all tested samples lost PrP detections under the non-denatured condition (Figures 3-20.E to H). Therefore, these ELISA results suggested that the modification of PrP^C levels were involved in the disease development in TSE-affected animals. However, it is unknown if the increase of PrP^C levels inhibited replications of the CWD inoculum and disease progressions in the

TSE-inoculated mice, which eventually maintained subclinical conditions. Since one of PrP^C functions is neuroprotection, the increased PrP^C levels could participate in preservative mechanisms for brains in the CWD inoculated sub-clinical mice against the persistence of the infection and disease development.

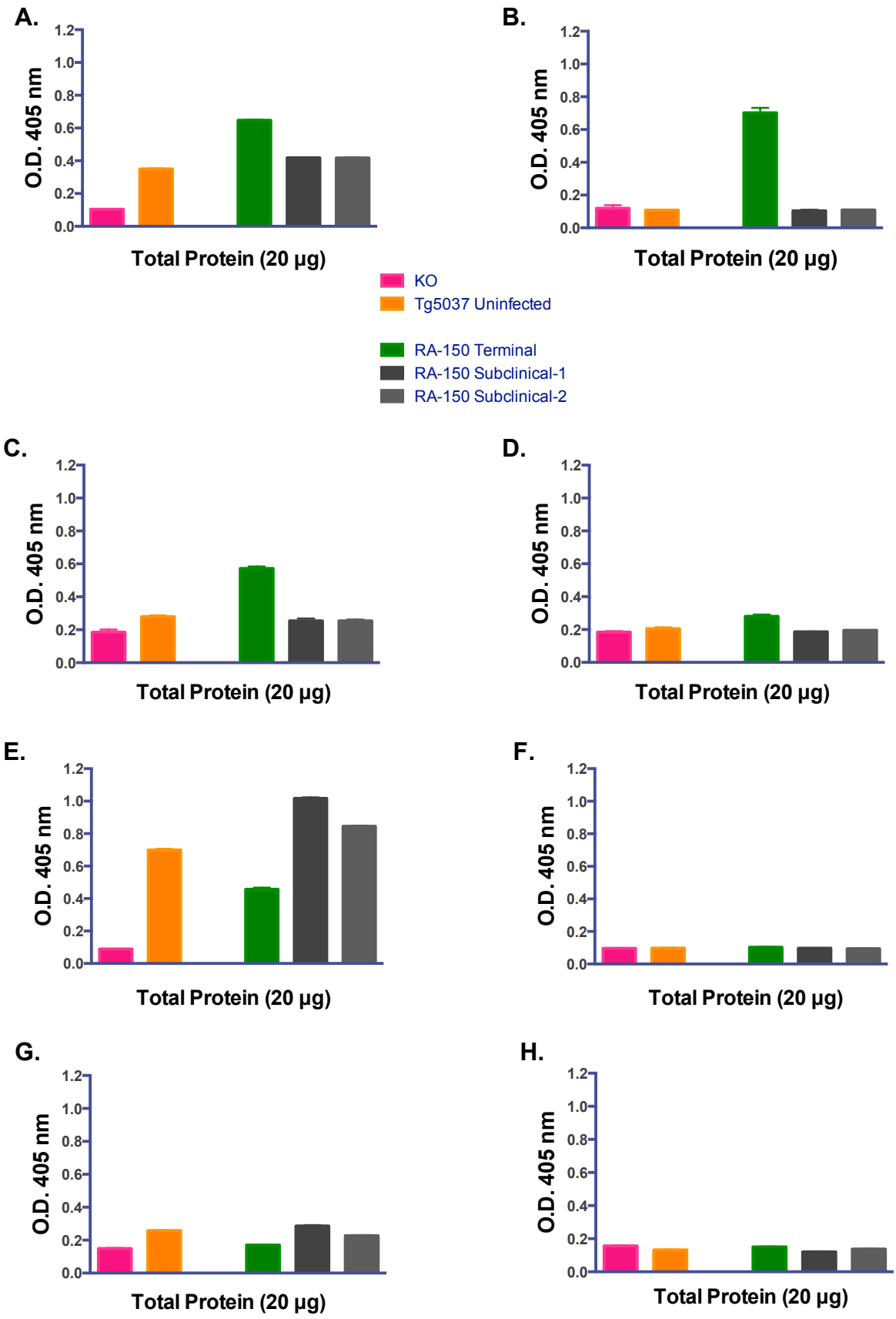
A.
B.
C.
D.
E.
F.
G.
H.
O.D. 405 nm
1.2
1.0
0.8
0.6
0.4
0.2
0.0
Total Protein (20 µg)
KO
Tg5037 Uninfected
RA-150 Terminal
RA-150 Subclinical-1
RA-150 Subclinical-2

Figure 3-21. PrP detections in BH samples from CWD-inoculated Tg5037(ElkPrP) mice with subclinical conditions.
The D-5 ELISA method with (A) non-PK but denaturation, (B) high PK with denaturation, (C) non-PK and non-denaturation, and (D) high PK with non-denaturation. The 7-5 ELISA method with (E) non-PK but denaturation, (F) high PK with denaturation, (G) non-PK and non-denaturation, and (H) high PK with non-denaturation. (n=3, each sample with 20μg total protein per well)

Range of PK-dose dependent responses

To confirm capacities of the PrP^{C} tolerance and the PrP^{Sc} resistance against PK digestions, the D-5 ELISA and 7-5 ELISA methods evaluated different doses of PK responses. Since the tested mouse BH samples from the RML bioassays above were limited, this ELISA experiment replaced those analyte to test another TSE-infected BH sample from the inoculation study TS-06 (RML-inoculations into FVB/n mice; animal number c280). Using BH samples from PrP-KO, uninfected FVB/n and RML-inoculated FVB/n mice (n=1 for each mouse type), various PK concentrations (0, 0.5, 1, 5, 10, 20, 50 and 100 μg/ml) were incubated at 37°C for one hour, followed by 2mM PMSF incubation on ice for 10 minutes. As described in the higher PK treatment study, the same procedures and preparations were performed in these ELISA experiments. Note: Sarkosyl was included for sample preparations in the study section with the Figure 3-15. Based on preliminary results, however, the tested PK concentrations showed different PrP detections under 0.1% or 2% Sarkosyl. To evaluate a PK efficacy properly, the following ELISA experiment excluded Sarkosyl in the sample preparation. Also, each prepared sample was coated into wells on ELISA plates pre-coated with the D18 or PRC7 capture antibody (well number = 4 for each as quadruplication).

Intriguingly, both the D-5 ELISA and 7-5 ELISA methods measured the peak of O.D. values at 10μg/ml PK treatment in the denatured RML-infected BH sample (Figures 3-22.A and B). It was unknown from this experiment how the 10μg/ml PK concentration enhanced PrP detections in TSE-infected material. In addition, the non-PK treated RML-infected BH sample had equivalent PrP detections to 50μg/ml PK treatment. These observations indicated that the difference between 0 and 10μg/ml

and/or between 10 and 50μg/ml PK treatment could reflect the amounts of PK-sensitive PrP^{Sc} agents in this infected BH sample. In contrast to the higher PK dose (50μg/ml) study by the 7-5 ELISA methods in the study section with the Figure 3-20 (Figure 3-20.P), the denatured RML-infected mouse BH sample did not exhibit much reductions of PrP detections at 50 and 100μg/ml PK concentrations in this study section of the D-5 ELISA and 7-5 ELISA experiments (Figures 3-22.A and B). As noticed above, this experiment tested a new RML-inoculated FVB/n mouse BH sample from a different inoculation experiment, because of limited BH amounts from RML-infected FVB/n mice in the RA-150 study. Thus, these outcomes possibly indicated that the under-glycosylated PrP generation might be dependent on animals, disease conditions and progressions, or inoculated TSE isolates. In addition, this experiment did not include Sarkosyl for the reason mentioned above. Therefore, these two factors were potentials for higher PrP detections under the PK digestion and denaturation in this experiment.

For the non-denatured condition, the D-5 ELISA and 7-5 ELISA method measured the complete elimination of PrP detections in both uninfected and infected samples at 10μg/ml and higher concentrations of PK treatments. These results indicated that detected PrP levels under the non-denatured condition were PrP^{C} levels (Figures 3-22.C to F). Moreover, the outcomes suggested that the maximum tolerant capacity of PrP^{C} molecules against PK digestion could be estimated as between 5-10μg/ml concentrations (Figure 3-22.E and F). Although the established ELISA protocols do not require the PK reagent for PrP detections in TSE-infected materials, the 10μg/ml PK treatment would enhance higher PrP^{Sc} detections in denatured BH samples for the ELISA methods in this dissertation.

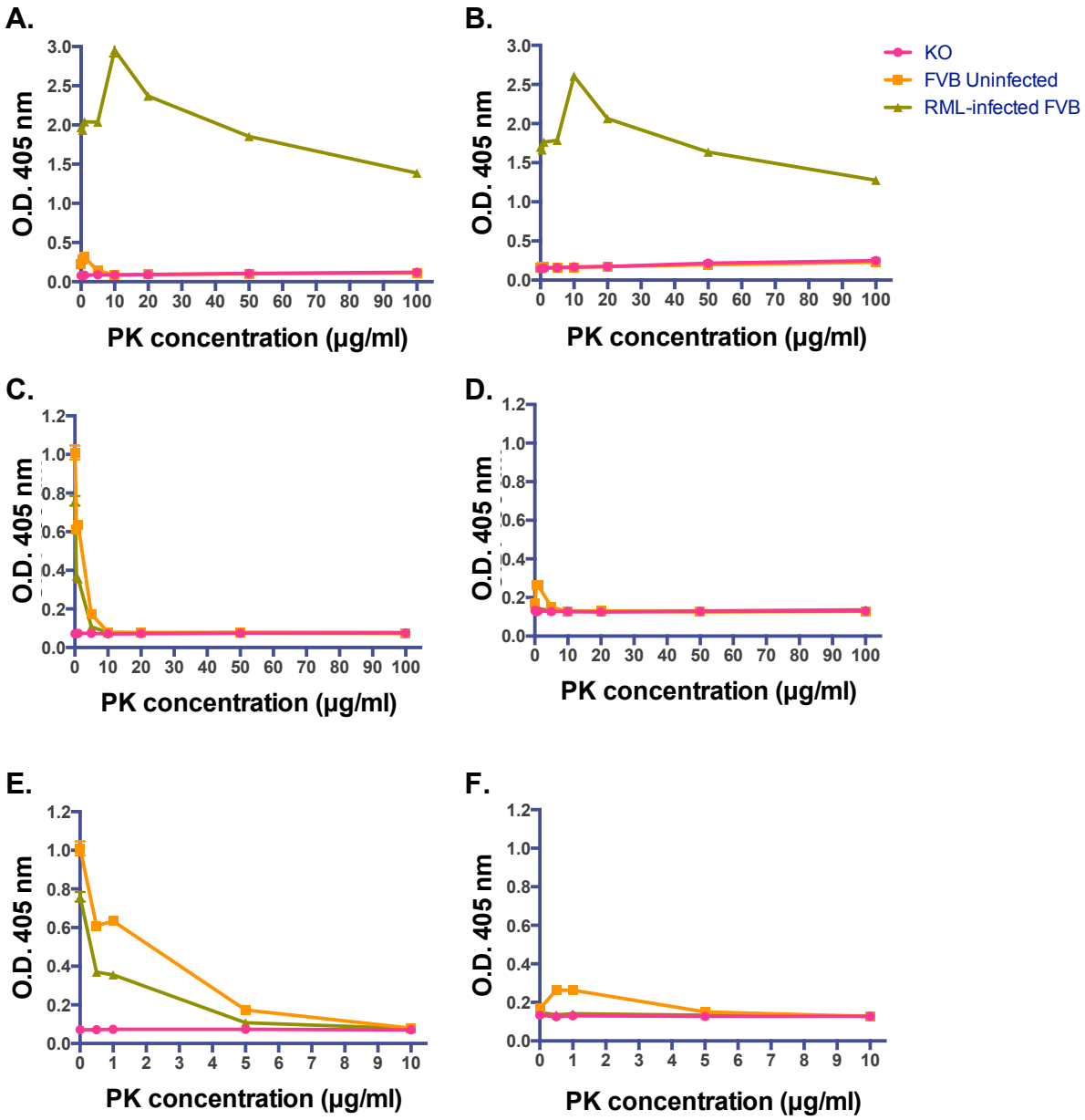

Figure 3-22. PK-dose dependences for PrP detections in the D-5 and 7-5 ELISA methods. Using a RML-inoculated FVB/n BH analyte and its control samples, PK with denaturation in (A) the D-5 ELISA method and (B) the 7-5 ELISA method; PK with non-denaturation in (C) the D-5 ELISA method and (D) the 7-5 ELISA method. Detected O.D values at lower PK concentrations in in (E) the D-5 ELISA method and (F) the 7-5 ELISA method. (n=3, each sample with 20µg total protein per well)

Supplemental application of chemicals that enhance PrP detection in Sandwich ELISA applications

Based on the finding in the study section with the Figure 3-20 that the 50μg/ml PK concentration reduced the PrP detection in the RML-infected mouse BH sample (Figure 3-20.P), the previous 7-5 ELISA experiment for its protocol optimizations was reviewed. For enhancing PrP detections by the 7-5 ELISA method, different reagents were tested to select effective detergents. Currently, Triton X-100 (TX100) is used in sample preparations for the 7-5 ELISA protocol. In addition, Sarkosyl is an effective reagent in WB for CWD-inoculated transgenic mouse BH samples. However, this reagent was influential for PrP detections in RML-inoculated murine BH samples in Sandwich ELISA methods. Therefore, the 7-5 ELISA method examined the efficacy of Sarkosyl with CWD-inoculated transgenic mouse BH samples. This experiment compared with TX100, Sarkosyl, and the mixture (TX100 and Sarkosyl) for sample preparations.

Here, it is important to note that the following ELISA procedures were slightly different from the current 7-5 ELISA protocol. Tested mouse BH samples included from PrP-KO, uninfected Tg5037 (ElkPrP), CWD (Bala05-0308 elk brain)-inoculated Tg5037 (inoculation experiment RA-150; animal number b582), uninfected Tg1563 (DeerPrP), and CWD (Bala05-0308)-inoculated Tg1536 (inoculation experiment RA-154; animal number B694): one mouse BH sample per each category (n=1). Initially, these BH samples were diluted by PBS with either 0.5% TX100, 0.4% Sarcosyl, or both. After the incubation for 75 minutes at 37°C, these detergent-treated samples were denatured with 4M GdnHCL for 15 minutes at 37°C. After 10-fold dilutions with 1% BSA-containing

PBS, these diluted samples was 300μg/ml protein concentration, and then 100μl of each prepared sample was coated into wells (well number = 2 as duplication; total protein 30μg per well). Subsequent procedures were performed under the current 7-5 ELISA protocol. Intriguingly, the use of 0.4% Sarkosyl reduced the O.D. value of the PrP detection in the CWD-inoculated Tg5037 (ElkPrP) mouse BH sample, compared to the same BH sample treated with TX100 (Figure 3-23.A).

This decreased PrP level was also similar O.D. values to the uninfected controls. These observations corresponded to the result from the RML-inoculated FVB/n mouse BH sample in the study section of the Figure 3-20, which was treated by PBS with 50μg/ml PK concentration and 2% Sarkosyl (Figure 3-20.P). Nevertheless, the D-5 ELISA and 7-5 ELISA methods for the PK-dose dependence showed significant O.D. values of PrP detections in the denatured RML-infected material with 50μg/ml or higher PK concentrations when Sarkosyl was excluded (Figures 3-22.A and B). These findings suggested that some TSE strains or animals might present dose-dependent sensitivities to Sarkosyl in Sandwich ELISA experiments. Indeed, the CWD-infected Tg5037 mouse BH sample reduced PrP detections with Sarkosyl treatment, compared to the infected Tg1536 (DeerPrP) mouse with the same inoculum (Figure 3-23.A). As described in the study section of the Figure 3-5, deer and elk PrP structures have one amino acid difference at the residue 226: deer has glutamine (abbreviated as Gln or Q), while elk has glutamic acid (abbreviated as Glu or E). In the globular domain of the PrP^C structure, this amino acid residue 226 exists in α-helix 3, and consists of the β2-α2 loop. The interaction between the α-helix 3 and the β2-α2 loop is influential for structural arrangements in the globular domain. These conformational influences in the PrP

tertiary structure have roles in the CWD prion replication and pathogenesis.[22] Since the CWD inoculum Bala05-0308 was originally isolated from elk, its interspecies transmission might have altered PrP^{Sc} structures for adapting in the new host Tg1536 (DeerPrP) mice through the interaction with deer PrP molecules and the further PrP replications. Therefore, this conformational compatibility might rearrange PrP structures between elk and deer, and possibly acquire resistance to Sarkosyl. Moreover, Sarkosyl can cause PrP aggregations that are not dependent on the PrP^{Sc} features, such as infectivity and PK resistance.[39] If this phenomenon occurred in the tested BH samples from the TSE mouse models above, the Sarkosyl-induced PrP aggregations might affect denaturation effects and/or reactivities of PRC7 and PRC5 mAbs to their binding epitopes.

The 7-5 ELISA studies above indicated that this PrP analytical method is sensitive to certain chemicals in sample preparations and experiments. In other words, non-tested reagents might have potentials to enhance PrP detections in the 7-5 ELISA method. In the literature search for establishing a Sandwich ELISA protocol, I recognized that some TSE researchers, such as Dr. Stanley Prusiner and Dr. Christine Sigurdson at the University of California, San Francisco, and San Diego, respectively, used buffers with extra reagents of sodium group/series for sample preparations and dilutions in ELISA methods: i.e. sodium bicarbonate ($NaHCO_3$) and sodium chloride (NaCl).[44,45] Since buffers for the 7-5 ELISA method did not contain these sodium reagents, several reagents were determined with denatured mouse BH samples under the 7-5 ELISA protocol. Further identifications would improve PrP^{Sc} detections in TSE diagnoses. The following three chemicals were selected as detergents for this aim: 1)

sodium hydroxide (NaOH), 2) sodium chloride (NaCl), and 3) Monosodium phosphate (NaH_2PO_4, also named as monobasic sodium phosphate and sodium dihydrogen phosphate). NaOH is known to convert a PK-resistant PrP^{Sc} agent into a PK-sensitive form, and also decrease prion infectivity.[46,47] However, 10mM NaOH did not eliminate PK-resistant PrP^{Sc} detections in scrapie-infected hamster BH samples under its dose-dependent dilutions and incubation-time points by WB assay.[46] Thus, an initial testing concentration of the three chemicals was 10mM for the evaluation if the 7-5 ELISA method would be able to detect PrP^{Sc} levels with 10mM NaOH. Each sodium product was prepared with PBS (no magnesium and calcium) for three different testing conditions in sample preparations under the 7-5 ELISA protocol: either 1) incubated with 1% TX100, 2) denatured with 5M GdnHCL, or 3) performed both 1) and 2) conditions. For the control (1% Tx100 only), PBS was added into testing BH samples, instead of the same volume of each chemical. Testing BH samples included PrP-KO, uninfected Tg5037 (ElkPrP), and CWD (Bala05-0308)-inoculated Tg5037 (inoculation study RA-150) mice: one sample from each category as n=1. Total protein 20μg of each prepared sample was applied to respective wells on a PRC7 pre-coated ELISA plate (well numbers = 2 as duplication).

Incubated with TX100 in the 1) condition, 10mM NaOH completely eliminated the PrP detection in the CWD-infected BH sample, equivalent to PrP-KO and uninfected mice (Figure 17-B). A previous article reported that the 10mM NaOH concentration did not eliminate the PrP detection in scrapie-inoculated hamster brains by WB assay.[46] Thus, the PrP reduction in the 7-5 ELISA method might be associated with different TSE isolates and host species: scrapie vs. CWD elk isolate, and hamster vs. transgenic

mouse with elk PrP expressions. Moreover, NaCl slightly enhanced the PrP detection in the infected BH sample, whereas NaH_2PO_4 decreased (Figure 3-23.B). These observations also resulted in other steps of the detergent with GdnHCL, and with both TX100 and GdnHCL (data not present). In addition, the 7-5 ELISA method determined NaCl dose-dependent responses (5, 10, 50, and 100mM) with TX100 treatment using the same tested BH samples above. However, all tested NaCl concentrations did not enhance PrP detections in CWD-infected mouse BH samples, compared to the same analyte with PBS (Figure 3-23.C).

For finding an effective detergent, the second approach evaluated sodium bicarbonate ($NaHCO_3$). Its different concentrations (5, 10, and 50mM) in 1% TX100-containing PBS (without magnesium and calcium) were applied to the same BH samples above. All processes and sample preparations were performed under the 7-5 ELISA protocol, as described in the study section of the Figure 3-16. Intriguingly, the supplemental addition of 50mM $NaHCO_3$ increased 1.3 fold of the O.D. value in the CWD-infected BH sample, compared to the same analyte with PBS (Figure 3-23.D).

Furthermore, 25, 50, and 100mM of $NaHCO_3$ were examined with the same BH samples. Indeed, the 25mM concentration showed an equivalent O.D. value of the PrP detection to 50mM and 100mM concentrations (Figure 3-23.E). These O.D. values in the detergent-treated BH samples from a CWD-infected mouse were approximately 1.25 times higher than the same analyte with PBS. Therefore, the use of at least 25mM $NaHCO_3$ could promote high PrP detections in CWD-infected materials. However, the application of this detergent might cause chemical reactions. It is known that the reaction of $NaHCO_3$ and hydrochloride (HCL) produces NaCl and carbonic acid (H_2CO_3).

Then, H_2CO_3 quickly decomposes to release water (H_2O) and carbon dioxide (CO_2). In addition, heating causes the thermal decomposition to $NaHCO_3$ that is converted to sodium carbonate (Na_2CO_3), H_2O, and CO_2. Even at room temperature, $NaHCO_3$ initiates the CO_2 production in diluted solutions. Thus, $NaHCO_3$ might cause extra dilutions of tested samples by the produced water, as a sequence of the reaction with GdnHCL and heating.

To avoid the potential of extra dilutions, I had an interest to test the $NaHCO_3$-converted product, sodium carbonate (Na_2CO_3), which is resistant to thermal decomposition even at higher temperatures. Since the temperature for the sample incubation was at 37°C in the ELISA protocol, Na_2CO_3 should be less reactive to this lower heating temperature during the sample preparation and subsequent processes on ELISA plates. Under the same procedures with sodium bicarbonate above, the 7-5 ELISA method analyzed 25, 50, and 100mM of Na_2CO_3 with the same CWD-sample group. In contrast to the results from $NaHCO_3$, the 25mM Na_2CO_3 concentration increased 1.4 times of the O.D. value in the CWD-infected material, compared to the same analyte with PBS (Figure 3-23.F). Also, the increase of Na_2CO_3 concentrations is predisposed to reduce PrP detections. This phenomenon might link to the potential production of NaOH in the samples, which the chemical reaction of Na_2CO_3 with H_2O produces NaOH and CO_2. In fact, the reduction of PrP detections was obvious under the low NaOH concentration (Figure 3-23.B). However, this NaOH production should occur when $NaHCO_3$ is applied, because Na_2CO_3 is the converted product from $NaHCO_3$.

To identify the reduction of PrP detections as specific to sodium carbonate Na_2CO_3, a chemical product of carbonate-bicarbonate buffer-capsule (Sigma-Aldrich) was tested. This chemical product contained both Na_2CO_3 and $NaHCO_3$ in equilibrium. Indeed, the aqueous solution of the chemical product has been used for coating capture antibodies in the 7-5 ELISA and D-5 ELISA protocols. Under the same procedure above, this combined chemical product of 25, 50, and 100mM was determined with the same CWD-sample group under the 7-5 ELISA protocol. Since this chemical contained higher Na_2CO_3 amounts from the product and the possible $NaHCO_3$ conversation, the reduction of PrP detections was predictable. However, the outcomes from the carbonate-bicarbonate product were similar to those from the sodium bicarbonate treatment (Figure 3-23.E and G). Although the mechanisms of reactions between PrP and these sodium products were unknown in these experiments, the results showed that 25mM of the three chemical products enhanced PrP detections in TSE-infected materials. One possible assumption was that efficacies of sodium bicarbonate and sodium carbonate might reveal binding epitopes of anti-PrP mAbs in the 7-5 ELISA method. Therefore, Na_2CO_3 and $NaHCO_3$ are effective supplemental detergents for the 7-5 ELISA protocol, especially for cases that additional enhancements of PrP detections would be required, such as limited amounts of testing samples for TSE diagnoses.

In past Sandwich ELISA experiments, PrP detections in TSE-infected materials were not successful when some buffers contained sodium deoxycholate (DOC: deoxycholic acid sodium salt) and/or sodium dodecyl sulfate (SDS). It was unknown how these chemicals interfered for PrP detections in the 7-5 ELISA method. DOC is one of the common components contained in lysis buffer for cell cultures. Previously, the 7-5

ELISA method measured the extracted samples of TSE-infected cells, treated by the lysis buffer with DOC. However, these samples did not exhibit PrP detections. Since the 7-5 ELISA method has been developed using mouse BH samples and recombinant PrP molecules, this protocol might be not applicable to cellular materials. In addition, SDS is one of the chemical materials in the application of PNGaseF that enzymatically removes *N*- and *O*-glycans from proteins (protein deglycosilation). The PNGaseF application was success for the WB assay to detect PrP levels in TSE-infected cellular extract samples.[20] The successful use of PNGaseF will promote more PrP detections by the PRC7 mAb, because all PNGaseF-treated PrP molecules would be unglycosyl forms. According to the results in this study section, doses of each chemical influenced PrP detections in the 7-5 ELISA method. Therefore, the following concentrations of DOC and SDS were evaluated under the same procedures and preparations with the CWD-sample group above with the 1% TX100: DOC = 0.1, 0.25, and 0.5%; and SDS = 0.1, 0.5, and 1%. In the 7-5 ELISA results, all DOC concentrations reduced O.D. values of PrP detections in the CWD-infected material (Figure 17-H). However, 0.1% SDS treatment enhanced PrP detections in the infected materials, while the increased concentrations reduced PrP detections (Figure 3-23.I). Thus, these outcomes suggested 1) no use of DOC for PrP detections in cellular extracts under the 7-5 ELISA protocol, and 2) minimal use of SDS at lower than 0.5% if needed.

Overall, the 7-5 ELISA approach must be sensitive to certain chemicals and concentrations that affect PrP detections. It is important to make sure what chemical components the testing sample and other materials contain, prior to the 7-5 ELISA analysis. Otherwise, false-negative results are serious concerns for TSE diagnoses. On

the other hand, sodium bicarbonate and sodium carbonate are effective chemicals for enhancing PrP detections in the 7-5 ELISA method.

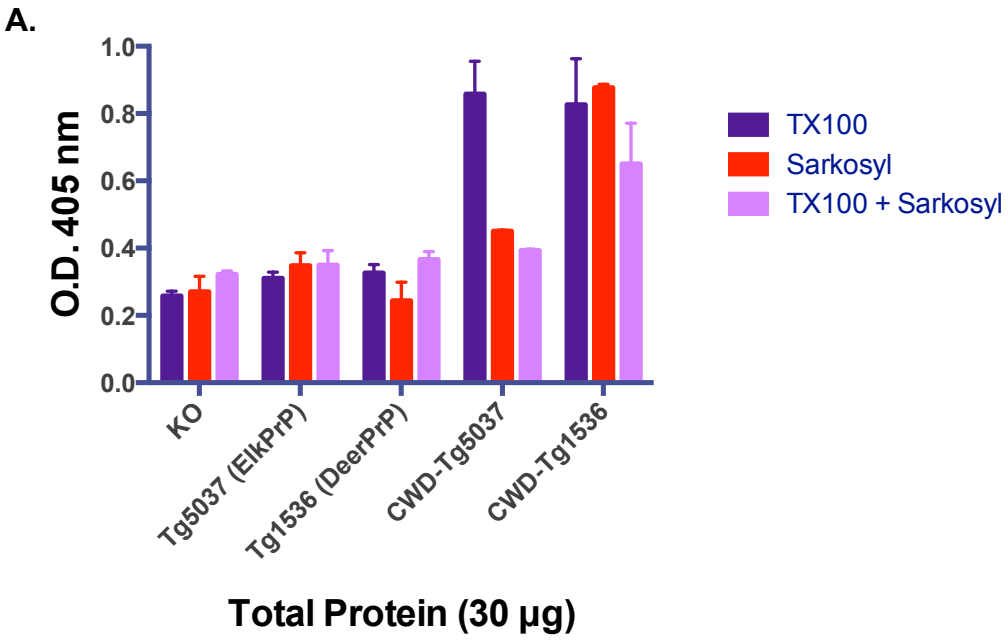

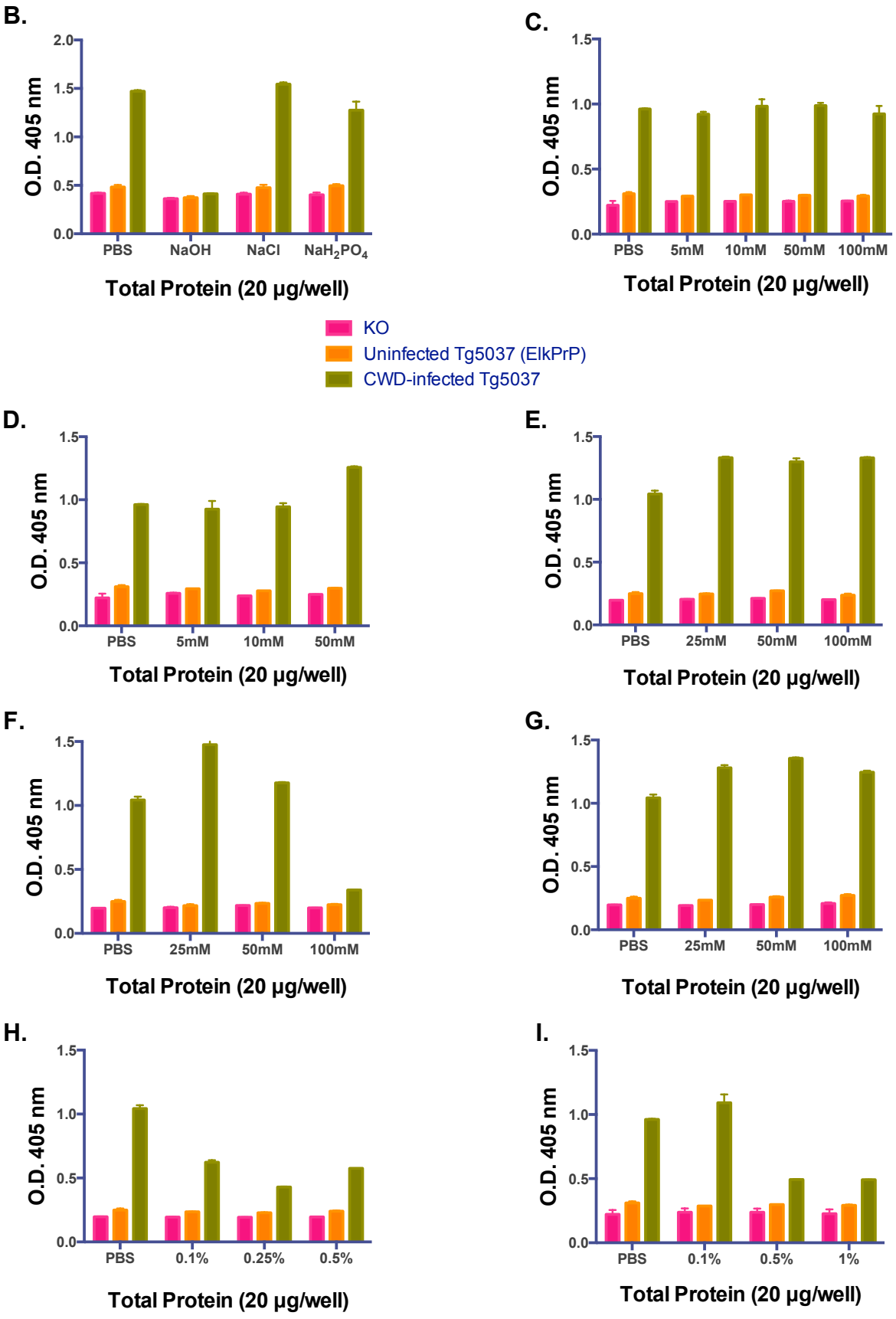
B.
O.D. 405 nm
2.0
1.5
1.0
0.5
0.0
PBS
NaOH
NaCl
NaH2PO4
Total Protein (20 µg/well)
C.
O.D. 405 nm
1.5
1.0
0.5
0.0
PBS
5mM
10mM
50mM
100mM
Total Protein (20 µg/well)
KO
Uninfected Tg5037 (ElkPrP)
CWD-infected Tg5037
D.
O.D. 405 nm
1.5
1.0
0.5
0.0
PBS
5mM
10mM
50mM
Total Protein (20 µg/well)
E.
O.D. 405 nm
1.5
1.0
0.5
0.0
PBS
25mM
50mM
100mM
Total Protein (20 µg/well)
F.
O.D. 405 nm
1.5
1.0
0.5
0.0
PBS
25mM
50mM
100mM
Total Protein (20 µg/well)
G.
O.D. 405 nm
1.5
1.0
0.5
0.0
PBS
25mM
50mM
100mM
Total Protein (20 µg/well)
H.
O.D. 405 nm
1.5
1.0
0.5
0.0
PBS
0.1%
0.25%
0.5%
Total Protein (20 µg/well)
I.
O.D. 405 nm
1.5
1.0
0.5
0.0
PBS
0.1%
0.5%
1%
Total Protein (20 µg/well)

Figure 3-23. Evalutions of supplemental reagents with TX100 for enhancing PrP detections in BH samples from CWD-mouse models. (A) Comparisons of TX100 and Sarkosyl in the 7-5 ELISA method with denatured analyte, (B) Comparisons of NaOH, NaCl, and NaH_2PO_4 with TX100 in the 7-5 ELISA method with denatured analyte, (C) NaCl-dose dependent responses in the 7-5 ELISA method, (D) sodium carbonate ($NaHCO_3$)-dose dependent responses in the 7-5 ELISA method with denatured analyte, (E) PrP detections with lower $NaHCO_3$ concentrations in the 7-5 ELISA method with denatured analyte, (F) PrP detections with sodium carbonate (Na_2CO_3) in the 7-5 ELISA method with denatured analyte, (G) PrP detections with sodium carbonate-bicarbonate reagent in the 7-5 ELISA method with denatured analyte, (H) PrP detections with sodium deoxycholate (DOC/SDS) in the 7-5 ELISA method with denatured analyte, and (I) applications of lower DOC concentrations. (n=3, each sample with 20µg total protein per well)

PK-sensitive PrP^{Sc} detections in mouse models of human inherited prion disease

Gerstmann-Sträussler-Scheinker syndrome (GSS) is an autosomal-dominant inherited TSE disease in humans, caused by mutation at the codon 102 on choromosome 20 of Prnp gene from Proline (P) to Leucine (L), referred to as P102L. Transgenic (Tg) mouse breed lines of GSS models have been established.[48-54] In this study section, experimental studies examined BH samples from a transgenic mouse breed line expressing the mutation P101L in the murine PrP gene, here denoted as Tg(GSS), corresponding to the human P102L GSS mutation.[19] These Tg(GSS) mice spontaneously developed the CNS dysfunction and reproduced the neuropathological features of GSS. Moreover, these Tg(GSS) mice generate PK-sensitive PrP forms.[19] In fact, GSS patients also exhibit abundant portions of PK-sensitive PrP^{Sc} agents in their brains.[55] Thus, the Tg(GSS) mice present GSS features clinically and molecularly. According to the laboratory database, hemizygous Tg464 mice of Tg(GSS) mouse breed lines overexpress murine PrP molecules with the mutation of the GSS-corresponding residue P101L, which are twelve times higher than the PrP^{C} expression in uninfected wild-type mice. Clinically, the Tg464 mice spontaneously exhibited onsets of neurological signs and disease developments. Moreover, the inoculation of brain materials from a spontaneously sick Tg464 mouse into immature host Tg464 mice at non-sick stages caused earlier disease progressions, compared to the scrapie sick day of the spontaneous GSS development in these mice.

Prior to the 7-5 ELISA experiment, WB with the PK reagent were performed with Tg464 mouse BH samples to confirm the non-existence of PK-resistant PrP^{Sc} molecules. Testing BH samples included three Tg464 mice at terminal stages from the

inoculation study KN-35, as well as negative and positive controls: PrP-KO, uninfected FVB/n, uninfected Tg4112 (MousePrP overexpression), and RML-inoculated FVB/m mice. The WB results indicated that PK-treated BH samples of all GSS mice lost PrP detections, similar to outcomes in uninfected wild-type FVB/n and Tg4112 mice. In contrast, the RML-infected BH sample exhibited PK-resistant PrP agents (Figure 3-24.A). Therefore, the Tg464 mouse breed line only expressed PK-sensitive PrP molecules in the disease condition, but not PK-resistant PrP^{Sc} forms.

1) GdnHCL-dose dependent responses of Tg(GSS) mouse BH samples by the 7-5 ELISA method: The dose dependence of GdnHCL denaturation was determined with Tg464 mice, if the spontaneous GSS mouse model would show the same outcomes from the 7-5 ELISA method above using other TSE strains and transgenic mice with different PrP species. Testing BH mouse samples included the three Tg464 mice (n=3), and controls of PrP-KO, uninfected FVB/n, and RML-inoculated FVB/n mice (n=1). Under the optimized 7-5 ELISA protocol, three different doses of GdnHCL (0M, 2.5M and 5M) were examined with these BH samples for denaturation. The final protein concentration of these prepared samples was 200μg/ml, and then 100μl of each sample was coated into wells (total protein per well = 20μg; well numbers for each sample = 3 as technical triplication). In the coated samples, the residual amounts of GdnHCL were 0, 0.25, and 0.5M for each denaturation category, respectively. In the results, 0M GdnHCL (only addition of 50mM Tris) denaturation did not enhance PrP detections in the RML-infected and the Tg(GSS) BH samples (Figure 3-24.B). However, the Tg464 mice showed low O.D. values of PrP detections that could arise from the features of transgenic mice with PrP overexpressions, based on the

experiments above. In contrast, the increased GdnHCL doses enhanced higher PrP detections in these disease mouse BH samples, especially at 5M GdnHCL (Figures 3-24.C and D). Thus, the optimized protocol maintained the 5M GdnHCL denaturation in Sandwich ELISA experiments with the Tg464 mice BH samples below. Based on these results, PrP molecules in the GSS mouse models should form abnormal PrP^{Sc} or PrP^{Sc}-like structures at their terminal stages, because the PRC7 mAb requires denaturation and renaturation of the PrP^{Sc} isoforms for these detections. Also, the tested Tg(GSS) transgenic mice generated unglycosyl and/or mono-1 glycosyl PrP forms that the PRC7 mAb can react with. Hence, under-glycosylated PrP^{Sc} forms could be PK-sensitive PrP agents in TSE-disease mice.

In the TSE pathogenesis, PK-sensitive PrP^{Sc} agents exhibit an equivalent infectivity and neurotoxicity to PK-resistant PrP^{Sc} agents in the same TSE strain.[41-43] These PK-sensitive PrP^{Sc} agents are also known as forming smaller oligomeric aggregates that induce neurotoxicity and neurodegeneration.[56-57] In fact, the small aggregate is a causal molecule of the protein misfolding and disease initiation, because smaller aggregates possess a higher seeding potency in the conformational conversion and replicative process, under a template-associated progression of the protein-only hypothesis.[58] Since the 7-5 ELISA protocol does not require the PK reagent, the established approaches should be capable of detecting small aggregates of PK-sensitive PrP^{Sc} forms in TSE-infected materials. According to the results, the 7-5 ELISA application presented a successful utility to evaluate PK-sensitive PrP^{Sc} agents in Tg464 mice. Indeed, this ELISA method highly detected these PrP^{Sc} agents in BH samples from the Tg(GSS) mice at not only terminal stages but also pre-clinical stages.

Therefore, the 7-5 ELISA method will be ultimately beneficial for detecting PK-sensitive PrP^{Sc} agents in TSE diagnostic investigations and understanding the TSE pathogenesis in research.

2) Different tissue-collecting time points from Tg(GSS) mice and the 7-5 ELISA approach: According to the laboratory database, many collected tissues from previous GSS mouse model studies were already used, and thus amounts of stored samples from Tg(GSS) mice were very limited. However, some brains from non-sick conditions of homozygous Tg464 mice were available for this ELISA experiment. This pilot study included five BH samples from non-sick Tg464 mice: 2 brains at 61 days, 1 brain at 81 days, and 2 brains at 142 days from their births, in addition to the three GSS-developed Tg464 mice above. Notably, these GSS mice were originated from the inoculation study KN-35: the inoculation of 1% crude brain homogenate from a spontaneously GSS-developed Tg464 mouse into young Tg464 mice at 40 days old (non-clinical sign). Their scrapie sick days were Mean ± SEM = 105.38 ± 2.03 days, whereas those in homozygous Tg464 mice with spontaneous disease developments were an average of 160 days. All BH samples from these non-sick and disease mice were prepared by the same procedures, including denaturation with 5M GdnHCL under the 7-5 ELISA protocol. Intriguingly, Tg464 mice with non-clinical signs exhibited higher PrP levels even from 61 days of birth. (Figure 3-24.E). Compared to the non-disease conditions, the 7-5 ELISA method measured the increased O.D. value in the disease conditions of Tg464 mice. These results indicated that the GSS mouse model highly generated under-glycosylated PrP^{Sc} forms from early lifetime after the birth. However, it is not confirmed if the higher PrP detections arose from the genetic GSS background or

the feature of PrP-overexpressing transgenic mouse breed lines, such as Tg4112 mouse with mouse PrP overexpressions.

3) Different tissue-collecting time points from Tg(GSS) mice and the D-5 ELISA approach: To evaluate modifications of PrP^{C} and PrP^{Sc} levels in disease progressions, the D-5 ELISA methods examined one BH sample from each tissue-collecting time point, under the denatured and non-denatured sample preparations: non-sick 61, 81, and 142 days after the birth, and a GSS-disease developed Tg464 mouse that the 7-5 ELISA method already tested. As described above, the D18 Fab Ab has unique characteristics for ELISA applications. This antibody requires denaturation to detect PrP^{Sc} levels in TSE-infected materials. In contrast, this antibody recognizes only PrP^{C} levels in uninfected and infected murine BH samples. Also, the D18 Fab Ab is capable of reacting with all four glycosyl PrP forms.

In this D-5 ELISA experiment, all procedures were performed by the optimized ELISA protocol. Each well on an ELISA plate contained total protein 20μg of each prepared sample (well number = 3 as technical replication). Intriguingly, the D-5 ELISA method detected an inverse proportion of PrP^{C} and PrP^{Sc} modifications in the GSS development, which PrP^{C} levels decreased, but PrP^{Sc} levels increased through their lifetimes (Figure 3-24.F). Compared to the 61 days at a non-sick state, the GSS condition increased approximately 1.3% of denatured PrP^{Sc} detections. In the non-denatured preparation, the GSS mouse decreased almost 1.3% of PrP^{C} detections in comparison to the 61 days BH sample. Thus, this PrP^{C} decrease might indicate conformational changing amounts or rates of the PrP^{C} molecule to the abnormal PrP^{Sc} structure, based on the protein-only hypothesis that the abnormal template conformer

interacts with the normal PrP molecule. In another aspect, the PrP^C decrease in the disease condition might reflect damages in the affected brain. The death of many affected cells should reduce total amounts of PrP^C detections in the tested brain sample. In contrast, the 7-5 ELISA method showed low O.D. values of PrP detections at all time points of Tg464 mouse BH samples (Figure 3-24.G). This observation indicated that tested Tg(GSS) mice generated less amounts of unglycosyl and/or mono-1 glycosyl PrP forms through disease developments. However, both denatured and non-denatured PrP detections in these analyte increased O.D. values from the 81 days after birth. Thus, this increase should be proof of under-glycosylated PrP generations in the TSE pathogenesis.

Based on the features of D18 and PRC7 antibodies, Tg464 mice generate both PrP^C and PrP^{Sc} isoforms with the GSS genetic background. In the D-5 ELISA method, the detected PrP level must be the PrP^C structure under the non-denaturation, whereas the denatured PrP levels indicate PrP^{Sc} conformations. Thus, PrP^C molecules with the P101L mutation in Tg464 mice initially formed α-helical structures, but subsequently misfolded to β-sheet rich structures in TSE conditions. Hence, the reduction of PrP^C detections reflects not only the PrP conformational change from the normal to abnormal isoform, but also the disease development and progression. At this point, however, it is unknown what factors trigger the conformational changes from PrP^C and PrP^{Sc} conformers in this spontaneous Tg(GSS) mouse model.

Supplementarily, the D-5 ELISA method determined PrP^C modulations in drug-induced mouse models of Parkinson's disease (PD), one of the major neurodegenerative disorders in humans (kindly provided by Dr. Ronald B. Tjalkens,

Department of Environmental and Radiological Health Sciences at Colorado State University; data not present). Under the non-denatured sample preparation, the D-5 ELISA method revealed the reduction of PrP^{C} levels in BH samples from the PD mouse models at the onset of clinical signs, compared to pre-treated mice. Moreover, these PD mouse BH samples were determined by Sandwich ELISA approaches using other capture antibodies PRC7 and POM2 mAbs. With the detecting antibody PRC5 mAb, a POM2-base ELISA approach showed similar reductions of PrP^{C} levels in the disease-developed PD mice. However, the 7-5 ELISA method did not measure PrP^{C} levels. These results suggested that the abundance of PrP^{C} molecules were a diglycosyl state in normal and PD conditions. Hence, the generation of under-glycosylated PrP forms should be a specific phenomenon in the TSE pathogenesis.

As the 7-5 ELISA method detected in Tg464 mice of the GSS model above (Figure 3-24.G), the modulation of PrP glycosylations might link to the conformational change from PrP^{C} and PrP^{Sc} structures, or the generation of abnormal PrP conformers in the GSS pathogenesis. Because the loss of glycans causes the instability of protein conformations, PrP molecules with glycosidic deficits might allow more replications of PrP^{Sc} isoforms via the interaction of these molecules and abnormal templates. To evaluate this potential implication, the 7-5 and D-5 ELISA approaches would be capable of analyzing modulations of the PrP^{Sc} glycosylation state and the PrP^{C} and PrP^{Sc} detection in longitudinal studies of the GSS disease development and progression in Tg464 mice.

For further identifications, these ELISA experiments should be applied for longitudinal studies in TSE mouse bioassays, such as the inoculation of a mouse-

adapted scrapie strain (i.e. RML and 22L) into a wild-type mouse breed line (i.e. FVB/n and C57BL6 mice). This experimental plan will reduce potential influences from unknown generations of under-glycosylated PrP forms that the 7-5 ELISA method detected in uninfected transgenic mouse breed lines. However, these longitudinal studies of TSE-mouse models would have technical limitations for monitoring PrP modulations. Brain biopsies must be difficult to repeat at different time points in a same animal, even collecting partial brain tissue samples. Because of mouse body size, this procedure is risky for maintaining mouse health conditions and lives for completing the studies. Therefore, timed-specimen collections should be a practical plan for this aim. For each specific time point of tissue collections, the same numbers of mice should be prepared at the beginning of the studies. Then, tissues would be collected at each time point for analyzing the disease progression and the correlative PrP^{C}-PrP^{Sc} modulation. As described above, the 7-5 ELISA and D-5 ELISA approaches are very sensitive to detect PrP quantities in testing samples, even subtle differences. Also, these Sandwich ELISA protocols are especially capable of measuring both PK-sensitive and resistant PrP^{Sc} isoforms in TSE-infected materials. Consequently, these approaches would be indispensable innovations for identifying the underlying mechanisms of the PrP^{Sc} formation during the TSE disease development.

A.

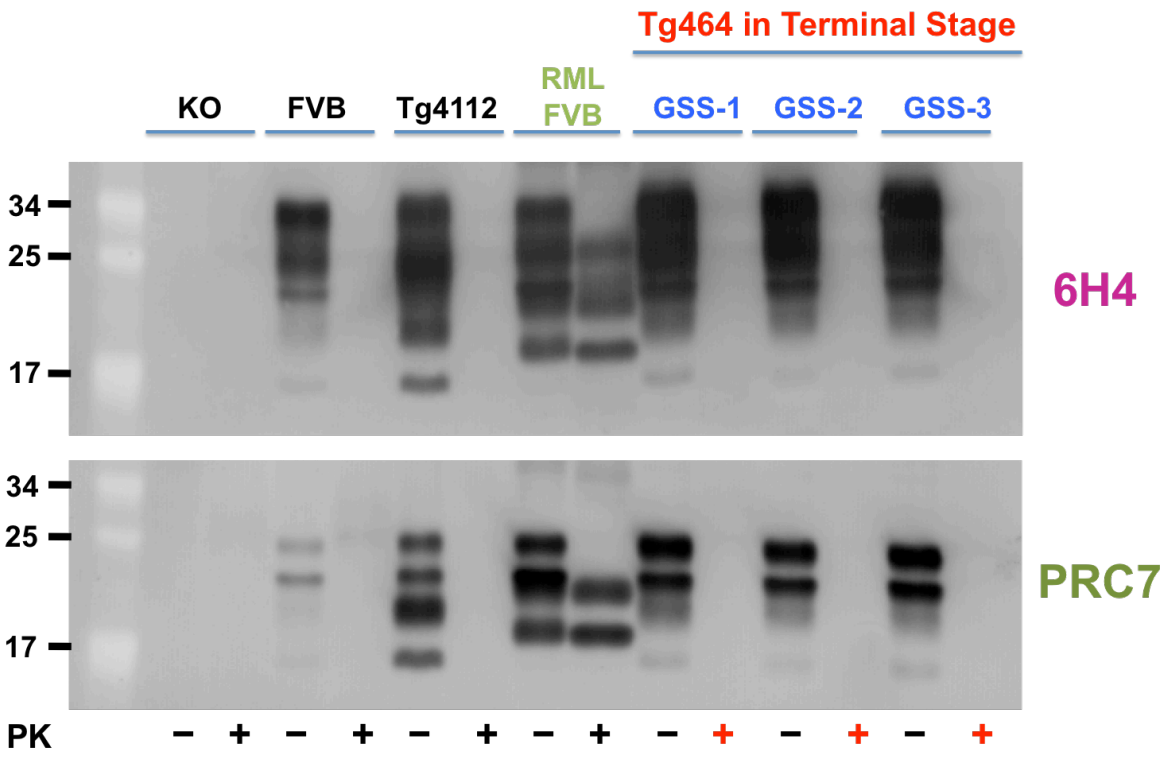
Tg464 in Terminal Stage
KO
FVB
Tg4112
RML FVB
GSS-1
GSS-2
GSS-3
34
25
17
6H4
34
25
17
PRC7
PK
– + – + – + – + – + – + – +

B.

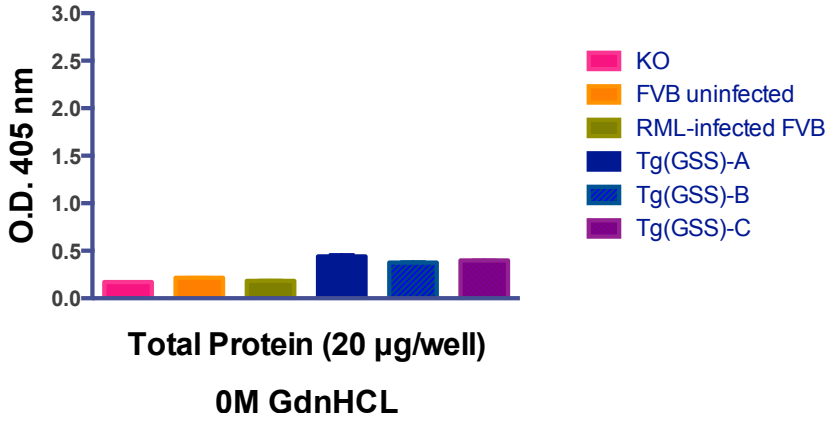
3.0
2.5
2.0
1.5
1.0
0.5
0.0
O.D. 405 nm
KO
FVB uninfected
RML-infected FVB
Tg(GSS)-A
Tg(GSS)-B
Tg(GSS)-C
Total Protein (20 µg/well)
0M GdnHCL

C.

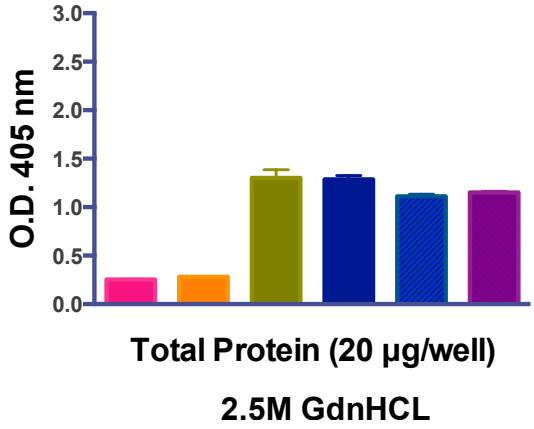
3.0
2.5
2.0
1.5
1.0
0.5
0.0
O.D. 405 nm
Total Protein (20 µg/well)
2.5M GdnHCL

D.

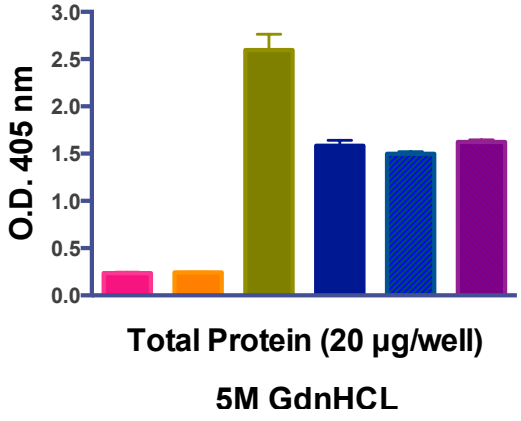
3.0
2.5
2.0
1.5
1.0
0.5
0.0
O.D. 405 nm
Total Protein (20 µg/well)
5M GdnHCL

E.

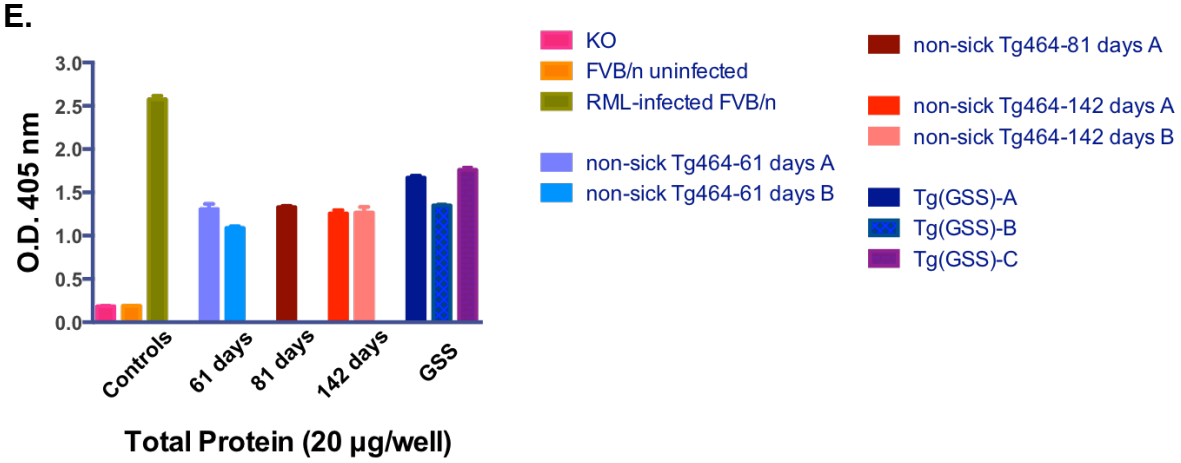
KO
FVB/n uninfected
RML-infected FVB/n
non-sick Tg464-61 days A
non-sick Tg464-61 days B
non-sick Tg464-81 days A
non-sick Tg464-142 days A
non-sick Tg464-142 days B
Tg(GSS)-A
Tg(GSS)-B
Tg(GSS)-C
O.D. 405 nm
3.0
2.5
2.0
1.5
1.0
0.5
0.0
Controls
61 days
81 days
142 days
GSS
Total Protein (20 µg/well)

F.

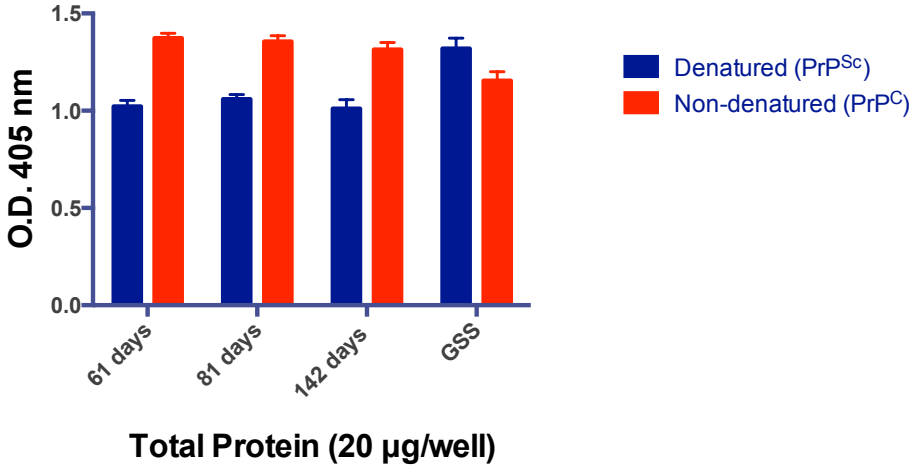
Denatured (PrP^Sc)
Non-denatured (PrP^C)
O.D. 405 nm
1.5
1.0
0.5
0.0
61 days
81 days
142 days
GSS
Total Protein (20 µg/well)

G.

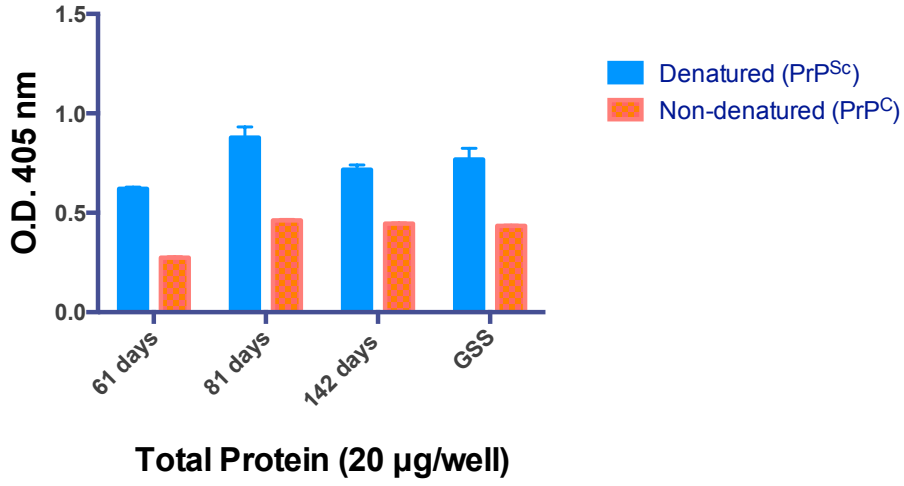
Denatured (PrP^Sc)
Non-denatured (PrP^C)
O.D. 405 nm
1.5
1.0
0.5
0.0
61 days
81 days
142 days
GSS
Total Protein (20 µg/well)

Figure 3-24. PK-sensitive PrP^{Sc} molecules in GSS-mouse models.
(A) Western blot (WB) analyses of PrP detections in BH samples from three Tg464 (GSS) mice with terminal stages. These mice did not exhibit PK-resistant PrP detections, compared to the RML-inoculated FVB/n BH analyte. 6H4 mAb for the upper analysis and PRC7 mAb for the lower analysis. (B) 0M GdnHCL, (C) 2.5M GdnHCL, and (D) 5M GdnHCL denaturations for BH samples of the disease Tg464 (GSS) mice without PK treatments for PrP detections by the 7-5 ELISA method. (E) the 7-5 ELISA method detected PrP levels in denatured BH samples from Tg464 (GSS) mice, at different ages with non-clinical conditions or GSS development, without PK treatments. Brains from non-sick mice were collected at 61, 81, and 142 days of ages. Brains from the diseased mice were collected at terminal stages. In both non-denatured and denatured BH samples, (F) the D-5 ELISA method measured all forms of the PrP glycosylation, and (G) the 7-5 ELISA method detected unglycosyl and mono-1 glycosyl PrP forms. Modulations of PrP levels in BH samples from Tg464 (GSS) mice at different-time points of tissue collections. Ages at 61, 81, and 142 days were no clinical signs. Brains from the diseased mice as GSS were collected at terminal stages. (n=3, each sample with 20μg total protein per well)

Discussions

The 7-5 ELISA method is an exceptionally sensitive approach for detecting PrP^{Sc} isoforms in a RML mouse scrapie-infected brain homogenate (BH) sample (Figures 3-1.A and B). The O.D. value differences between TSE-infected and uninfected or PrP-KO mouse are statistically significant (n=3 for technical repeats; $p<0.0001$). Biological replicates (n=3) of three mouse groups (TSE-infected, uninfected, and PrP-KO) showed specificities of the 7-5 ELISA method for the PrP detection in BH samples from RML-inoculated FVB/n, CWD-inoculated Tg5037 and CWD-inoculated Tg1536 mice (Figures 3-2.A, B and C). At the 20μg amount of total protein, the differences of O.D. values between TSE-infected and uninfected BH samples are statistically significant ($p<0.01$-0.0001). These differences arose from the PRC7 mAb feature that only reacts with unglycosyl and mono-1 glycosyl PrP forms. Hence, the 7-5 ELISA results indicate that under-glycosylated PrP forms are highly generated in TSE-infected animals during the disease development, but not in uninfected animals because PrP^{C} molecules normally preserve the diglycosyl form. Therefore, the PrP glycosidic state could be implicated with mechanisms of the TSE pathogenesis.

Furthermore, the 7-5 ELISA method is capable of detecting PrP levels in BH samples from TSE-infected mouse models with different PrP species backgrounds, such as mice, elk, deer, sheep, or mink (Figures 3-3.A to E). According to the protein dose-dependent approach, tested TSE-infected BH samples obviously exhibited the increased PrP detection at higher amounts of total protein, while uninfected controls did not show any or subtle change (Figures 3-3.A to E). Indeed, these outcomes were observed in the four different TSEs: RML (mouse-adapted scrapie), CWD, sheep

scrapie, and TME. Based on high PrP detections in TSE-infected mouse BH samples, the 7-5 ELISA method revealed that these disease animals preferentially generated under-glycosylated PrP forms in their brains. At the same tested total protein, the 7-5 ELISA method intriguingly detected different PrP levels of mouse BH samples among the five mouse-adapted scrapie strains (Figures 3-4.A to E). Although all strains exhibited significantly higher PrP detections than controls, these O.D values showed strain differences in inoculated mice. Hence, these results suggested that the generation and quantity of under-glycosylated PrP forms might be dependent on distinct PrP^{Sc} strains in infected hosts. In addition, each strain presented different responses to concentrations of the denaturant, guanidine hydrochloride (GdnHCL), under the 7-5 ELISA method analyses at the 20μg of total protein per BH sample. Thus, this ELISA application additionally evaluated different denaturants and reagents with various prion isolates and strains. Possibly, these responses for chemicals reflect differences of conformational stabilities among prion isolates and strains. In diagnostic and analytical aspects, the 3-5M range of GdnHCL should be applicable for denaturation to detect higher amounts of PrP molecules in TSE-infected materials (Figures 3-4.A to E).

In CWD mouse models, the 7-5 ELISA method found that structure rearrangements of PrP^{Sc} agents between different species were dependent on the origin of CWD isolates and the conformational compatibility of PrP molecules. The inoculation of moose-CWD isolate (08W-11,741) into Tg1536 (DeerPrP expression) mice enhanced the detection of under-glycosylated PrP forms in these BH samples, compared to the PrP level of the moose-CWD BH inoculum at the same amount of total protein (Figure 3-5.C). In contrast, moose-CWD inoculated Tg5037 (ElkPrP) mice did

not increase PrP detections. These observations could be associated with identical primary PrP structures in deer (Odocoileus species) and Shira's moose (Alces alces shirasi). However, the PrP structure of elk is different from deer and moose at the amino acid residue 226 in the globular domain, which is considerably essential for the CWD prion propagation and disease development.[22] The experimental results suggested that the conformational compatibility was a critical factor for PrP^{Sc} transmissions between different species, as well as its structure rearrangement and propagation in infected hosts. In fact, the inoculation of a CWD isolate from elk (99W12389) did not enhance the generation of under-glycosylated PrP forms in Tg1536 (DeerPrP) mice (Figure 3-5.D). However, the 7-5 ELISA method showed higher detections of under-glycosylated PrP forms in Tg1536 (DeerPrP) mice with inoculations of the murine-brain isolate, originated from the elk CWD 99W12389-infected Tg5037 (ElkPrP) mouse (Figure 3-5.E). Moreover, the inoculation of another elk CWD isolate (Bala04) also exhibited the same observation in these transgenic mice (Figures 3-5.F and G). These outcomes indicated that the passage of cervid CWD inocula into differing transgenic mice with cervid PrP expressions enhanced the adaptation and propagation of infected PrP^{Sc} agents in new murine hosts, even though their PrP structures were different. Hence, the predominant adaptation and selection of the infected PrP^{Sc} structure reflect the interspecies transmission of TSEs in new hosts. Thus, the 7-5 ELISA results revealed that some factors in CWD-infected murine hosts could be involved in the mechanism of the PrP^{Sc} adaptation and propagation, which should be dependent on the structural arrangement and conformational compatibility between different PrP species backgrounds.

Furthermore, the 7-5 ELISA method measured the non-enhanced PrP level in transgenic mice with mink PrP expressions (TgF431) that were inoculated with the three different TME isolates from mink (#58 NBP, 10^{-5} cloned TME 941031 and 10^{-5} cloned TME 941201), compared to analyte of these mink TME brain inocula at the same amount of total protein (Figure 3-6.B, C and D). These results might suggest that the structural arrangement of mink TME PrP agents was not well promoted in murine hosts to generate and propagate this abnormal PrP^{Sc} agent, because of the conformational incompatibility between these two different PrP species backgrounds. Possibly, some other factors in hosts implicated the compatibility for propagations of the heterogeneous PrP^{Sc} agent. In fact, experimental transmissions of TME isolates are not successful into several wild-type mouse breed lines because of possible biological reasons, while Syrian golden hamsters have been used in TME transmissible studies.[3,59] Moreover, black ferret, a close mustelid to mink, was less susceptible to the TME infection and disease development, compared to mink.[60] As described above in deer and elk, mink and ferret have differences in amino acid sequences of the PrP genes at two codons: phenylalanine (Phe or F) vs. lysine (Lys or L) at 179, and arginine (Arg or R) vs. glutamine (Glu or Q) at 224, respectively (mink vs. ferret). Therefore, the amino acid differences (cervid at 224 and mustelid at 226) in the globular domain of the PrP structure could be important factors in the conformational compatibility for the adaptation, structure rearrangement and propagation of infected PrP^{Sc} agents in new hosts, especially interspecies transmissions of TSEs. After the adaption of infected PrP^{Sc} conformers, these hosts predominantly would generate these pathogenic agents more than native PrP^{C} molecules. The infected animals would present clinical signs and

disease developments of the TSE strain phenotype, such as drowsy (DY) and hyper (HY) observations of TME isolates.[3,61]

In comparison to the cervid prion cell assay (CPCA), the 7-5 ELISA approach demonstrated its potential utility to estimate the prion infectivity and titration (Figures 3-7.A to D, and 3-8). This pilot application provided a new scope of the 7-5 ELISA method in the TSE research for further investigations. In addition, the CPCA results with the PRC7 mAb indicated that SMB-PS cells expressed similar levels of under-glycosylated PrP forms to those of SMB cells under the non- PK treatment (Figures 3-9.A to F). These SMB cells are a scrapie-infected clonal cell line, originally derived from the mouse brain with the inoculation of the mouse-adapted scrapie strain Chandler.[13] In contrast, SMB-PS cells are the permanently cured SMB cells with the treatment of pentosan sulphate (PS) that do not express PK-resistant PrP molecules even after 50 passages.[14] Moreover non-infected RK13 cells with murine PrP expressions (RKM7) did not exhibit the PrP detection. Although an abundance of normal PrP^{C} molecules states the diglycosyl form, the PRC7 mAb only reacts with unglycosyl and mono-1 glycosyl PrP forms. These SMB results indicated that RKM7 cells did not generate under-glycosylated PrP forms under the non-TSE infection condition. Hence, TSE-infected cells would continue to generate under-glycosylated PrP forms even after a cure from the PrP^{Sc}-producing condition. Based on these outcomes, SMB-PS cells might have dysfunctions in the process of protein glycosylations, even though this cell line does not express PK-resistant PrP molecules.

In this dissertation, the central hypothesis proposed that the detection of under-glycosylated PrP forms is a hallmark of TSEs as a diagnostic biomarker for the disease

progression. In fact, the 7-5 ELISA method highly detected the mono-1 glycosyl and/or unglycosyl PrP forms in BH samples from TSE-infected animals, whereas non-infected materials did not present or only expressed subtle levels of PrP detections. Therefore, the loss of full glycosylation on the PrP structure could be one of the pathological mechanisms in the TSE etiology. Thus, the 7-5 ELISA method should be applicable for monitoring and profiling modulations of under-glycosylated PrP forms through the TSE disease development and progression.

In addition to the establishment of the 7-5 ELISA method, another Sandwich ELISA protocol was innovated for measuring only PrP^{C} or total PrP^{Sc} levels. The D-5 ELISA method is a unique application of the D18 Fab Ab and PRC5 mAb as capture and detecting antibodies, respectively. Notably, this Fab Ab requires denaturation to detect PrP27-30 rod isolated from a scrapie prion, which is the protease-resistant core of an infectious PrP^{Sc} isoform and important for its infectivity and pathogenesis.[15,27,28] Without the sample denaturation process, the D18 Fab Ab was not able to measure the PrP27-30 rod by ELISA methods.[15] Since this antibody can detect all four glycosylated PrP forms (unglycosyl, mono-1 glycosyl, mono-2 glycosyl, and diglycosyl), the use of D18 Fab Ab can measure total amounts of PrP^{Sc} agents in testing samples. In contrast, the 7-5 ELISA method specifically detects unglycosyl and mono-1 glycosyl PrP forms with which the PRC7 mAb only reacts (but PRC5 mAb can bind to all four glycosylated PrP forms). Importantly, the D18 Fab Ab reactivity to normal PrP^{C} molecules was applied for a therapeutic strategy, which this antibody could interfere with the interaction of PrP^{C} and PrP^{Sc} isoforms.[29] Since this study was performed without the sample denaturation, the D18 application in ELISA methods would be capable of analyzing only

normal PrP^C isoforms in non-denatured samples. Based on these characteristic features of the D18 Fab Ab, the D-5 ELISA protocol analyzes PrP^{Sc} or PrP^C levels in testing samples with or without denaturation, respectively.

For GdnHCL-denatured murine BH samples, the D-5 ELISA method detected higher O.D. values of PrP levels in TSE-inoculated mice, compared to the control BH samples (Figure 3-13.A). These findings resulted in two different inocula (RML and 22L) of mouse-adapted scrapie prions in FVB and C57BL6 wild-type mice, respectively. Furthermore, this new Sandwich ELISA approach revealed the decrease of PrP^C levels in the infected BH samples without denaturation (Figure 3-13.B). Therefore, these pilot studies suggested that the D-5 ELISA approach would be capable of analyzing the modulation of normal PrP^C and abnormal PrP^{Sc} levels in the TSE disease state by different sample preparations. Possibly, the loss of PrP^C levels causes functional abnormalities in the infected animals through the TSE disease development.

To find an optimized concentration of the D18 Fab Ab as a capture antibody in a Sandwich ELISA method, different concentrations of this Ab were examined with the RML-infected mouse BH sample and its controls (PrP KO and uninfected FVB mice). For both denatured and non-denatured sample conditions, the 20 μg/ml D18-coating concentration showed the highest O.D. values of PrP detections in the RML-infected sample (Figures 3-14.A to D). Also, the 5μg/ml concentration could be a minimum amount for coating the D18 Fab Ab, which exhibited a higher PrP detection, similar to the 20 μg/ml concentration. Intriguingly, the D-5 ELISA method determined that GdnHCL was effective for the sample denaturation to detect higher PrP levels in the TSE-infected material, compared to GdnSCN (Figures 3-15.A and B). For the dose-

dependent study, at least 4M concentration of GdnHCL was necessary to measure higher O.D. values in BH samples by the D-5 ELISA method (Figure 3-16.B). In the Chapter 2, the 7-5 ELISA method also showed similar outcomes that 4-5M GdnHCL enhanced higher PrP detections in TSE-infected BH samples (Figure 2-16.A to C, Chapter 2). Thus, higher GdnHCL concentrations are essential for enhancing higher detections of PrP^{Sc} levels in denatured TSE-infected materials by Sandwich ELISA methods. However, PrP levels in TSE-infected materials decreased with prolonged coating times on ELISA plates, pre-coated with capture antibodies for the D-5 and 7-5 ELISA methods (Figures 3-17.A and B). In these experiments, prepared samples exhibited aggregated clusters around the 20-minute time point during waiting times for coating on the plates. This aggregation was increasingly observed according to the time course, but a reason or cause of this cluster aggregation was unclear. These observations suggested that testing samples must be coated on the prepared ELISA plates immediately after processes of sample denaturation and dilution.

Using the RML-inoculated BH sample and its controls, multiple capture antibodies were compared in the Sandwich ELISA approach with the detecting antibody PRC5 mAb under the 7-5 and D-5 ELISA protocols (Figures 3-18.A to L). This study evaluated specificities of these two Sandwich ELISA methods for the PrP detection in TSE-infected materials. The six capture antibodies were categorized into the three groups, based on binding epitopes of these antibodies on domains of the PrP structure: 1) structured globular domain of C terminus (PRC7, D18, 6H4); 2) unstructured flexible domain at N terminus (POM2, SAF-32); and 3) hydrophobic core region adjacent to the cleavage of unstructured and structured domains between N- and C-termini (mAb132).

Except for the mAb 132, other capture antibodies were able to detect higher PrP levels in the denatured RML-infected BH sample, compared to its control, using the detecting antibody PRC5 mAb for Sandwich ELISA methods (Figures 3-18.A to F). Specifically, the capture antibodies binding to the C terminus of the PrP structure (the Group 1) showed significantly higher PrP detections in the infected materials than other antibody groups (Figure 3-18.A to C). Intriguingly, the POM2 mAb detected high PrP levels in the denatured uninfected FVB/n BH sample (Figure 3-18.D). In contrast, PRC7, D18, and 6H4 mAbs measured no or subtle amounts, compared with a PrP-KO mouse BH sample (Figure 3-18.A to C). These results indicated that the POM2 mAb exhibited high binding probabilities to PrP conformers, because of its four different binding epitopes at the N-terminus. In addition, denaturation was not influential to the unstructured flexible domain of the N-terminus in the PrP structure.

Moreover, PRC7, SAF-32, and mAb132 mAbs were not capable of measuring PrP levels in tested samples under the non-denatured condition. D18 and 6H4 mAbs measured higher PrP^C levels in the uninfected BH sample, compared to the RML-infected material. However, the POM2 capture antibody showed similar values of the PrP detections in both infected and uninfected BH samples. Therefore, these observations suggested the following possibilities about PrP^C detections in TSE-infected animals: 1) decreased PrP^C levels reflect the reduced amount of PrP productions in TSE-infected cells or the loss of PrP^C-expressing cells (cell death); and 2) the PrP^C molecule might have the conformational modification on its structured globular domain of the C-terminus, because the PrP detection targeting to the N-terminus did not show clear differences between infected and uninfected BH samples. Since TSEs alter the

PrP conformation from a predominantly α-helix PrP^{C} structure to a β-sheet rich PrP^{Sc} structure, targeting the structured globular domain of the C-terminus could be an appropriate approach to evaluate PrP levels between TSE-infected and uninfected samples. Thus, the D-5 ELISA approaches can be useful to analyze PrP conformational modulations in TSE-infected samples with or without denaturation.

To determine modulations of PrP levels observed above, both the 7-5 ELISA and D-5 ELISA methods evaluated BH samples from various murine models of different TSE inocula with and without GdnHCL denaturation: RML mouse-adapted scrapie, CWD (Bala05-0308), CWD (99W12389), sheep scrapie, and TME 941031 (Figures 3-19.A to Y). Testing BH samples included all TSE-infected mice and their controls with different PrP species background. With denaturation, the 7-5 ELISA method specifically measured high PrP levels in all infected samples (Figures 3-19.A, E, I, M, Q, U, and Y). This finding indicated preferential generations of unglycosyl and mono-1 glycosyl PrP forms during the disease development and terminal stage. Also, the D-5 ELISA method detected increases of total PrP levels in these TSE-infected mice with denaturation (Figures 3-19.B, F, J, N, R, and V). Since the D18 Fab Ab requires denaturation to detect PrP^{Sc} agents, the majority of the detected PrP molecules must be the pathological conformers. According to the D-5 ELISA results without denaturation, the infected mice decreased PrP^{C} levels at terminal stages of the TSE progression. Since these mice increased total PrP (PrP^{Sc}) amounts, modulations of PrP^{C} and PrP^{Sc} levels could implicate with pathological developments and progressions of various TSEs in different species backgrounds.

In addition, these PrP modulations might affect PrP^C-mediated functions. Intriguingly, the 7-5 ELISA and D-5 ELISA methods did not measure abnormal PrP^C-PrP^{Sc} modulations in sub-clinical conditions of Tg5037 mice with CWD inoculations (Figures 3-21.A to H). In fact, these sub-clinical animals exhibited similar PrP levels to uninfected Tg5037 mice. However, uninfected transgenic mice with PrP overexpressions spontaneously developed neurological dysfunctions and progressions.[34] In the laboratory database, some records indicated spontaneous disease developments in uninfected transgenic mice with PrP overexpressions. Therefore, excessive PrP generations could be toxic to mice and could induce pathological conditions in the nervous system.

Based on the outcome from the uninfected transgenic mice, the D-5 ELISA method detected GdnHCL-resistant PrP^C molecules (Figures 3-19.E to Y). Also, the 7-5 ELISA method measured the generation of under-glycosylated PrP forms under the non-TSE condition both with and without denaturation. A transgenic mouse breed line with murine PrP expressions (Tg4112) exhibited these PrP detections in BH samples. Their PrP molecules, including under-glycosylated forms, were resistant to a lower dose of proteinase K (PK) (Figures 3-20.C and J). These observations suggested that under-glycosylated PrP forms generated in transgenic mice might have different conformations, compared to the normal PrP^C structure that is PK-sensitive and the diglycosyl form. In addition to detectable amounts of total PrP levels, the glycosylation state could be essential in maintaining healthy conditions and developing pathological abnormalities. As an example, congenital disorder of glycosylation is known as causing severe neurological dysfunctions due to the defective or deficient modulation of

glycosylations.[62,63] Therefore, the ELISA approaches could evaluate the PrP detection and glycosylation states as possible underlying mechanisms of the PrP abnormality, converting from normal to pathological/toxic conformers in the condition with PrP overexpressions or excessive generations.

In a transgenic mouse model of Gerstmann-Sträussler-Scheinker syndrome (GSS), the pilot study evaluated the PrP modulations through the disease course. The 7-5 and D-5 ELISA methods were capable of measuring PK-sensitive PrP molecules in the GSS mouse model. Similar to animal TSEs described above, higher doses of GdnHCL denaturation were necessary to detect and enhance PrP levels in BH samples from spontaneously disease-developed Tg464 mice (GSS-developed mice) using the 7-5 ELISA method (Figures 3-24.B to D). Compared to the younger ages of the hemizygous Tg464 mice without any clinical signs, the 7-5 ELISA method increased detections of under-glycosylated PrP forms in the GSS-developed mice (Figure 3-24.E). Intriguingly, the D-5 ELISA method identified the time-dependent (longitudinal) modulation of PrP^{C} and PrP^{Sc} detections in BH samples from Tg464 mice at pre- and post- onset of GSS clinical signs (Figure 3-24.F). As described above, the D-5 ELISA method is capable of detecting only PrP^{C} molecules without denaturation, or PrP^{Sc} agents with denaturation, based on the feature of the D18 Fab Ab reactivity. Under the D-5 ELISA approach, PrP^{Sc} levels did not change in the GdnHCL-treated BH samples of Tg464 mice at three different time points, prior to the onset of clinical signs. Also, these PrP^{Sc} levels are lower O.D. values than PrP^{C} levels (detected without denaturation) in the same animals. The Tg464 mouse with GSS clinical signs exhibited a higher PrP^{Sc} detection than the PrP^{C} level (Figure 3-24.F). In addition, tested Tg464 mice decreased

PrP^{C} levels toward to the GSS disease onset. These observations indicated that these Tg464 mice exhibited clinical signs when the PrP^{Sc} level exceeded the PrP^{C} level. Moreover, these PrP modulations might affect physiological functions in which PrP^{C} isoforms mediate. Eventually, GSS-developed mice would present clinical signs and neurological deficits. Notably, these D-5 ELISA results identified that Tg464 mice with the P101L mutation generated both PrP^{C} isoforms and PrP^{Sc} conformers. Hence, some factors or mechanisms initiated the conformational conversion from mutated PrP^{C} molecules to pathological structures. In this aspect, the 7-5 ELISA results indicated one possibility for this misfolding mechanism (Figure 3-24.G). At the second earliest time point (81 days) in Tg464 mice, the detectable level of under-glycosylated PrP forms increased. In contrast, PrP^{C} levels decreased from 81 days to the GSS onset (Figure 3-24.F). These observations suggested that the generation of under-glycosylated PrP forms could be pathological evidence at early stages of the TSE disease progression. Possibly, under-glycosylated PrP forms were immature states of the PrP^{C} generation in Tg464 mice. Or, the TSE development might defect or impair the glycosidic process through the PrP^{C} synthesis in affected cells.

As proposed, the loss of full glycosylation implicates with the TSE pathogenesis. Since glycosylation is important to preserve the protein structure and stability, the glycosidic modulation can initiate unstable conditions for maintaining proper PrP^{C} conformations. Consequently, these unstable states might be prone to alter PrP^{C} structures abnormally. These aberrant formations would impair functions of normal prion protein during the disease development. Therefore, the generation of under-glycosylated PrP forms must be a hallmark of TSEs as a diagnostic biomarker for the

disease progression. Obviously, the 7-5 ELISA and D-5 ELISA methods are capable of analyzing PrP modulations in the TSE disease development. For future directions, these established analytical methods would be applicable for longitudinal and kinetic studies of the PrP modulation (both PrP^{C} and PrP^{Sc} levels) in TSE mouse models. In addition to histological and other standard PrP analyses, electrodiagnoses (i.e. EEG, EMG) and biomechanical gait analyses would be useful tools for evaluating neurological functions and abnormalities. In the diagnostic advantages for detecting PK-sensitive PrP molecules, the 7-5 and D-5 ELISA approaches will provide more accurate PrP^{Sc} analyses in the TSE research and public health, including human and veterinary medical fields.

REFERENCES

1. Chandler RL. Encephalopathy in mice produced by inoculation with scrapie brain material. *Lancet* 1961;1:1378–9.
2. Weissmann C, Fischer M, Raeber A, Büeler H, Sailer A, Shmerling D, *et al.* The use of transgenic mice in the investigation of transmissible spongiform encephalopathies. *Rev - Off Int Epizoot* 1998;17:278–90.
3. Bartz JC, Bessen RA, McKenzie D, Marsh RF, Aiken JM. Adaptation and selection of prion protein strain conformations following interspecies transmission of transmissible mink encephalopathy. *J Virol* 2000;74:5542–7.
4. Barron RM, Thomson V, King D, Shaw J, Melton DW, Manson JC. Transmission of murine scrapie to P101L transgenic mice. *J Gen Virol* 2003;84:3165–72.
5. Agrimi U, Nonno R, Dell'Omo G, Di Bari MA, Conte M, Chiappini B, *et al.* Prion protein amino acid determinants of differential susceptibility and molecular feature of prion strains in mice and voles. *PLoS Pathog* 2008;4:e1000113.
6. Groschup MH, Buschmann A. Rodent models for prion diseases. *Vet Res* 2008;39:32.
7. Di Bari MA, Chianini F, Vaccari G, Esposito E, Conte M, Eaton SL, *et al.* The bank vole (Myodes glareolus) as a sensitive bioassay for sheep scrapie. *J Gen Virol* 2008;89:2975–85.
8. Di Bari MA, Nonno R, Castilla J, D'Agostino C, Pirisinu L, Riccardi G, *et al.* Chronic wasting disease in bank voles: characterisation of the shortest incubation time model for prion diseases. *PLoS Pathog* 2013;9:e1003219.
9. Watts JC, Prusiner SB. Mouse models for studying the formation and propagation of prions. *J Biol Chem* 2014;289:19841–9.
10. Bian J, Napier D, Khaychuck V, Angers R, Graham C, Telling G. Cell-based quantification of chronic wasting disease prions. *J Virol* 2010;84:8322–6.
11. Bian J, Kang H-E, Telling GC. Quinacrine promotes replication and conformational mutation of chronic wasting disease prions. *Proc Natl Acad Sci USA* 2014;111:6028–33.
12. Klöhn P-C, Stoltze L, Flechsig E, Enari M, Weissmann C. A quantitative, highly sensitive cell-based infectivity assay for mouse scrapie prions. *Proc Natl Acad Sci USA* 2003;100:11666–71.
13. Clarke MC, Haig DA. Evidence for the multiplication of scrapie agent in cell culture. *Nature* 1970;225:100–1.
14. Birkett CR, Hennion RM, Bembridge DA, Clarke MC, Chree A, Bruce ME, *et al.* Scrapie strains maintain biological phenotypes on propagation in a cell line in culture. *EMBO J* 2001;20:3351–8.
15. Williamson RA, Peretz D, Pinilla C, Ball H, Bastidas RB, Rozenshteyn R, *et al.* Mapping the prion protein using recombinant antibodies. *J Virol* 1998;72:9413–8.
16. Féraudet C, Morel N, Simon S, Volland H, Frobert Y, Créminon C, *et al.* Screening of 145 anti-PrP monoclonal antibodies for their capacity to inhibit PrP^{Sc} replication in infected cells. *J Biol Chem* 2005;280:11247–58.

17. Kim C-L, Umetani A, Matsui T, Ishiguro N, Shinagawa M, Horiuchi M. Antigenic characterization of an abnormal isoform of prion protein using a new diverse panel of monoclonal antibodies. *Virology* 2004;320:40–51.
18. Yamasaki T, Suzuki A, Shimizu T, Watarai M, Hasebe R, Horiuchi M. Characterization of intracellular localization of PrP(Sc) in prion-infected cells using a mAb that recognizes the region consisting of aa 119-127 of mouse PrP. *J Gen Virol* 2012;93:668–80.
19. Nazor KE, Kuhn F, Seward T, Green M, Zwald D, Pürro M, *et al.* Immunodetection of disease-associated mutant PrP, which accelerates disease in GSS transgenic mice. *EMBO J* 2005;24:2472–80.
20. Kang H-E, Weng CC, Saijo E, Saylor V, Bian J, Kim S, *et al.* Characterization of conformation-dependent prion protein epitopes. *J Biol Chem* 2012;287:37219–32.
21. Saijo E, Kang H-E, Bian J, Bowling KG, Browning S, Kim S, *et al.* Epigenetic dominance of prion conformers. *PLoS Pathog* 2013;9:e1003692.
22. Angers R, Christiansen J, Nalls AV, Kang H-E, Hunter N, Hoover E, *et al.* Structural effects of PrP polymorphisms on intra- and interspecies prion transmission. *Proc Natl Acad Sci USA* 2014;111:11169–74.
23. Baeten LA, Powers BE, Jewell JE, Spraker TR, Miller MW. A natural case of chronic wasting disease in a free-ranging moose (Alces alces shirasi). *J Wildl Dis* 2007;43:309–14.
24. Kreeger TJ, Montgomery DL, Jewell JE, Schultz W, Williams ES. Oral transmission of chronic wasting disease in captive Shira's moose. *J Wildl Dis* 2006;42:640–5.
25. Angers RC, Seward TS, Napier D, Green M, Hoover E, Spraker T, *et al.* Chronic wasting disease prions in elk antler velvet. *Emerging Infect Dis* 2009;15:696–703.
26. Angers RC, Kang H-E, Napier D, Browning S, Seward T, Mathiason C, *et al.* Prion strain mutation determined by prion protein conformational compatibility and primary structure. *Science* 2010;328:1154–8.
27. Gabizon R, McKinley MP, Prusiner SB. Purified prion proteins and scrapie infectivity copartition into liposomes. *Proc Natl Acad Sci USA* 1987;84: 4017–21.
28. Gabizon R, Prusiner SB. Prion liposomes. *Biochem J* 1990;266:1–14.
29. Peretz D, Williamson RA, Kaneko K, Vergara J, Leclerc E, Schmitt-Ulms G, *et al.* Antibodies inhibit prion propagation and clear cell cultures of prion infectivity. *Nature* 2001;412:739–43.
30. Prion 2015 poster abstracts. *Prion* 2015;9 Suppl 1:S11-99.
31. Tanaka M, Fujiwara A, Suzuki A, Yamasaki T, Hasebe R, Masujin K, *et al.* Comparison of abnormal isoform of prion protein in prion-infected cell lines and primary-cultured neurons by PrPSc-specific immunostaining. *J Gen Virol* 2016;97:2030–42.
32. Shan Z, Yamasaki T, Suzuki A, Hasebe R, Horiuchi M. Establishment of a simple cell-based ELISA for the direct detection of abnormal isoform of prion protein from prion-infected cells without cell lysis and proteinase K treatment. *Prion* 2016;10:305–18.

33. Yamasaki T, Suzuki A, Hasebe R, Horiuchi M. Flow Cytometric Detection of PrP^{Sc} in Neurons and Glial Cells from Prion-Infected Mouse Brains. *J Virol* 2018;92:.
34. Westaway D, DeArmond SJ, Cayetano-Canlas J, Groth D, Foster D, Yang SL, *et al.* Degeneration of skeletal muscle, peripheral nerves, and the central nervous system in transgenic mice overexpressing wild-type prion proteins. *Cell* 1994;76:117–29.
35. Yuan J, Xiao X, McGeehan J, Dong Z, Cali I, Fujioka H, *et al.* Insoluble aggregates and protease-resistant conformers of prion protein in uninfected human brains. *J Biol Chem* 2006;281:34848–58.
36. Yuan J, Dong Z, Guo J-P, McGeehan J, Xiao X, Wang J, *et al.* Accessibility of a critical prion protein region involved in strain recognition and its implications for the early detection of prions. *Cell Mol Life Sci* 2008;65:631–43.
37. Zou W-Q, Zhou X, Yuan J, Xiao X. Insoluble cellular prion protein and its association with prion and Alzheimer diseases. *Prion* 2011;5:172–8.
38. Zou RS, Fujioka H, Guo J-P, Xiao X, Shimoji M, Kong C, *et al.* Characterization of spontaneously generated prion-like conformers in cultured cells. *Aging (Albany NY)* 2011;3:968–84.
39. Xiong LW, Raymond LD, Hayes SF, Raymond GJ, Caughey B. Conformational change, aggregation and fibril formation induced by detergent treatments of cellular prion protein. *J Neurochem* 2001;79:669–78.
40. Horiuchi M, Baron GS, Xiong LW, Caughey B. Inhibition of interactions and interconversions of prion protein isoforms by peptide fragments from the C-terminal folded domain. *J Biol Chem* 2001;276:15489–97.
41. Cronier S, Gros N, Tattum MH, Jackson GS, Clarke AR, Collinge J, *et al.* Detection and characterization of proteinase K-sensitive disease-related prion protein with thermolysin. *Biochem J* 2008;416:297–305.
42. Sandberg MK, Al-Doujaily H, Sharps B, De Oliveira MW, Schmidt C, Richard-Londt A, *et al.* Prion neuropathology follows the accumulation of alternate prion protein isoforms after infective titre has peaked. *Nat Commun* 2014;5:4347.
43. Sajnani G, Silva CJ, Ramos A, Pastrana MA, Onisko BC, Erickson ML, *et al.* PK-sensitive PrP is infectious and shares basic structural features with PK-resistant PrP. *PLoS Pathog* 2012;8:e1002547.
44. Peretz D, Scott MR, Groth D, Williamson RA, Burton DR, Cohen FE, *et al.* Strain-specified relative conformational stability of the scrapie prion protein. *Protein Sci* 2001;10:854–63.
45. Bett C, Joshi-Barr S, Lucero M, Trejo M, Liberski P, Kelly JW, *et al.* Biochemical properties of highly neuroinvasive prion strains. *PLoS Pathog* 2012;8:e1002522.
46. Käsermann F, Kempf C. Sodium hydroxide renders the prion protein PrP^{Sc} sensitive to proteinase K. *J Gen Virol* 2003;84:3173–6.
47. Unal A, Thyer J, Uren E, Middleton D, Braun M, Maher D. Investigation by bioassay of the efficacy of sodium hydroxide treatment on the inactivation of mouse-adapted scrapie. *Biologicals* 2007;35:161–4.
48. Prusiner SB. Molecular biology and transgenetics of prion diseases. *Crit Rev Biochem Mol Biol* 1991;26:397–438.

49. Hsiao K, Prusiner SB. Molecular genetics and transgenic model of Gertsmann-Sträussler-Scheinker disease. *Alzheimer Dis Assoc Disord* 1991;5:155–62.
50. Hsiao K, Scott M, Foster D, DeArmond SJ, Groth D, Serban H, *et al.* Spontaneous neurodegeneration in transgenic mice with prion protein codon 101 proline----leucine substitution. *Ann N Y Acad Sci* 1991;640:166–70.
51. Yang W, Cook J, Rassbach B, Lemus A, DeArmond SJ, Mastrianni JA. A New Transgenic Mouse Model of Gerstmann-Straussler-Scheinker Syndrome Caused by the A117V Mutation of PRNP. *J Neurosci* 2009;29:10072–80.
52. Asante EA, Linehan JM, Smidak M, Tomlinson A, Grimshaw A, Jeelani A, *et al.* Inherited prion disease A117V is not simply a proteinopathy but produces prions transmissible to transgenic mice expressing homologous prion protein. *PLoS Pathog* 2013;9:e1003643.
53. Asante EA, Grimshaw A, Smidak M, Jakubcova T, Tomlinson A, Jeelani A, *et al.* Transmission Properties of Human PrP 102L Prions Challenge the Relevance of Mouse Models of GSS. *PLoS Pathog* 2015;11:e1004953.
54. Mercer RCC, Daude N, Dorosh L, Fu Z-L, Mays CE, Gapeshina H, *et al.* A novel Gerstmann-Sträussler-Scheinker disease mutation defines a precursor for amyloidogenic 8 kDa PrP fragments and reveals N-terminal structural changes shared by other GSS alleles. *PLoS Pathog* 2018;14:e1006826.
55. Zou W-Q, Zheng J, Gray DM, Gambetti P, Chen SG. Antibody to DNA detects scrapie but not normal prion protein. *Proc Natl Acad Sci USA* 2004;101: 1380–5.
56. Tzaban S, Friedlander G, Schonberger O, Horonchik L, Yedidia Y, Shaked G, *et al.* Protease-sensitive scrapie prion protein in aggregates of heterogeneous sizes. *Biochemistry* 2002;41:12868–75.
57. Collinge J, Clarke AR. A general model of prion strains and their pathogenicity. *Science* 2007;318:930–6.
58. Silveira JR, Raymond GJ, Hughson AG, Race RE, Sim VL, Hayes SF, *et al.* The most infectious prion protein particles. *Nature* 2005;437:257–61.
59. Taylor DM, Dickinson AG, Fraser H, Marsh RF. Evidence that transmissible mink encephalopathy agent is biologically inactive in mice. *Neuropathol Appl Neurobiol* 1986;12:207–15.
60. Bartz JC, McKenzie DI, Bessen RA, Marsh RF, Aiken JM. Transmissible mink encephalopathy species barrier effect between ferret and mink: PrP gene and protein analysis. *J Gen Virol* 1994;75 (Pt 11):2947–53.
61. Bartz JC, Kincaid AE, Bessen RA. Retrograde transport of transmissible mink encephalopathy within descending motor tracts. *J Virol* 2002;76:5759–68.
62. Jaeken J. Congenital disorders of glycosylation. *Handb Clin Neurol* 2013;113:1737–43.
63. Parkinson WM, Dookwah M, Dear ML, Gatto CL, Aoki K, Tiemeyer M, *et al.* Synaptic roles for phosphomannomutase type 2 in a new Drosophila congenital disorder of glycosylation disease model. *Dis Model Mech* 2016;9:513–27.

CHAPTER 4

EVALUATION OF THE UTILITY OF THE 7-5 ELISA METHOD AS A DIAGNOSTIC TOOL FOR TSES IN CERVIDS

Summary

This dissertation hypothesizes that the generation of under-glycosylated PrP forms is a key hallmark of diagnostic biomarkers for the TSE-infection state and disease progression. In this chapter, the 7-5 ELISA method evaluated cervid tissue samples to address this hypothesis in chronic wasting disease (CWD). Successfully, the 7-5 ELISA method detected under-glycosylated PrP forms in CWD-infected BH samples from elk, deer and moose, but not in the CWD-negative control. Importantly, the ELISA result corresponded to WB in tested deer brain samples. Moreover, the 7-5 ELISA method could detect PrP levels in CWD-infected analyte that WB could not identify. Hence, the analytical sensitivity of the 7-5 ELISA method could overcome a threshold limitation of WB for the PrP detection. In addition, the 7-5 ELISA method detected higher PrP levels in non-nervous tissues from CWD-positive cervid, compared to the uninfected control. These observations indicated that CWD-positive animals prominently generated under-glycosylated PrP forms in both nervous and non-nervous tissues and organs. Therefore, the 7-5 ELISA method is a useful tool to determine under-glycosylated PrP forms, which are hallmark biomarkers in the TSE pathogenesis and diagnosis.

Introduction

CWD is the first TSE, identified in free-ranging (wild) animal populations. This infectious disease occurs only in the family Cervidae (cervid ruminants), such as mule deer, white-tailed deer, black-tailed deer, elk, moose, and reindeer.[1] CWD-affected cervid has also been found in the captivity nature. After the first identification in 1967 (later published as the TSE pathology in 1980), CWD incidences have pandemically expanded throughout the US, Canada, South Korea, and Norway.[2-6] In North America, CWD has annually spread its incidences throughout geographical ranges. However, causative factors for geographic distributions of the CWD prevalence are not confirmed yet.[7]

CWD agents transmit through horizontal (animals to animals) and vertical (maternal) pathways.[8-13] Dependent on herds and living areas, the CWD morbidity varies from 1% to over 90% rates.[2,8,14-17] In fact, cervid animals that are born and/or live in endemic CWD areas suffer from higher rates of the disease occurrence and prevalence. For instance, elk in the Rocky Mountain area exhibited 80% rate of the mother-to-offspring transmissions in CWD-infected dams.[12]

In public health, the CWD transmission is not evident from cervids to humans via the consumption of venison or related products. However, a recent study revealed that CWD agents converted recombinant human PrP^{C} molecules, and also formed amyloid aggregations.[18] Since antler velvets and skeletal muscles of CWD-infected animals contain infectious PrP^{Sc} isoforms, the longitudinal consumption of these products could be a source of CWD transmissions to humans, which ingested CWD agents might remain and accumulate in human bodies.[19-24] Thus, CWD might expand a potential risk

to develop a new variant of food-borne diseases as zoonotic TSE in humans. Therefore, CWD surveillance and research are still important subjects in public health. To prevent potential CWD transmissions, sensitive analytical methods are critically important for detecting PrP^{Sc} agents and TSE infection states.

For this aim, PrP glycosylations are distinctive targets that influence PrP^{Sc} isoforms for crossing the species barriers and forming PK-resistances with conformational stabilities.[25-27] Although CWD-infected brain samples abundantly exhibit diglycosyl forms, these samples also highly express under-glycosylated forms.[1,28] Thus, monitoring the PrP-glycosidic patterns and PrP-expressional modifications would be enable to evaluate the TSE infection state and the transmissive efficiency between different species. Therefore, targeting abnormalities of the PrP glycosylation will be essential approaches to eradicate future TSE epidemics, resulting in preventive managements for human populations from potential CWD exposures. In this chapter, the 7-5 ELISA method will demonstrate its analytical feature and utility in the CWD diagnosis using cervid tissue analyte.

Materials and Methods

The 7-5 ELISA method for Cervid Tissues

At first, the PRC7 mAb, a capture antibody of the 7-5 ELISA method, was diluted with a coating buffer (0.05M Carbonate-Bicarbonate in distilled water) to be 20μg/ml concentration. Subsequently, 100μl of the diluted PRC7 solution was added per well on a 96-well ELISA plate (Nunc MaxiSorp® flat-bottom 96-well plate, Thermo Fisher Scientific, Rochester, New York, USA). This ELISA plate was incubated overnight at

4°C. After removing all solutions from the ELISA plate, 200µl of a blocking buffer, which contained 3% of bovine serum albumin (BSA: Sigma-Aldrich Co. LLC, St. Louis, Missouri, USA) into 1X phosphate buffered saline (PBS: no calcium and magnesium, HyClone Laboratories, Inc. GE Healthcare Life Sciences, Logan, Utah, USA), was added into each well to minimize non-specific binding sites on well surfaces. The plate was incubated at 37°C for one hour. During this incubation time, testing brain/tissue homogenate samples were prepared for coating into wells on the plate. In this Chapter 4, all testing homogenate samples were analyzed with 200µg/ml of each sample as the final protein concentration. For planning a technical triplicate (testing three wells per sample) with coating 100µl of the processed sample (200µg/ml) per well (total protein 20µg in each well), 400µl of the final volume was prepared for each analyte. As the first step (sample dilution), testing homogenate samples were diluted with 1X PBS (no calcium and magnesium) to be 5.87mg/ml. Second (detergent), 10% Triton X-100 (TX100) was added into each homogenate sample to be 1% concentration: 1.5µl of 10% TX100 in 1X PBS was added into 13.5µl of the diluted homogenate sample (5.87mg/ml) (= total 15µl volume of 5.33mg/ml protein concentration with 1% TX100 at this point). This mixed analyte was incubated for one hour at 37°C with 1000rpm agitation. Third (denaturation), the incubated sample (15µl) was mixed with 25µl of 8M guanidine hydrochloride (GdnHCL: G3272, Sigma-Aldrich Co. LLC, St. Louis, Missouri, USA) in 1X TBS-Tween buffer (TBST: 50mM Tris, 150mM NaCl, 0.05% Tween-20 in distilled water, pH 7.6). In this denaturation step, a final concentration of GdnHCL was 5M in 40µl of the sample volume that contained 2mg/ml concentration of a testing homogenate sample. This mixture was incubated for 15 minutes at 37°C with 1000rpm

agitation. Fourth (10-time dilution), immediately after the incubation, 360µl of a dilution buffer (1% BSA-containing PBS: no calcium and magnesium) was added into each denatured sample, and then mixed together. At this final step of the sample preparation, the total sample volume was 400µl (200µg/ml concentration of a testing homogenate sample) with 0.5M GdnHCL. Once the incubation of the blocking process was completed, all blocking solutions were removed from the ELISA plate. Subsequently, the plate was washed three times with 1X TBST by a plate washer (the Finstruments™ Microplate Washer, MTX Lab Systems, Inc. Vienna, Virginia, USA). Thereafter, 100µl of each prepared homogenate sample (200µg/ml) was transferred into each designated well (total protein 20µg per well; well number = 3 as a technical triplicate) on the processed ELISA plate. This sample-coated plate was incubated overnight at 4°C. Followed by this incubation, the plate was emptied and washed three times with 1X TBST by the plate washer. The detecting antibody PRC5 mAb was diluted as 1:5,000 ratio in a dilution buffer (1% BSA-containing PBS without calcium and magnesium). After adding 100µl of the diluted PRC5 solution per well for all testing wells, the ELISA plate was incubated for one hour at 37°C. After that, the plate was evacuated and washed three times with 1X TBST by the plate washer. At the same time, a horseradish peroxidase (HRP)-conjugated secondary antibody (Goat Anti-Mouse IgG2a HRP conjugate, 1mg/ml, Alpha Diagnostic Intl. Inc. Texas, USA) was prepared to be 1:5,000 ratio in a dilution buffer. Once all solutions were cleared from the plate, 100µl of the diluted secondary antibody solution was added into each well for all testing wells on the plate. Following one hour incubation of the plate at 37°C, all solutions were removed from the plate, which was washed seven times with 1X TBST by the plate washer.

ABTS® Peroxidase Substrate (KPL, Inc. Maryland, USA) was applied to the plate for evaluating an enzymatic reaction and color development under the manufacturer's protocol. The absorbency of each well on the ELISA plate was analyzed by an ultramicroplate reader (ELx808 Absorbance Reader, BioTek Instruments, Inc, Winooski, Vermont, USA) at a wavelength of 405nm.

Tested tissue homogenate samples

Brain and non-brain tissue samples derived from cervid (deer, elk, and moose) were homogenated to 10% in cold 1X PBS by an automatic tissue homogenizer (FastPrep®-24 Instrument, MP Biomedicals LLC, Solon. Ohio, USA) under the manufacturer's protocol, and then repeatedly extracted using different sizes of syringe needles. A protein concentration of each homogenate sample was measured by an ultramicroplate reader (ELx808 Absorbance Reader, BioTek Instruments, Inc, Winooski, Vermont, USA), using the BCA Protein Assay Kit (Pierce™ BCA Protein Assay Kit) under the manufacturer's protocol. All prepared samples were evaluated by the 7-5 ELISA method, under the protocol above, in the following three different sections for each experimental purpose.

1) Pilot applications of cervid tissue samples with the 7-5 ELISA method: The utility of the 7-5 ELISA method was evaluated specifically for PrP^{Sc} detections in infected materials with chronic wasting disease (CWD). The following brain homogenate (BH) samples were derived from CWD negative and positive cervid (Table 4). This experiment also included PrP-KO mouse BH samples. As noted below, there are three genotypes of the prion protein gene (PRNP) at the codon 132 of elk: MM, ML, and ML

(M = Methionine; L = Leucine).[29] In addition, three pairs of brain and lymph node tissue samples from the same three animals (one elk, one whitetail deer and one red deer) were provided by Ms. Carla Calvi, a former research coordinator in the CSU Prion Research Center, who initially obtained the samples from Dr. Mark Zabel's laboratory in the Department of Microbiology, Immunology and Pathology at Colorado State University (Table 5). The 7-5 ELISA method analyzed these paired tissue samples with the controls (PrP-KO mouse and CWD-negative elk BH samples).

2) Testing non-brain tissue samples from cervids by the 7-5 ELISA method: Multiple types of tissue samples isolated from one CWD-negative (#502) and two CWD-positive deer (#782 and #785, experimentally inoculated) were kindly provided by Dr. Edward Hoover's laboratory. In addition to the brain samples (obex) from these three deer, the 7-5 ELISA method examined six other non-brain tissue samples: parotid lymph node, tonsil, vagus nerve, third eyelid, muscle and rectum (Table 6). BH samples from PrP-KO, uninfected FVB/n, and RML (Rocky Mountain Laboratories strain)-inoculated FVB/n mice were included as the negative and positive controls of the 7-5 ELISA method.

Table 4. Tested brain samples by the 7-5 ELISA method for detecting CWD prion

Sample	Species	Tissue	CWD
PrP-KO A	Mouse	Brain	Negative
PrP-KO B	Mouse	Brain	Negative
PrP-KO C	Mouse	Brain	Negative
FR56.98	Deer	Brain	Negative
AK03008	Elk (ML)*	Brain	Negative
AK03024	Elk (LL)*	Brain	Negative
Db99	Deer	Brain	Positive
99W12389	Elk (MM)*	Brain	Positive
03-3297	Elk (ML)*	Brain	Positive
03-3355	Elk (LL)*	Brain	Positive
08W-11,741	Moose	Brain	Positive

*M = Methionine (Met); L = Leucine (Leu)

Table 5. Paired tissue samples derived from CWD-positive cervid

Species	CWD	Brain	Lymph node
Elk	Positive	Tested	Tested
Whitetail deer	Positive	Tested	Tested
Red deer	Positive	Tested	Tested

Note: The 6 control BH samples in Table 1 (PrP-KO A B C, FR56.98, AK03008 and AK03024) were included in this 7-5 ELISA experiment.

Table 6. Deer tissue samples from Dr. Edward Hoover's Laboratory

Deer	CWD	Obex	PLD*	Tonsil	VN**	TE***	Muscle	RM****
#502	Negative	Tested	Tested	Tested	Tested	Tested	Tested	Tested
#782	Positive	Tested	Tested	Tested	Tested	Tested	Tested	Tested
#785	Positive	Tested	Tested	Tested	Tested	Tested	Tested	Tested

*PLD = parotid lymph node; VN= vagus nerve; ***TE= Third eyelid; ****RM=Rectum

3) Sensitivity of the 7-5 ELISA method for subtle PrP levels in CWD-affected elk brain samples:

Elk brain samples from two different herds. Dr. Tracy Nichols, the USDA National Wildlife Research Center (NWRC), in Fort Collins, Colorado, kindly provided eleven CWD-positive elk brain samples, which Dr. Jeffrey Christiansen, a postdoctoral fellow in the Prion Research Center at CSU, initially obtained. Based on the sample background information from Dr. Nichols, these elk showed clinical signs of CWD disease developments. The elk brain samples were originated from two herd groups: Syb and NWRC. The Syb group of elk herd was settled into the highly CWD-affected research site in Wyoming for CWD exposures. Seven Syb elk died in short terms after their settlement. The NWRC group of elk with "T" numbers was herded in the low CWD-contaminated area near Fort Collins, Colorado. Four NWRC animals showed clinical signs terminally, and the CWD infection state was confirmed with immunohistochemistry (IHC) for these four brains. However, western blot (WB) analyses using proteinase K (PK) could not detect PK-resistant PrP agents (=PrP^{Sc}) in the 6 brain samples (3 Syb and 3 NWRC elk) among the 11 elk (7 Syb and 4 NWRC elk), which Dr. Christiansen tested with the PRC5 mAb that can react with all four states of PrP glycosylated forms (Figure 3-A). To evaluate the threshold limitation to detect subtle amounts of PrP^{Sc} agents and the existences of PK-sensitive PrP^{Sc} forms in these CWD-infected elk, the 7-5 ELISA method was applied to all elk brain samples above. This experiment also determined a sensitivity of this ELISA approach for CWD detections. In addition, two BH samples from CWD-negative elk were analyzed: AK03008 and AK03024 were isolated from elk in a certain CWD-free island in Alaska. The controls in the 7-5 ELISA

experiment included murine BH samples from PrP-KO, uninfected wild-type FVB/n, RML-inoculated FVB/n, uninfected Tg5037 (ElkPrP), and CWD (Bala05 strain)-inoculated Tg5037 mice.

Table 7. Elk brain samples from two herd groups and control samples

Species	TSE state	Numbers	Animals
Elk Syb	CWD (Wyoming)	7	Syb 7, Syb 13, Syb 21, Syb 27, Syb 35, Syb J19, Syb J27
Elk NWRC	CWD (Colorado)	4	T45-7353, T56-1821, T56-4100, T90-3137
Elk Alaska	Negative	2	AK03008 (Elk-1 CWD-), AK03024 (Elk-2 CWD-)
Mouse	Negative	1	PrP-KO
Mouse	Negative	1	FVB/n
Mouse	Negative	1	Tg5037 (ElkPrP)
Mouse	RML	1	FVB/n
Mouse	CWD (Bala05, Canada)	1	Tg5037 (ElkPrP)

Multiple CWD-positive cervid brain samples. The CWD infection states of multiple cervid brain samples isolated were previously confirmed.[30] Among these CWD-positive brain samples that were stored at -80°C, Dr. Jeffrey Christiansen re-examined 18 samples by WB analyses with the PRC5 mAb. However, seven of the 18 CWD-positive brain samples did not show clear observations of PK-resistant PrP existences (Figure 3-D to 3-F). Therefore, the 7-5 ELISA method was applied to determine existing PrP^{Sc} agents in these cervid brain samples below. These PrP^{Sc} agents might be

sensitive to PK reagents. All testing samples were listed below, including controls (Table 8).

As described in the 7-5 ELISA method protocol above, tested tissue samples in this Chapter were examined at the final total protein 20μg per well (well number = 3 as technical replication for each individual) on ELISA plates.

Table 8. List of testing CWD-positive cervid brains and controls

Species	TSE state	Numbers	BH samples of Animals
Mouse	Negative	1	PrP-KO (whole brain)
Deer	Negative	3	FPS 6.98 (brain cerebral cortex), #694 (midbrain), #695 (midbrain)
Elk	Negative	2	AK03008 (elk ML: obex), AK03024 (elk LL: obex)
Deer	CWD	7	Dp99, 978-24384, D10, 001-39697, 989-09147, HP2, CSU-135
Elk	CWD	11	99W12389 (elk MM), Bala 1A (01-0306), Bala 2A (02-0306), Bala 3A (03-0306), Bala 4A (04-0306), 03W3297 (elk ML), 03-03355 (elk LL), 012-09442, 012-22012, 14-005 NPS, 001-44720
Moose	CWD	2	08W-11,741, Bala 13 Moose TSE

Western blot analyses for cervid tissues

All results and images of WB analyses were provided by courtesy of Dr. Jeffrey Christiansen. The WB protocol was previously published.[31-33] According to these

references, the protocol was described as following. Each BH sample was digested with 100μg/ml PK in cold lysis buffer for one hour at 37°C. After this incubation, PMSF (2μM at a final concentration in each digested sample) terminated this enzymatic digestion, and then the prepared samples were boiled for 10 minutes. Proteins were resolved by SDS-PAGE and transferred to Immobilon-FL PVDF (Polyvinylidene Difluoride) membranes (Millipore, Billerica, USA). These membranes were probed with primary mAbs followed by the HRP–conjugated anti-mouse secondary antibody (GE Healthcare, Little Chalfont, UK). Protein was visualized by chemiluminescence using ECL Plus (GE Healthcare, Piscataway, USA) and an FLA-5000 scanner (Fujifilm Life Science, Woodbridge, USA).[31-33]

Results

Pilot results of the 7-5 ELISA method with cervid tissue samples

Based on the optimized Sandwich ELISA protocol, the 7-5 ELISA method analyzed the following BH samples in three ca tegories: three PrP-KO mice, three CWD negative cervids (one deer and two elk), and five CWD-infected cervids (three elk, one deer, and one moose). At the total protein amount 20μg per well for each sample (well number = 3 as technical triplicate), the 7-5 ELISA method detected high PrP levels in the three CWD-infected materials (99W12389, Db99, and 08W-11,741), originally derived from different species (elk, deer, and moose, respectively) (Figure 4-1.A). In contrast, PrP detections in all CWD negative samples were equivalent O.D. values to the PrP-KO mice. However, the two CWD positive elk BH samples (03-3297 and 03-3355) showed lower O.D. values. Notably, these two samples have been stored in -80°C freezers for many years. In the results from the study section with the Figure 2-19 in Chapter 2, similar low PrP detections were observed in the BH samples from TSE-infected mouse models, which were also stored long term at -80°C (Figure 2-19). Thus, storage conditions and terms of testing samples could be influential factors for the 7-5 ELISA method to detect PrP levels in TSE-infected materials. However, the causal mechanisms of longer storage and ultralow temperature are not clarified for the PrP detection in the 7-5 ELISA method at this point. In another aspect, these results reflected a technical limitation to collect small tissue pieces with rich PrP^{Sc} amounts from large organs for diagnostic analyses. Indeed, PrP^{Sc} distributions in brains and other organs should not be dependent on CWD-affected animals. Thus, different

samples have various ranges of PrP^{Sc} amounts possibly, even if isolated from the same animal.

In addition, the 7-5 ELISA method evaluated the paired homogenate samples of brain and lymph nodes from the same cervid: one elk, one whitetail deer, and one red deer. Under the same procedures above, total protein 20μg of each prepared sample was coated per well on an ELISA plate (well numbers = 3). The 7-5 ELISA method detected equivalent O.D values of PrP levels in lymph nodes and brains from these infected animals (Figure 2-1.B). WB analyses also presented the same observations, performed by Ms. Calvi (data not present). These outcomes suggested that under-glycosylated PrP forms were generated and/or propagated in lymph nodes through the CWD infection and disease development. Consequently, the 7-5 ELISA method is exceptionally capable of detecting PrP^{Sc} levels in non-nervous tissues, possibly corresponding to PrP^{Sc} levels in brains for CWD diagnosis. To determine expressions and distributions of under-glycosylated PrP forms throughout the body of a CWD-affected cervid, the 7-5 ELISA method should examine more peripheral nervous tissues and non-nervous tissues.

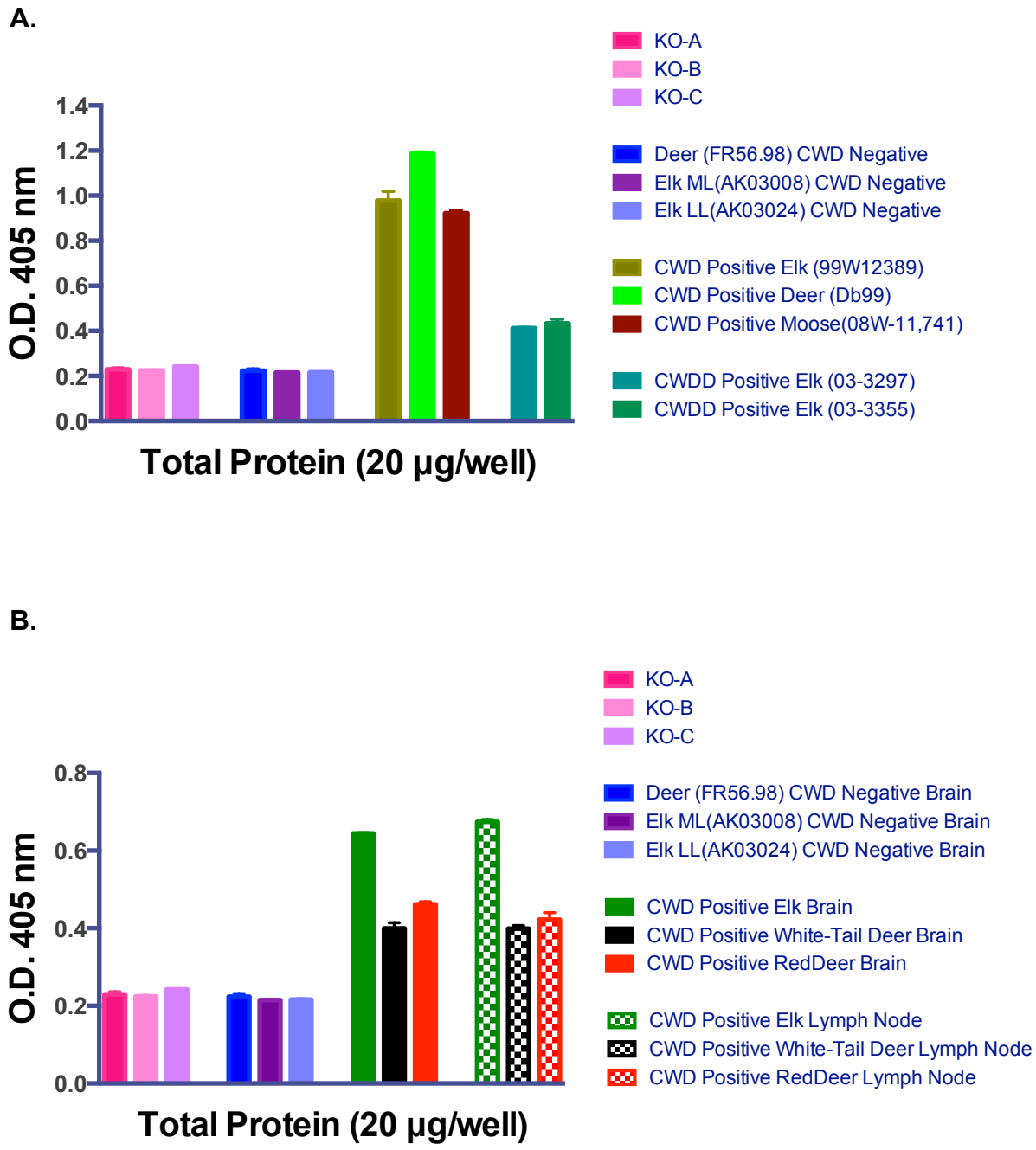

Figure 4-1. PrP detections in cervid tissues with CWD infections by the 7-5 ELISA method. (A) evaluations of CWD infectious states with detectable PrP levels, and (B) comparisons of PrP detections in brains and lymph nodes from same animals. (n=3, each sample with 20µg total protein amount)

Testing non-brain tissue samples from cervids by the 7-5 ELISA method

From Dr. Edward Hoover's laboratory, multiple tissue samples isolated from one CWD-negative (#502) and two CWD-positive deer (#782 and #785, experimentally inoculated) were kindly provided for testing with the 7-5 ELISA method. According to the information from Ms. Amy Nalls in Dr. Hoover's laboratory, the CWD infection state of these samples was previously examined by WB analyses and real-time quaking-induced conversion (RT-QuIC). In addition to brain samples (obex) from the three deer, the 7-5 ELISA method also examined the following six tissue samples: parotid lymph node, tonsil, vagus nerve, third eyelid, muscle, and rectum. The controls for this ELISA method included BH samples from PrP-KO, uninfected FVB and RML-inoculated FVB mice. In the sample preparation, all samples were prepared with 1% TX100 and 5M GdnHCL under the current 7-5 ELISA protocol. The final total protein coating on ELISA plates was 20μg per well (well number = 3 as technical replication) for each sample. The 7-5 ELISA results for PrP detections in these deer tissue samples are following:

1) Obex: Both #782 and 785 CWD-positive deer showed higher O.D. values of PrP levels, compared to the CWD-negative deer (#502) (Figure 4-2.A). Remarkably, #785 sample exhibited almost a four-times higher PrP level than #782 value. The O.D. value of #785 sample exhibited a high PrP detection, similarly to RML-infected FVB. In contrast, the O.D value of #782 sample accounted for the range of average PrP levels in CWD-inoculated Tg1563 (deerPrP) mice, based on the 7-5 ELISA data in Chapter 3. These results indicated that under-glycosylated PrP forms were highly generated in the CWD infection and disease development, especially in #785 animal.

2) Parotid lymph node and tonsil: Corresponding to the obex results, these lymphoid tissues from the CWD-positive deer showed different PrP detections that #785 presented a higher O.D. value than #782 (Figures 4-2.B and C). Although the PrP levels in the CWD-positive lymphoid samples were small amounts, *p*-values between infected and uninfected samples were $p<0.001$ as technical replications. Intriguingly, these results indicated that under-glycosylated PrP forms were generated in lymphoid tissues in the CWD infection state. These PrP detections in lymph nodes might be utilized to estimate the generated amounts of these PrP forms in brains from same animals.

3) Vagus nerve, third eyelid, muscle, and rectum: In contrast to the results from brains and lymphoid tissues, O.D. values in these four samples between the two CWD-positive deer showed almost no difference (Figure 4-2.D to G). The PrP levels in the infected samples were small quantities, compared to the uninfected samples. However, *p*-values between infected and uninfected samples were $p<0.01$-0.0001 as technical replications. Therefore, the 7-5 ELISA method is extremely sensitive to detect subtle levels of PrP^{Sc} agents in non-nervous tissue and/or peripheral tissues in CWD-infected deer.

Overall, the 7-5 ELISA method could detect higher O.D. values of PrP levels in all seven different tissue samples from CWD-infected deer at the total protein amount 20μg, compared to uninfected deer tissues. Since non-nervous tissue and peripheral tissues have lower PrP^{C} expressions than brain, this analysis might decrease the chance of PrP^{Sc} detections in these tissues from TSE-infected individuals. However, the 7-5 ELISA method is capable of determining the existence of under-glycosylated PrP^{Sc} forms in non-nervous tissues and peripheral tissues. These results suggested that

under-glycosylated PrP forms (unglycosyl and mono-1 glycosyl forms by PRC7 mAb) can be generated or accumulated in these tissues during CWD infection and disease development. For further studies, the increase of testing total protein would enhance PrP^{Sc} detections in non-nervous tissues and peripheral tissues in TSE diagnoses.

A.

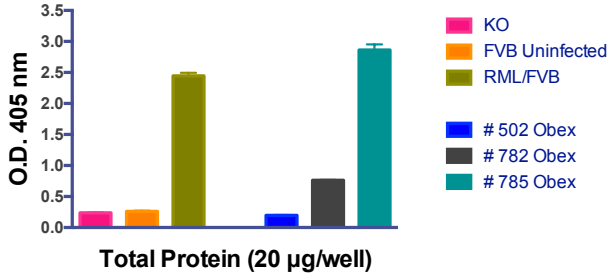
O.D. 405 nm
3.5
3.0
2.5
2.0
1.5
1.0
0.5
0.0
KO
FVB Uninfected
RML/FVB
502 Obex
782 Obex
785 Obex
Total Protein (20 µg/well)

B.

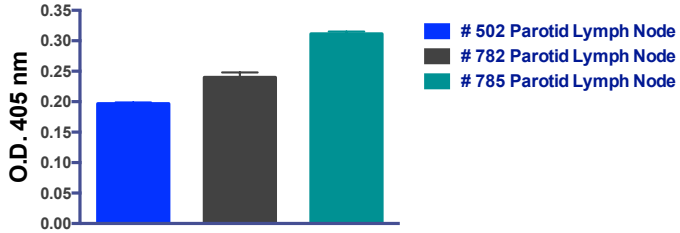
O.D. 405 nm
0.35
0.30
0.25
0.20
0.15
0.10
0.05
0.00
502 Parotid Lymph Node
782 Parotid Lymph Node
785 Parotid Lymph Node
Total Protein (20 µg)

C.

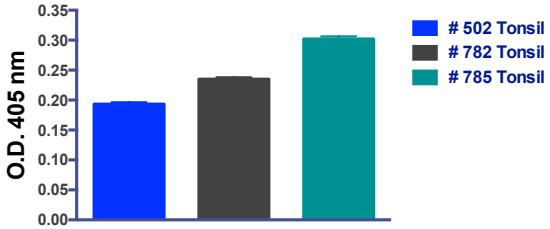
O.D. 405 nm
0.35
0.30
0.25
0.20
0.15
0.10
0.05
0.00
502 Tonsil
782 Tonsil
785 Tonsil
Total Protein (20 µg)

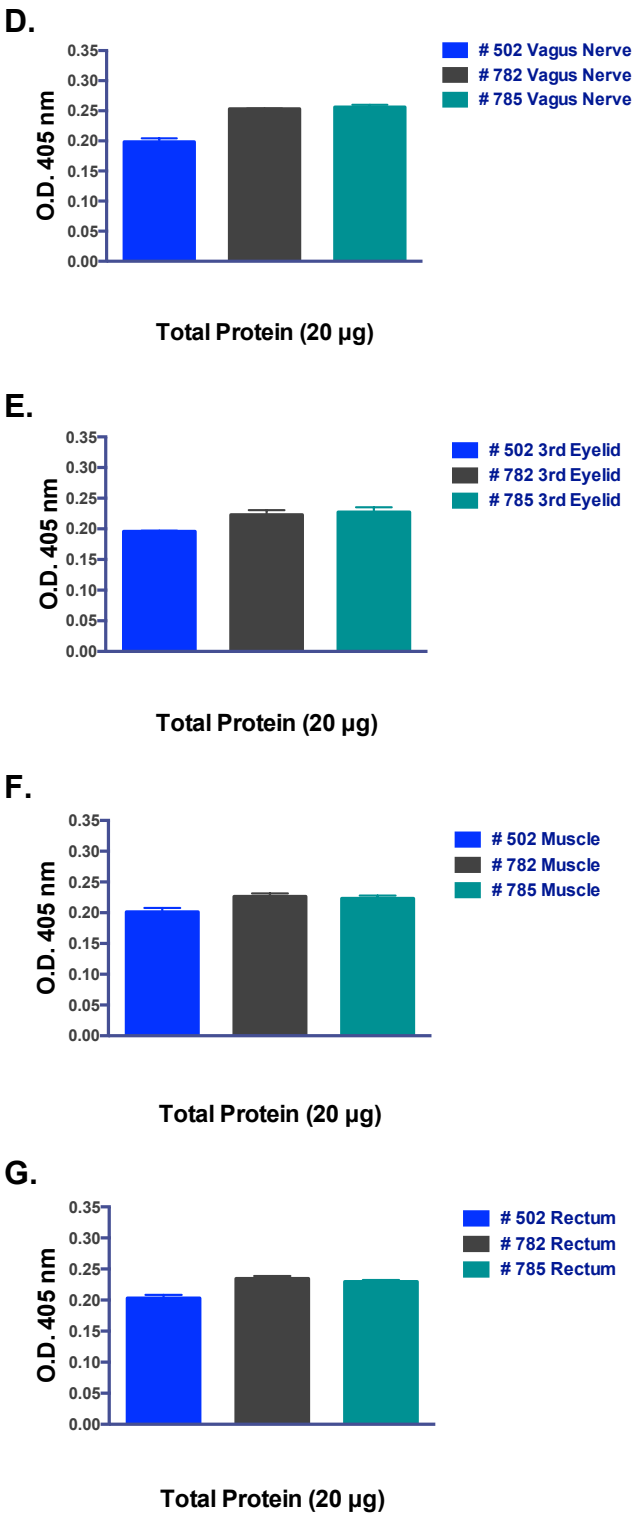

Figure 4-2. PrP detections in analyte from CWD-positive deer by the 7-5 ELISA method. (A) obex, (B) parotid lymph node, (C) tonsil, (D) vagus nerve, (E) third eyelid, (F) muscle, and (G) rectum (n=3, each sample with 20µg total protein amount)

Sensitivity of the 7-5 ELISA method for subtle PrP levels in CWD-infected brain samples

1) Elk brain samples from two different herds: Corresponding to the WB results (Figure 4-3.A), the 7-5 ELISA method measured low O.D. values in the six samples that did not present PK-resistant PrP levels in WB analyses. Other CWD-positive samples showed higher PrP levels over 1.0 O.D value at least (Figure 4-3.B). Also, the control samples for this ELISA method supported that this analysis worked properly. Focusing on the six materials with non PK-resistant PrP agents, the ELISA method detected higher O.D. values (at least 0.2 difference) in all non-PK resistant CWD-infected samples, compared to CWD-negative elk samples (Figure 4-3.C). In technical replication, *p*-values between each CWD sample and uninfected sample were $p<0.0001$. Therefore, these results suggested that the 7-5 ELISA method is exceptionally sensitive to detect subtle PrP^{Sc} amounts in CWD-infected materials that WB assay using PRC5 mAb and PK could not measure. Possibly, these PrP levels detected by the 7-5 ELISA method might be PK-sensitive PrP^{Sc} agents with under-glycosylated forms through CWD infection and disease progression.

2) Multiple CWD-positive cervid brain samples: Instead of the past confirmation for the CWD infection states, the WB results showed no or little detection of PK-resistant PrP agents in seven brain samples (001-44720, 03-03355, 012-22012, 3A(Bala 3A), 03W3297, 7138, and Bala 13 Moose) among the 18 CWD-positive cervids (Figures 4-3.D to F). To evaluate the existence of PrP^{Sc} agents in these samples, the 7-5 ELISA method analyzed PrP detections in the 17 CWD-positive (not including the sample 7138) and 4 negative samples, previously tested by WB analyses above.

Additionally, two CWD-positive brain samples and one negative deer brain sample were included. All sample information below was based on records in the laboratory database.

List of the cervid brain samples

CWD-negative state

- **Deer (3 brain samples):** FPS 6.98 (brain cerebral cortex), #694 (midbrain), #695 (midbrain)
- **Elk (2 brain samples):** AK03008 (elk ML: obex), AK03024 (elk LL: obex)

CWD-positive state

- **Deer (7 brain samples from mule deer):** Dp99, 978-24384, D10, 001-39697, 989-09147, HP2, CSU-135
- **Elk (11 brain samples):** 99W12389 (elk MM), 03W3297 (elk ML), 03-03355 (elk LL), Bala 1A (01-0306), Bala 2A (02-0306), Bala 3A (03-0306), Bala 4A (04-0306), 012-09442, 012-22012, 14-005 NPS, 001-44720
- **Moore (2 brain samples):** 08W-11,741, Bala 13 Moose TSE

Under the same 7-5 ELISA procedures in this study section, all cervid brain samples listed above were prepared for coating on ELISA plates. The final total protein of each prepared sample was 20μg per well for triplicates. In addition, one PrP-KO mouse BH sample was examined as a negative control for the PrP detection in the 7-5 ELISA method. Intriguingly, PrP-KO mouse BH sample showed a slightly higher O.D. value than all CWD-negative brain samples (Figures 4-3.G to J). Possibly, the anti-mouse IgG2a antibody with HRP (used as a secondary antibody for the 7-5 ELISA

method) caused this increased O.D. value in the mouse sample. This antibody can react with any murine IgG2a even in the PrP-KO mouse sample, whereas cervid tissues do not have murine IgG2a.

Unexpectedly, the 7-5 ELISA method showed similar O.D. values between all CWD negative controls and the six CWD-positive brain samples (001-44720, 03-03355, 012-22012, Bala 3A, 03W3297, 7138, and Bala 13 Moose), and WB analyses could not measure clear detections of PK-resistant PrP agents (Figures 4-3.G to J). This ELISA observation corresponded to the WB result. Hence, WB analyses and the 7-5 ELISA method indicated no detectable amount of PrP^{Sc} agents in these six CWD-positive brain samples. In the study section with the Figure 4-1 of this Chapter 4, however, the 7-5 ELISA method also measured two (03W3297 and 03-03355) of the six samples for the PrP^{Sc} detection (Figure 4-1.A). In that past experiment (Year 2013), the 7-5 ELISA application detected small amounts of PrP levels in these CWD-positive brain samples. In contrast, the analytical assay in this study (Year 2015) could not measure these PrP levels in the same tested samples after a two-year storage from brain homogenizations. Indeed, the 7-5 ELISA method also determined similar observations in other CWD-positive elk brain samples. These infection states were previously confirmed by PMCA in Dr. Mark Zabel's laboratory, and the samples have been stored over 3-7 years in -80°C freezers (data not present here). Thus, the cold temperature might have caused denaturation (cold denaturation) for PrP^{Sc} conformers in the six CWD-positive brain samples during -80°C storage for couple years.

If a denatured protein could not renature to its structured form, the two conformational-dependent anti-PrP mAbs (PRC7 and PRC5 mAbs) would not be able to

react with unfolding or partially unfolded PrP structures. In addition, PrP^{Sc} conformers after longer storage at the ultralow temperature might decrease these tolerances to detergents, denaturants and other factors for protein renaturations or stabilities. Especially, the PrP structure that the 7-5 ELISA method can detect are unglycosyl and mono-1 glycosyl forms. These glycosidic PrP forms must be less stable conformations than a diglycosyl PrP form. Since the other tested 14 CWD-positive samples showed clearly high O.D. values of PrP levels by the 7-5 ELISA method, the capacity of temperature resistance could be dependent on glycosylation states and possibly TSE strain differences.

Overall, the 7-5 ELISA method is capable of detecting PrP molecules in CWD-infected materials isolated from elk, deer and moose, but not in CWD-negative cervid samples. However, this analytical assay is only available to measure existing amounts of conformational PrP structures after denaturation and renaturation. Because of large brain sizes in cervid, higher total proteins of testing samples should enhance the PrP^{Sc} detection by the 7-5 ELISA method. Moreover, other additional reagents should be applicable to improve PrP^{Sc} detections in TSE-infected materials, such as the use of PK 10μg for enzymatic digestions that increased O.D. values for RML-inoculated FVB mouse brain samples (Figure 3-20, Chapter 3).

A.

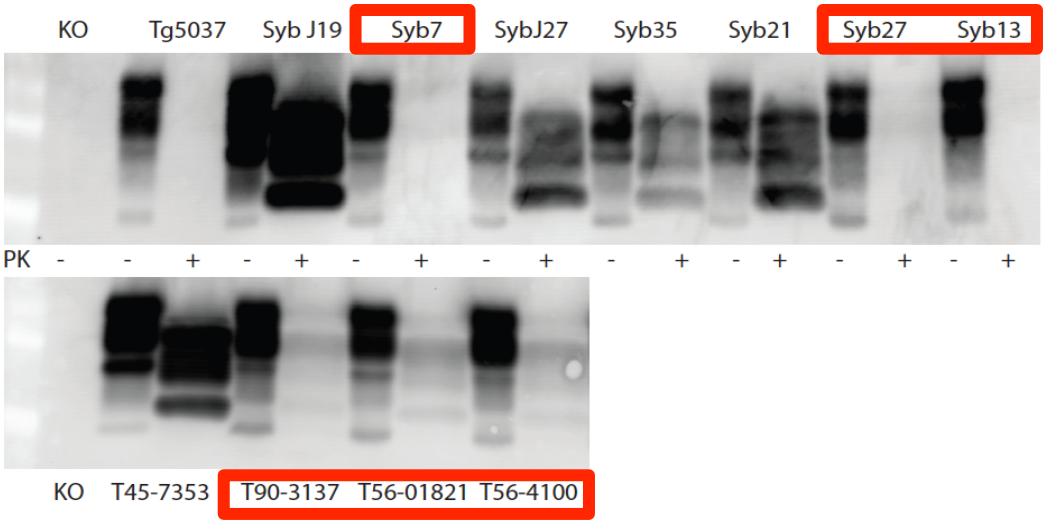

(Courtesy by Dr. Jeffrey Christiansen)

B.

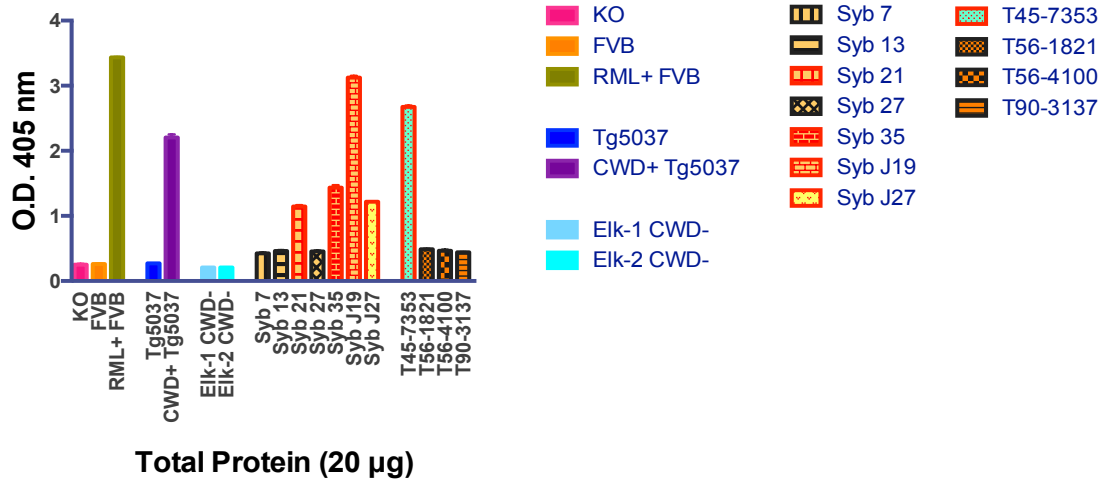

Total Protein (20 µg)

C.

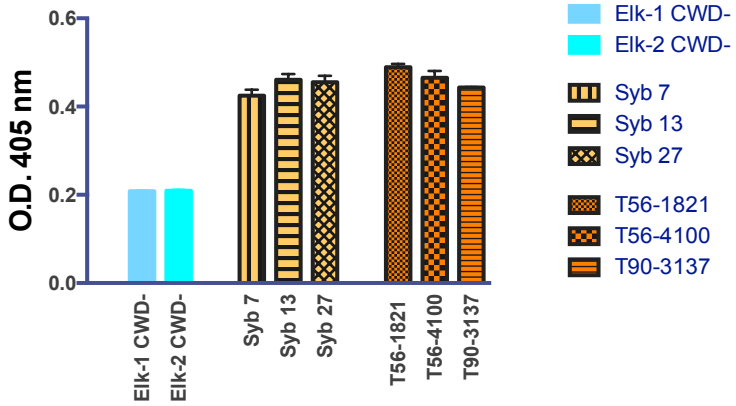

Total Protein (20 µg)

D.

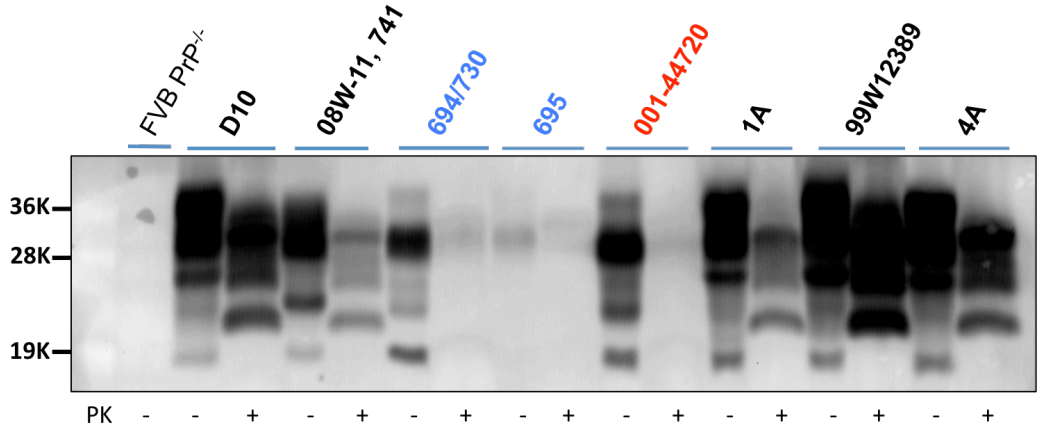

E.

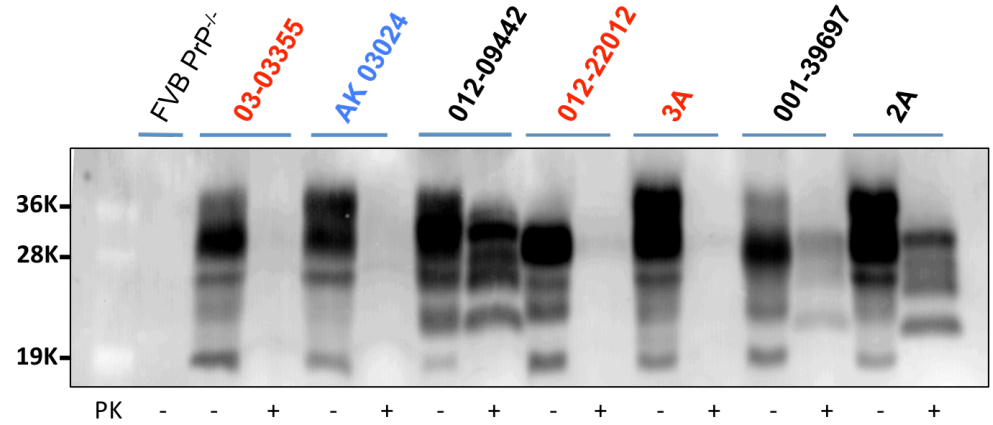

F.

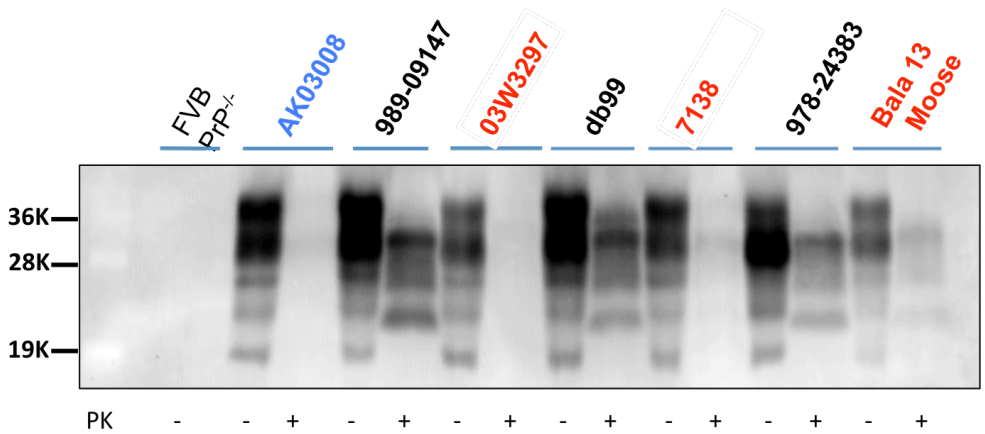

(Courtesy by Dr. Jeffrey Christiansen)

G.

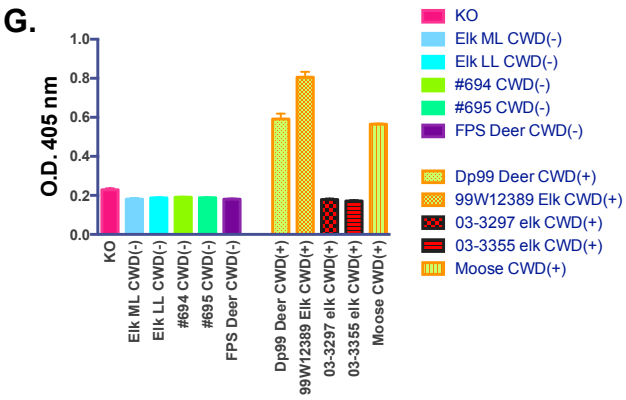
O.D. 405 nm
1.0
0.8
0.6
0.4
0.2
0.0
KO
Elk ML CWD(-)
Elk LL CWD(-)
#694 CWD(-)
#695 CWD(-)
FPS Deer CWD(-)
Dp99 Deer CWD(+)
99W12389 Elk CWD(+)
03-3297 elk CWD(+)
03-3355 elk CWD(+)
Moose CWD(+)
KO
Elk ML CWD(-)
Elk LL CWD(-)
#694 CWD(-)
#695 CWD(-)
FPS Deer CWD(-)
Dp99 Deer CWD(+)
99W12389 Elk CWD(+)
03-3297 elk CWD(+)
03-3355 elk CWD(+)
Moose CWD(+)

H.

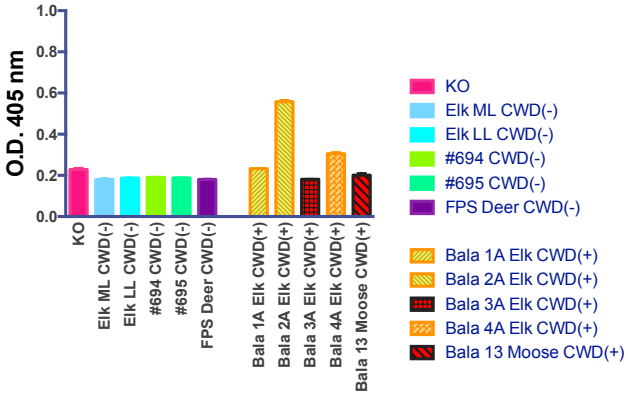
O.D. 405 nm
1.0
0.8
0.6
0.4
0.2
0.0
KO
Elk ML CWD(-)
Elk LL CWD(-)
#694 CWD(-)
#695 CWD(-)
FPS Deer CWD(-)
Bala 1A Elk CWD(+)
Bala 2A Elk CWD(+)
Bala 3A Elk CWD(+)
Bala 4A Elk CWD(+)
Bala 13 Moose CWD(+)
KO
Elk ML CWD(-)
Elk LL CWD(-)
#694 CWD(-)
#695 CWD(-)
FPS Deer CWD(-)
Bala 1A Elk CWD(+)
Bala 2A Elk CWD(+)
Bala 3A Elk CWD(+)
Bala 4A Elk CWD(+)
Bala 13 Moose CWD(+)

I.

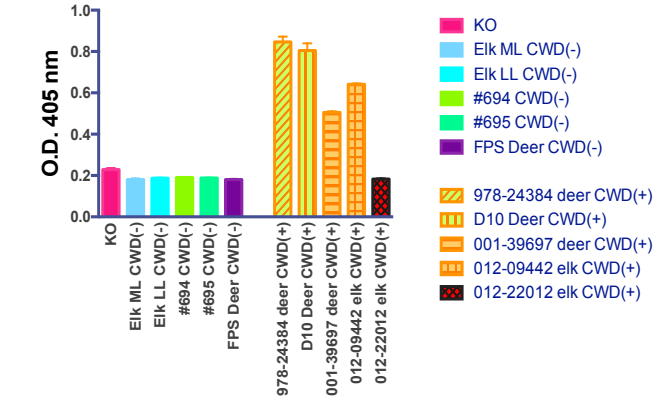
O.D. 405 nm
1.0
0.8
0.6
0.4
0.2
0.0
KO
Elk ML CWD(-)
Elk LL CWD(-)
#694 CWD(-)
#695 CWD(-)
FPS Deer CWD(-)
978-24384 deer CWD(+)
D10 Deer CWD(+)
001-39697 deer CWD(+)
012-09442 elk CWD(+)
012-22012 elk CWD(+)
KO
Elk ML CWD(-)
Elk LL CWD(-)
#694 CWD(-)
#695 CWD(-)
FPS Deer CWD(-)
978-24384 deer CWD(+)
D10 Deer CWD(+)
001-39697 deer CWD(+)
012-09442 elk CWD(+)
012-22012 elk CWD(+)

J.

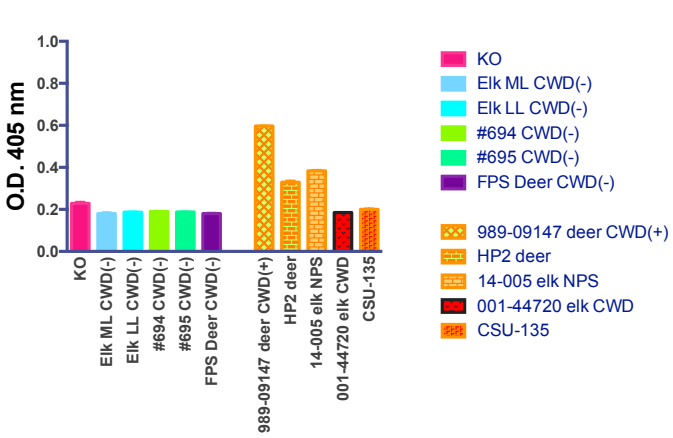
O.D. 405 nm
1.0
0.8
0.6
0.4
0.2
0.0
KO
Elk ML CWD(-)
Elk LL CWD(-)
#694 CWD(-)
#695 CWD(-)
FPS Deer CWD(-)
989-09147 deer CWD(+)
HP2 deer
14-005 elk NPS
001-44720 elk CWD
CSU-135
KO
Elk ML CWD(-)
Elk LL CWD(-)
#694 CWD(-)
#695 CWD(-)
FPS Deer CWD(-)
989-09147 deer CWD(+)
HP2 deer
14-005 elk NPS
001-44720 elk CWD
CSU-135

Figure 4-3. Sensitive PrP detections by the 7-5 ELISA method for CWD-infected BH samples. (A) PK-resistant PrP levels in diseased elk BH samples from CWD-epidemic areas by WB analysis with PRC5 mAb. (B) The 7-5 ELISA application for all tested elk BH samples in WB, and (C) the detection of subtle PrP levels in the CWD-positive BH samples that WB did not measure. (n=3, each sample with 20μg total protein amount)
(D), (E), and (F) PK-resistant PrP levels in BH samples from CWD-positive elk by a WB analyses with PRC5 mAb. Highlighted samples in Red exhibit no to little measurements of PK-resistant PrP materials, whereas these samples were previously confirmed as the CWD positive.
(G), (H), (I), and (J) The 7-5 ELISA application for all tested elk BH samples in WB. (n=3, each sample with 20μg total protein amount)

Discussions

In the previous chapters, the 7-5 ELISA method detected high levels of under-glycosylated PrP forms in brain homogenate (BH) samples from mouse models of several transmissible spongiform encephalopathies (TSEs), but not in uninfected mice. As proposed, the loss of full glycosylation is implicated in pathological mechanisms of TSEs. Because of the unstable conformation, under-glycosylated PrP forms might promote conformational alterations of the normal PrP structure to the pathologic isoform. Eventually, this conformational modulation would impair the PrP physiology and induce the TSE disease progression. Therefore, this dissertation hypothesized that the generation of under-glycosylated PrP forms is a key hallmark of diagnostic biomarkers for the TSE-infection state and disease progression. In this chapter, the 7-5 ELISA method evaluated cervid tissue samples to address this hypothesis in chronic wasting disease (CWD).

The 7-5 ELISA method successfully demonstrated the existence of under-glycosylated PrP forms in CWD-infected BH samples from three different cervid species (deer, elk, and moose) (Figure 4-1.A). In contrast, BH samples from CWD-negative deer and elk showed similar O.D. values to PrP-KO mice. In addition, this analytical approach was capable of detecting lower amounts of these PrP forms in CWD-positive elk BH samples (Figure 4-1.A). Intriguingly, the 7-5 ELISA method detected under-glycosylated PrP forms in other types of tissue samples from CWD-positive deer and elk, such as lymph nodes and muscles, compared to the uninfected deer (Figures 4-1.B, 4-2.B to G). Although these PrP detections showed lower O.D. values, the 7-5 ELISA method was sensitive to detect subtle amounts of the under-glycosylated PrP

forms in CWD-positive tissue samples, compared to the controls. These results indicated the utility of the 7-5 ELISA method for testing non-nervous tissues from cervid in CWD diagnostic examinations. In clinical and diagnostic situations, tissue sample collections from the body surface of animals are convenient and quick approaches with the uses of disposable tools, such as a needle and blade. In general, brain biopsy and neurosurgical procedures (e.g. craniotomy) for tissue collections require special instruments and handling techniques, as well as longer procedure times. Without proper sterilizations to inactivate TSE pathogens, the reuse of medical instruments with potential PrP^{Sc} contaminations would be a causal source of iatrogenic transmissions in TSEs.[34] The 7-5 ELISA results demonstrated its ability to evaluate the TSE infection state in tissue samples, easily collected in the clinic and the field. For a future direction, the 7-5 ELISA method should be applied for more additional samples of brain and other tissues to establish a diagnostic standard scale. These outcomes would also determine distributions or ranges of under-glycosylated PrP levels in CWD-positive and negative animals.

In addition, sensitive PrP^{Sc} detections are critical to develop a new analytical system in the TSE diagnosis and research. Dr. Hoover's laboratory, the provider of tissue samples from deer with oral inoculations of CWD-positive brain materials, detected very high amounts of PK-resistant PrP agents in the deer brain by WB analyses. The 7-5 ELISA method also measured similar results in the same sample (Figure 4-2.A). Hence, the ELISA application and result corresponded to the WB analysis in tested deer brain samples. In addition, the 7-5 ELISA method determined different levels of under-glycosylated PrP forms between CWD-positive deer at the

same protein amount (total protein 20μg per each well on an ELISA plate). These outcomes indicated that the 7-5 ELISA method would be applicable for quantitative analyses of under-glycosylated PrP forms in TSE-infected animals. In further longitudinal or kinetic studies, a quantitative application of the 7-5 ELISA method would evaluate outcomes with background information of each tested animal, including the TSE-incubation time and clinical signs.

Moreover, the 7-5 ELISA method demonstrated its exceptional sensitivity for the PrP detection in CWD-infected animals that WB analyses with the PRC5 mAb and PK digestion could not identify (Figures 4-3.A to C). Tested elk brain samples were collected from two different herds in CWD-contaminated locations. Prior to this dissertation experiment, the sample providers evaluated clinical signs and CWD-infection states of these elk herds. Among BH samples from the eleven CWD-positive elk, WB analyses could not detect PK-resistant PrP agents in six animals. However, the 7-5 ELISA method detected higher PrP levels in these six BH samples, compared to the CWD-negative elk and uninfected mice (PrP-KO, FVB and Tg5037). The other five CWD-positive BH samples exhibited high PrP levels in this ELISA method (Figure 4-3.B). These observations indicated that CWD-positive animals prominently generated under-glycosylated PrP forms. Although several factors might affect PrP detections, such as tissues, animals, disease stages, sampling and storage conditions, the 7-5 ELISA method could overcome a threshold limitation of WB analyses (with PRC5 mAb and PK digestion) for the PrP detection. Potentially, the PrP levels that the 7-5 ELISA method detected in cervid tissues were PK-sensitive PrP^{Sc} forms.

For further analyses, the 7-5 ELISA method examined additional BH samples from CWD-positive cervid that were previously confirmed for infection states (based on the laboratory database). Initially, WB analyses with the PRC5 mAb examined existences of PK-resistant PrP agents in BH samples of 18 CWD-positive cervid. However, the samples from seven animals (001-44720, 03-03355, 012-22012, 3A(Bala 3A), 03W3297, 7138, and Bala 13 Moose) showed no or little amounts of PK-resistant PrP agents (Figures 4-3.D to F). Previously, the four CWD isolates (001-44720, 012-22012, 03W3297, and 7138) exhibited high detections of PK-resistant PrP agents, in addition to these transmissions to Tg1536 mice.[30] Thus, these CWD isolates might have lost detectable amounts of PrP^{Sc} agents in brains during the -80°C storage. In fact, the 7-5 ELISA method measured low O.D. values in six CWD-positive BH samples (03W3297, 03-03355, Bala 3A, Bala 13 Moose, 012-22012, and 001-44720), similar to detected PrP levels in all CWD negative controls (Figures 4-3.G to J). PrP^{Sc} amounts in these CWD-positive brain samples might be undetectable quantities by this assay. Furthermore, the 7-5 ELISA method previously detected small amounts of PrP levels (PrP^{Sc} detections) in 03W3297 and 03-03355 CWD isolates (Figures 4-1.A, Chapter 4). In contrast, this later ELISA experiment could not measure these PrP levels after two years, possibly due to long-term storages of the same brain samples and these defrostings. Moreover, the 7-5 ELISA method showed similar observations in other CWD-positive elk brain samples, stored over 3-7 years in -80°C freezers (data not present). Previously, Protein Misfolding Cyclic Amplification (PMCA) confirmed these infection states in Dr. Mark Zabel's laboratory. Since the binding epitopes of PRC7 and PRC5 mAbs localize in the structured globular domains of the PrP structure, these

conformation-dependent anti-PrP mAbs require renaturation of denatured PrP^{Sc} agents for these detections. Otherwise, these two mAbs would not be able to react with unfolded or partially unfolded PrP molecules. Therefore, PrP^{Sc} conformers in these samples might lose structural stabilities or conformations during the storage term, caused by cold temperature-mediated denaturation.

As examined in the Chapter 2, the 7-5 ELISA method could not measure the PrP level in the RML-inoculated FVB mouse BH sample when treated with β-mercaptoethanol (βME), compared with PrP-KO and uninfected FVB mice (Figure 2-12.A, Chapter 2). Since this reagent cleaves disulfide bonds in structured globular domains of proteins and also disrupts protein conformational structure, both PRC7 and PRC5 mAb cannot recognize PrP molecules with non-conformational conditions. In addition, PrP^{Sc} conformers after longer storages at the ultralow temperature might decrease tolerances to detergents, denaturants and other factors for the protein renaturation or stability. Thus, unglycosyl and mono-1 glycosyl PrP forms with which the PRC7 mAb reacts might reduce conformational stabilities, compared to a diglycosyl PrP form. Also, these tolerances could be dependent on isolates or strains (Figures 4-3.G to J). Therefore, the 7-5 ELISA method might have a potential utility to determine the capacity of temperature resistance and conformational stability, based on PrP glycosylation states

To evaluate these possibilities described above and enhance PrP detections, PMCA can be applied to amplify PrP^{Sc} isoforms in the BH samples from CWD-positive animals, in which the 7-5 ELISA method and/or WB analysis did not detect PrP^{Sc} levels.[35-37] Real-time quaking induced conversion (RT-Quic) assay also would be a

useful method for this purpose.[38] These amplified products should consist of conformational PrP structures. Subsequently, PRC7 and PRC5 mAbs in the 7-5 ELISA method and WB analysis will be capable of determining the existence of pathologic PrP isoforms in amplified products of each brain sample. In addition, tissues from TSE isolates should be examined by the 7-5 ELISA method, prior to infections of these inocula into cell cultures and mice. Quantities of under-glycosylated PrP^{Sc} forms in the inocula might influence prion infectivity, replication, propagation, and incubation time for *in vitro* and *in vivo* studies. This approach will provide quality controls of stored tissue samples and TSE-infection/inoculation experiments. Otherwise, unexpected outcomes or failures of experiments would delay planned research projects if amounts of under-glycosylated PrP^{Sc} forms were limited in each testing sample. Therefore, the ELISA application will be useful for the quality management of these experiments.

Overall, the 7-5 ELISA method is capable of detecting PrP molecules in CWD-infected materials isolated from elk, deer and moose, but not in CWD-negative cervid tissue samples. However, this analytical assay is only available to measure existing amounts of conformational PrP structures in testing samples after denaturation and renaturation. Based on protein-dose dependent studies, it is clear that increases of total proteins enhance the PrP^{Sc} detection in TSE-infected tissue samples by the 7-5 ELISA method. Unlike mice, large volumes of tissue samples are available to collect easily from cervid because of their large body size. Thus, CWD diagnostic examinations should examine higher total proteins of testing samples, rather than the 20μg we tested in this Chapter 4. Furthermore, other additional reagents might be capable of increasing PrP^{Sc} detections in TSE-infected materials, such as the use of PK 10μg for enzymatic

digestions that increased O.D. values for the RML-inoculated FVB mouse brain sample (Figure 3-15, Chapter 3). As hypothesized, the 7-5 ELISA method prominently detected under-glycosylated PrP forms in CWD-positive tissue samples. These results indicate that the generation of under-glycosylated PrP forms is a key hallmark of diagnostic biomarkers for the TSE-infection state and disease progression. Therefore, the 7-5 ELISA method will be available to utilize as a novel sensitive analytical assay for TSE diagnosis, resulting in beneficial impacts for the fields of veterinary medicine and public health.

REFERENCES

1. Belay ED, Maddox RA, Williams ES, Miller MW, Gambetti P, Schonberger LB. Chronic wasting disease and potential transmission to humans. *Emerging Infect Dis* 2004;10:977–84.
2. Williams ES, Young S. Chronic wasting disease of captive mule deer: a spongiform encephalopathy. *J Wildl Dis* 1980;16:89–98.
3. Kahn S, Dubé C, Bates L, Balachandran A. Chronic wasting disease in Canada: Part 1. *Can Vet J* 2004;45:397–404.
4. Argue CK, Ribble C, Lees VW, McLane J, Balachandran A. Epidemiology of an outbreak of chronic wasting disease on elk farms in Saskatchewan. *Can Vet J* 2007;48:1241–8.
5. Dubé C, Mehren KG, Barker IK, Peart BL, Balachandran A. Retrospective investigation of chronic wasting disease of cervids at the Toronto Zoo, 1973-2003. *Can Vet J* 2006;47:1185–93.
6. Benestad SL, Mitchell G, Simmons M, Ytrehus B, Vikøren T. First case of chronic wasting disease in Europe in a Norwegian free-ranging reindeer. *Vet Res* 2016;47:88.
7. Williams ES, Miller MW. Chronic wasting disease in deer and elk in North America. *Rev - Off Int Epizoot* 2002;21:305–16.
8. Miller MW, Williams ES, McCarty CW, Spraker TR, Kreeger TJ, Larsen CT, *et al.* Epizootiology of chronic wasting disease in free-ranging cervids in Colorado and Wyoming. *J Wildl Dis* 2000;36:676–90.
9. Miller MW, Williams ES. Prion disease: horizontal prion transmission in mule deer. *Nature* 2003;425:35–6.
10. Miller MW, Williams ES, Hobbs NT, Wolfe LL. Environmental sources of prion transmission in mule deer. *Emerging Infect Dis* 2004;10:1003–6.
11. Nalls AV, McNulty E, Powers J, Seelig DM, Hoover C, Haley NJ, *et al.* Mother to offspring transmission of chronic wasting disease in reeves' muntjac deer. *PLoS ONE* 2013;8:e71844.
12. Selariu A, Powers JG, Nalls A, Brandhuber M, Mayfield A, Fullaway S, *et al.* In utero transmission and tissue distribution of chronic wasting disease-associated prions in free-ranging Rocky Mountain elk. *J Gen Virol* 2015;96:3444–55.
13. Nalls AV, McNulty E, Hoover CE, Pulscher LA, Hoover EA, Mathiason CK. Infectious Prions in the Pregnancy Microenvironment of Chronic Wasting Disease-Infected Reeves' Muntjac Deer. *J Virol* 2017;91:.
14. Williams ES, Young S. Spongiform encephalopathy of Rocky Mountain elk. *J Wildl Dis* 1982;18:465–71.
15. Miller MW, Wild MA, Williams ES. Epidemiology of chronic wasting disease in captive Rocky Mountain elk. *J Wildl Dis* 1998;34:532–8.
16. Wild MA, Spraker TR, Sigurdson CJ, O'Rourke KI, Miller MW. Preclinical diagnosis of chronic wasting disease in captive mule deer (Odocoileus hemionus) and white-tailed deer (Odocoileus virginianus) using tonsillar biopsy. *J Gen Virol* 2002;83:2629–34.

17. Miller MW, Wild MA. Epidemiology of chronic wasting disease in captive white-tailed and mule deer. *J Wildl Dis* 2004;40:320–7.
18. Davenport KA, Henderson DM, Mathiason CK, Hoover EA. Assessment of the PrPc Amino-Terminal Domain in Prion Species Barriers. *J Virol* 2016;90:10752–61.
19. Sleivert G, Burke V, Palmer C, Walmsley A, Gerrard D, Haines S, *et al.* The effects of deer antler velvet extract or powder supplementation on aerobic power, erythropoiesis, and muscular strength and endurance characteristics. *Int J Sport Nutr Exerc Metab* 2003; 13:251–65.
20. Syrotuik DG, MacFadyen KL, Harber VJ, Bell GJ. Effect of elk velvet antler supplementation on the hormonal response to acute and chronic exercise in male and female rowers. *Int J Sport Nutr Exerc Metab* 2005;15:366–85.
21. Angers RC, Browning SR, Seward TS, Sigurdson CJ, Miller MW, Hoover EA, *et al.* Prions in skeletal muscles of deer with chronic wasting disease. *Science* 2006;311:1117.
22. Angers RC, Seward TS, Napier D, Green M, Hoover E, Spraker T, *et al.* Chronic wasting disease prions in elk antler velvet. *Emerging Infect Dis* 2009;15:696–703.
23. Gilbey A, Perezgonzalez JD. Health benefits of deer and elk velvet antler supplements: a systematic review of randomised controlled studies. *N Z Med J* 2012;125:80–6.
24. Cox HD, Eichner D. Detection of human insulin-like growth factor-1 in deer antler velvet supplements. *Rapid Commun Mass Spectrom* 2013;27:2170–8.
25. Priola SA, Lawson VA. Glycosylation influences cross-species formation of protease-resistant prion protein. *EMBO J* 2001;20:6692–9.
26. Lawson VA, Collins SJ, Masters CL, Hill AF. Prion protein glycosylation. *J Neurochem* 2005;93:793–801.
27. Wiseman FK, Cancellotti E, Piccardo P, Iremonger K, Boyle A, Brown D, *et al.* The glycosylation status of PrPC is a key factor in determining transmissible spongiform encephalopathy transmission between species. *J Virol* 2015;89:4738–47.
28. Race RE, Raines A, Baron TGM, Miller MW, Jenny A, Williams ES. Comparison of abnormal prion protein glycoform patterns from transmissible spongiform encephalopathy agent-infected deer, elk, sheep, and cattle. *J Virol* 2002;76:12365–8.
29. Spraker TR, O'Rourke KI, Gidlewski T, Powers JG, Greenlee JJ, Wild MA. Detection of the abnormal isoform of the prion protein associated with chronic wasting disease in the optic pathways of the brain and retina of Rocky Mountain elk (Cervus elaphus nelsoni). *Vet Pathol* 2010;47:536–46.
30. Angers RC, Kang H-E, Napier D, Browning S, Seward T, Mathiason C, *et al.* Prion strain mutation determined by prion protein conformational compatibility and primary structure. *Science* 2010;328:1154–8.
31. Kang H-E, Weng CC, Saijo E, Saylor V, Bian J, Kim S, *et al.* Characterization of conformation-dependent prion protein epitopes. *J Biol Chem* 2012;287:37219–32.

32. Saijo E, Kang H-E, Bian J, Bowling KG, Browning S, Kim S, *et al.* Epigenetic dominance of prion conformers. *PLoS Pathog* 2013;9:e1003692.
33. Bian J, Kang H-E, Telling GC. Quinacrine promotes replication and conformational mutation of chronic wasting disease prions. *Proc Natl Acad Sci USA* 2014;111:6028–33.
34. Rutala WA, Weber DJ, Society for Healthcare Epidemiology of America. Guideline for disinfection and sterilization of prion-contaminated medical instruments. *Infect Control Hosp Epidemiol* 2010;31:107–17.
35. Haley NJ, Seelig DM, Zabel MD, Telling GC, Hoover EA. Detection of CWD prions in urine and saliva of deer by transgenic mouse bioassay. *PLoS ONE* 2009;4:e4848.
36. Haley NJ, Mathiason CK, Zabel MD, Telling GC, Hoover EA. Detection of sub-clinical CWD infection in conventional test-negative deer long after oral exposure to urine and feces from CWD+ deer. *PLoS ONE* 2009;4:e7990.
37. Pulford B, Spraker TR, Wyckoff AC, Meyerett C, Bender H, Ferguson A, *et al.* Detection of PrPCWD in feces from naturally exposed Rocky Mountain elk (Cervus elaphus nelsoni) using protein misfolding cyclic amplification. *J Wildl Dis* 2012;48:425–34.
38. Henderson DM, Manca M, Haley NJ, Denkers ND, Nalls AV, Mathiason CK, *et al.* Rapid antemortem detection of CWD prions in deer saliva. *PLoS ONE* 2013;8:e74377.

CHAPTER 5

OVERALL CONCLUSION AND FUTURE DIRECTIONS

Overall Conclusion

TSEs are fatal neurodegenerative disorders that transmit horizontally and environmentally in humans and animals. Currently, CWD outbreaks have emerged in not only North America, but also Asia and Europe. Although various analytical methods have been applied to the TSE diagnoses, each method has both advantages and limitations, such as technical processes.[1,2] Because of the existence of PK-sensitive PrP^{Sc} pathogens that implicate with neurotoxicity and lethal outcomes, the application of PK reagents might result in false negative detections in the traditional TSE diagnostic methods.[3-5] However, early detections and preventions of TSEs are critically important to eradicate further epidemic incidences throughout the world. In this dissertation, the overreaching goal set aims to establish new analytical systems for the TSE diagnoses without the use of PK reagents.

For these purposes, the first part of this dissertation investigated new Sandwich ELISA protocols that could overcome some limitations of the current TSE diagnoses. In order to evaluate capabilities of the in-house anti-PrP mAbs, PRC7 and PRC5, the Indirect ELISA method was beneficial as an initial approach. Using recombinant prion protein (RecPrP) of elk and mouse species, these two mAbs demonstrated detectable abilities of PrP particles for the Indirect ELISA application. In addition, each mAb presented similar O.D. values for denatured and non-denatured RecPrP samples (Figure 2-1, Chapter 2). Since PRC5 and PRC7 mAbs are conformation-dependent

antibodies, these results indicated that the denatured PrP particles refolded (renatured) to these native conformations. Furthermore, the Sandwich ELISA method proved specificities of these mAbs for the PrP detection. In fact, the combination of the capture PRC7 antibody with the detecting PRC5 antibody (the 7-5 ELISA method) showed increased PrP detections under the RecPrP-dose dependence for both elk and mouse species. Corresponding to the Indirect ELISA results, the 7-5 ELISA method also showed similar O.D. values in detections of denatured and non-denatured RecPrP samples (Figure 2-2, Chapter 2). At a certain dose of guanidine hydrochloride (GdnHCL), some PrP particles might not have renatured to the native folding structures. As a result, the 7-5 ELISA method reduced the detection of denatured RecPrP particles. Hence, these observations indicated that PRC5 and/or PRC7 could not bind to unfolded conditions of PrP particles. Thus, the 7-5 ELISA method demonstrated the property of the conformational-dependent recognition, because of only detecting the structured PrP particles.

Conversely, this detectable specificity was a potential concern for applying to brain samples from TSE-affected animals. Since the RecPrP conformations were non-glycosylated forms, the PRC7 mAb could bind to these particles without glycosidic restrictions, such as mono-2 glycosyl and diglycosyl forms. In contrast to this concern, the 7-5 ELISA method was particularly capable of detecting GdnHCL-resistant PrP agents in brain homogenates (BH) from TSE-inoculated mice. This analytical ability indicated that the detected particles were unglycosyl and/or mono-1 glycosyl PrP^{Sc} forms because the PRC7 mAb only bound to those two forms. Thus, the 7-5 ELISA method clarified the generation of under-glycosylated PrP forms in the TSE disease

development. These evidences supported this dissertation hypothesis that an under-glycosylated PrP form would be the hallmark as an essential diagnostic biomarker to evaluate the TSE-infection state and disease progression. Therefore, the 7-5 ELISA method proved a potential utility as a new analytical system for the TSE diagnosis. Followed by optimizing a procedure protocol, the 7-5 ELISA method increased its detectability of PrP^{Sc} agents in BH samples from TSE-infected mice. To confirm the conformation-dependent feature of this analytical method, β-mercaptoethanol (βME) was applied to cleave disulfide bonds of the structural globular domain in the PrP structure. In fact, βME-treated BH samples lost protein folding and stability, resulting in no PrP detection by the 7-5 ELISA method (Figure 2-12, Chapter 2). These outcomes indicated that the 7-5 ELISA method has the characteristic feature of the conformation-dependent PrP detection.

In the second part of this dissertation, the 7-5 ELISA method showed an exceptional sensitivity for the PrP^{Sc} detection in BH samples from various transgenic-mouse models of different TSE diseases (Figure 3-1, 3-2, and 3-3, Chapter 3). The capability of this analytical assay indicated the abundant existences of under-glycosylated PrP^{Sc} forms at the terminal stage of the disease progression in mice. Hence, TSE-affected brains generated under-glycosylated PrP^{Sc} forms throughout different species and with various PrP^{Sc} strains. Notably, strain differences exhibited variances in generations, quantities, and conformational stabilities among the detected PrP^{Sc} agents in inoculated hosts (Figures 3-4, Chapter 3). Thus, the 7-5 ELISA method distinguished strain differences, based on the detections of under-glycosylated PrP^{Sc} forms. In addition, this analytical assay demonstrated another capability to estimate

prion infectivity and titration, in comparison to CPCA results with the PRC7 mAb (Figures 3-7, 3-8, 3-9, 3-10, and 3-11, Chapter 3). These outcomes indicated the implication of under-glycosylated PrP^{Sc} forms in the TSE infection. The glycosidic deficit on the PrP conformation should be associated with the TSE pathogenesis. The unstable structures of under-glycosylated PrP forms might link to conformational alterations of the normal PrP^{C} structure to the pathologic isoform. Therefore, the 7-5 ELISA method can be applied to evaluate the kinematic modulations of under-glycosylated PrP agents during the TSE disease progression.

In the third part of the dissertation, the 7-5 ELISA method detected the existence and implication of under-glycosylated PrP forms in tissue samples (brains, peripheral nerves, lymph nodes, muscles, skins) from different cervid species with CWD infections (Figure 4-1 and 4-2, Chapter 4). This analytical approach was capable of detecting subtle amounts of the PrP^{Sc} agents in CWD-positive samples, which western blot analyses did not detect (Figures 4-3, Chapter 4). These results indicated the utility of the 7-5 ELISA method for testing non-nervous tissues from cervid for CWD diagnostic examinations. In clinical and diagnostic situations, this sensitivity for PrP^{Sc} detections in non-CNS tissues could be essential to diagnose TSE states conveniently and quickly, rather than brain collections. Using disposable tools, these easier procedures would be beneficial for avoiding a potential risk of the iatrogenic TSE transmission. As hypothesized, the 7-5 ELISA method measured significant levels of under-glycosylated PrP forms, predominantly generated in various TSE diseases. Therefore, the detection of under-glycosylated PrP forms is a key hallmark of diagnostic biomarkers for TSE-infection states and disease progression. Eventually, the 7-5 ELISA method will provide

its utility as a new sensitive analytical assay for TSE diagnosis and PrP^{Sc} analysis, resulting in beneficial impacts for the fields of veterinary medicine and public health.

Furthermore, the D-5 ELISA method also demonstrated a unique feature of PrP^{Sc} and PrP^{C} detections. Since D18 Fab Ab and PRC5 mAb can bind to all four glycosyl PrP forms, the D-5 ELISA method is capable of detecting PrP molecules with any glycosylated states. With or without the denaturation process, this assay could measure total PrP^{Sc} or PrP^{C} levels in testing BH samples, respectively. For GdnHCL-denatured murine BH samples, the D-5 ELISA method measured higher O.D. values of PrP detections in TSE-inoculated individuals, compared to the control BH samples (Figure 4-9.A, Chapter 4). In contrast, this new approach revealed the decrease of PrP^{C} levels in these infected BH samples without denaturation (Figure 4-9.B, Chapter 4). These results proved that the D-5 ELISA approach could analyze modulations of normal PrP^{C} and abnormal PrP^{Sc} levels in TSE disease states by a single change in sample preparations. Therefore, the loss of PrP^{C} isoforms should correlate with the cause of the functional abnormality in TSE-infected animals through disease progressions. Based on the comparison study of capture antibodies (Figures 4-13, Chapter 4), the PrP^{C} decline might reflect the following possibilities: 1) the reduced generation of PrP^{C} isoforms; 2) the death of PrP^{C}-expressing cells; and 3) the conformational modification of the structured globular domain on PrP^{C} isoforms. Thus, the D-5 ELISA approaches would be capable of monitoring the PrP^{C} deficiency, the PrP conformational modulation, and the PrP^{Sc} propagation through longitudinal periods of the TSE disease course. Modulations of PrP^{C} and PrP^{Sc} levels could be involved in the pathological development and progression among various TSE diseases, strains and species backgrounds. For

instance, the D-5 ELISA approaches detected the increased PrP^{Sc} levels and the decreased PrP^{C} levels in BH samples from the diseased mice (terminal stages) of different TSE models (Figures 4-14, Chapter 4). Interestingly, these PrP modulations did not present clear differences between uninfected control mice and CWD-inoculated mice with asymptomatic conditions (Figures 4-15, Chapter 4). The pilot study of the GSS mouse models also proved phenomena of these PrP variances from asymptomatic states to clinical disease onsets (Figures 4-17, Chapter 4). Remarkably, these D-5 ELISA results identified that the GSS mice with the corresponding gene mutation exhibited both PrP^{C} isoforms and PrP^{Sc} conformers. This finding is essential to determine how mutated PrP^{C} molecules misfold to pathological structures and what influential factors initiate the PrP transformations. In addition, these PrP modulations should affect physiological functions of PrP^{C} isoforms. Therefore, these impairments would develop neurological abnormalities and deficits in affected mice.

Overall, the 7-5 ELISA and the D-5 ELISA methods indicated three possible aspects of the TSE pathogenesis. As proposed, the loss of full glycosylation should correlate with pathological alterations of the PrP structure in the TSE disease development. Since glycosylation is an important factor to preserve protein structure, its modulation can initiate unstable conditions for maintaining the proper PrP conformation. Consequently, this unstable state could alter the PrP structure pathologically. Eventually, these aberrant formations could lead to the impairment of the PrP^{C} functions in physiology. Possibly, PrP^{Sc} conformers can interact with other molecules that the normal PrP^{C} structure does not bind to. Or, this opposite phenomenon might occur during the TSE disease development. This aspect arises from the PRC7 reactivity to

under-glycosylated PrP^{Sc} forms. This mAb cannot bind to the abundance of native PrP^{C} structures with two glycans. Therefore, the loss of glycans might escalate or interfere with molecular interactions abnormally, resulting in the impairment of PrP^{C} functions. Subsequently, the toxic gain or functional loss of these interactions could trigger pathogenic alterations in cellular biology and physiology. These pathogenic mechanisms are common in other neurodegenerative diseases, such as AD, PD, ALS, HD, and frontotemporal dementia.[6] Declines of PrP^{C} productions and expressions affect these normal functions and cause pathogenic alterations. In conclusion, the monitor of PrP^{C}-PrP^{Sc} variances is a valuable analysis to understand disease stages and prognoses. The generation of under-glycosylated PrP forms must be a characteristic feature of TSEs as a diagnostic biomarker for disease infection and progression. Based on all findings in this dissertation, the 7-5 ELISA and D-5 ELISA methods have exceptional capabilities of analyzing PrP modulations in the TSE disease development.

Future Directions

Unfolded protein responses are the central role of pathological mechanisms for disturbing protein conformations in neurodegenerative diseases including TSEs.[7,8] The predominance of partially unfolded PrP forms appears in the process of conformational conversions to misfolded structures.[9] These immature or intermediate conformations should be under-glycosylated forms of PrP molecules, in an alteration from PrP^{C} to PrP^{Sc} structures and/or during new PrP^{Sc} replication and generation. Thus, I propose that the PrP^{Sc} conformers in under-glycosylated or immature/intermediate states are fully or partially unfolding conditions. In this dissertation, PRC7 mAb and the 7-5 ELISA

method could not detect PrP^{Sc} levels (under-glycosylated forms) without denaturation. These observations indicated that denaturation might induce a renaturation process for unfolding PrP^{Sc} forms to PrP^{C} or its equivalent structure that PRC7 could bind to.

As a future direction, I hypothesize that the PrP glycosylation state changes during different stages of the TSE pathogenesis, especially for under-glycosylated PrP forms. For this aim, the 7-5 ELISA method would be applicable to determine the modulation of glycosylated PrP formations at different time points, through the disease course of asymptomatic, symptomatic, and progressive conditions in TSE-mouse models. This experimental project can investigate the under-glycosylated PrP formation and variance during the PrP^{Sc} replication and generation. This longitudinal approach will identify the kinetic changes of the PrP glycosidic state as involved in the disease development. Furthermore, the D-5 ELISA methods would investigate PrP modulations (both PrP^{C} and PrP^{Sc}) in longitudinal and kinetic studies using TSE mouse models. Besides histological analyses and other standard PrP analyses, electrodiagnoses (i.e. EEG) and biomechanical gait analyses will be supportive approaches if applicable. In the diagnostic application for the CWD infectious state, the two Sandwich ELISA approaches would establish the scale ranges of PrP levels in normal/uninfected, asymptomatic, and early to terminal stages of disease courses via large sample studies of cervid tissues and live animals. For kinetic and longitudinal analyses, fluids (i.e. blood, saliva, urine) and cutaneous/subcutaneous tissues will be practical samples to monitor the modulation of PrP^{C}-PrP^{Sc} variances as well as the PrP^{Sc} appearance. Based on the diagnostic advantages of these ELISA methods, the detectable property of PK-sensitive PrP forms will provide more accurate analyses for these pathogenic alterations

in TSE research, veterinary medicine, and public health. For human medicine, the 7-5 and D-5 ELISA methods might have a beneficial impact applying to major disorders including DM and cancer.[10-15] Recent studies have revealed the interaction or implication of PrP^C isoforms with disease-related molecules in non-TSE neurodegenerative pathologies, such as AD, PD, HD, and ALS.[16-36] Theoretically, these Sandwich ELISA protocols can be utilized for these neurological diseases by only a single modification.

In further expansions, the 7-5 and D-5 ELISA utilities can be applicable to traumatic brain injury (TBI). Recently, TBI has had serious attention through the world, because of prominent causes for mortality and morbidity.[37,38] The TBI severity has a classification with three grades: mild, moderate, and severe. Acute TBI causes short-term complications, such as subdural hematoma and catastrophic brain injury, which a severe TBI grade might result in death. In contrast, the low severity of TBI, such as mild TBI and concussion, causes functional impairments and axonal injuries in brains, rather than gross structural damages. Military professionals and contact-sports athletes who have histories of TBI, such as concussions or head trauma, are prone to exhibit a typical brain lesion, called chronic traumatic encephalopathy (CTE).[39,40] Over the past decades, trauma-mediated degenerations in brains are commonly recognized in boxers who have had repetitive impacts to their brains.[41] At present, CTE induces severe issues in sports and recreational activities.[42] In the US, the annual incidence of concussions is estimated as 3.8 million people. These issues mostly occur in competitive sports events and recreational activities.[43] Possibly, 50% of the concussion cases are not reported. Any sports have potential risks for concussions, while sports

with frequent physical contacts have higher incidences, such as American football, soccer, basketball, hockey (field and ice), and rugby. Currently, the US public perception has increased the awareness of CTE in contact-sports athletes, particularly in National Football League (NFL) players.[44] Both media and scientific fields have investigated the connections of repetitive mild TBI with CTE in American football players, leading to other neurodegenerative developments and deaths. Over 3,000 former NFL players and their families have argued that the NFL failed to acknowledge and address the risks of repetitive TBI as leading to developments of neurodegenerative disorders such as CTE, AD and PD. The damaged brains would induce neurological impairments and psychiatric abnormalities. Thus, the medical and legal investigations of CTE in the NFL are indispensable from a forensic psychiatry perspective. Now, this attention is more focused on high school football players and their parents for the risks of silent CTE developments and future clinical onsets. Thus, it is critical how children in contact sports can prevent potential risks of neurological impairments, which would influence their educational abilities and long-term lives with good health.

In the CTE progression, affected people show various clinical symptoms, such as cognitive impairment, mood change, and behavioral abnormality.[39,40] Their brains exhibit aberrant depositions of hyper phosphorylated tau proteins, which are characteristic features of the CTE diagnosis at postmortem autopsies. A recent study found the correlation that increased levels of phosphorylated tau proteins were implicated with PrP^C expression levels in the brain and blood, following severe TBI.[45] This correlation linked to observations of clinical dysfunctions, such as cognitive impairments. Thus, PrP^C isoforms should be associated with the mechanism of TBI-

related pathogenesis. Nevertheless, the tau deposition is a detectable feature with other factors, such as genetic mutations, drugs, toxins, aging, environmental factors, and postmortem brain processing. Possibly, athletes with these backgrounds might have greater susceptibilities for developing CTE and other neurodegenerative diseases, as resulted from TBI and its delayed complications. Intriguingly, athletes who had sport-related concussions exhibited a significant increase of PrP^C levels in their plasma.[46] Thus, the measurement of plasma PrP^C levels can be a reliable diagnostic biomarker for the assessments of the TBI severity and prognosis. However, the implication of PrP^C isoforms is not well understood in TBI and CTE yet.

Furthermore, numbers of media reports have reinforced the implications of mental health problems and CTE in former professional athletes (contact sports) and military veterans who had repetitive TBI.[47,48] CTE could implicate to their underlying suicidality, resulting from posttraumatic stress disorder (PTSD) and depression. Possibly, proteinopathy in the CTE development might be a causative factor in these clinical features, similar to other neurodegenerative diseases. Thus, additional researches are necessary to identify mediators or moderators of mental health problems and suicidality in neuropathology of TBI and CTE, especially for pathogenic and molecular mechanisms. An experimental study reported that TBI impaired expression levels of GABA-receptor subunits in brains, which affect these associated pathways of signaling transductions.[49] Since GABAergic synaptic systems inhibit excitable neuronal circuits in the brain, reductions of GABA receptors influence sensitivities to neurotransmitters and result in hyperexcitable consequences.[50,51]

In addition, PrP^C defects diminish fast inhibitions of post-synaptic potential via GABA receptors. Thus, PrP^C alterations impair the receptor activities in neuronal circuits, leading to aberrant changes in neurophysiology.[52] These abnormalities disrupt Ca^{2+} homeostasis and cause depolarizations in the brains, which provoke clinical onsets in individuals with brain lesions.[51] Moreover, synaptic PrP^C depositions progress neuronal degenerations in brains.[53,54] These pathologic progressions link to the loss of inhibitory GABA receptors in the brain. The synaptic degenerations exacerbate axonal transports and PrP^C activities, eventually causing apoptotic cell death and pathogenic development in the brain.[55] Hence, PrP^C expressions are relative factors in TBI-mediated changes in brains. In mouse models, blast-induced TBI increases PrP^C levels in plasma after the injury.[56] This PrP^C increase indicates that blast waves disrupt brains and dislodge extracellular-localized PrP^C molecules, leading to elevated PrP^C concentrations through the systemic circulation. In fact, the plasma PrP^C level is correlated to increasing the blast intensity. Therefore, the PrP^C level should be a valuable biomarker to detect and evaluate TBI, its severity and delayed complications. To investigate the PrP^C implication in TBI and CTE pathogeneses, I assume that the established methods in this dissertation, especially the D-5 ELISA without denaturation, would be capable of understanding the PrP^C modulation in the disease progression and prognosis. Ultimately, PrP^C isoforms might be the targeting molecules for novel therapeutic innovations in brain damages, not only for TBI and CTE, but also stroke and other neurological disorders.

REFERENCES

1. Gavier-Widén D, Stack MJ, Baron T, Balachandran A, Simmons M. Diagnosis of transmissible spongiform encephalopathies in animals: a review. *J Vet Diagn Invest* 2005;17:509–27.
2. Lukan A, Vranac T, Curin Šerbec V. TSE diagnostics: recent advances in immunoassaying prions. *Clin Dev Immunol* 2013;2013:360604.
3. Tzaban S, Friedlander G, Schonberger O, Horonchik L, Yedidia Y, Shaked G, *et al.* Protease-sensitive scrapie prion protein in aggregates of heterogeneous sizes. *Biochemistry* 2002;41:12868–75.
4. Nazor KE, Kuhn F, Seward T, Green M, Zwald D, Pürro M, *et al.* Immunodetection of disease-associated mutant PrP, which accelerates disease in GSS transgenic mice. *EMBO J* 2005;24:2472–80.
5. Thackray AM, Hopkins L, Bujdoso R. Proteinase K-sensitive disease-associated ovine prion protein revealed by conformation-dependent immunoassay. *Biochem J* 2007;401:475–83.
6. Westergard L, Christensen HM, Harris DA. The cellular prion protein (PrP(C)): its physiological function and role in disease. *Biochim Biophys Acta* 2007;1772:629–44.
7. Halliday M, Mallucci GR. Review: Modulating the unfolded protein response to prevent neurodegeneration and enhance memory. *Neuropathol Appl Neurobiol* 2015;41:414–27.
8. Scheper W, Hoozemans JJM. The unfolded protein response in neurodegenerative diseases: a neuropathological perspective. *Acta Neuropathol* 2015;130:315–31.
9. Moulick R, Das R, Udgaonkar JB. Partially Unfolded Forms of the Prion Protein Populated under Misfolding-promoting Conditions: CHARACTERIZATION BY HYDROGEN EXCHANGE MASS SPECTROMETRY AND NMR. *J Biol Chem* 2015;290:25227–40.
10. Strom A, Wang G-S, Reimer R, Finegood DT, Scott FW. Pronounced cytosolic aggregation of cellular prion protein in pancreatic beta-cells in response to hyperglycemia. *Lab Invest* 2007;87:139–49.
11. Mehrpour M, Codogno P. Prion protein: From physiology to cancer biology. *Cancer Lett* 2010;290:1–23.
12. Bitel CL, Feng Y, Souayah N, Frederikse PH. Increased expression and local accumulation of the prion protein, Alzheimer Aβ peptides, superoxide dismutase 1, and nitric oxide synthases 1 & 2 in muscle in a rabbit model of diabetes. *BMC Physiol* 2010;10:18.
13. Antony H, Wiegmans AP, Wei MQ, Chernoff YO, Khanna KK, Munn AL. Potential roles for prions and protein-only inheritance in cancer. *Cancer Metastasis Rev* 2012;31:1–19.
14. Santos TG, Lopes MH, Martins VR. Targeting prion protein interactions in cancer. *Prion* 2015;9:165–73.
15. Mukherjee A, Soto C. Prion-Like Protein Aggregates and Type 2 Diabetes. *Cold Spring Harb Perspect Med* 2017;7:.

16. Dupuis L, Mbebi C, Gonzalez de Aguilar J-L, Rene F, Muller A, de Tapia M, *et al.* Loss of prion protein in a transgenic model of amyotrophic lateral sclerosis. *Mol Cell Neurosci* 2002;19:216–24.
17. Eikelenboom P, Bate C, Van Gool WA, Hoozemans JJM, Rozemuller JM, Veerhuis R, *et al.* Neuroinflammation in Alzheimer's disease and prion disease. *Glia* 2002;40:232–9.
18. Castellani RJ, Perry G, Smith MA. Prion disease and Alzheimer's disease: pathogenic overlap. *Acta Neurobiol Exp (Wars)* 2004;64:11–7.
19. Lee K-J, Panzera A, Rogawski D, Greene LE, Eisenberg E. Cellular prion protein (PrPC) protects neuronal cells from the effect of huntingtin aggregation. *J Cell Sci* 2007;120:2663–71.
20. Laurén J, Gimbel DA, Nygaard HB, Gilbert JW, Strittmatter SM. Cellular prion protein mediates impairment of synaptic plasticity by amyloid-beta oligomers. *Nature* 2009;457:1128–32.
21. Kellett KAB, Hooper NM. Prion protein and Alzheimer disease. *Prion* 2009;3:190–4.
22. Steinacker P, Hawlik A, Lehnert S, Jahn O, Meier S, Görz E, *et al.* Neuroprotective function of cellular prion protein in a mouse model of amyotrophic lateral sclerosis. *Am J Pathol* 2010;176:1409–20.
23. Olanow CW, McNaught K. Parkinson's disease, proteins, and prions: milestones. *Mov Disord* 2011;26:1056–71.
24. Westaway D, Jhamandas JH. The P's and Q's of cellular PrP-Aβ interactions. *Prion* 2012;6:359–63.
25. Ashe KH, Aguzzi A. Prions, prionoids and pathogenic proteins in Alzheimer disease. *Prion* 2013;7:55–9.
26. Zhou J, Liu B. Alzheimer's disease and prion protein. *Intractable Rare Dis Res* 2013;2:35–44.
27. Dohler F, Sepulveda-Falla D, Krasemann S, Altmeppen H, Schlüter H, Hildebrand D, *et al.* High molecular mass assemblies of amyloid-β oligomers bind prion protein in patients with Alzheimer's disease. *Brain* 2014;137: 873–86.
28. Goedert M. NEURODEGENERATION. Alzheimer's and Parkinson's diseases: The prion concept in relation to assembled Aβ, tau, and α-synuclein. *Science* 2015;349:1255555.
29. Falker C, Hartmann A, Guett I, Dohler F, Altmeppen H, Betzel C, *et al.* Exosomal cellular prion protein drives fibrillization of amyloid beta and counteracts amyloid beta-mediated neurotoxicity. *J Neurochem* 2016;137: 88–100.
30. Salazar SV, Strittmatter SM. Cellular prion protein as a receptor for amyloid-β oligomers in Alzheimer's disease. *Biochem Biophys Res Commun* 2017;483:1143–7.
31. Hartmann A, Muth C, Dabrowski O, Krasemann S, Glatzel M. Exosomes and the Prion Protein: More than One Truth. *Front Neurosci* 2017;11:194.
32. Onodera T. Dual role of cellular prion protein in normal host and Alzheimer's disease. *Proc Jpn Acad, Ser B, Phys Biol Sci* 2017;93:155–73.

33. Urrea L, Ferrer I, Gavín R, Del Río JA. The cellular prion protein (PrPC) as neuronal receptor for α-synuclein. *Prion* 2017;11:226–33.
34. Aulić S, Masperone L, Narkiewicz J, Isopi E, Bistaffa E, Ambrosetti E, *et al.* α-Synuclein Amyloids Hijack Prion Protein to Gain Cell Entry, Facilitate Cell-to-Cell Spreading and Block Prion Replication. *Sci Rep* 2017;7:10050
35. Ferreira DG, Temido-Ferreira M, Miranda HV, Batalha VL, Coelho JE, Szegö ÉM, *et al.* α-synuclein interacts with PrPCto induce cognitive impairment through mGluR5 and NMDAR2B. *Nat Neurosci* 2017;20:1569–79.
36. Purro SA, Nicoll AJ, Collinge J. Prion Protein as a Toxic Acceptor of Amyloid-β Oligomers. *Biol Psychiatry* 2018;83:358–68.
37. Levin HS, Diaz-Arrastia RR. Diagnosis, prognosis, and clinical management of mild traumatic brain injury. *Lancet Neurol* 2015;14:506–17.
38. Ling H, Hardy J, Zetterberg H. Neurological consequences of traumatic brain injuries in sports. *Mol Cell Neurosci* 2015;66:114–22.
39. Wilk JE, Thomas JL, McGurk DM, Riviere LA, Castro CA, Hoge CW. Mild traumatic brain injury (concussion) during combat: lack of association of blast mechanism with persistent postconcussive symptoms. *J Head Trauma Rehabil* 2010;25:9–14.
40. Davis GA, Castellani RJ, McCrory P. Neurodegeneration and sport. *Neurosurgery* 2015;76:643–55; discussion 655-656.
41. Koliatsos VE, Xu L. The Problem of Neurodegeneration in Cumulative Sports Concussions: Emphasis on Neurofibrillary Tangle Formation. In: Kobeissy FH, editor. *Brain Neurotrauma: Molecular, Neuropsychological, and Rehabilitation Aspects*. Boca Raton (FL): CRC Press/Taylor & Francis; 2015.
42. Love S, Solomon GS. Talking with parents of high school football players about chronic traumatic encephalopathy: a concise summary. *Am J Sports Med* 2015;43:1260–4.
43. Harmon KG, Drezner JA, Gammons M, Guskiewicz KM, Halstead M, Herring SA, *et al.* American Medical Society for Sports Medicine position statement: concussion in sport. *Br J Sports Med* 2013;47:15–26.
44. Korngold C, Farrell HM, Fozdar M. The National Football League and chronic traumatic encephalopathy: legal implications. *J Am Acad Psychiatry Law* 2013;41:430–6.
45. Rubenstein R, Chang B, Grinkina N, Drummond E, Davies P, Ruditzky M, *et al.* Tau phosphorylation induced by severe closed head traumatic brain injury is linked to the cellular prion protein. *Acta Neuropathol Commun* 2017;5:30.
46. Pham N, Akonasu H, Shishkin R, Taghibiglou C. Plasma soluble prion protein, a potential biomarker for sport-related concussions: a pilot study. *PLoS ONE* 2015;10:e0117286.
47. Iverson GL. Chronic traumatic encephalopathy and risk of suicide in former athletes. *Br J Sports Med* 2014;48:162–5.
48. Iverson GL. Suicide and Chronic Traumatic Encephalopathy. *J Neuropsychiatry Clin Neurosci* 2016;28:9–16.
49. Raible DJ, Frey LC, Cruz Del Angel Y, Russek SJ, Brooks-Kayal AR. GABA(A) receptor regulation after experimental traumatic brain injury. *J Neurotrauma* 2012;29:2548–54.

50. Armijo JA, Valdizán EM, De Las Cuevas I, Cuadrado A. [Advances in the physiopathology of epileptogenesis: molecular aspects]. *Rev Neurol* 2002;34:409–29.
51. Aroniadou-Anderjaska V, Fritsch B, Qashu F, Braga MFM. Pathology and pathophysiology of the amygdala in epileptogenesis and epilepsy. *Epilepsy Res* 2008;78:102–16.
52. Blumenfeld H. Cellular and network mechanisms of spike-wave seizures. *Epilepsia* 2005;46 Suppl 9:21–33.
53. Ferrer I, Puig B, Blanco R, Martí E. Prion protein deposition and abnormal synaptic protein expression in the cerebellum in Creutzfeldt-Jakob disease. *Neuroscience* 2000;97:715–26.
54. Hüls S, Högen T, Vassallo N, Danzer KM, Hengerer B, Giese A, *et al.* AMPA-receptor-mediated excitatory synaptic transmission is enhanced by iron-induced α-synuclein oligomers. *J Neurochem* 2011;117:868–78.
55. Ferrer I. Synaptic pathology and cell death in the cerebellum in Creutzfeldt-Jakob disease. *Cerebellum* 2002;1:213–22.
56. Pham N, Sawyer TW, Wang Y, Jazii FR, Vair C, Taghibiglou C. Primary blast-induced traumatic brain injury in rats leads to increased prion protein in plasma: a potential biomarker for blast-induced traumatic brain injury. *J Neurotrauma* 2015;32:58–65.